

8-2013

Design of Cable-to-Post Attachments for Use in a Non-Proprietary, High-Tension, Cable Median Barrier

Ronald K. Faller

University of Nebraska - Lincoln, rfaller1@unl.edu

Robert W. Bielenberg

University of Nebraska - Lincoln, rbielenberg2@unl.edu

Dean L. Sicking

University of Nebraska - Lincoln, dsicking1@unl.edu

Cody S. Stolle

University of Nebraska at Lincoln, cstolle2@unl.edu

Karla A. Lechtenberg

University of Nebraska - Lincoln, kpolivka2@unl.edu

See next page for additional authors

Follow this and additional works at: <http://digitalcommons.unl.edu/ndor>



Part of the [Transportation Engineering Commons](#)

Faller, Ronald K.; Bielenberg, Robert W.; Sicking, Dean L.; Stolle, Cody S.; Lechtenberg, Karla A.; Rosenbaugh, Scott K.; Bateman, Ryan J.; and Reid, John D., "Design of Cable-to-Post Attachments for Use in a Non-Proprietary, High-Tension, Cable Median Barrier" (2013). *Nebraska Department of Transportation Research Reports*. 111.
<http://digitalcommons.unl.edu/ndor/111>

This Article is brought to you for free and open access by the Nebraska LTAP at DigitalCommons@University of Nebraska - Lincoln. It has been accepted for inclusion in Nebraska Department of Transportation Research Reports by an authorized administrator of DigitalCommons@University of Nebraska - Lincoln.

Authors

Ronald K. Faller, Robert W. Bielenberg, Dean L. Sicking, Cody S. Stolle, Karla A. Lechtenberg, Scott K. Rosenbaugh, Ryan J. Bateman, and John D. Reid



*Midwest States Regional Pooled Fund Research Program
Fiscal Years 2009-2012 (Years 19 and 22)
Research Project Number TPF-5(091) and TPF-5(193)
NDOR Sponsoring Agency Code RFPF-09-01 and RFPF-12-CABLE 1&2*

DESIGN OF CABLE-TO-POST ATTACHMENTS FOR USE IN A NON-PROPRIETARY, HIGH-TENSION, CABLE MEDIAN BARRIER

Submitted by

Ryan J. Bateman, M.S.C.E., E.I.T.
Former Graduate Research Assistant

Ronald K. Faller, Ph.D., P.E.
Research Associate Professor
MwRSF Director

Robert W. Bielenberg, M.S.M.E., E.I.T.
Research Associate Engineer

Dean L. Sicking, Ph.D., P.E.
Emeritus Professor

John D. Reid, Ph.D.
Professor

Cody S. Stolle, Ph.D., E.I.T.
Post-Doctoral Research Assistant

Karla A. Lechtenberg, M.S.M.E., E.I.T.
Research Associate Engineer

Scott K. Rosenbaugh, M.S.C.E., E.I.T.
Research Associate Engineer

MIDWEST ROADSIDE SAFETY FACILITY

Nebraska Transportation Center
University of Nebraska-Lincoln
130 Whittier Research Center
2200 Vine Street
Lincoln, Nebraska 68583-0853
(402) 472-0965

Submitted to

MIDWEST STATES REGIONAL POOLED FUND PROGRAM

Nebraska Department of Roads
1500 Nebraska Highway 2
Lincoln, Nebraska 68502

MwRSF Research Report No. TRP-03-285-13

August 29, 2013

TECHNICAL REPORT DOCUMENTATION PAGE

1. Report No. TRP-03-285-13	2.	3. Recipient's Accession No.	
4. Title and Subtitle Design of Cable-to-Post Attachments for Use in a Non-Proprietary, High-Tension, Cable Median Barrier		5. Report Date August 29, 2013	
		6.	
7. Author(s) Bateman, R.J., Faller, R.K., Bielenberg, R.W., Sicking, D.L., Reid, J.D., Stolle, C.S., Lechtenberg, K.A., Rosenbaugh, S.K.		8. Performing Organization Report No. TRP-03-285-13	
9. Performing Organization Name and Address Midwest Roadside Safety Facility (MwRSF) Nebraska Transportation Center University of Nebraska-Lincoln 130 Whittier Research Center 2200 Vine Street Lincoln, Nebraska 68583-0853		10. Project/Task/Work Unit No.	
		11. Contract © or Grant (G) No. TPF-5(091) Sup. #1 TPF-5(193) Sup. #44 & 45	
12. Sponsoring Organization Name and Address Midwest States Regional Pooled Fund Program Nebraska Department of Roads 1500 Nebraska Highway 2 Lincoln, Nebraska 68502		13. Type of Report and Period Covered Final Report: 2011-2013	
		14. Sponsoring Agency Code RPFP-09-01 RPFP-12-CABLE 1&2	
15. Supplementary Notes Prepared in cooperation with U.S. Department of Transportation, Federal Highway Administration.			
16. Abstract <p>Cable median barriers are widely used across the country to prevent cross-median crashes. Several years ago, the Midwest States Pooled Fund Program contracted with the Midwest Roadside Safety Facility (MwRSF) to develop a new, non-proprietary, high-tension, 4-cable median barrier. In the Fall of 2011 and following two failed full-scale vehicle crash tests on prototype barrier systems, it was determined that design modifications were necessary to improve barrier performance. In addition, members of the Midwest States Pooled Fund Program desired to redirect the development effort.</p> <p>Both of the barrier system failures which prompted the re-design effort could be partially attributed to the manner in which the cables were attached to the posts. Therefore, the cable-to-post attachments at all four cable heights were to be re-designed.</p> <p>The first step in this effort was to determine the minimum design loads associated with horizontal and vertical curves as a function of post spacing. Once the design loads were known, target capacities for the lateral and vertical cable release out of the cable-to-post attachments were determined. The target vertical and lateral cable release capacities for the lower three cables were 225 lb (1.00 kN) and 6.00 kips (26.7 kN), respectively. The top cable-to-post attachment had a target range of 100 to 200 lb (445 to 890 N) for both the lateral and vertical cable release capacities.</p> <p>MwRSF performed seventy dynamic component tests, forty-five static component tests, and one bogie impact test on prototype cable-to-post attachments. Finally, a cable-to-post attachment, consisting of a bolted tabbed bracket, was recommended for use with the lower three cables and provided lateral and vertical cable release capacities of 6.10 kips (27.1 kN) and 346 lb (1.54 kN), respectively. Further, a top cable-to-post attachment, consisting of a straight brass rod with bent ends, was recommended for placement in a notch and provided a vertical and lateral cable release capacity of approximately 175 lb (778 N).</p>			
17. Document Analysis/Descriptors High-Tension, Median, Cable Barrier, Cable Hardware, Crash Test, Highway Safety, Roadside Appurtenances		18. Availability Statement No restrictions. Document available from: National Technical Information Services, Springfield, Virginia 22161	
19. Security Class (this report) Unclassified	20. Security Class (this page) Unclassified	21. No. of Pages 570	22. Price

DISCLAIMER STATEMENT

This report was completed with funding from the Federal Highway Administration, U.S. Department of Transportation. The contents of this report reflect the views and opinions of the authors who are responsible for the facts and the accuracy of the data presented herein. The contents do not necessarily reflect the official views or policies of the state highway departments participating in the Midwest States Regional Pooled Fund Program nor the Federal Highway Administration, U.S. Department of Transportation. This report does not constitute a standard, specification, regulation, product endorsement, or an endorsement of manufacturers.

UNCERTAINTY OF MEASUREMENT STATEMENT

The Midwest Roadside Safety Facility (MwRSF) has determined the uncertainty of measurements for several parameters involved in standard full-scale crash testing and non-standard testing of roadside safety features. Information regarding the uncertainty of measurements for critical parameters is available upon request by the sponsor and the Federal Highway Administration. Test nos. HTCUB-38 through HTCUB-65, HTTB-1 through HTTB-40, KR-1 through KR-36, and TCT-1 through TCT-9 were non-certified component tests conducted for research and development purposes only.

INDEPENDENT APPROVING AUTHORITY

The Independent Approving Authority (IAA) for the data contained herein was Dr. Jennifer Schmidt, Post-Doctoral Research Assistant.

ACKNOWLEDGEMENTS

The authors wish to acknowledge several sources that made a contribution to this project: (1) the Midwest States Regional Pooled Fund Program funded by the Illinois Department of Transportation, Iowa Department of Transportation, Kansas Department of Transportation, Minnesota Department of Transportation, Missouri Department of Transportation, Nebraska Department of Roads, Ohio Department of Transportation, South Dakota Department of Transportation, Wisconsin Department of Transportation, and Wyoming Department of Transportation for sponsoring this project; and (2) MwRSF personnel for constructing the barriers and conducting the crash tests.

Acknowledgement is also given to the following individuals who made a contribution to the completion of this research project.

Midwest Roadside Safety Facility

J.C. Holloway, M.S.C.E., E.I.T., Test Site Manager
J.D. Schmidt, Ph.D., E.I.T., Post-Doctoral Research Assistant
A.T. Russell, B.S.B.A., Shop Manager
K.L. Krenk, B.S.M.A., Maintenance Mechanic
S.M. Tighe, Laboratory Mechanic
D.S. Charroin, Laboratory Mechanic
Undergraduate and Graduate Research Assistants

Illinois Department of Transportation

David Piper, P.E., Safety Implementation Engineer (retired)
Priscilla A. Tobias, P.E., State Safety Engineer/Bureau Chief
Tim Sheehan, P.E., Safety Design Unit Chief

Iowa Department of Transportation

Chris Poole, P.E., Litigation/Roadside Safety Engineer

Kansas Department of Transportation

Ron Seitz, P.E., Bureau Chief
Rod Lacy, P.E., Metro Engineer
Scott King, P.E., Road Design Leader

Minnesota Department of Transportation

Michael Elle, P.E., Design Standard Engineer

Missouri Department of Transportation

Joseph G. Jones, P.E., Engineering Policy Administrator

Nebraska Department of Roads

Phil TenHulzen, P.E., Design Standards Engineer
Jodi Gibson, Research Coordinator

Ohio Department of Transportation

Michael Bline, P.E., Standards and Geometrics Engineer
Maria Rupp, P.E., Roadway Standards Engineer

South Dakota Department of Transportation

David Huft, Research Engineer
Bernie Clocksin, Lead Project Engineer

Wisconsin Department of Transportation

Jerry Zogg, P.E., Chief Roadway Standards Engineer
John Bridwell, P.E., Standards Development Engineer
Erik Emerson, P.E., Standards Development Engineer

Wyoming Department of Transportation

William Wilson, P.E., Architectural and Highway Standards Engineer

Federal Highway Administration

John Perry, P.E., Nebraska Division Office
Danny Briggs, Nebraska Division Office

TABLE OF CONTENTS

TECHNICAL REPORT DOCUMENTATION PAGE	i
DISCLAIMER STATEMENT	ii
UNCERTAINTY OF MEASUREMENT STATEMENT.....	ii
INDEPENDENT APPROVING AUTHORITY.....	ii
ACKNOWLEDGEMENTS.....	iii
TABLE OF CONTENTS.....	v
LIST OF FIGURES	xi
LIST OF TABLES	xxii
1 INTRODUCTION	1
1.1 Problem Statement.....	1
1.2 Research Objective	3
1.3 Research Approach	3
1.4 Order of Report.....	3
2 LITERATURE REVIEW	7
2.1 Introduction.....	7
2.2 Cable-to-Post Attachments	7
2.3 A-Pillar Testing and Design.....	23
3 PROJECT BACKGROUND	25
3.1 Introduction.....	25
3.2 Improved Low-Tension Cable Median Barrier.....	25
3.3 High-Tension, Cable Median Barrier	30
3.3.1 Curved Keyway Bracket Development	30
3.3.2 Phase I Full-Scale Crash Tests.....	34
3.3.3 Keyway Bolt Development.....	37
3.3.4 Phase II Full-Scale Crash Tests	40
3.4 Conclusions.....	47
4 DETERMINATION OF DESIGN LOADS	49
4.1 Introduction.....	49
4.2 Prior Cable-to-Post Attachments—Capacity and Performance	49
4.3 Minimum Design Loads Due to Vertical Curves	50
4.4 Minimum Design Loads Due to Horizontal Curves	56
4.5 Target Lateral and Vertical Cable Release Capacities.....	60
5 OVERVIEW OF IMPROVED KEYWAY BOLTS—ROUND 1.....	61
5.1 Introduction.....	61

5.1.1 Dynamic Bogie Tests.....	61
5.1.2 Keyway Bolt Basics.....	61
5.2 First Round Design Modifications.....	63
5.2.1 Small Oversized Keyway.....	63
5.2.2 Large Oversized Keyway.....	64
5.2.3 Modified Keyway Bolt	65
6 CABLE-TO-POST ATTACHMENT DYNAMIC COMPONENT TEST CONDITIONS	67
6.1 Purpose.....	67
6.2 Scope.....	67
6.3 Test Facility	68
6.4 Equipment and Instrumentation.....	68
6.4.1 Bogie.....	68
6.4.2 Load Cell.....	69
6.4.3 Optic Speed Trap	70
6.4.4 Digital Photography	70
6.4.5 Test Jig.....	70
6.5 Data Processing.....	71
6.6 Loading Event Determination.....	72
6.7 Results.....	72
7 DYNAMIC COMPONENT TESTS—KEYWAY BOLTS, ROUND 1	74
7.1 Results.....	74
7.1.1 Test No. HTCUB-38 (A449 KB, Small, Vertical)	87
7.1.2 Test No. HTCUB-39 (A449 KB, Small, Vertical)	90
7.1.3 Test No. HTCUB-40 (A449 KB, Large, Vertical).....	93
7.1.4 Test No. HTCUB-41 (A449 KB, Large, Vertical).....	96
7.1.5 Test No. HTCUB-42 (C1018 KB, Small, Vertical).....	99
7.1.6 Test No. HTCUB-43 (C1018 KB, Small, Vertical).....	102
7.1.7 Test No. HTCUB-44 (C1018 KB, Large, Vertical).....	105
7.1.8 Test No. HTCUB-45 (C1018 KB, Large, Vertical).....	108
7.1.9 Test No. HTCUB-46 (A449 KB, Small, Lateral)	111
7.1.10 Test No. HTCUB-47 (A449 KB, Small, Lateral)	114
7.1.11 Test No. HTCUB-48 (A449 KB, Large, Lateral)	117
7.1.12 Test No. HTCUB-49 (A449 KB, Large, Lateral)	120
7.1.13 Test No. HTCUB-50 (C1018 KB, Small, Lateral)	123
7.1.14 Test No. HTCUB-51 (C1018 KB, Small, Lateral)	126
7.1.15 Test No. HTCUB-52 (C1018 KB, Large, Lateral)	129
7.1.16 Test No. HTCUB-53 (C1018 KB, Large, Lateral)	132
7.1.17 Test No. HTCUB-54 (C1018 Mod. KB, Large, Lateral).....	135
7.1.18 Test No. HTCUB-55 (C1018 Mod. KB, Large, Lateral).....	138
7.1.19 Test No. HTCUB-56 (C1018 Mod. KB, Large, Vertical)	141
7.1.20 Test No. HTCUB-57 (C1018 Mod. KB, Large, Vertical)	144
7.2 Discussion.....	147
8 OVERVIEW OF IMPROVED KEYWAY BOLTS—ROUND 2.....	149
8.1 Introduction.....	149

8.2 Extended Moment Arm Concepts.....	149
8.3 Extended Keyway Bolts.....	154
8.3.1 Computer Simulations	154
8.3.2 Prototype Extended Keyway Bolts	159
8.3.3 Dynamic Bogie Tests.....	160
9 DYNAMIC COMPONENT TESTS—EXTENDED KEYWAY BOLTS, ROUND 2.....	161
9.1 Results.....	161
9.1.1 Test No. HTCUB-58 (C1018 Ext. KB, Original, Vertical)	163
9.1.2 Test No. HTCUB-59 (C1018 Ext. KB, Original, Vertical)	166
9.1.3 Test No. HTCUB-60 (C1018 Ext. KB, Original, Lateral).....	169
9.1.4 Test No. HTCUB-61 (C1018 Ext. KB, Original, Lateral).....	172
9.1.5 Test No. HTCUB-62 (C1018 Ext. KB, Modified, Lateral)	175
9.1.6 Test No. HTCUB-63 (C1018 Ext. KB, Modified, Lateral)	178
9.1.7 Test No. HTCUB-64 (C1018 Ext. KB, Modified, Vertical).....	181
9.1.8 Test No. HTCUB-65 (C1018 Ext. KB, Modified, Vertical).....	184
9.2 Discussion	187
10 OVERVIEW OF CRIMP-IN-PLACE TABBED BRACKETS, ROUND 1	188
10.1 Introduction.....	188
10.1.1 Dynamic Bogie Tests	188
10.1.2 Tabbled Bracket Basics.....	189
10.2 Crimp-In-Place Tabbled Brackets.....	189
10.2.1 Round 1 Design Equations.....	190
10.2.2 Dimensions and Structural Capacities	194
11 DYNAMIC COMPONENT TESTS—CRIMP-IN-PLACE TABBED BRACKETS, ROUND 1	199
11.1 Results.....	199
11.1.1 Test No. HTTB-1 (TB V1, Crimp, Lateral).....	241
11.1.2 Test No. HTTB-2 (TB V1, Crimp, Lateral).....	244
11.1.3 Test No. HTTB-3 (TB V2, Crimp, Lateral).....	247
11.1.4 Test No. HTTB-4 (TB V2, Crimp, Lateral).....	250
11.1.5 Test No. HTTB-5 (TB V1, Crimp, Vertical)	253
11.1.6 Test No. HTTB-6 (TB V1, Crimp, Vertical)	256
11.1.7 Test No. HTTB-7 (TB V2, Crimp, Vertical)	259
11.1.8 Test No. HTTB-8 (TB V2, Crimp, Vertical)	262
11.2 Discussion	265
12 OVERVIEW OF BOLTED TABBED BRACKETS—ROUND 2	267
12.1 Introduction.....	267
12.1.1 Dynamic Bogie Tests.....	267
12.2 Bolted Tabbled Brackets.....	267
12.2.1 Round 2 Design Equations.....	268
12.2.2 Dimensions and Structural Capacities	273
13 DYNAMIC COMPONENT TESTS—TABBED BRACKETS, ROUND 2.....	278
13.1 Results.....	278

13.1.1 Test No. HTTB-9 (TB V3, Bolted, Vertical).....	281
13.1.2 Test No. HTTB-9R (TB V3, Bolted, Vertical)	283
13.1.3 Test No. HTTB-10 (TB V3, Bolted, Vertical).....	286
13.1.4 Test No. HTTB-11 (TB V3, Bolted, Lateral)	289
13.1.5 Test No. HTTB-12 (TB V3, Bolted, Lateral)	292
13.1.6 Test No. HTTB-12R (TB V3, Bolted, Lateral).....	295
13.1.7 Test No. HTTB-13 (TB V4, Bolted, Vertical).....	298
13.1.8 Test No. HTTB-14 (TB V4, Bolted, Vertical).....	301
13.1.9 Test No. HTTB-15 (TB V4, Bolted, Lateral)	304
13.1.10 Test No. HTTB-16 (TB V4, Bolted, Lateral)	307
13.2 Discussion	310
14 OVERVIEW OF BOLTED TABBED BRACKETS—ROUND 3	312
14.1 Introduction.....	312
14.1.1 Dynamic Bogie Tests.....	312
14.2 Bolted Tabbed Bracket Design Modifications.....	312
14.2.1 Round 3 Design Equations.....	313
14.2.2 Dimensions and Structural Capacities	317
15 DYNAMIC COMPONENT TESTS—TABBED BRACKETS, ROUND 3.....	331
15.1 Results.....	331
15.1.1 Test No. HTTB-17 (TB V5, Bolted, Vertical).....	335
15.1.2 Test No. HTTB-18 (TB V5, Bolted, Vertical).....	338
15.1.3 Test No. HTTB-19 (TB V5, Bolted, Vertical).....	341
15.1.4 Test No. HTTB-20 (TB V8, Bolted, Vertical).....	344
15.1.5 Test No. HTTB-21 (TB V8, Bolted, Lateral)	347
15.1.6 Test No. HTTB-22 (TB V8, Bolted, Lateral)	350
15.1.7 Test No. HTTB-23 (TB V5, Bolted, Lateral)	353
15.1.8 Test No. HTTB-24 (TB V5, Bolted, Lateral)	356
15.1.9 Test No. HTTB-25 (TB V6, Bolted, Lateral)	359
15.1.10 Test No. HTTB-26 (TB V6, Bolted, Lateral)	362
15.1.11 Test No. HTTB-27 (TB V7, Bolted, Lateral)	365
15.1.12 Test No. HTTB-28 (TB V7, Bolted, Lateral)	368
15.1.13 Test No. HTTB-29 (TB V9, Bolted, Lateral)	371
15.1.14 Test No. HTTB-30 (TB V9, Bolted, Lateral)	374
15.1.15 Test No. HTTB-31 (TB V10, Bolted, Lateral)	377
15.1.16 Test No. HTTB-32 (TB V10, Bolted, Lateral)	380
15.1.17 Test No. HTTB-33 (TB V6, Bolted, Vertical).....	383
15.1.18 Test No. HTTB-34 (TB V6, Bolted, Vertical).....	385
15.1.19 Test No. HTTB-35 (TB V7, Bolted, Vertical).....	387
15.1.20 Test No. HTTB-36 (TB V7, Bolted, Vertical).....	390
15.1.21 Test No. HTTB-37 (TB V10, Bolted, Vertical).....	393
15.1.22 Test No. HTTB-38 (TB V10, Bolted, Vertical).....	396
15.1.23 Test No. HTTB-39 (TB V6, Bolted, Vertical).....	399
15.1.24 Test No. HTTB-40 (TB V6, Bolted, Vertical).....	402
15.2 Discussion	404

16 CABLE-TO-POST ATTACHMENT CONCLUSIONS	407
16.1 Summary of Design and Testing Efforts	407
16.2 Selection of Cable-to-Post Attachment.....	409
17 TOP CABLE-TO-POST ATTACHMENT DETAILS	413
17.1 Introduction.....	413
17.1.1 Static Tensile Testing.....	414
17.2 Top Cable-to-Post Attachment Design Concepts	415
17.2.1 Web-Inserted Curved Rods.....	415
17.2.2 Revised Web-Inserted Curved Rods.....	415
17.2.3 Squeeze-In-Place Curved Rods.....	416
17.2.4 HellermannTyton Stainless Steel Cable Ties.....	417
17.2.5 Straight Rods.....	418
18 TOP CABLE-TO-POST ATTACHMENT STATIC TEST CONDITIONS.....	420
18.1 Purpose.....	420
18.2 Scope.....	420
18.3 Testing Facility	420
18.4 Equipment and Instrumentation.....	420
18.4.1 MTS 810	421
18.4.2 Test Jig	421
18.4.3 Digital Photography	422
19 TOP CABLE-TO-POST ATTACHMENT STATIC TESTING RESULTS AND DISCUSSION	423
19.1 Results.....	423
19.2 Web-Inserted Curved Rods.....	423
19.2.1 Test Nos. KR-1 and KR-2 (Web, 1/16-in. Brass).....	426
19.2.2 Test Nos. KR-3 and KR-4 (Web, 3/32-in. Brass).....	428
19.2.3 Test Nos. KR-5 and KR-6 (Web, 1/8-in. Brass).....	430
19.2.4 Test Nos. KR-7 and KR-8 (Web, 3/32-in. Stainless).....	432
19.2.5 Test Nos. KR-9 and KR-10 (Web, 1/8-in. Stainless).....	434
19.3 Squeeze-In-Place Curved Rods.....	436
19.3.1 Test Nos. KR-11 and KR-12 (Squeeze, 1/16-in. Brass)	438
19.3.2 Test Nos. KR-13 and KR-14 (Squeeze, 3/32-in. Brass)	440
19.3.3 Test Nos. KR-15 and KR-16 (Squeeze, 1/8-in. Brass)	442
19.3.4 Test Nos. KR-17 and KR-18 (Squeeze, 3/32-in. Stainless).....	444
19.3.5 Test Nos. KR-19 and KR-20 (Squeeze, 1/8-in. Stainless).....	446
19.4 HellermannTyton Stainless Steel Cable Ties.....	448
19.4.1 Tests that timed out.....	450
19.4.2 Test Nos. TCT-4, TCT-6 and TCT-7 (Ties, 0.31-in.).....	450
19.4.3 Test Nos. TCT-8 and TCT-9 (Ties, 0.18-in.).....	453
19.5 Revised Web-Inserted Curved Rods.....	455
19.5.1 Test Nos. KR-21 and KR-22 (Rev. Web, 1/8-in. Brass).....	457
19.5.2 Test Nos. KR-23 and KR-24 (Rev. Web, 1/8-in. Stainless)	459
19.6 Straight Rods.....	461
19.6.1 Test No. KR-25 (Straight, 1/8-in. Brass)	463

19.6.2 Test No. KR-26 (Straight, 1/8-in. Brass)	465
19.6.3 Test Nos. KR-27 and KR-28 (Straight, 1/8-in. Stainless).....	467
19.6.4 Test Nos. KR-29 and KR-30 (Straight, 3/16-in. Brass).....	469
19.6.5 Test Nos. KR-31 and KR-32 (Straight, 3/16-in. Stainless).....	471
19.6.6 Test Nos. KR-33 and KR-34 (Straight, 1/4-in. Brass).....	473
19.6.7 Test Nos. KR-35 and KR-36 (Straight, 1/4-in. Stainless).....	475
19.7 Discussion	477
20 TOP CABLE-TO-POST ATTACHMENT—BOGIE IMPACT TEST CONDITIONS	480
20.1 Purpose.....	480
20.2 Test Setup and Details	480
20.3 Test Facility	495
20.4 Equipment and Instrumentation.....	495
20.4.1 Bogie	495
20.4.2 Accelerometers	496
20.4.3 Optic Speed Trap	497
20.4.4 Pressure Tape Switches.....	498
20.4.5 Digital Photography	498
21 TOP CABLE-TO-POST ATTACHMENT—TEST RESULTS.....	499
21.1 Test No. HTTC-1 and Results	499
21.2 Discussion, Summary, Conclusions, and Recommendations	505
22 SUMMARY, CONCLUSIONS, AND RECOMMENDATIONS	506
22.1 Summary and Conclusions	506
22.1.1 Research Objective	506
22.1.2 Research Approach	506
22.1.3 Determination of Design Loads	507
22.1.4 Determining the Target Capacities	508
22.1.5 Keyway Bolts.....	509
22.1.6 Tabbed Brackets.....	510
22.1.7 Top Cable-to-Post Attachments	515
22.2 Recommendations.....	515
23 REFERENCES	517
24 APPENDICES	524
Appendix A. Proprietary Cable Barrier Systems	525
Appendix B. Full-Scale Crash Test Summary Sheets—Cable Barrier Testing	527
Appendix C. Derivation of Cable Slope Changes.....	537
Appendix D. CAD Details for Top Cable-to-Post Attachments	542
Appendix E. Material Specifications	555

LIST OF FIGURES

Figure 1. Weak-Steel Post Cable Guardrail [11]	9
Figure 2. Cable Hook Bolt [11]	9
Figure 3. Shouldered Cable Hook Bolt [11]	10
Figure 4. Typical Brifen WRSF.....	11
Figure 5. Brifen WRSF TL-4 Line Post Assembly [22]	12
Figure 6. Gibraltar TL-4 (3 Cable) Line Post Details [32]	13
Figure 7. Installation of Gibraltar's Hairpin and Lockplate [32].....	13
Figure 8. Nu-Cable TL-4 Cable-to-Post Attachments [33]	14
Figure 9. Nu-Cable TL-4 Line Post Detail, Median Configuration [33]	15
Figure 10. Safence Cable-to-Post Attachment Details [41].....	16
Figure 11. Safence with Side Hooks [49]	16
Figure 12. Trinity Highway Products' CASS [62]	17
Figure 13. CASS Wave-Shaped Slot [50].....	18
Figure 14. CASS Hook Bolts [50]	18
Figure 15. Armorwire Cable Barrier Line Post Assembly [63].....	19
Figure 16. Armorwire Cable Barrier Line Post Photographs [63].....	19
Figure 17. Typical A-Pillar	23
Figure 18. Cable Barrier System, Test No. CMB-1.....	26
Figure 19. Rigid Cable Bracket Detail, Test No. CMB-2.....	27
Figure 20. Cable Barrier System, Test No. CMB-2.....	27
Figure 21. Rigid Cable Bracket Detail, Test No. CMB-3.....	29
Figure 22. Cable Barrier System, Test No. CMB-3.....	29
Figure 23. U-Bolt Concepts	31
Figure 24. Curved Keyway Bracket with Shoulder Bolts.....	32
Figure 25. Curved Keyway Bracket Details	32
Figure 26. Curved Keyway Brackets Installed on Post	33
Figure 27. Cable Snag Resulting in Crushed A-Pillar, Test No. 4CMB-3	36
Figure 28. Keyway Bolt Details.....	38
Figure 29. Keyway Details	38
Figure 30. Keyway Bolts Installed on Post.....	39
Figure 31. Post Rotation Test with A449 Keyway Bolts, Test No. HTCC-4	41
Figure 32. Impact with Post and Barrier Override, Test No. 4CMB-5.....	43
Figure 33. A-Pillar Beginning to Crush, Test No. 4CMBLT-1	45
Figure 34. Vehicle Damage, Test No. 4CMBLT-1	45
Figure 35. Typical Parabolic Vertical Curve	51
Figure 36. Cable System on a Parabolic Vertical Curve	52
Figure 37. Change in Slope Between Post Spans	53
Figure 38. Free Body Diagram of Cable-to-Post Attachment on Vertical Curve.....	54
Figure 39. Cable Barrier on a Horizontal Curve.....	56
Figure 40. Free Body Diagram of a Post within a Horizontal Curve	57
Figure 41. Maximum Post Spacing vs. Horizontal Curve Radius	58
Figure 42. Keyway Bolt—(a) Design Details and (b) Seated in Keyway	62
Figure 43. Dual-Width Keyway.....	63
Figure 44. Small Oversized Keyway—(a) Dimensions and (b) With Keyway Bolt Installed	64
Figure 45. Large Oversized Keyway—(a) Dimensions and (b) With Keyway Bolt Installed	65

Figure 46. Modified Keyway Bolt—(a) Dimensions and (b) Installed in Large Oversized Keyway.....	66
Figure 47. Rigid Frame Bogie on Guidance Track.....	69
Figure 48. Test Jig.....	71
Figure 49. Bogie Test Setup, Test Nos. HTCUB-38 through HTCUB-65.....	75
Figure 50. Test Jig Details, Test Nos. HTCUB-38 through HTCUB-65.....	76
Figure 51. Test Jig Setup, Test Nos. HTCUB-38 through HTCUB-65.....	77
Figure 52. Reinforcement for S3x5.7 (S76x8.5), Test Nos. HTCUB-38 through HTCUB-65.....	78
Figure 53. Reinforcing Gussets and S3x5.7 (S76x8.5) Sections for Oversized Keyways, Test Nos. HTCUB-38 through HTCUB-65.....	79
Figure 54. S3x5.7 (S76x8.5) Sections for Dual-Width Keyways, Test Nos. HTCUB-38 through HTCUB-65.....	80
Figure 55. Keyway Bolt and Modified Keyway Bolt Details, Test Nos. HTCUB-38 through HTCUB-65.....	81
Figure 56. Extended Keyway Bolt Details, Test Nos. HTCUB-38 through HTCUB-65.....	82
Figure 57. Bogie Testing Matrix, Test Nos. HTCUB-38 through HTCUB-65.....	83
Figure 58. Bill of Materials, Test Nos. HTCUB-38 through HTCUB-65.....	84
Figure 59. Force-Time Data, Test No. HTCUB-38.....	88
Figure 60. Pre-Test and Post-Test Photographs, Test No. HTCUB-38.....	89
Figure 61. Sequential Photographs, Test No. HTCUB-38.....	89
Figure 62. Force-Time Data, Test No. HTCUB-39.....	91
Figure 63. Pre-Test and Post-Test Photographs, Test No. HTCUB-39.....	92
Figure 64. Sequential Photographs, Test No. HTCUB-39.....	92
Figure 65. Force-Time Data, Test No. HTCUB-40.....	94
Figure 66. Pre-Test and Post-Test Photographs, Test No. HTCUB-40.....	95
Figure 67. Sequential Photographs, Test No. HTCUB-40.....	95
Figure 68. Force-Time Data, Test No. HTCUB-41.....	97
Figure 69. Pre-Test and Post-Test Photographs, Test No. HTCUB-41.....	98
Figure 70. Sequential Photographs, Test No. HTCUB-41.....	98
Figure 71. Force-Time Data, Test No. HTCUB-42.....	100
Figure 72. Pre-Test and Post-Test Photographs, Test No. HTCUB-42.....	101
Figure 73. Sequential Photographs, Test No. HTCUB-42.....	101
Figure 74. Force-Time Data, Test No. HTCUB-43.....	103
Figure 75. Pre-Test and Post-Test Photographs, Test No. HTCUB-43.....	104
Figure 76. Sequential Photographs, Test No. HTCUB-43.....	104
Figure 77. Force-Time Data, Test No. HTCUB-44.....	106
Figure 78. Pre-Test and Post-Test Photographs, Test No. HTCUB-44.....	107
Figure 79. Sequential Photographs, Test No. HTCUB-44.....	107
Figure 80. Force-Time Data, Test No. HTCUB-45.....	109
Figure 81. Pre-Test and Post-Test Photographs, Test No. HTCUB-45.....	110
Figure 82. Sequential Photographs, Test No. HTCUB-45.....	110
Figure 83. Force-Time Data, Test No. HTCUB-46.....	112
Figure 84. Pre-Test and Post-Test Photographs, Test No. HTCUB-46.....	113
Figure 85. Sequential Photographs, Test No. HTCUB-46.....	113
Figure 86. Force-Time Data, Test No. HTCUB-47.....	115
Figure 87. Pre-Test and Post-Test Photographs, Test No. HTCUB-47.....	116
Figure 88. Sequential Photographs, Test No. HTCUB-47.....	116

Figure 89. Force-Time Data, Test No. HTCUB-48	118
Figure 90. Pre-Test and Post-Test Photographs, Test No. HTCUB-48	119
Figure 91. Sequential Photographs, Test No. HTCUB-48.....	119
Figure 92. Force-Time Data, Test No. HTCUB-49	121
Figure 93. Pre-Test and Post-Test Photographs, Test No. HTCUB-49	122
Figure 94. Sequential Photographs, Test No. HTCUB-49.....	122
Figure 95. Force-Time Data, Test No. HTCUB-50	124
Figure 96. Pre-Test and Post-Test Photographs, Test No. HTCUB-50	125
Figure 97. Sequential Photographs, Test No. HTCUB-50.....	125
Figure 98. Force-Time Data, Test No. HTCUB-51	127
Figure 99. Pre-Test and Post-Test Photographs, Test No. HTCUB-51	128
Figure 100. Sequential Photographs, Test No. HTCUB-51.....	128
Figure 101. Force-Time Data, Test No. HTCUB-52	130
Figure 102. Pre-Test and Post-Test Photographs, Test No. HTCUB-52	131
Figure 103. Sequential Photographs, Test No. HTCUB-52.....	131
Figure 104. Force-Time Data, Test No. HTCUB-53	133
Figure 105. Pre-Test and Post-Test Photographs, Test No. HTCUB-53	134
Figure 106. Sequential Photographs, Test No. HTCUB-53.....	134
Figure 107. Force-Time Data, Test No. HTCUB-54	136
Figure 108. Pre-Test and Post-Test Photographs, Test No. HTCUB-54	137
Figure 109. Sequential Photographs, Test No. HTCUB-54.....	137
Figure 110. Force-Time Data, Test No. HTCUB-55	139
Figure 111. Pre-Test and Post-Test Photographs, Test No. HTCUB-55	140
Figure 112. Sequential Photographs, Test No. HTCUB-55.....	140
Figure 113. Force-Time Data, Test No. HTCUB-56.....	142
Figure 114. Pre-Test and Post-Test Photographs, Test No. HTCUB-56	143
Figure 115. Sequential Photographs, Test No. HTCUB-56.....	143
Figure 116. Force-Time Data, Test No. HTCUB-57	145
Figure 117. Pre-Test and Post-Test Photographs, Test No. HTCUB-57	146
Figure 118. Sequential Photographs, Test No. HTCUB-57.....	146
Figure 119. Moment Arm Concept—(a) Cantilever Beam and (b) Keyway Bolt.....	149
Figure 120. Button Snag in the Load Cell Data.....	152
Figure 121. Extended-Moment-Arm Keyway Bolts—(a) Baseline, (b) AISI C1018, and (c) ASTM A449	153
Figure 122. Extended Moment-Arm Concepts—(a) Concept 1 and (b) Concept 2	154
Figure 123. Baseline Keyway Bolt Model.....	155
Figure 124. Keyway Bolt Models—(a) Baseline and (b) Extended	157
Figure 125. LS-DYNA Model Cable-Bolt Vertical Forces	157
Figure 126. Simulations—(a) Baseline Model and (b) Extended Keyway Bolt Model	158
Figure 127. Extended Keyway Bolt Prototype	159
Figure 128. Dual-Width Keyways—(a) Original and (b) Modified	160
Figure 129. Force-Time Data, Test No. HTCUB-58	164
Figure 130. Pre-Test and Post-Test Photographs, Test No. HTCUB-58	165
Figure 131. Sequential Photographs, Test No. HTCUB-58.....	165
Figure 132. Force-Time Data, Test No. HTCUB-59	167
Figure 133. Pre-Test and Post-Test Photographs, Test No. HTCUB-59	168
Figure 134. Sequential Photographs, Test No. HTCUB-59.....	168

Figure 135. Force-Time Data, Test No. HTCUB-60	170
Figure 136. Pre-Test and Post-Test Photographs, Test No. HTCUB-60	171
Figure 137. Sequential Photographs, Test No. HTCUB-60.....	171
Figure 138. Force-Time Data, Test No. HTCUB-61	173
Figure 139. Pre-Test and Post-Test Photographs, Test No. HTCUB-61	174
Figure 140. Sequential Photographs, Test No. HTCUB-61.....	174
Figure 141. Force-Time Data, Test No. HTCUB-62	176
Figure 142. Pre-Test and Post-Test Photographs, Test No. HTCUB-62	177
Figure 143. Sequential Photographs, Test No. HTCUB-62.....	177
Figure 144. Force-Time Data, Test No. HTCUB-63	179
Figure 145. Pre-Test and Post-Test Photographs, Test No. HTCUB-63	180
Figure 146. Sequential Photographs, Test No. HTCUB-63.....	180
Figure 147. Force-Time Data, Test No. HTCUB-64	182
Figure 148. Pre-Test and Post-Test Photographs, Test No. HTCUB-64	183
Figure 149. Sequential Photographs, Test No. HTCUB-64.....	183
Figure 150. Force-Time Data, Test No. HTCUB-65	185
Figure 151. Post-Test Photograph, Test No. HTCUB-65	186
Figure 152. Sequential Photographs, Test No. HTCUB-65.....	186
Figure 153. Tabbed Brackets—(a) Crimp-In-Place and (b) Bolted.....	189
Figure 154. Installed Crimp-In-Place Tabbed Bracket	190
Figure 155. Tabbed Bracket—(a) Laterally Loaded and (b) Vertically Loaded	191
Figure 156. Dimensions and Failure Locations for Tabbed Bracket	191
Figure 157. End Reactions for Use in the Design Equations.....	192
Figure 158. Side Views of Tabbed Bracket Version 1—Before and After Installation	195
Figure 159. Flat Pattern for Tabbed Bracket Version 1	195
Figure 160. Tabbed Bracket Version 1 Keyway.....	196
Figure 161. Side Views of Tabbed Bracket Version 2—Before and After Installation	197
Figure 162. Flat Pattern of Tabbed Bracket Version 2	197
Figure 163. Tabbed Bracket Version 2 Keyway.....	197
Figure 164. Bogie Test Setup, Test Nos. HTTPB-1 through HTTPB-40	200
Figure 165. Test Jig Details, Test Nos. HTTPB-1 through HTTPB-40.....	201
Figure 166. Test Jig Setup for Tabbed Bracket Versions 1 and 2, Test Nos. HTTPB-1 through HTTPB-40.....	202
Figure 167. Reinforced S3x5.7 (S76x8.5) Section Version 1 Details, Test Nos. HTTPB-1 through HTTPB-40.....	203
Figure 168. Reinforced S3x5.7 (S76x8.5) Section Version 1 Details, Test Nos. HTTPB-1 through HTTPB-40.....	204
Figure 169. Reinforced S3x5.7 (S76x8.5) Section Version 2 Details, Test Nos. HTTPB-1 through HTTPB-40.....	205
Figure 170. Reinforced S3x5.7 (S76x8.5) Section Version 2 Details, Test Nos. HTTPB-1 through HTTPB-40.....	206
Figure 171. Reinforcing Gusset Details, Test Nos. HTTPB-1 through HTTPB-40	207
Figure 172. Test Jig Setup for Tabbed Bracket Versions 3 and 4, Test Nos. HTTPB-1 through HTTPB-40.....	208
Figure 173. Reinforced S3x5.7 (S76x8.5) Section Version 3 Details, Test Nos. HTTPB-1 through HTTPB-40.....	209

Figure 174. Reinforced S3x5.7 (S76x8.5) Section Version 3 Details, Test Nos. HTTPB-1 through HTTPB-40.....	210
Figure 175. Reinforced S3x5.7 (S76x8.5) Section Version 4 Details, Test Nos. HTTPB-1 through HTTPB-40.....	211
Figure 176. Test Jig Setup for Tabbed Bracket Version 5 through 10, Test Nos. HTTPB-1 through HTTPB-40.....	212
Figure 177. Mounting Plate Details, Test Nos. HTTPB-1 through HTTPB-40.....	213
Figure 178. Reinforced C-Section Details, Test Nos. HTTPB-1 through HTTPB-40.....	214
Figure 179. C-Section Details, Test Nos. HTTPB-1 through HTTPB-40	215
Figure 180. C-Section Details, Test Nos. HTTPB-1 through HTTPB-40	216
Figure 181. Tabbed Bracket Version 1, Test Nos. HTTPB-1 through HTTPB-40.....	217
Figure 182. Version 1 Flat Pattern, Test Nos. HTTPB-1 through HTTPB-40.....	218
Figure 183. Tabbed Bracket Version 2, Test Nos. HTTPB-1 through HTTPB-40.....	219
Figure 184. Version 2 Flat Pattern, Test Nos. HTTPB-1 through HTTPB-40.....	220
Figure 185. Tabbed Bracket Version 3, Test Nos. HTTPB-1 through HTTPB-40.....	221
Figure 186. Version 3 Flat Pattern, Test Nos. HTTPB-1 through HTTPB-40.....	222
Figure 187. Tabbed Bracket Version 4, Test Nos. HTTPB-1 through HTTPB-40.....	223
Figure 188. Version 4 Flat Pattern, Test Nos. HTTPB-1 through HTTPB-40.....	224
Figure 189. Tabbed Bracket Version 5, Test Nos. HTTPB-1 through HTTPB-40.....	225
Figure 190. Version 5 Flat Pattern, Test Nos. HTTPB-1 through HTTPB-40.....	226
Figure 191. Tabbed Bracket Version 6, Test Nos. HTTPB-1 through HTTPB-40.....	227
Figure 192. Version 6 Flat Pattern, Test Nos. HTTPB-1 through HTTPB-40.....	228
Figure 193. Tabbed Bracket Version 7, Test Nos. HTTPB-1 through HTTPB-40.....	229
Figure 194. Version 7 Flat Pattern, Test Nos. HTTPB-1 through HTTPB-40.....	230
Figure 195. Tabbed Bracket Version 8, Test Nos. HTTPB-1 through HTTPB-40.....	231
Figure 196. Version 8 Flat Pattern, Test Nos. HTTPB-1 through HTTPB-40.....	232
Figure 197. Tabbed Bracket Version 9, Test Nos. HTTPB-1 through HTTPB-40.....	233
Figure 198. Version 9 Flat Pattern, Test Nos. HTTPB-1 through HTTPB-40.....	234
Figure 199. Tabbed Bracket Version 10, Test Nos. HTTPB-1 through HTTPB-40.....	235
Figure 200. Version 10 Flat Pattern, Test Nos. HTTPB-1 through HTTPB-40.....	236
Figure 201. Bogie Test Matrix, Test Nos. HTTPB-1 through HTTPB-40	237
Figure 202. Bill of Materials, Test Nos. HTTPB-1 through HTTPB-40	238
Figure 203. Bill of Materials, Test Nos. HTTPB-1 through HTTPB-40	239
Figure 204. Force-Time Data, Test No. HTTPB-1	242
Figure 205. Pre-Test and Post-Test Photographs, Test No. HTTPB-1	243
Figure 206. Sequential Photographs, Test No. HTTPB-1	243
Figure 207. Force-Time Data, Test No. HTTPB-2	245
Figure 208. Pre-Test and Post-Test Photographs, Test No. HTTPB-2	246
Figure 209. Sequential Photographs, Test No. HTTPB-2.....	246
Figure 210. Force-Time Data, Test No. HTTPB-3	248
Figure 211. Pre-Test and Post-Test Photographs, Test No. HTTPB-3	249
Figure 212. Sequential Photographs, Test No. HTTPB-3.....	249
Figure 213. Force-Time Data, Test No. HTTPB-4	251
Figure 214. Pre-Test and Post-Test Photographs, Test No. HTTPB-4	252
Figure 215. Sequential Photographs, Test No. HTTPB-4.....	252
Figure 216. Force-Time Data, Test No. HTTPB-5	254
Figure 217. Pre-Test and Post-Test Photographs, Test No. HTTPB-5	255

Figure 218. Sequential Photographs, Test No. HTTB-5.....	255
Figure 219. Force-Time Data, Test No. HTTB-6	257
Figure 220. Pre-Test and Post-Test Photographs, Test No. HTTB-6	258
Figure 221. Sequential Photographs, Test No. HTTB-6.....	258
Figure 222. Force-Time Data, Test No. HTTB-7	260
Figure 223. Pre-Test and Post-Test Photographs, Test No. HTTB-7	261
Figure 224. Sequential Photographs, Test No. HTTB-7.....	261
Figure 225. Force-Time Data, Test No. HTTB-8	263
Figure 226. Pre-Test and Post-Test Photographs, Test No. HTTB-8	264
Figure 227. Sequential Photographs, Test No. HTTB-8.....	264
Figure 228. Installed Bolted Tabbed Bracket	268
Figure 229. Bolted Tabbed Bracket—(a) Laterally Loaded and (b) Vertically Loaded.....	268
Figure 230. Dimensions and Failure Locations for Bolted Tabbed Bracket Design	269
Figure 231. End Reactions for Use in the Design Equations.....	269
Figure 232. Side View of Tabbed Bracket Version 3.....	274
Figure 233. Flat Pattern of Tabbed Bracket Version 3	274
Figure 234. Tabbed Bracket Version 3 Keyway.....	275
Figure 235. Side View of Tabbed Bracket Version 4.....	276
Figure 236. Flat Pattern of Tabbed Bracket Version 4	276
Figure 237. Tabbed Bracket Version 4 Keyway.....	277
Figure 238. Pre-Test and Post-Test Photographs, Test No. HTTB-9	282
Figure 239. Sequential Photographs, Test No. HTTB-9.....	282
Figure 240. Force-Time Data, Test No. HTTB-9R	284
Figure 241. Pre-Test and Post-Test Photographs, Test No. HTTB-9R	285
Figure 242. Sequential Photographs, Test No. HTTB-9R	285
Figure 243. Force-Time Data, Test No. HTTB-10	287
Figure 244. Pre-Test and Post-Test Photographs, Test No. HTTB-10	288
Figure 245. Sequential Photographs, Test No. HTTB-10.....	288
Figure 246. Force-Time Data, Test No. HTTB-11	290
Figure 247. Pre-Test and Post-Test Photographs, Test No. HTTB-11	291
Figure 248. Sequential Photographs, Test No. HTTB-11.....	291
Figure 249. Force-Time Data, Test No. HTTB-12	293
Figure 250. Pre-Test and Post-Test Photographs, Test No. HTTB-12	294
Figure 251. Sequential Photographs, Test No. HTTB-12.....	294
Figure 252. Correction of a Fabrication Flaw.....	296
Figure 253. Force-Time Data, Test No. HTTB-12R	296
Figure 254. Pre-Test and Post-Test Photographs, Test No. HTTB-12R	297
Figure 255. Sequential Photographs, Test No. HTTB-12R	297
Figure 256. Force-Time Data, Test No. HTTB-13	299
Figure 257. Pre-Test and Post-Test Photographs, Test No. HTTB-13	300
Figure 258. Sequential Photographs, Test No. HTTB-13.....	300
Figure 259. Force-Time Data, Test No. HTTB-14	302
Figure 260. Pre-Test and Post-Test Photographs, Test No. HTTB-14	303
Figure 261. Sequential Photographs, Test No. HTTB-14.....	303
Figure 262. Force-Time Data, Test No. HTTB-15	305
Figure 263. Pre-Test and Post-Test Photographs, Test No. HTTB-15	306
Figure 264. Sequential Photographs, Test No. HTTB-15.....	306

Figure 265. Force-Time Data, Test No. HTTB-16	308
Figure 266. Pre-Test and Post-Test Photographs, Test No. HTTB-16	309
Figure 267. Sequential Photographs, Test No. HTTB-16	309
Figure 268. Round 3 Bolted Tabbed Bracket	313
Figure 269. Bolted Tabbed Bracket—(a) Laterally Loaded and (b) Vertically Loaded	313
Figure 270. Dimensions and Failure Locations for Bolted Tabbed Bracket	314
Figure 271. Side View of Tabbed Bracket Version 5	318
Figure 272. Flat Pattern of Tabbed Bracket Version 5	318
Figure 273. Tabbed Bracket Version 5 Keyway	319
Figure 274. Side View of Tabbed Bracket Version 6	320
Figure 275. Flat Pattern of Tabbed Bracket Version 6	320
Figure 276. Tabbed Bracket Version 6 Keyway	321
Figure 277. Side View of Tabbed Bracket Version 7	322
Figure 278. Flat Pattern of Tabbed Bracket Version 7	322
Figure 279. Tabbed Bracket Version 7 Keyway	323
Figure 280. Side View of Tabbed Bracket Version 8	324
Figure 281. Flat Pattern of Tabbed Bracket Version 8	324
Figure 282. Tabbed Bracket Version 8 Keyway	325
Figure 283. Side View of Tabbed Bracket Version 9	326
Figure 284. Flat Pattern of Tabbed Bracket Version 9	327
Figure 285. Tabbed Bracket Version 9 Keyway	327
Figure 286. Side View of Tabbed Bracket Version 10	328
Figure 287. Flat Pattern of Tabbed Bracket Version 10	329
Figure 288. Tabbed Bracket Version 10 Keyway	329
Figure 289. Force-Time Data, Test No. HTTB-17	336
Figure 290. Pre-Test and Post-Test Photographs, Test No. HTTB-17	337
Figure 291. Sequential Photographs, Test No. HTTB-17	337
Figure 292. Force-Time Data, Test No. HTTB-18	339
Figure 293. Pre-Test and Post-Test Photographs, Test No. HTTB-18	340
Figure 294. Sequential Photographs, Test No. HTTB-18	340
Figure 295. Force-Time Data, Test No. HTTB-19	342
Figure 296. Pre-Test and Post-Test Photographs, Test No. HTTB-19	343
Figure 297. Sequential Photographs, Test No. HTTB-19	343
Figure 298. Force-Time Data, Test No. HTTB-20	345
Figure 299. Pre-Test and Post-Test Photographs, Test No. HTTB-20	346
Figure 300. Sequential Photographs, Test No. HTTB-20	346
Figure 301. Force-Time Data, Test No. HTTB-21	348
Figure 302. Pre-Test and Post-Test Photographs, Test No. HTTB-21	349
Figure 303. Sequential Photographs, Test No. HTTB-21	349
Figure 304. Force-Time Data, Test No. HTTB-22	351
Figure 305. Pre-Test and Post-Test Photographs, Test No. HTTB-22	352
Figure 306. Sequential Photographs, Test No. HTTB-22	352
Figure 307. Force-Time Data, Test No. HTTB-23	354
Figure 308. Pre-Test and Post-Test Photographs, Test No. HTTB-23	355
Figure 309. Sequential Photographs, Test No. HTTB-23	355
Figure 310. Force-Time Data, Test No. HTTB-24	357
Figure 311. Pre-Test and Post-Test Photographs, Test No. HTTB-24	358

Figure 312. Sequential Photographs, Test No. HTTPB-24.....	358
Figure 313. Force-Time Data, Test No. HTTPB-25	360
Figure 314. Pre-Test and Post-Test Photographs, Test No. HTTPB-25	361
Figure 315. Sequential Photographs, Test No. HTTPB-25.....	361
Figure 316. Force-Time Data, Test No. HTTPB-26	363
Figure 317. Pre-Test and Post-Test Photographs, Test No. HTTPB-26	364
Figure 318. Sequential Photographs, Test No. HTTPB-26.....	364
Figure 319. Force-Time Data, Test No. HTTPB-27	366
Figure 320. Pre-Test and Post-Test Photographs, Test No. HTTPB-27	367
Figure 321. Sequential Photographs, Test No. HTTPB-27	367
Figure 322. Force-Time Data, Test No. HTTPB-28	369
Figure 323. Pre-Test and Post-Test Photographs, Test No. HTTPB-28	370
Figure 324. Sequential Photographs, Test No. HTTPB-28.....	370
Figure 325. Force-Time Data, Test No. HTTPB-29	372
Figure 326. Pre-Test and Post-Test Photographs, Test No. HTTPB-29	373
Figure 327. Sequential Photographs, Test No. HTTPB-29.....	373
Figure 328. Force-Time Data, Test No. HTTPB-30	375
Figure 329. Pre-Test and Post-Test Photographs, Test No. HTTPB-30	376
Figure 330. Sequential Photographs, Test No. HTTPB-30.....	376
Figure 331. Force-Time Data, Test No. HTTPB-31	378
Figure 332. Pre-Test and Post-Test Photographs, Test No. HTTPB-31	379
Figure 333. Sequential Photographs, Test No. HTTPB-31.....	379
Figure 334. Force-Time Data, Test No. HTTPB-32	381
Figure 335. Pre-Test and Post-Test Photographs, Test No. HTTPB-32	382
Figure 336. Sequential Photographs, Test No. HTTPB-32.....	382
Figure 337. Pre-Test and Post-Test Photographs, Test No. HTTPB-33	384
Figure 338. Sequential Photographs, Test No. HTTPB-33.....	384
Figure 339. Pre-Test and Post-Test Photographs, Test No. HTTPB-34	386
Figure 340. Sequential Photographs, Test No. HTTPB-34.....	386
Figure 341. Force-Time Data, Test No. HTTPB-35	388
Figure 342. Pre-Test and Post-Test Photographs, Test No. HTTPB-35	389
Figure 343. Sequential Photographs, Test No. HTTPB-35.....	389
Figure 344. Force-Time Data, Test No. HTTPB-36	391
Figure 345. Pre-Test and Post-Test Photographs, Test No. HTTPB-36	392
Figure 346. Sequential Photographs, Test No. HTTPB-36.....	392
Figure 347. Force-Time Data, Test No. HTTPB-37	394
Figure 348. Pre-Test and Post-Test Photographs, Test No. HTTPB-37	395
Figure 349. Sequential Photographs, Test No. HTTPB-37.....	395
Figure 350. Force-Time Data, Test No. HTTPB-38	397
Figure 351. Pre-Test and Post-Test Photographs, Test No. HTTPB-38	398
Figure 352. Sequential Photographs, Test No. HTTPB-38.....	398
Figure 353. Force-Time Data, Test No. HTTPB-39	400
Figure 354. Pre-Test and Post-Test Photographs, Test No. HTTPB-39	401
Figure 355. Sequential Photographs, Test No. HTTPB-39.....	401
Figure 356. Pre-Test and Post-Test Photographs, Test No. HTTPB-40	403
Figure 357. Sequential Photographs, Test No. HTTPB-40.....	403
Figure 358. Bolted Tabbed Bracket Version 8 and Keyway Version 8.....	411

Figure 359. Bolted Tabbed Bracket Version 10 and Keyway Version 10.....	411
Figure 360. Web-Inserted Curved Rod Example.....	415
Figure 361. 1/8-in. (3.2-mm) Web-Inserted Curved Rod—(a) Original and (b) Revised	416
Figure 362. Squeeze-In-Place Curved Rod Example	417
Figure 363. HellermannTyton Stainless Steel Cable Tie Example.....	418
Figure 364. Straight Rod Example.....	419
Figure 365. Test Jig for Static Tests	422
Figure 366. Example of Web-Inserted Curved Rod Test	425
Figure 367. Force Versus Displacement, Test Nos. KR-1 and KR-2	426
Figure 368. Pre-Test and Post-Test Photographs, Test No. KR-1	427
Figure 369. Pre-Test and Post-Test Photographs, Test No. KR-2	427
Figure 370. Force Versus Displacement, Test Nos. KR-3 and KR-4	428
Figure 371. Pre-Test and Post-Test Photographs, Test No. KR-3	429
Figure 372. Pre-Test and Post-Test Photographs, Test No. KR-4	429
Figure 373. Force Versus Displacement, Test Nos. KR-5 and KR-6	430
Figure 374. Pre-Test and Post-Test Photographs, Test No. KR-5	431
Figure 375. Pre-Test and Post-Test Photographs, Test No. KR-6	431
Figure 376. Force Versus Displacement, Test Nos. KR-7 and KR-8	432
Figure 377. Pre-Test and Post-Test Photographs, Test No. KR-7	433
Figure 378. Pre-Test and Post-Test Photographs, Test No. KR-8	433
Figure 379. Force Versus Displacement, Test Nos. KR-9 and KR-10	434
Figure 380. Pre-Test and Post-Test Photographs, Test No. KR-9	435
Figure 381. Pre-Test and Post-Test Photographs, Test No. KR-10	435
Figure 382. Example of Squeeze-In-Place Curved Rod Test	437
Figure 383. Force Versus Displacement, Test Nos. KR-11 and KR-12	438
Figure 384. Pre-Test Photograph, Test No. KR-11	439
Figure 385. Pre-Test Photograph, Test No. KR-12	439
Figure 386. Force Versus Displacement, Test Nos. KR-13 and KR-14	440
Figure 387. Pre-Test Photograph, Test No. KR-13	441
Figure 388. Pre-Test Photograph, Test No. KR-14	441
Figure 389. Force Versus Displacement, Test Nos. KR-15 and KR-16	442
Figure 390. Pre-Test Photograph, Test No. KR-15	443
Figure 391. Pre-Test Photograph, Test No. KR-16	443
Figure 392. Force Versus Displacement, Test Nos. KR-17 and KR-18	444
Figure 393. Pre-Test Photograph, Test No. KR-17	445
Figure 394. Pre-Test Photograph, Test No. KR-18	445
Figure 395. Force Versus Displacement, Test Nos. KR-19 and KR-20	446
Figure 396. Pre-Test Photograph, Test No. KR-19	447
Figure 397. Pre-Test Photograph, Test No. KR-20	447
Figure 398. Example of HellermannTyton Stainless Steel Cable Tie Test	449
Figure 399. Force Versus Displacement, Test Nos. TCT-4, TCT-6 and TCT-7	451
Figure 400. Pre-Test and Post-Test Photographs, Test No. TCT-4	451
Figure 401. Pre-Test and Post-Test Photographs, Test No. TCT-6	452
Figure 402. Pre-Test and Post-Test Photographs, Test No. TCT-7	452
Figure 403. Force Versus Displacement, Test Nos. TCT-8 and TCT-9	453
Figure 404. Pre-Test and Post-Test Photographs, Test No. TCT-8	454
Figure 405. Pre-Test and Post-Test Photographs, Test No. TCT-9	454

Figure 406. Example Revised Web-Inserted Curved Rod Test	456
Figure 407. Force Versus Displacement, Test Nos. KR-21 and KR-22	457
Figure 408. Pre-Test and Post-Test Photographs, Test No. KR-21	458
Figure 409. Pre-Test and Post-Test Photographs, Test No. KR-22	458
Figure 410. Force Versus Displacement, Test Nos. KR-23 and KR-24	459
Figure 411. Pre-Test and Post-Test Photographs, Test No. KR-23	460
Figure 412. Pre-Test and Post-Test Photographs, Test No. KR-24	460
Figure 413. Example of Straight Rod Test	462
Figure 414. Force Versus Displacement, Test No. KR-25	463
Figure 415. Pre-Test and Post-Test Photographs, Test No. KR-25	464
Figure 416. Force Versus Displacement, Test No. KR-26	465
Figure 417. Pre-Test and Post-Test Photographs, Test No. KR-26	466
Figure 418. Force Versus Displacement, Test Nos. KR-27 and KR-28	467
Figure 419. Pre-Test and Post-Test Photographs, Test No. KR-27	468
Figure 420. Pre-Test and Post-Test Photographs, Test No. KR-28	468
Figure 421. Force Versus Displacement, Test Nos. KR-29 and KR-30	469
Figure 422. Pre-Test and Post-Test Photographs, Test No. KR-29	470
Figure 423. Pre-Test and Post-Test Photographs, Test No. KR-30	470
Figure 424. Force Versus Displacement, Test No. KR-31 and KR-32	471
Figure 425. Pre-Test and Post-Test Photographs, Test No. KR-31	472
Figure 426. Pre-Test and Post-Test Photographs, Test No. KR-32	472
Figure 427. Force Versus Displacement, Test Nos. KR-33 and KR-34	473
Figure 428. Pre-Test and Post-Test Photographs, Test No. KR-33	474
Figure 429. Pre-Test and Post-Test Photographs, Test No. KR-34	474
Figure 430. Force Versus Displacement, Test Nos. KR-35 and KR-36	475
Figure 431. Pre-Test and Post-Test Photographs, Test No. KR-35	476
Figure 432. Pre-Test and Post-Test Photographs, Test No. KR-36	476
Figure 433. Lateral Resistance of the Straight Rod and V-Notch	478
Figure 434. Bogie Test Setup, Test No. HTTC-1	482
Figure 435. Cable Anchor Details, Test No. HTTC-1	483
Figure 436. Post with Straight Rod Details, Test No. HTTC-1	484
Figure 437. Post Details, Test No. HTTC-1	485
Figure 438. Straight Rod Details, Test No. HTTC-1	486
Figure 439. Anchorage Details, Test No. HTCC-1	487
Figure 440. Cable Anchor Bracket Details, Test No. HTTC-1	488
Figure 441. Cable Release Lever Assembly Details, Test No. HTTC-1	489
Figure 442. Cable Anchor Bracket Component Details, Test No. HTTC-1	490
Figure 443. Cable Anchor Bracket Component Details, Test No. HTTC-1	491
Figure 444. Cable Release Lever Component Details, Test No. HTTC-1	492
Figure 445. Cable End Assembly and Cable Spice Assembly Details, Test No. HTTC-1	493
Figure 446. Bill of Materials, Test No. HTTC-1	494
Figure 447. Rigid-Frame Bogie Aligned for Test No. HTTC-1	496
Figure 448. Pre-Test Photograph of Cable Barrier System, Test No. HTTC-1	499
Figure 449. Pre-Test and Post-Test Photographs for Post No. 3, Test No. HTTC-1	500
Figure 450. Pre-Test and Post-Test Photographs for Post No. 4, Test No. HTTC-1	501
Figure 451. Pre-Test and Post-Test Photographs for Post No. 5, Test No. HTTC-1	501
Figure 452. Sequential Photographs for Camera AOS5, Test No. HTTC-1	502

Figure 453. Sequential Photographs for Camera AOS6, Test No. HTTC-1.....	503
Figure 454. Sequential Photographs for Camera AOS7, Test No. HTTC-1.....	504
Figure 455. Maximum Post Spacing vs. Horizontal Curve Radius	508
Figure 456. Bolted Tabbed Bracket—(a) Laterally Loaded and (b) Vertically Loaded.....	511
Figure 457. Bolted Tabbed Bracket Dimensions.....	511
Figure 458. End Reactions for Use in the Design Equations.....	512
Figure A-1. Cable Barrier Resource Chart [15].....	526
Figure B-1. Test Results Summary (English), Test No. CMB-1 [70]	528
Figure B-2. Test Results Summary (English), Test No. CMB-2 [70]	529
Figure B-3. Test Results Summary (English), Test No. CMB-3 [70]	530
Figure B-4. Test Results Summary (English), Test No. 4CMB-1 [2]	531
Figure B-5. Test Results Summary (English), Test No. 4CMB-2 [2]	532
Figure B-6. Test Results Summary (English), Test No. 4CMB-3 [2]	533
Figure B-7. Test Results Summary (English), Test No. 4CMB-4 [3]	534
Figure B-8. Test Results Summary (English), Test No. 4CMB-5 [3]	535
Figure B-9. Test Results Summary (English), Test No. 4CMBLT-1 [4]	536
Figure C-1. Derivation of Slope Change, Sheet ¼	538
Figure C-2. Derivation of Slope Change, Sheet 2/4	539
Figure C-3. Derivation of Slope Change, Sheet ¾	540
Figure C-4. Derivation of Slope Change, Sheet 4/4	541
Figure D-1. S3x5.7 (S76x8.5) Section Hole Details.....	543
Figure D-2. 1/16 in. (1.6 mm) Diameter, Web-Inserted Curved Rod Detail.....	544
Figure D-3. 3/32 in. (2.4 mm) Diameter, Web-Inserted Curved Rod Detail.....	545
Figure D-4. 1/8 in. (3.2 mm) Diameter, Web-Inserted Curved Rod Detail.....	546
Figure D-5. 1/16 in. (1.6 mm) Diameter, Squeeze-In-Place Curved Rod Detail.....	547
Figure D-6. 3/32 in. (2.4 mm) Diameter, Squeeze-In-Place Curved Rod Detail.....	548
Figure D-7. 1/8 in. (3.2 mm) Diameter, Squeeze-In-Place Curved Rod Detail.....	549
Figure D-8. Cable Tie Concepts	550
Figure D-9. 1/8 in. (3.2 mm) Diameter, Revised Web-Inserted Curved Rod Detail.....	551
Figure D-10. 1/8 in. (3.2 mm) Diameter, Straight Rod with Bent Ends Detail	552
Figure D-11. 3/16 in. (4.8 mm) Diameter, Straight Rod with Bent Ends Detail	553
Figure D-12. 1/4 in. (6.4 mm) Diameter, Straight Rod with Bent Ends Detail	554
Figure E-1. AISI C1018 Keyway Bolts	556
Figure E-2. ¼ in. (6.4 mm) Diameter, C360 Brass Round Bar	557
Figure E-3. 1/8 in. (3.2 mm) Diameter, T-304 Stainless Steel Round Bar.....	558
Figure E-4. 3/16 in. (4.8 mm) Diameter, C360 Brass Round Bar	559
Figure E-5. 3/32 in. (2.4 mm) Diameter, T-303 Stainless Steel Round Bar.....	560
Figure E-6. 3/32 in. (2.4 mm) Diameter, C360 Brass Round Bar	561
Figure E-7. 1/16 in. (1.6 mm) Diameter, C360 Brass Round Bar	562
Figure E-8. 1/8 in. (3.2 mm) Diameter C360 Brass Round Bar	563
Figure E-9. ¼ in. (6.4 mm) Diameter, T-304 Stainless Steel Round Bar	564
Figure E-10. 3/16 in. (4.8 mm) Diameter, T-304 Stainless Steel Round Bar.....	565
Figure E-11. 10-Gauge Sheet Steel.....	566
Figure E-12. 11-Gauge Sheet Steel.....	567
Figure E-13. 12-Gauge Sheet Steel.....	568
Figure E-14. 14-Gauge Sheet Steel.....	569

LIST OF TABLES

Table 1. FHWA Eligibility Letters for Selected Cable Barriers [65]	21
Table 2. Summary of Full-Scale Vehicle Crash Tests into Low- and High-Tension, Cable Barrier Systems	46
Table 3. Design Speed vs. Minimum Curve Radius	59
Table 4. Bogie Weights.....	69
Table 5. Summary of Dynamic Component Testing of Keyway Bolts, Round 1	85
Table 6. Summary of Dynamic Component Testing of Extended Keyway Bolts, Round 2	162
Table 7. Expected Release Loads for Round 1 Crimp-In-Place Tabbed Brackets	198
Table 8 Summary of Dynamic Component Testing on Crimp-In-Place Tabbed Brackets, Round 1	240
Table 9 Calculated Bearing Strengths with $\sigma_u = 70$ ksi (483 MPa).....	272
Table 10. Expected Release Loads for Round 2 Bolted Tabbed Brackets	277
Table 11. Summary of Dynamic Component Testing on Bolted Tabbed Brackets, Round 2	279
Table 12. Expected Release Loads for Round 3 Bolted Tabbed Brackets	330
Table 13. Summary of Dynamic Component Testing on Bolted Tabbed Brackets, Round 3	332
Table 14. Expected vs. Observed Lateral Release Loads for Ideal Bolted Tabbed Brackets	405
Table 15. Expected vs. Observed Vertical Release Loads for Bolted Tabbed Brackets	406
Table 16. Summary of Design Concepts for Cable-to-Post Attachments	408
Table 17. Round Rod or Bar Material-Type, Size, and Strength.....	414
Table 18. Test Matrix and Results for Web-Inserted Curved Rods.....	424
Table 19. Test Matrix and Results for Squeeze-In-Place Curved Rods	436
Table 20. Test Matrix and Results for HellermannTyton Stainless Steel Cable Ties.....	448
Table 21. Test Matrix and Results for Revised Web-Inserted Curved Rods.....	455
Table 22. Test Matrix and Results for Straight Rods.....	461
Table 23. Average Vertical Release Loads for Top Cable-to-Post Attachments	477

1 INTRODUCTION

1.1 Problem Statement

Several years ago, researchers at the Midwest Roadside Safety Facility (MwRSF) of the University of Nebraska-Lincoln (UNL) were contracted by the Midwest States Pooled Fund Program to develop a new, non-proprietary, high-tension cable median barrier. The barrier system was to be developed to meet the Test Level 3 (TL-3) impact safety requirements published by the American Association of State Highway and Transportation Officials (AASHTO) and entitled the *Manual for Assessing Safety Hardware* (MASH) [1]. Initially, the new barrier system was being designed for use at any lateral position within a highway median with side slopes as steep as 4V:1H.

Within the noted R&D program, five full-scale vehicle crash tests were performed on prototype high-tension cable barrier systems placed in 4V:1H V-ditches [2-3], and one full-scale vehicle crash test was conducted on a similar system installed on level terrain [4]. Of those six crash tests, three of the barriers succeeded in meeting the MASH TL-3 impact safety requirements, and three did not. The two most recent crash tests were test nos. 4CMB-5 and 4CMBLT-1, both of which failed, thus prompting this redesign effort.

In test no. 4CMB-5 [3], a 5,149-lb (2,336-kg) pickup truck (2270P vehicle) impacted the cable barrier system at a speed of 61.8 mph (99.5 km/h) and at a 26.5-degree angle. The barrier was located on the front slope of a 46-ft (14-m) wide, 4V:1H sloped V-ditch, 12 ft (3.6 m) laterally away from the front slope break point. The critical impact point was targeted to be 12-in. (305-mm) upstream from a support post. As the impacted post rotated backward and downward, it pushed the cables on the non-impact side and pulled the cables on the impact side along with it. The top cable was on the non-impact side. As a result, the vehicle overrode the top cable and was not captured, ultimately resulting in a failure of the barrier system.

In test no. 4CMBLT-1 [4], a 3,470-lb (1,574-kg) passenger car (1500A vehicle) impacted the cable barrier system at a speed of 62.2 mph (100.1 km/h) and at a 25.3-degree angle. For this scenario, the barrier system was placed on level terrain. The critical impact point was determined to occur between two posts. As the vehicle was being redirected, the third cable from the ground heavily interacted with the vehicle and crushed the A-pillar, thus resulting in a failure of the barrier system due to excessive penetration into the vehicle's occupant compartment. Of particular note, the third cable was still attached to the post immediately downstream from the vehicle when it began to crush the A-pillar.

Both barrier system failures could be partially attributed to the manner in which the cables were attached to the posts. In the case of test no. 4CMB-5, the impacted post itself—not the attachment—laterally pushed the top cable as it rotated backward and downward. As the post continued to rotate, the top cable began to engage the cable-to-post attachment vertically, but was unable to be released away from the post. During this event, the upper cable was pulled downward an estimated 20 in. (508 mm).

In the case of test no. 4CMBLT-1, the third cable that crushed the A-pillar was on the impact side of the posts. Just before the A-pillar was crushed, the third cable was still attached to the post immediately downstream from the vehicle, while laterally being pushed into the front of the post and slightly wedged upward on the cable-to-post attachment. From the high-speed video, the downstream post did not appear to bend backward much under this initial lateral load, and the cable-to-post attachment did not release the cable under this vertical load.

In 2011 and following the failure of test nos. 4CMB-5 and 4CMBLT-1, it was determined that design modifications were necessary to improve barrier performance. In addition, members of the Midwest States Pooled Fund Program desired to redirect the development effort.

1.2 Research Objective

The research objective of the portion of the project reported herein was to design new cable-to-post attachments to improve the safety performance of the non-proprietary, high-tension, 4-cable median barrier system. The modified cable barrier system would be designed for use in median ditches with 6V:1H or flatter side slopes and using a 0 to 4 ft (0 to 1.2 m) lateral placement away from the edge of the shoulder or slope break point. However, the state DOTs may desire to select the system configuration so that the barrier would provide satisfactory safety performance when positioned anywhere in a 6V:1H or flatter median ditch. In addition, it was hopeful that the cable barrier system could later be modified for use in 4V:1H sloped medians, including at 0 to 4 ft (0 to 1.2 m) as well as anywhere in the ditch. Finally, the modified cable barrier system would be designed to meet the Test Level 3 impact safety standards provided in MASH.

1.3 Research Approach

The research objective was completed in four steps: (1) determine the minimum design loads associated with horizontal and vertical curves as a function of post spacing; (2) determine target capacities for the vertical and lateral cable release out of the cable-to-post attachments at all four cable heights; (3) design and test cable-to-post attachments for the bottom three cables; and (4) design and test cable-to-post attachments for the top cable. Steps 3 and 4 were ongoing, with cable-to-post attachments constantly being designed, tested, modified and re-tested until final recommendations were ready to be made.

1.4 Order of Report

Chapter 1 introduces the problems with the cable-to-post attachments in the most recent full-scale vehicle crash tests, states the objective of designing new cable-to-post attachments, and lays out the research approach.

Chapter 2 is intended to familiarize the reader with cable-to-post attachments used within other, federally-approved cable barrier systems. It also contains a brief discussion on the design and testing of passenger vehicles, including the roof and A-pillar.

Chapter 3 is intended to familiarize the reader with each of the six full-scale vehicle crash tests which MwRSF has performed on prototype high-tension cable barrier systems, as well as three full-scale vehicle crash tests which were performed on prototype low-tension cable barrier systems. It also contains details about the R&D programs utilized to explore new cable-to-post attachments.

Chapter 4 is a discussion of the design loads. It contains equations for the design loads associated with horizontal and vertical curves as a function of post spacing, as well as new targets for the lateral and vertical release loads of the cable-to-post attachments.

Chapter 5 discusses the Round-1 modifications to the keyway bolts and their keyways. Keyway bolts were one of two major categories of cable-to-post attachments which were considered for the bottom three cables. Chapter 5 shows details and dimensions for concepts that made it to component-level testing and discusses the thought process behind each.

Chapter 6 contains details about the conditions of the dynamic component tests on keyway bolts and tabbed brackets.

Chapter 7 presents and discusses the results of Round 1 of dynamic component tests on the keyway bolts.

Chapter 8 discusses the Round-2 modifications to the keyway bolts, which resulted in the extended keyway bolts.

Chapter 9 presents and discusses the results of Round 2 of dynamic component tests on the extended keyway bolts.

Chapter 10 discusses the crimp-in-place tabbed bracket concepts. Tabbed brackets were the other major category of cable-to-post attachments, besides keyway bolts, which were considered for the bottom three cables. There were three rounds of design modifications, testing and evaluation on tabbed brackets. Chapter 10 shows details for crimp-in-place tabbed brackets of Round 1 and includes equations that were used to predict their lateral and vertical release loads.

Chapter 11 presents and discusses the results of Round 1 of dynamic component tests on the crimp-in-place tabbed brackets.

Chapter 12 shows details for the bolted tabbed brackets of Round 2 and includes equations that were used to predict their lateral and vertical release loads.

Chapter 13 presents and discusses the results of Round 2 of dynamic component tests on the bolted tabbed brackets.

Chapter 14 shows details for the bolted tabbed brackets of Round 3 and includes equations that were used to predict their lateral and vertical release loads.

Chapter 15 presents and discusses the results of Round 3 of dynamic component tests on the bolted tabbed brackets.

Chapter 16 summarizes the results of the dynamic component tests on the keyway bolts and tabbed brackets and explains how one concept was chosen as the cable-to-post attachment that would be used for the bottom three cables.

Chapter 17 discusses the top cable-to-post attachment concepts that were tested in quasi-static component tests.

Chapter 18 contains details about the conditions of the quasi-static component tests on top cable-to-post attachment concepts.

Chapter 19 presents and discusses the results of quasi-static component tests on the top cable-to-post attachment concepts. One of the concepts was selected for further component testing.

Chapter 20 contains details about the conditions of a bogie impact test that was used to evaluate the top cable-to-post attachment that was chosen.

Chapter 21 presents and discusses the results of the bogie impact test and makes a recommendation concerning the top cable-to-post attachment.

Chapter 22 summarizes the design effort, draws conclusions about the design of cable-to-post attachments, and recommends the cable-to-post attachments to be used.

2 LITERATURE REVIEW

2.1 Introduction

Cross-median crashes result in a disproportionately high number of fatalities when compared with other run-off-road events [5]. Cable median barriers have been demonstrated to be effective in preventing cross-median crashes [6], but they also increase crash frequency [7]. When it comes to current cable median barriers and their associated hardware, room for continued improvement exists, especially cable-to-post attachments. As such, a literature review was performed to focus on the current methods for connecting wire rope cables to vertical support posts.

2.2 Cable-to-Post Attachments

Previously, MwRSF researchers performed a thorough literature review of cable barrier testing as well as summarized typical hardware and configurations, which was published in 2010 [8]. MwRSF had also performed an extensive patent search in order to ensure that any new hardware did not violate others' intellectual property [9]. Based on these prior investigations, some of the various cable-to-post attachments are highlighted below. It should be noted that cable-to-post attachments are responsible for connecting horizontal cables to posts and withstanding vehicle impact forces until cables are released away from posts, either vertically or horizontally. A well-designed cable-to-post attachment should develop the full moment capacity of the post about the strong axis of bending when pulled laterally, but release when pulled vertically so that the cable does not clamp down on an impacting vehicle's A-pillar and crush it. The intended function of the cable-to-post attachments will be discussed in more detail in Chapters 3 and 4.

Between 1960 and 1965, the New York State Department of Public Works (NYSDPW) crash tested several guardrail systems [10]. Some of them were cable barriers. The first cable

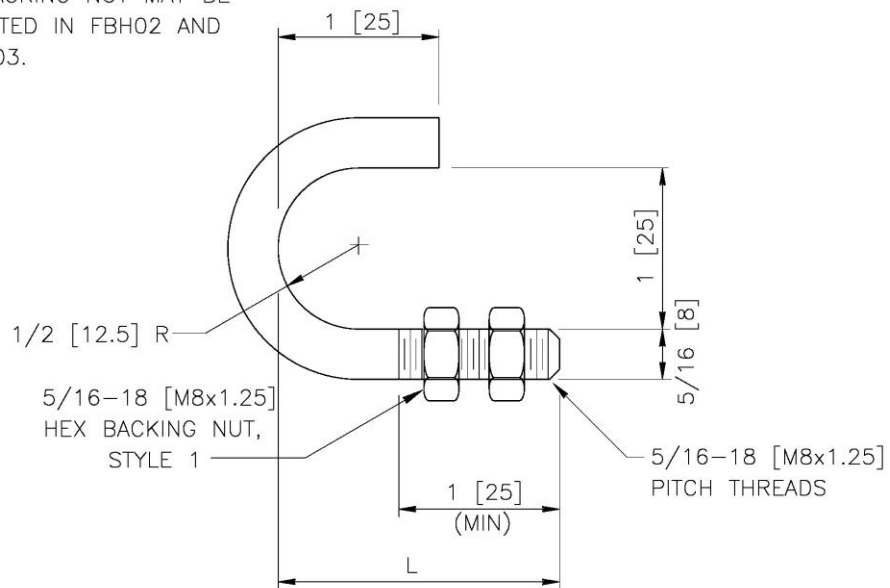
barrier crash test had an undesirable result, leading to many conclusions about how cable barriers should be designed. Among those conclusions was the assertion that, in order to prevent posts from pulling the cables down during impact events, cables should not be securely fastened to the posts. Later, a new cable barrier design was selected for crash testing, which included three cables attached to S3x5.7 (S76x8.5) steel posts with 1/4-in. (6-mm) J bolts. The relatively weak J bolts opened up as the post deflected, allowing the cable to nearly stay at its original elevation, preventing the car from climbing up the cable. This case demonstrates how an undesirable behavior was observed in a crash test, traced back to the cable-to-post attachments, and subsequently changed.

Cable J bolts are still commonly used today. The American Association of State Highway and Transportation Officials, (AASHTO) Task Force 13 published *A Guide to Standardized Highway Barrier Hardware* [11]. Among other systems and components, the hardware guide contains drawings and specifications for a nonproprietary, low-tension, 3-cable guardrail that was successfully crash tested according to the National Cooperative Highway Research Program (NCHRP) Report No. 350, Test Level 3 (TL-3) requirements [12]. Additional information regarding its recommended use can be found in Federal Highway Administration (FHWA) eligibility letter nos. B-64 [13] and B-64sup [14]. The system, shown in Figure 1, uses 5/16-in. (8-mm) J bolts to attach the cables to S3x5.7 (S76x8.5) steel posts. Several J bolt variations may be used and are shown in Figures 2 and 3.



Figure 1. Weak-Steel Post Cable Guardrail [11]

NOTE: A BACKING NUT MAY BE OMITTED IN FBH02 AND FBH03.



DESIGNATOR	L
FBH01	1.75 [45]
FBH02	4.5 [115]
FBH03	7 [180]

Figure 2. Cable Hook Bolt [11]

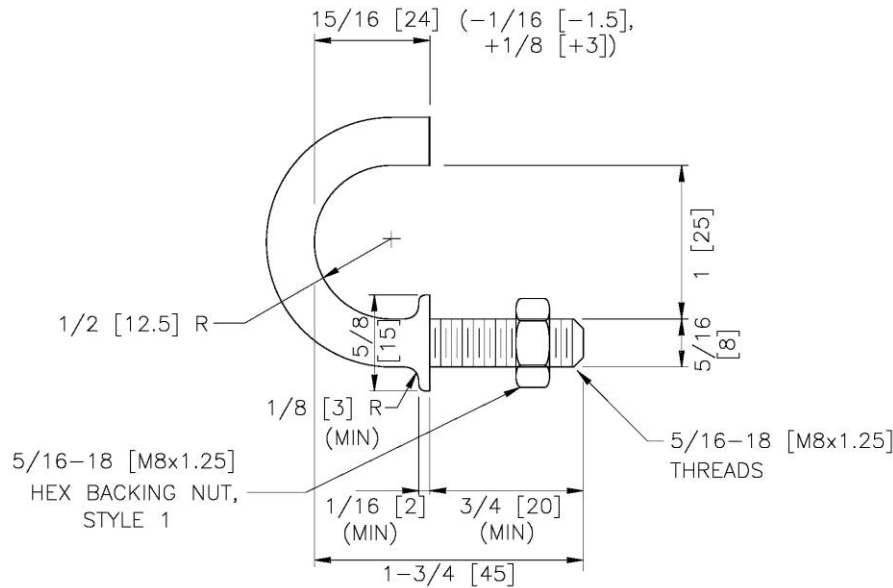


Figure 3. Shouldered Cable Hook Bolt [11]

There are also several proprietary cable barriers which use different methods for attaching the cables to the posts. Under an FHWA contract, KLS Engineering recently developed resource charts which provide general information about several commonly-used roadside safety systems [15]. A cable barrier resource chart from that document is shown in Appendix A. Researchers and designers are encouraged to visit the manufacturers' web sites to obtain more information on each cable barrier system. The cable-to-post attachment methods for each of the barrier systems denoted on that chart are presented herein. The systems represent the most common high-tension cable barriers currently being used in the United States.

The Brifen Wire Rope Safety Fence (WRSF) is a high-tension, cable barrier system [16]. It has different configurations (both 3- and 4-strand) which have been successfully crash tested according to the NCHRP Report No. 350 TL-3 and TL-4 requirements. More detailed information is provided in FHWA eligibility letter nos. B-82 [17], B-82B [18], B-82C [19], B-82C1 [20], and B-82B1 [21]. For the common Brifen system, the top cable is placed in a slot located in the center of a Z-shaped post and covered with a post cap. The other cables sit on

exterior locating pegs and are weaved around the line posts. Typical Brifen systems are shown in Figures 4 and 5 with the express written consent of Brifen USA, Inc.



Figure 4. Typical Brifen WRSF

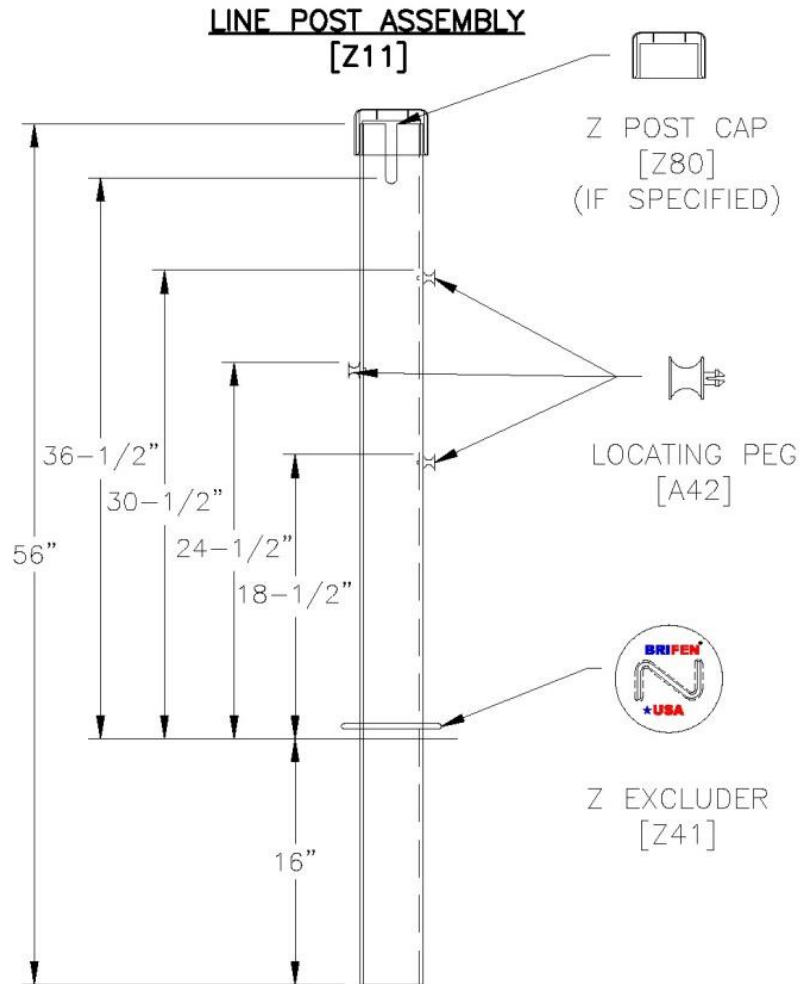


Figure 5. Brifen WRSF TL-4 Line Post Assembly [22]

The Gibraltar Cable Barrier System is another high-tension, cable barrier system [23]. It also has different configurations (both 3- and 4-strand) which have been successfully crash tested according to the NCHRP Report No. 350 TL-3 and TL-4 requirements. More detailed information is provided in FHWA eligibility letter nos. B-137 [24], B-137A [25], B-137B [26], B-147A [27], B-137C (HSA) [28], B-137A1 [29], B-137C (HSSD) [30], and B-137D [31]. For the common Gibraltar system, the cables are attached to C-section posts with a single steel hair pin. The TL-4, 3-cable version is shown in Figures 6 and 7.

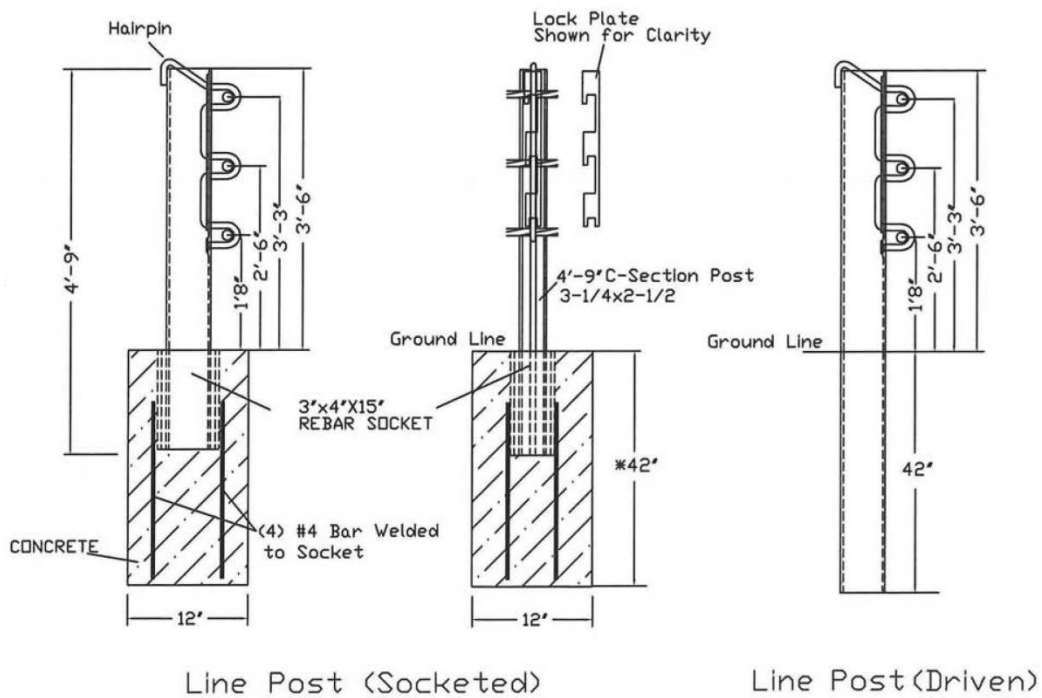


Figure 6. Gibraltar TL-4 (3 Cable) Line Post Details [32]



Figure 7. Installation of Gibraltar's Hairpin and Lockplate [32]

Nucor Steel Marion manufactures the Nu-Cable high-tension, cable barrier system [33]. The Nu-Cable barrier has different configurations (both 3- and 4-strand) which have been successfully crash tested according to the NCHRP Report No. 350 TL-3 and TL-4 requirements. More detailed information is provided in FHWA eligibility letter nos. B-96 [34], B-96A [35], B-167 [36], B-183 [37], B-184 [38], B-193 (REVISED) [39], and B-184A [40]. For a common Nucor Steel Marion system, the top two cables are held in place by a cable hanger and hanger strap. The other cables are held in place by locking hook bolts, which differ according to the side of the post to which the cable is being attached. There are two different configurations—roadside and median. For the median configuration, the bottom cables are placed on alternating sides and use two different locking hook bolts. The roadside configuration has both bottom cables on the same side and use the same type of locking hook bolt. The cable-to-post attachments for the TL-4 system are shown in Figure 8. The line post detail for the median configuration is shown in Figure 9.

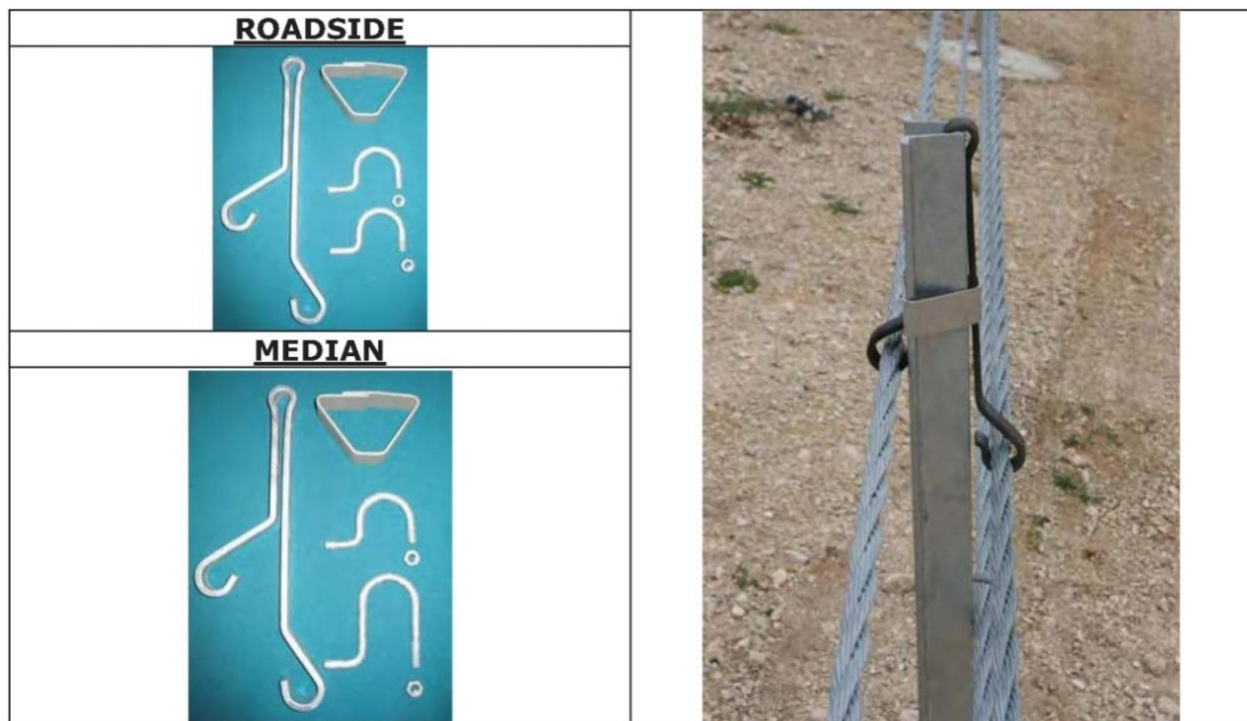


Figure 8. Nu-Cable TL-4 Cable-to-Post Attachments [33]

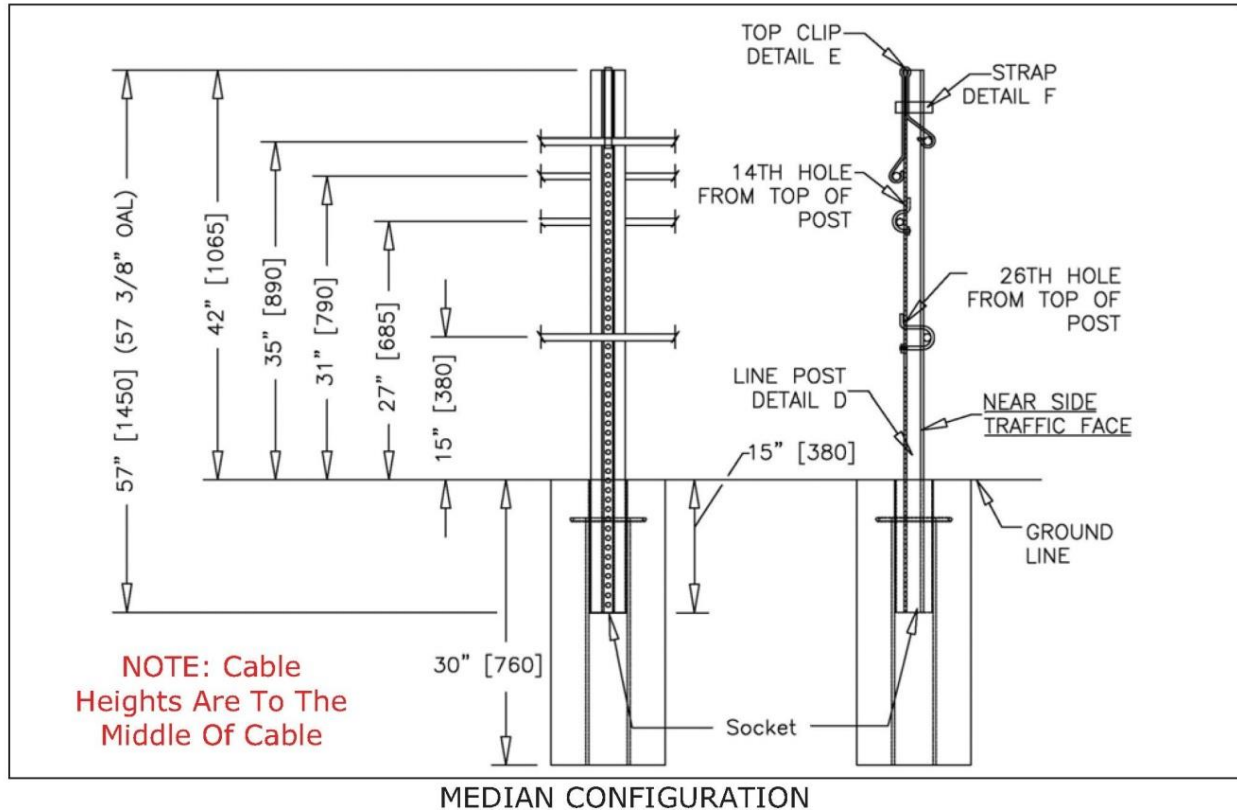


Figure 9. Nu-Cable TL-4 Line Post Detail, Median Configuration [33]

Gregory Industries, Inc. promotes the Blue Systems, Inc. Safence cable barrier system in the U.S. The Safence system has different configurations (both 3- and 4-strand) which have been successfully crash tested according to the NCHRP Report No. 350 TL-3 and TL-4 requirements [41]. More detailed information is provided in FHWA eligibility letter nos. B-88 [42], B-88A [43], B-88B [44], B-88C [45], B-88D [46], B-88E [47], and B-88F [48]. For common systems, all of the cables are inserted in the web of the post and separated by plastic spacers. Two different posts can be used—an I-shaped post or a Safence C-post. Attachment details for the common 3- and 4-strand configurations for both posts are shown in Figure 10. MwRSF performed a full-scale vehicle crash test on a Safence cable barrier system placed on a 4V:1H side slope in which the bottom cable was fastened to the side of the post with a 3/16-in. (4.8-mm) diameter side hook [49]. A line post and side hook detail for that system is shown in Figure 11.

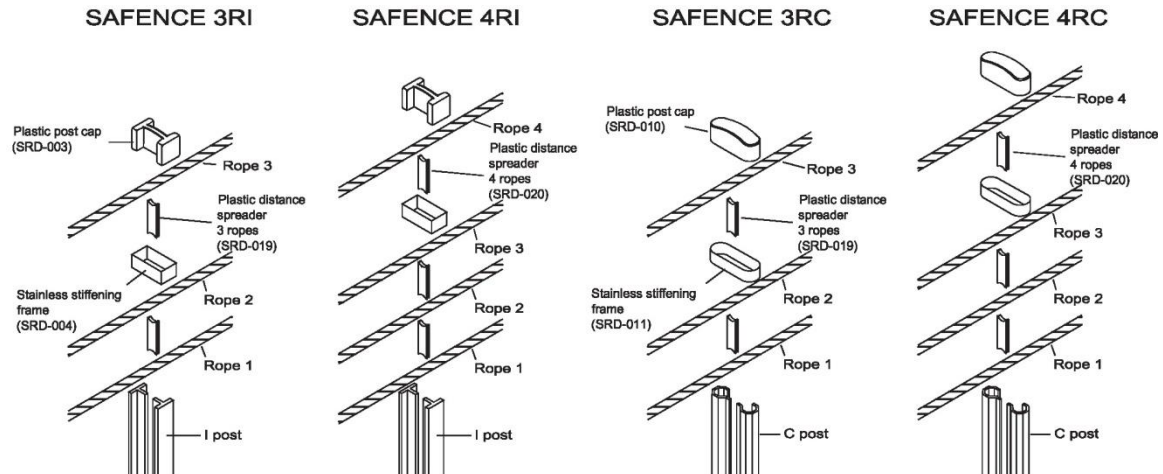


Figure 10. Safence Cable-to-Post Attachment Details [41]

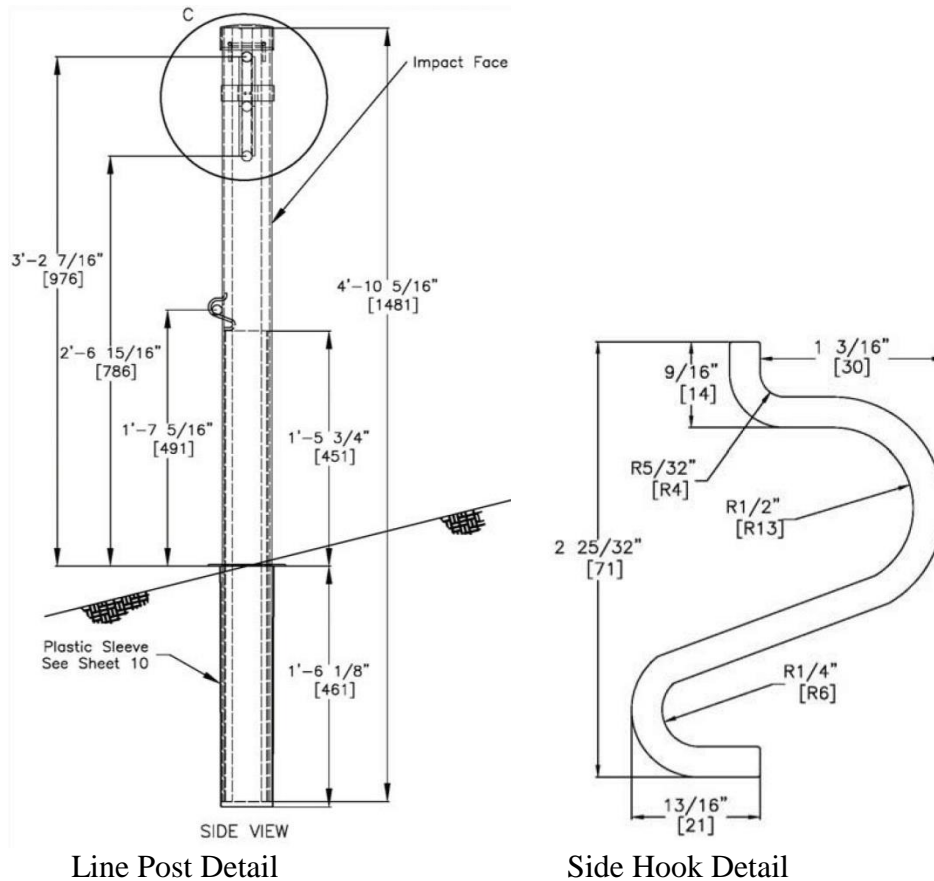


Figure 11. Safence with Side Hooks [49]

Trinity Highway Products manufactures the Cable Safety System (CASS). CASS is a high-tension, cable barrier system which has different configurations (both 3- and 4-strand) and

has been successfully crash tested according to the NCHRP Report No. 350 TL-3 and TL-4 requirements [50]. More detailed information is provided in FHWA eligibility letter nos. B-119 [51], B-119A [52], B-119B [53], B-141 [54], B-141A [55], B-141B [56], B-157 [57], B-141C [58], B-141E [59], B-141D [60], and B-232 [61]. The line posts have a wave-shaped slot in the center of the post. For the typical CASS system, all of the cables are placed in the slot and separated by plastic spacers. For the TL-3 CASS system for placement on 4V:1H side slopes, the bottom cable is attached to the side of the post with a cable lock bolt. The support posts that are located closer to the end terminal are different. These posts use hook bolts to attach the cables to the flanges. A typical CASS system is shown in Figure 12. The wave shape of the upper slot is shown in Figure 13, while the CASS hook bolts, used on the posts closer to the terminals, are depicted in Figure 14.



Figure 12. Trinity Highway Products' CASS [62]

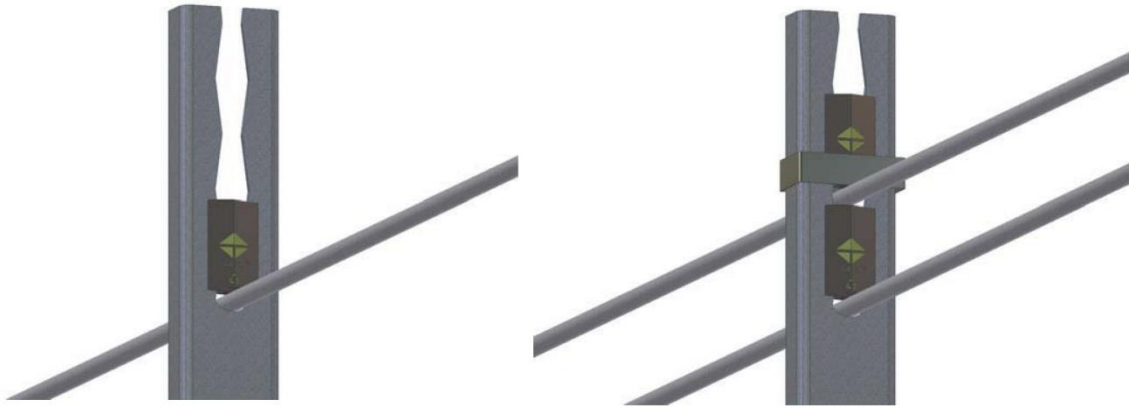


Figure 13. CASS Wave-Shaped Slot [50]

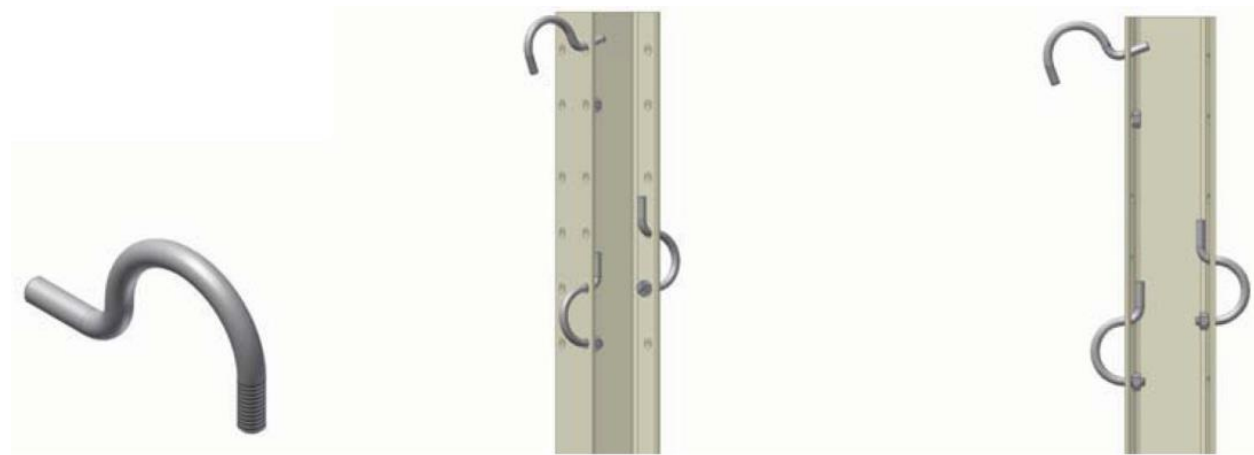


Figure 14. CASS Hook Bolts [50]

Armorflex of New Zealand manufactures the Armorwire Cable Barrier system [63], a high-tension cable barrier with different configurations (both 3- and 4-strand). The Armorwire Cable Barrier system has been successfully crash tested according to the NCHRP Report No. 350 TL-3 and TL-4 requirements. More detailed information is provided in FHWA eligibility letter no. B-222 [64]. The line posts are hollow, oval steel tubes. For a typical system, the cables are placed in top and side slots, and a plastic post cap is inserted in the top end. A drawing of a line post assembly is shown in Figure 15. Photographs of a line post before and after inserting the post cap are shown in Figure 16.

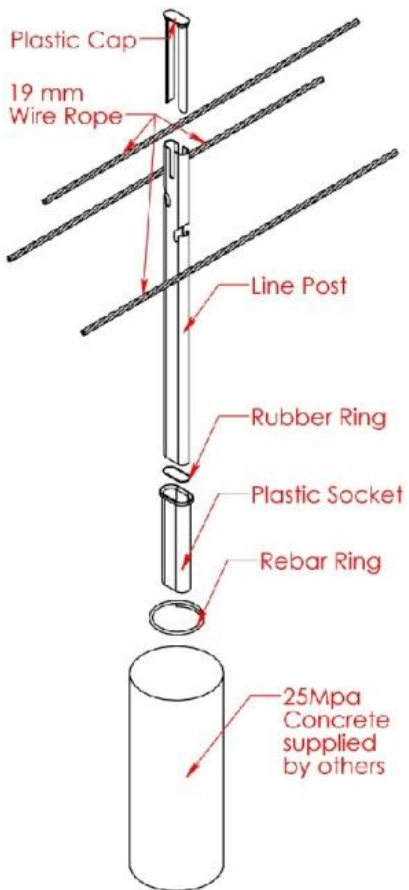


Figure 15. Armorwire Cable Barrier Line Post Assembly [63]



Before Post Cap Installation

After Post Cap Installation

Figure 16. Armorwire Cable Barrier Line Post Photographs [63]

Eligibility letters for previously noted cable barrier systems can be found on the FHWA web site at http://safety.fhwa.dot.gov/roadway_dept/policy_guide/road_hardware/barriers/, keyword: “Cable Barrier” [65]. A summary of the cable barrier systems and eligibility letters is provided in Table 1.

Table 1. FHWA Eligibility Letters for Selected Cable Barriers [65]

Letter No.	Date	Submitted By:	Test Level	Device Description
B-64	2/14/2000	N/A	3	SGR01c Generic 3-strand cable barrier
B-64sup	9/12/2005	N/A	3	SGR01a-b Generic 3-strand cable barrier
B-161	7/3/2007	NYSDOT	3	Generic 4-strand cable barrier
B-227	1/6/2012	WSDOT	3	Generic high-tension 3-strand cable barrier
B-82	4/10/2001	Brifen Ltd.	3	4-strand Brifen WRSF
B-82B	3/27/2005	Hill & Smith Ltd.	4	4-strand Brifen WRSF
B-82C	5/26/2005	Hill & Smith Ltd.	3	3-strand Brifen WRSF
B-82C1	4/13/2006	Hill & Smith Ltd.	3	3-strand Brifen WRSF with reduced post spacing
B-82B1	5/9/2006	Brifen Ltd.	3	4-strand Brifen WRSF on 4V:1H slope
B-137	6/13/2005	Gibraltar	3	3-strand Gibraltar Cable Barrier
B-137A	7/13/2005	Gibraltar	4	3-strand Gibraltar Cable Barrier
B-137B	4/3/2006	Gibraltar	4	3-strand Gibraltar Cable Barrier with alternative post spacing
B-147A	6/16/2006	Gibraltar	3	Gibraltar cable to W-beam transition
B-137C (HSA)	7/12/2006	Gibraltar	3	3-strand Gibraltar Cable Barrier on 4V:1H slope
B-137A1	10/27/2006	Gibraltar	4	4-strand Gibraltar Cable Barrier
B-137C (HSSD)	1/8/2008	Gibraltar	4	Revised anchor design for 4-strand Gibraltar Cable Barrier
B-137D	2/8/2008	Gibraltar	4	Four point anchorage to 4-strand Gibraltar Cable Barrier
B-96	8/30/2002	Nucor Steel Marion Inc.	3	3-strand guardrail with Marion Steel U-Channel posts
B-96A	10/12/2005	Nucor Steel Marion Inc.	3	Variations on 3-strand guardrail with Marion Steel U-channel posts
B-167	2/24/2008	Nucor Steel Marion Inc.	4	4-strand Nucor Wire Rope Barrier System
B-183	11/26/2008	Nucor Steel Marion Inc.	3 & 4	Nu-Cable systems using plastic or steel sockets
B-184	12/9/2008	Nucor Steel Marion Inc.	4	Revised hanging clip for Nucor Steel posts
B-193 (REVISED)	7/27/2009	Nucor Steel Marion Inc.	3	4-strand Nu-Cable system on 4V:1H slope
B-184A	8/3/2009	Nucor Steel Marion Inc.	4	Nu-Cable with 20-ft spacing

Table 1. FHWA Eligibility Letters for Selected Cable Barriers [65] (Continued)

Letter No.	Date	Submitted By:	Test Level	Device Description
B-88	7/13/2001	Blue Systems AB	3	4-strand Safence
B-88A	1/28/2004	Safence, Inc.	3	4-strand Safence for roadside applications
B-88B	6/8/2004	Blue Systems AB	3	4-strand Safence with posts set in concrete footings
B-88C	5/26/2005	Safence, Inc.	3	4-strand Safence with alternative posts (C-channel)
B-88D	12/27/2006	Safence, Inc.	4	3-strand Safence
B-88E	7/31/2007	Safence, Inc.	4	4-strand Safence with different cable heights
B-88F	12/23/2008	Safence, Inc.	3	3-strand Safence on 4V:1H slope
B-119	5/13/2003	Trinity Highway Products	3	3-strand CASS
B-119A	5/15/2003	Trinity Highway Products	3	3-strand CASS with 5 m post spacing
B-119B	8/28/2003	Trinity Highway Products	3	3-strand CASS with 2 m post spacing with concrete footings
B-141	11/17/2005	Trinity Highway Products	3 & 4	3-strand CASS TL-3 and CASS TL-4 with S4x7.7 driven posts
B-141A	5/2/2006	Trinity Highway Products	3	3-strand CASS TL-3 with driven posts at 20-ft post spacing
B-141B	5/8/2006	Trinity Highway Products	3	3-strand CASS TL-3 with 32.5-ft post spacing
B-157	4/23/2007	Trinity Highway Products	4	4-strand CASS system with S4x7.7 posts & terminal
B-141C	11/14/2008	Trinity Highway Products	3	3-strand CASS on 4V:1H slope
B-141E	2/20/2009	Trinity Highway Products	3	4-strand CASS with C-Channel posts
B-141D	3/19/2009	Trinity Highway Products	4	3-strand CASS on 6V:1H or flatter slopes
B-232	5/4/2012	Trinity Highway Products	3	CASS S3 on 4V:1H slope
B-222	1/27/2012	Armorflex	3 & 4	3- and 4-strand Armorwire Barrier

2.3 A-Pillar Testing and Design

Thus far, details for common cable-to-post attachments used in federally-approved cable barriers were investigated and have been presented as it is important to be aware of the state-of-the-practice. However, it was deemed valuable to briefly explore the testing and design of motor vehicle roof structures; since, cable interaction with A-pillars was observed in several MwRSF full-scale vehicle crash tests noted previously and also discussed in Chapter 3. For this reason, the testing and design of vehicle roof structures (e.g., A-pillar) were also investigated.

A-pillars are the front-most structural members which support the roof of a vehicle, as shown in Figure 17. B- and C-pillars are also used to support the roof structure. The roof and its supporting pillars are configured to mitigate concerns for excessive crush of the occupant compartment during vehicle rollovers. As such, vehicles must comply with roof crush testing standards.



Figure 17. Typical A-Pillar

There are currently two standard roof crush tests: Federal Motor Vehicle Safety Standard (FMVSS) 216a [66] and the Insurance Institute for Highway Safety's (IIHS) Roof Strength Test [67]. Both are quasi-static tests in which a rigid plate is pushed into the corner of the roof, and the force is measured through 5 in. (127 mm) of deflection. According to FMVSS 216a, which took effect on September 1, 2012, the crush resistance must exceed three times the vehicle weight. The old standard, FMVSS 216, set in 1973, only required one and a half times the vehicle weight [68]. By September 1, 2017, all vehicles must satisfy the new FMVSS 216a standard, which may result in stronger, more robust A-pillars. It should be noted that many of the vehicles currently on the road already comply with the updated standard.

In general, A-pillars have been getting stronger, sturdier, and ultimately thicker. One unfortunate consequence of this is reduced visibility for the driver, putting pedestrians and bicyclists at risk, especially when the driver is making a left turn [69]. Clearly, there are competing goals. Increased driver visibility demands that the A-pillar be smaller, while increased safety in the event of a rollover crash demands that the A-pillar be stronger. One solution could be to use stronger materials.

From the available literature, no evidence was found which denoted that motor vehicle manufacturers were particularly concerned with A-pillar crushing or cutting as a result of vehicular collisions with cable barriers, which is not surprising. However, one may assume that stiffening and strengthening the A-pillars to meet more stringent rollover requirements could partially and indirectly address concerns for A-pillar crushing or cutting.

3 PROJECT BACKGROUND

3.1 Introduction

Over the years, cable-to-post attachments have played a central role in the effort to develop an improved, non-proprietary, cable median barrier. MwRSF has conducted nine full-scale crash tests on low- and high-tension cable barrier systems as well as hundreds of static and dynamic component tests.

3.2 Improved Low-Tension Cable Median Barrier

Before MwRSF began developing a high-tension cable median barrier, the Midwest States Pooled Fund Program funded an effort to develop an improved, low-tension, cable median barrier [70]. Three low-tension, cable barrier prototypes were designed and full-scale crash tested. Each of the three differed from the generic, low-tension, 3-cable guardrail in three main ways. First, a fourth cable was incorporated into the barrier system in order to reduce the potential for under-ride. Second, the cable spacing was expanded in order cover more area. Third, the post spacing was shortened in order to reduce barrier deflections. Each design was tested once.

The first design, tested in full-scale crash test no. CMB-1, used M8x6.5 (M203x9.7) line posts, spaced at 6 ft (1.8 m) centers. The system was 486 ft (148 m) in length, consisted of 80 posts, and was placed on level terrain. Standard cable hook bolts, as shown in Figure 3 in the previous chapter, attached the cables to the posts. From post to post, the cables alternated from the front flange to the back flange, creating a woven pattern. A pre-test photograph from test no. CMB-1 is shown in Figure 18.



Figure 18. Cable Barrier System, Test No. CMB-1

For test no. CMB-1, a 1,969-lb (893-kg) small car (820C vehicle) impacted the barrier at a speed of 60.6 mph (97.6 km/h) and at a 19.7-degree angle. The impact point was 33 in. (846 mm) upstream from post no. 41. The vehicle was contained, but it rolled over as it was redirecting. The cable barrier was determined to be unacceptable according to the TL-3 safety performance criteria for test designation no. 3-10 found in NCHRP Report No. 350. More information about the prototype barrier system and the test, including the test summary sheet, is provided in Appendix B, Figure B-1.

The second design used S3x5.7 (S76x8.5) line posts spaced at 8 ft (2.4 m) centers. The system was 484 ft (148 m) in length, consisted of 61 posts, and was placed on level terrain. Rigid

cable brackets, made from ½-in. (13-mm) thick A36 steel plate, were welded to the posts, and the cables were set in them. The cables were not weaved, although the cables alternated from front side to backside of post as a function of height. A detail of the rigid cable bracket is shown in Figure 19. A pre-test photograph of a line post is shown in Figure 20.

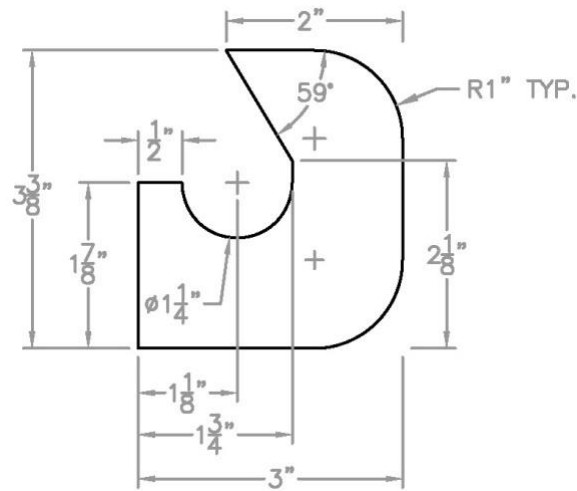


Figure 19. Rigid Cable Bracket Detail, Test No. CMB-2



Figure 20. Cable Barrier System, Test No. CMB-2

For test no. CMB-2, a 1,960-lb (889-kg) small car (820C vehicle) impacted the system at a speed of 62.8 mph (101.1 km/h) and at a 19.7-degree angle. The impact point was 48 in. (1,219 mm) upstream from post 31. The vehicle was adequately contained. The left-front tire became snagged on a post as the vehicle was being redirected. As a result of the snag, the vehicle yawed counterclockwise away from the barrier before coming to rest. In spite of this motion, the vehicle intrusion into adjacent traffic lanes was minimal. The cable barrier was determined to be acceptable according to the TL-3 safety performance criteria for test designation no. 3-10 found in NCHRP Report No. 350. More information about the prototype barrier system and the test, including the test summary sheet, is provided in Appendix B, Figure B-2.

For this test, the cable behavior upon release from the posts was particularly interesting. Since the brackets were open at the top, the upper two cables were prematurely released away from a significant number of posts beyond the impact region. This behavior was due to a stress wave which propagated through the cables. There was a concern that such premature cable release would result in reduced energy dissipation, which could contribute to reduced vehicle containment. On a positive note, the easy vertical release prevented the cables from clamping down on the A-pillar and crushing it—a problem encountered in future barrier designs.

Similar to the design used in test no. CMB-2, the third configuration used S3x5.7 (S76x8.5) line posts spaced at 8 ft (2.4 m) centers. The system was 484 ft (148 m) in length, consisted of 61 posts, and was placed on level terrain. The shape of the rigid cable brackets was changed slightly. Retainer bolts were also added above the cable brackets to prevent premature cable release. A detail of the rigid cable bracket is shown in Figure 21. A pre-test photograph of a line post is shown in Figure 22.

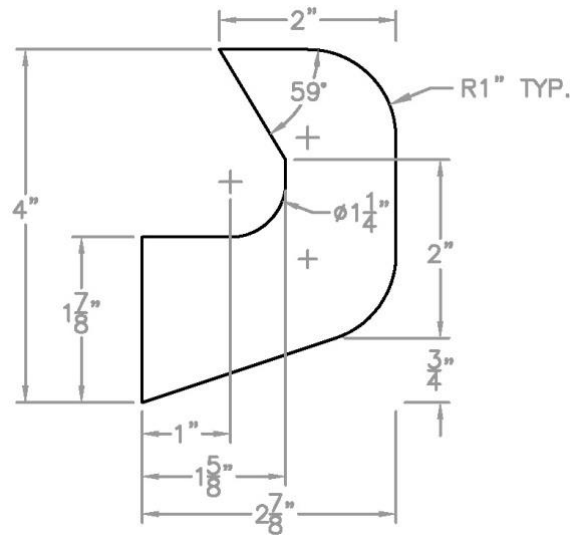


Figure 21. Rigid Cable Bracket Detail, Test No. CMB-3



Figure 22. Cable Barrier System, Test No. CMB-3

For test no. CMB-3, a 4,459-lb (2,023-kg) pickup truck (2000P vehicle) impacted the system at a speed of 60.8 mph (97.8 km/h) and at a 25.4-degree angle. The impact point was 48

in. (1,219 mm) upstream from post no. 31. The vehicle was adequately contained and safely redirected. Because of the retainer bolts, the top two cables were retained on the posts that were outside of the impact region. The cable barrier was determined to be acceptable according to the TL-3 safety performance criteria for test designation no. 3-11 found in NCHRP Report No. 350. More information about the prototype barrier system and the test, including the test summary sheet, is provided in Appendix B, Figure B-3.

Despite the successful crash tests on the improved low-tension, cable barrier systems installed on level terrain, the member states of the Midwest States Pooled Fund Program ultimately decided to redirect the cable barrier R&D program. In addition, the cable-to-post attachments, consisting of brackets welded to the posts, were not desirable.

3.3 High-Tension, Cable Median Barrier

The objective of the new effort was to design an improved, non-proprietary, high-tension, cable median barrier that for use on generally flat terrain as well as anywhere within a depressed median with side slopes as steep as 4V:1H. The 4-cable barrier system was to be crash tested and evaluated according to the TL-3 safety performance criteria found in the *Manual for Assessing Safety Hardware* (MASH) [1].

3.3.1 Curved Keyway Bracket Development

Before a new high-tension, cable barrier system could be crash tested, an effort was undertaken to design a completely new cable-to-post attachment. This R&D effort was summarized in an MwRSF research report [9]. Ninety-nine static component tests and fourteen dynamic component tests were performed. In these tests, the attachments were subjected to vertical or lateral loads until failure. The static component tests, which included both slotted bracket and U-bolt concepts, were very similar to those later described in Chapter 18. Designers set target lateral and vertical release loads of 6.00 kips (26.7 kN) and 1.00 kips (4.45 kN),

respectively. Ultimately, one of the slotted bracket concepts—the curved keyway bracket—was chosen for further testing, but the U-bolt concepts which featured keyways and slotted upper holes in the post, as shown in Figure 23, also performed very well and were the inspiration behind the keyway bolts in a later R&D effort [71].

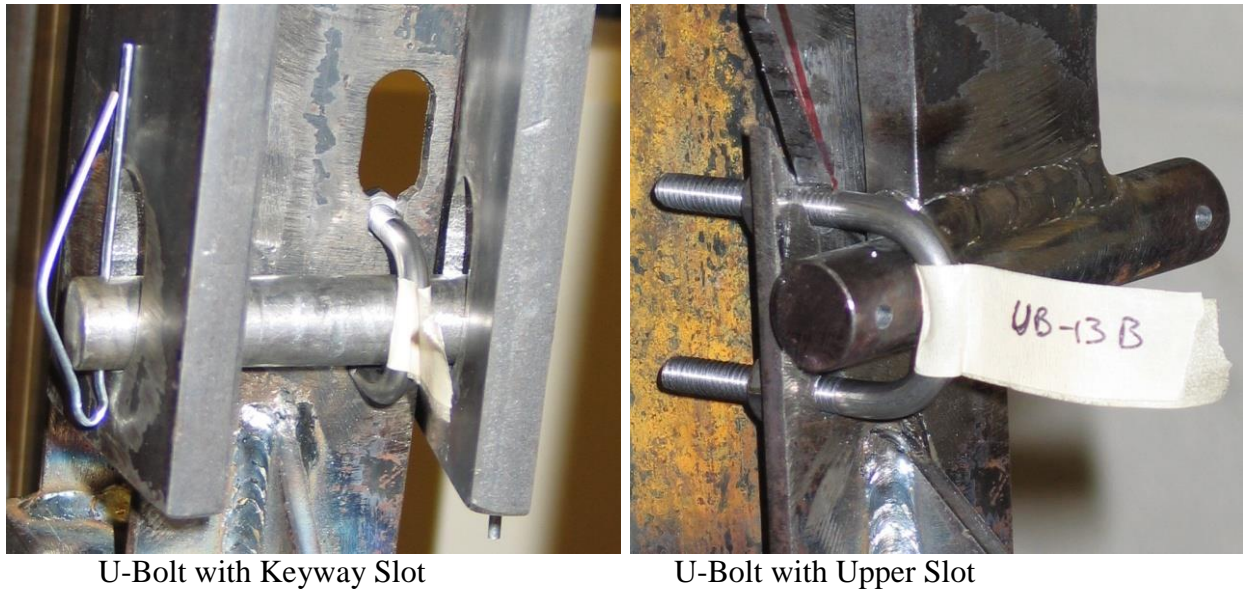


Figure 23. U-Bolt Concepts

The dynamic component tests were very similar to those later described in Chapter 6, but with slight adjustments to the test jig in order to accommodate the different cable-to-post attachments. The cable-to-post attachment that was chosen—the curved keyway bracket—was fabricated from 1/8-in. (3-mm) thick A36 sheet steel. Each bracket was attached to the flange of the post with two SAE grade 5, 5/16-in. (8-mm) shoulder hex bolts with nuts and washers. Curved keyway bracket details are shown with the shoulder bolts in Figure 24, and without the shoulder bolts in Figure 25. A photograph of a curved keyway brackets installed on a post is shown in Figure 26.

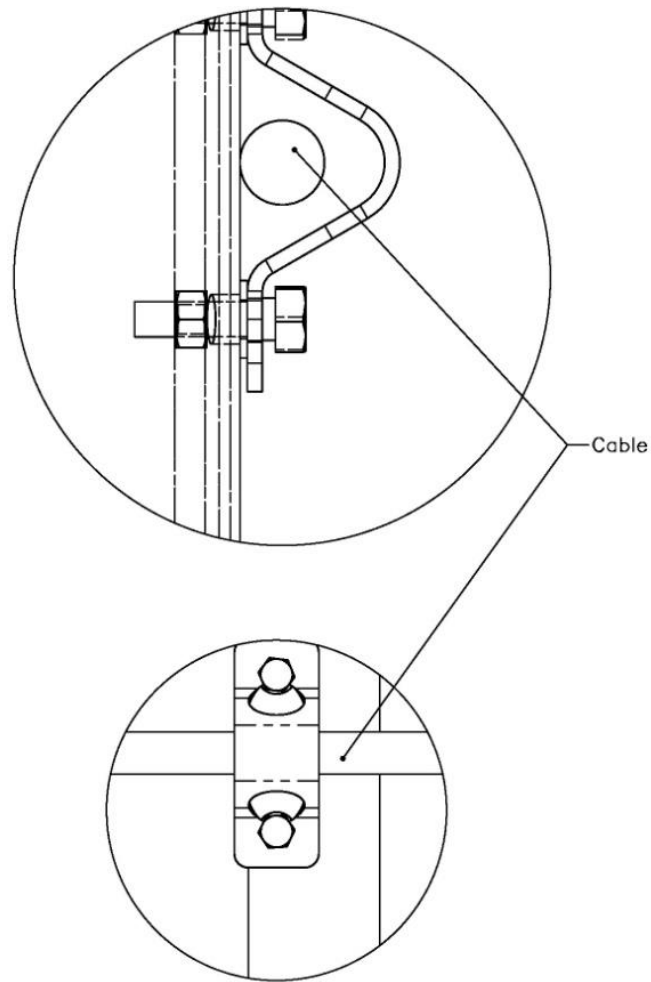


Figure 24. Curved Keyway Bracket with Shoulder Bolts

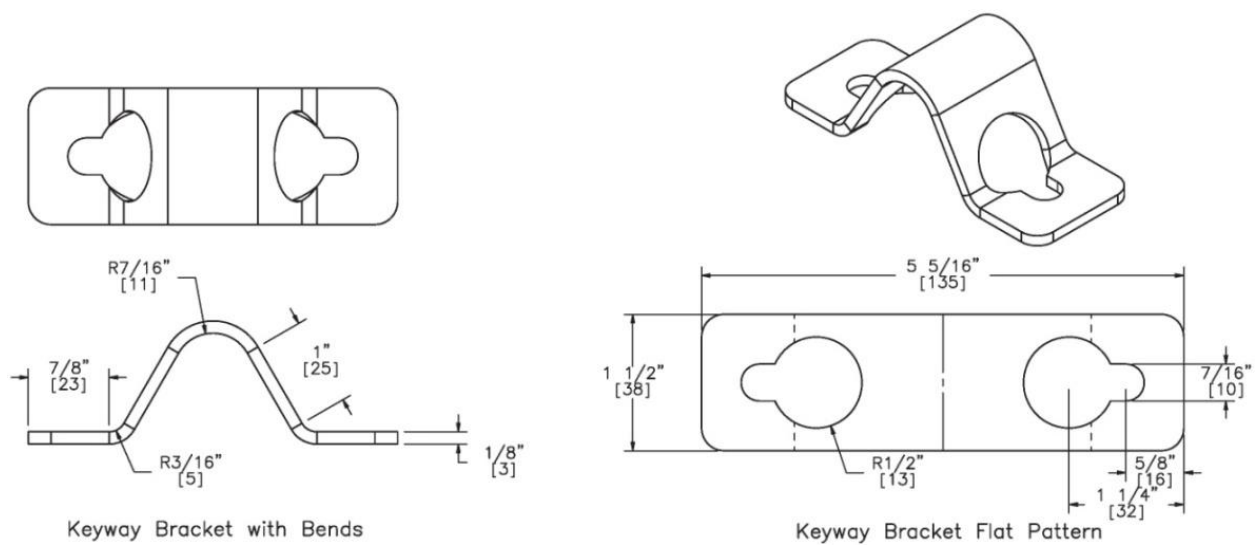


Figure 25. Curved Keyway Bracket Details



Figure 26. Curved Keyway Brackets Installed on Post

Since the cable-to-post attachments would be loaded dynamically during an impact event, dynamic component tests were an especially important part of the evaluation process. The curved keyway brackets had lateral and vertical release loads of 5.72 kips (25.4 kN) and 1.17 kips (5.20 kN), respectively. It was believed that this would provide sufficient lateral strength to develop the full moment capacity of the post, and a sufficiently low vertical strength to prevent cables from being pulled down too far by rotating posts or clamping down and crushing a vehicle's A-pillar.

3.3.2 Phase I Full-Scale Crash Tests

Phase I consisted of three full-scale vehicle crash tests [2]. The cable barrier system used S3x5.7 (S76x8.5) line posts spaced at 16 ft (4.9 m). The system was 608 ft (148 m) in length, consisted of 40 posts, and was placed in a 46-ft (14-m) wide, 4V:1H V-ditch. The cables were pre-tensioned to a target load of 4,213 lb (18.7 kN). The location of the barrier in the V-ditch was different for each of the three tests. Curved keyway brackets attached the cables to the posts.

For test no. 4CMB-1, a 4,988-lb (2,263-kg) pickup truck (2270P vehicle) impacted the high-tension, 4-cable median barrier at a speed of 61.8 mph (99.4 km/h) and at a 27.9-degree angle. The barrier system was located on the front slope of the V-ditch, 12 ft (3.6 m) laterally away from the front slope break point. The point of impact was 36 in. (914 mm) downstream from post no. 15. The vehicle was adequately contained and redirected. It remained upright, and there were no significant penetrations into the occupant compartment. The test was determined to be acceptable according to the TL-3 safety performance criteria for test designation no. 3-11 found in MASH. More information about the prototype barrier system and the test, including the test summary sheet, is provided in Appendix B, Figure B-4.

For test no. 4CMB-2, a 2,557-lb (1,160-kg) small car (1100C vehicle) impacted the high-tension, 4-cable median barrier at a speed of 62.7 mph (100.9 km/h) and at a 26.8-degree angle. The barrier system was located on the back slope of the V-ditch, 4 ft (1.2 m) laterally away from the bottom of the ditch. The point of impact was 64 in. (1,626 mm) downstream from post no. 17. In order to increase the likelihood of under-ride, a soft soil condition was used for the ditch bottom. Prior to contact with the barrier, the vehicle made contact with the back slope. The vehicle undercarriage and wheels penetrated into and gouged the soft soil, resulting in loss of vehicle speed prior to impact with the barrier. As a result of these occurrences, the vehicle's front end penetrated slightly under the bottom cable. However, the barrier system still contained the

vehicle, which remained upright. No significant penetrations into the occupant compartment occurred. In addition, the longitudinal OIV exceeded the MASH limit of 40 ft/s (12.2 m/s) when considering the loss in vehicle speed during tire rutting and soil plowing prior to vehicle contact with the barrier. Therefore, the test was determined to be marginally acceptable according to the TL-3 performance criteria for test designation no. 3-10 found in MASH when the barrier was placed near the ditch bottom configured with a soft soil condition. More information about the prototype barrier system and the test, including the test summary sheet, is provided in Appendix B, Figure B-5.

For test no. 4CMB-3, a 2,586-lb (1,173-kg) small car (1100C vehicle) impacted the high-tension, 4-cable median barrier at a speed of 62.0 mph (99.8 km/h), at a 27.2-degree angle. The barrier system was located on the back slope of the V-ditch, 4 ft (1.2 m) laterally away from the bottom of the ditch. The point of impact was 64 in. (1,626 mm) downstream from post no. 16. In contrast to the soft soil condition of test no. 4CMB-2, the soil at the bottom of the ditch was heavily compacted for this test. Similar to the previous test, the vehicle made contact with the back slope before making contact with the barrier. Upon impact with the barrier, the vehicle was adequately contained and remained upright, but the A-pillar was crushed by a cable, resulting in significant damage to the roof, windshield, and penetration into the occupant compartment. The cable crushed the A-pillar, because it was snagged on one of the shoulder bolts that corresponded to the curved keyway brackets, as shown in Figure 27. Therefore, due to the excessive occupant compartment penetrations, the test did not meet the TL-3 safety performance criteria for test designation no. 3-10 found in MASH when the barrier was placed near the ditch bottom with a strong/stiff soil condition. More information about the prototype barrier system and the test, including the test summary sheet, is provided in Appendix B, Figure B-6.



Figure 27. Cable Snag Resulting in Crushed A-Pillar, Test No. 4CMB-3

3.3.3 Keyway Bolt Development

After full-scale crash test no. 4CMB-3, it was clear that the curved keyway brackets required redesign or replacement in order to improve barrier performance. As a result, MwRSF began an effort to redesign the cable-to-post attachments. For this effort, three main objectives were followed: (1) the cable-to-post attachments should meet or maintain the vertical and lateral release behavior provided by the curved keyway brackets; (2) the hardware should prevent cable snagging; and (3) the cable-to-post attachments should be simplified by minimizing the number of connecting parts. This R&D effort was summarized in an MwRSF research report [71].

MwRSF performed thirty-seven dynamic component tests (test nos. HTCUB-1 through HTCUB-37), and six steel-framed bogie vehicle impact tests (test nos. HTCC-1 through HTCC-6). Dynamic component tests were used to obtain the lateral and vertical release loads of a particular cable-to-post attachment, and steel-framed bogie vehicle impact tests were used to obtain information about how far a post with that attachment might rotate before releasing the cable, during a simulated impact event.

The cable-to-post attachments that were tested in this effort were known as keyway bolts. Keyway bolts were deliberately curved to avoid jagged protrusions, thus avoiding the problem which caused the barrier system to fail in test no. 4CMB-3. The first keyway bolts were fabricated from AISI C1018 steel round bar and had lateral and vertical release loads of 6.47 kips (28.8 kN) and 0.81 kips (3.60 kN), respectively. Stronger keyway bolts, fabricated from ASTM A449 steel round bar, were also tested. The stronger keyway bolts were found to have lateral and vertical release loads of 8.00 kips (35.6 kN) and 1.18 kips (5.25 kN), respectively. Keyway bolt details are shown in Figure 28. Details for the corresponding keyway are shown in Figure 29. The keyway bolts installed in and actual post are shown in Figure 30.

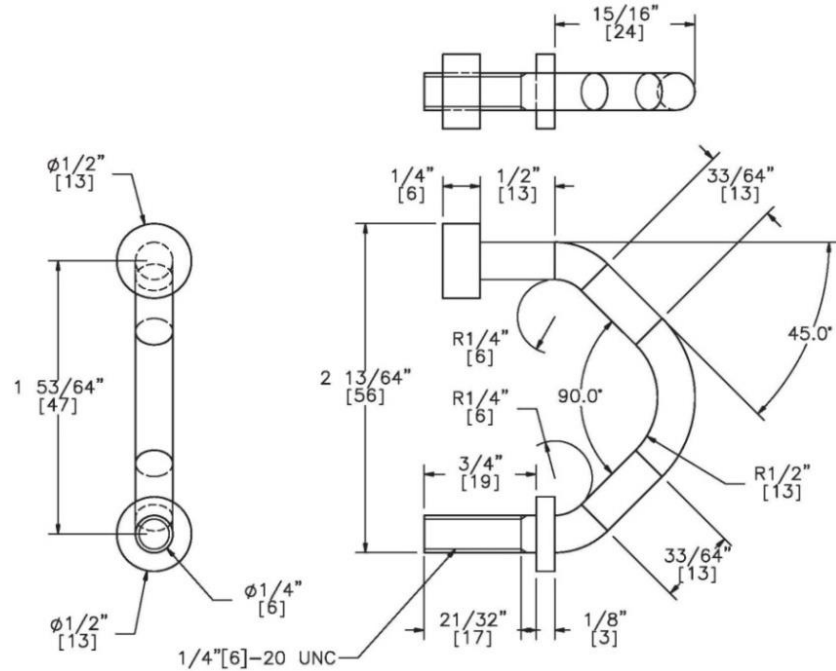


Figure 28. Keyway Bolt Details

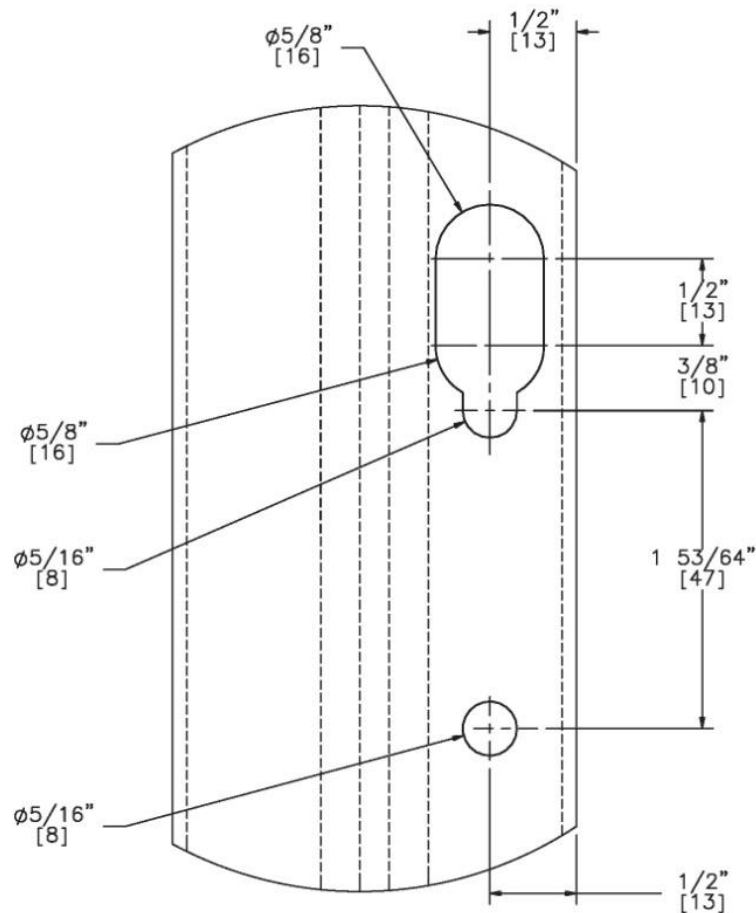


Figure 29. Keyway Details



Figure 30. Keyway Bolts Installed on Post

Besides lateral and vertical release loads, energy absorption was another important criterion used for evaluating cable-to-post attachments. When a cable barrier system is laterally loaded, it deflects backward and causes the posts to yield and rotate. For a given steel section, more post rotation results in more energy absorption.

In test nos. HTCC-1 through HTCC-6, a steel-framed bogie vehicle impacted a simplified, single-cable system in a perpendicular orientation and at a target speed of 17.0 mph (27.4 km/h). The basic test setup consisted of four S3x5.7 (S76x8.5) posts, spaced at 16 ft (1.9 m) centers, with a tensioned cable mounted along all four posts. For a given test, only one type of cable-to-post attachment was being evaluated. The cable, which was pre-tensioned to 4,000 lb (17.8 kN), was mounted at a height of 34-½ in. (876 mm) above the ground. The bogie impacted the cable at the midpoint of a 16-ft (4.9-m) span between two of the posts. The cable-to-post attachments on the two posts adjacent to the span were on alternating sides. In this configuration, the bogie pushed the cable away from one post while pushing the cable into the other post. Upon

impact, the posts would begin to rotate until the cable-to-post attachments released the cable. The resulting post rotation angles were measured. The purpose of these tests was to compare the post rotations that could be achieved for cable barrier systems with different cable-to-post attachments.

The post rotations achieved by the C1018 keyway bolts, A449 keyway bolts, and curved keyway brackets were 18 degrees, 34 degrees, and 33 degrees, respectively. As a result, the A449 keyway bolts were chosen over the C1018 keyway bolts. High-speed video images from test no. HTCC-4, in which the A449 keyway bolts were evaluated, are shown in Figure 31. Additional information and test results are provided in an MwRSF research report [71].

3.3.4 Phase II Full-Scale Crash Tests

Phase II consisted of three full-scale vehicle crash tests. The cable barrier system used S3x5.7 (S76x8.5) line posts spaced at 16 ft (4.9 m) centers. The system was 608 ft (148 m) in length and consisted of 40 posts. For the first two tests (test nos. 4CMB-4 and 4CMB-5), the barrier systems were placed in a 46-ft (14-m) wide, 4V:1H V-ditch [3]. The location of the barrier in the V-ditch was different for both tests. For the third test (test no. 4CMBLT-1), the barrier system was placed on level terrain [4]. For all three tests, the cables were attached to the posts with A449 keyway bolts.



Bogie Impacts Cable



Cable Releases from Post

Figure 31. Post Rotation Test with A449 Keyway Bolts, Test No. HTCC-4

For test no. 4CMB-4, a 2,574-lb (1,168-kg) small car (1100C vehicle) impacted the high-tension, 4-cable median barrier at a speed of 61.1 mph (98.4 km/h) and at a 25.8-degree angle. The barrier system was located on the back slope of the V-ditch, 4 ft (1.2 m) laterally away from the bottom of the ditch. The point of impact was 64 in. (1,626 mm) downstream from post no. 16. Similar to test no. 4CMB-3, the soil in the region of the impact was heavily compacted. The vehicle made contact with the back slope before contacting the barrier. Upon impact with the barrier, the vehicle was adequately contained and redirected. It remained upright, and there were no significant penetrations into the occupant compartment. The test was determined to be acceptable according to the TL-3 safety performance criteria for test designation no. 3-10 found in MASH. More information about the prototype barrier system and the test, including the test summary sheet, is provided in Appendix B, Figure B-7.

For test no. 4CMB-5, a 5,149-lb (2,336-kg) pickup truck (2270P vehicle) impacted the high-tension, 4-cable median barrier at a speed of 61.8 mph (99.5 km/h) and at a 26.5-degree angle. The barrier was located on the front slope of the V-ditch, 12 ft (3.6 m) laterally from the front slope break point. The point of impact was 12 in. (305 mm) upstream of post no. 15. The left-front bumper impacted the post, causing it to begin to rotate downward. As the post rotated, all of the cables were pulled down with it, including the top cable. This action allowed the vehicle to completely override the barrier, as shown in Figure 32. Only the right-rear wheel was snagged by a cable. As a result, the vehicle impacted the back slope and rolled over. The test failed to meet the TL-3 safety performance criteria for test designation no. 3-10 found in MASH. More information about the prototype barrier system and the test, including the test summary sheet, is provided in Appendix B, Figure B-8.



Impact, Time = 0.000 sec



Override, Time = 0.090 sec

Figure 32. Impact with Post and Barrier Override, Test No. 4CMB-5

The system failure of full-scale crash test no. 4CMB-5 demonstrated another critical vulnerability for cable barriers installed within sloped median ditches. Specifically, there is increased likelihood for barrier override when a 2270P vehicle impacts the cable barrier just upstream from a post. In order to increase the likelihood of vehicle capture, the top cable-to-post attachments must release the cable away from a post very quickly to prevent it from being pulled down and/or the top cable must be positioned higher.

For test no. 4CMBLT-1, a 3,470-lb (1,574-kg) passenger car (1500A vehicle) impacted the high-tension, 4-cable median barrier at a speed of 62.2 mph (100.1 km/h) and at a 25.3-degree angle. The barrier system was placed on level terrain. The point of impact was 64 in. (1,626 mm) downstream from post no. 16. Upon impact with the barrier, the vehicle was adequately contained, redirected, and remained upright, but the A-pillar was crushed by a cable, resulting in significant damage to the roof, windshield, and penetration into the occupant compartment. When the A-pillar was being crushed, the critical cable was still attached to the downstream post, as shown in Figure 33. The resulting damage is shown in Figure 34. The test failed to meet the TL-3 performance criteria found in MASH. More information about the system and the test, including the test summary sheet, is provided in Appendix B, Figure B-9.

For convenience, all nine full-scale vehicle crash tests into the prototype low- and high-tension, cable barriers are summarized in Table 2.



Figure 33. A-Pillar Beginning to Crush, Test No. 4CMBLT-1



Figure 34. Vehicle Damage, Test No. 4CMBLT-1

Table 2. Summary of Full-Scale Vehicle Crash Tests into Low- and High-Tension, Cable Barrier Systems

Test No.	System Description	Cable-to-Post Attachments	Vehicle	Pass/Fail	Notes
CMB-1	Low-tension, 4-cable median barrier on level terrain, weaved cables	Standard cable hook bolts	Small car (820C)	Fail	Vehicle rolled over
CMB-2	Low-tension, 4-cable median barrier on level terrain	Rigid cable brackets	Small car (820C)	Pass	
CMB-3	Low-tension, 4-cable median barrier on level terrain	Rigid cable brackets with retainer bolts	Pickup (2000P)	Pass	
4CMB-1	High-tension, 4-cable median barrier on 4V:1H sloped V-ditch	Curved keyway brackets	Pickup (2270P)	Pass	
4CMB-2	High-tension, 4-cable median barrier on 4V:1H sloped V-ditch, soft soil in impact region	Curved keyway brackets	Small car (1100C)	Marginal Pass	Longitudinal OIV exceeded 40 ft/s (12.2 m/s) MASH limit when considering vehicle speed loss from tire rutting and soil plowing prior to barrier contact
4CMB-3	High-tension, 4-cable median barrier on 4V:1H sloped V-ditch, heavily compacted soil in impact region	Curved keyway brackets	Small car (1100C)	Fail	A-pillar was crushed
4CMB-4	High-tension, 4-cable median barrier on 4V:1H sloped V-ditch, heavily compacted soil in impact region	A449 keyway bolts	Small car (1100C)	Pass	
4CMB-5	High-tension, 4-cable median barrier on 4V:1H sloped V-ditch	A449 keyway bolts	Pickup (2270P)	Fail	Vehicle overrode barrier and rolled over
4CMBLT-1	High-tension, 4-cable median barrier on level terrain	A449 keyway bolts	Passenger car (1500A)	Fail	A-pillar was crushed

3.4 Conclusions

Following a review of MwRSF's full-scale crash testing program on cable barriers, two problems were very clearly identified that were directly related to the behavior of the cable-to-post attachments. The first problem was excessive penetration into the occupant compartment due to A-pillar crushing. The second problem was barrier override when the vehicle impacted the system at a post. Both problems were caused by failure of cables to adequately release from the posts.

A-pillar crushing had now occurred on more than one occasion, manifesting itself first in full-scale crash test no. 4CMB-3, and again in full-scale crash test no. 4CMBLT-1. In test no. 4CMB-3, the A-pillar was crushed because a protruding shoulder bolt snagged one of the cables, restricting it from releasing upward along a post. The snagging problem was solved by replacing the keyway brackets with the keyway bolts in test no. 4CMB-4. However, the A-pillar was again crushed by a cable in test no. 4CMBLT-1, where several factors may have contributed to this result. The keyway bolt delayed cable release away from the downstream post. Ideally, a cable with the potential to crush the A-pillar should be allowed to slide up and over the A-pillar rather than cutting into it. Thus, several design changes were considered in an attempt to mitigate this type of failure and are provided below:

- Decrease cable pre-tension to reduce the load imparted to the A-pillar;
- Alter cable heights or vertical cable spacing;
- Choose a weaker post to encourage the post to bend more when loaded laterally, giving the cable more freedom to deflect;
- Change the number of cables used.
- Move top cable-to-post attachments from side of post to middle of post;
- Modify keyway on post to allow the button head of keyway bolt to release quicker; and

- Re-design cable-to-post attachments to provide lower vertical release loads.

Even though all of these modifications were to be considered in the next full-scale crash test, the R&D effort described herein only addressed the last three suggestions.

As previously noted, vehicle override was observed in test no. 4CMB-5. It was learned that a cable barrier is particularly susceptible to this type of failure when a vehicle impacts just upstream of a post. It has been believed that this behavior may be mitigated with the use of cable-to-post attachments which release the top cable away from posts much quicker rather than allowing it to be pulled down with the rotating post. Quick cable release could be achieved with a reduced lateral and/or vertical capacity for the top cable-to-post attachment.

With these two problems clearly identified, the next step was to determine the minimum design loads associated with horizontal and vertical curves as a function of post spacing, and to determine target capacities for the vertical and lateral cable release out of the cable-to-post attachments at all four cable heights. This process is presented in Chapter 4.

4 DETERMINATION OF DESIGN LOADS

4.1 Introduction

Following the system failures observed in full-scale crash test nos. 4CMB-5 and 4CMBLT-1, as discussed in Chapter 3, an effort was initiated to re-design the cable-to-post attachment hardware and associated release mechanisms. Thus, it was deemed necessary to determine: (1) the minimum design loads associated with horizontal and vertical curves as a function of post spacing and (2) the desired capacities for vertical and lateral cable release out of the cable-to-post attachments at all four cable heights.

4.2 Prior Cable-to-Post Attachments—Capacity and Performance

The curved keyway brackets, as shown in Figures 25 and 26 of Chapter 3, had lateral and vertical release loads of 5.72 kips (25.4 kN) and 1.00 kips (4.45 kN), respectively [9]. The shoulder bolts, which attached the curved keyway bracket to the post, were relatively bulky and protruded away from the post at a right angle. In full-scale crash test no. 4CMB-3, the impacting vehicle's A-pillar was crushed by a restrained cable that vertically snagged on a protruding shoulder bolt.

The A449 keyway bolts, as shown in Figures 28 through 30 of Chapter 3, had lateral and vertical release loads of 8.00 kips (35.6 kN) and 1.18 kips (5.25 kN), respectively [71]. The keyway bolts did not show the same tendency to snag the lower cables as observed with the protruding shoulder bolt of the curved keyway brackets. However, the A449 keyway bolts may have excessively delayed cable release away from a post, which likely contributed to significant crushing of the vehicle's A-pillar in test no. 4CMBLT-1. Furthermore, test no. 4CMB-5 demonstrated that the A449 keyway bolts were too strong in the vertical direction and demonstrated a propensity for pulling cables down when positioned on the back side of a rotating

post, thus compromising the capture of a 2270P vehicle. Therefore, the release behavior needed to be changed.

4.3 Minimum Design Loads Due to Vertical Curves

Cable median barriers installed along roadways with changes in vertical and horizontal alignment will encounter load conditions which tend to push cables against the post, pull cables away from posts, lift cables up, or push cables down at the cable-to-post attachment. A vertical change in cable slope between posts will result in a vertical force being applied at the point where the slope changes (i.e., the cable-to-post attachment).

Cable tension also increases when the ambient air temperature decreases in a cable barrier with rigid anchors at the ends. On the contrary, cable tension decreases when the ambient air temperature increases. The expansion or contraction of a fixed-length, anchored cable will result in changes in axial stress according to Hooke's Law.

Vertical curves along roadways are designed to be parabolic in shape. For a parabolic curve, the rate of change of the slope (the slope gradient) is constant. The AASHTO Green Book, *A Policy on Geometric Design of Highways and Streets* [72] refers to the tangent slopes of the roadway as grades, which are expressed as percents—not the actual decimal form. A vertical curve with horizontal length, L , and tangent grades, G_1 and G_2 , at its ends, as shown in Figure 35, will have a value, K , associated with it such that $K = L/A$, where A is the algebraic difference between the two tangent grades.

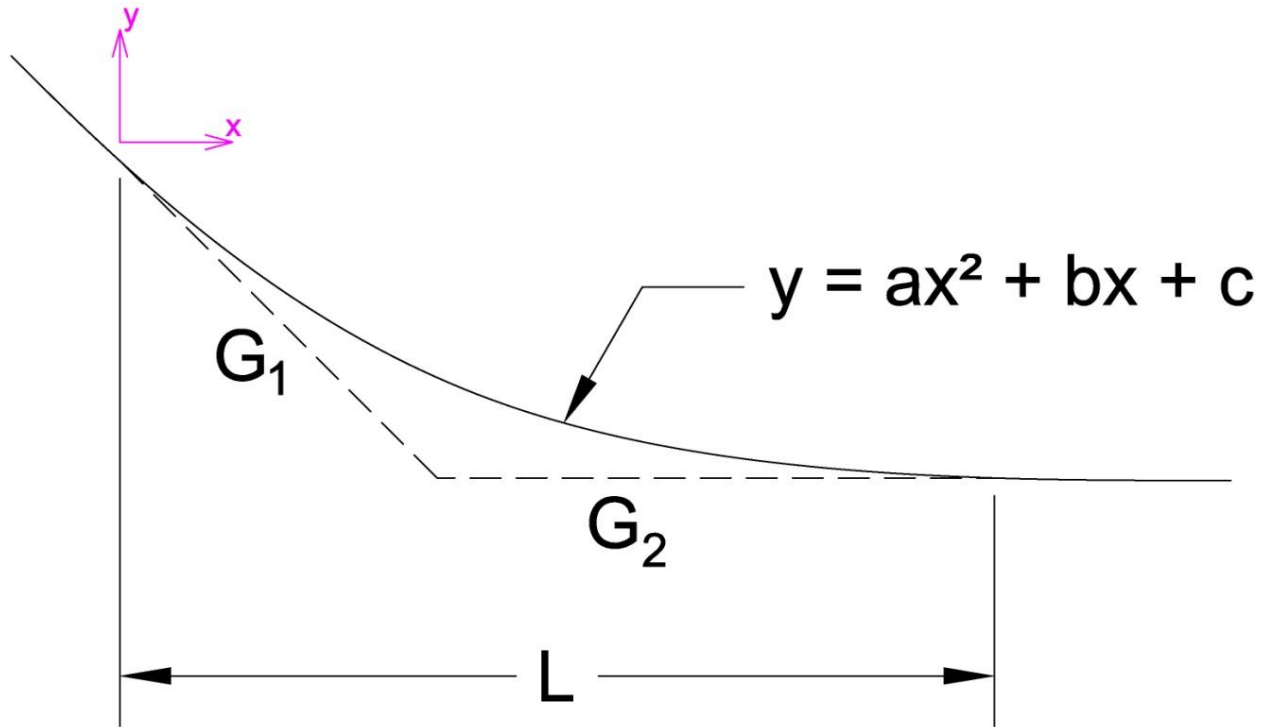


Figure 35. Typical Parabolic Vertical Curve

As noted previously, a change in the slope of the cable between adjacent post spans will result in a net vertical force on the cable-to-post attachment. This change in the slope will be a function of the post spacing and the slope gradient of the vertical curve. In reality, the posts will be spaced evenly along the parabolic curve. However, the post spacing was assumed to occur at horizontal distance increments, s , as shown in Figure 36. This assumption is actually conservative; since, if the spacing, s , were along the curve, the horizontal distance between posts would be less than s .

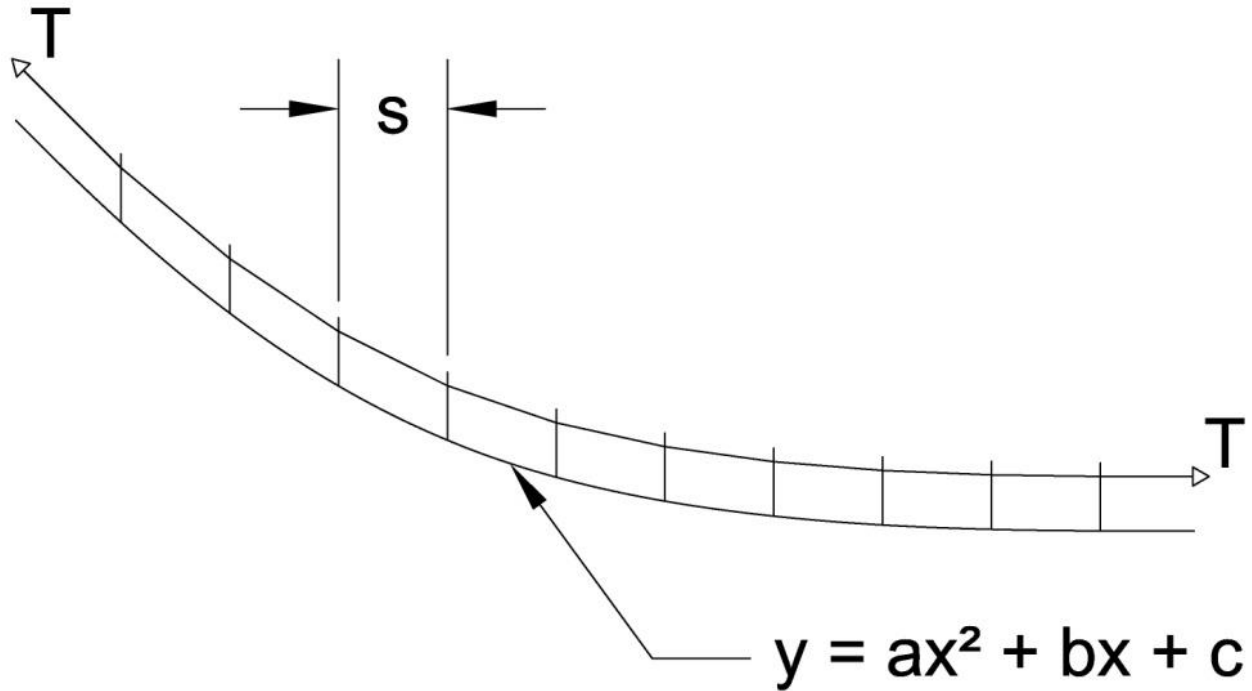


Figure 36. Cable System on a Parabolic Vertical Curve

The general equation for a parabola is given below.

$$y = ax^2 + bx + c$$

Where y = vertical coordinate of the roadway
 x = horizontal coordinate of the roadway
 a , b , and c are arbitrary coefficients

The first derivative provides the general form of the equation for the slope gradient and is given by Equation 4.1.

$$\frac{dy}{dx} = 2ax + b \quad (4.1)$$

If the origin is placed at the beginning of the vertical curve, where the tangent grade is G_1 (a percent), the slope gradient at $x = 0$ is given by Equation 4.2.

$$\left(\frac{dy}{dx}\right)_{x=0} = b = \frac{G_1}{100} \quad (4.2)$$

Where G_1 = tangent grade (as a percent) at the beginning of the vertical curve (i.e., $x = 0$)

At $x = L$, the end of the curve, the tangent grade is G_2 (a percent), as shown in Equation 4.3.

$$\left(\frac{dy}{dx}\right)_{x=L} = 2aL + b = 2aL + \frac{G_1}{100} = \frac{G_2}{100} \quad (4.3)$$

Where $L =$ horizontal length of curve
 $G_2 =$ tangent grade (as a percent) at the end of the vertical curve (i.e., $x = L$)

Solving for “a” in Equation 4.3 gives Equation 4.4.

$$a = \frac{G_2 - G_1}{200L} = \frac{A}{200L} = \frac{1}{200\left(\frac{L}{A}\right)} \quad (4.4)$$

Where $A =$ algebraic difference between the two tangent grades

Recall that $K = L/A$. Therefore, the coefficient, a , can be expressed in terms of K , as shown in Equation 4.5.

$$a = \frac{1}{200K} \quad (4.5)$$

It can be shown that the difference in the slope of the cable between two adjacent spans of cable, as shown in Figure 37, is given by Equation 4.6. This derivation is provided in Appendix C.

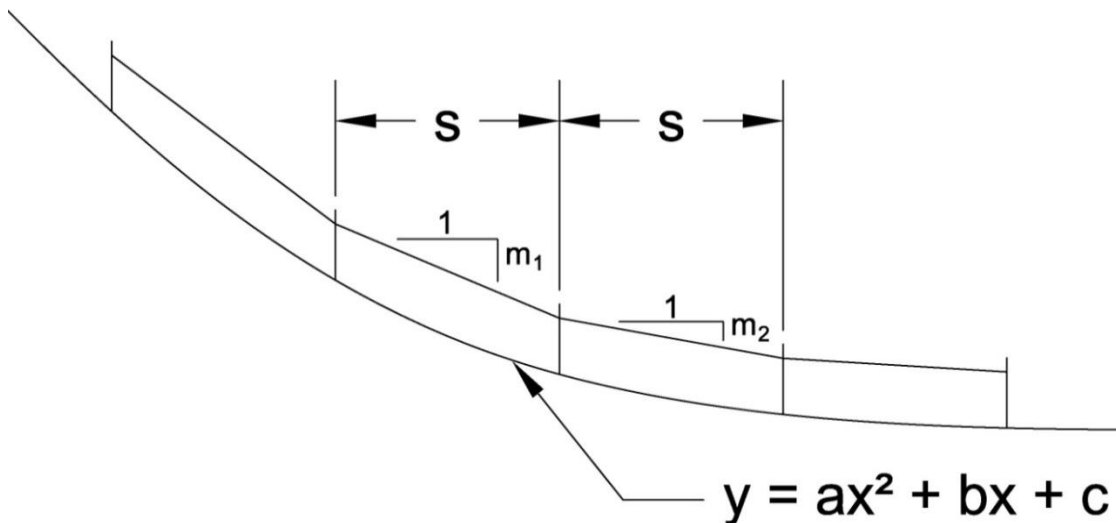


Figure 37. Change in Slope Between Post Spans

$$m_2 - m_1 = 2as = \frac{s}{100K} \quad (4.6)$$

Where m_1 = cable slope on left side of attachment (see Figure 37)
 m_2 = cable slope on right side of attachment (see Figure 37)
 s = post spacing

A free body diagram of the forces acting on the cable-to-post attachment between the two spans of cable with slopes m_1 , and m_2 , is shown in Figure 38.

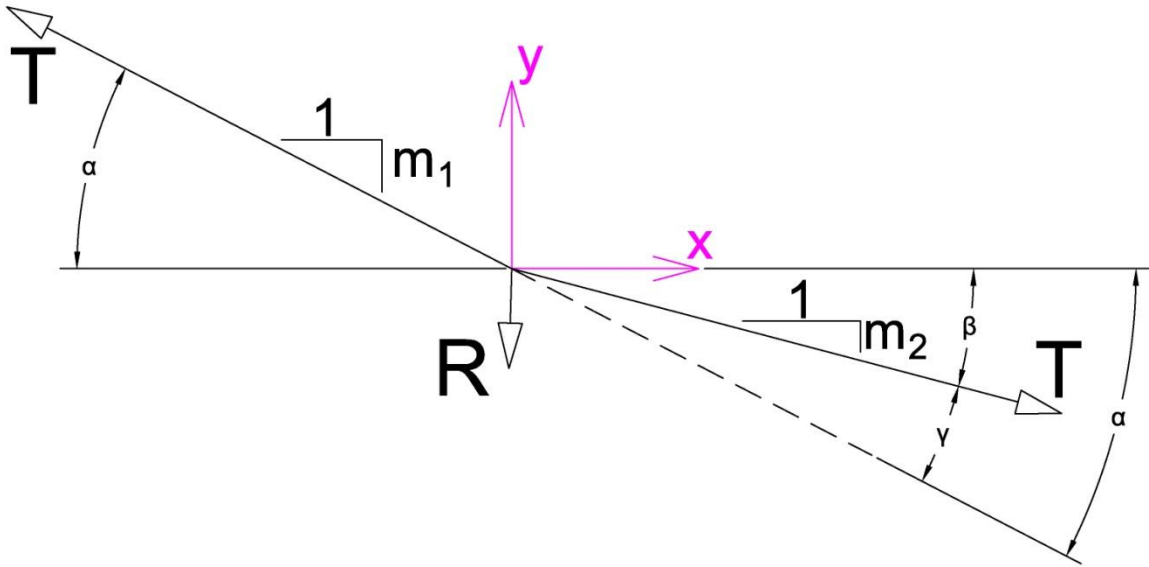


Figure 38. Free Body Diagram of Cable-to-Post Attachment on Vertical Curve

The y-direction forces were set equal to zero.

$$\sum F_y = -R_v + T \sin \alpha - T \sin \beta = 0$$

$$R_v = T(\sin \alpha - \sin \beta) \quad (4.7)$$

Where R_v = vertical reaction of the cable-to-post attachment
 T = cable tension
 α = reference angle (see Figure 38)
 β = reference angle (see Figure 38)

The reference angle, α , is the sum of the other two reference angles, β and γ .

$$\sin \alpha = \sin(\beta + \gamma) = \sin \beta \cos \gamma + \cos \beta \sin \gamma \quad (4.8)$$

Where γ = difference angle (see Figure 38)

The difference angle, γ , as shown in Figure 38, will be very small.

$$\cos \gamma \approx 1, \sin \gamma \approx \tan \gamma \approx \gamma$$

Therefore, Equation 4.8 becomes Equation 4.9.

$$\sin \alpha \approx \sin \beta + \tan \gamma \cos \beta \quad (4.9)$$

The tangent of the angle, γ , is the difference of the two slopes, m_1 and m_2 . Therefore, Equation 4.7 can be combined with Equations 4.9 and 4.6.

$$R_V = T(\sin \alpha - \sin \beta) = T(\tan \gamma \cos \beta) = T(m_2 - m_1) \cos \beta$$

$$R_V = T \frac{s}{100K} \cos \beta \quad (4.10)$$

Equation 4.11 gives the maximum vertical reaction of the cable-to-post attachment, which will occur when the value of β is zero (i.e., one of the cable spans has a horizontal slope).

$$(R_V)_{Max} = T \frac{s}{100K} \quad (4.11)$$

Where $T =$ cable tension
 $s =$ post spacing
 $K =$ horizontal length per percent algebraic difference
 in intersecting grades

The Green Book [72] specifies minimum K-values for different types of curves and for different highway design speeds. This guidance accounts for stopping and passing sight distance. For more information on highway design geometry, refer to the Green Book. There are two types of vertical curves—sag and crest. Their names describe their shapes. In a crest, the curvature is negative, and the net vertical force on the cable-to-post attachments as a result of the change in slope between two adjacent post spans will be in the downward direction. In a sag, the curvature is positive, and the net vertical force will be in the upward direction.

The K-value for a sag vertical curve on a highway with a design speed of 40 mph (72 km/h) is 64 ft (19.5 m). For an 8-kip (36-kN) cable tension, the change in the slope of the cable

between two adjacent, 16-ft (4.9-m) post spans, on a 40-mph (64 km/h) sag vertical curve, will produce a 20-lb (89-N) uplift force at the cable-to-post attachments. For comparison, the weight of a 16-ft (4.9-m) length of cable is approximately 13 lb (58 N). The design speed for most highways will be greater than 40 mph (64 km/h), so the K-values will be greater than 64 ft (19.5 m), resulting in even smaller vertical forces on the cable-to-post attachments. As the rest of the analysis will show, the pre-impact, vertical loads on the cable-to-post attachments were relatively insignificant.

4.4 Minimum Design Loads Due to Horizontal Curves

In the same way, a horizontal change in cable slope between posts may result in a lateral force being applied on the cable-to-post attachments, depending on which side of the post the cable is positioned.

For a given cable tension, lateral forces on the cable-to-post attachments vary with the post spacing and radius of the cable curve. A hypothetical horizontal curve is shown in Figure 39, and a free body diagram of a post within that curve is shown in Figure 40.

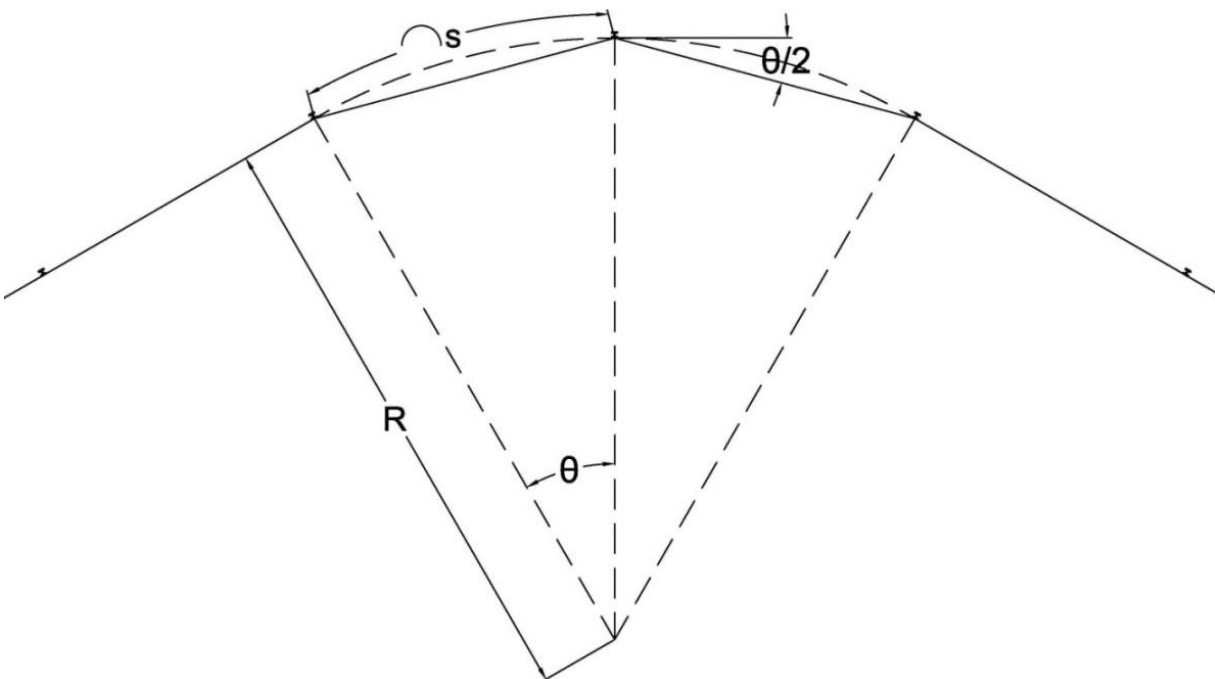


Figure 39. Cable Barrier on a Horizontal Curve

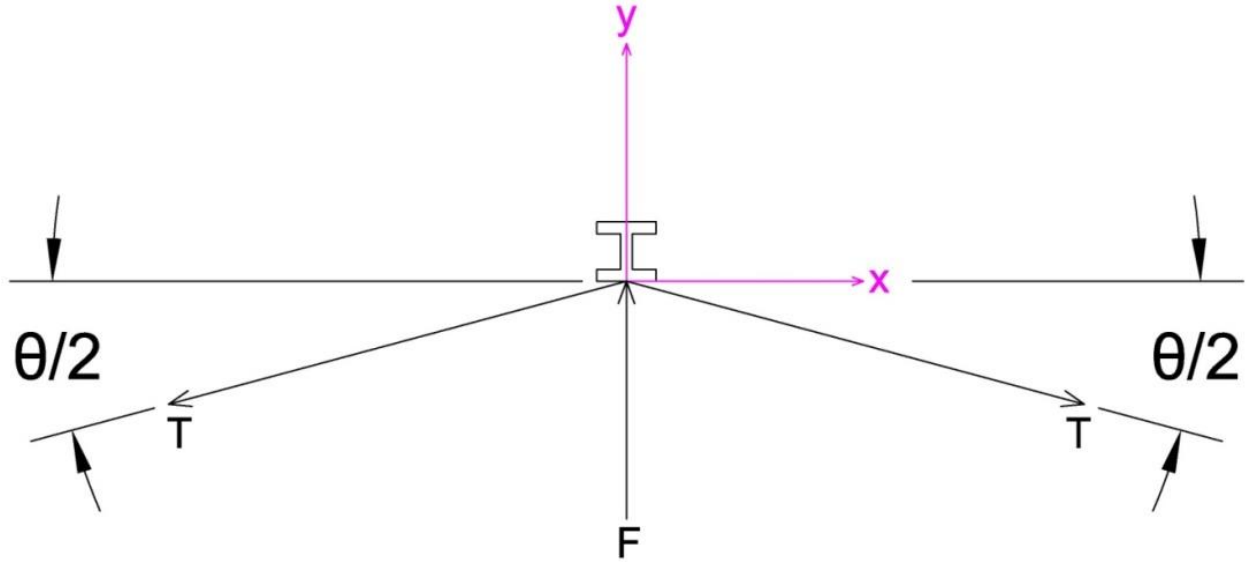


Figure 40. Free Body Diagram of a Post within a Horizontal Curve

For large radius, R and small angle, θ , the straight line distance between the posts (i.e. the post spacing) and the arc length, s , are approximately equal. Summing the y-direction (lateral) forces in Figure 40, gives Equation 4.12.

$$\sum F_y = F - 2T \sin \frac{\theta}{2} = 0$$

$$F = 2T \sin \frac{\theta}{2} \quad (4.12)$$

Where T = cable tension
 θ = reference angle (see Figures 39 and 40)

The curve radius, R , will be much larger than the post spacing, s . The arc length and the post spacing are approximately equal. Therefore, θ will be small and approximately equal to $\sin \theta$.

$$\sin \theta \approx \theta \approx \frac{s}{R}$$

$$F = 2T \sin \frac{\theta}{2} \approx 2T \left(\frac{\theta}{2} \right) = T\theta \approx T \left(\frac{s}{R} \right) \quad (4.13)$$

Equation 4.13 is a useful relationship for determining the maximum allowable post spacing on a horizontal curve. All previous full-scale crash tests used a post spacing of 16 ft (4.9 m). For a design cable tension of 8 kips (36 kN) and lateral cable-to-post attachment strength, F , the maximum allowable post spacing as a function of the curve radius is shown in Figure 41.

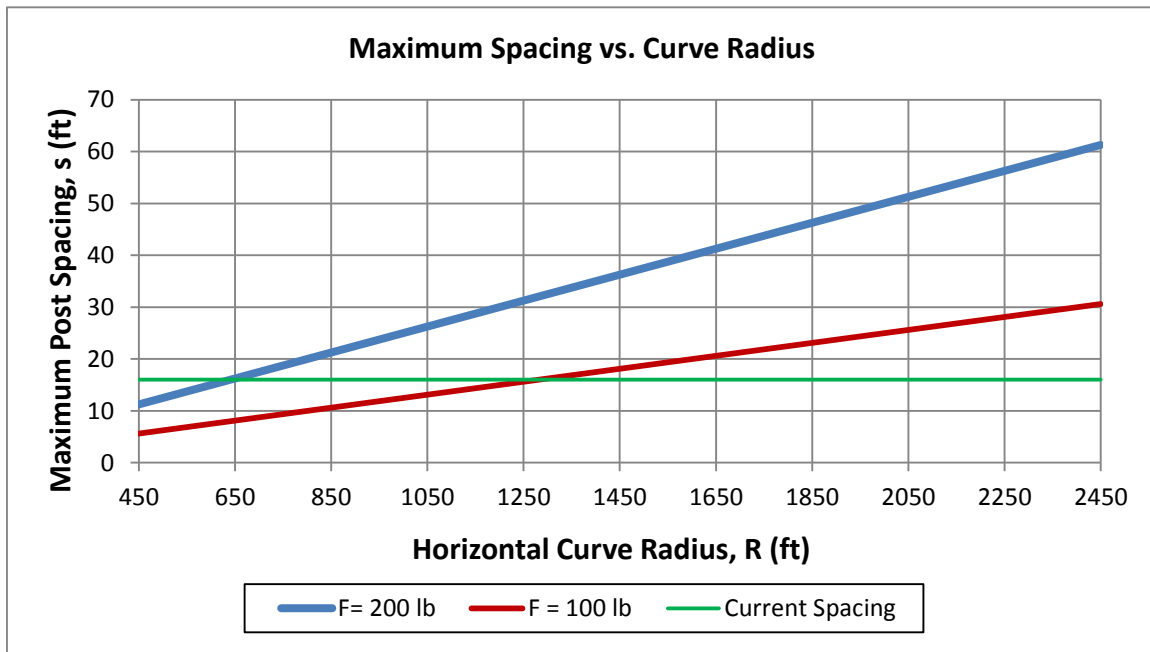


Figure 41. Maximum Post Spacing vs. Horizontal Curve Radius

The cable barrier's radius will be related to the roadway curve radius. The Green Book [72] specifies minimum radii for given design speeds and super-elevations. For a super-elevation of 8.0%, the minimum radii for different design speeds are shown in Table 3.

Table 3. Design Speed vs. Minimum Curve Radius

Design Speed mph (km/h)	Minimum Curve Radius ft (m)
40 (64)	444 (135)
45 (72)	587 (179)
50 (80)	758 (231)
55 (89)	960 (293)
60 (97)	1,200 (366)
65 (105)	1,480 (451)
70 (113)	1,810 (552)
75 (121)	2,210 (674)
80 (129)	2,675 (814)

The high-tension, cable median barrier will be used primarily for highways with design speeds greater than 55 mph (89 km/h), so the curve radius is not likely to be less than 960 ft (293 m). Due to concerns for the top cable to be pulled downward when the post is impacted by a vehicle (as seen in full scale test no. 4CMB-5), the lateral strength of the top cable-to-post attachments should be limited.

As shown in Figure 41 for a 16-ft (4.9-m) post spacing, a 200-lb (8905-N) lateral strength of the top cable-to-post attachment would be adequate for curve radii greater than 640 ft (195 m), covering the full range of design speeds of 55 mph (89 km/h) or greater. For a 16-ft (4.9-m) post spacing, a 100-lb (445-N) lateral strength of the top cable-to-post attachment would be adequate for curve radii greater than 1,280 ft (390 m), but if the post spacing were decreased to 12 ft (3.7 m), it would be adequate for curve radii greater than 960 ft (293 m).

These numbers are based on a design tension of 8,000 lb (36 kN). For cable tensions higher than 8,000 lb (36 kN), the post spacing would probably need to be decreased even further, depending on the curve radius and the actual lateral cable-to-post attachment strength. Thus, Equation 4.13 should be used to determine the limits for post spacing for different horizontal

curve radii based on a maximum cable tension and the actual lateral cable release capacity of the selected cable-to-post attachment.

4.5 Target Lateral and Vertical Cable Release Capacities

In light of all of these observations, some targets were set to guide the design process. The desired behavior was more important than the target strength. The top cable-to-post attachments would need to hold the cable in place before an impact, but easily and quickly release the cable when a post was impacted and began to rotate backward and downward. A target range of 100 to 200 lb (445 to 890 N) was chosen for the lateral and vertical cable release loads for the top cable-to-post attachment.

As a starting point, a target vertical release of 225 lb (1.00 kN) was set for the lower three cable-to-post attachments. This value reflected a significant reduction from the 1.18-kip (5.25-kN) vertical resistance of the keyway bolts used in the most recent designs. The goal was to ensure that if a vehicle's A-pillar became positioned under the cable and began to push up on it (as observed in full scale crash test no. 4CMBLT-1), the cable would quickly release away from the post, introducing slack to the cable so that the normal force exerted by the cable on the A-pillar would not crush the A-pillar. In addition to the targeted vertical cable release load, the lower three cable-to-post attachments would be designed with a targeted lateral release load of 6.00 kips (26.7 kN). The goal was for the cable-to-post attachments to be able to develop the full moment capacity of the post when loaded laterally.

5 OVERVIEW OF IMPROVED KEYWAY BOLTS—ROUND 1

5.1 Introduction

Previously, the desired vertical and lateral cable release loads for the cable-to-post attachments at all four cable heights were determined. Thus, the next step was to design and test new cable-to-post attachments for the bottom three cables. The obvious place to start was with the keyway bolts that had been used in the most recent full-scale vehicle crash tests. The keyway bolt concept was desirable for three main reasons. First, it employed two different release mechanisms. When pulled laterally, the button head would become caught in the narrow part of the keyway, and the cable would continue to pull on the bolt until it fractured through the threads. When pulled vertically, the bolt would bend upward and allow the button head to rotate up and out of the keyway. These two different release mechanisms allowed the vertical and lateral release behaviors to be treated independently to some degree. Second, the bolt was deliberately curved to avoid jagged, right-angle protrusions from extending off of the flange, which may tend to snag cables. Third, it was simple, consisting of only two pieces—a bolt and nut.

5.1.1 Dynamic Bogie Tests

All of the designs presented in this chapter were later tested and evaluated using dynamic bogie testing described in Chapter 6, unless otherwise noted. Different load orientations were used in order to determine the vertical and lateral release loads for each concept under dynamic loading conditions.

5.1.2 Keyway Bolt Basics

The keyway bolts used in test nos. 4CMB-4, 4CMB-5, and 4CMBLT-1 had been designed, tested, and evaluated in a previous component testing effort by MwRSF [71]. The final keyway bolts from that design effort consisted of a 1/4-in. (6-mm) diameter, curved shaft, a 1/2-in.

(13-mm) diameter by ¼-in. (6-mm) thick button head at one end, and a shoulder and threads at the other end, as shown in Figure 42a. The threaded end was inserted into the bottom hole and was secured to the flange of the S3x5.7 (S76x8.5) steel post with a ¼-in. (6-mm), SAE grade 8 nut, while the button-head end sat in the narrow part of the keyway, as shown in Figure 42b. The keyway bolts were made of galvanized, ASTM A449 steel, which had a minimum yield strength of 92 ksi (630 MPa) and a minimum ultimate tensile strength of 120 ksi (830 MPa). AISI C1018 keyway bolts were also tested. The AISI C1018 steel had a minimum yield strength of 54 ksi (370 MPa) and a minimum ultimate tensile strength of 64 ksi (440 MPa).

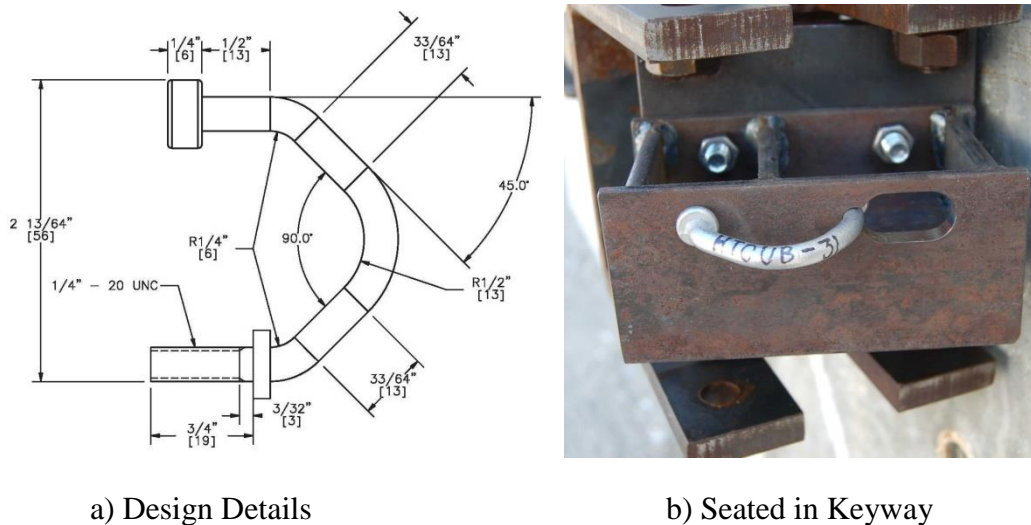


Figure 42. Keyway Bolt—(a) Design Details and (b) Seated in Keyway

The dual-width keyway consisted of a 5/16-in. (8-mm) diameter hole, where the upper shaft of the keyway bolt was positioned, overlapped by a 5/8-in. (16-mm) diameter hole, which was part of a longer slotted opening, as shown in Figure 43. The dual-width feature allowed the button head to be caught in the narrow part of the keyway when pulled laterally but clear the wide part of the keyway when pulled vertically. The main problem with the keyway bolt in the dual-width keyway was the tendency for the button head to scrape against the inside of the flange

when the bolt was pulled vertically. This scraping action contributed to much higher vertical release loads than if the button head had been free of scraping.

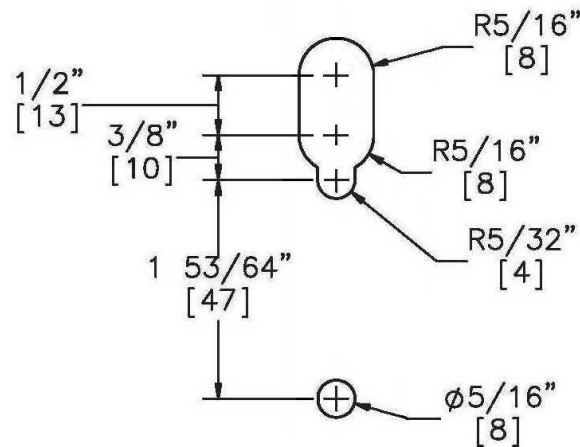


Figure 43. Dual-Width Keyway

The ASTM A449 keyway bolts, used with the dual-width keyway, had a vertical release load of 1.18 kips (5.25 kN) and a lateral release load of 8.00 kips (35.6 kN). The AISI C1018 keyway bolts, used in the same keyway, had vertical and lateral release loads of 0.81 kips (3.60 kN) and 6.47 kips (28.8 kN) respectively.

5.2 First Round Design Modifications

For the first round of design modifications, three slightly different keyway bolts were considered, along with two different keyways. A total of twenty bogie tests were performed, as later discussed in Chapter 7. There were a total of four tests for each concept—two for each load orientation—in order to test their vertical and lateral strengths. Each concept, and the thought process behind it, will be discussed in detail in Subsections 5.2.1 through 5.2.3.

5.2.1 Small Oversized Keyway

It was primarily the top two cables which had caused the problems which led to failures in full-scale crash test nos. 4CMB-5 and 4CMBLT-1. The oversized keyways were originally designed with only the top two cables in mind. If they were going to be used at all, then they

would only be used for those two cables. The bottom two cables would use the same dual-width keyway that had been used previously.

For both of the oversized keyways, the narrow part was eliminated, as shown by the top hole in Figure 44a. The small oversized keyway was designed so that when viewed from the inside of the flange, the button head of the keyway bolt overlapped the bottom of the keyway by 1/16 in. (2 mm). When the small oversized keyway was compared to the dual-width keyway, it could be seen that there was significantly less backside flange area for the button head to scrape against when pulled vertically as well as significantly less area for the button head to bear against when pulled laterally. Both the lateral and vertical release loads would likely be affected.

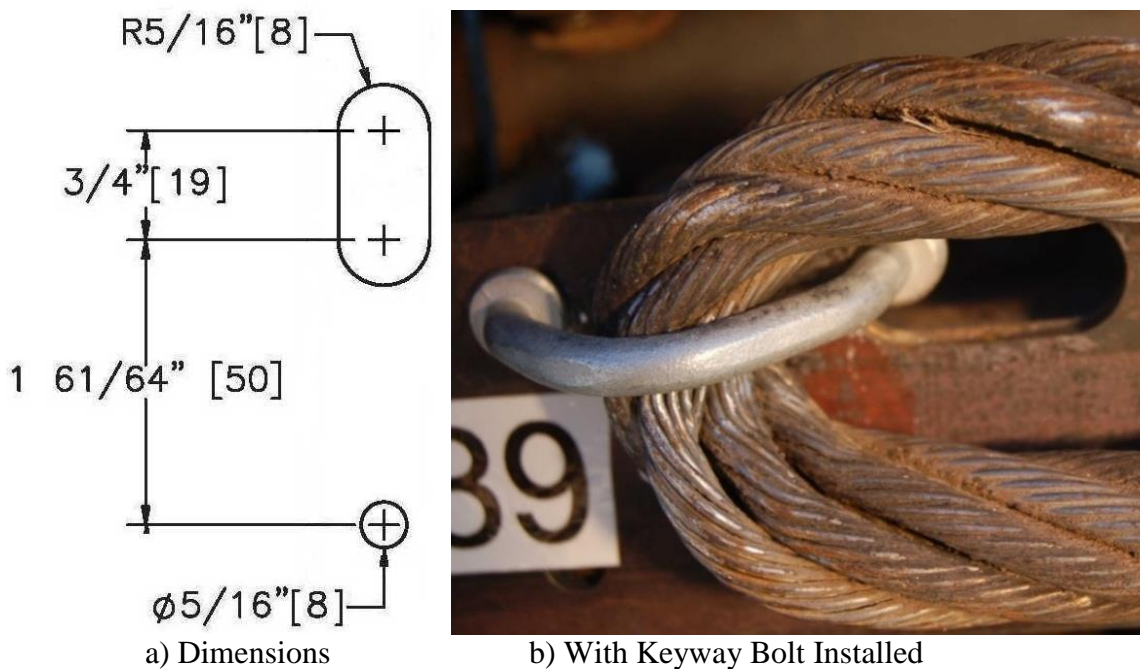


Figure 44. Small Oversized Keyway—(a) Dimensions and (b) With Keyway Bolt Installed

5.2.2 Large Oversized Keyway

The small and large oversized keyways were nearly identical. The large oversized keyway, as shown in Figure 45, was 1/8 in. (3 mm) longer than the small oversized keyway. Thus, the button head of the keyway bolt did not overlap the bottom of the keyway. The large

oversized keyway was tested to determine a baseline release behavior when the button head of the keyway bolt did not contact the inside of the flange. Testing would demonstrate whether the absence of the 1/16-in. (2-mm) overlap between the button head of the keyway bolt and the bottom of the large oversized keyway would affect release loads.

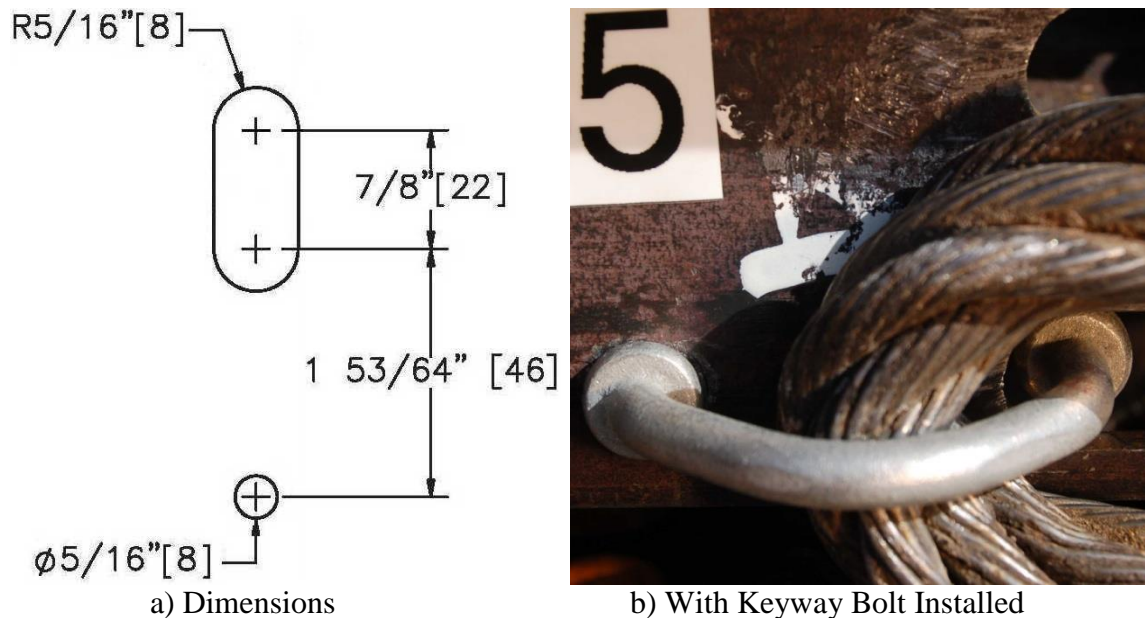


Figure 45. Large Oversized Keyway—(a) Dimensions and (b) With Keyway Bolt Installed

5.2.3 Modified Keyway Bolt

The last concept that would be tested in the first round of modifications was the modified keyway bolt placed in the large oversized keyway. Originally, the modified keyway bolt would be tested with both oversized keyways. However, it was apparent that the small oversized keyway performed inconsistently when the bolt was loaded laterally. Thus, the modified keyway bolt was only tested with the large oversized keyway. The modified keyway bolt, as shown in Figure 46, was designed and tested with the dual-width keyway that was used in the previous cable-to-post attachment testing program [71]. Only the AISI C1018 modified keyway bolts were tested.



b) Installed in Large Oversized Keyway

Figure 46. Modified Keyway Bolt—(a) Dimensions and (b) Installed in Large Oversized Keyway

The modified keyway bolt was shaped differently than the original keyway bolts. Due to its shape, the cable load direction would be perpendicular to the modified keyway bolt at the point of contact when pulled vertically. Testing would demonstrate whether this difference in the shape of the bolt would affect the release behavior.

6 CABLE-TO-POST ATTACHMENT DYNAMIC COMPONENT TEST CONDITIONS

6.1 Purpose

Dynamic component tests were used to evaluate the structural capacity and behavior of the cable-to-post attachments before implementation into a barrier system and subjected to a full-scale crash test. These component tests were designed with two purposes in mind: (1) to demonstrate the performance of the various cable-to-post attachment designs when subjected to cable loads at dynamic speeds and (2) to measure the fracture and release loads of the attachment. It should be noted that the cable used in the dynamic bogie tests was a ¾-in. (19-mm) diameter 6x19 wire rope, and the actual cable used in the high-tension cable barrier was a ¾-in. (19-mm) diameter 3x7 wire rope.

6.2 Scope

A series of twenty-eight bogie tests were conducted on different keyway bolt designs, as presented in Chapters 7 and 9. In addition, forty-two bogie tests were conducted on different tabbed bracket designs, as discussed in Chapters 11, 13, and 15. These tests consisted of attaching one end of a cable to a bogie and the other end to the cable-to-post attachment. The cable-to-post attachment was mounted to a rigid post section which was contained within the test jig. The test jig was fixed to a steel shaft outfitted with a load cell, which later was anchored to a rigid concrete block. The bogie was then set in motion, away from the bracket, placing a dynamic load on the connection until cable release from or fracture of the attachment occurred. The target cable speed was 5.0 mph (8.0 km/h). An adjustable plate was used with the post, which allowed the cable to be pulled at either a 90-degree or 0-degree angle to the face of the post, simulating either a lateral or vertical load condition.

6.3 Test Facility

Physical testing was conducted at the MwRSF outdoor testing facility, which is located at the Lincoln Air Park on the northwest side of the Lincoln Municipal Airport. The facility is approximately 5 miles (8 km) northwest from UNL's city campus.

6.4 Equipment and Instrumentation

Several types of equipment and instrumentation were utilized to collect and record data during the cable-to-post attachment dynamic component tests, including a bogie vehicle, a 50-kip (222-kN) load cell, accelerometers, an optic speed trap, high-speed and standard-speed digital video cameras, and digital still cameras.

6.4.1 Bogie

A rigid-frame bogie was used to pull on a cable which was anchored to the cable-to-post attachment. The bogie with the test setup is shown in Figure 47. The bogie weights were different for each round of tests, as shown in Table 4. A pickup truck, with a reverse cable tow system, was used to propel the bogie along a guidance track to a target speed of 5.0 mph (8.0 km/h). The pickup truck braked allowing the bogie to be free rolling as the bogie approached the end of the guidance system and applied the load to the cable-to-post attachment.



Figure 47. Rigid Frame Bogie on Guidance Track

Table 4. Bogie Weights

Test Nos.	Bogie Weight, lb (kg)
HTCUB-38 through HTCUB-47, HTCUB-50 and HTCUB-51	1,616 (733)
HTCUB-48, HTCUB-49, and HTCUB-52 through HTCUB-57	1,612 (731)
HTCUB-58 through HTCUB-61	1,528 (693)
HTCUB-62 through HTCUB-65	1,861 (844)
HTTB-1 through HTTB-8	1,765 (800)
HTTB-9 through HTTB-16	1,866 (846)
HTTB-17 through HTTB-40	Not weighed

6.4.2 Load Cell

A 50-kip (222-kN) capacity load cell was used to measure the force exerted on the test article by the cable until the cable released. This load cell was placed in a tension configuration between the post section and the anchor plate mounted on the rigid concrete block.

6.4.3 Optic Speed Trap

The retroreflective optic speed trap was used to determine the speed of the bogie vehicle before impact for test nos. HTCUB-38 through HTCUB-47, HTCUB-50 and HTCUB-51, and HTCUB-58 through HTCUB-61. Five retroreflective targets, spaced at 4-in. (102-mm) intervals, were applied to the side of the bogie vehicle and used to break the beam of light. When the emitted beam of light was returned to the Emitter/Receiver, a signal was sent to the Optic Control Box, which in turn sent a signal to the data computer as well as activated the External LED box. The computer and data acquisition system recorded the signals and the associated time. The speed was then calculated using the spacing between the retroreflective targets and the time between the signals. LED lights and high-speed digital video analysis are only used as a backup in the event that vehicle speeds cannot be determined from the electronic data.

6.4.4 Digital Photography

Two AOS X-PRI high-speed digital video cameras and one JVC digital video camera were used to document test nos. HTCUB-38 through HTCUB-61. One AOS X-PRI high-speed digital video cameras and one JVC digital video camera were used to document test nos. HTCUB-62 through HTCUB-65, HTTPB-1 through HTTPB-8, and HTTPB-17 through HTTPB-40. One AOS S-VIT high-speed digital camera and one JVC digital video camera were used to document test nos. HTTPB-9 through HTTPB-16. The AOS high-speed cameras had a frame rate of 500 frames per second and the JVC digital video camera had a frame rate of 29.97 frames per second. A Nikon D50 digital still camera was also used to document pre- and post-test conditions for all tests.

6.4.5 Test Jig

The test jig was mounted to a small section of steel post as well as a steel shaft, which was anchored to a mounting plate placed on the side of a rigid block. The test article (either a

keyway bolt or tabbed bracket) was attached to the post section. The test jig could be adjusted to change the angle at which the cable pulled on the test article. The steel tube or shaft was attached to the mounting plate by a cylindrical joint which allowed a tension load cell to be used to measure the loads. A looped cable was placed through the test article, as shown in Figure 48. The other end of the cable was attached to the bogie, which was towed to a speed of approximately 5 mph (8 km/h).



Figure 48. Test Jig

6.5 Data Processing

Force data was measured with the load cell transducer and filtered using the SAE Class 60 Butterworth filter conforming to the SAE J211 specifications [73]. Filtered voltage data was converted to load using the following equation:

$$Load = \left[\frac{1}{Gain} \right] \left[\frac{Filtered Load Cell Data}{\left(\frac{(Calibration Factor)(Excitation Voltage)}{Full - Scale Load} \right) \left(\frac{1 V}{1000 mV} \right)} \right]$$

Details behind the theory and equations used for processing and filtering the load cell data are located in SAE J211. The gain and excitation voltage were recorded in the field book for each test. The full-scale load was 50 kips (222 kN). The calibration factor varied depending on the specific load cell being used. The load cell data was recorded in a data file and processed in a specifically designed Excel spreadsheet.

6.6 Loading Event Determination

Once the data was processed, the period of the loading event was determined. In the data set and before the load was applied, the data signal oscillated between positive and negative values, close to zero. The peak load time was easily distinguishable as a large, positive spike in the voltage data. The loading event was the prolonged, positive voltage data period which included the peak load time and lasted until the data went negative again. After the loading event, the data returned to an oscillating positive and negative pattern until the end of recording.

Once the loading event was determined, the data was matched up with the high-speed video. However, it was somewhat difficult to distinguish the beginning of the loading event when using the high-speed video. It was much easier to distinguish the release of the test article, and hence, the end of the loading event in the video footage. Thus, the beginning of the loading event (time zero in the high-speed video) was found by subtracting the duration of the loading event (obtained from the load cell data) from the clearly distinguishable release of the cable in the high-speed video.

6.7 Results

The goal of dynamic component testing was to determine the release behavior of a given cable-to-post attachment design. The peak forces were obtained from the load cell data, and the behavior of the cable and the cable-to-post attachment at those peaks was observed from the

high-speed video. Test results for the keyway bolts as well as the tabbed brackets are given in Chapters 7, 9, 11, 13, and 15.

7 DYNAMIC COMPONENT TESTS—KEYWAY BOLTS, ROUND 1

7.1 Results

In an effort to reach the simplest solution possible, the first part of the re-design effort for the cable-to-post attachments involved making slight modifications to the keyway bolts that had been used previously. This task was accomplished by varying the shape of the bolt, the steel grade of the bolt, and the shape of the keyway. There were two rounds of design modifications on the keyway bolts, followed by component testing and evaluation for each round. Twenty dynamic component tests (test nos. HTCUB-38 through HTCUB-57) were performed in the first round. They are presented in this chapter. Eight more dynamic component tests (test nos. HTCUB-58 through HTCUB-65) were performed in the second round, as discussed later in Chapters 8 and 9. Each individual concept was tested twice in its vertical orientation and twice in its lateral orientation in order to find the strength of the connection in those directions. For the sake of convenience, the consolidated drawing set for both rounds of dynamic component testing of the keyway bolts is shown in Figures 49 through 58. A summary of the test matrix and results for the first round of dynamic components tests is provided in Table 5.

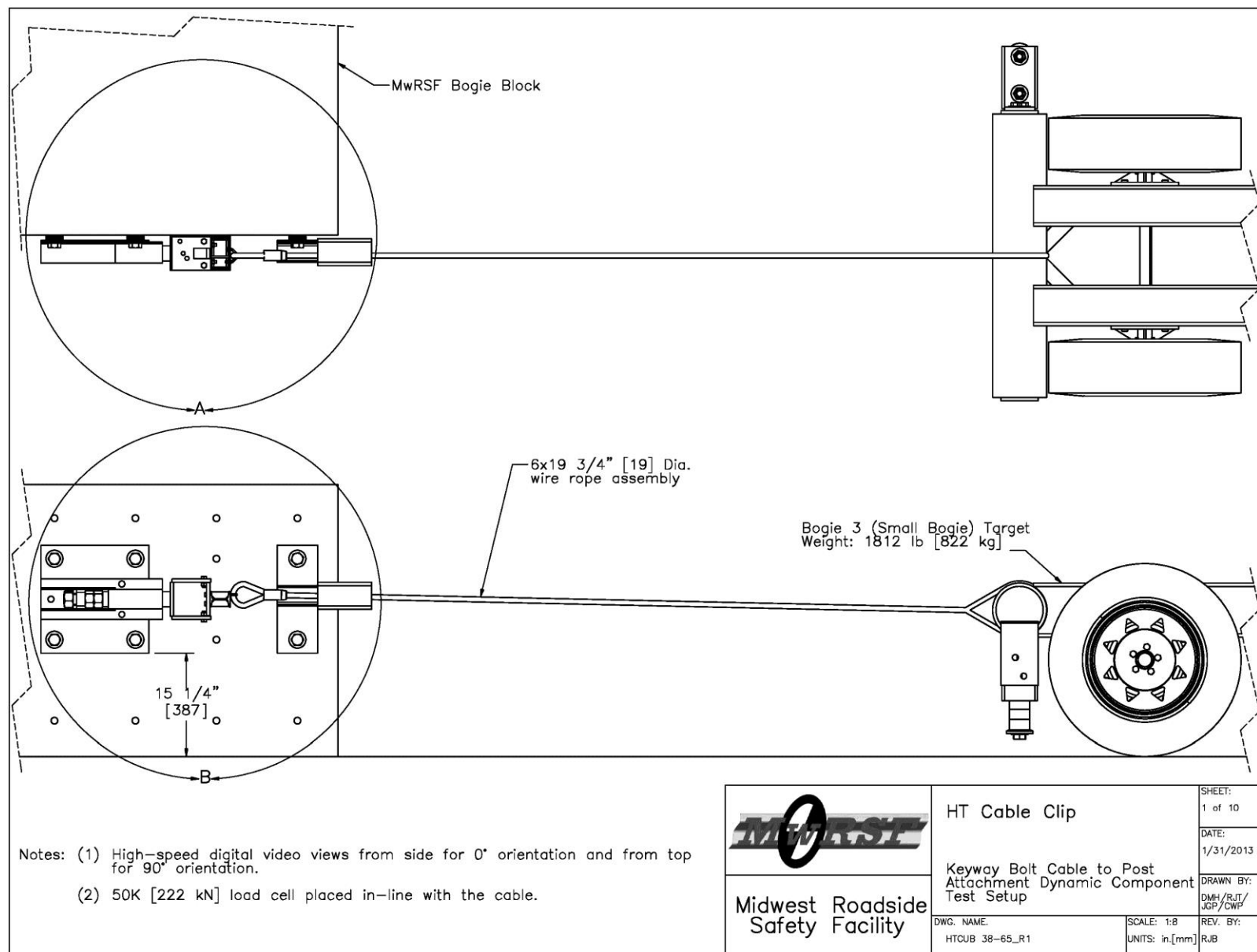


Figure 49. Bogie Test Setup, Test Nos. HTCUB-38 through HTCUB-65

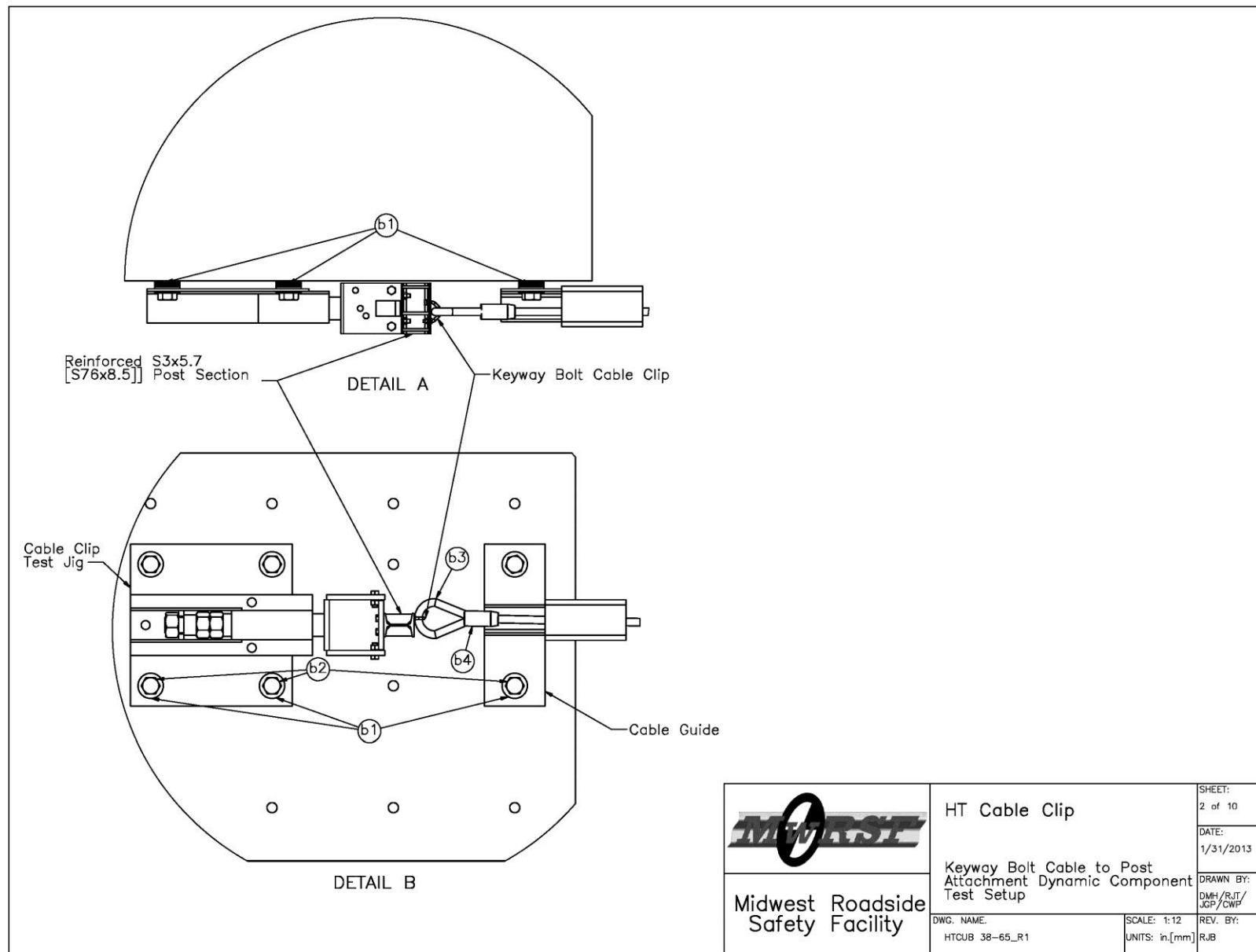


Figure 50. Test Jig Details, Test Nos. HTCUB-38 through HTCUB-65

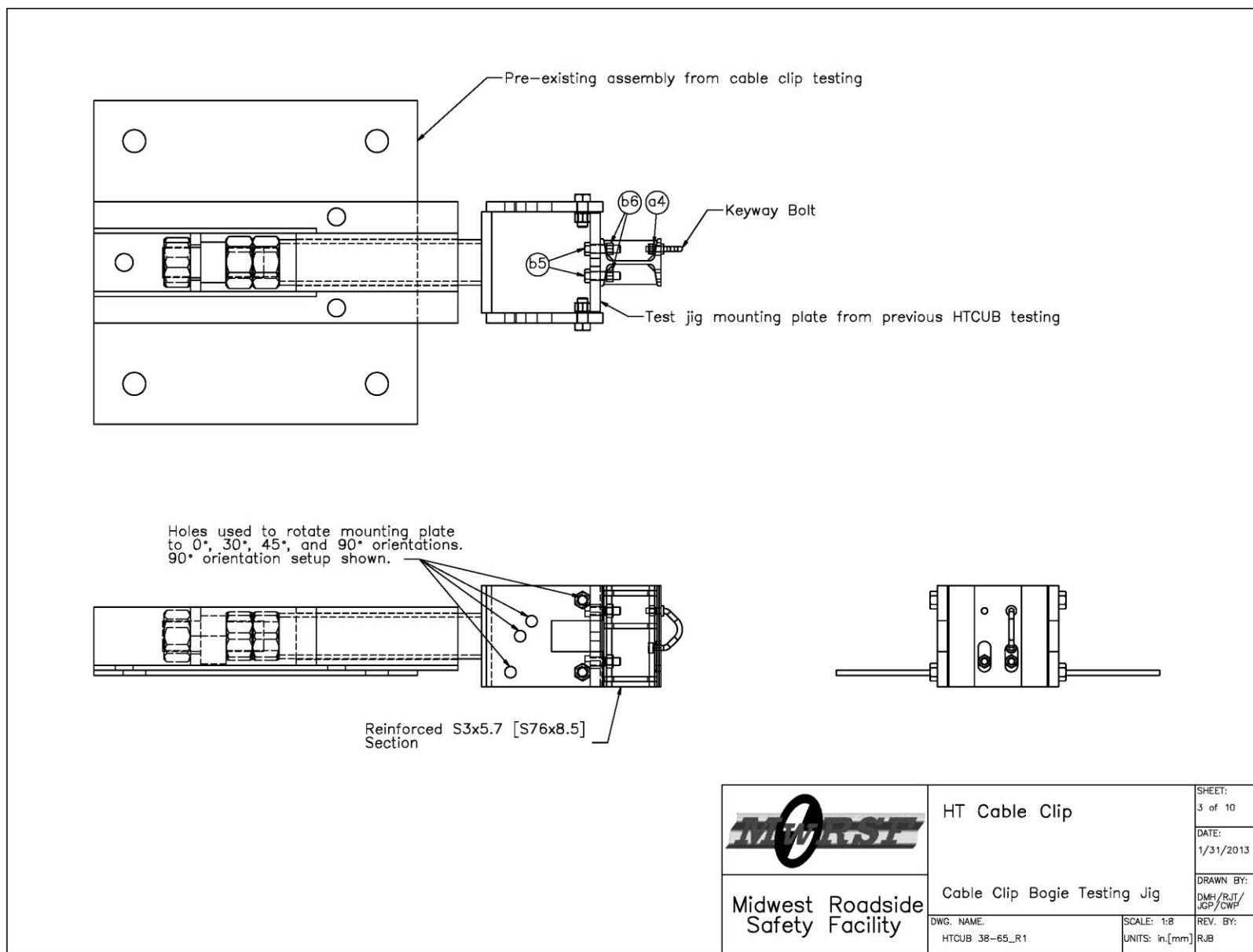


Figure 51. Test Jig Setup, Test Nos. HTCUB-38 through HTCUB-65

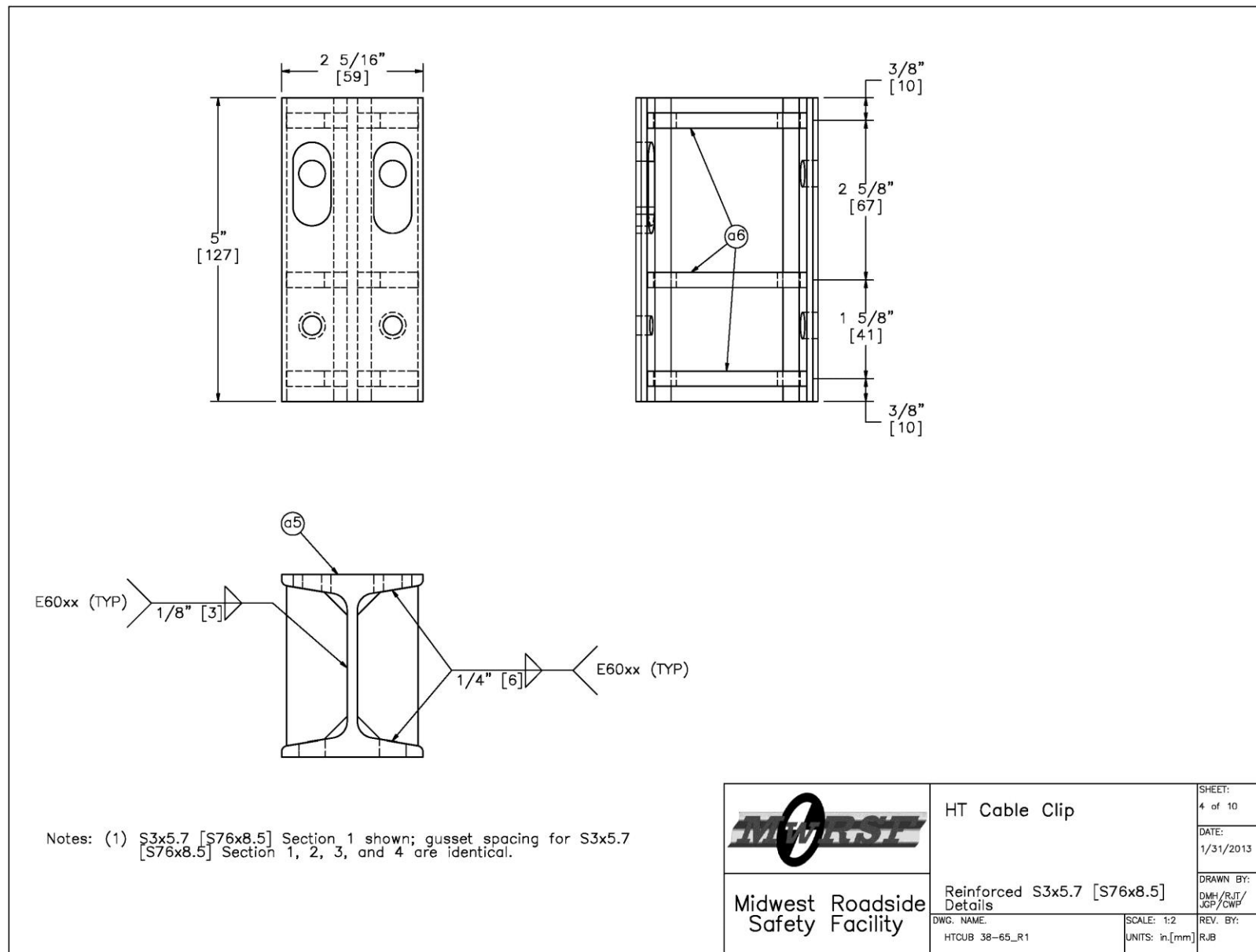


Figure 52. Reinforcement for S3x5.7 (S76x8.5), Test Nos. HTCUB-38 through HTCUB-65

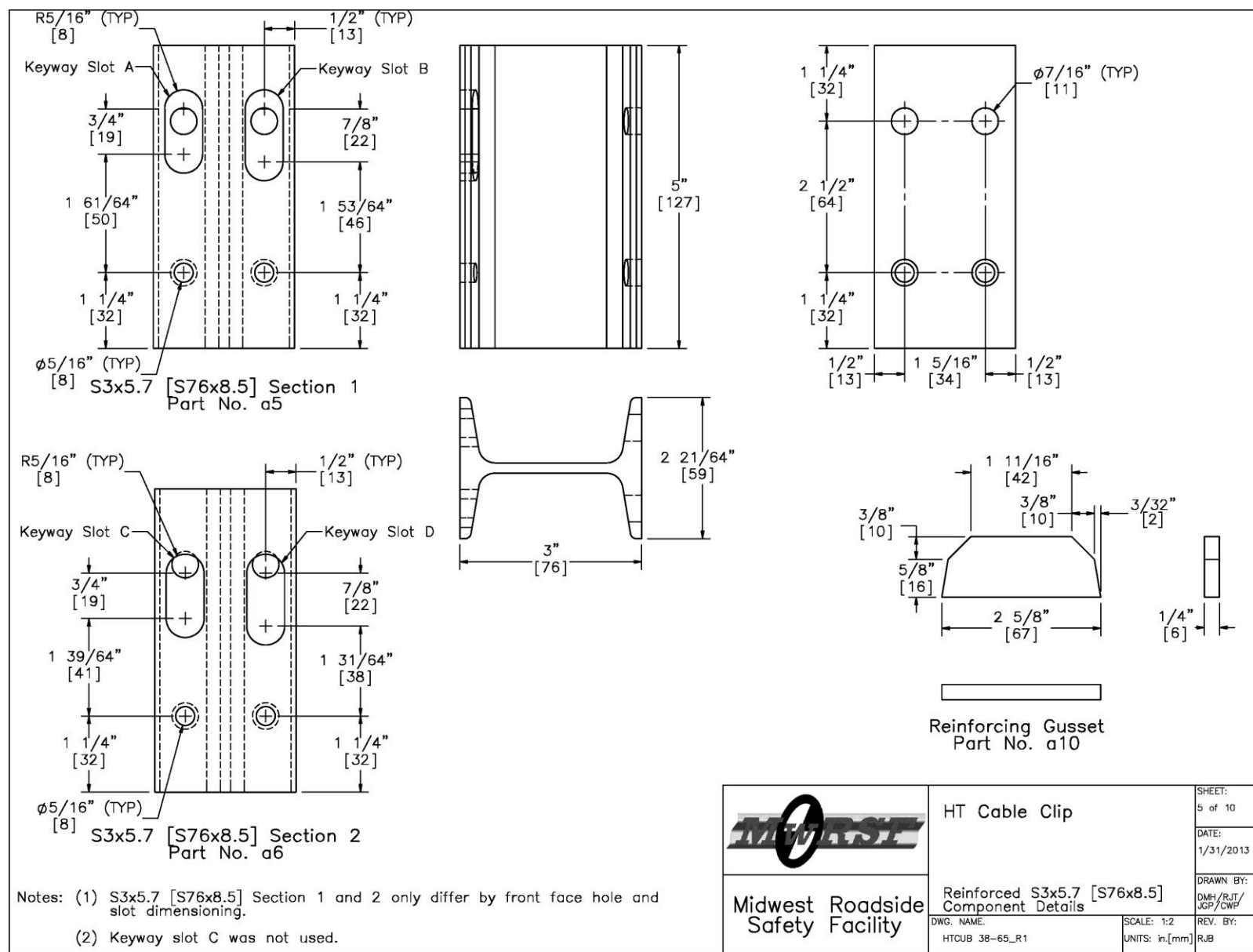


Figure 53. Reinforcing Gussets and S3x5.7 (S76x8.5) Sections for Oversized Keyways, Test Nos. HTCUB-38 through HTCUB-65

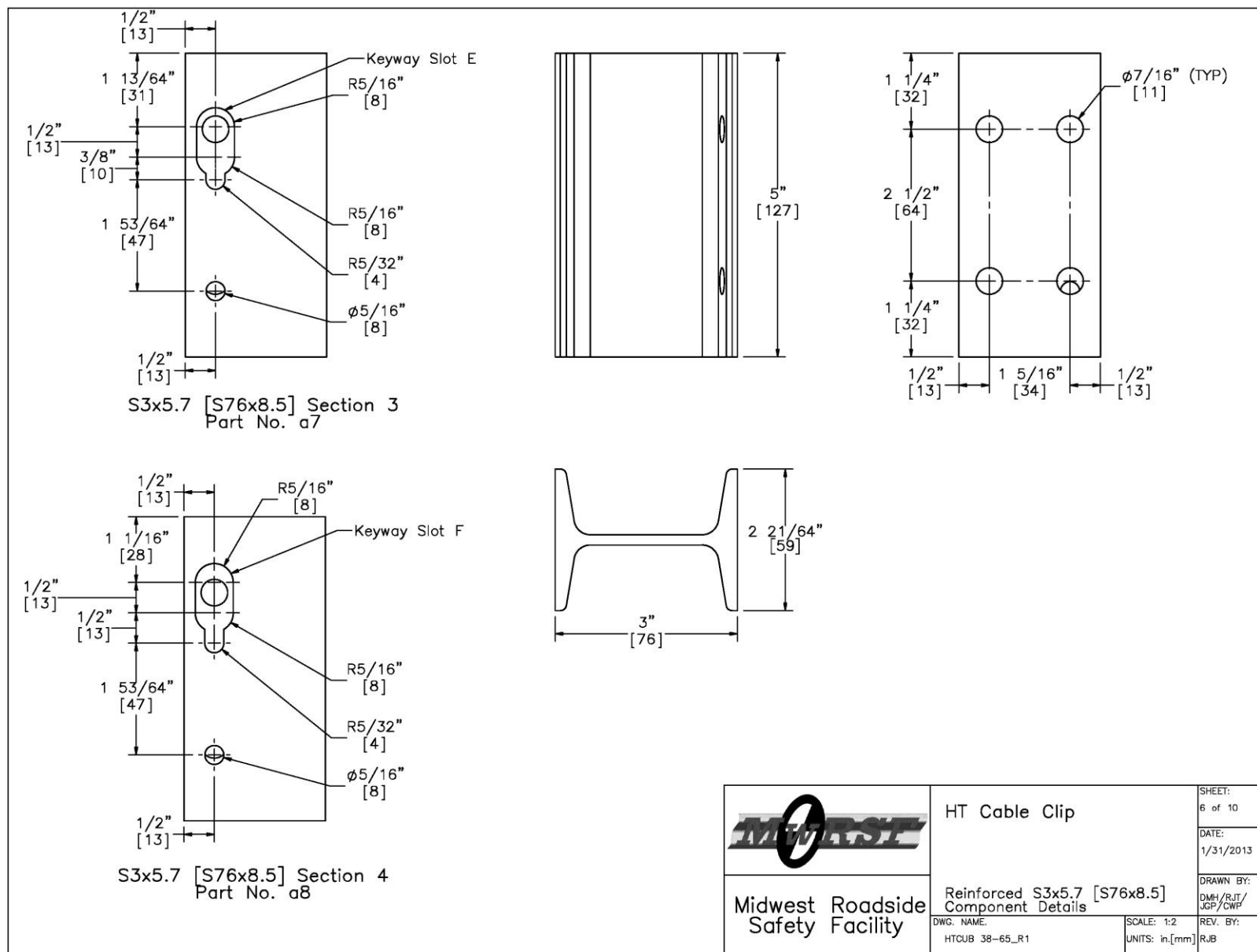


Figure 54. S3x5.7 (S76x8.5) Sections for Dual-Width Keyways, Test Nos. HTCUB-38 through HTCUB-65

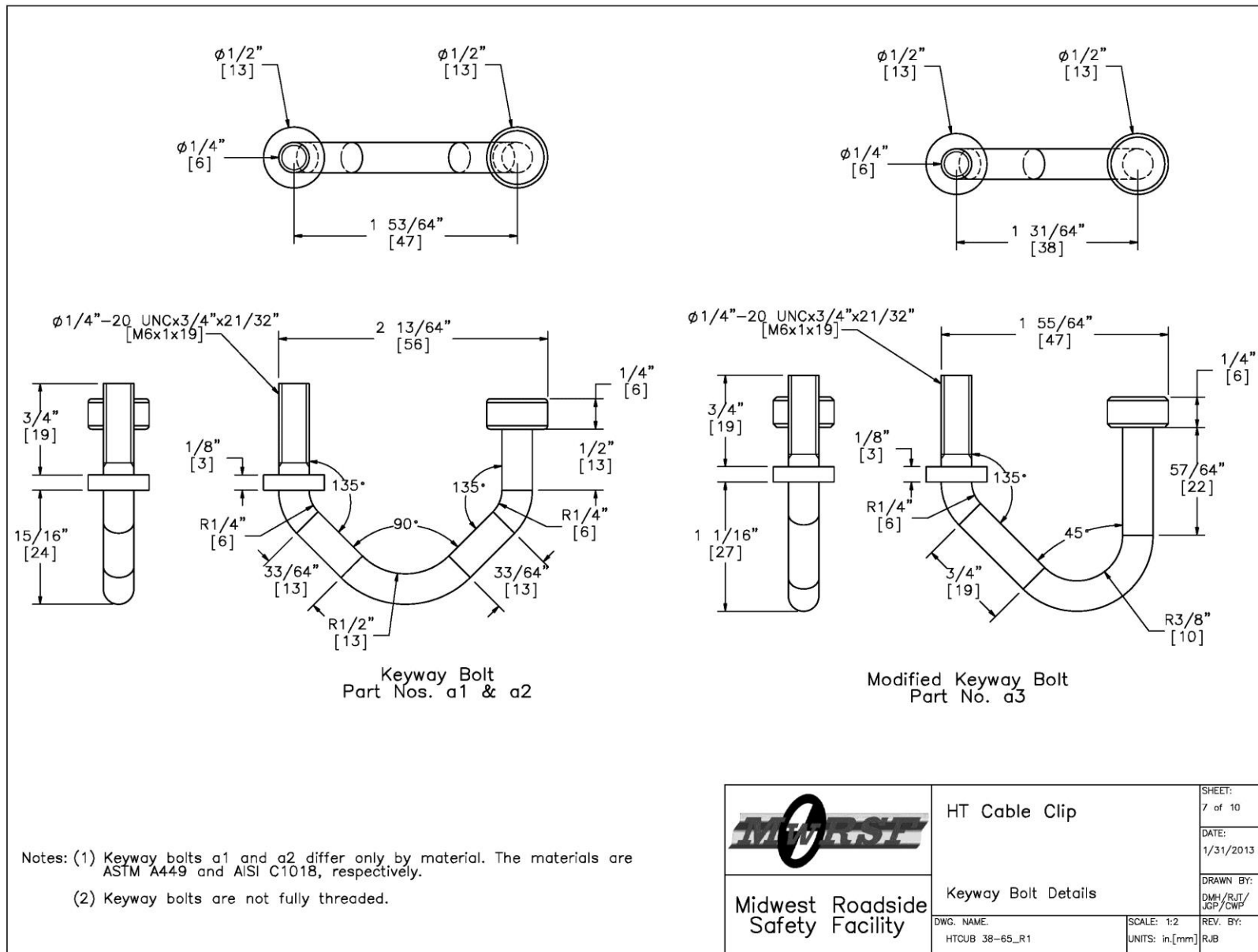


Figure 55. Keyway Bolt and Modified Keyway Bolt Details, Test Nos. HTCUB-38 through HTCUB-65

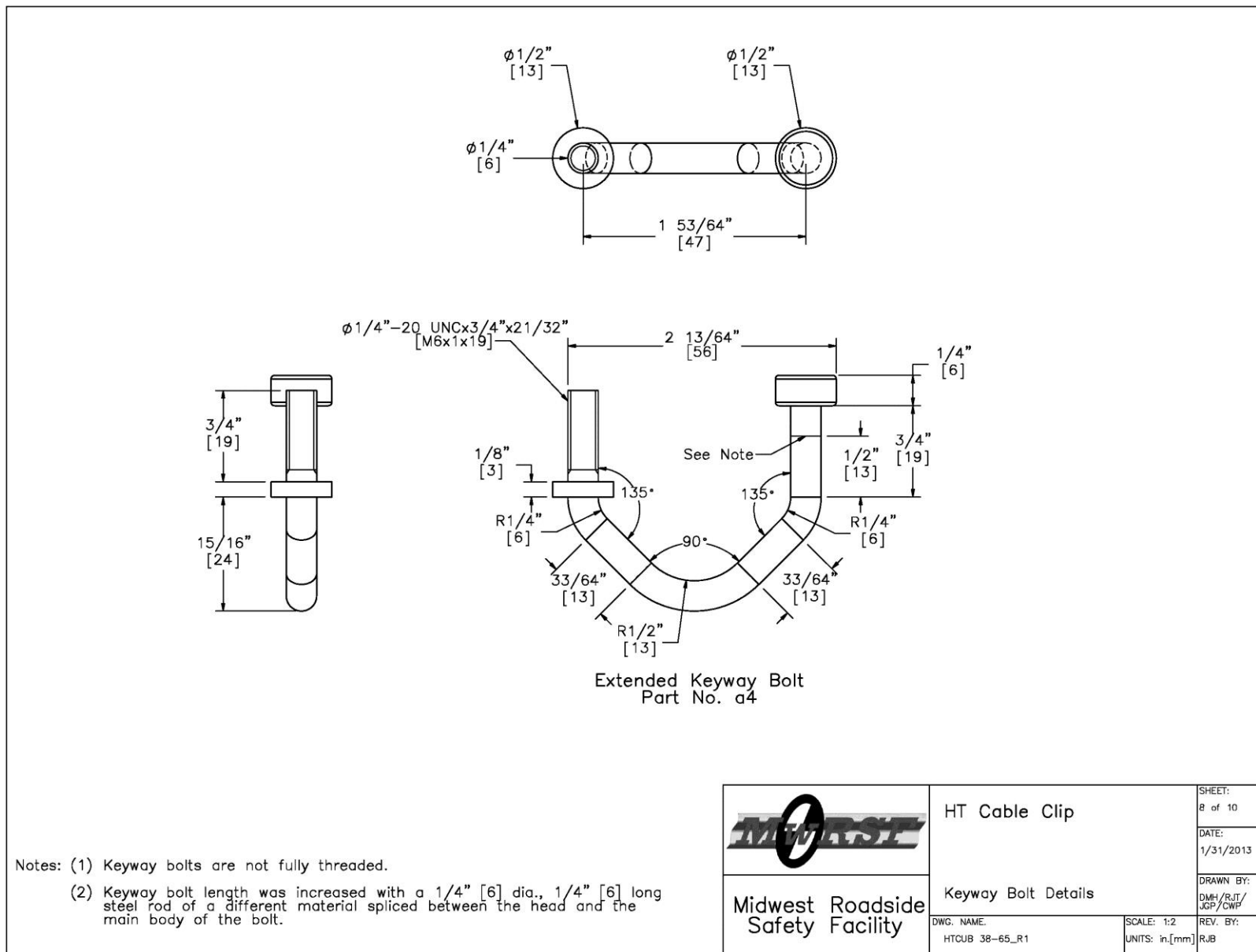


Figure 56. Extended Keyway Bolt Details, Test Nos. HTCUB-38 through HTCUB-65

Bogie Testing Matrix				
Test Qty.	Keyway Bolt	Orientation deg.	Load Direction	Keyway Slot
2	a1	0	Vertical	A
2	a1	90	Lateral	A
2	a1	0	Vertical	B
2	a1	90	Lateral	B
2	a2	0	Vertical	A
2	a2	90	Lateral	A
2	a2	0	Vertical	B
2	a2	90	Lateral	B
2	a3	0	Vertical	D
2	a3	90	Lateral	D
2	a4	0	Vertical	E
2	a4	90	Lateral	E
2	a4	0	Vertical	F
2	a4	90	Lateral	F



	HT Cable Clip		SHEET: 9 of 10
	Test Matrix		DATE: 1/31/2013
Midwest Roadside Safety Facility	DWG. NAME: HTCUB 38-65_R1	SCALE: 1:64 UNITS: in.[mm]	DRAWN BY: DMH/RJT/ JGP/CWP
			REV. BY: RJB

Figure 57. Bogie Testing Matrix, Test Nos. HTCUB-38 through HTCUB-65

Item No.	Qty.	Description	Material Specification
a1	8	1/4" [6] Dia. Keyway Bolt	ASTM A449 Galv.
a2	8	1/4" [6] Dia. Keyway Bolt	AISI C1018 Galv.
a3	4	1/4" [6] Dia. Modified Keyway Bolt	AISI C1018 Galv.
a4	8	1/4" [6] Dia. Extended Keyway Bolt	AISI C1018 Galv.
a5	1	S3x5.7 [S76x8.5], 5" [127] Long Post Section - 1	ASTM A572 GR50-07/ASTM A709 GR50-09A/ASTM A992-06A
a6	1	S3x5.7 [S76x8.5], 5" [127] Long Post Section - 2	ASTM A572 GR50-07/ASTM A709 GR50-09A/ASTM A992-06A
a7	1	S3x5.7 [S76x8.5], 5" [127] Long Post Section - 3	ASTM A572 GR50-07/ASTM A709 GR50-09A/ASTM A992-06A
a8	1	S3x5.7 [S76x8.5], 5" [127] Long Post Section - 4	ASTM A572 GR50-07/ASTM A709 GR50-09A/ASTM A992-06A
a9	28	1/4" [6] Dia. UNC Hex Nut High Topped	SAE Grade 8 Galv.
a10	24	2 5/8"x1"x1/4" [67x25x6] Gusset	ASTM A36
b1	36	1" [25] Dia. Plain Round Washer	ASTM F436
b2	6	1" [25] Dia. UNC, 2 1/2"x1 3/4" [25x64x44] Heavy Hex Bolts	ASTM A307
b3	1	3/4" [19] Dia. 6x19 Wire Rope	-
b4	1	3/4" [19] Mechanical Splice	-
b5	4	3/8" [10] Dia. UNC, 1 1/2 [38] Long Heavy Hex Bolt	ASTM A307
b6	4	3/8" [10] UNC Hex Nut	ASTM A563
-	-	Cable Clip Bogie Test Jig (Pre-Existing in Field)	-
-	-	Cable Guide (Pre-Existing in Field)	-



**Midwest Roadside
Safety Facility**

HT Cable Clip

Bill of Materials

SHEET:
10 of 10

DATE:
1/31/2013

DRAWN BY:
DMH/RJT/
JGP/CWP

DWG. NAME:
HTCUB 38-65_R1

SCALE: 1:64
UNITS: in./mm

REV. BY:
RJB

Table 5. Summary of Dynamic Component Testing of Keyway Bolts, Round 1

Test No.	Load Direction	Test Article	Material	Keyway Slot	Release Load kips (kN)	Test Result
HTCUB-38	Vertical	Keyway Bolt, a1	ASTM A449	Small Oversized, A	0.49 (2.2)	Free release through keyway, button snag load = 0.93 kips (4.1 kN)
HTCUB-39	Vertical	Keyway Bolt, a1	ASTM A449	Small Oversized, A	0.46 (2.0)	Free release through keyway, button snag load = 0.84 kips (3.7 kN)
HTCUB-40	Vertical	Keyway Bolt, a1	ASTM A449	Large Oversized, B	0.49 (2.2)	Free release through keyway, button snag load = 0.88 kips (3.9 kN)
HTCUB-41	Vertical	Keyway Bolt, a1	ASTM A449	Large Oversized, B	0.42 (1.9)	Free release through keyway, button snag load = 0.75 kips (3.3 kN)
HTCUB-42	Vertical	Keyway Bolt, a2	AISI C1018	Small Oversized, A	0.31 (1.4)	Free release through keyway, button snag load = 0.53 kips (2.4 kN)
HTCUB-43	Vertical	Keyway Bolt, a2	AISI C1018	Small Oversized, A	0.39 (1.7)	Free release through keyway, button snag load = 0.52 kips (2.3 kN)
HTCUB-44	Vertical	Keyway Bolt, a2	AISI C1018	Large Oversized, B	0.28 (1.2)	Free release through keyway, button snag load = 0.48 kips (2.1 kN)
HTCUB-45	Vertical	Keyway Bolt, a2	AISI C1018	Large Oversized, B	0.38 (1.7)	Free release through keyway, button snag load = 0.60 kips (2.7 kN)
HTCUB-46	Lateral	Keyway Bolt, a1	ASTM A449	Small Oversized, A	1.14 (5.07)	Free release through keyway
HTCUB-47	Lateral	Keyway Bolt, a1	ASTM A449	Small Oversized, A	5.05 (22.5)	Button caught on bottom of keyway, release through keyway
HTCUB-48	Lateral	Keyway Bolt, a1	ASTM A449	Large Oversized, B	0.84 (3.74)	Free release through keyway
HTCUB-49	Lateral	Keyway Bolt, a1	ASTM A449	Large Oversized, B	1.22 (5.43)	Free release through keyway

Table 5. Summary of Dynamic Component Testing of Keyway Bolts, Round 1 (Continued)

Test No.	Load Direction	Test Article	Material	Keyway Slot	Release Load kips (kN)	Test Result
HTCUB-50	Lateral	Keyway Bolt, a2	AISI C1018	Small Oversized, A	0.53 (2.4)	Free release through keyway
HTCUB-51	Lateral	Keyway Bolt, a2	AISI C1018	Small Oversized, A	0.54 (2.4)	Free release through keyway
HTCUB-52	Lateral	Keyway Bolt, a2	AISI C1018	Large Oversized, B	0.54 (2.4)	Free release through keyway
HTCUB-53	Lateral	Keyway Bolt, a2	AISI C1018	Large Oversized, B	1.53 (6.81)	Free release through keyway
HTCUB-54	Lateral	Modified Keyway Bolt, a3	AISI C1018	Large Oversized, D	2.90 (12.9)	Button caught on side of keyway, release through keyway
HTCUB-55	Lateral	Modified Keyway Bolt, a3	AISI C1018	Large Oversized, D	0.80 (3.6)	Free release through keyway
HTCUB-56	Vertical	Modified Keyway Bolt, a3	AISI C1018	Large Oversized, D	1.71 (7.61)	Button rubbed on side of keyway as it released, button snag load = 0.67 kips (3.0 kN)
HTCUB-57	Vertical	Modified Keyway Bolt, a3	AISI C1018	Large Oversized, D	1.17 (5.20)	Button rubbed on side of keyway as it released, button snag load = 0.70 kips (3.1 kN)

7.1.1 Test No. HTCUB-38 (A449 KB, Small, Vertical)

For test no. HTCUB-38, the cable pulled on the ASTM A449 keyway bolt at an angle of 0 degrees, parallel to the front face of the flange, thus imparting a vertical load. The keyway bolt was attached to the front flange with one grade 8 nut. The small oversized keyway was used for this test. As the cable pulled on the bolt, the bolt was bent upward and out of the keyway freely with a maximum release load of 494 lb (2.20 kN). A peak load of 932 lb (4.15 kN) occurred as the cable became snagged on the button head, after the button head had already cleared the keyway. The force versus time plot is shown in Figure 59. Pre- and post-test photographs are shown in Figure 60. Sequential photographs are shown in Figure 61.

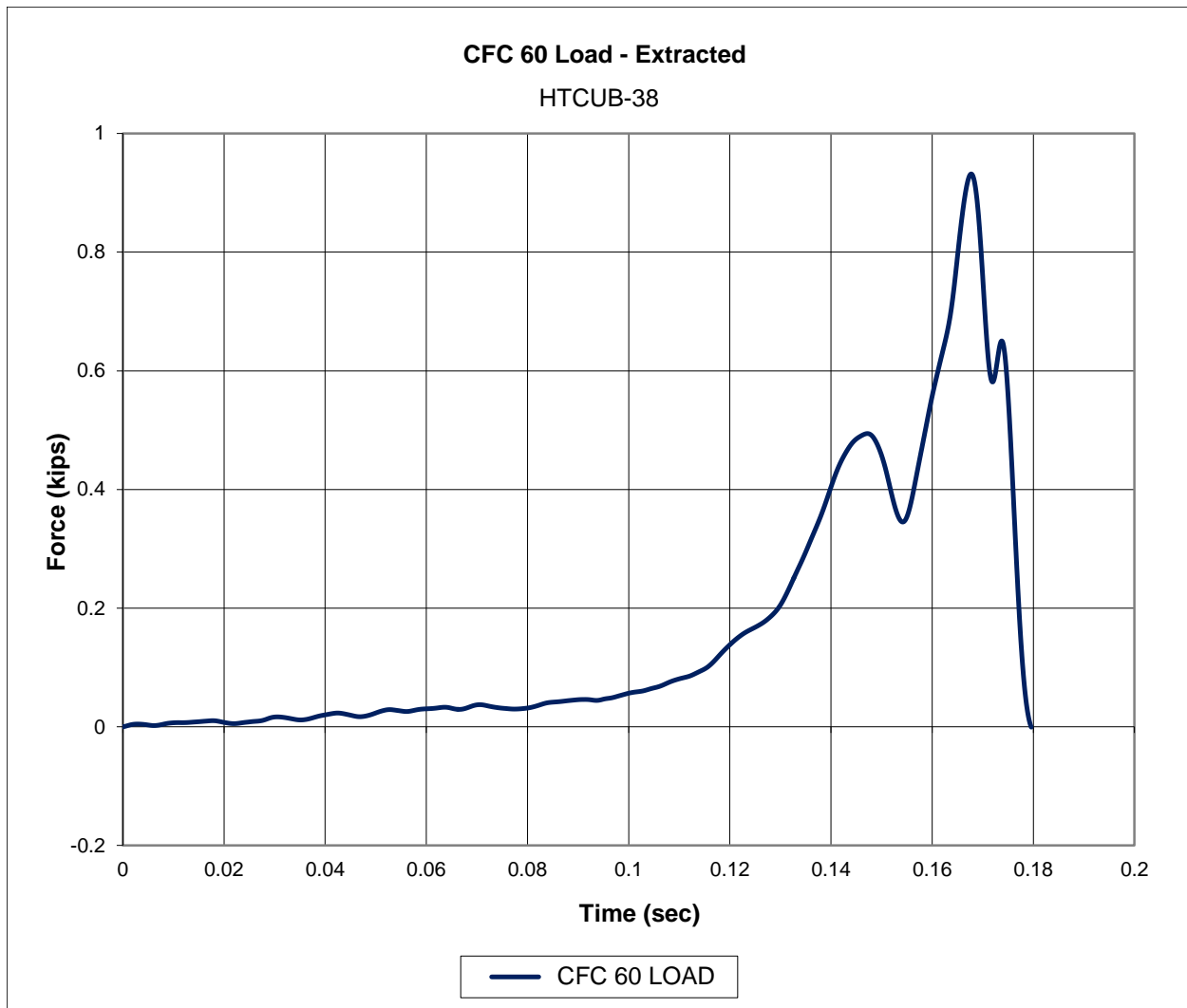
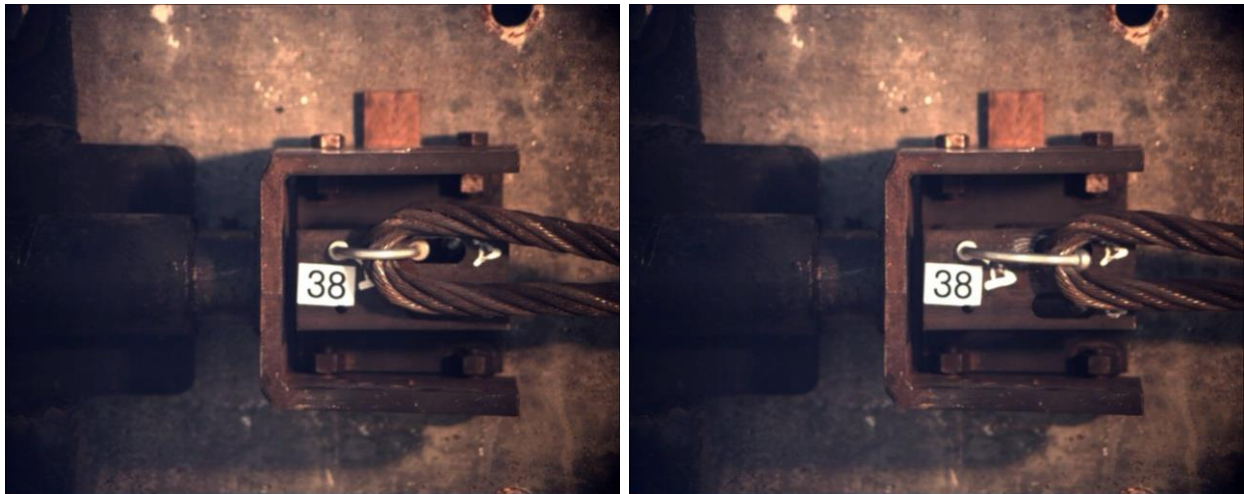


Figure 59. Force-Time Data, Test No. HTCUB-38

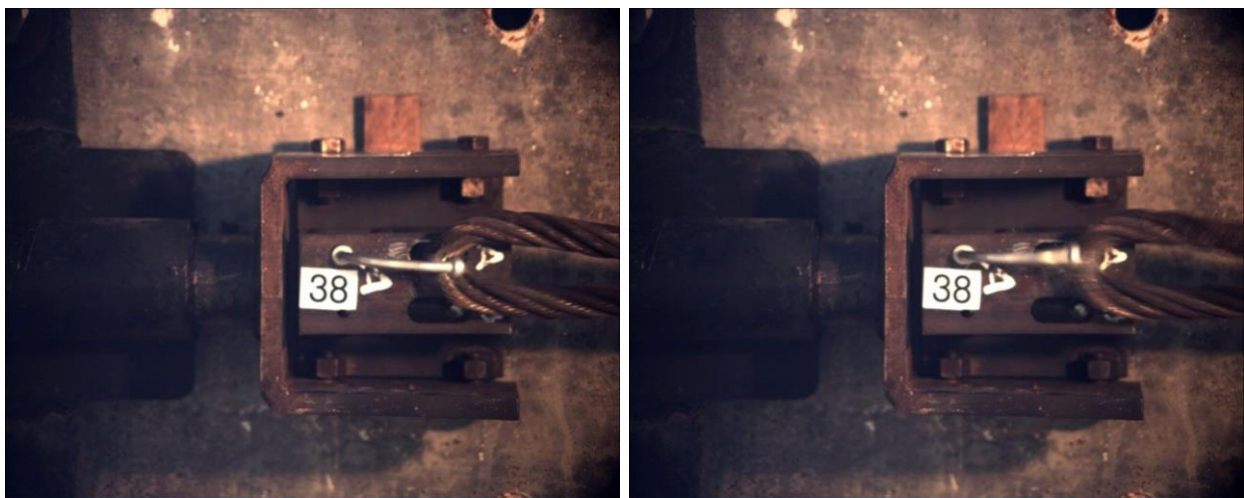


Figure 60. Pre-Test and Post-Test Photographs, Test No. HTCUB-38



Time = 0 sec

Time = 0.172 sec



Time = 0.176 sec

Time = 0.180 sec, Release

Figure 61. Sequential Photographs, Test No. HTCUB-38

7.1.2 Test No. HTCUB-39 (A449 KB, Small, Vertical)

For test no. HTCUB-39, the cable pulled on the ASTM A449 keyway bolt at an angle of 0 degrees, parallel to the front face of the flange, thus imparting a vertical load. The keyway bolt was attached to the front flange with one grade 8 nut. The small oversized keyway was used for this test. As the cable pulled on the bolt, the bolt was bent upward and out of the keyway freely with a maximum release load of 459 lb (2.04 kN). A peak load of 844 lb (3.75 kN) occurred as the cable became snagged on the button head, after the button head had already cleared the keyway. The force versus time plot is shown in Figure 62. Pre- and post-test photographs are shown in Figure 63. Sequential photographs are shown in Figure 64.

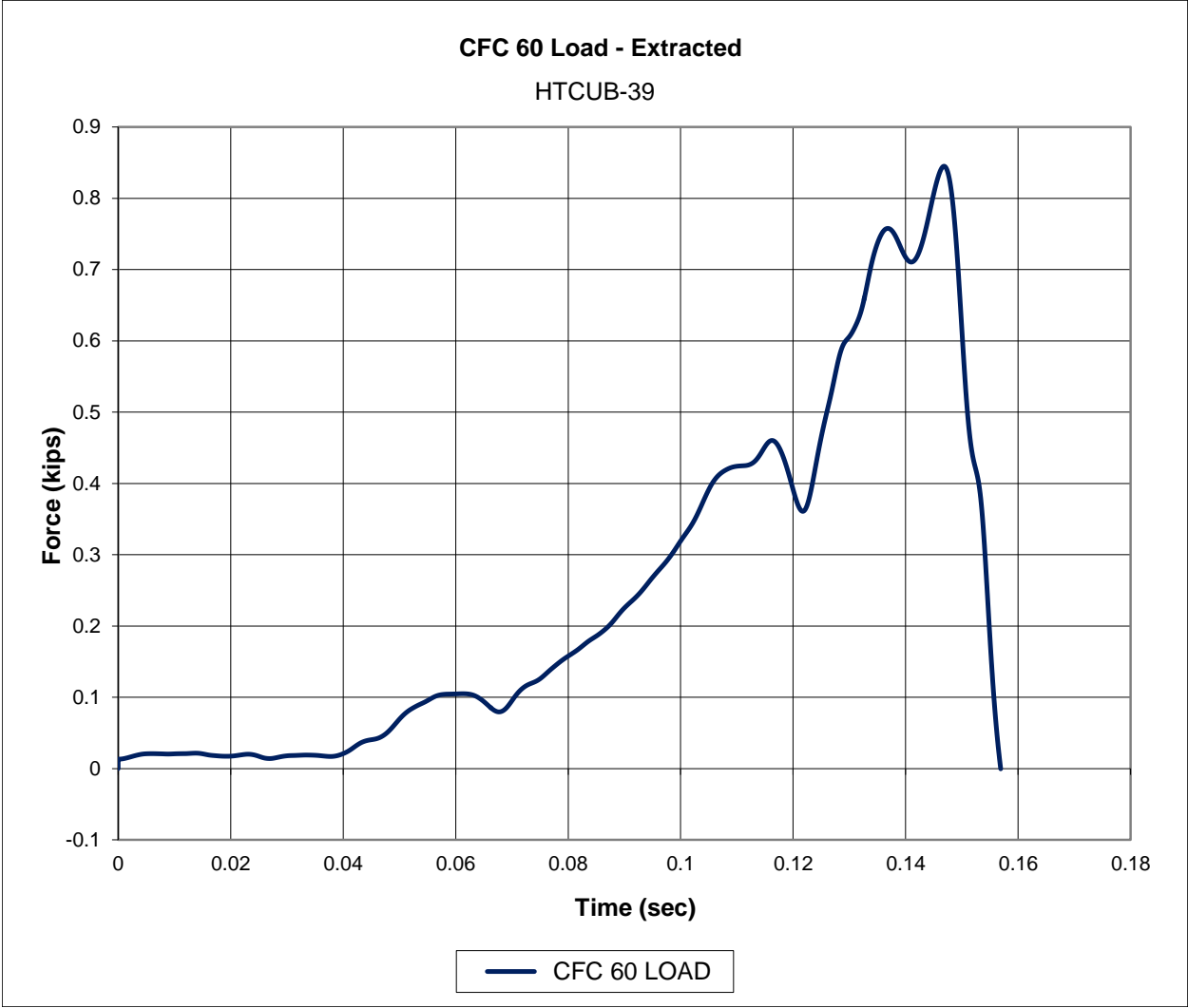


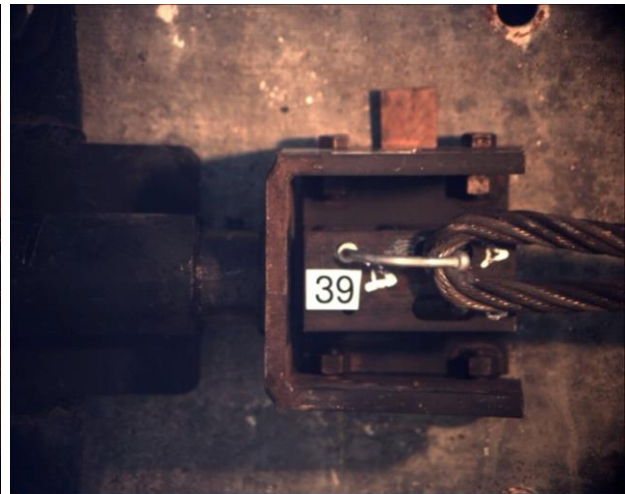
Figure 62. Force-Time Data, Test No. HTCUB-39



Figure 63. Pre-Test and Post-Test Photographs, Test No. HTCUB-39



Time = 0 sec



Time = 0.244 sec



Time = 0.248 sec



Time = 0.252 sec, Release

Figure 64. Sequential Photographs, Test No. HTCUB-39

7.1.3 Test No. HTCUB-40 (A449 KB, Large, Vertical)

For test no. HTCUB-40, the cable pulled on the ASTM A449 keyway bolt at an angle of 0 degrees, parallel to the front face of the flange, thus imparting a vertical load. The keyway bolt was attached to the front flange with one grade 8 nut. The large oversized keyway was used for this test. As the cable pulled on the bolt, the bolt was bent upward and out of the keyway freely with a maximum release load of 489 lb (2.18 kN). A peak load of 879 lb (3.91 kN) occurred as the cable became snagged on the button head, after the button head had already cleared the keyway. The force versus time plot is shown in Figure 65. Pre- and post-test photographs are shown in Figure 66. Sequential photographs are shown in Figure 67.

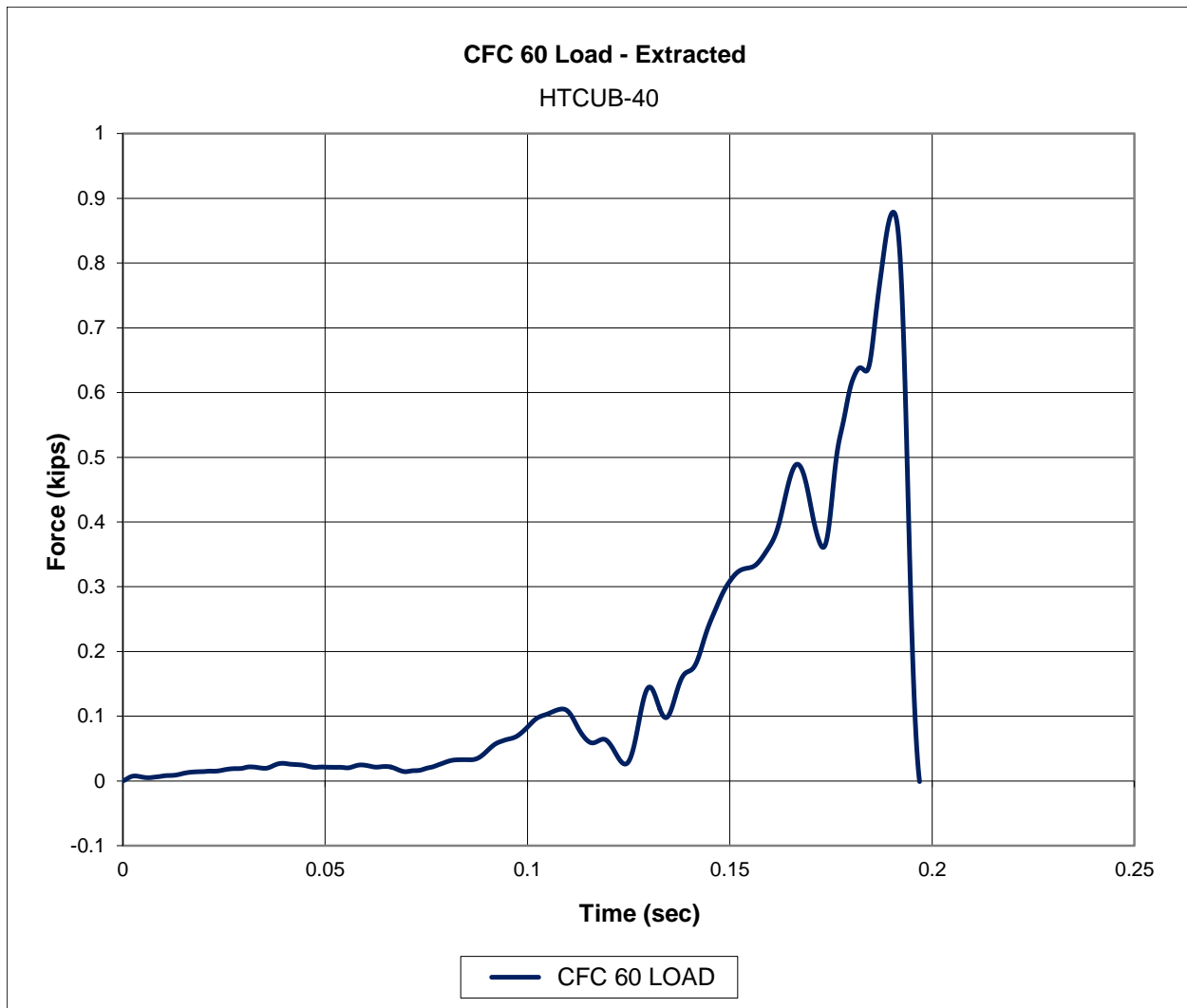
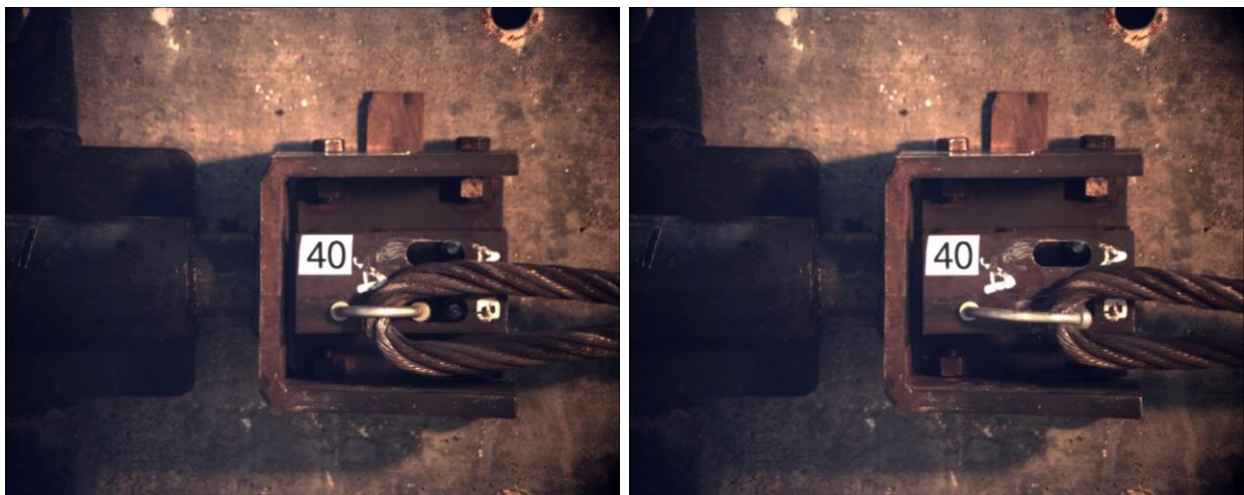


Figure 65. Force-Time Data, Test No. HTCUB-40

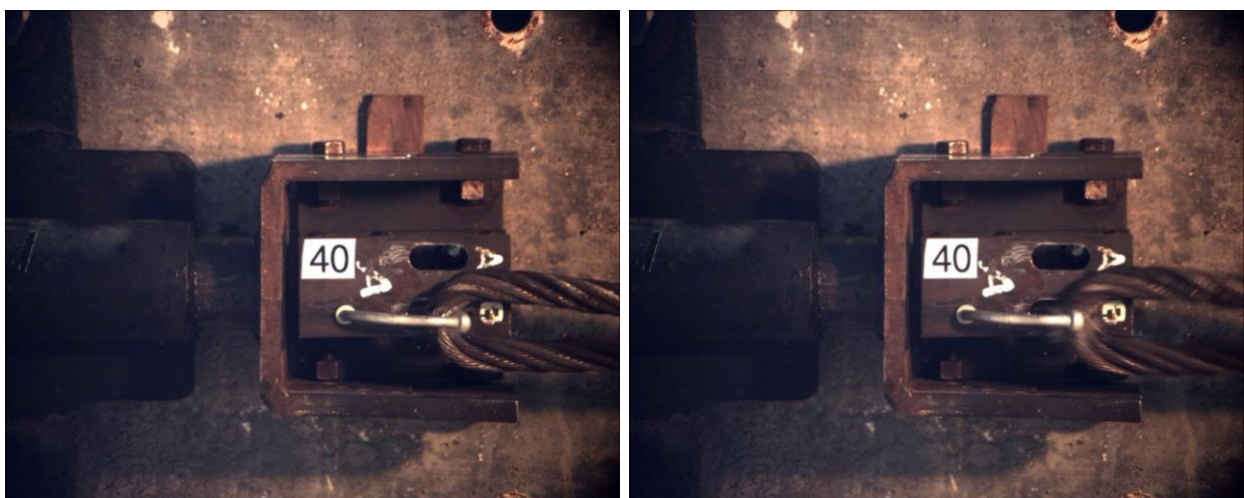


Figure 66. Pre-Test and Post-Test Photographs, Test No. HTCUB-40



Time = 0 sec

Time = 0.188 sec



Time = 0.192 sec

Time = 0.196 sec, Release

Figure 67. Sequential Photographs, Test No. HTCUB-40

7.1.4 Test No. HTCUB-41 (A449 KB, Large, Vertical)

For test no. HTCUB-41, the cable pulled on the ASTM A449 keyway bolt at an angle of 0 degrees, parallel to the front face of the flange, thus imparting a vertical load. The keyway bolt was attached to the front flange with one grade 8 nut. The large oversized keyway was used for this test. As the cable pulled on the bolt, the bolt was bent upward and out of the keyway freely with a maximum release load of 415 lb (1.85 kN). A peak load of 748 lb (3.33 kN) occurred as the cable became snagged on the button head, after the button head had already cleared the keyway. The force versus time plot is shown in Figure 68. Pre- and post-test photographs are shown in Figure 69. Sequential photographs are shown in Figure 70.

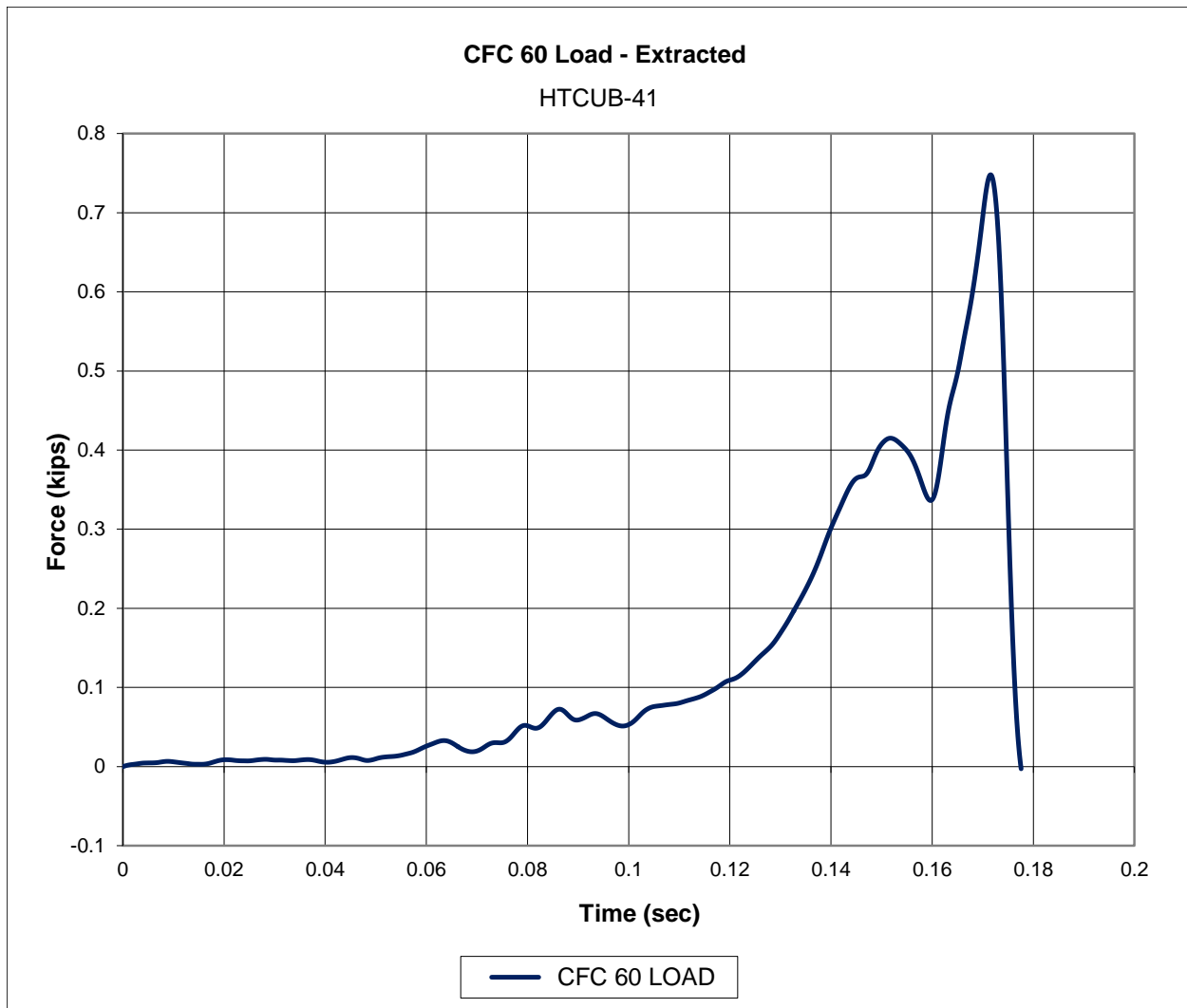


Figure 68. Force-Time Data, Test No. HTCUB-41

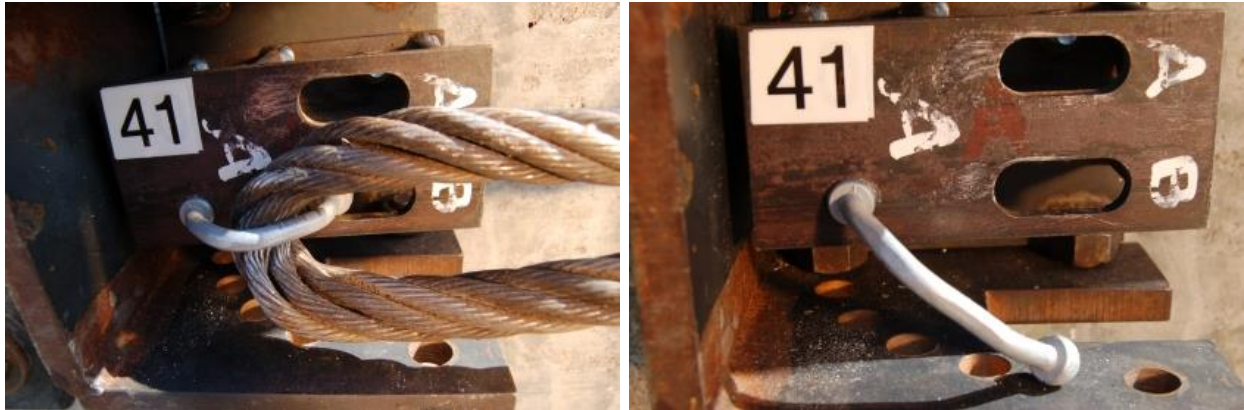
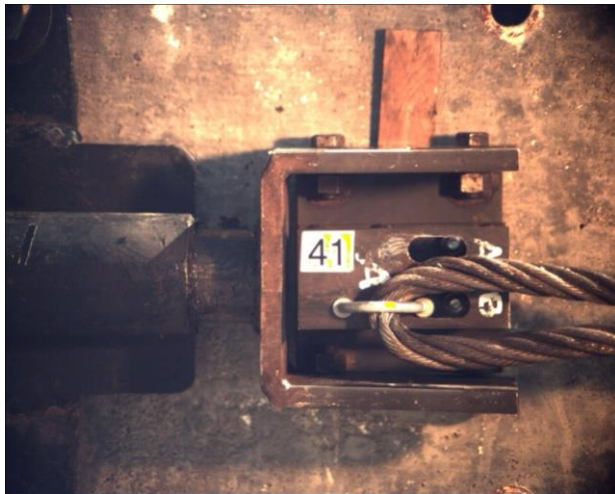
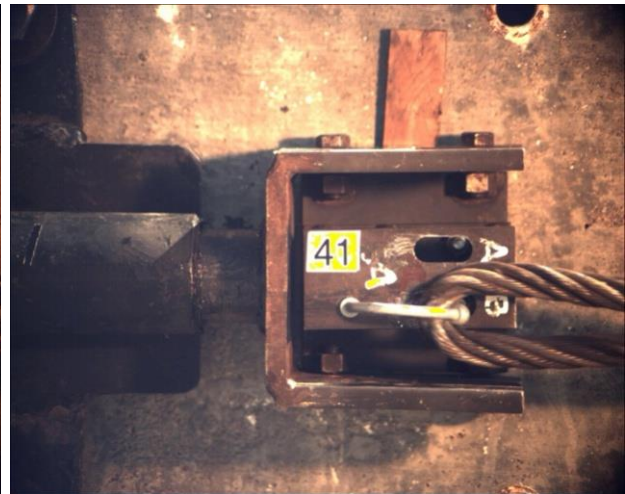


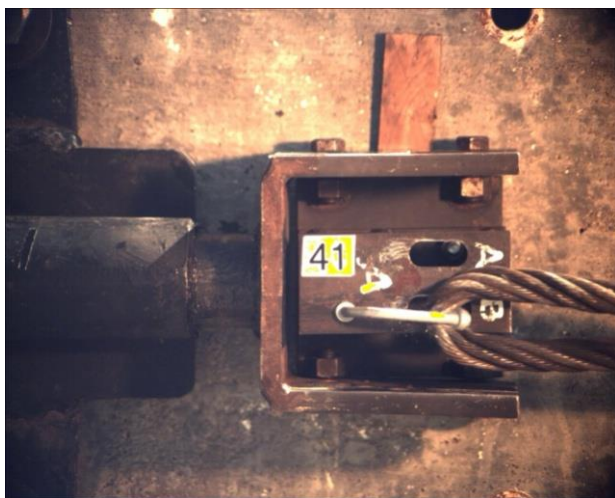
Figure 69. Pre-Test and Post-Test Photographs, Test No. HTCUB-41



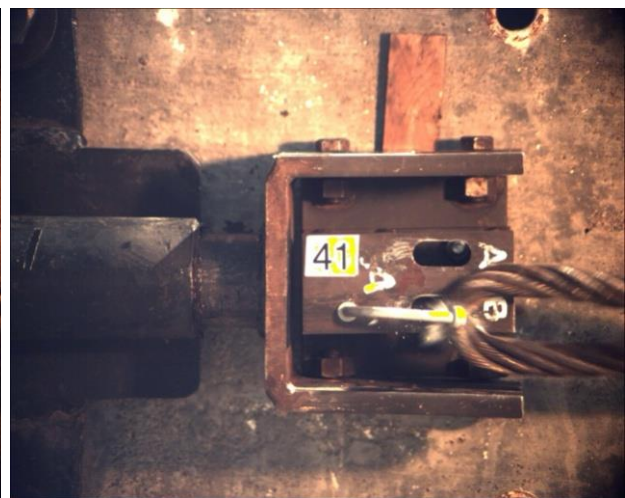
Time = 0 sec



Time = 0.170 sec



Time = 0.174 sec



Time = 0.178 sec, Release

Figure 70. Sequential Photographs, Test No. HTCUB-41

7.1.5 Test No. HTCUB-42 (C1018 KB, Small, Vertical)

For test no. HTCUB-42, the cable pulled on the AISI C1018 keyway bolt at an angle of 0 degrees, parallel to the front face of the flange, thus imparting a vertical load. The keyway bolt was attached to the front flange with one grade 8 nut. The small oversized keyway was used for this test. As the cable pulled on the bolt, the bolt was bent upward and out of the keyway freely with a maximum release load of 305 lb (1.36 kN). A peak load of 533 lb (2.37 kN) occurred as the cable became snagged on the button head, after the button head had already cleared the keyway. The force versus time plot is shown in Figure 71. Pre- and post-test photographs are shown in Figure 72. Sequential photographs are shown in Figure 73.

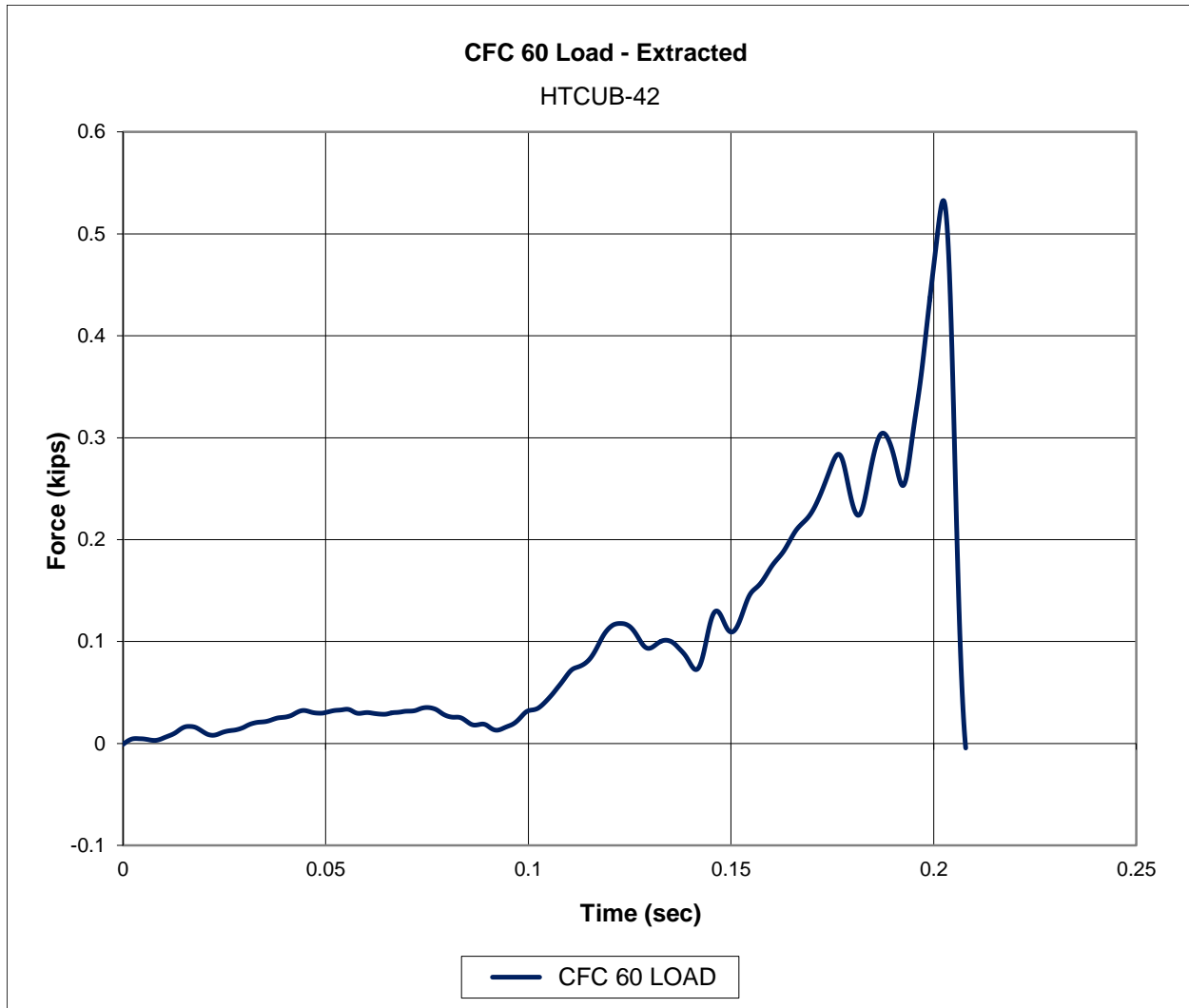
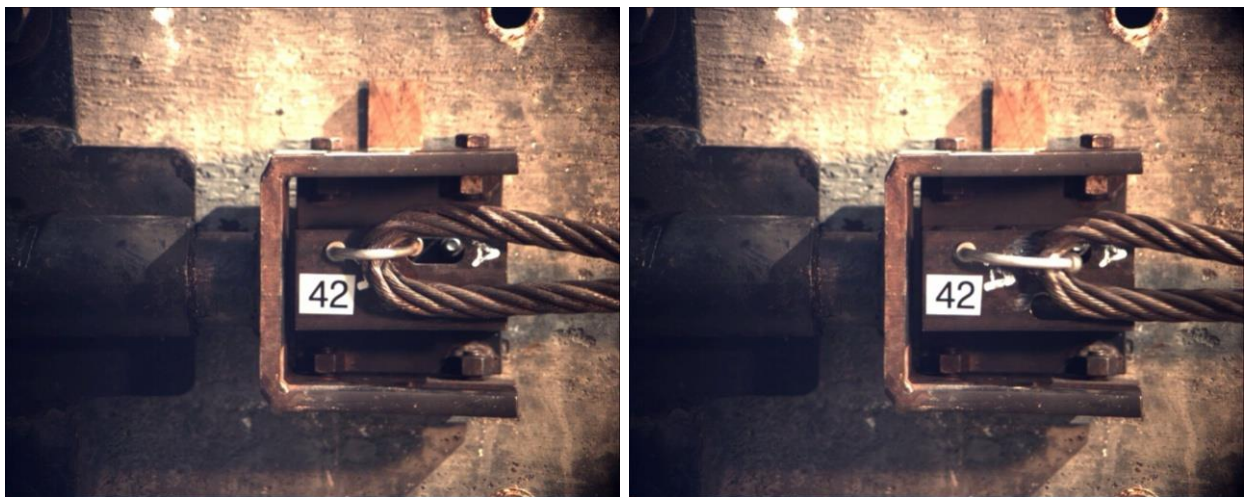


Figure 71. Force-Time Data, Test No. HTCUB-42

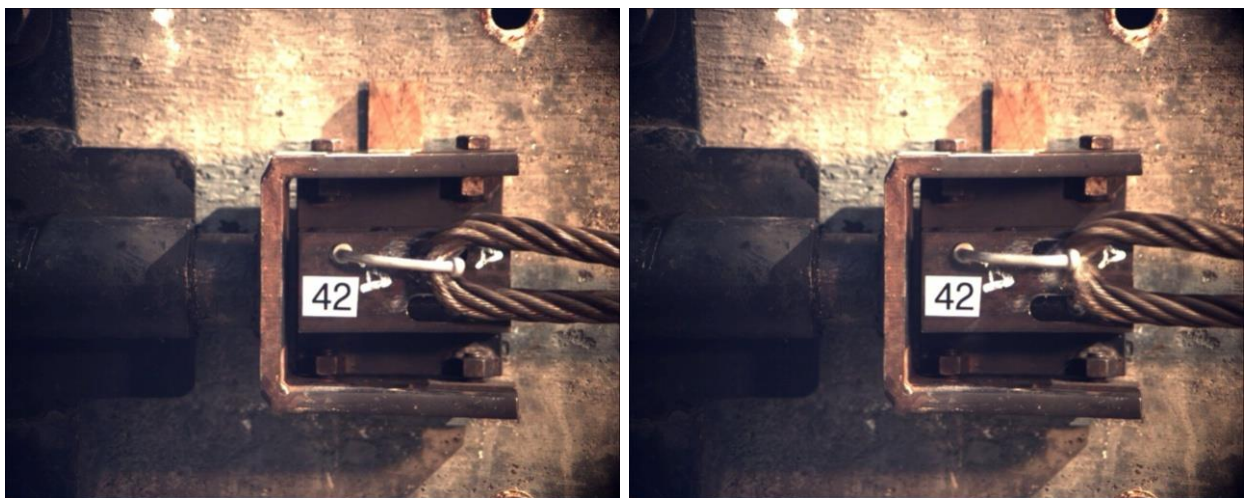


Figure 72. Pre-Test and Post-Test Photographs, Test No. HTCUB-42



Time = 0 sec

Time = 0.200 sec



Time = 0.204 sec

Time = 0.208 sec, Release

Figure 73. Sequential Photographs, Test No. HTCUB-42

7.1.6 Test No. HTCUB-43 (C1018 KB, Small, Vertical)

For test no. HTCUB-43, the cable pulled on the AISI C1018 keyway bolt at an angle of 0 degrees, parallel to the front face of the flange, thus imparting a vertical load. The keyway bolt was attached to the front flange with one grade 8 nut. The small oversized keyway was used for this test. As the cable pulled on the bolt, the bolt was bent upward and out of the keyway freely with a maximum release load of 390 lb (1.73 kN). A peak load of 516 lb (2.30 kN) occurred as the cable became snagged on the button head, after the button head had already cleared the keyway. The force versus time plot is shown in Figure 74. Pre- and post-test photographs are shown in Figure 75. Sequential photographs are shown in Figure 76.

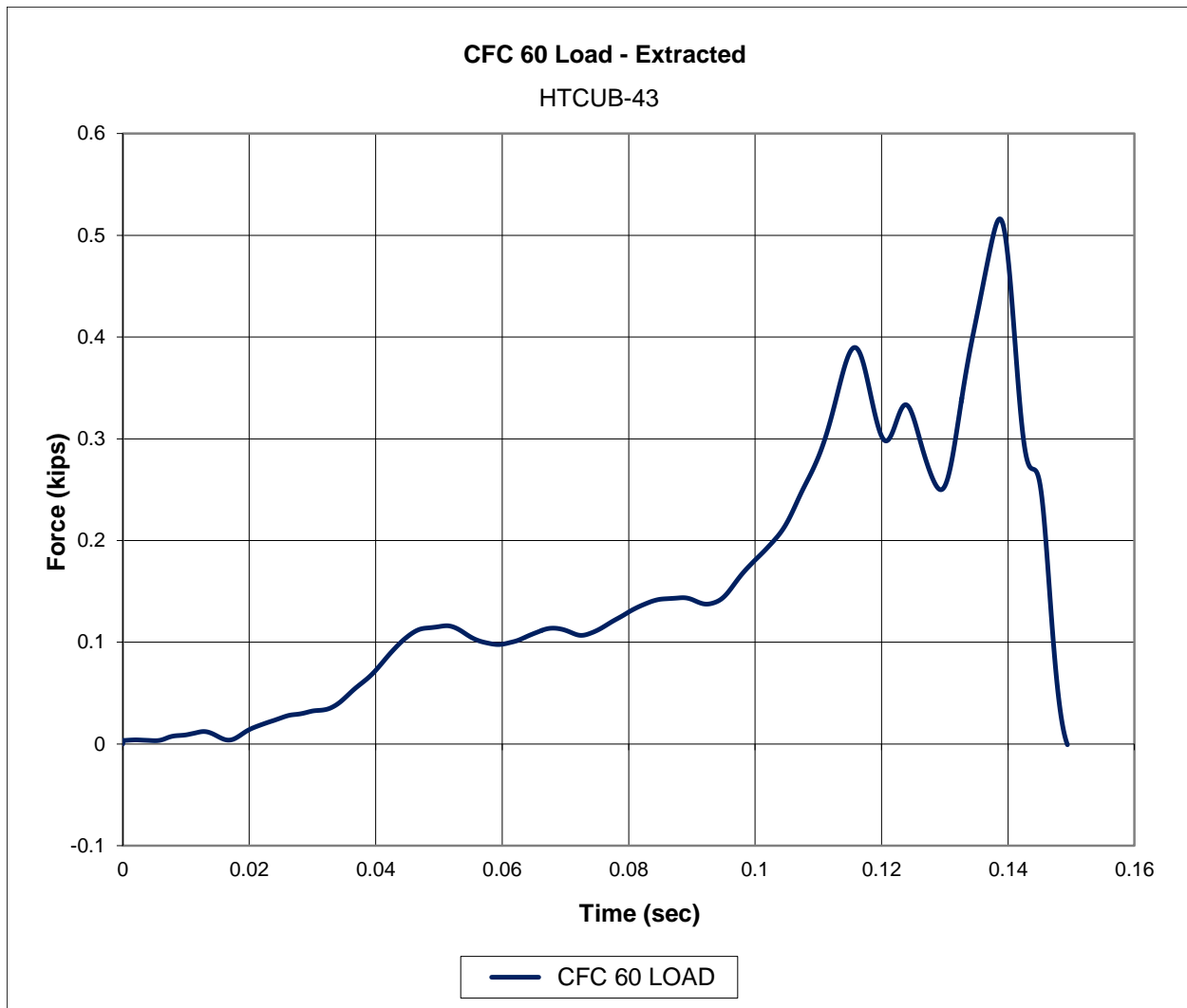
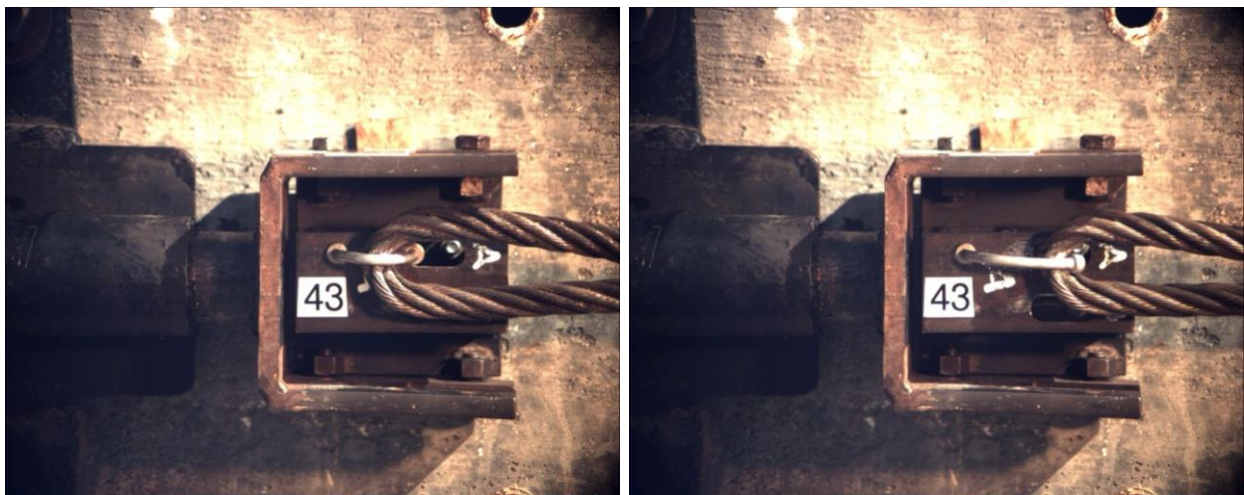


Figure 74. Force-Time Data, Test No. HTCUB-43

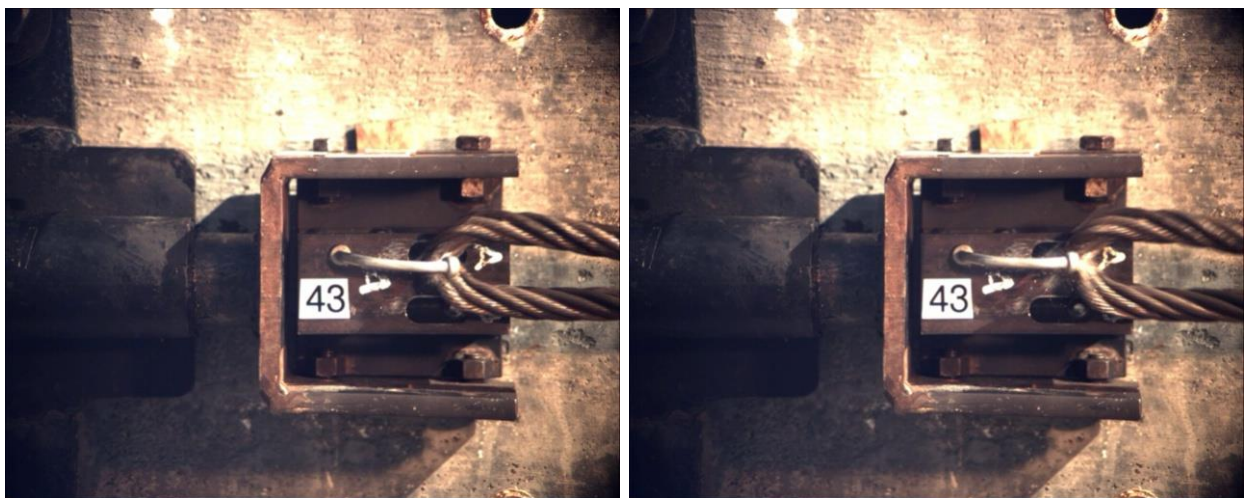


Figure 75. Pre-Test and Post-Test Photographs, Test No. HTCUB-43



Time = 0 sec

Time = 0.242 sec



Time = 0.246 sec

Time = 0.250 sec, Release

Figure 76. Sequential Photographs, Test No. HTCUB-43

7.1.7 Test No. HTCUB-44 (C1018 KB, Large, Vertical)

For test no. HTCUB-44, the cable pulled on the AISI C1018 keyway bolt at an angle of 0 degrees, parallel to the front face of the flange, thus imparting a vertical load. The keyway bolt was attached to the front flange with one grade 8 nut. The large oversized keyway was used for this test. As the cable pulled on the bolt, the bolt was bent upward and out of the keyway freely with a maximum release load of 282 lb (1.25 kN). A peak load of 475 lb (2.11 kN) occurred as the cable became snagged on the button head, after the button head had already cleared the keyway. The force versus time plot is shown in Figure 77. Pre- and post-test photographs are shown in Figure 78. Sequential photographs are shown in Figure 79.

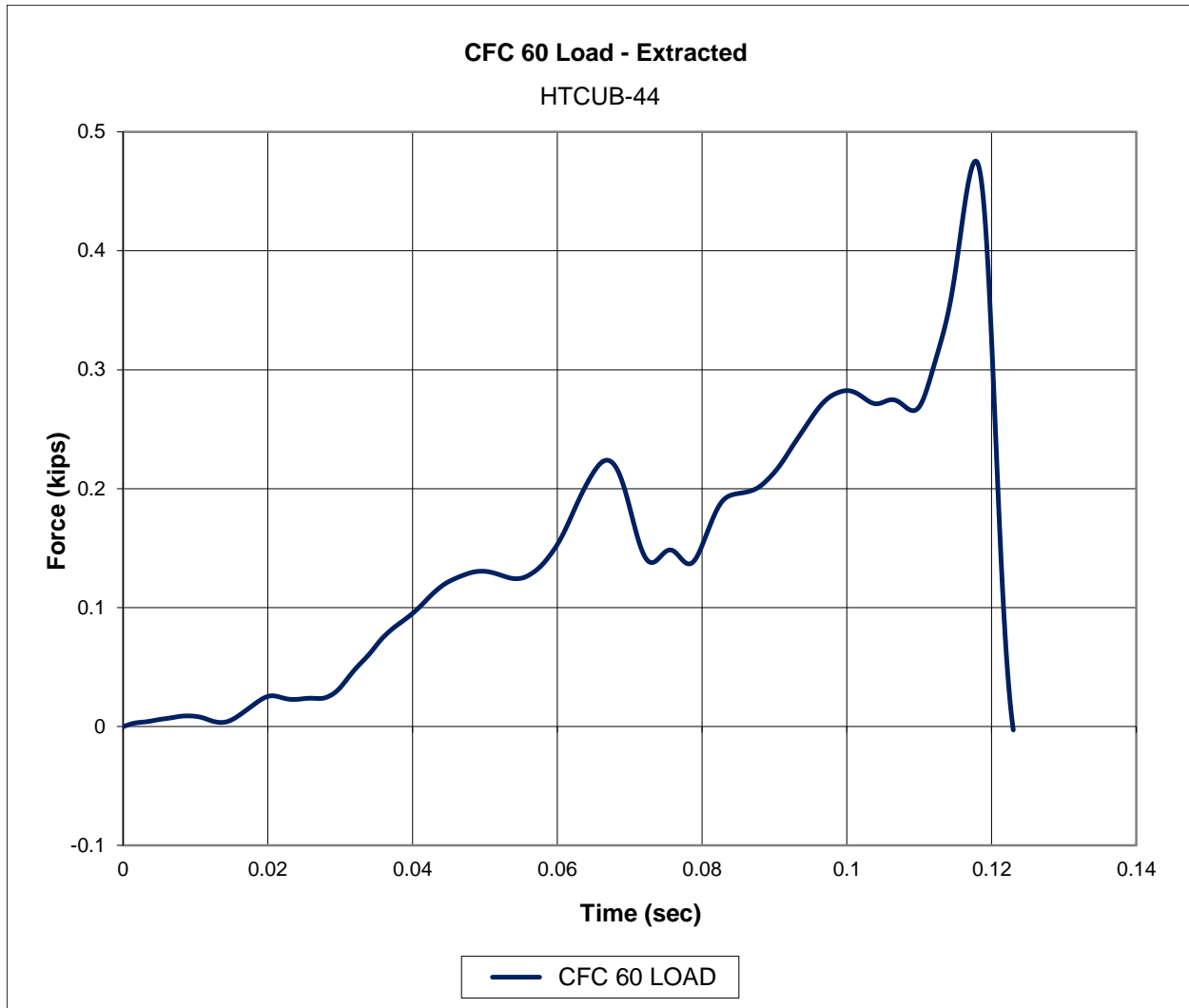
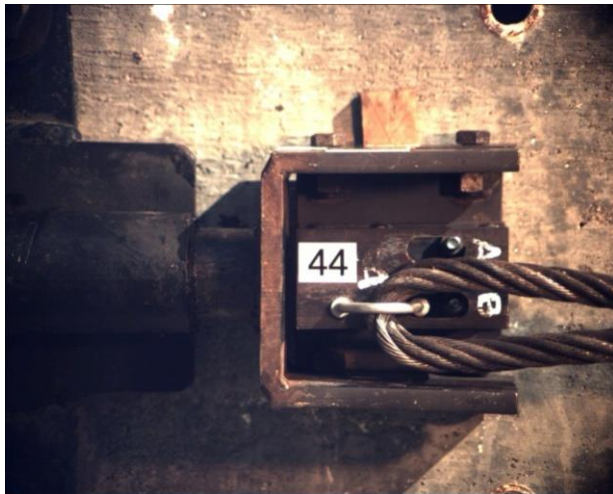


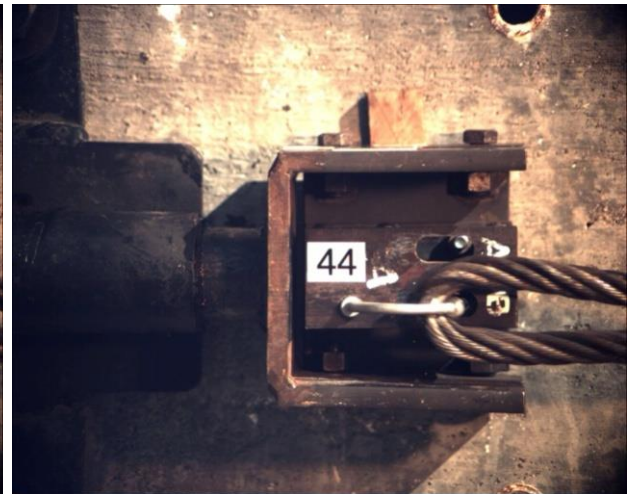
Figure 77. Force-Time Data, Test No. HTCUB-44



Figure 78. Pre-Test and Post-Test Photographs, Test No. HTCUB-44



Time = 0 sec



Time = 0.116 sec



Time = 0.120 sec



Time = 0.124 sec, Release

Figure 79. Sequential Photographs, Test No. HTCUB-44

7.1.8 Test No. HTCUB-45 (C1018 KB, Large, Vertical)

For test no. HTCUB-45, the cable pulled on the AISI C1018 keyway bolt at an angle of 0 degrees, parallel to the front face of the flange, thus imparting a vertical load. The keyway bolt was attached to the flange with one grade 8 nut. The large oversized keyway was used for this test. As the cable pulled on the bolt, the bolt was bent upward and out of the keyway freely with a maximum release load of 379 lb (1.69 kN). The peak load of 601 lb (2.67 kN) occurred as the cable became snagged on the button head, after the button head had already cleared the keyway. The force versus time plot is shown in Figure 80. Pre- and post-test photographs are shown in Figure 81. Sequential photographs are shown in Figure 82.

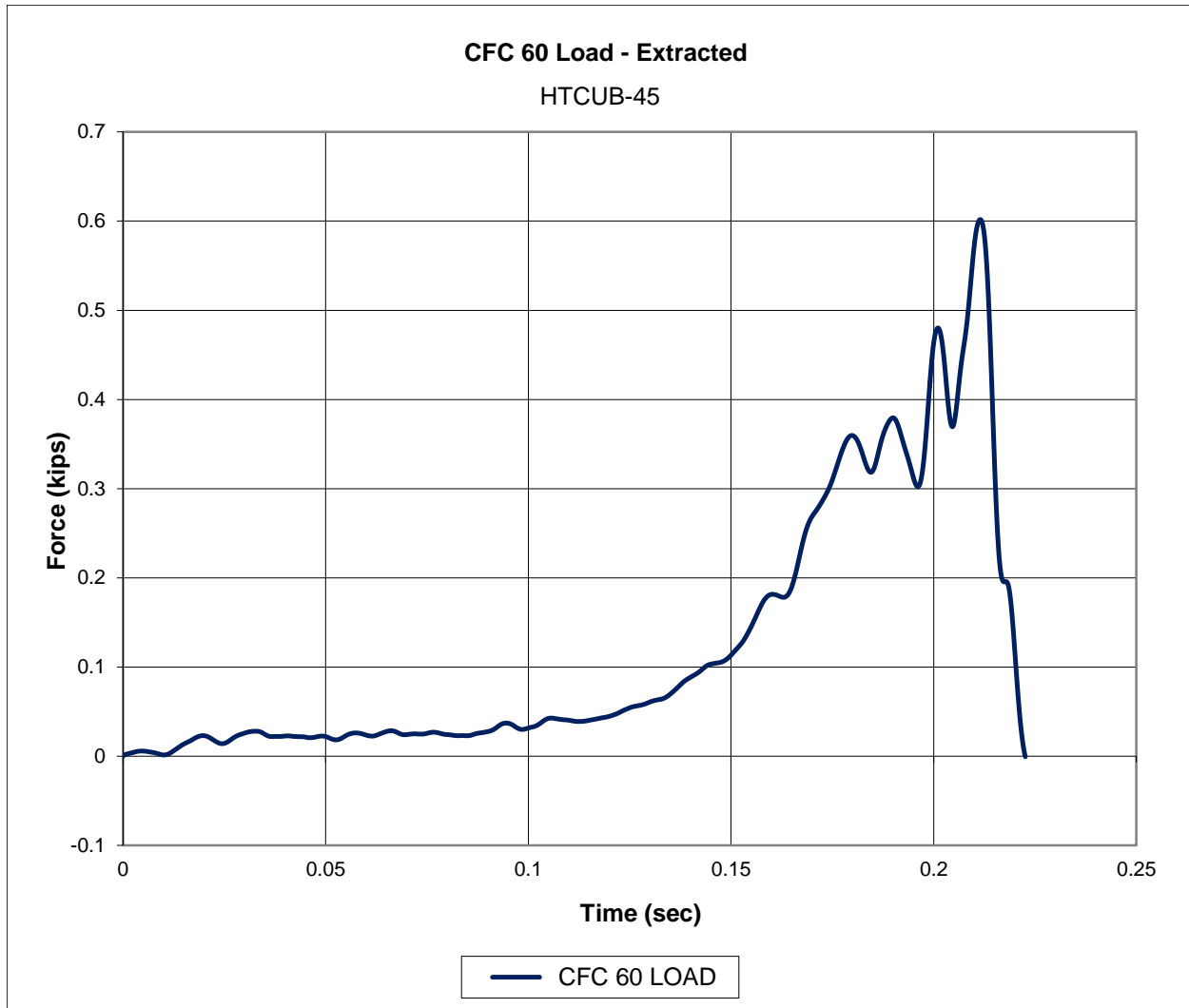


Figure 80. Force-Time Data, Test No. HTCUB-45



Figure 81. Pre-Test and Post-Test Photographs, Test No. HTCUB-45

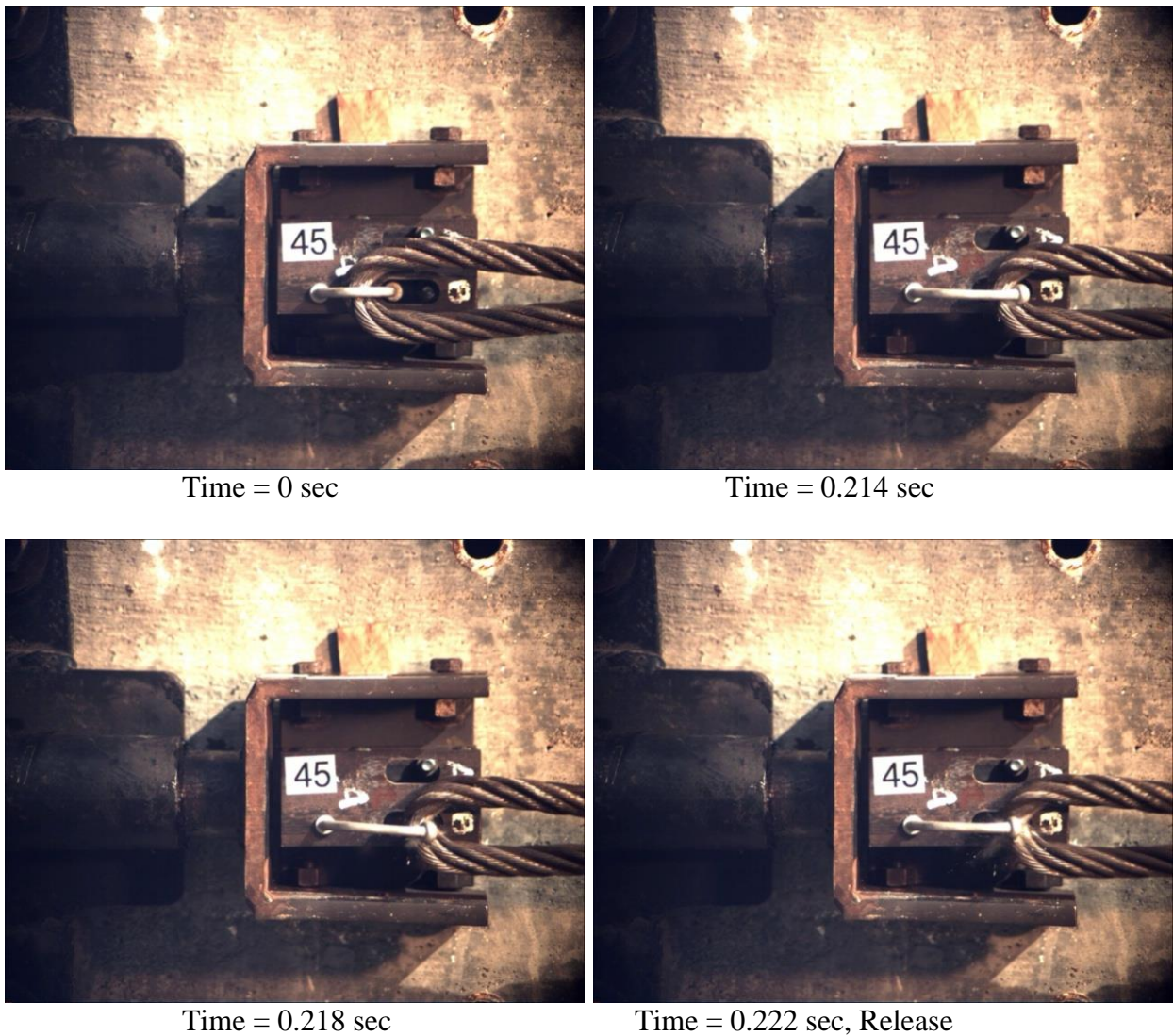


Figure 82. Sequential Photographs, Test No. HTCUB-45

7.1.9 Test No. HTCUB-46 (A449 KB, Small, Lateral)

For test no. HTCUB-46, the cable pulled on the ASTM A449 keyway bolt at an angle of 90 degrees, perpendicular to the front face of the flange, thus imparting a lateral load. The keyway bolt was attached to the front flange with one grade 8 nut. The small oversized keyway was used for this test. As the cable began to pull on the bolt, the button head was not caught or snagged on the bottom or side of the keyway but released through the keyway freely. A peak load of 1.14 kips (5.07 kN) occurred as the bolt was bent straight out by the cable. The force versus time plot is shown in Figure 83. Pre- and post-test photographs are shown in Figure 84. Sequential photographs are shown in Figure 85.

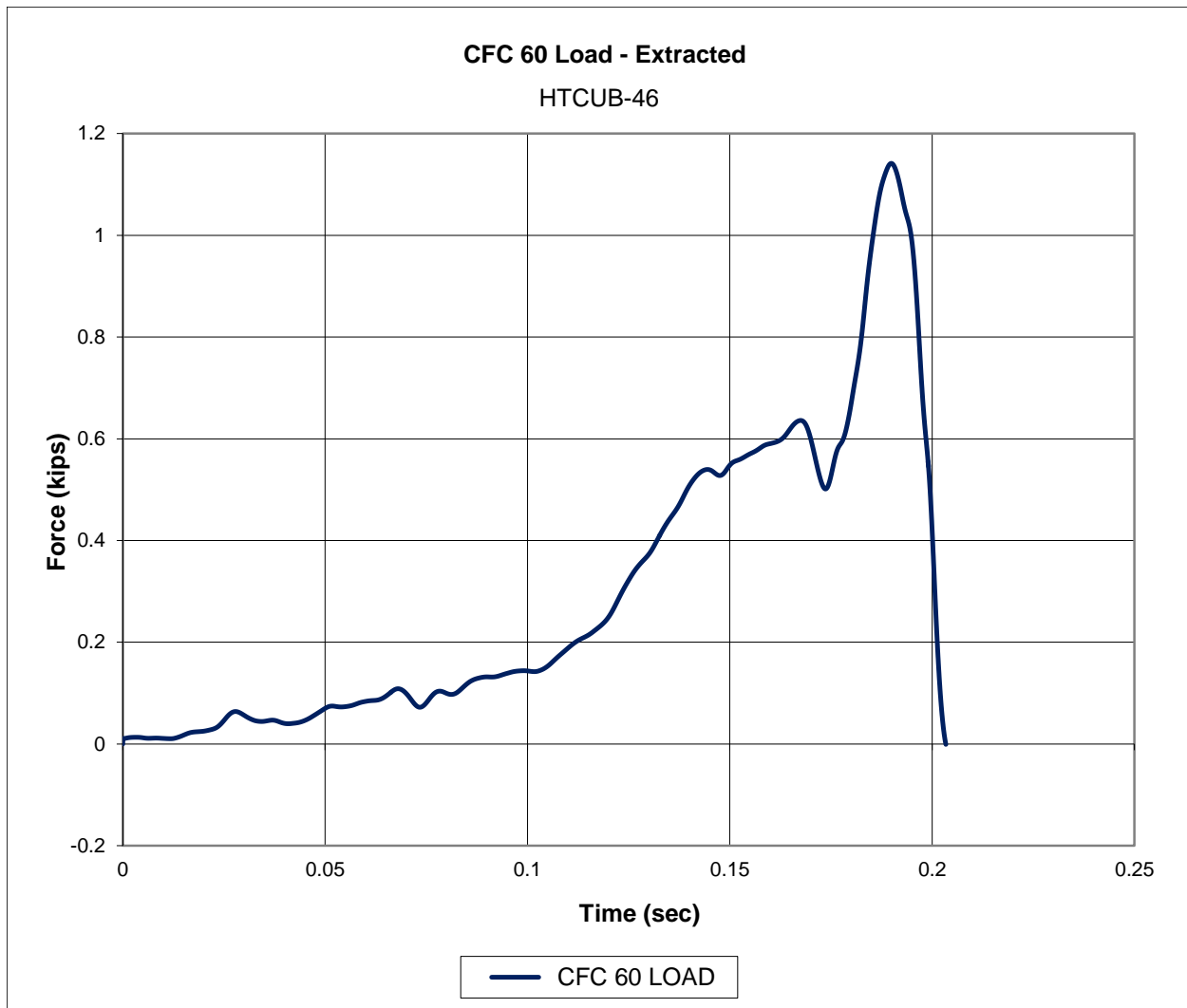
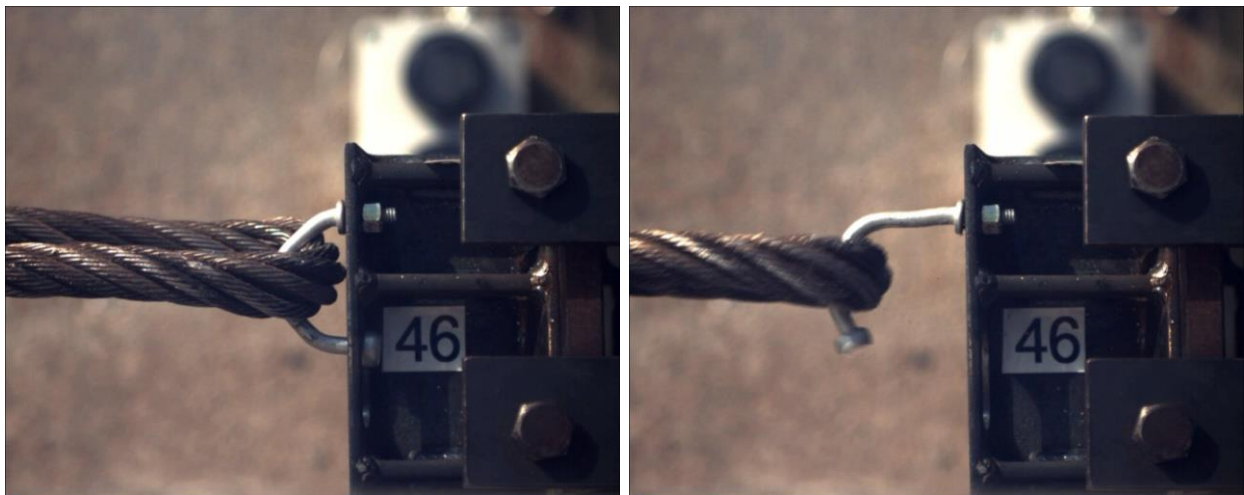


Figure 83. Force-Time Data, Test No. HTCUB-46

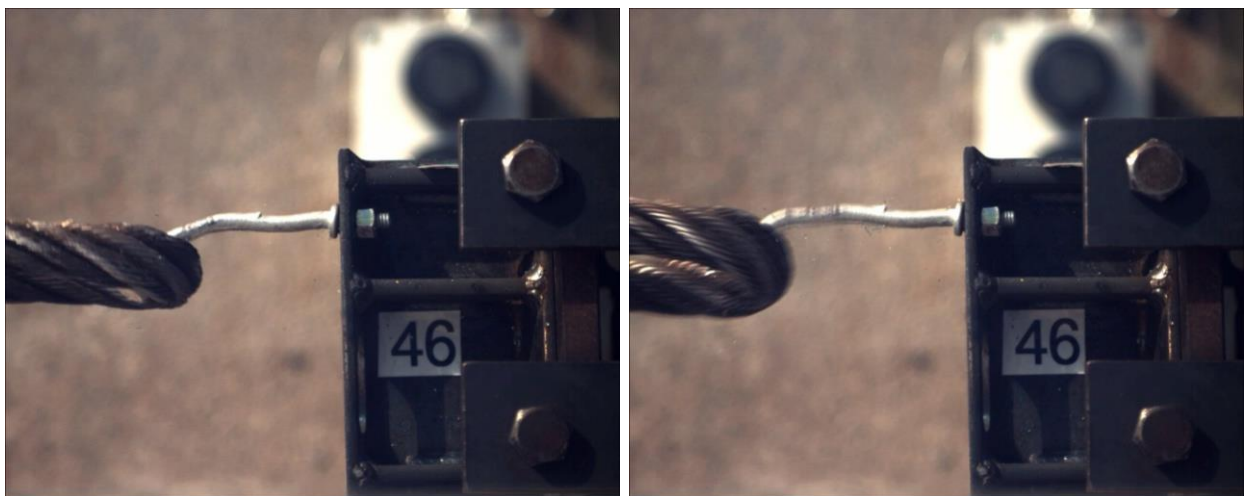


Figure 84. Pre-Test and Post-Test Photographs, Test No. HTCUB-46



Time = 0 sec

Time = 0.324 sec



Time = 0.344 sec

Time = 0.352 sec, Release

Figure 85. Sequential Photographs, Test No. HTCUB-46

7.1.10 Test No. HTCUB-47 (A449 KB, Small, Lateral)

For test no. HTCUB-47, the cable pulled on the ASTM A449 keyway bolt at an angle of 90 degrees, perpendicular to the front face of the flange, thus imparting a lateral load. The keyway bolt was attached to the front flange with one grade 8 nut. The small oversized keyway was used for this test. As the cable began to pull on the bolt, the button head was caught on the bottom of the keyway. A peak load of 5.05 kips (22.5 kN) occurred while the button head was caught on the bottom of the keyway, as the cable continued to pull on the bolt. Finally, the button head slipped off, and the cable released as it straightened out the bolt. The force versus time plot is shown in Figure 86. Pre- and post-test photographs are shown in Figure 87. Sequential photographs are shown in Figure 88.

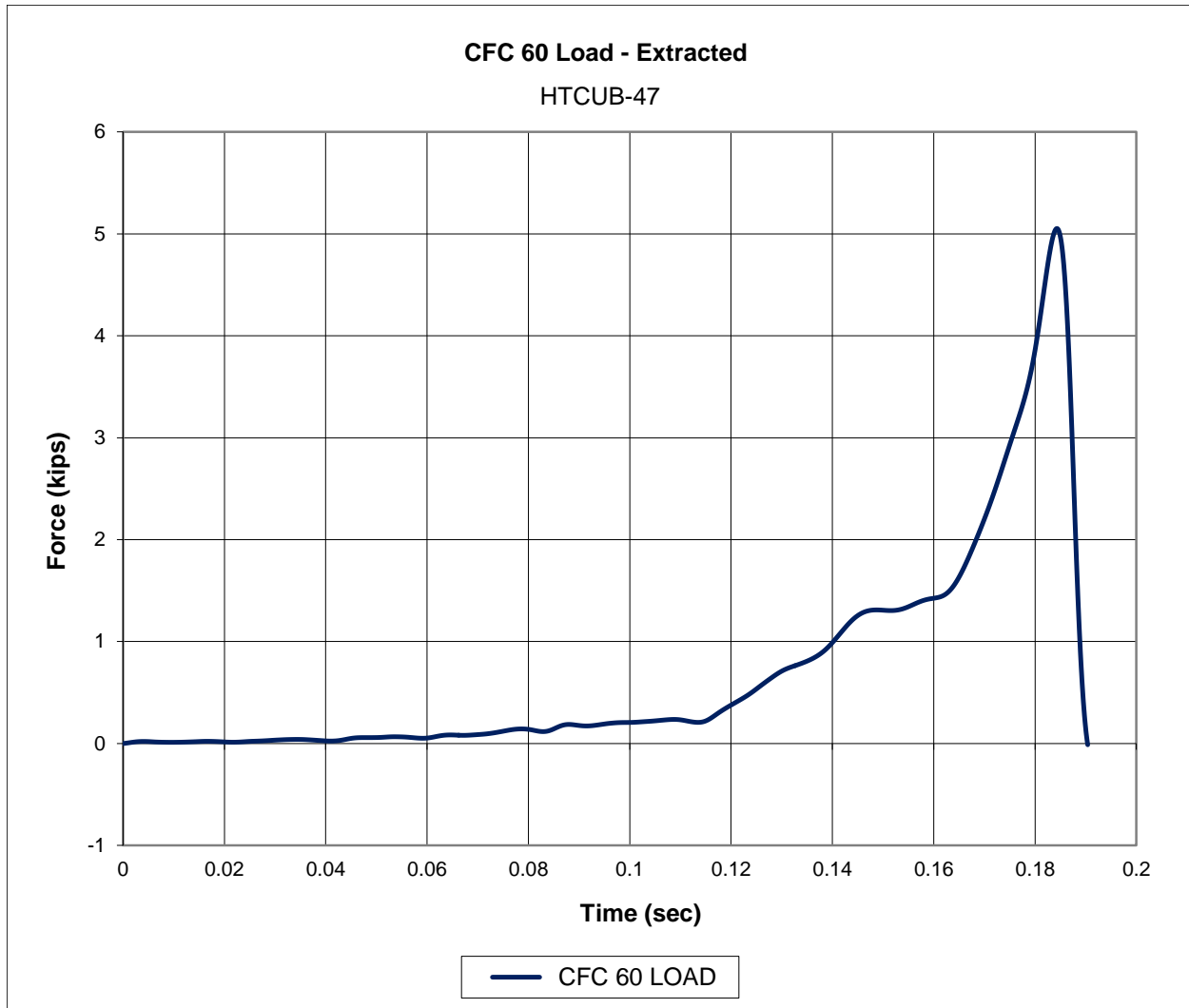


Figure 86. Force-Time Data, Test No. HTCUB-47



Figure 87. Pre-Test and Post-Test Photographs, Test No. HTCUB-47



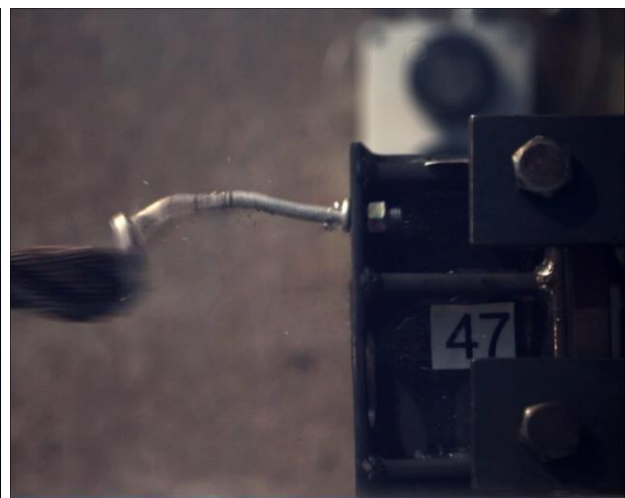
Time = 0 sec



Time = 0.162 sec



Time = 0.182 sec



Time = 0.192 sec, Release

Figure 88. Sequential Photographs, Test No. HTCUB-47

7.1.11 Test No. HTCUB-48 (A449 KB, Large, Lateral)

For test no. HTCUB-48, the cable pulled on the ASTM A449 keyway bolt at an angle of 90 degrees, perpendicular to the front face of the flange, thus imparting a lateral load. The keyway bolt was attached to the front flange with one grade 8 nut. The large oversized keyway was used for this test. As the cable began to pull on the bolt, the button head was not caught or snagged on the bottom or side of the keyway but released through the keyway freely. A peak load of 840 lb (3.74 kN) occurred as the bolt was bent straight out by the cable. The force versus time plot is shown in Figure 89. Pre- and post-test photographs are shown in Figure 90. Sequential photographs are shown in Figure 91.

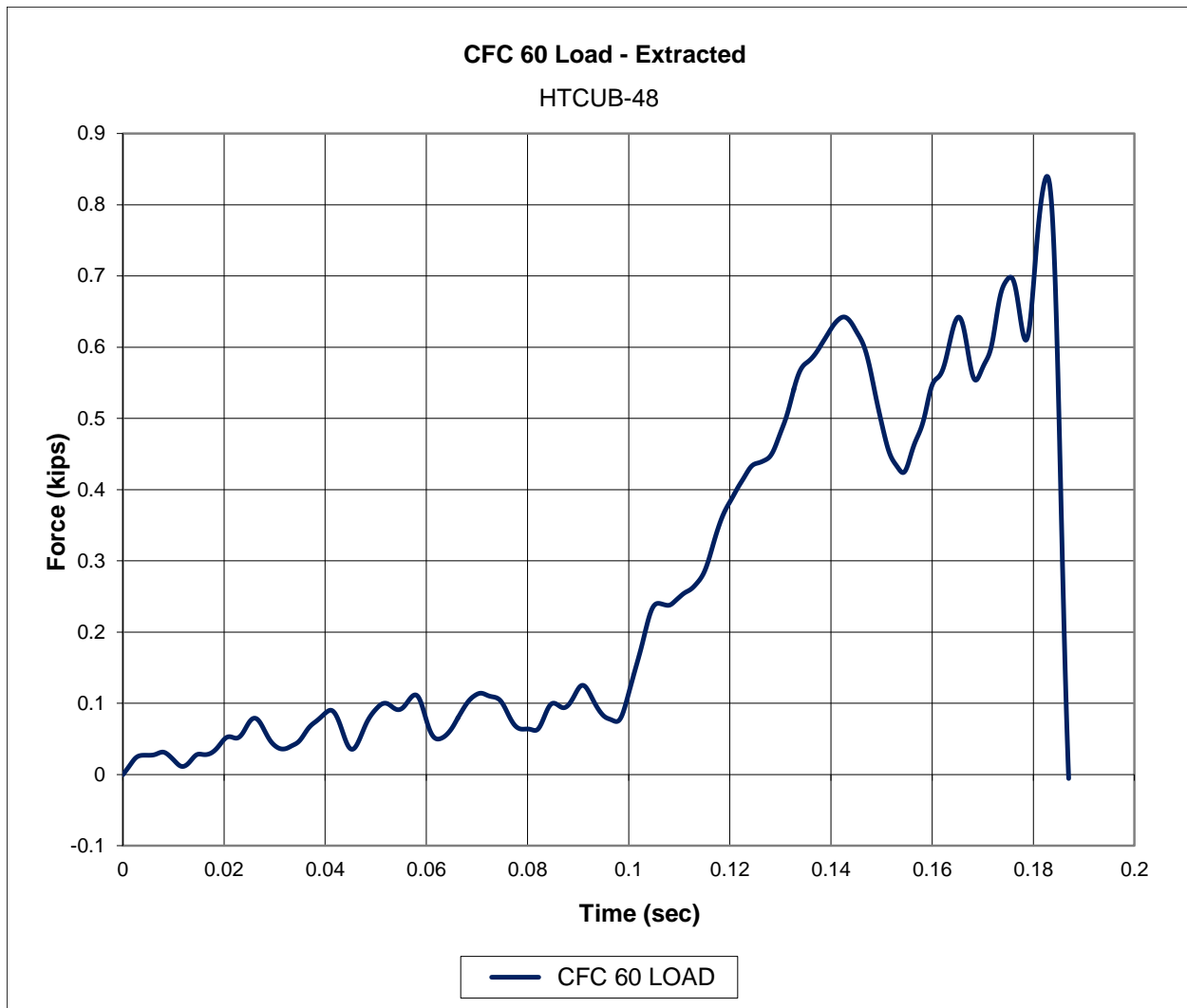


Figure 89. Force-Time Data, Test No. HTCUB-48



Figure 90. Pre-Test and Post-Test Photographs, Test No. HTCUB-48

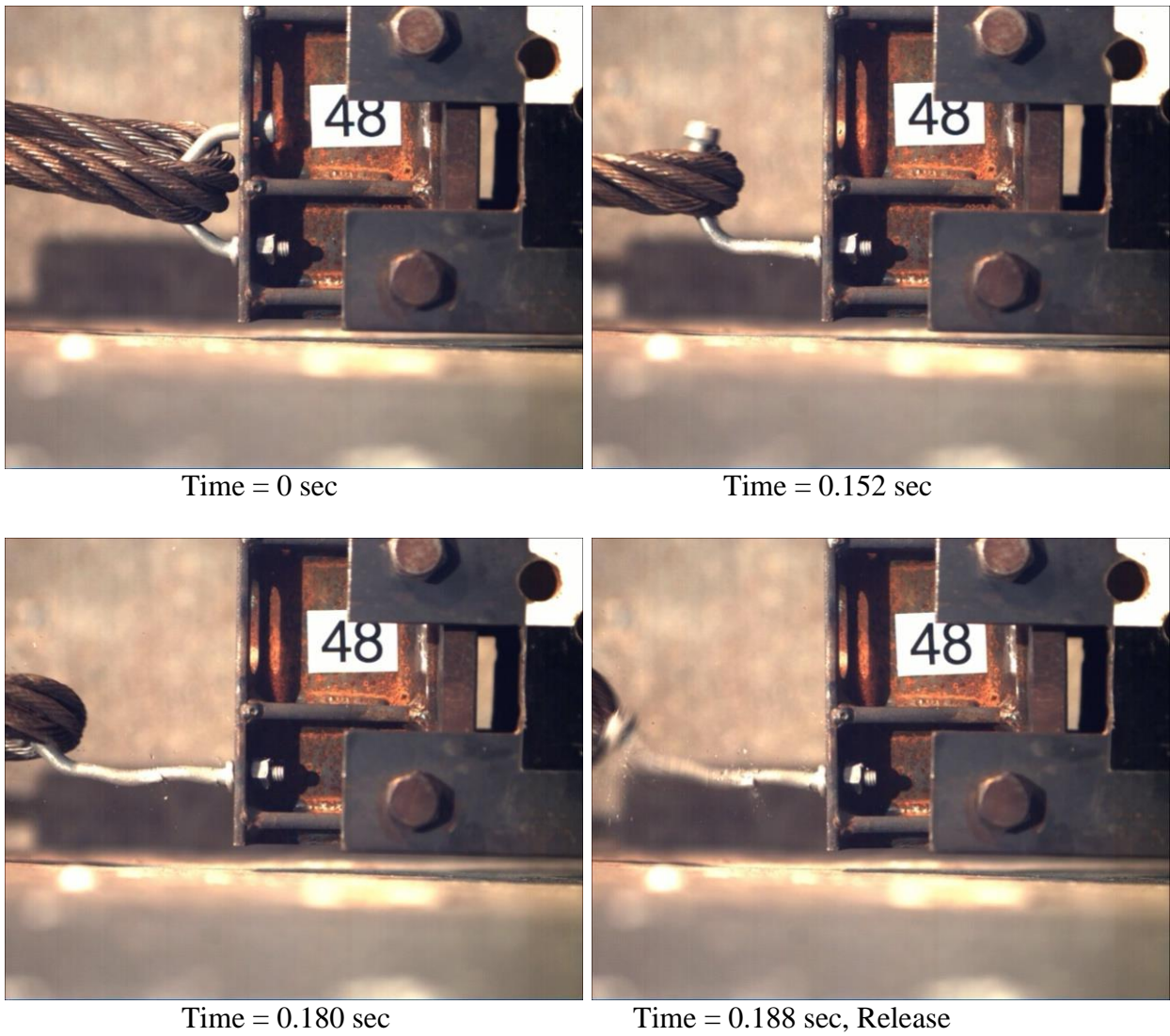


Figure 91. Sequential Photographs, Test No. HTCUB-48

7.1.12 Test No. HTCUB-49 (A449 KB, Large, Lateral)

For test no. HTCUB-49, the cable pulled on the ASTM A449 keyway bolt at an angle of 90 degrees, perpendicular to the front face of the flange, thus imparting a lateral load. The keyway bolt was attached to the front flange with one grade 8 nut. The large oversized keyway was used for this test. As the cable began to pull on the bolt, the button head was not caught or snagged on the bottom or side of the keyway but released through the keyway freely. A peak load of 1.22 kips (5.43 kN) occurred as the bolt was bent straight out by the cable. The force versus time plot is shown in Figure 92. Pre- and post-test photographs are shown in Figure 93. Sequential photographs are shown in Figure 94.

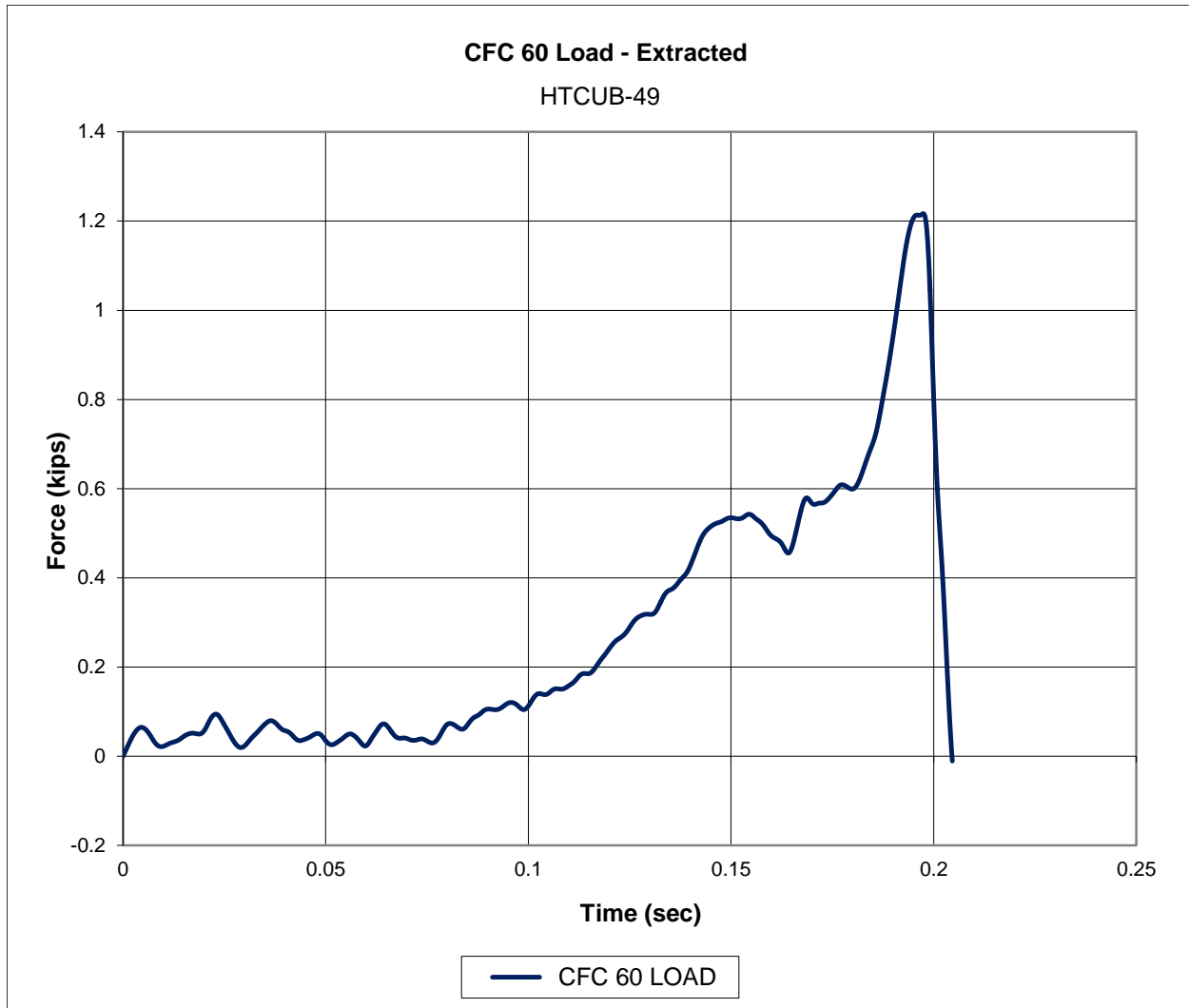
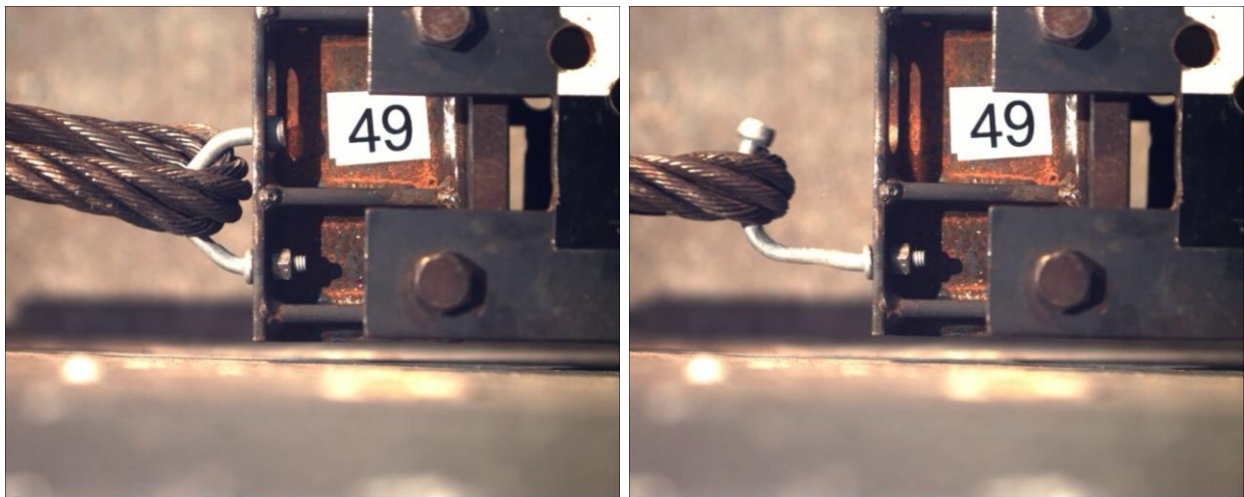


Figure 92. Force-Time Data, Test No. HTCUB-49

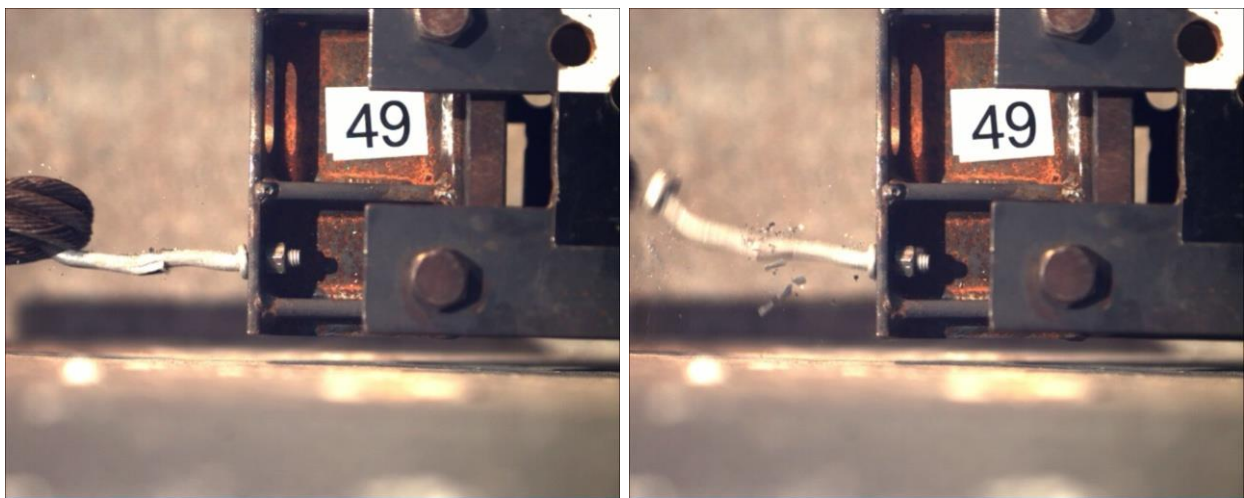


Figure 93. Pre-Test and Post-Test Photographs, Test No. HTCUB-49



Time = 0 sec

Time = 0.160 sec



Time = 0.196 sec

Time = 0.204 sec, Release

Figure 94. Sequential Photographs, Test No. HTCUB-49

7.1.13 Test No. HTCUB-50 (C1018 KB, Small, Lateral)

For test no. HTCUB-50, the cable pulled on the AISI C1018 keyway bolt at an angle of 90 degrees, perpendicular to the front face of the flange, thus imparting a lateral load. The keyway bolt was attached to the front flange with one grade 8 nut. The small oversized keyway was used for this test. As the cable began to pull on the bolt, the button head was not caught or snagged on the bottom or side of the keyway but released through the keyway freely. A peak load of 531 lb (2.36 kN) occurred as the bolt was bent straight out by the cable. The force versus time plot is shown in Figure 95. Pre- and post-test photographs are shown in Figure 96. Sequential photographs are shown in Figure 97.

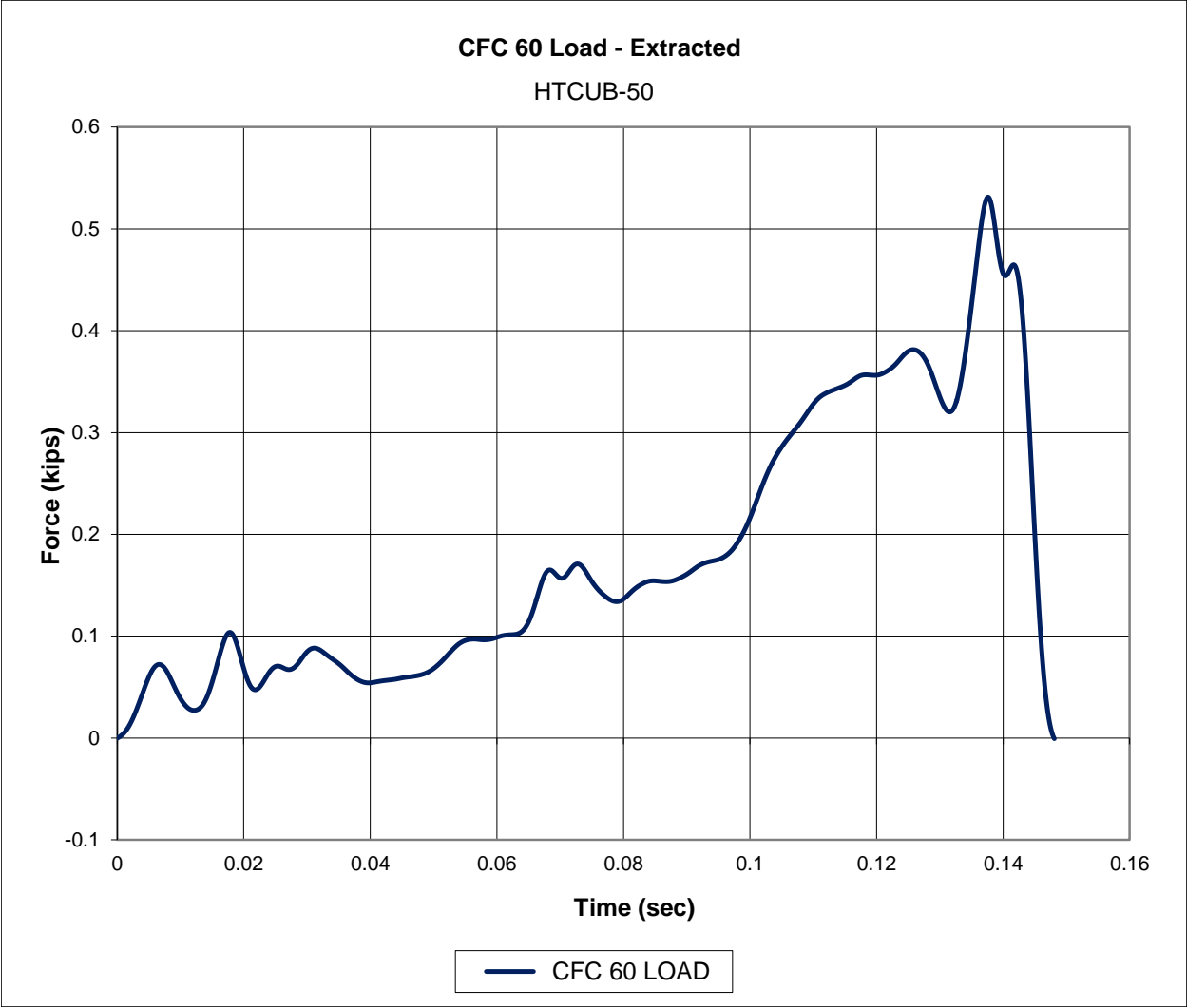
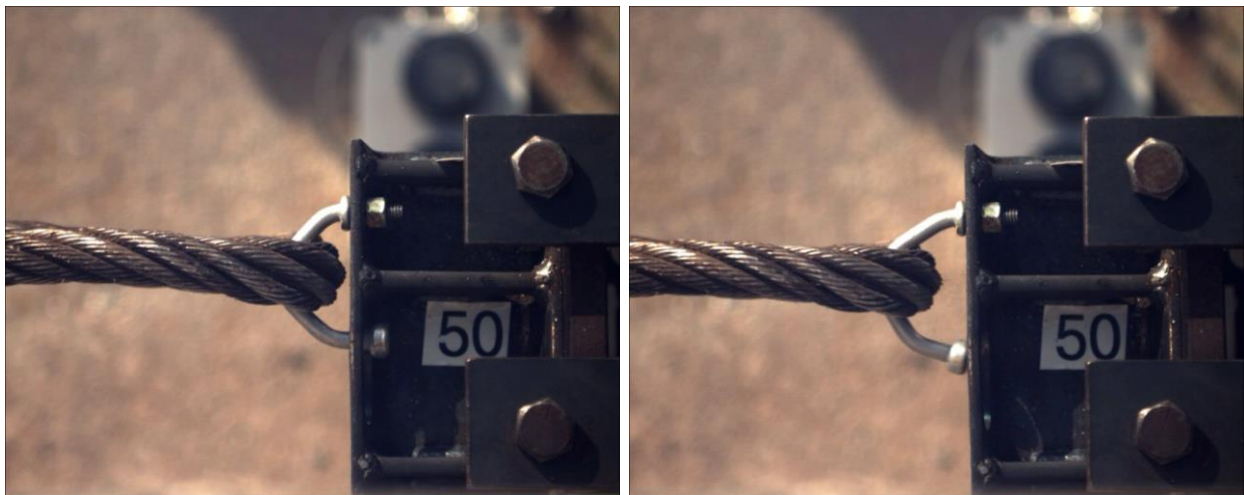


Figure 95. Force-Time Data, Test No. HTCUB-50

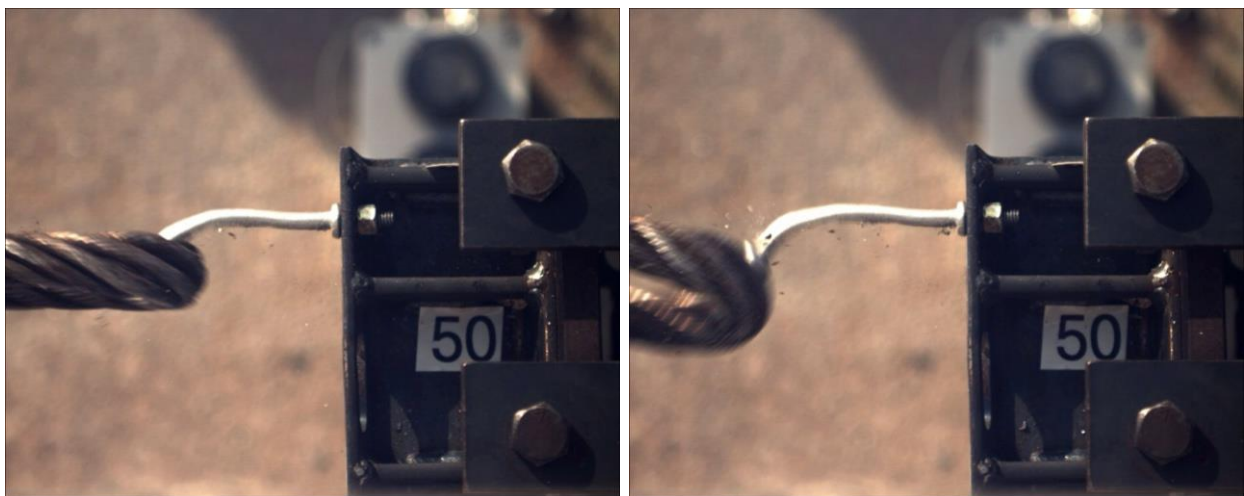


Figure 96. Pre-Test and Post-Test Photographs, Test No. HTCUB-50



Time = 0 sec

Time = 0.120 sec



Time = 0.140 sec

Time = 0.148 sec, Release

Figure 97. Sequential Photographs, Test No. HTCUB-50

7.1.14 Test No. HTCUB-51 (C1018 KB, Small, Lateral)

For test no. HTCUB-51, the cable pulled on the AISI C1018 keyway bolt at an angle of 90 degrees, perpendicular to the front face of the flange, thus imparting a lateral load. The keyway bolt was attached to the front flange with one grade 8 nut. The small oversized keyway was used for this test. As the cable began to pull on the bolt, the button head was not caught or snagged on the bottom or side of the keyway but released through the keyway freely. A peak load of 538 lb (2.39 kN) occurred as the bolt was bent straight out by the cable. The force versus time plot is shown in Figure 98. Pre- and post-test photographs are shown in Figure 99. Sequential photographs are shown in Figure 100.

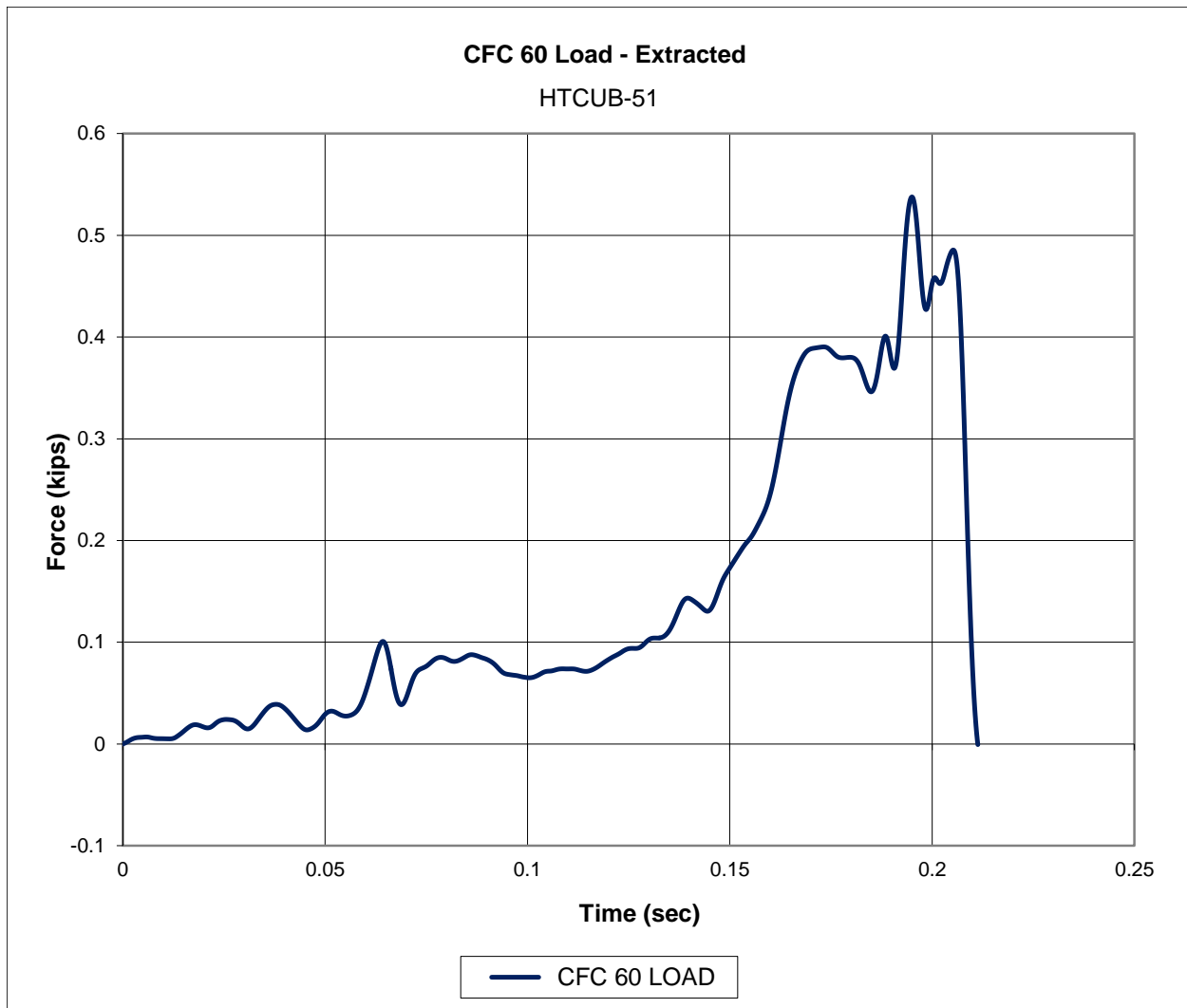
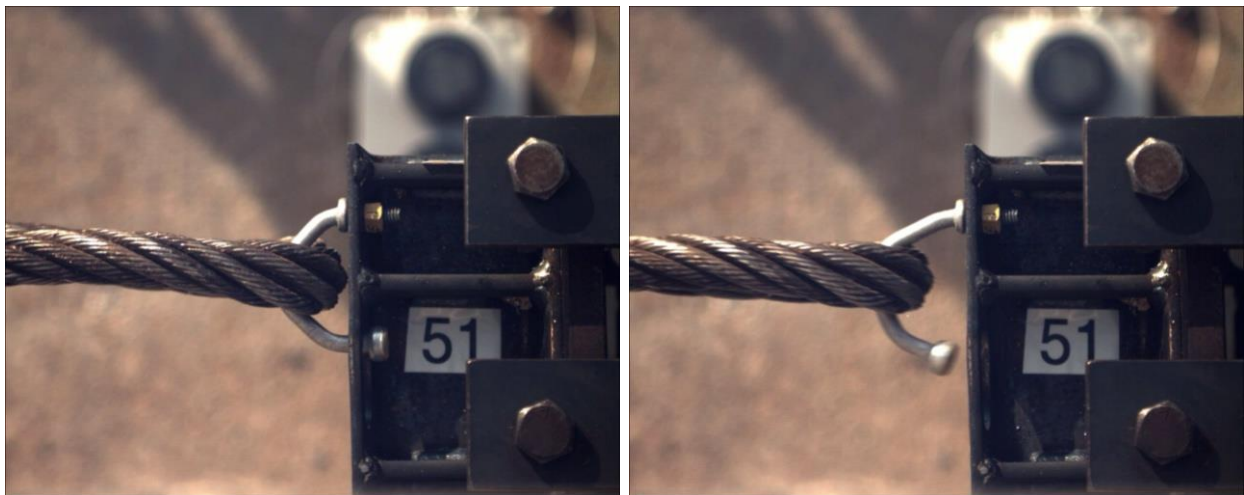


Figure 98. Force-Time Data, Test No. HTCUB-51

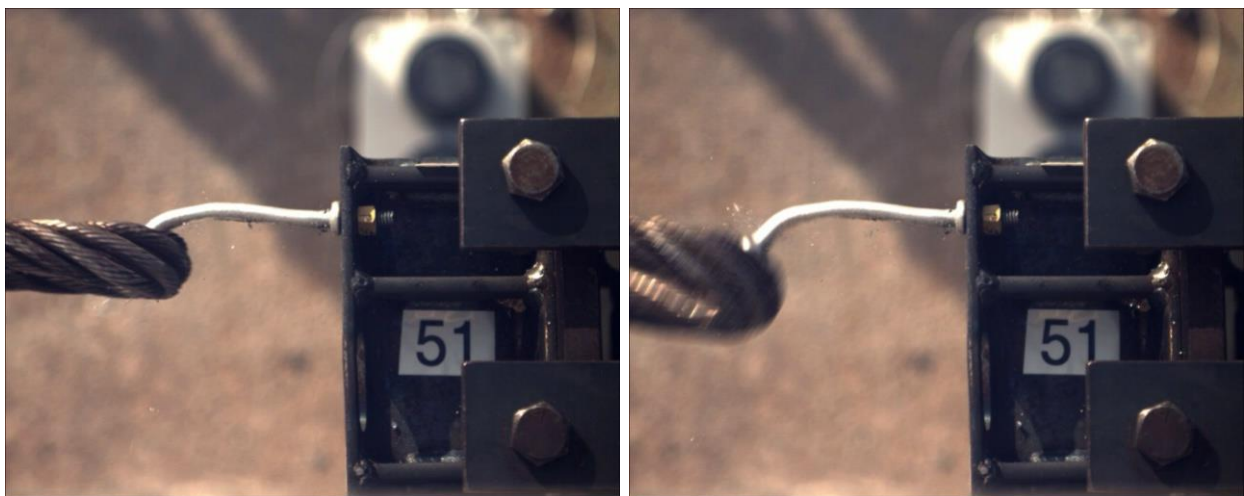


Figure 99. Pre-Test and Post-Test Photographs, Test No. HTCUB-51



Time = 0 sec

Time = 0.176 sec



Time = 0.204 sec

Time = 0.212 sec, Release

Figure 100. Sequential Photographs, Test No. HTCUB-51

7.1.15 Test No. HTCUB-52 (C1018 KB, Large, Lateral)

For test no. HTCUB-52, the cable pulled on the AISI C1018 keyway bolt at an angle of 90 degrees, perpendicular to the front face of the flange, thus imparting a lateral load. The keyway bolt was attached to the front flange with one grade 8 nut. The large oversized keyway was used for this test. As the cable began to pull on the bolt, the button head was not caught or snagged on the bottom or side of the keyway but released through the keyway freely. A peak load of 544 lb (2.42 kN) occurred as the bolt was bent straight out by the cable. The force versus time plot is shown in Figure 101. Pre- and post-test photographs are shown in Figure 102. Sequential photographs are shown in Figure 103.

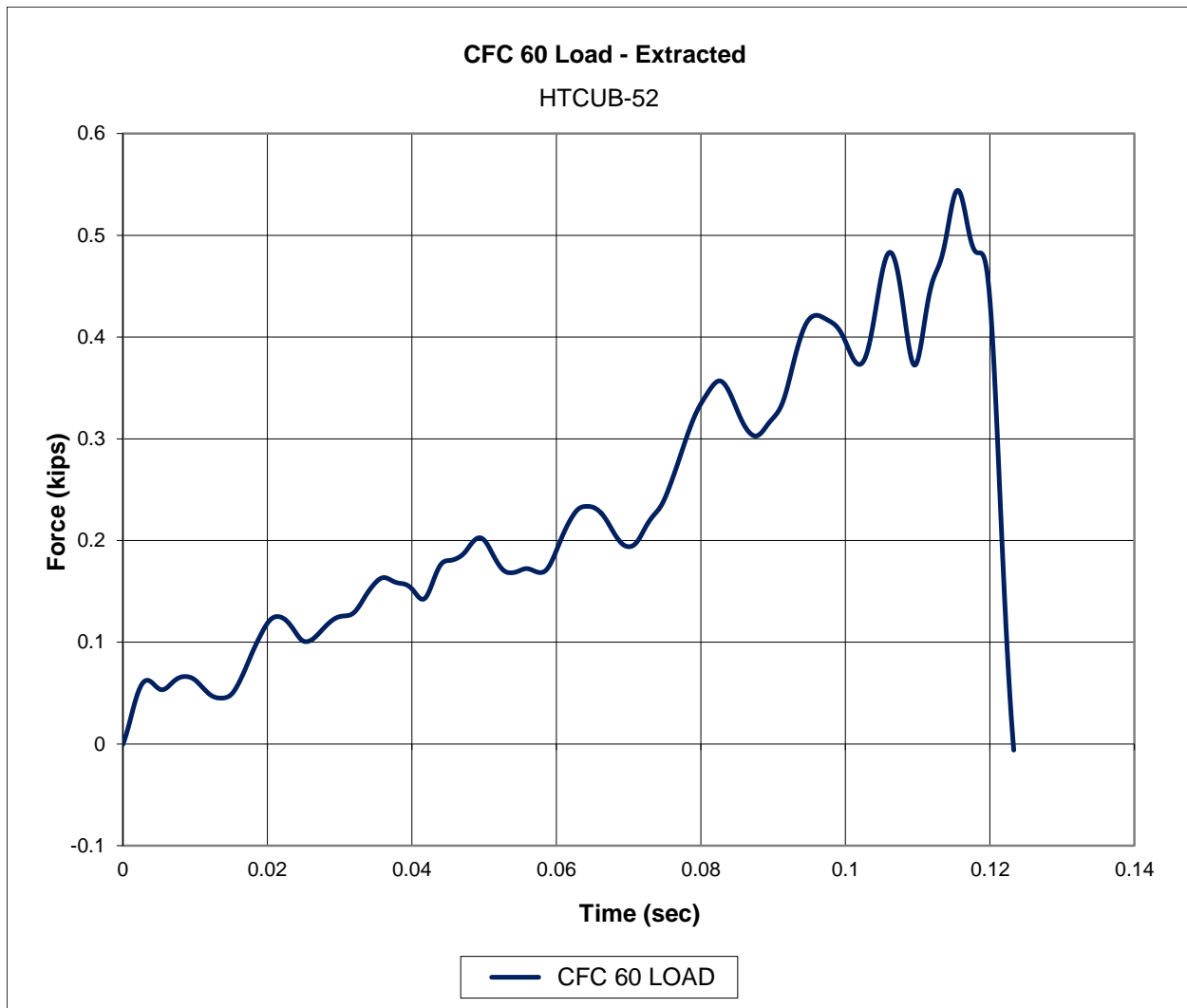


Figure 101. Force-Time Data, Test No. HTCUB-52

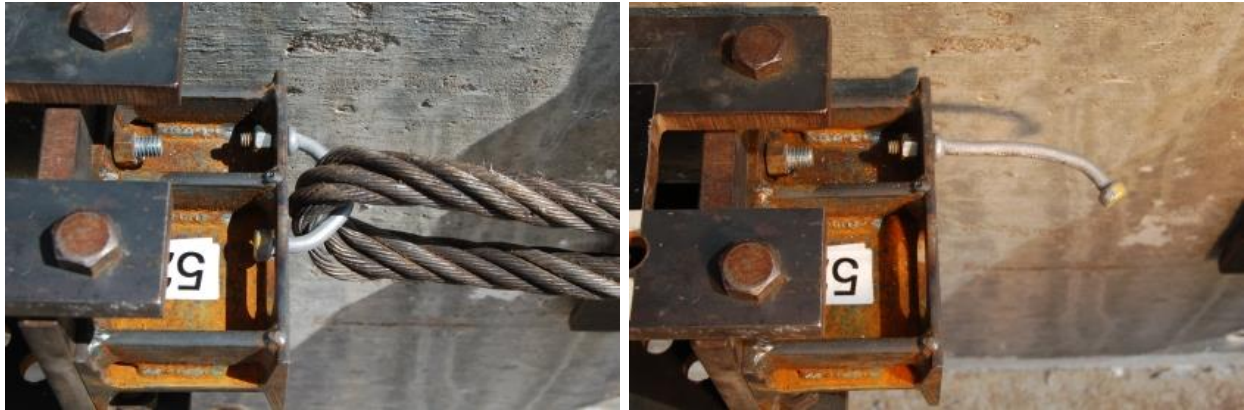
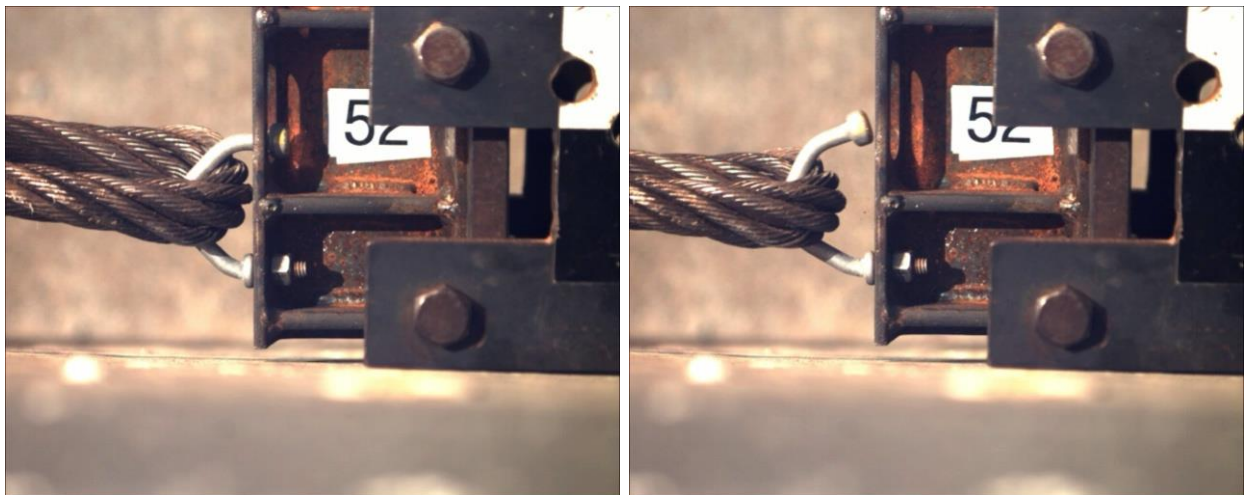
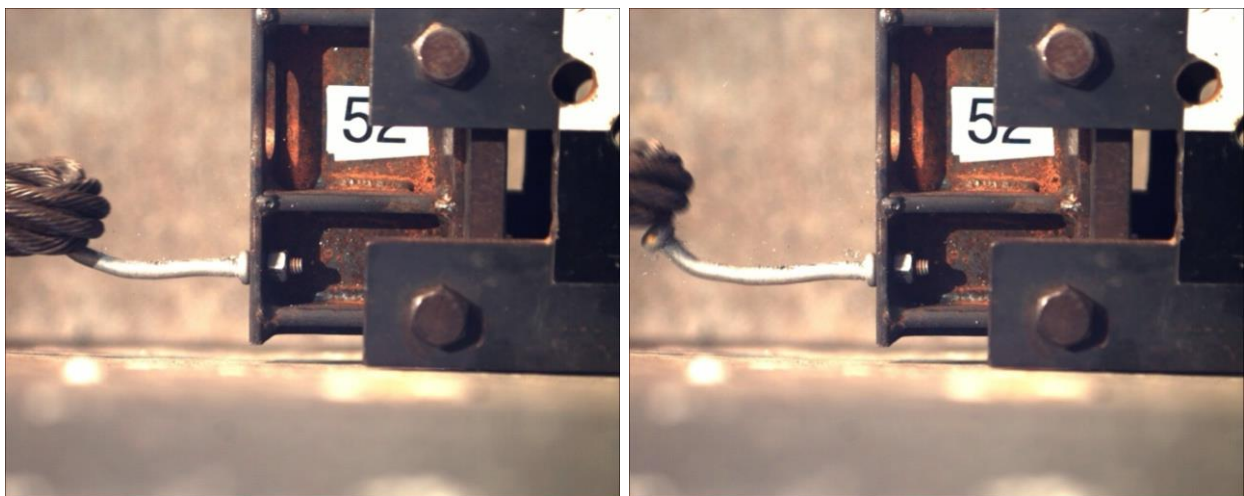


Figure 102. Pre-Test and Post-Test Photographs, Test No. HTCUB-52



Time = 0 sec

Time = 0.088 sec



Time = 0.116 sec

Time = 0.124 sec, Release

Figure 103. Sequential Photographs, Test No. HTCUB-52

7.1.16 Test No. HTCUB-53 (C1018 KB, Large, Lateral)

For test no. HTCUB-53, the cable pulled on the AISI C1018 keyway bolt at an angle of 90 degrees, perpendicular to the front face of the flange, thus imparting a lateral load. The keyway bolt was attached to the front flange with one grade 8 nut. The large oversized keyway was used for this test. As the cable began to pull on the bolt, the button head was not caught or snagged on the bottom or side of the keyway, but released through the keyway freely. A peak load of 1.53 kips (6.81 kN) occurred as the bolt was bent straight out by the cable. The force versus time plot is shown in Figure 104. Pre- and post-test photographs are shown in Figure 105. Sequential photographs are shown in Figure 106.

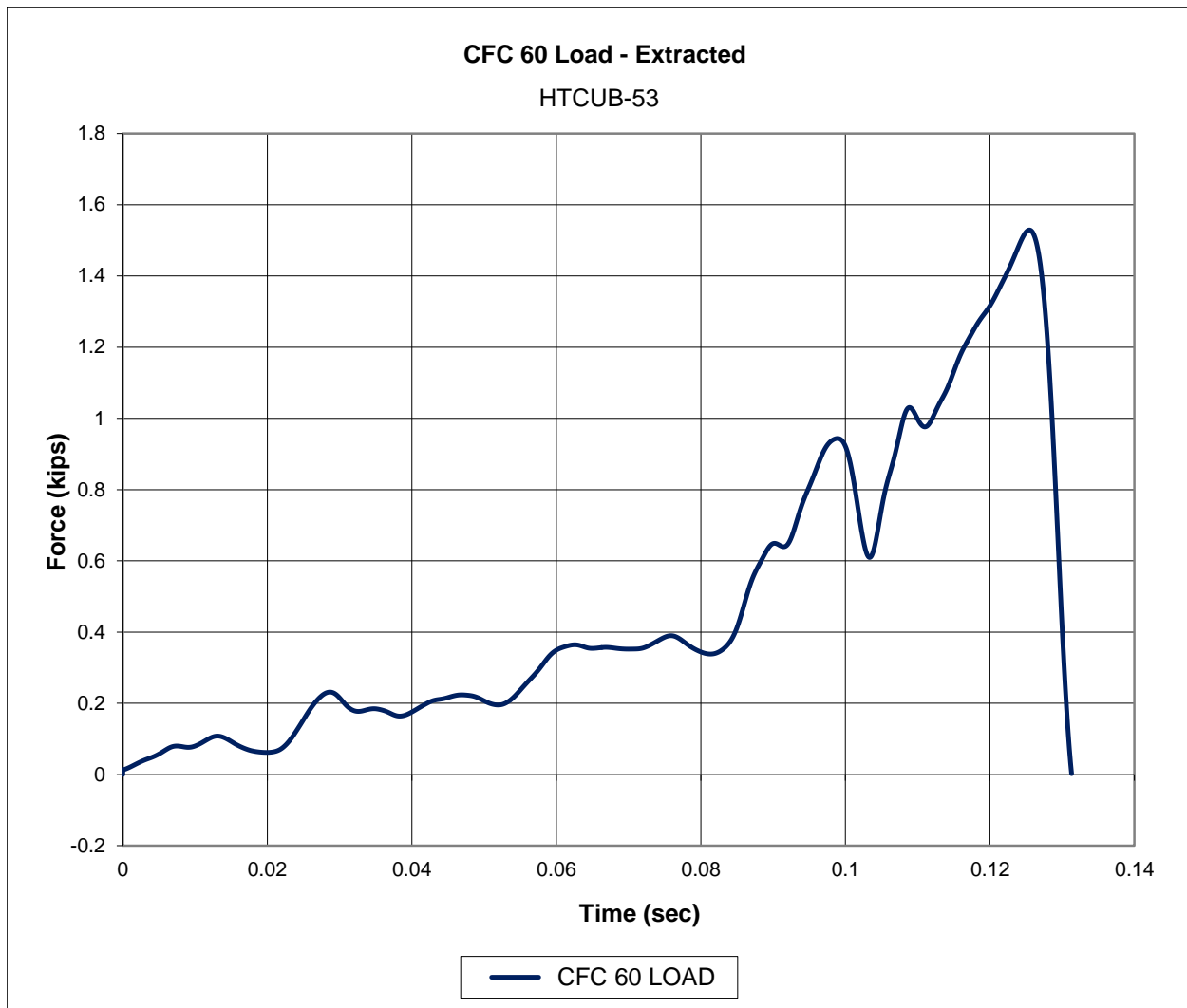


Figure 104. Force-Time Data, Test No. HTCUB-53

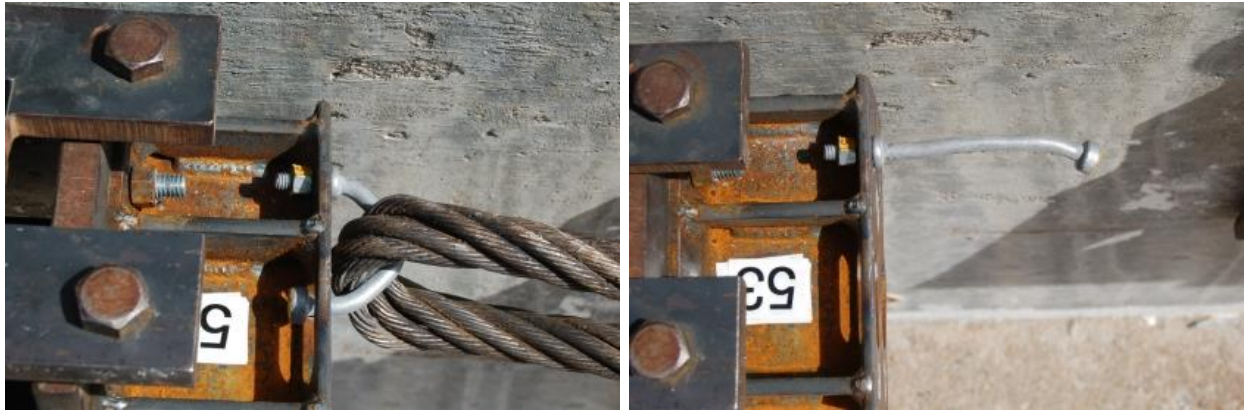
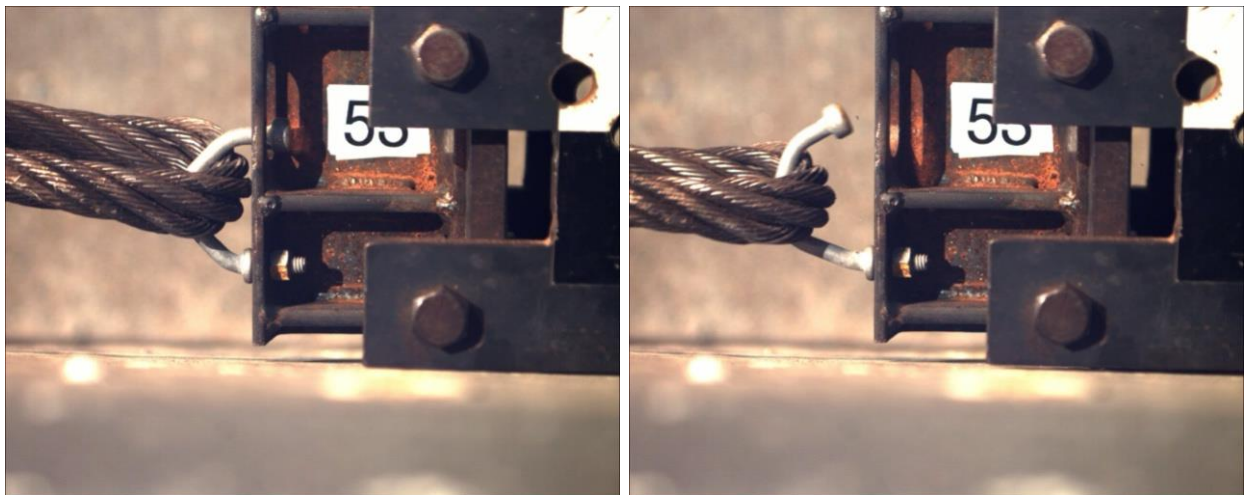
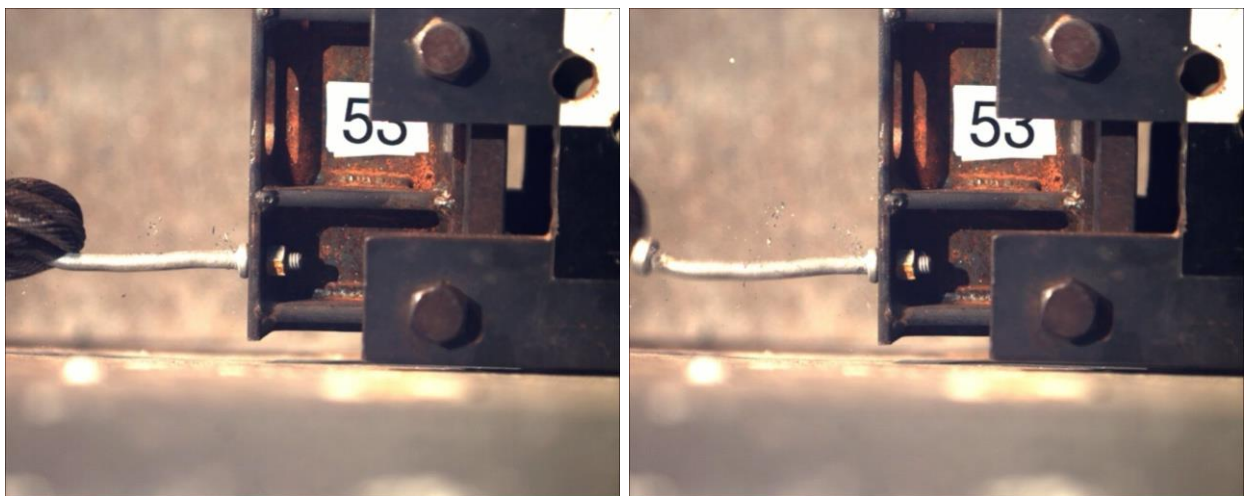


Figure 105. Pre-Test and Post-Test Photographs, Test No. HTCUB-53



Time = 0 sec

Time = 0.086 sec



Time = 0.124 sec

Time = 0.132 sec, Release

Figure 106. Sequential Photographs, Test No. HTCUB-53

7.1.17 Test No. HTCUB-54 (C1018 Mod. KB, Large, Lateral)

For test no. HTCUB-54, the cable pulled on the AISI C1018, modified keyway bolt at an angle of 90 degrees, perpendicular to the front face of the flange, thus imparting a lateral load. The keyway bolt was attached to the front flange with one grade 8 nut. The large oversized keyway was used for this test. As the cable began to pull on the bolt—before the bolt began to bend—it rotated about its fixed end so that the end of the shaft, just before the button head, came to rest against the side of the keyway. A peak load of 2.90 kips (12.9 kN) occurred as the cable continued to pull on the bolt. Finally, the button head slipped out, and the cable was released as the bolt was straightened. The force versus time plot is shown in Figure 107. Pre- and post-test photographs are shown in Figure 108. Sequential photographs are shown in Figure 109.

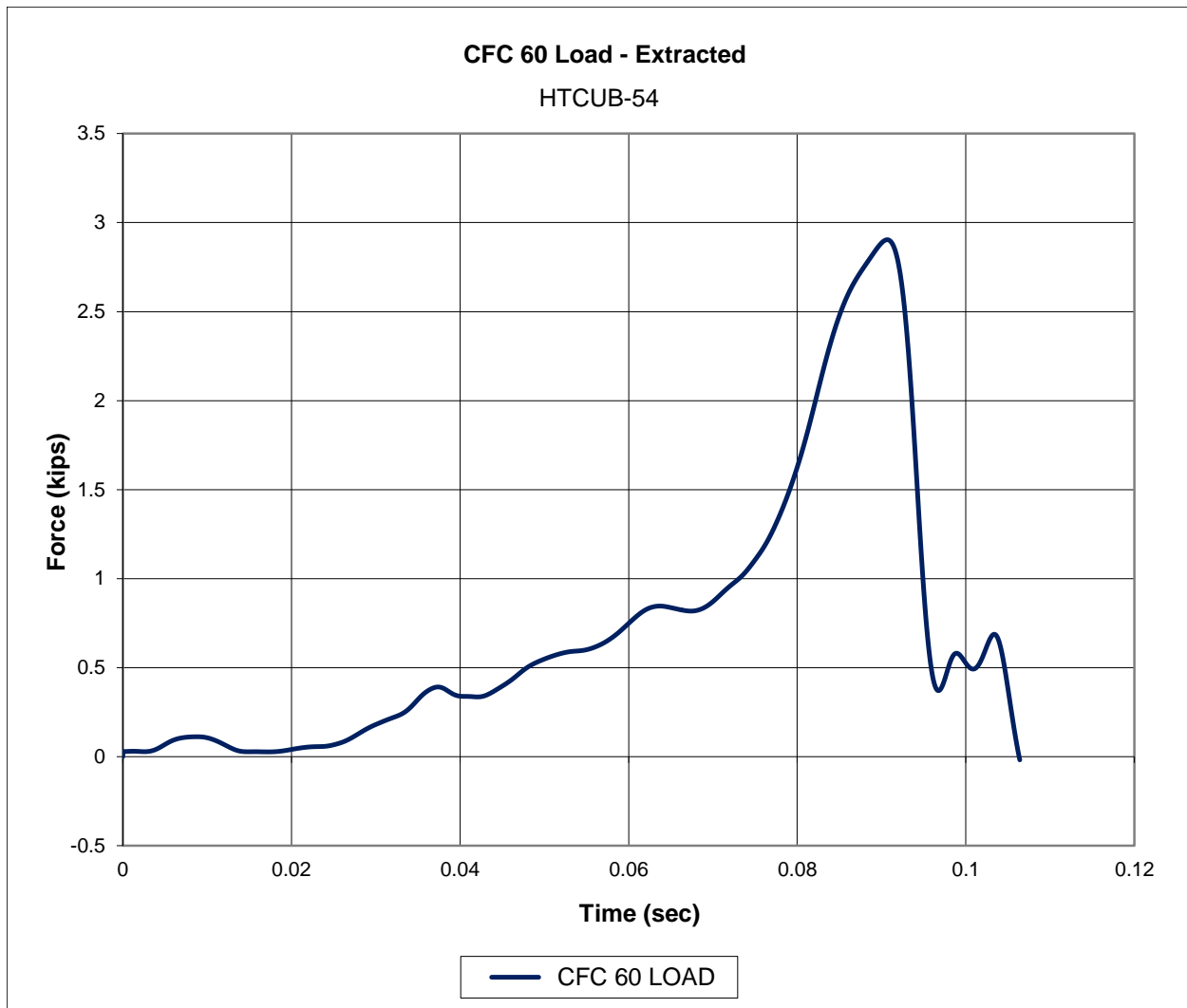


Figure 107. Force-Time Data, Test No. HTCUB-54

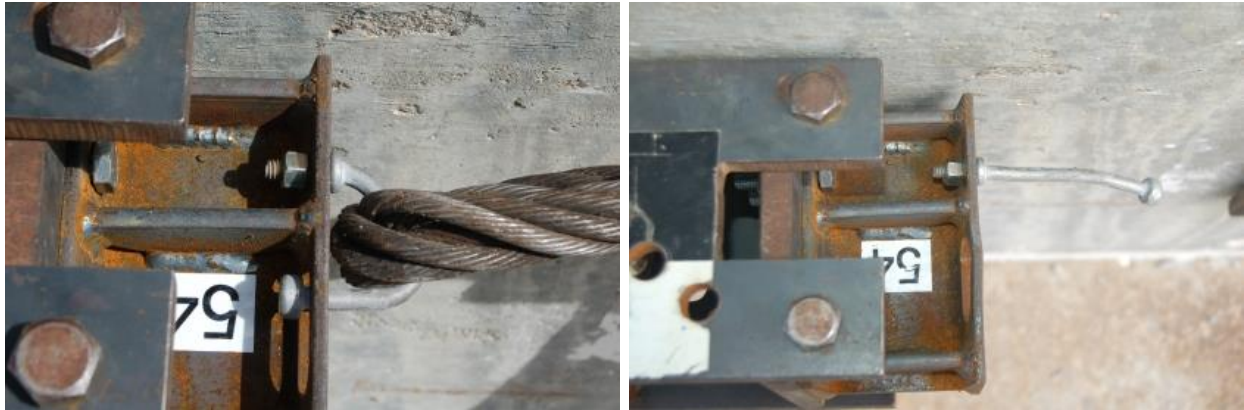
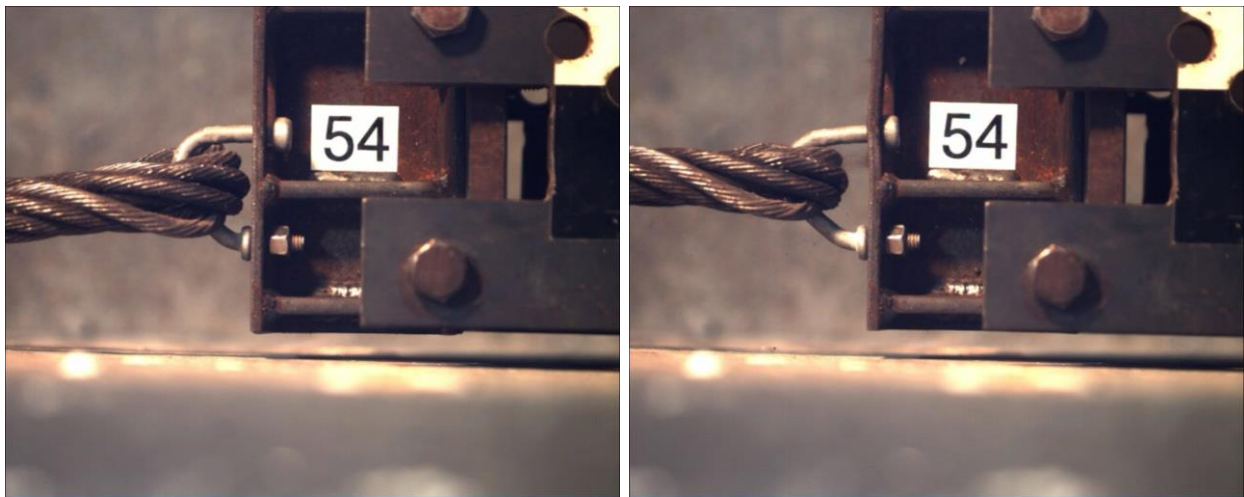
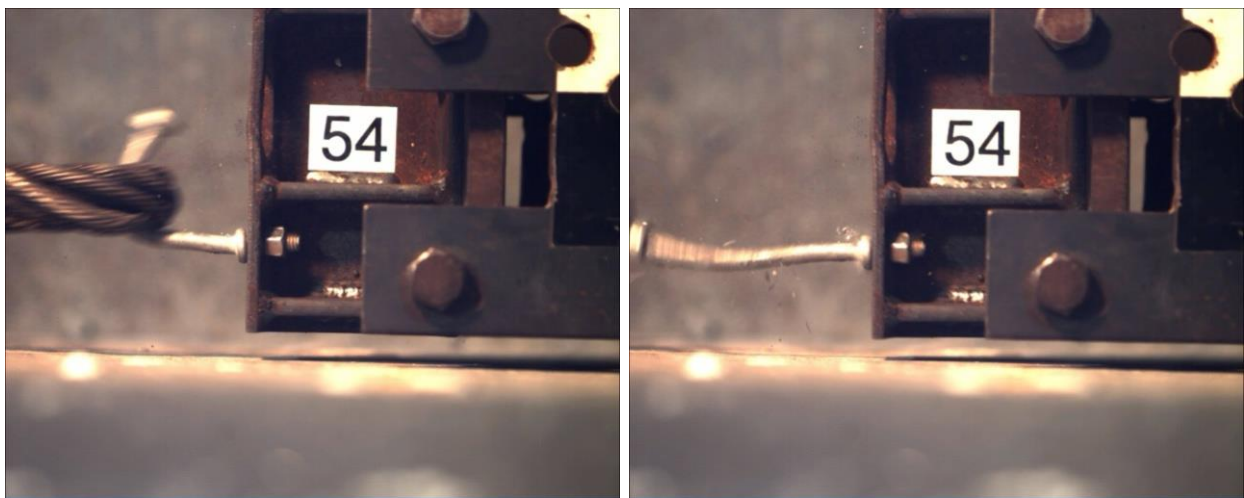


Figure 108. Pre-Test and Post-Test Photographs, Test No. HTCUB-54



Time = 0 sec

Time = 0.214 sec



Time = 0.218 sec

Time = 0.226 sec, Release

Figure 109. Sequential Photographs, Test No. HTCUB-54

7.1.18 Test No. HTCUB-55 (C1018 Mod. KB, Large, Lateral)

For test no. HTCUB-55, the cable pulled on the AISI C1018, modified keyway bolt at an angle of 90 degrees, perpendicular to the front face of the flange, thus imparting a lateral load. The keyway bolt was attached to the front flange with one grade 8 nut. The large oversized keyway was used for this test. As the cable began to pull on the bolt, the button head was not caught or snagged on the bottom or side of the keyway but released through the keyway freely. A peak load of 798 lb (3.55 kN) occurred as the bolt was bent straight out by the cable. The force versus time plot is shown in Figure 110. Pre- and post-test photographs are shown in Figure 111. Sequential photographs are shown in Figure 112.

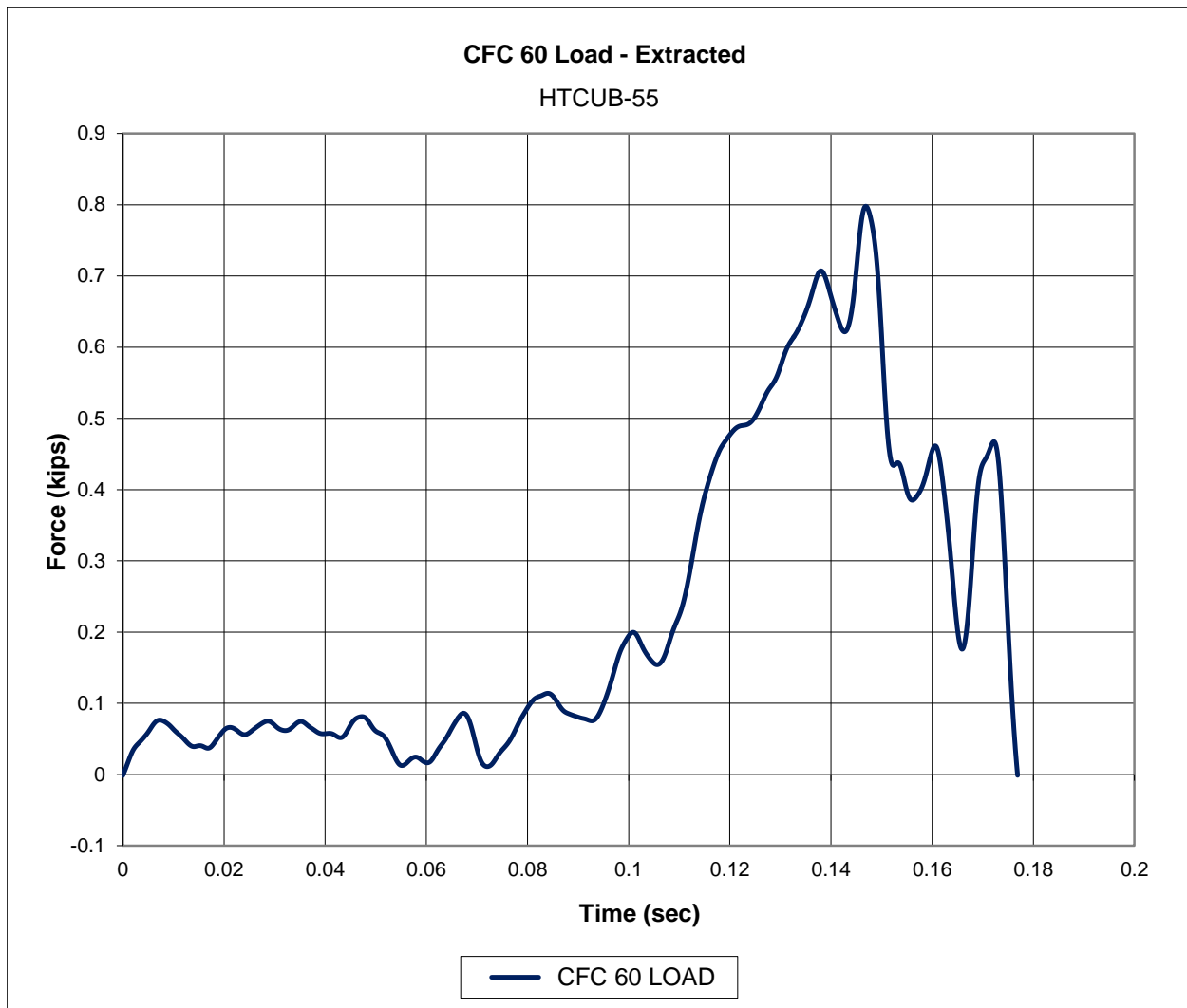


Figure 110. Force-Time Data, Test No. HTCUB-55

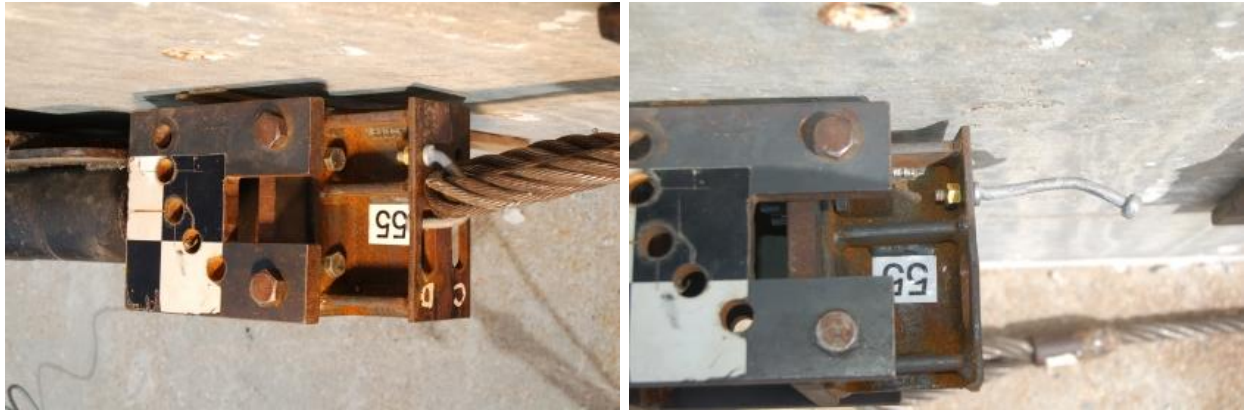
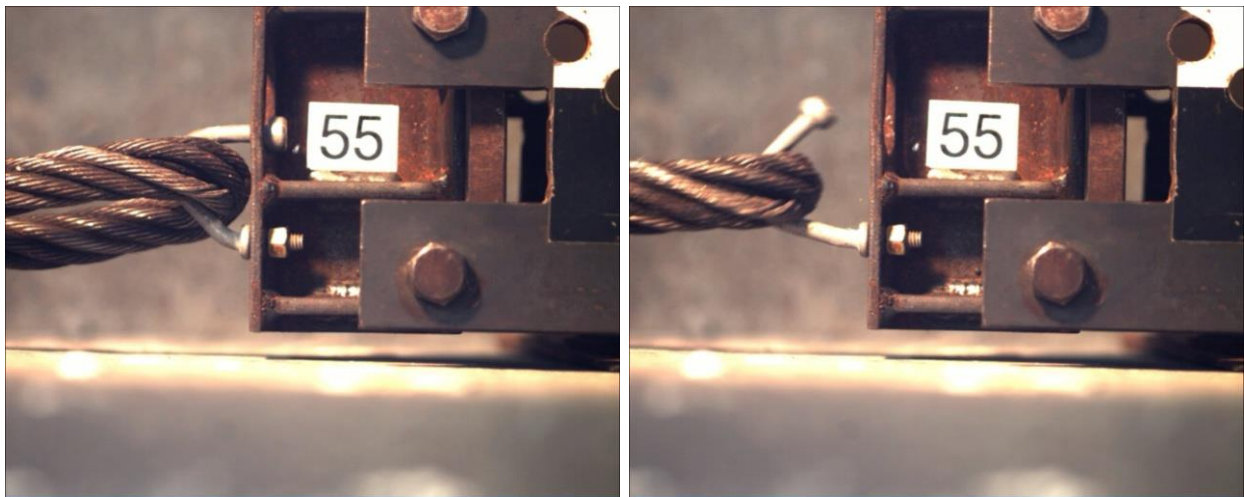
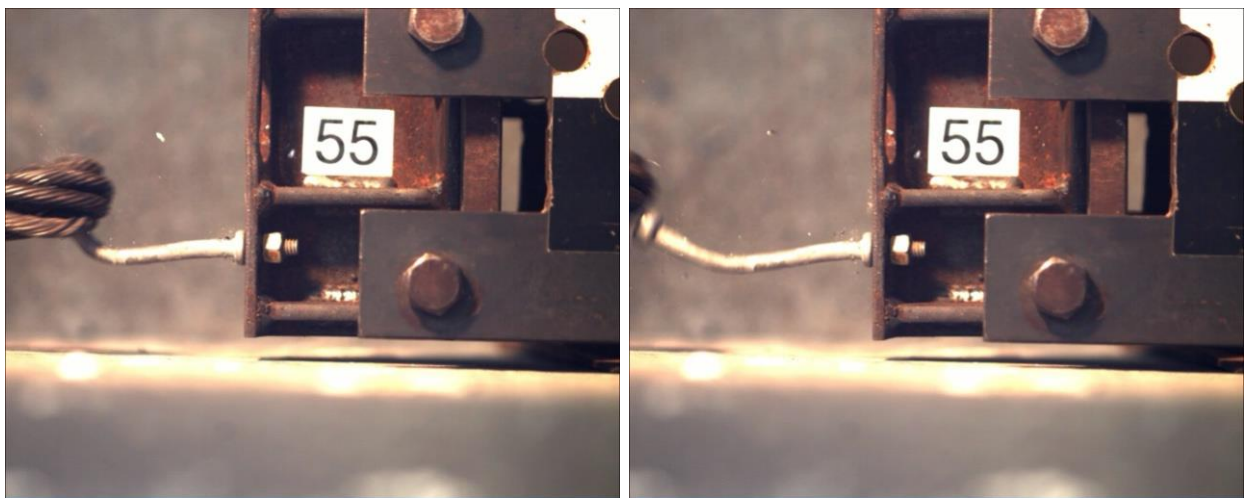


Figure 111. Pre-Test and Post-Test Photographs, Test No. HTCUB-55



Time = 0 sec

Time = 0.140 sec



Time = 0.160 sec

Time = 0.176 sec, Release

Figure 112. Sequential Photographs, Test No. HTCUB-55

7.1.19 Test No. HTCUB-56 (C1018 Mod. KB, Large, Vertical)

For test no. HTCUB-56, the cable pulled on the AISI C1018, modified keyway bolt at an angle of 0 degrees, parallel to the front face of the flange, thus imparting a vertical load. The keyway bolt was attached to the front flange with one grade 8 nut. The large oversized keyway was used for this test. As the cable began to pull on the bolt, the button head was caught on the side of the keyway. A peak load of 1.71 kips (7.61 kN) occurred as the button head rubbed against the back of the flange, while the bolt was being pulled upward. Finally, the button head slipped off the side of the keyway and released through it. A smaller button snag load of 671 lb (2.98 kN) occurred after the button head cleared the keyway. The force versus time plot is shown in Figure 113. Pre- and post-test photographs are shown in Figure 114. Sequential photographs are shown in Figure 115.

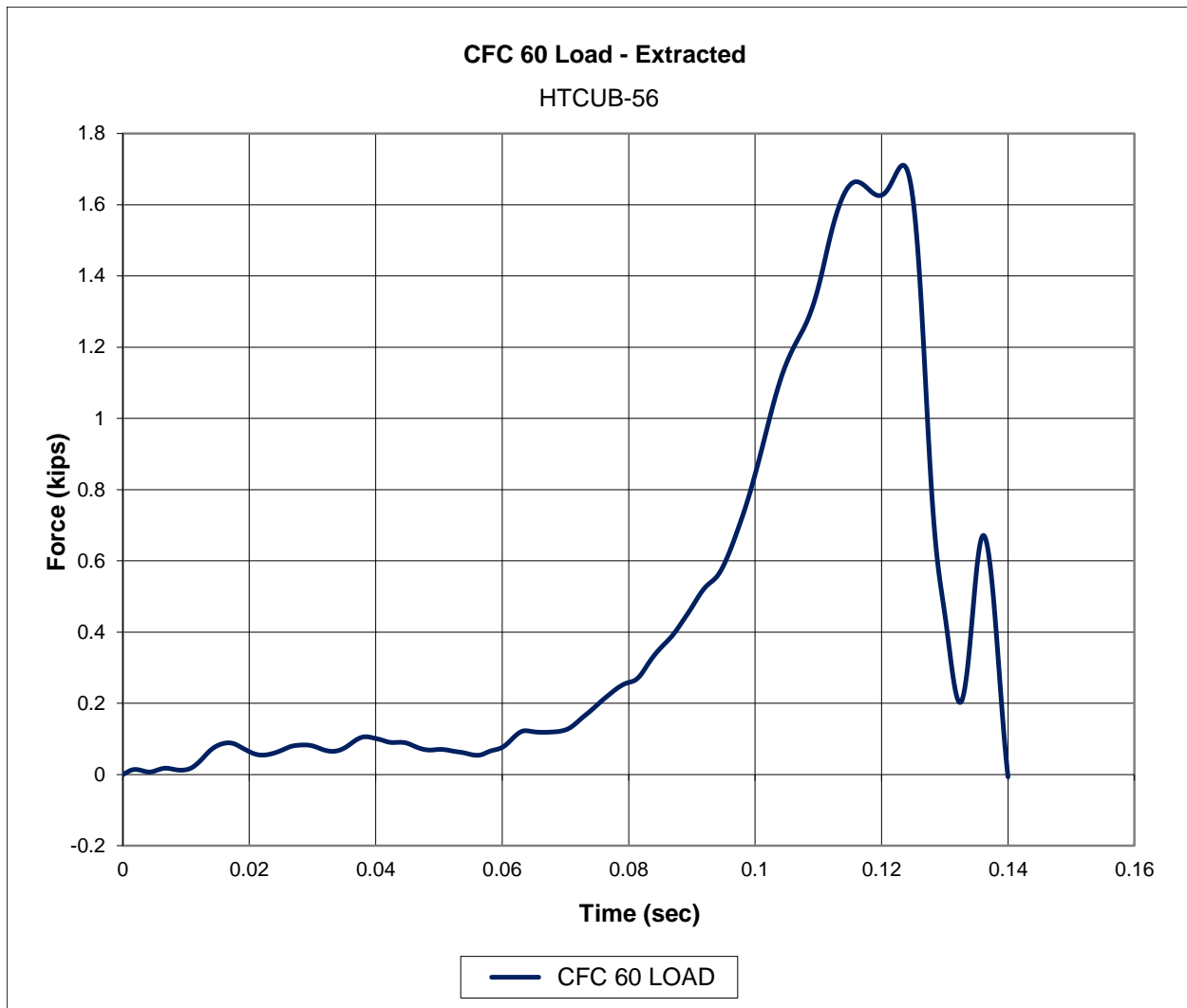
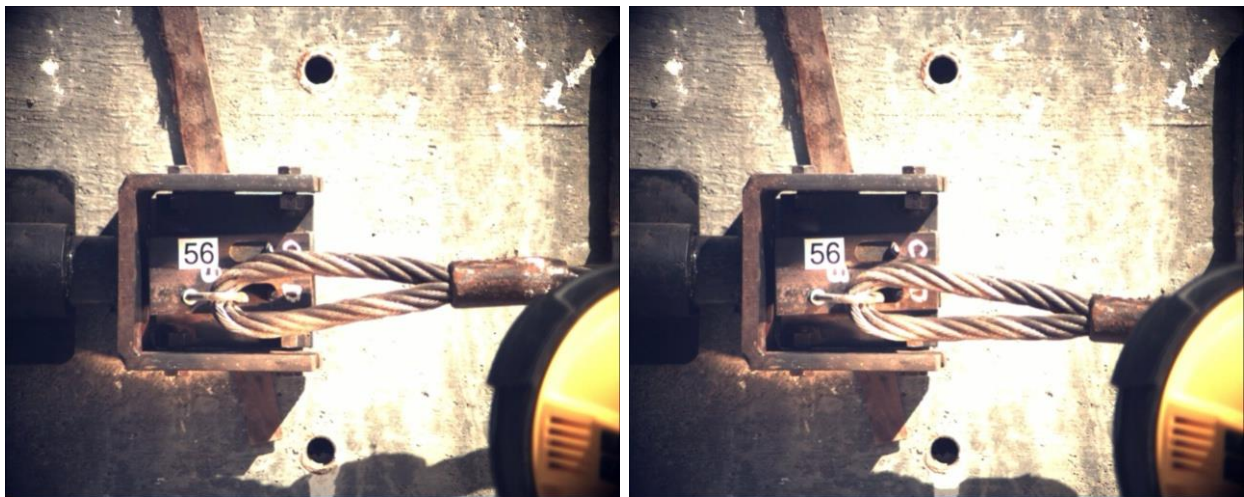


Figure 113. Force-Time Data, Test No. HTCUB-56

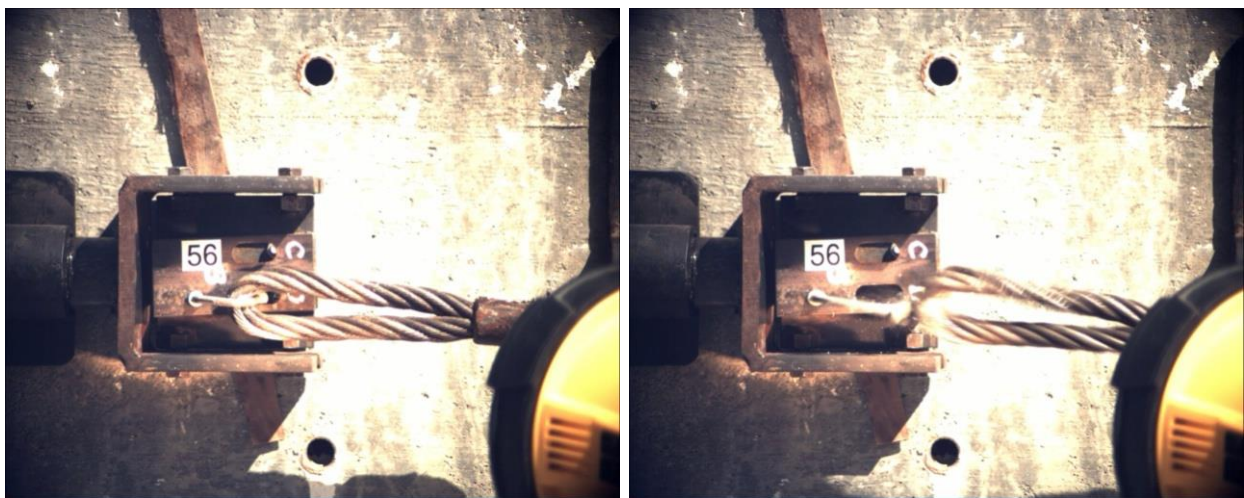


Figure 114. Pre-Test and Post-Test Photographs, Test No. HTCUB-56



Time = 0 sec

Time = 0.098 sec



Time = 0.122 sec

Time = 0.140 sec, Release

Figure 115. Sequential Photographs, Test No. HTCUB-56

7.1.20 Test No. HTCUB-57 (C1018 Mod. KB, Large, Vertical)

For test no. HTCUB-57, the cable pulled on the AISI C1018, modified keyway bolt at an angle of 0 degrees, parallel to the front face of the flange, thus imparting a vertical load. The keyway bolt was attached to the front flange with one grade 8 nut. The large oversized keyway was used for this test. As the cable began to pull on the bolt, the button head was caught on the side of the keyway. A peak load of 1.17 kips (5.20 kN) occurred as the button head rubbed against the back of the flange, while the bolt was being pulled upward. Finally, the button head slipped off the side of the keyway and released through it. A smaller button snag load of 704 lb (3.13 kN) occurred after the button head cleared the keyway. The force versus time plot is shown in Figure 116. Pre- and post-test photographs are shown in Figure 117. Sequential photographs are shown in Figure 118.

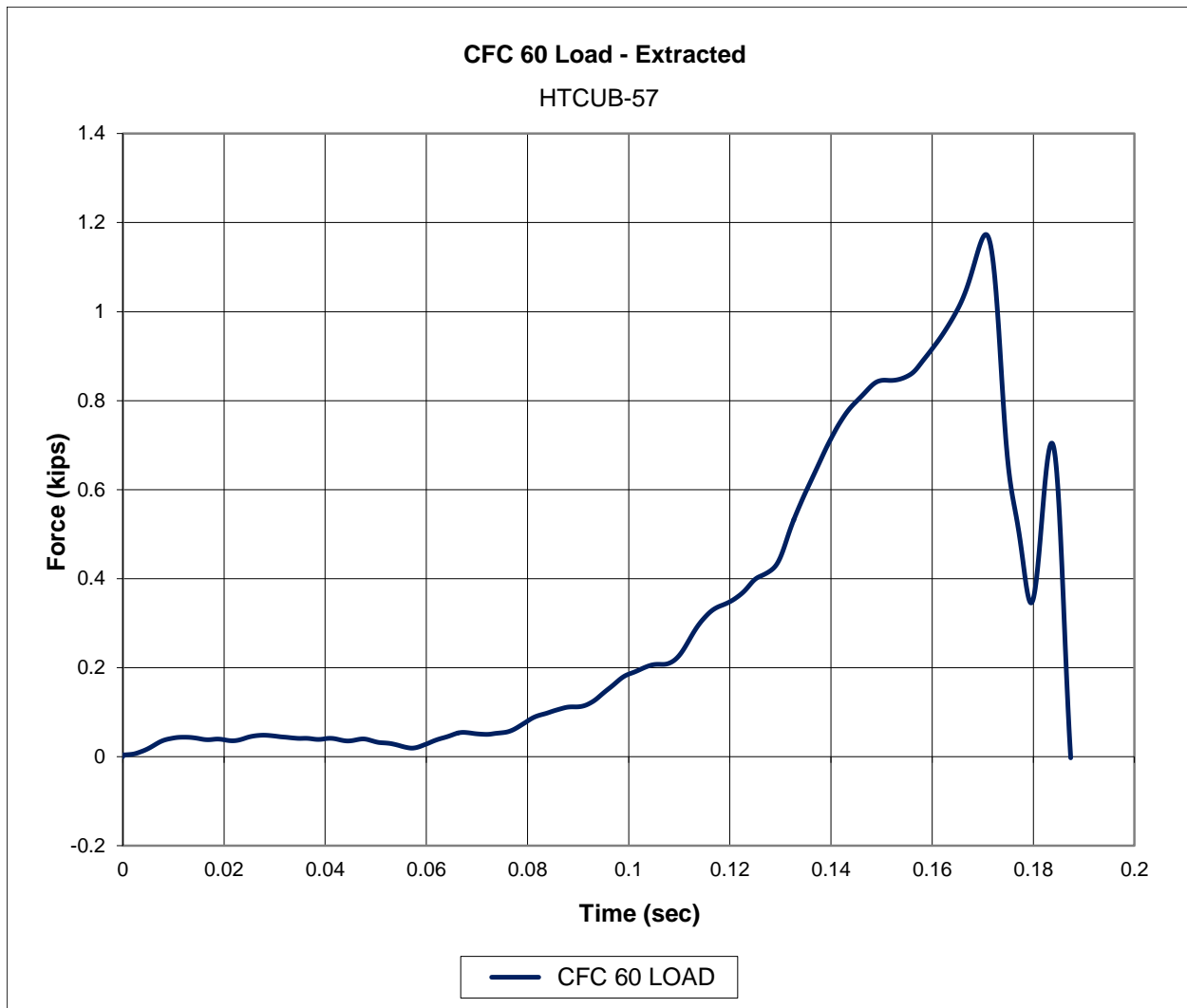


Figure 116. Force-Time Data, Test No. HTCUB-57

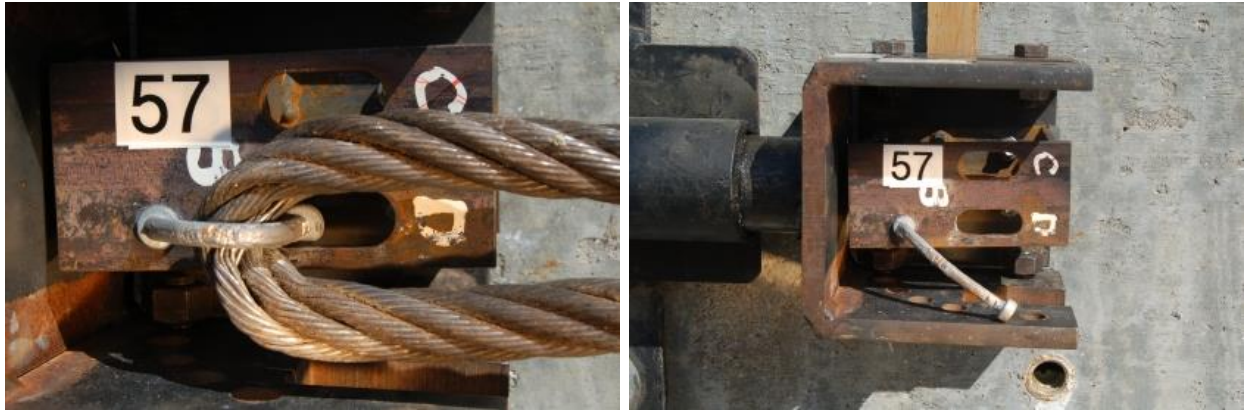


Figure 117. Pre-Test and Post-Test Photographs, Test No. HTCUB-57

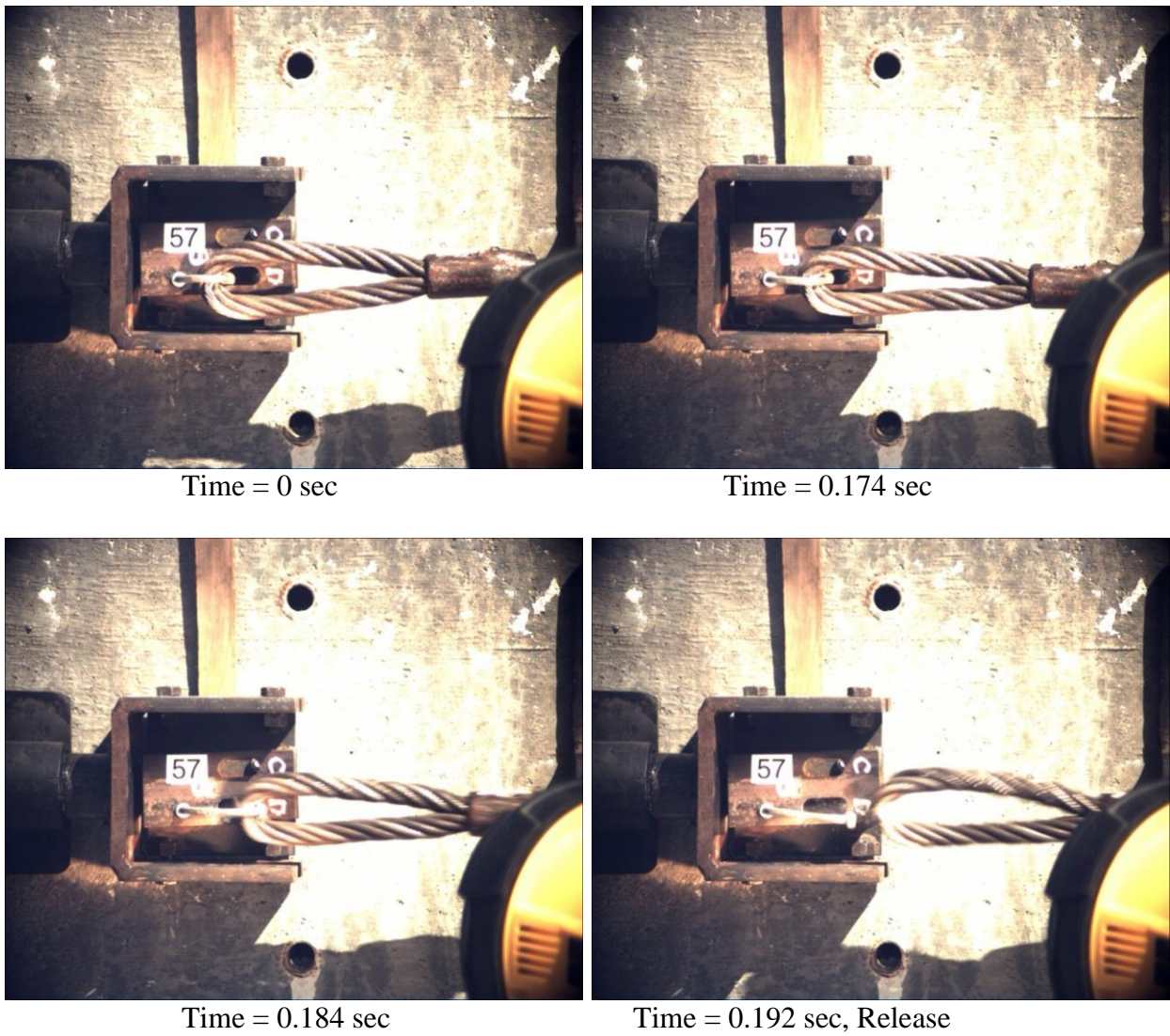


Figure 118. Sequential Photographs, Test No. HTCUB-57

7.2 Discussion

Twenty dynamic component tests were performed in the first round, which focused on reducing both the lateral and vertical release loads. To that end, these tests were successful. This goal was accomplished by making the keyways larger as well as by reducing or eliminating the contact surface area between the button head of the bolt and the backside of the flange.

Due to the 1/16-in. (2-mm) design overlap between the button head of the keyway bolts and the bottom of the small oversized keyway, the lateral release loads of the keyway bolts were expected to be much higher when placed in the small oversized keyway versus the large oversized keyway. In general, this was not the case. In three out of four lateral pull tests on keyway bolts placed in small oversized keyways, the button head slipped out of the keyway freely, demonstrating that the minimum overlap of 1/16 in. (2 mm) was ineffective. As such, the keyway bolts would not be able to achieve the target lateral release load of 6.00 kips (26.7 kN) when placed in either of the small or large oversized keyways.

When pulled vertically, both oversized keyways were expected to allow the button heads of the keyway bolts to properly release without scraping against the back side of the flange. When a free release behavior was observed, the vertical release loads were much lower than 1.18 kips (5.25 kN), as observed for the A449 keyway bolts in the dual width keyways. However, in the case of test nos. HTCUB-56 and HTCUB-57, the button head of the modified keyway bolts drifted to the side of the keyway prior to loading. As a result, when the modified keyway bolts were pulled vertically, the button heads scraped against the back side of the front flange but alongside the edge of the keyway, causing vertical release loads as high as 1.71 kips (7.61 kN), which was undesirable.

After careful consideration based on group discussions in several design meetings, none of the Round 1 designs were believed to provide the ideal release behavior. The lateral release

loads were too low and the vertical release loads were too high. Thus, oversized keyways were not used with the second round of keyway bolt modifications, as described in Chapters 8 and 9.

8 OVERVIEW OF IMPROVED KEYWAY BOLTS—ROUND 2

8.1 Introduction

After the first round of tests, some decisions were made about the future of the keyway bolts. Based on these discussions, it was determined that no further tests would be performed on keyway bolts installed in small or large oversized keyways. In tests to follow, some variation of the dual-width keyway would be used. The focus of the design effort shifted toward the keyway bolt itself. More specifically, it was highly desirable to achieve cable release at a lower vertical load, while maintaining an adequate lateral release load. To accomplish this goal, it would be necessary to take a closer look at the keyway bolts.

8.2 Extended Moment Arm Concepts

One way to decrease the vertical release of the cable would be to extend the moment arm of the applied force and the critical bending location. This concept can also be applied to the keyway bolts, as shown in Figure 119. The moment arm in Figure 119b is from the center of the cable (where the vertical force can be assumed to act) to the center of the outermost point of the bolt (where the maximum moment will be).

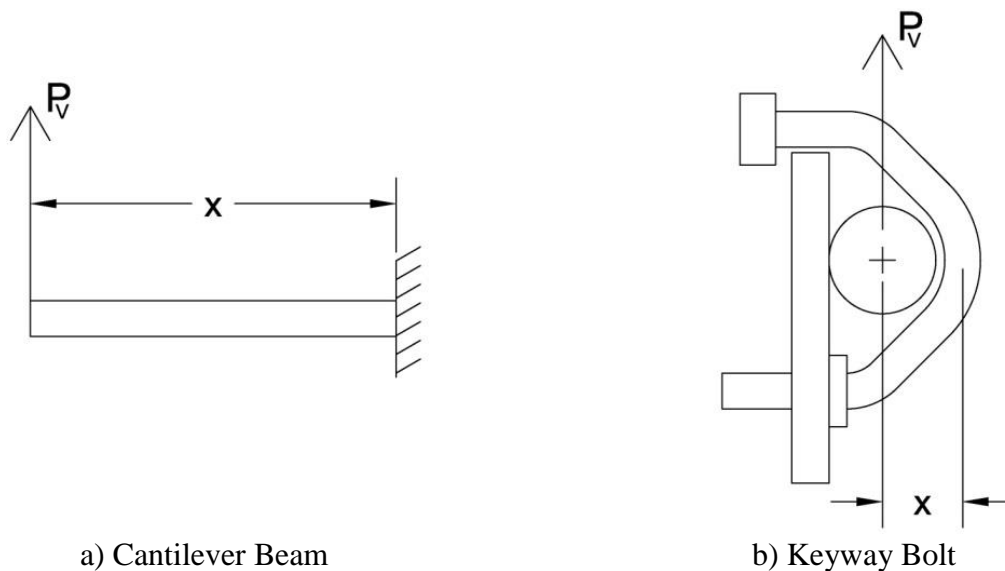


Figure 119. Moment Arm Concept—(a) Cantilever Beam and (b) Keyway Bolt

An equation was derived for the maximum vertical load that could be resisted by the keyway bolt. A pure plastic bending condition was assumed. The bending moment resistance for a pure plastic bending condition is given below.

$$M_p = Z\sigma_y$$

Where M_p = plastic moment
 Z = plastic section modulus
 σ_y = yield strength of the bolt

For a circular cross-section,

$$Z = \frac{d^3}{6}$$

Where d = diameter of the cross-section

Under dynamic loading conditions, a dynamic magnification factor is often used to account for strain rate effects. For the derivation of these equations, a dynamic magnification factor of 1.5 was assumed. This factor is empirical, and it is based on observations of steel guardrail or bridge rail posts placed in rigid foundations and subjected to a cantilevered load condition in bending [12]. To solve for the maximum vertical load that could be resisted by the keyway bolt, the applied moment was equated to the plastic bending resistance under dynamic loading conditions.

$$P_v x = 1.5M_p$$

$$P_V = \frac{1.5M_P}{x} = \frac{1.5\sigma_y Z}{x} = \frac{1.5\sigma_y \left(\frac{d^3}{6}\right)}{x} = \frac{\sigma_y d^3}{4x} \quad (8.1)$$

Where P_v = vertical release load of bolt
 x = moment arm (see Figure 119b)

The length of the moment arm, as defined in Figure 119b, was 0.56 in. (14 mm), and the diameter of the bolt was 1/4 in. (6 mm). Equation 4.1 provides a maximum vertical release load of 642 lb (2.86 kN) and 377 lb (1.68 kN) for the ASTM A449 and AISI C1018 bolts, respectively.

Equation 4.1 assumes that there is free release through the keyway without button head scraping on the back side surface of the front flange. It also does not account for the cable snagging on the button, or “button snag”. Button snag was observed in the first round of keyway bolt component tests. It would occur near the end of the release, after the button head had cleared the keyway but as the cable became momentarily snagged on the button. It was clearly distinguishable in the high-speed video footage and was characterized by a force spike in the load cell data. In most cases where button snag was distinguishable in the load cell data, there was a dip in the measured force just before an abrupt spike. An example of this behavior is shown in Figure 120. The load cell force peaked and began to dip around 0.15 sec, just before spiking due to button snag.

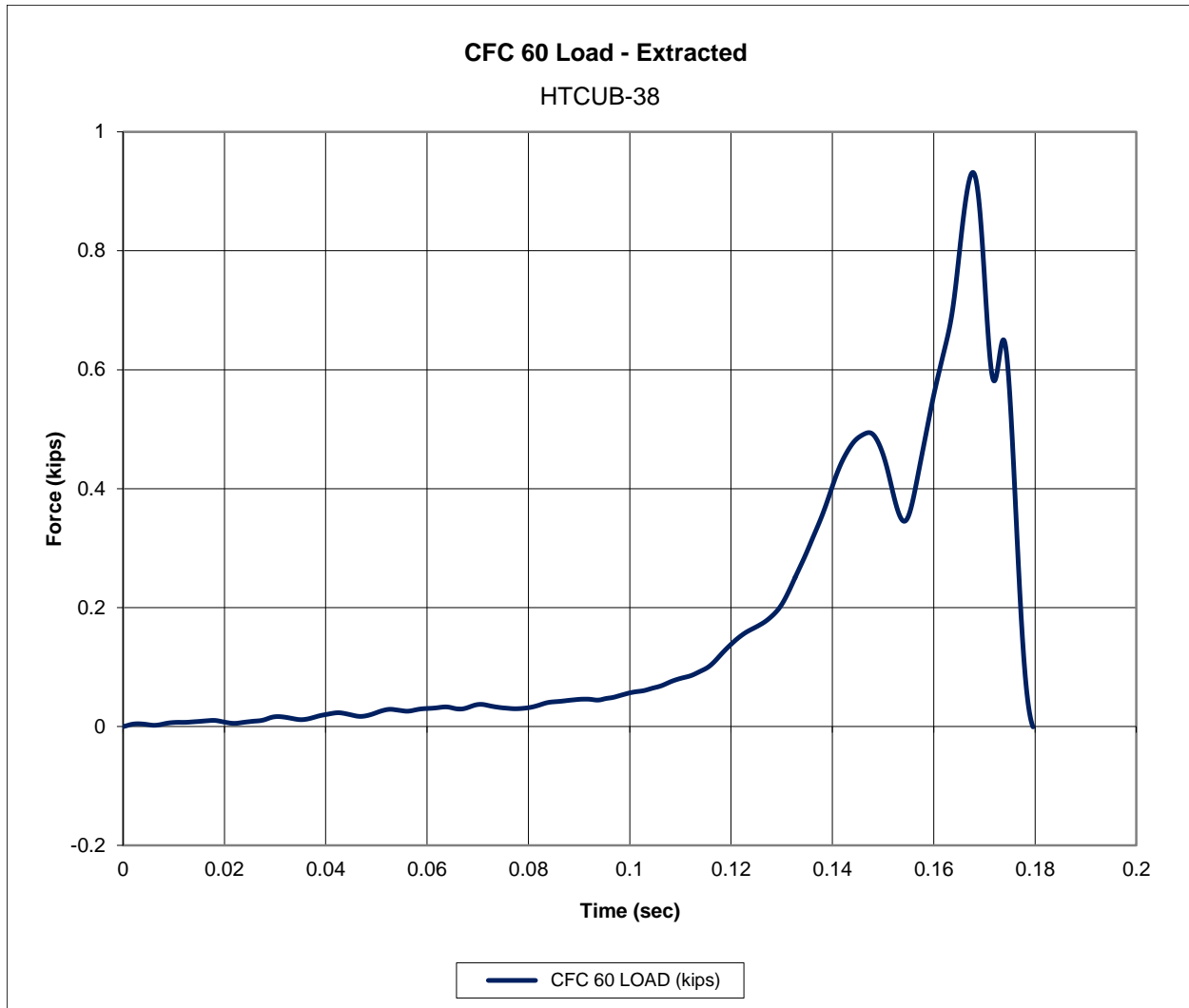


Figure 120. Button Snag in the Load Cell Data

After considering the actual conditions of the cable barrier, it was understood that the cable would not be wrapped (i.e., looped) around the cable-to-post attachment in the same manner as used in the component tests. Thus, it was assumed that the button snag phenomenon was unique to the component tests and therefore could be disregarded. If the button snag load was clearly distinguishable, it was not considered to be the critical peak load; since, it was not expected to occur in the actual cable barrier system.

Equation 8.1 served as a starting point for determining the required moment arm to reduce the vertical release load to 225 lb (1.00 kN)—the target set in the initial design meetings

and as discussed in Chapter 4. Accordingly, the required moment arms for the keyway bolts would be 1.60 in. (41 mm) for the ASTM A449 steel, and 0.938 in. (24 mm) for the AISI C1018 bolts, in order to keep the same curved shape, as shown in Figure 121.

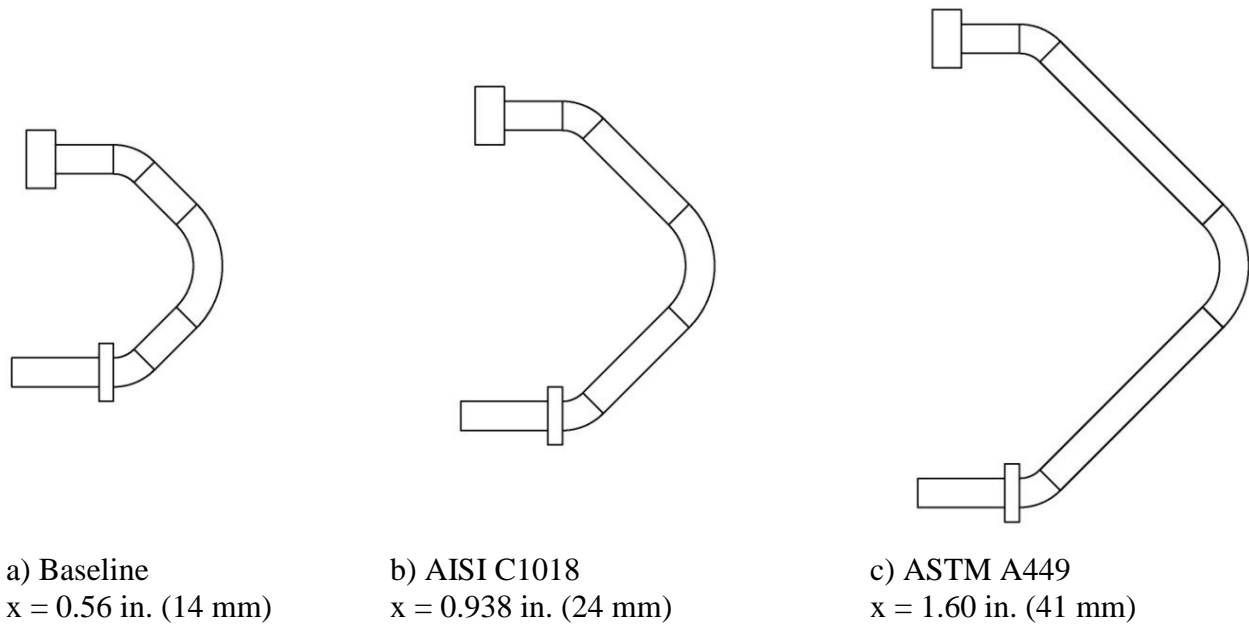


Figure 121. Extended-Moment-Arm Keyway Bolts—(a) Baseline, (b) AISI C1018, and (c) ASTM A449

The problem with the extended moment arm concepts was that there was so much more free space where the cables could float. For quality control reasons, it was preferable to have the cable confined to a smaller space so that the cable height would be consistent. One potential solution would be to bend the bolts in a way in which the cable's space would be more confined, while at the same time providing a long moment arm. Some of these concepts were actually drawn up, but the prototypes would be rather ridiculous and result in uneconomical bolts, as shown in Figure 122. The bolt in Figure 122a might have worked, but it provides an opportunity for installers to place the cable in the lower space. To eliminate installation error, a bolt concept with confined space was configured, as shown in Figure 122b. These two concepts were deemed too complicated. Thus, extended moment-arm concepts were not pursued any further.

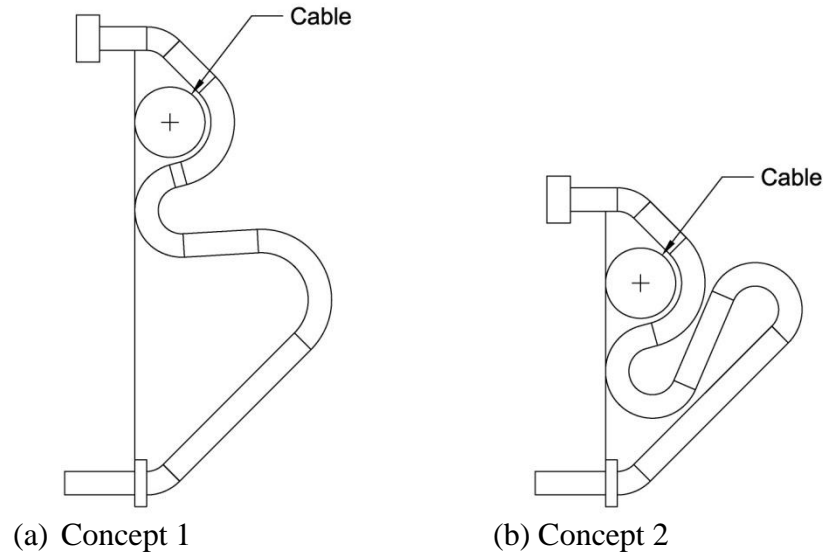


Figure 122. Extended Moment-Arm Concepts—(a) Concept 1 and (b) Concept 2

8.3 Extended Keyway Bolts

The oversized keyway tests showed that when button head scraping was eliminated, the vertical release loads were drastically reduced. The main reason for the scraping with the original keyway bolt installed in the dual-width keyway was the button head's close proximity to the backside surface of the post's front flange. This button head scraping could be reduced or eliminated with an extension added to the keyway bolt so that the button head was seated farther away from the inside of the front flange.

8.3.1 Computer Simulations

Before proceeding with dynamic component testing, the extended keyway bolt concept was investigated through the use of computer simulations. As part of a previous effort, MwRSF researchers developed an LS-DYNA computer simulation model of a vertical pull test on an ASTM A449 keyway bolt placed in a dual-width keyway. The model was based on test no. HTCUB-32, a dynamic component test (similar to the tests described in Chapter 6) from a previous cable-to-post attachment testing program [71]. The model is shown in Figure 123. For

details regarding the development and verification of the model, refer to the MwRSF research report [74].

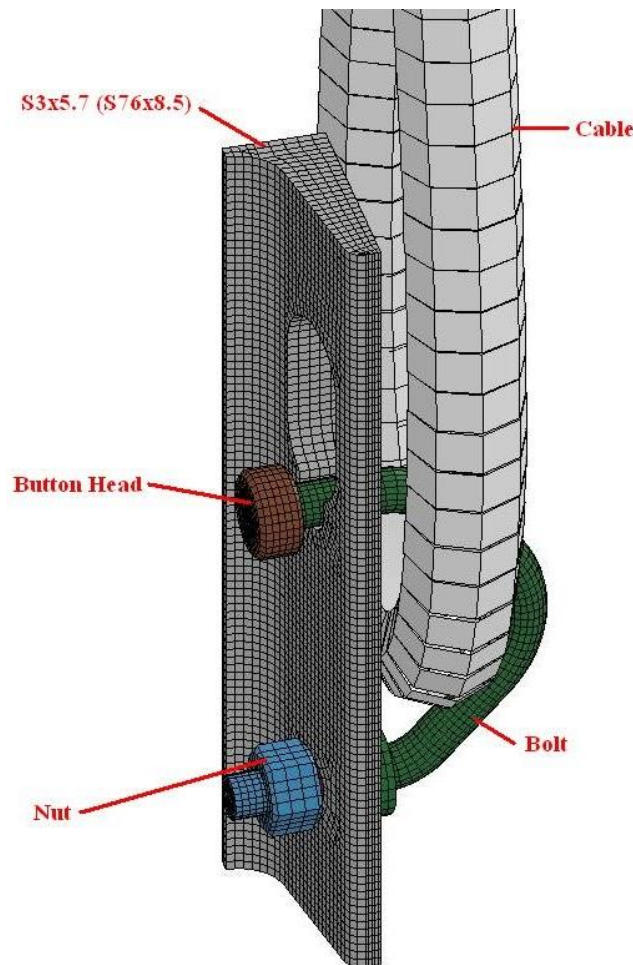


Figure 123. Baseline Keyway Bolt Model

Solid elements were used to model the bolt, nut, button head, and S3x5.7 (S76x8.5) post section. The 1/4-in. (6-mm) diameter keyway bolt was modeled with 59 elements in the cross-section, each having an average side length of 0.039 in. (1.0 mm). The elements in the button head were similar in size to those used for the bolt. A piecewise linear elastic-plastic material model was used to define properties of the ASTM A449 steel of the bolt and button head. A different piecewise linear elastic-plastic material model was used to define properties of the ASTM A36 steel used for the S3x5.7 (S76x8.5) post section. The nut was defined with a rigid

material model. All of the solid elements were single-point integrated. The elements of the bolt threads were given a pre-defined stress to simulate the bolt pre-tension. The friction coefficient between the bolt, the button head, and the post was 0.13.

The $\frac{3}{4}$ -in. (19-mm) diameter 7x19 wire rope (cable) was modeled with Belytschko-Schwer beam elements, and the *MAT_MOMENT_CURVATURE_BEAM material model in LS-DYNA. Bending, torsional, and tensile stiffness were approximated. The friction coefficient between the wire rope and the bolt was 0.10.

A load was applied to the end of the cable, with the load-time history of the applied load taken directly from the load cell data of test no. HTCUB-32. Fracture resistance, bolt deformation times, onset of visible plastic deformation, and cable motion observed from high-speed film were compared to simulation results, and material properties were updated until the simulation results were within an acceptable margin of error. This calibrated system was then used for the baseline model.

In order to model the extended keyway bolt concept, the shaft of the baseline keyway bolt was extended by $\frac{1}{4}$ in. (6 mm), as shown in Figure 124. Everything else was exactly the same as the baseline model. As a result of the extension, there was a significant reduction in the maximum loads, as shown in Figure 125. This result was observed because the button head scraping was eliminated in the extended keyway bolt model, resulting in a much quicker release of the button head through the keyway, as shown in Figure 126.

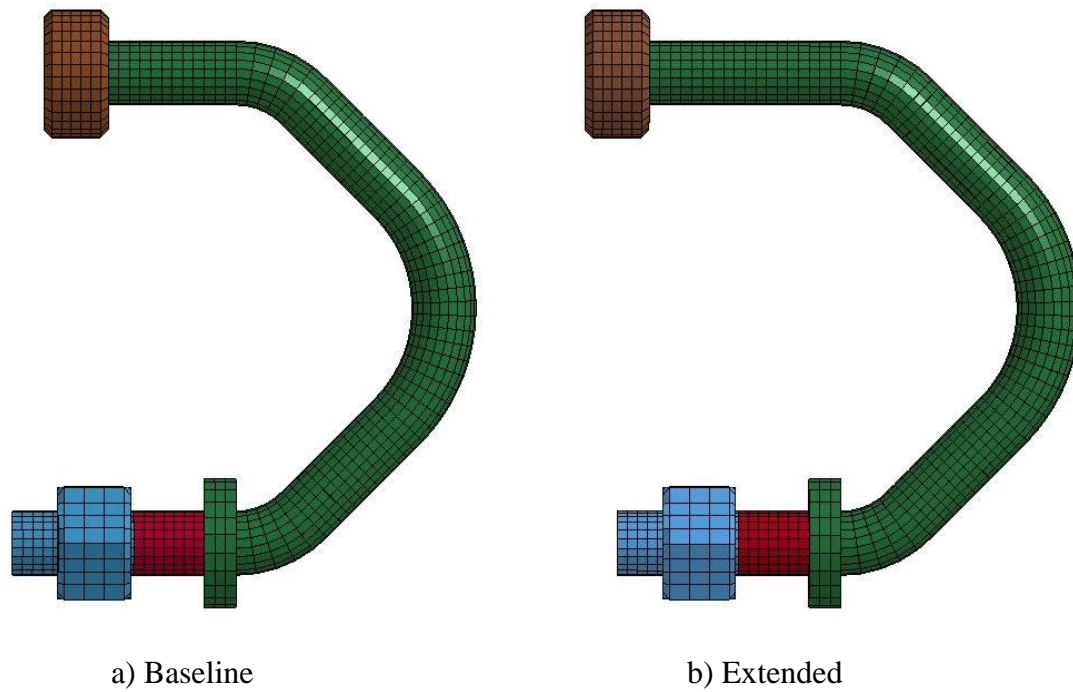


Figure 124. Keyway Bolt Models—(a) Baseline and (b) Extended

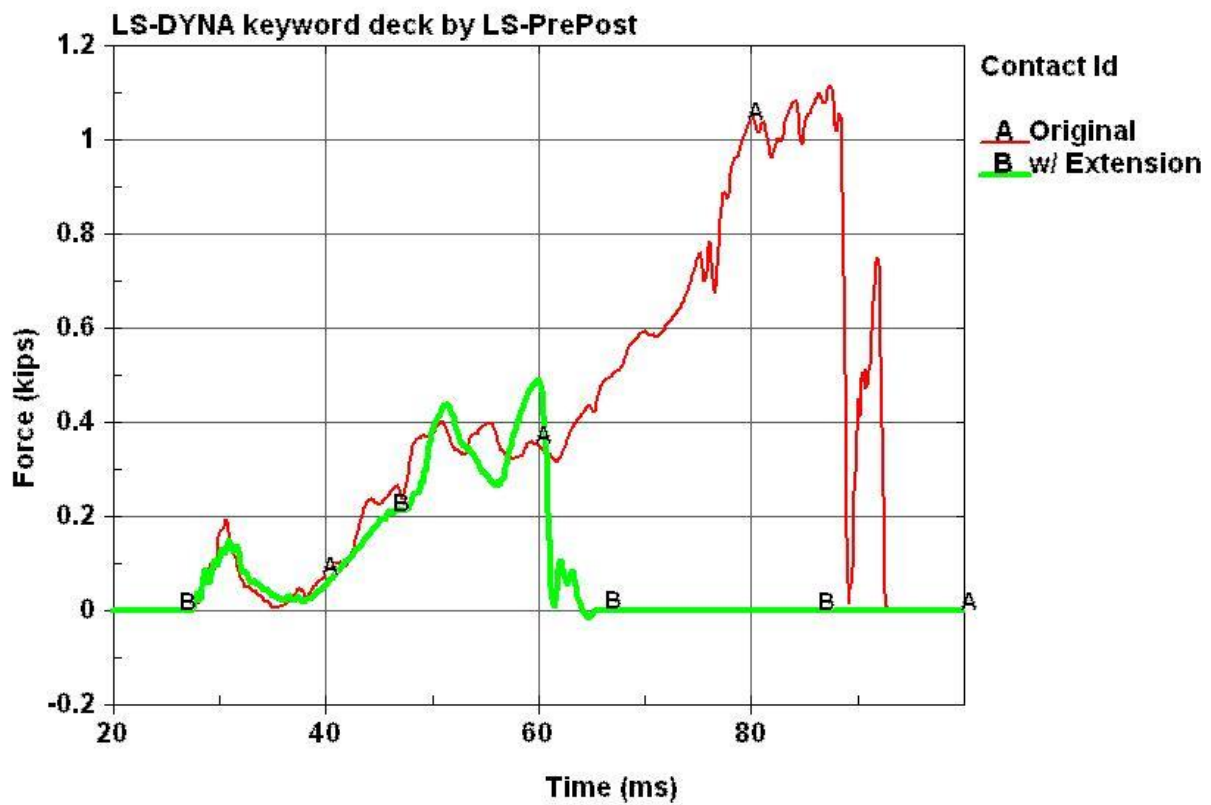
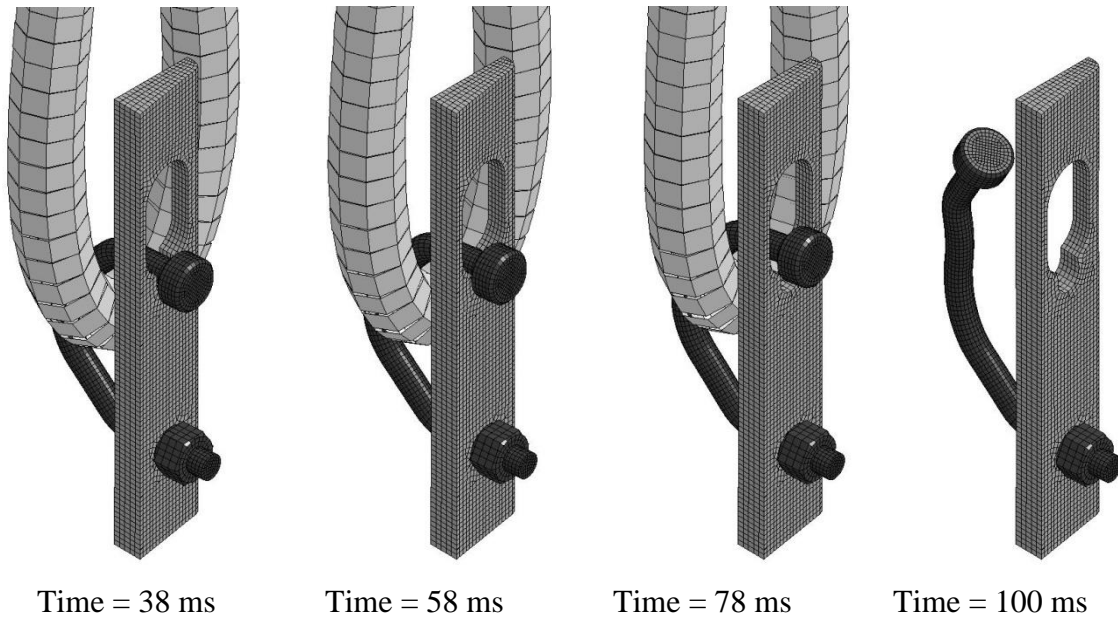
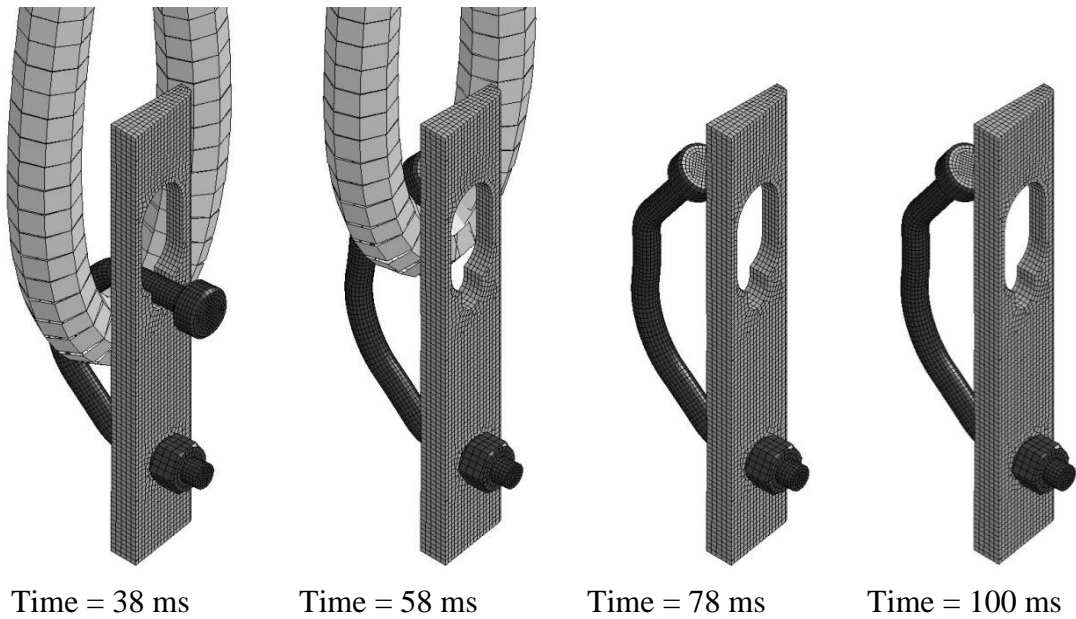


Figure 125. LS-DYNA Model Cable-Bolt Vertical Forces



a) Baseline Model



b) Extended Keyway Bolt Model

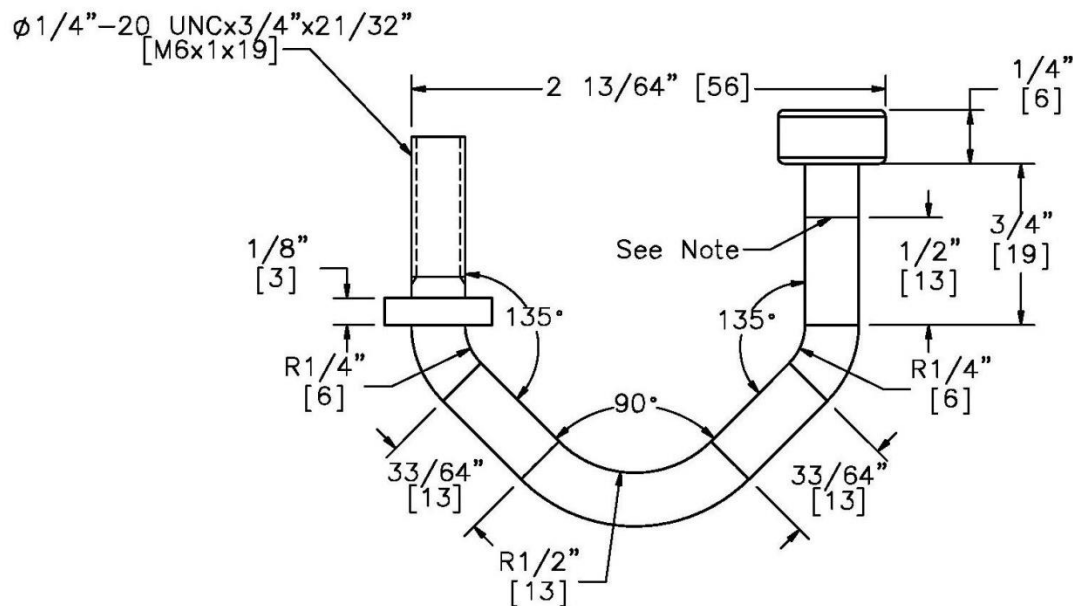
Figure 126. Simulations—(a) Baseline Model and (b) Extended Keyway Bolt Model

According to the LS-DYNA models, a ¼-in. (6-mm) extension of the shaft of the keyway bolt showed a propensity to reduce the maximum vertical release load from 1.1 kips (4.9 kN) to

0.5 kips (2.2 kN). Based on this limited simulation effort, it was believed that the next step should be component testing.

8.3.2 Prototype Extended Keyway Bolts

The acquisition of new bolts that were fabricated to be just $\frac{1}{4}$ in. (6 mm) longer would have been costly and require considerable time. Instead, extended keyway bolts were fabricated using the AISI C1018 keyway bolts that were already on hand. To make these prototypes, the button head was cut off, and a $\frac{1}{4}$ -in. (6-mm) piece of round steel bar was welded to the cut keyway bolt. Then, the button head was welded to the other end of the short segment. Details for the prototype are shown in Figure 127.



Notes: (1) Keyway bolt length was increased with a $1/4"$ [6] dia., $1/4"$ [6] long steel rod of a different material spliced between the head and the main body of the bolt.

Figure 127. Extended Keyway Bolt Prototype

Two different keyways were tested in combination with the extended keyway bolts—the original dual-width keyway and the modified dual-width keyway. The narrow part of the

modified dual-width keyway was 1/8 in. (3 mm) deeper than that of the original dual-width keyway, as shown in Figure 128. The increased depth of the lower slot of the modified dual-width keyway was expected to increase the likelihood that the button head would become caught when the keyway bolt was pulled laterally.

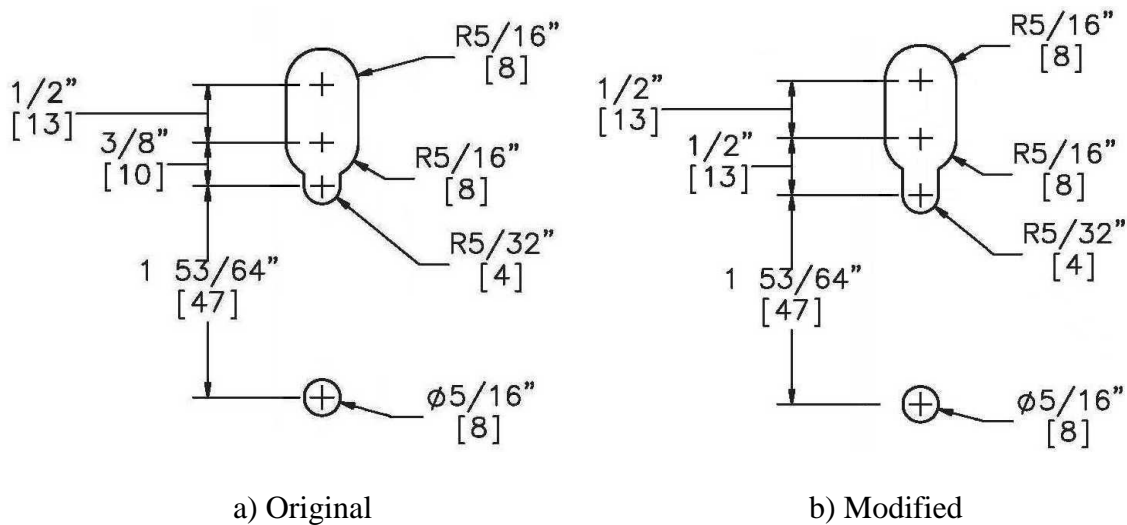


Figure 128. Dual-Width Keyways—(a) Original and (b) Modified

8.3.3 Dynamic Bogie Tests

The extended keyway bolts were tested and evaluated using the same dynamic bogie testing procedures described in Chapter 6. Different load orientations were used in order to determine the vertical and lateral release loads for each concept under dynamic loading conditions. The test results for the extended keyway bolts are presented in Chapter 9.

9 DYNAMIC COMPONENT TESTS—EXTENDED KEYWAY BOLTS, ROUND 2

9.1 Results

There were two rounds of design modifications on the keyway bolts, followed by component testing and evaluation for each round. Twenty dynamic component tests (test nos. HTCUB-38 through HTCUB-57) were performed in the first round, as described in Chapter 7. Eight more dynamic component tests (test nos. HTCUB-58 through HTCUB-65) were performed in the second round, as discussed in this chapter. Each individual concept was tested twice in its vertical orientation and twice in its lateral orientation in order to find the strength of the connection in those directions. For the sake of convenience, the consolidated drawing set for both rounds of keyway bolt dynamic component tests was shown in Figures 49 through 58, located in Chapter 7. A summary of the test matrix and results for the second round of dynamic components tests is provided in Table 6.

Table 6. Summary of Dynamic Component Testing of Extended Keyway Bolts, Round 2

Test No.	Load Direction	Test Article	Material	Keyway Slot	Release Load, kips (kN)	Test Results
HTCUB-58	Vertical	Extended Keyway Bolt, a4	AISI C1018	Original dual-width, E	0.38 (1.7)	Free release through keyway, button snag load = 0.46 kips (2.0 kN)
HTCUB-59	Vertical	Extended Keyway Bolt, a4	AISI C1018	Original dual-width, E	0.44 (2.0)	Free release through keyway, button snag load = 0.39 kips (1.7 kN)
HTCUB-60	Lateral	Extended Keyway Bolt, a4	AISI C1018	Original dual-width, E	3.53 (15.7)	Button caught in narrow part of keyway, released through keyway
HTCUB-61	Lateral	Extended Keyway Bolt, a4	AISI C1018	Original dual-width, E	1.75 (7.78)	Button caught in narrow part of keyway, released through keyway
HTCUB-62	Lateral	Extended Keyway Bolt, a4	AISI C1018	Modified dual-width, F	5.71 (25.4)	Button caught in narrow part of keyway, fracture through weld of extension
HTCUB-63	Lateral	Extended Keyway Bolt, a4	AISI C1018	Modified dual-width, F	4.62 (20.6)	Button caught in narrow part of keyway, fracture through weld of extension
HTCUB-64	Vertical	Extended Keyway Bolt, a4	AISI C1018	Modified dual-width, F	0.59 (2.6)	Free release through keyway, button snag load = 0.33 kips (1.5 kN), crack in weld
HTCUB-65	Vertical	Extended Keyway Bolt, a4	AISI C1018	Modified dual-width, F	0.39 (1.7)	Free release through keyway, button snag load = 0.44 kips (2.0 kN), crack in weld

9.1.1 Test No. HTCUB-58 (C1018 Ext. KB, Original, Vertical)

For test no. HTCUB-58, the cable pulled on the AISI C1018, extended keyway bolt at an angle of 0 degrees, parallel to the face of the flange, thus imparting a vertical load. The keyway bolt was attached to the front flange with one grade 8 nut. The original dual-width keyway was used for this test. As the cable began to pull on the bolt, the bolt was bent upward. The button head released through the keyway freely with a maximum release load of 380 lb (1.69 kN). A peak load of 455 lb (2.02 kN) occurred as the cable became snagged on the button head, after the button head had already cleared the keyway. The force versus time plot is shown in Figure 129. Pre- and post-test photographs are shown in Figure 130. Sequential photographs are shown in Figure 131.

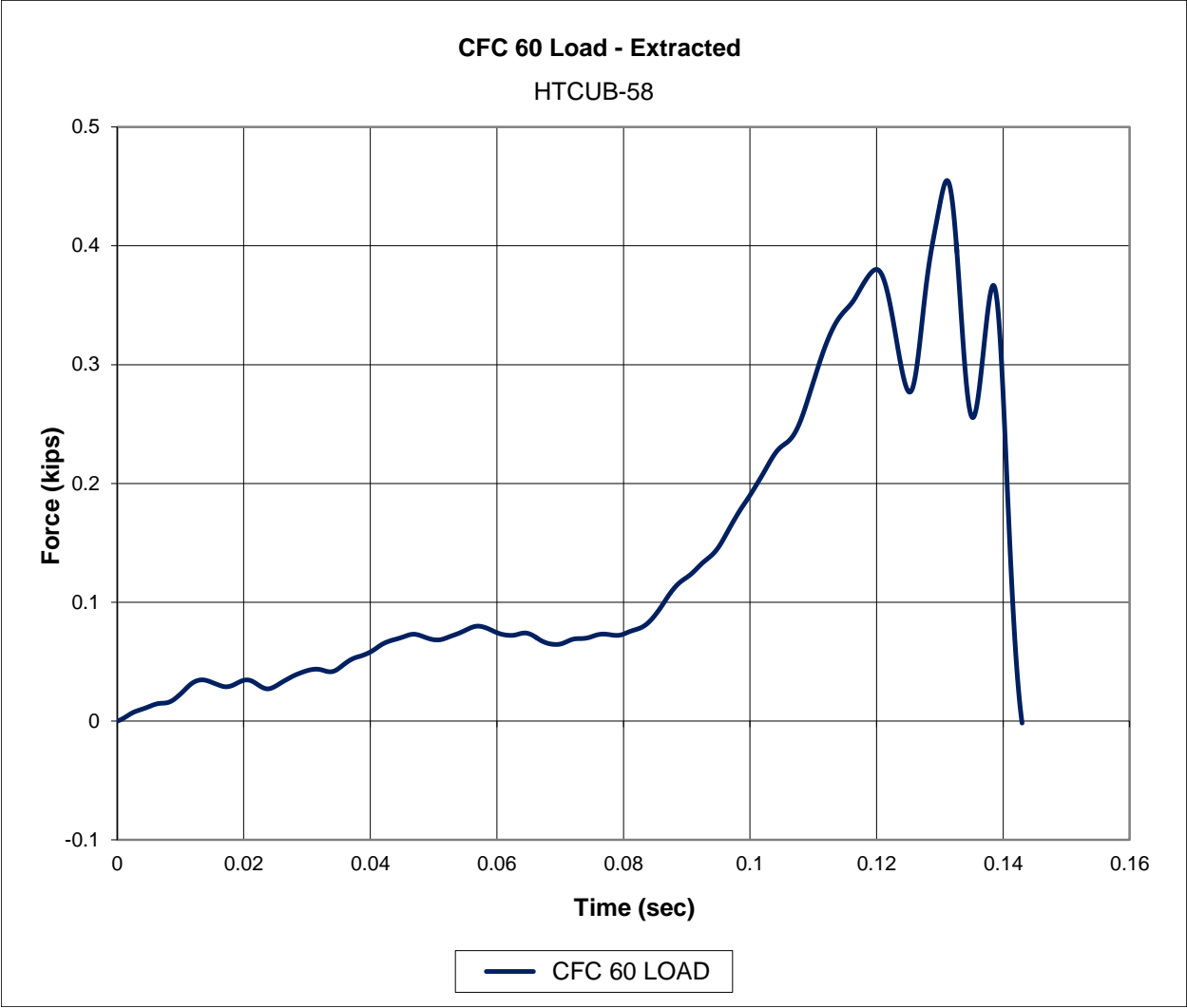


Figure 129. Force-Time Data, Test No. HTCUB-58



Figure 130. Pre-Test and Post-Test Photographs, Test No. HTCUB-58

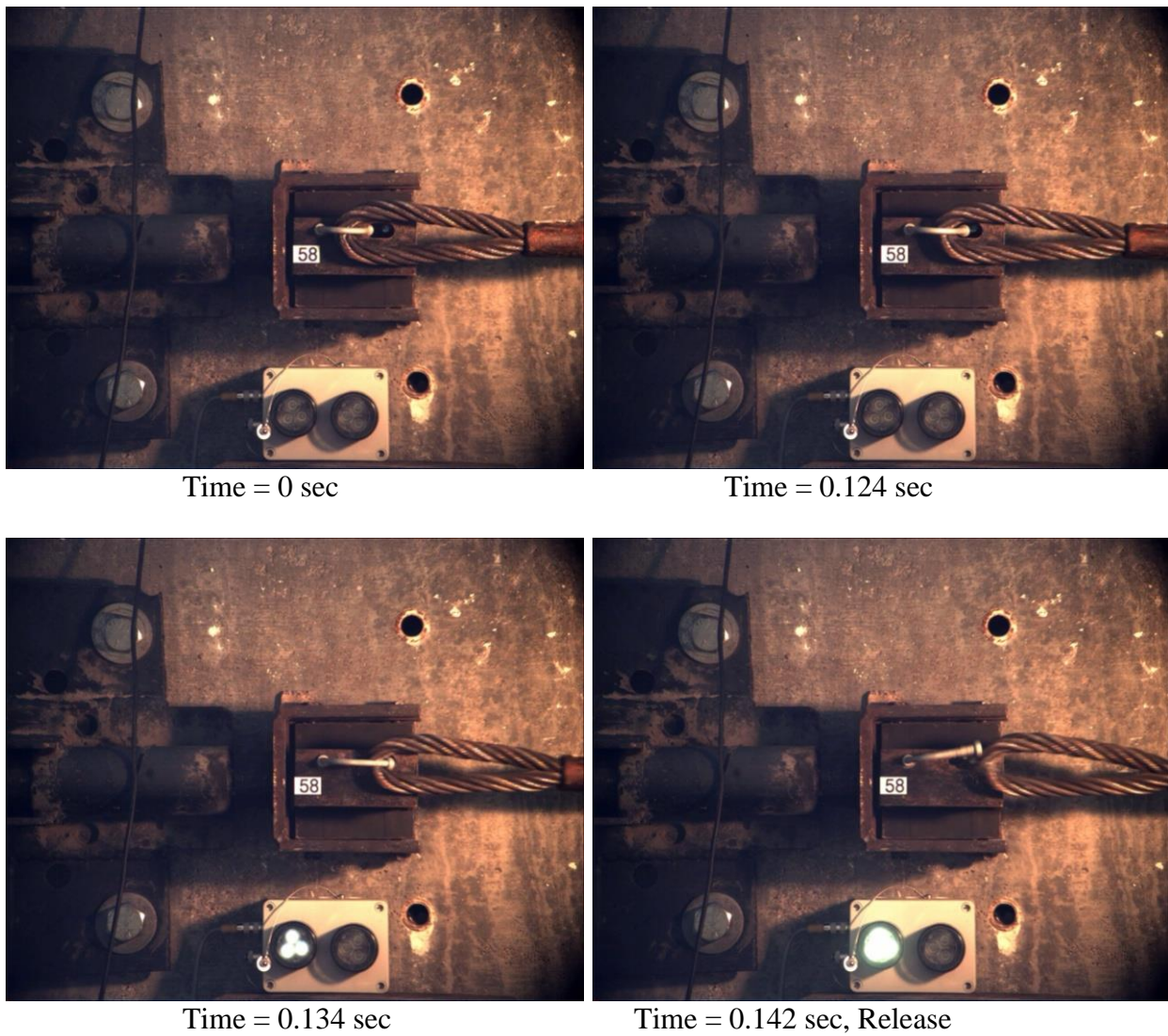


Figure 131. Sequential Photographs, Test No. HTCUB-58

9.1.2 Test No. HTCUB-59 (C1018 Ext. KB, Original, Vertical)

For test no. HTCUB-59, the cable pulled on the AISI C1018, extended keyway bolt at an angle of 0 degrees, parallel to the front face of the flange, thus imparting a vertical load. The keyway bolt was attached to the front flange with one grade 8 nut. The original dual-width keyway was used for this test. As the cable began to pull on the bolt, the bolt was bent upward. The button head released out of the keyway freely with a maximum release load of 440 lb (1.96 kN). A smaller button snag load of 387 lb (1.72 kN) occurred after the button head had already cleared the keyway. The force versus time plot is shown in Figure 132. Pre- and post-test photographs are shown in Figure 133. Sequential photographs are shown in Figure 134.

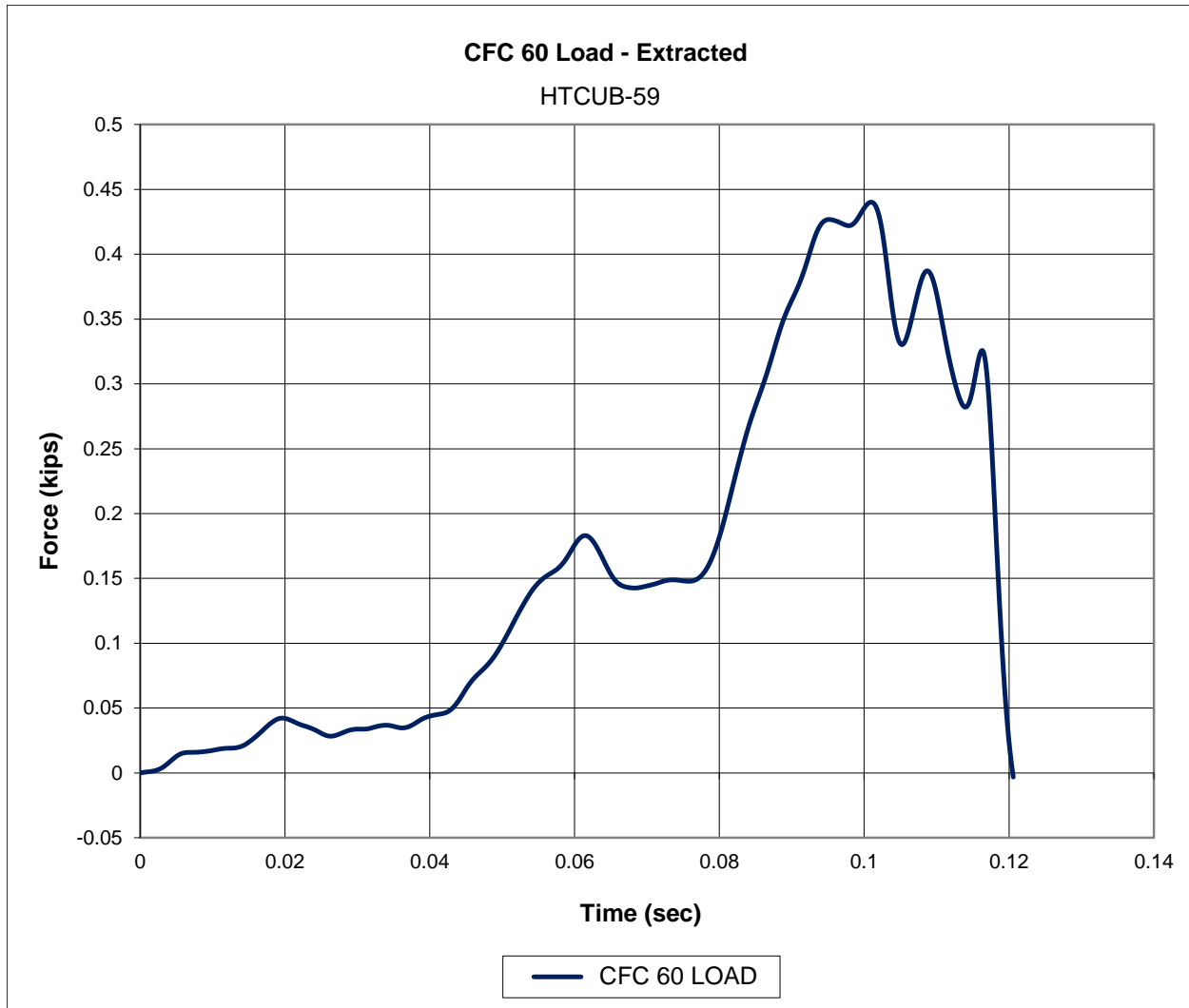


Figure 132. Force-Time Data, Test No. HTCUB-59

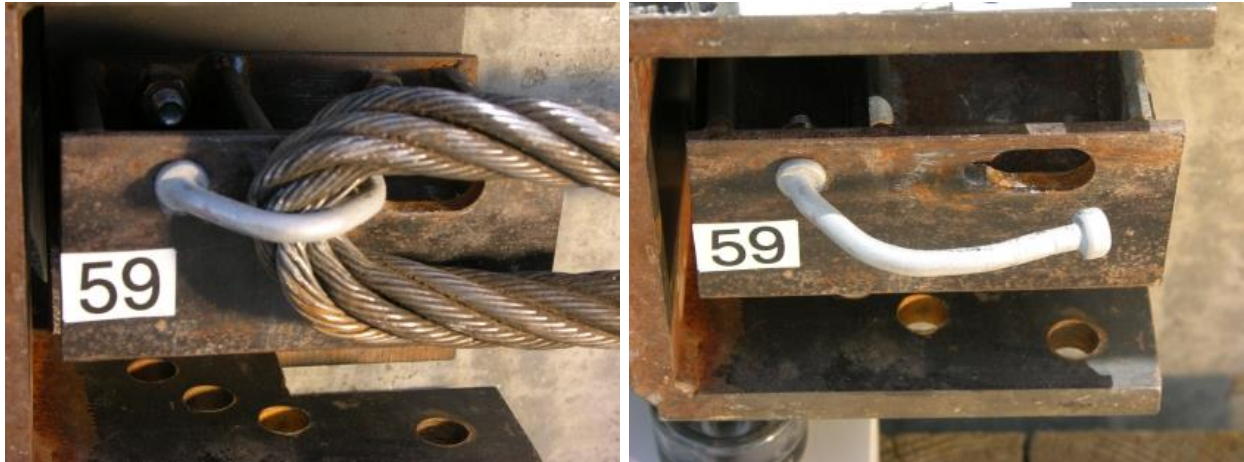
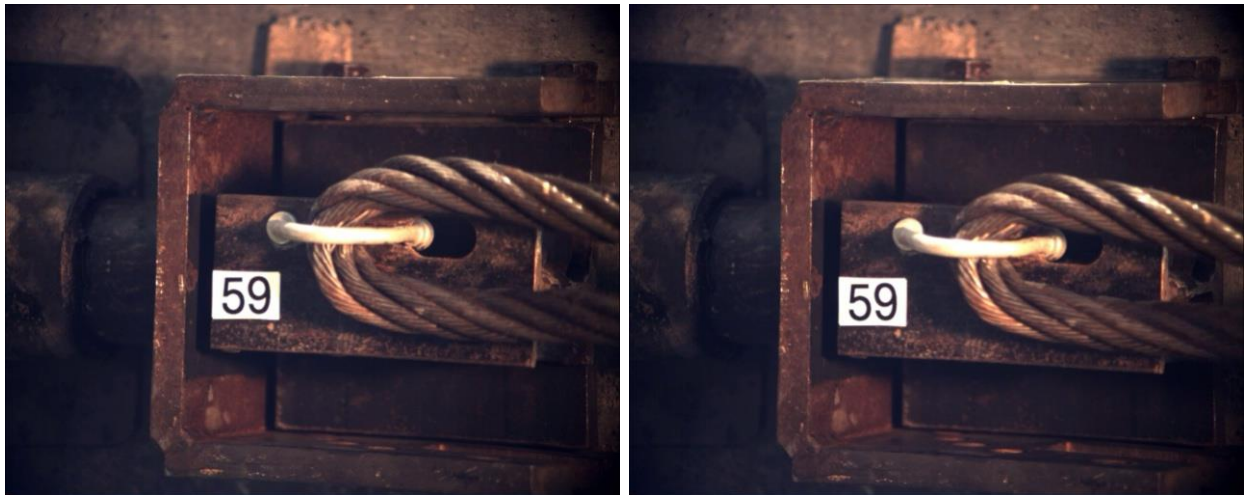
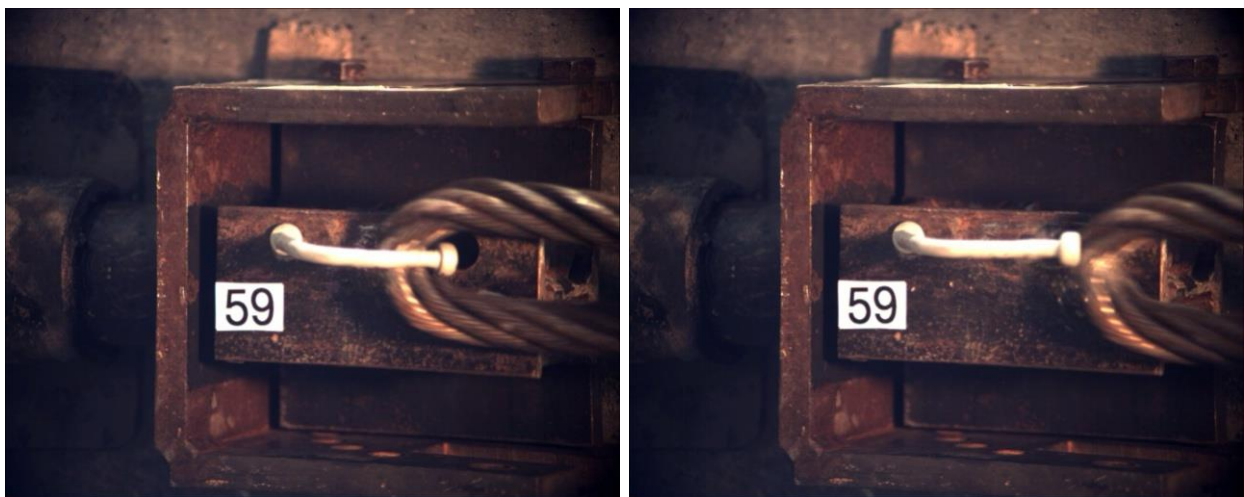


Figure 133. Pre-Test and Post-Test Photographs, Test No. HTCUB-59



Time = 0 sec

Time = 0.102 sec



Time = 0.112 sec

Time = 0.120 sec, Release

Figure 134. Sequential Photographs, Test No. HTCUB-59

9.1.3 Test No. HTCUB-60 (C1018 Ext. KB, Original, Lateral)

For test no. HTCUB-60, the cable pulled on the AISI C1018, extended keyway bolt at an angle of 90 degrees, perpendicular to the front face of the flange, thus imparting a lateral load. The keyway bolt was attached to the front flange with one grade 8 nut. The original dual-width keyway was used for this test. As the cable pulled on the bolt, the button head was caught in the narrow part of the keyway. The cable continued to pull on the bolt until the button head slipped out of the keyway with a release load of 3.53 kips (15.7 kN). The force versus time plot is shown in Figure 135. Pre- and post-test photographs are shown in Figure 136. Sequential photographs are shown in Figure 137.

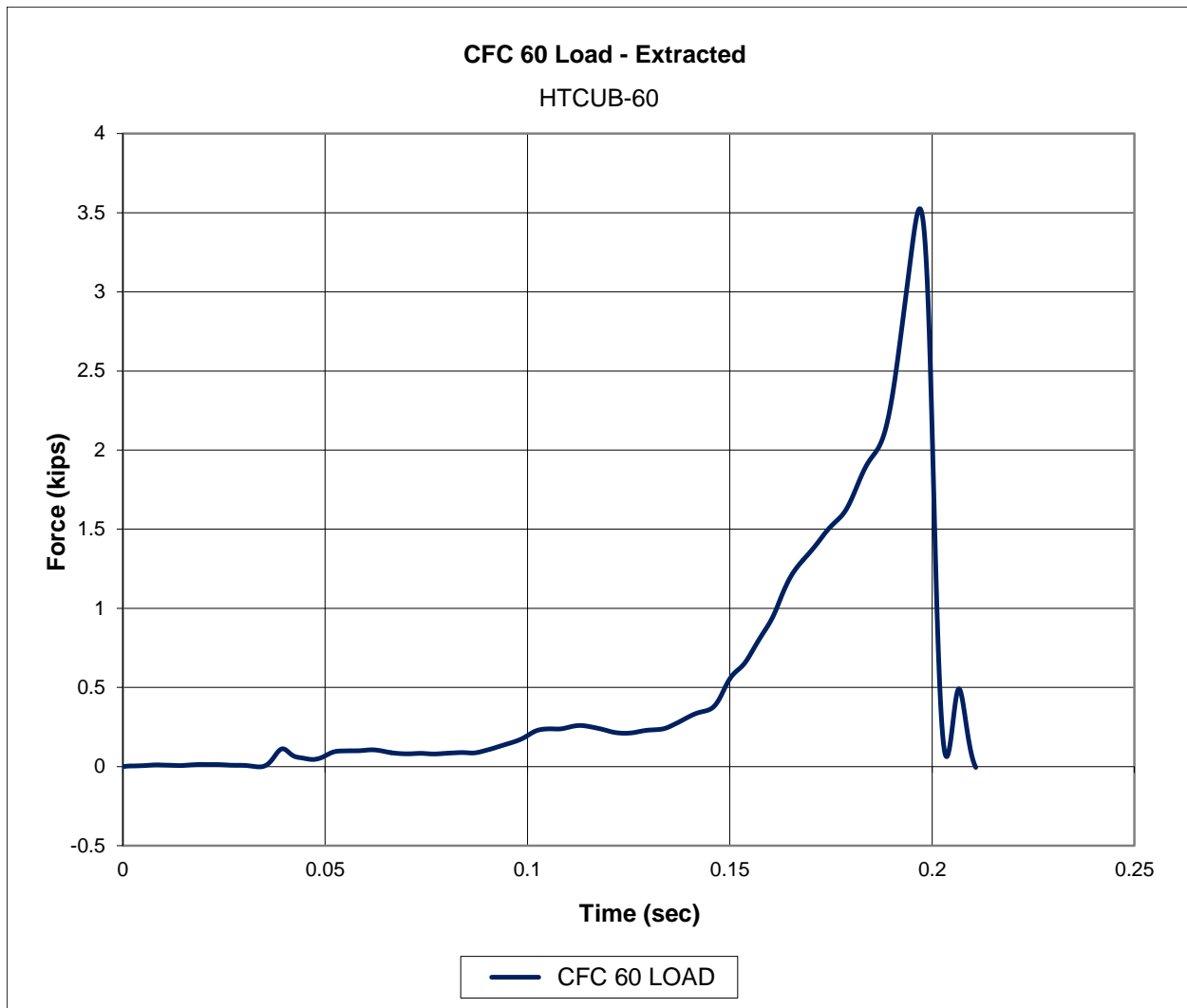


Figure 135. Force-Time Data, Test No. HTCUB-60



Figure 136. Pre-Test and Post-Test Photographs, Test No. HTCUB-60

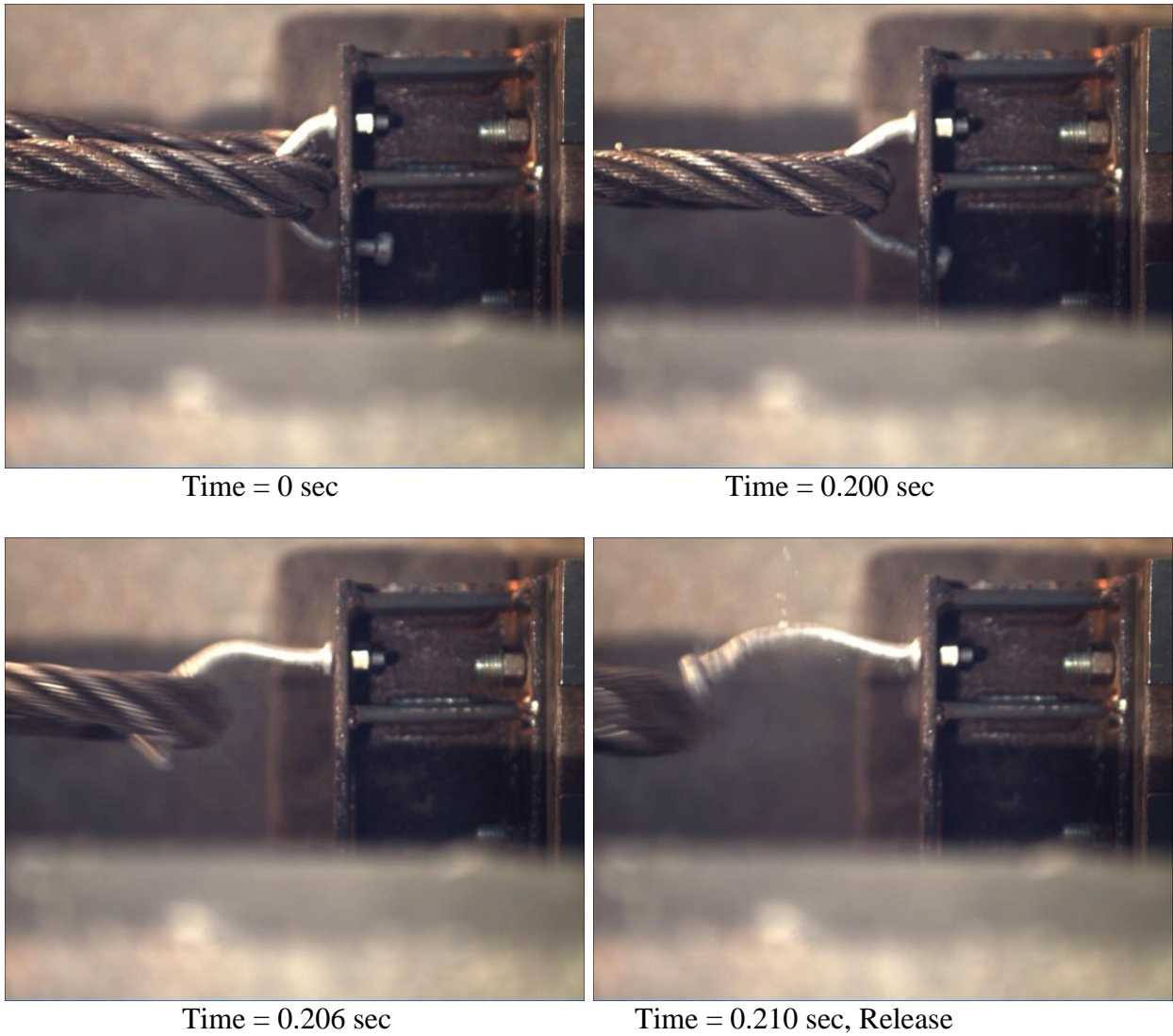


Figure 137. Sequential Photographs, Test No. HTCUB-60

9.1.4 Test No. HTCUB-61 (C1018 Ext. KB, Original, Lateral)

For test no. HTCUB-61, the cable pulled on the AISI C1018, extended keyway bolt at an angle of 90 degrees, perpendicular to the front face of the flange, thus imparting a lateral load. The keyway bolt was attached to the front flange with one grade 8 nut. The original dual-width keyway was used for this test. As the cable pulled on the bolt, the button head was caught in the narrow part of the keyway. The cable continued to pull on the bolt until the button head slipped out of the keyway with a release load of 1.75 kips (7.78 kN). The force versus time plot is shown in Figure 138. Pre- and post-test photographs are shown in Figure 139. Sequential photographs are shown in Figure 140.

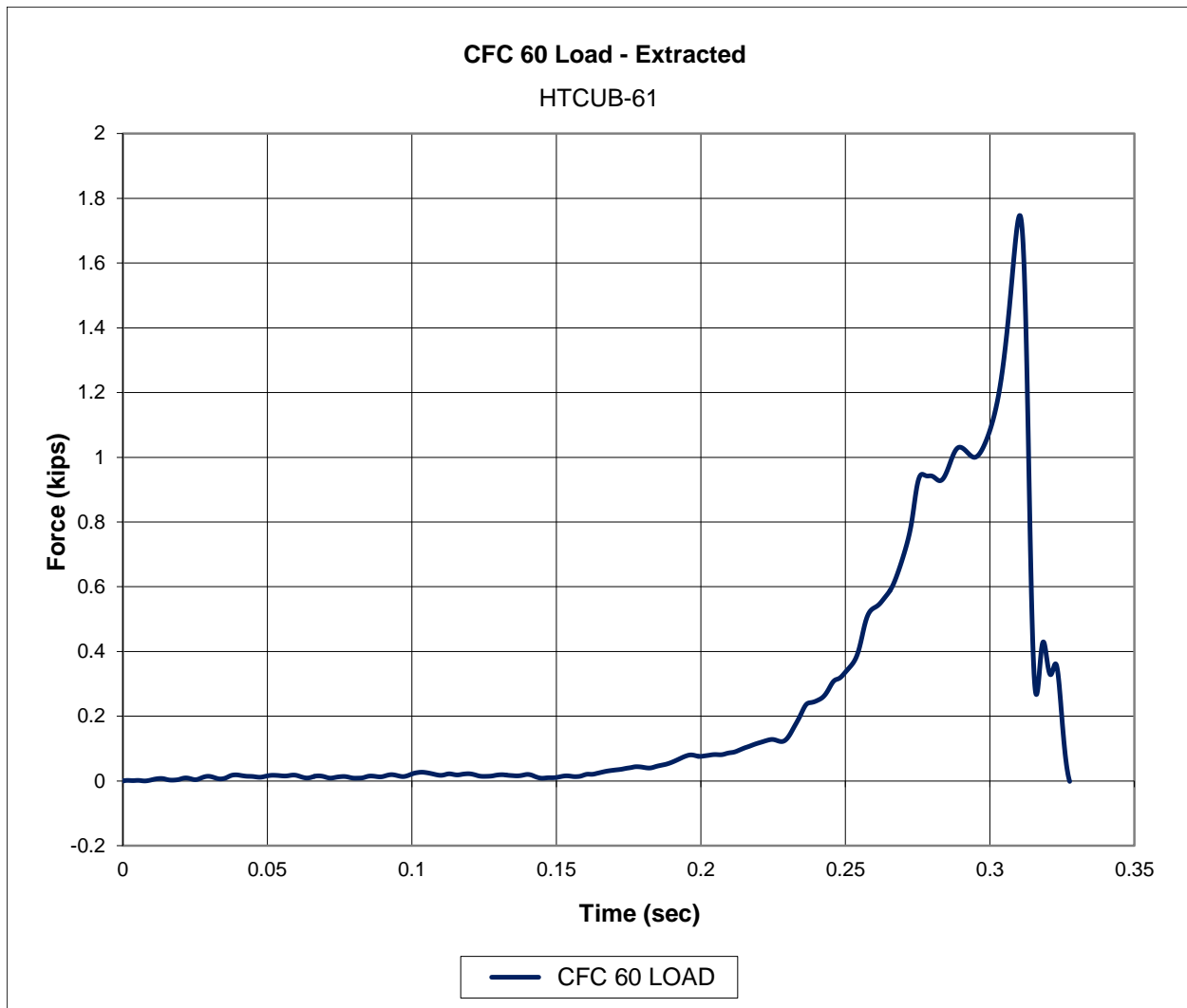
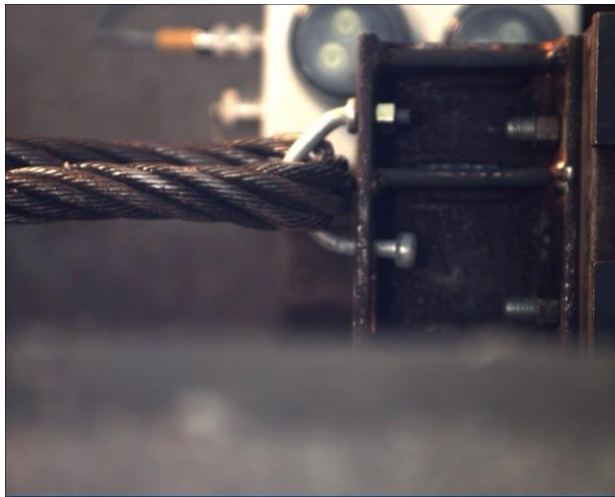


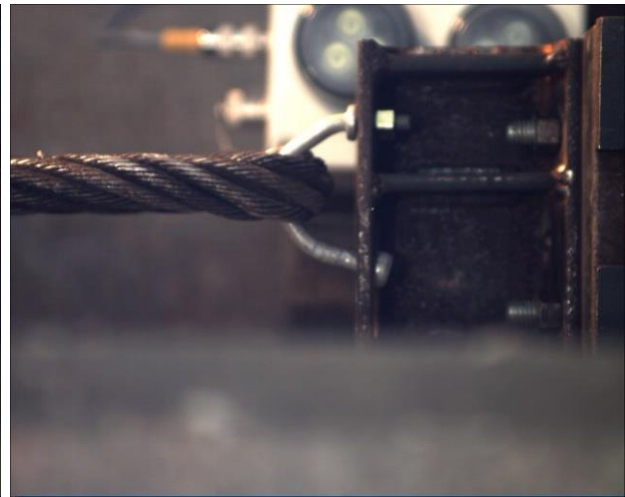
Figure 138. Force-Time Data, Test No. HTCUB-61



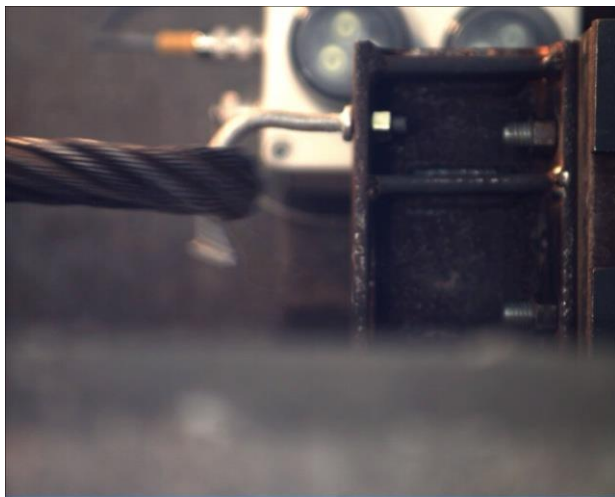
Figure 139. Pre-Test and Post-Test Photographs, Test No. HTCUB-61



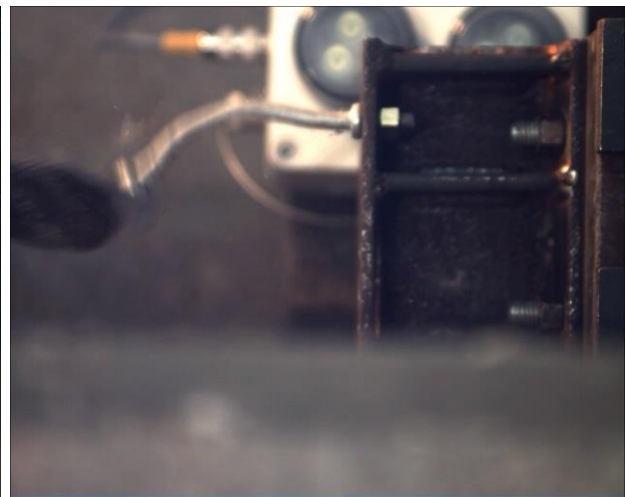
Time = 0 sec



Time = 0.312 sec



Time = 0.320 sec



Time = 0.328 sec, Release

Figure 140. Sequential Photographs, Test No. HTCUB-61

9.1.5 Test No. HTCUB-62 (C1018 Ext. KB, Modified, Lateral)

For test no. HTCUB-62, the cable pulled on the AISI C1018, extended keyway bolt at an angle of 90 degrees, perpendicular to the front face of the flange, thus imparting a lateral load. The keyway bolt was attached to the front flange with one grade 8 nut. The modified dual-width keyway was used for this test. As the cable pulled on the bolt, the button head was caught in the narrow part of the keyway. The cable continued to pull on the bolt until the bolt fractured through the weld of the ¼-in. (6-mm) extension with a peak load of 5.71 kips (25.4 kN). The force versus time plot is shown in Figure 141. Pre- and post-test photographs are shown in Figure 142. Sequential photographs are shown in Figure 143.

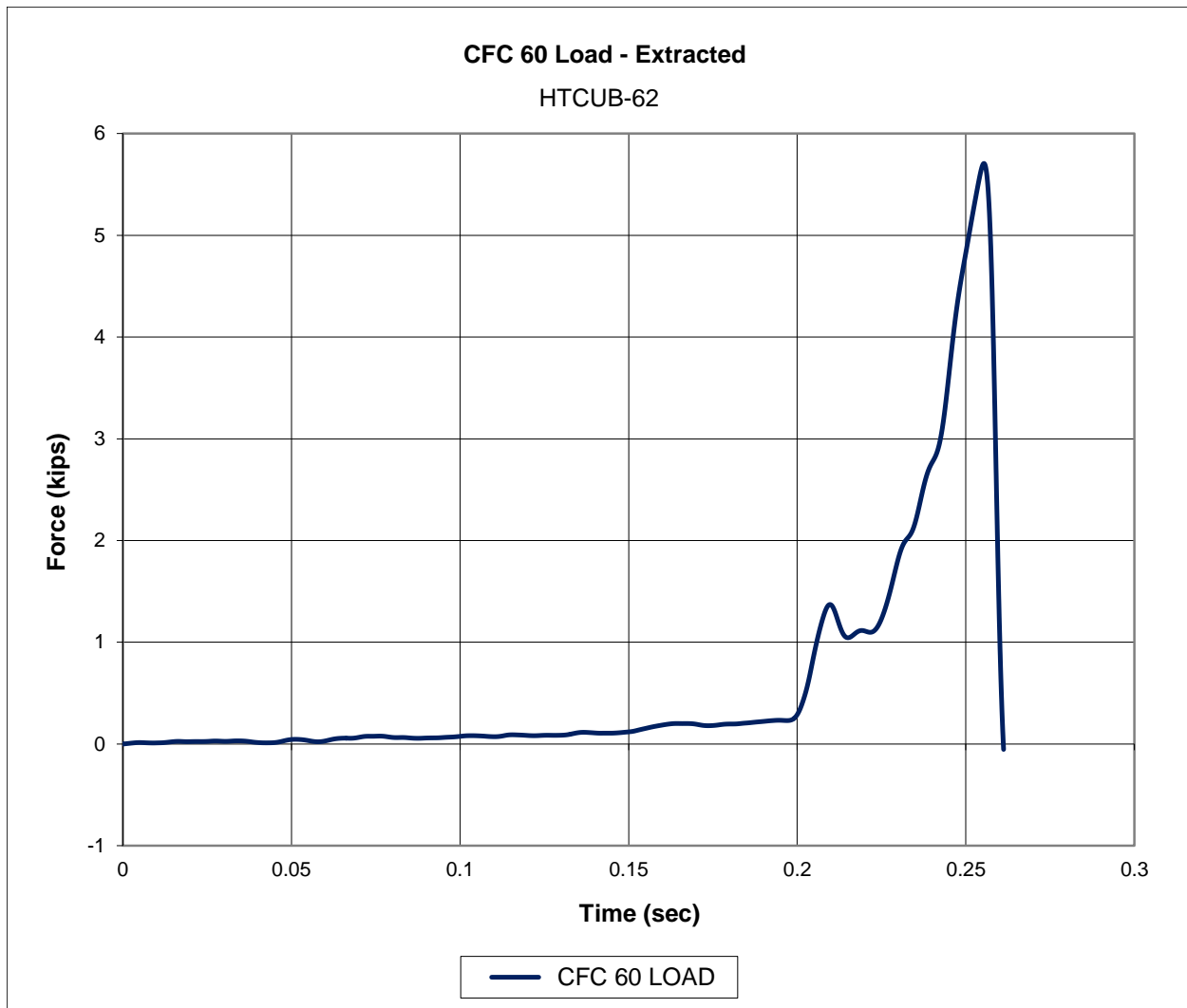


Figure 141. Force-Time Data, Test No. HTCUB-62

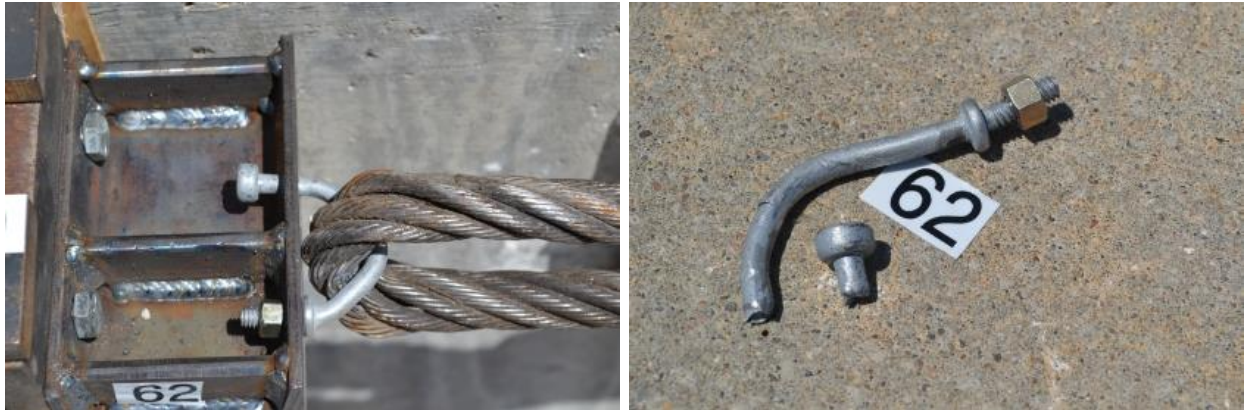


Figure 142. Pre-Test and Post-Test Photographs, Test No. HTCUB-62

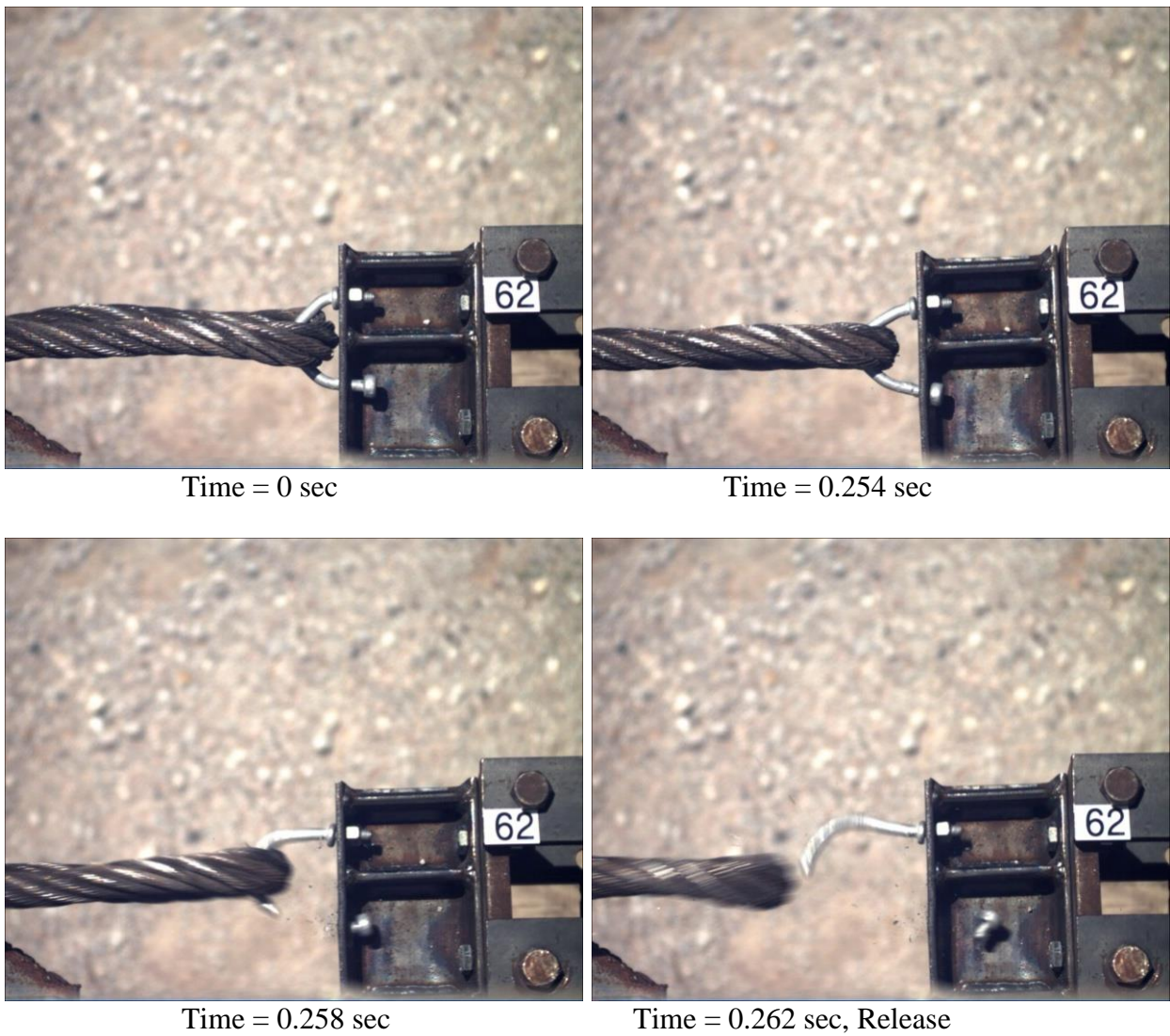


Figure 143. Sequential Photographs, Test No. HTCUB-62

9.1.6 Test No. HTCUB-63 (C1018 Ext. KB, Modified, Lateral)

For test no. HTCUB-63, the cable pulled on the AISI C1018, extended keyway bolt at an angle of 90 degrees, perpendicular to the front face of the flange, thus imparting a lateral load. The keyway bolt was attached to the front flange with one grade 8 nut. The modified dual-width keyway was used for this test. As the cable pulled on the bolt, the button head was caught in the narrow part of the keyway. The cable continued to pull on the bolt until the bolt fractured through the weld of the ¼-in. (6-mm) extension with a peak load of 4.62 kips (20.6 kN). The force versus time plot is shown in Figure 144. Pre- and post-test photographs are shown in Figure 145. Sequential photographs are shown in Figure 146.

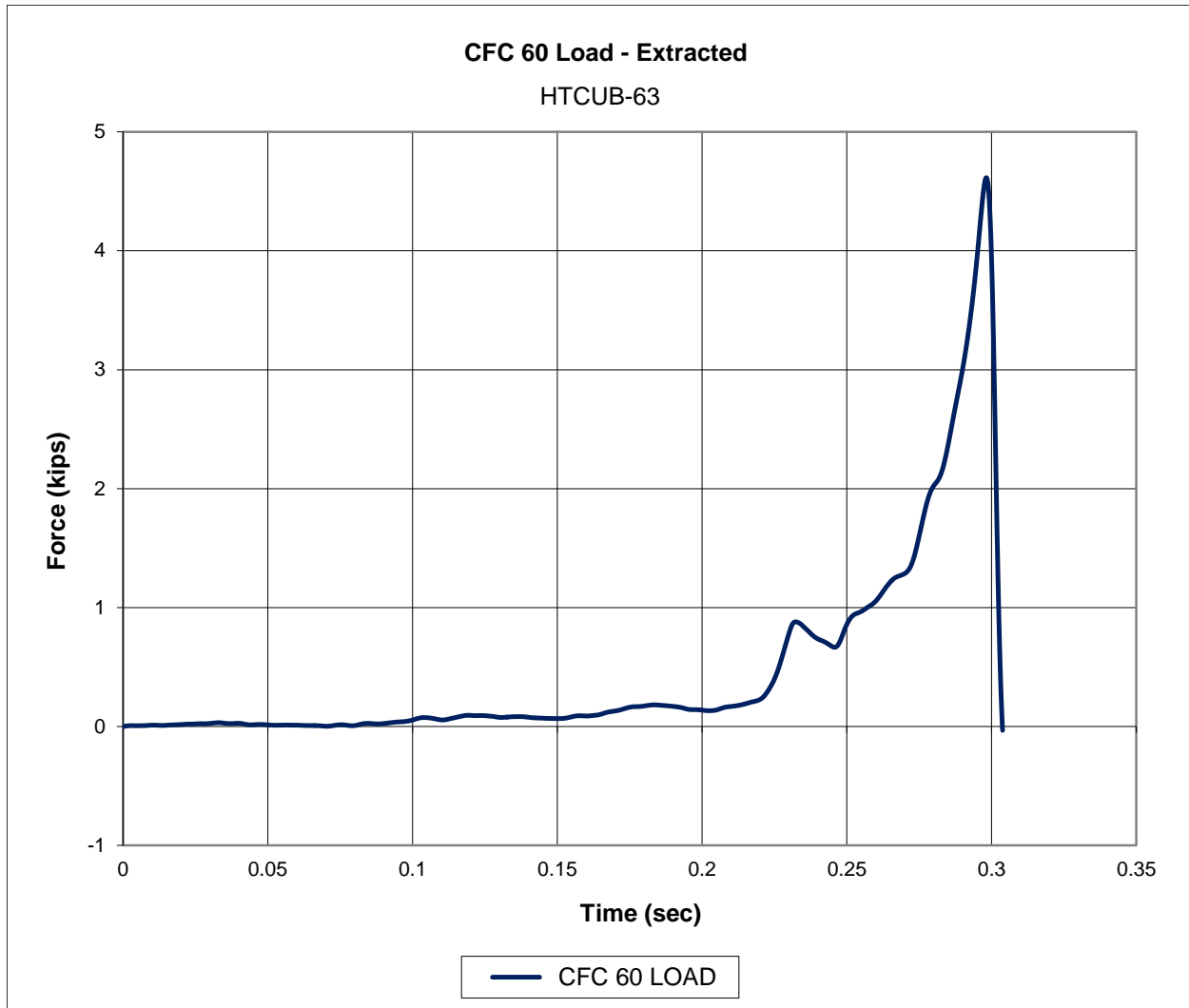


Figure 144. Force-Time Data, Test No. HTCUB-63

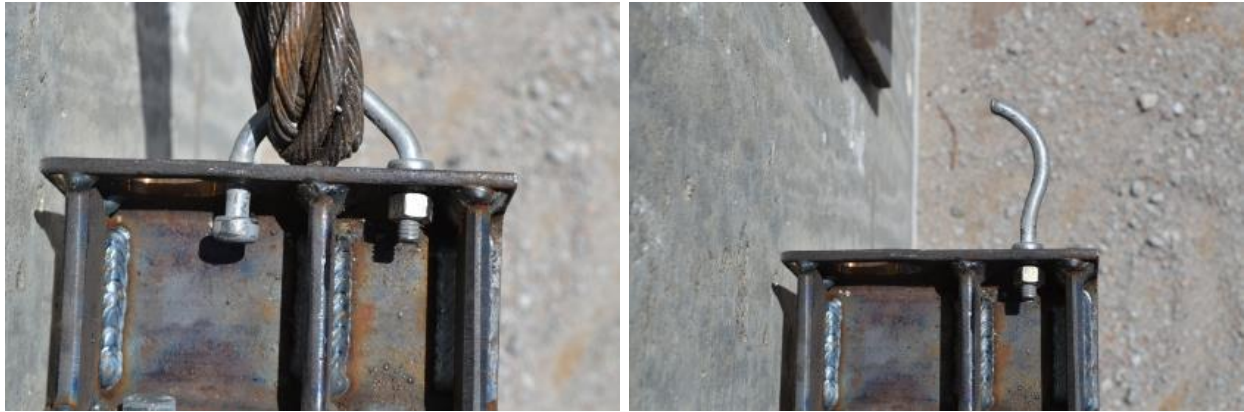
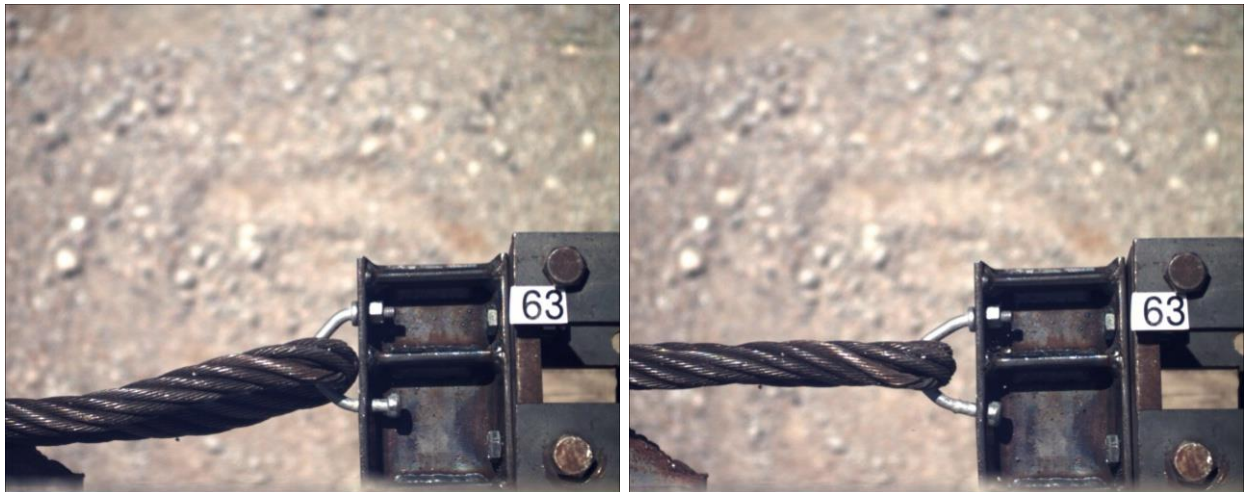
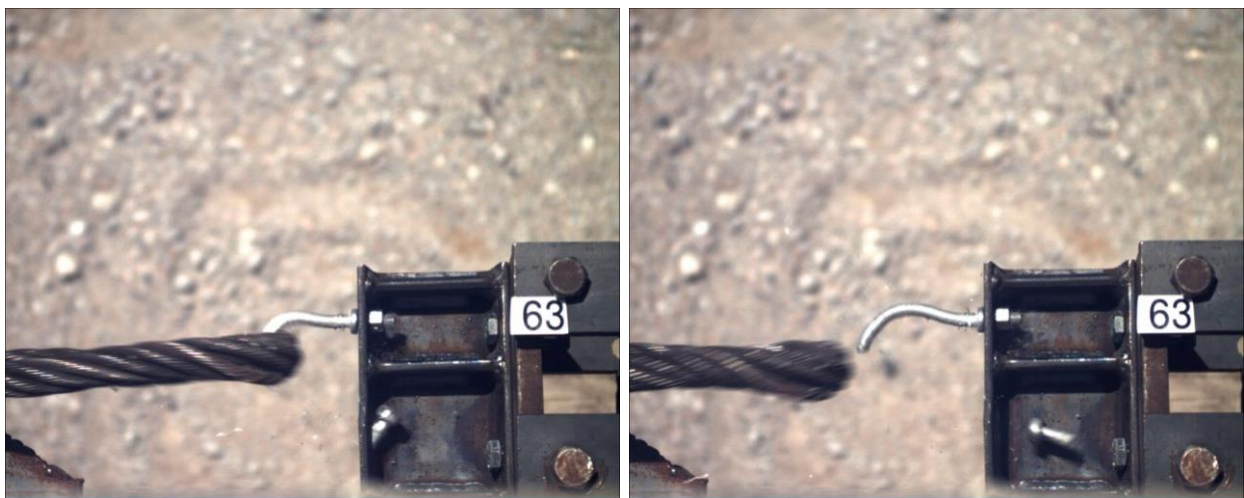


Figure 145. Pre-Test and Post-Test Photographs, Test No. HTCUB-63



Time = 0 sec

Time = 0.296 sec



Time = 0.300 sec

Time = 0.304 sec, Release

Figure 146. Sequential Photographs, Test No. HTCUB-63

9.1.7 Test No. HTCUB-64 (C1018 Ext. KB, Modified, Vertical)

For test no. HTCUB-64, the cable pulled on the AISI C1018, extended keyway bolt at an angle of 0 degrees, parallel to the front face of the flange, thus imparting a vertical load. The keyway bolt was attached to the front flange with one grade 8 nut. The modified dual-width keyway was used for this test. As the cable pulled on the bolt, the bolt was bent upward and out of the keyway freely with a maximum release load of 585 lb (2.60 kN). After the button head cleared the keyway, the cable became snagged on the button head. During the course of the test, a crack developed in the weld of the extension on the bolt, but the weld did not fracture completely. The load from the cable snagging on the button was 333 lb (1.48 kN). The force versus time plot is shown in Figure 147. Pre- and post-test photographs are shown in Figure 148. Sequential photographs are shown in Figure 149.

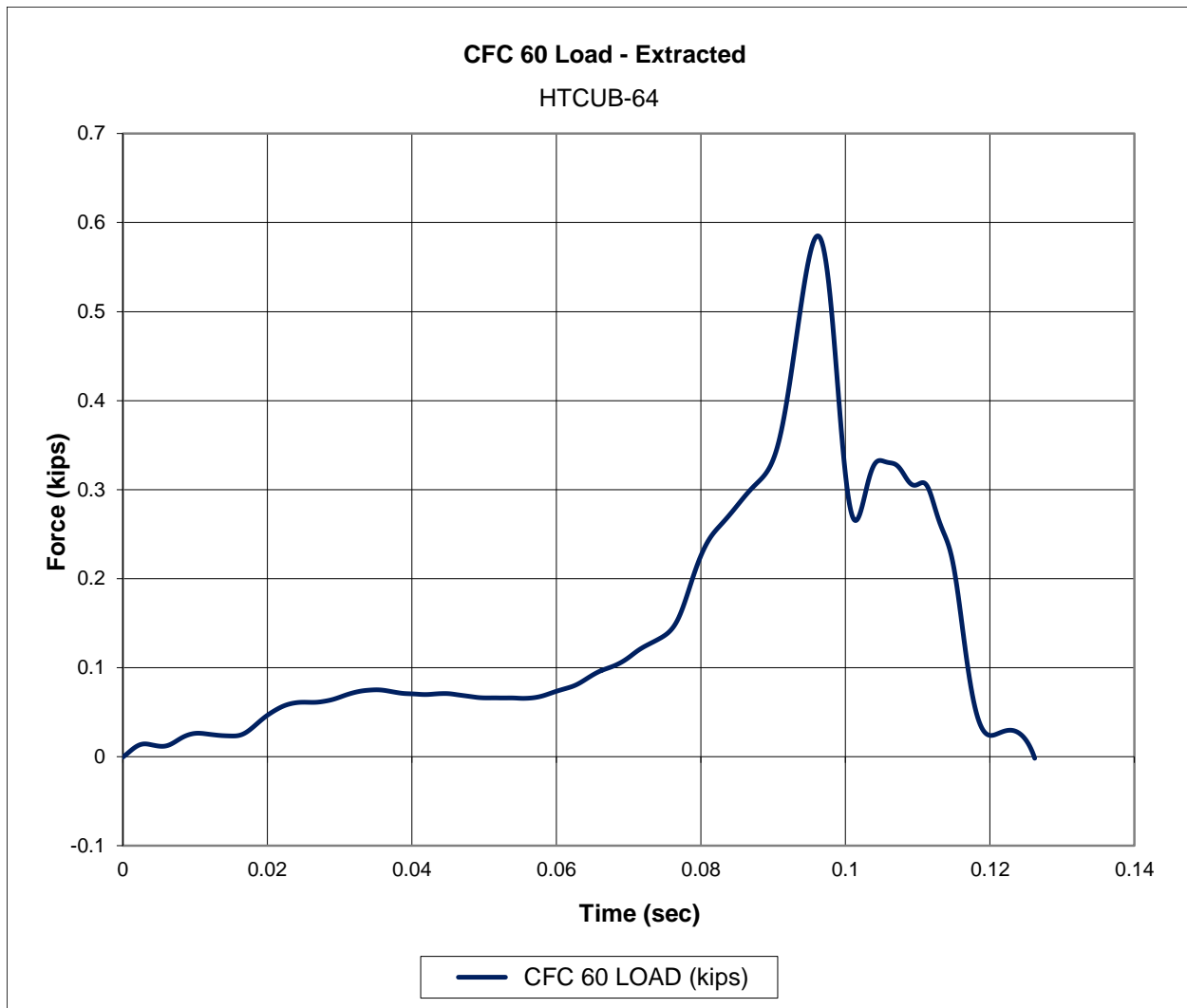


Figure 147. Force-Time Data, Test No. HTCUB-64

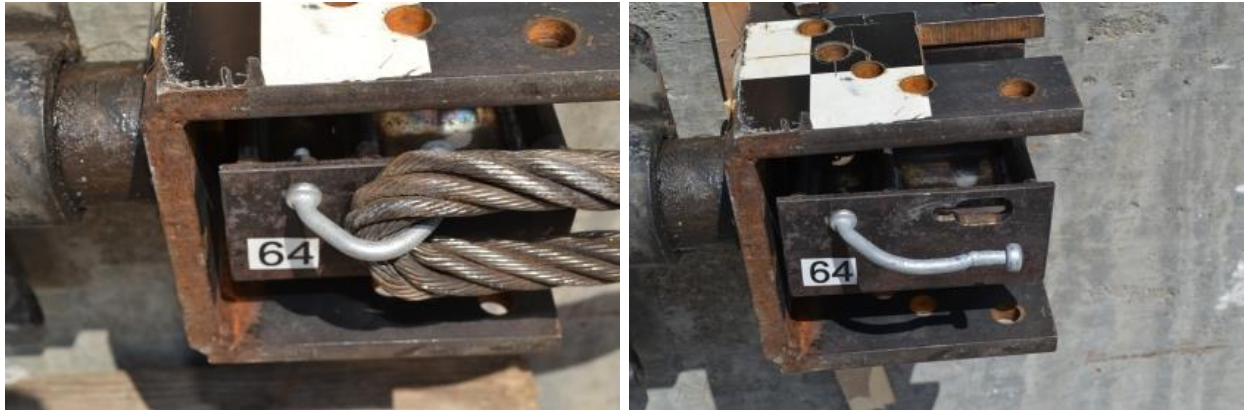
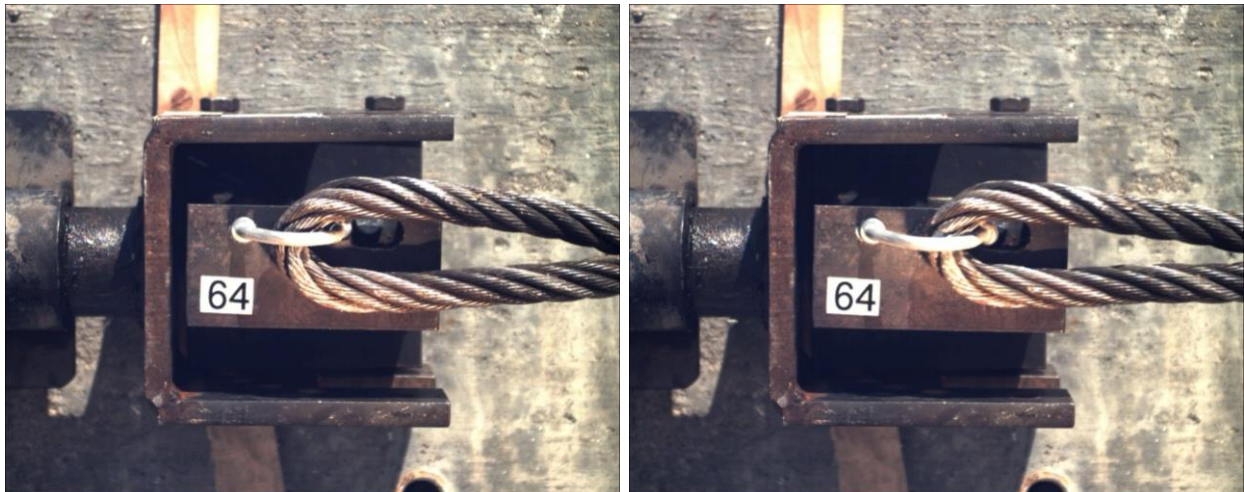
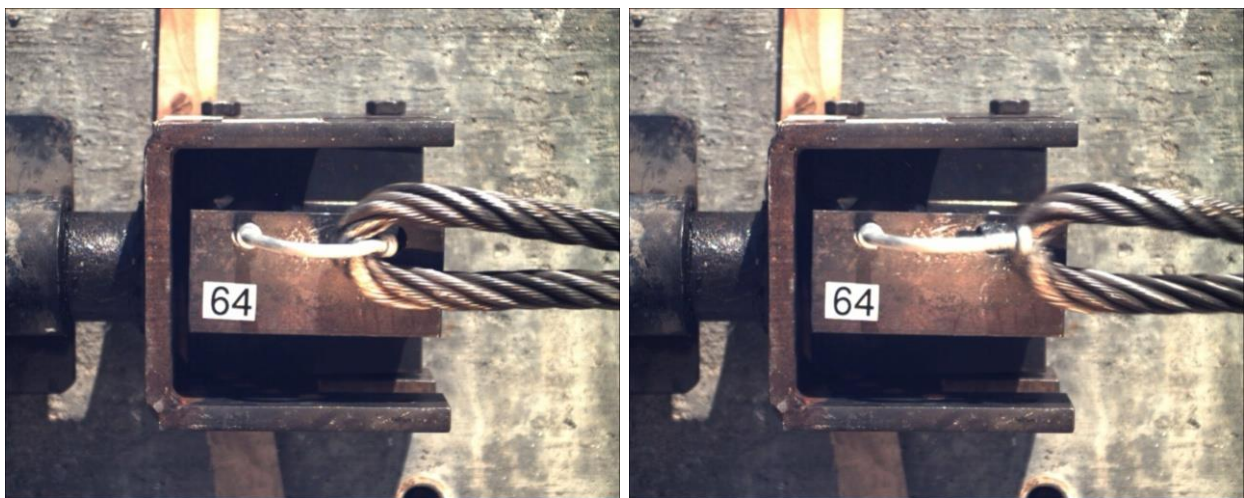


Figure 148. Pre-Test and Post-Test Photographs, Test No. HTCUB-64



Time = 0 sec

Time = 0.110 sec



Time 0.118 sec

Time = 0.126 sec, Release

Figure 149. Sequential Photographs, Test No. HTCUB-64

9.1.8 Test No. HTCUB-65 (C1018 Ext. KB, Modified, Vertical)

For test no. HTCUB-65, the cable pulled on the AISI C1018, extended keyway bolt at an angle of 0 degrees, parallel to the front face of the flange, thus imparting a vertical load. The keyway bolt was attached to the front flange with one grade 8 nut. The modified dual-width keyway was used for this test. As the cable pulled on the bolt, the bolt was bent upward and out of the keyway freely with a maximum release load of 387 lb (1.72 kN). A peak load of 442 lb (1.97 kN) occurred after the button head cleared the keyway but as the cable became snagged on the button head. During the course of the test, a crack developed in the weld of the extension on the bolt, but the weld did not fracture completely. The force versus time plot is shown in Figure 150. No pre-test photograph was taken. The post-test photograph is shown in Figure 151. Sequential photographs are shown in Figure 152.

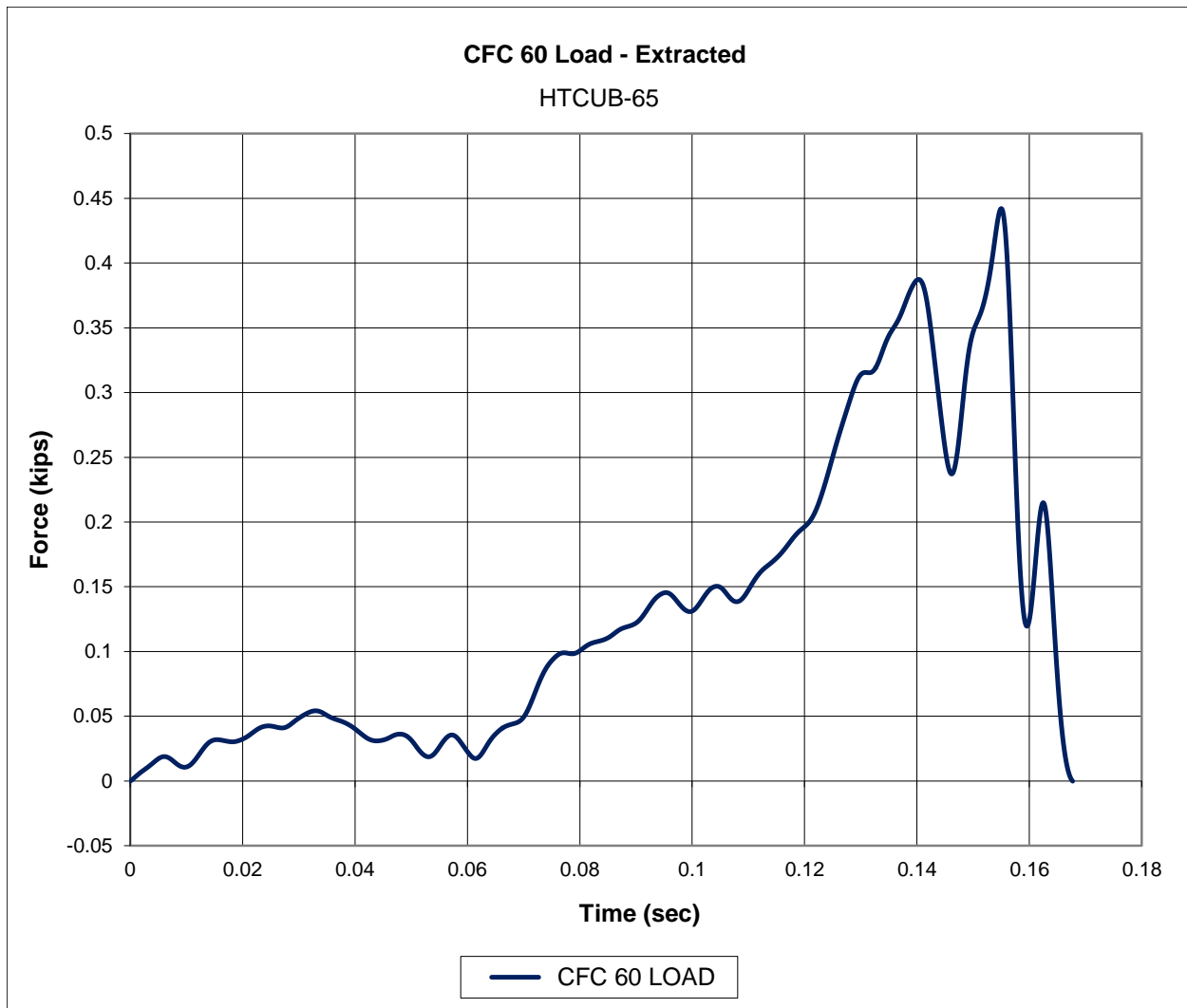
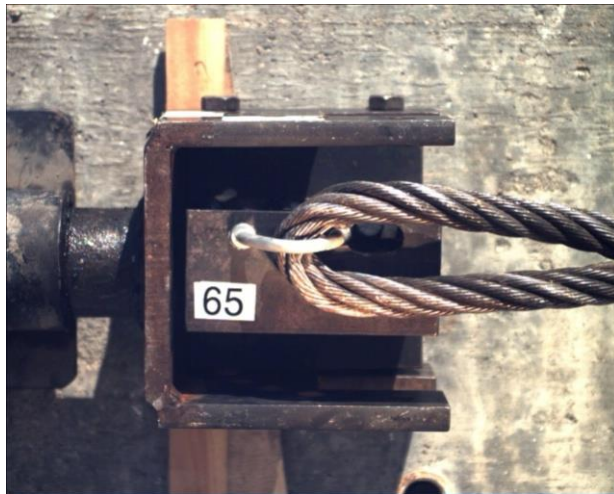


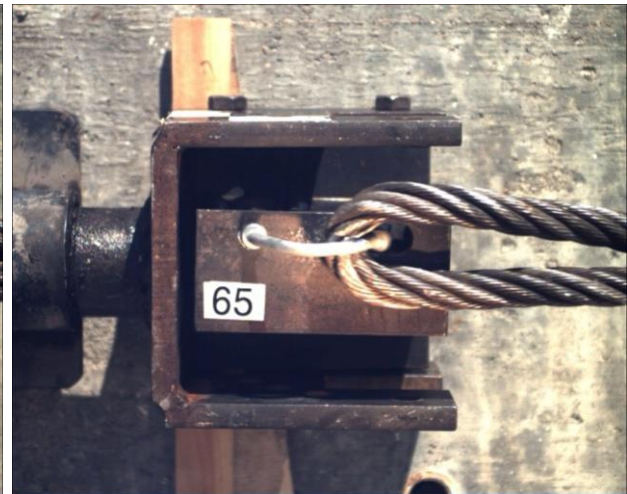
Figure 150. Force-Time Data, Test No. HTCUB-65



Figure 151. Post-Test Photograph, Test No. HTCUB-65



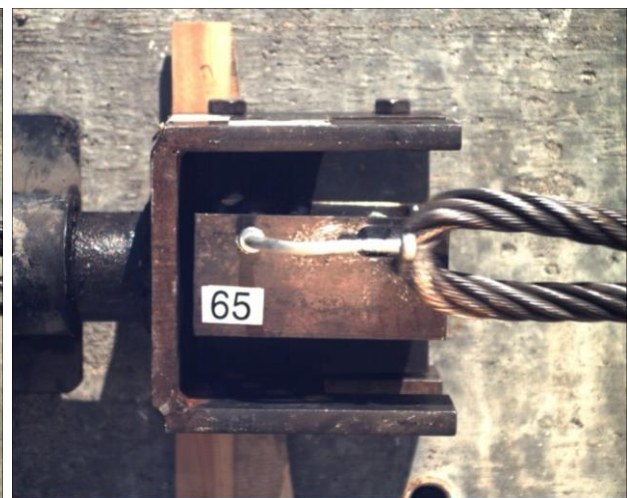
Time = 0 sec



Time = 0.152 sec



Time = 0.160 sec



Time = 0.168 sec, Release

Figure 152. Sequential Photographs, Test No. HTCUB-65

9.2 Discussion

The extended keyway bolts performed well when combined with the modified dual-width keyway. When pulled vertically, the button head released through the keyway freely. When pulled laterally, the button head became caught in the narrow part of the keyway, and the prototype bolt fractured through the weld of the extension.

The average vertical release load of the extended keyway bolts placed in the modified dual-width keyway was 486 lb (2.16 kN), and the average lateral release load was 5.17 kips (23.0 kN). During testing, several prototypes fractured through the weld of the extension—a weak spot that would not exist in the part if it were fabricated from one solid piece. However, it was believed that the lateral release of an extended keyway bolt (specially fabricated from one continuous round bar) would be higher. For lateral component test nos. HTCUB-23 and HTCUB-28 on the AISI C1018 keyway bolts from the previous testing program [71], the button heads became caught in the narrow part of the keyways as observed in test nos. HTCUB-62 and HTCUB-63. Subsequently, the bolts fractured through the threads with an average load of 6.47 kips (28.8 kN). Therefore, it was assumed that properly manufactured extended keyway bolts would also fracture through their threads with a lateral release load of 6.47 kips (28.8 kN).

The C1018 extended keyway bolts reduced the vertical release load from 1.18 kips (5.25 kN) to 486 lb (2.16 kN), although an even lower vertical release load was desired. Extending the moment arm was deemed impractical. A reduction in bolt diameter would decrease the bending strength and the vertical release load. Unfortunately, the tensile strength would also be decreased, which would reduce the lateral release load. Rather than pursue more keyway bolt concepts, new cable-to-post concepts were developed and are described in detail within Chapter 10.

10 OVERVIEW OF CRIMP-IN-PLACE TABBED BRACKETS, ROUND 1

10.1 Introduction

Following the investigation of the extended keyway bolts, it was deemed necessary to continue the effort to develop new cable-to-post attachments for use with the high-tension, cable barrier system. The extended keyway bolts seemed to be a good option, but it seemed prudent to cultivate multiple options, especially since the extended keyway bolts did not satisfy the initial target for the vertical release load of 225 lb (1.00 kN) or less. Toward the end of the investigative effort to modify the keyway bolts—even as dynamic component tests were in the queue—new cable-to-post attachment prototypes were being conceived. From the ongoing brainstorming of concepts, tabbed brackets, fabricated from sheet steel, were proposed.

There were two main variations of the tabbed bracket configurations, crimp-in-place and bolted, which referenced the method of attachment to the post. For both variations, the head of the bracket was designed to catch in the narrow part of a keyway when pulled laterally and release through the wider part of a keyway when pulled vertically. In this way, the tabbed brackets were very similar to the keyway bolts. Their main advantage over the keyway bolts was the “tune-ability” of their lateral and vertical release strengths. Cross-sectional properties, such as tensile area and plastic modulus, were easier to modify for the designer.

10.1.1 Dynamic Bogie Tests

All prototype designs noted in this chapter were later tested according to the dynamic bogie testing setup and procedures described in Chapter 6. Different load orientations were used in order to determine the vertical and lateral release loads for each concept under dynamic loading conditions.

10.1.2 Tabbed Bracket Basics

The tabbed brackets were to be fabricated from hot-rolled ASTM A1011 HSLA Grade 50 sheet steel. Similar to the keyway bolts, the tabbed brackets would utilize a type of dual-width keyway. Two variations of the tabbed brackets were configured—crimp-in-place and bolted. An example of each type of tabbed bracket is shown in Figure 153.

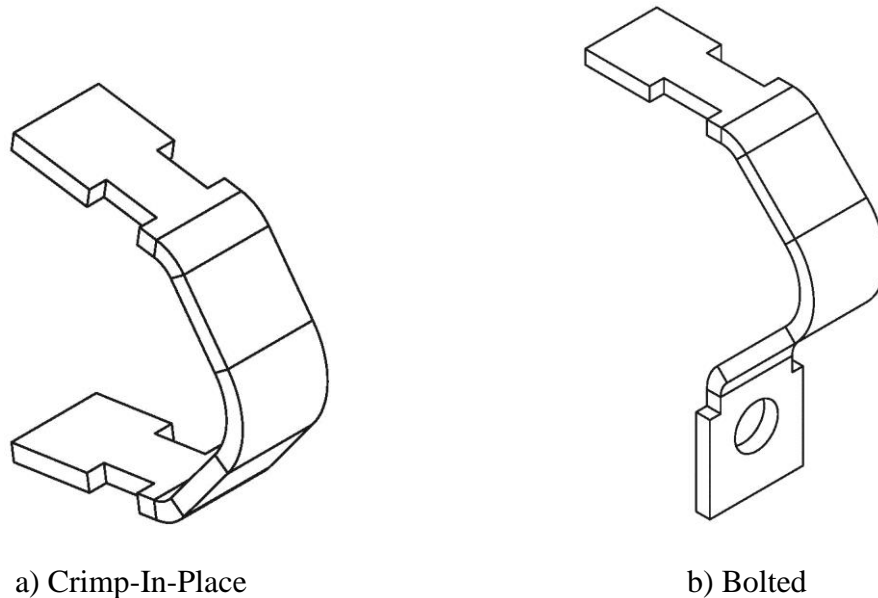


Figure 153. Tabbed Brackets—(a) Crimp-In-Place and (b) Bolted

The crimp-in-place tabbed brackets had two keyways where the top and bottom ends of the brackets were inserted into the post. The bracket was crimped into place following cable placement and insertion into post. The top of the bolted tabbed bracket was inserted only into one keyway at the top, while the bottom end was bolted to the front or back flange of the post with an SAE Grade 5 hex cap screw (i.e., bolt) and nut.

10.2 Crimp-In-Place Tabbed Brackets

The research and development of the tabbed brackets consisted of three rounds of design, testing, and evaluation. Crimp-in-place tabbed brackets were developed in the first round.

“Crimp-in-place” refers to the method of attachment to the support posts following cable insertion. The crimp-in-place tabbed brackets consisted of only one part. These brackets were inserted into the top and bottom keyways and crimped into place with channel-lock pliers, thus eliminating the need for extra parts, such as bolts, nuts, and washers. An example of an installed crimp-in-place tabbed bracket is shown in Figure 154.



Figure 154. Installed Crimp-In-Place Tabbed Bracket

10.2.1 Round 1 Design Equations

Equations were developed to guide the design process as well as to determine the actual dimensions of the prototype tabbed brackets. The dimensions, idealized load orientations, and assumed failure mechanisms and locations that were used in the development of the design equations, are shown in Figures 155 and 156.

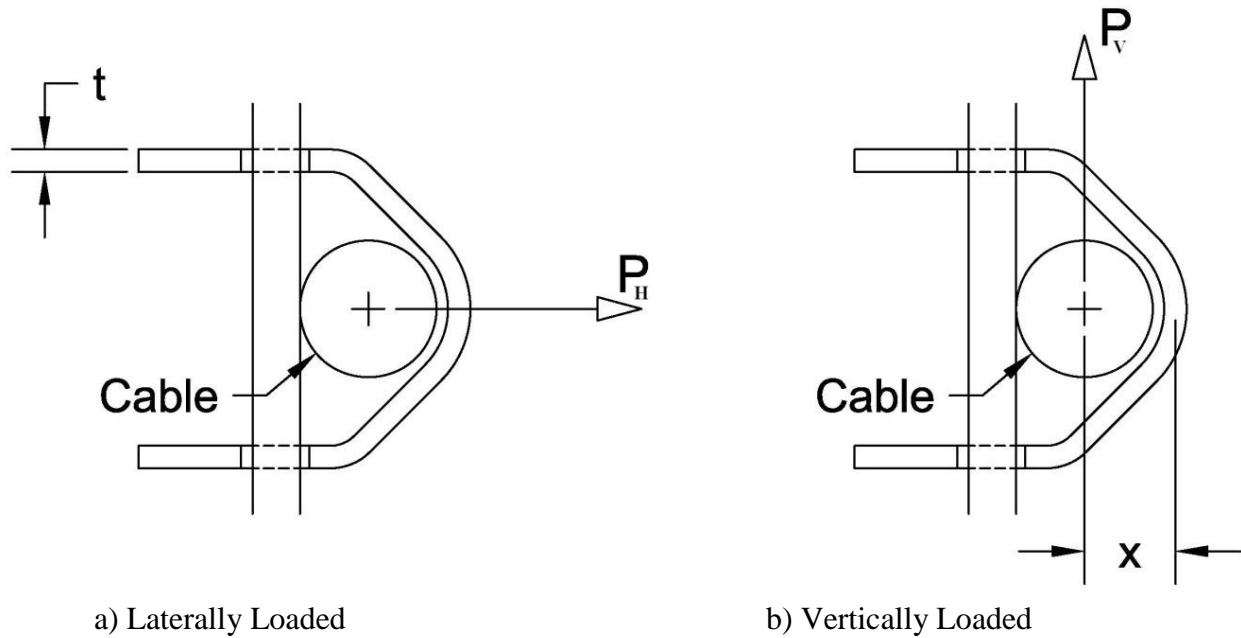


Figure 155. Tabbed Bracket—(a) Laterally Loaded and (b) Vertically Loaded

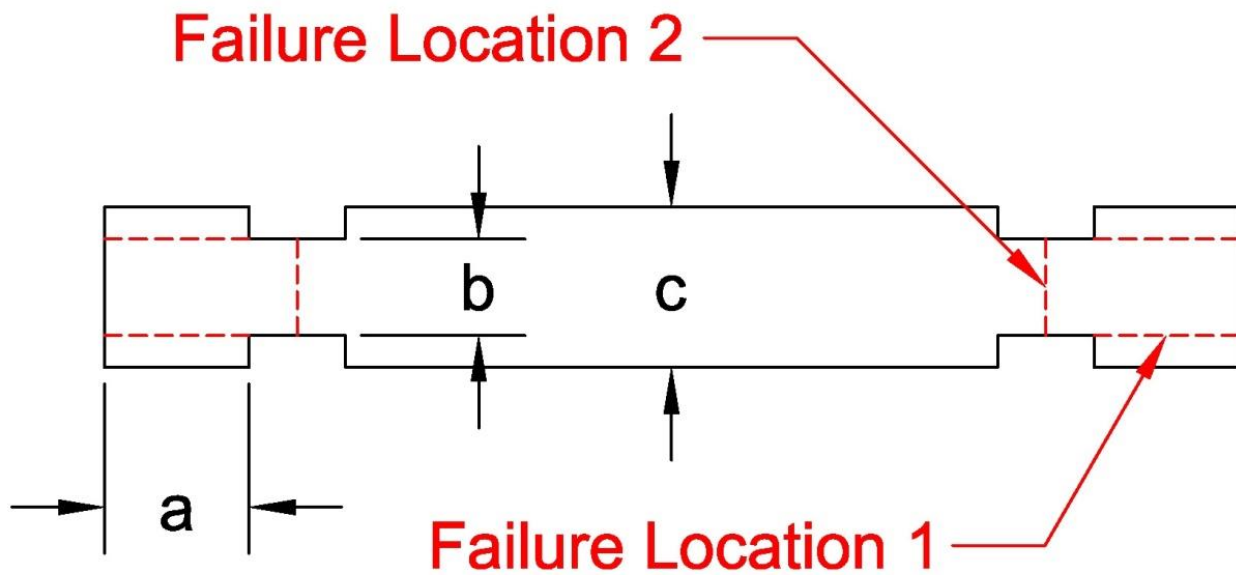


Figure 156. Dimensions and Failure Locations for Tabbed Bracket

For the lateral loading condition, as shown in Figure 155a, two failure locations were assumed in the bracket, as shown in Figure 157, thus resulting in two separate equations. It should be noted that dynamic magnification factors were not used in the first round equations as

they were not deemed necessary. One half of the horizontal load, P_H , was assumed to be distributed to each end of the tabbed bracket, as shown in Figure 157.

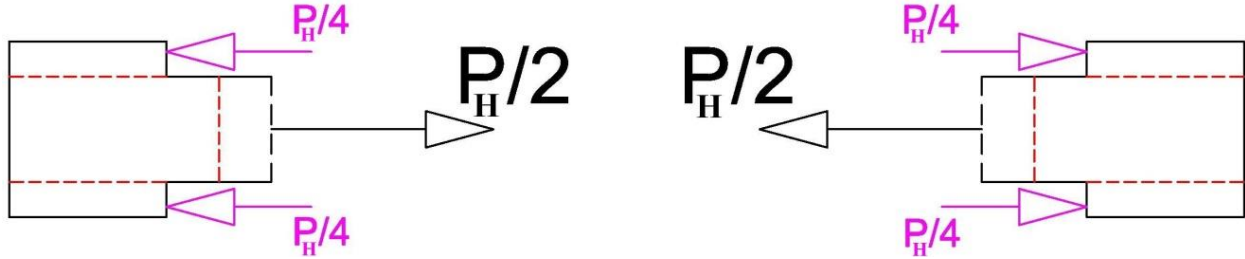


Figure 157. End Reactions for Use in the Design Equations

Failure location 1 was assumed to be a pure shear fracture. For pure shear, the shear yield strength is the tensile yield strength divided by the square root of three. This result corresponds to the maximum octahedral shear stress condition [75]. The same factor can be used with the ultimate tensile strength to obtain the ultimate shear strength. The lateral load needed to cause failure at location 1 for four surfaces was calculated using Equation 10.1. The steps used to derive the equation are also provided. The first step was to equate the end reaction to the available shear resistance.

$$\text{End Reaction} = \frac{P_{H_1}}{2} = A_1 \tau_u$$

Where A_1 = shear area for failure location 1 (two surfaces)
 τ_u = ultimate shear strength

$$\frac{P_{H_1}}{2} = (2at) \frac{\sigma_u}{\sqrt{3}}$$

$$P_{H_1} = \frac{4}{\sqrt{3}} at \sigma_u \quad (10.1)$$

Where σ_u = ultimate tensile strength
 a = length of head (see Figure 156)
 t = thickness (see Figure 155a)

Failure location 2 was assumed to be a pure tensile fracture. The lateral load needed to cause failure at location 2 for two surfaces was calculated using Equation 10.2. The steps used to derive the equation are also provided. The first step was to equate the end reaction with the available tensile resistance.

$$\text{End Reaction} = \frac{P_{H_2}}{2} = A_2 \sigma_u$$

Where A_2 = tensile area for failure location 2 (one surface)

$$\frac{P_{H_2}}{2} = (bt) \sigma_u$$

$$P_{H_2} = 2bt \sigma_u \quad (10.2)$$

Where σ_u = ultimate tensile strength
b = width of neck (see Figure 156)
t = thickness (see Figure 155a)

The expected lateral release load was determined to be the lesser of Equations 10.1 and 10.2.

The vertical release load was assumed to occur in pure, plastic bending. As noted previously, no dynamic magnification factor was used in the equations from the first round. The moment arm, x, was measured between the center of the cable and the mid-plane of the outer bracket, as shown in Figure 156b. The vertical release load for the cable was calculated using Equation 10.3. The steps used to derive the equation are also provided.

$$P_V x = M_P$$

Where x = moment arm (see Figure 155b)
 M_P = plastic moment

$$P_V = \frac{M_P}{x} = \frac{Z\sigma_y}{x} = \frac{\left(\frac{ct^2}{4}\right)\sigma_y}{x} = \frac{ct^2\sigma_y}{4x} \quad (10.3)$$

Where σ_y = yield strength
Z = plastic section modulus
c = width where bending occurs (see Figure 156)
t = thickness (see Figure 155a)

When calculating the shear and tensile capacities of the Round 1 tabbed brackets, the steel strengths were 50 ksi (345 MPa) for the yield strength and 70 ksi (483 MPa) for the ultimate tensile strength. The actual strengths can be found on the material testing reports, as provided in Appendix E.

10.2.2 Dimensions and Structural Capacities

There were two versions of the crimp-in-place tabbed brackets. Tabbed bracket Version 1 was fabricated from 10-gauge, grade 50 sheet steel. Using the design equations, the predicted lateral and vertical capacities were 5.88 kips (26.2 kN) and 224 lb (996 N), respectively. Side views of the Version 1 bracket are shown in Figure 158. A flat pattern of the tabbed bracket is shown in Figure 159. The keyway corresponding to the Version 1 bracket is shown in Figure 160.

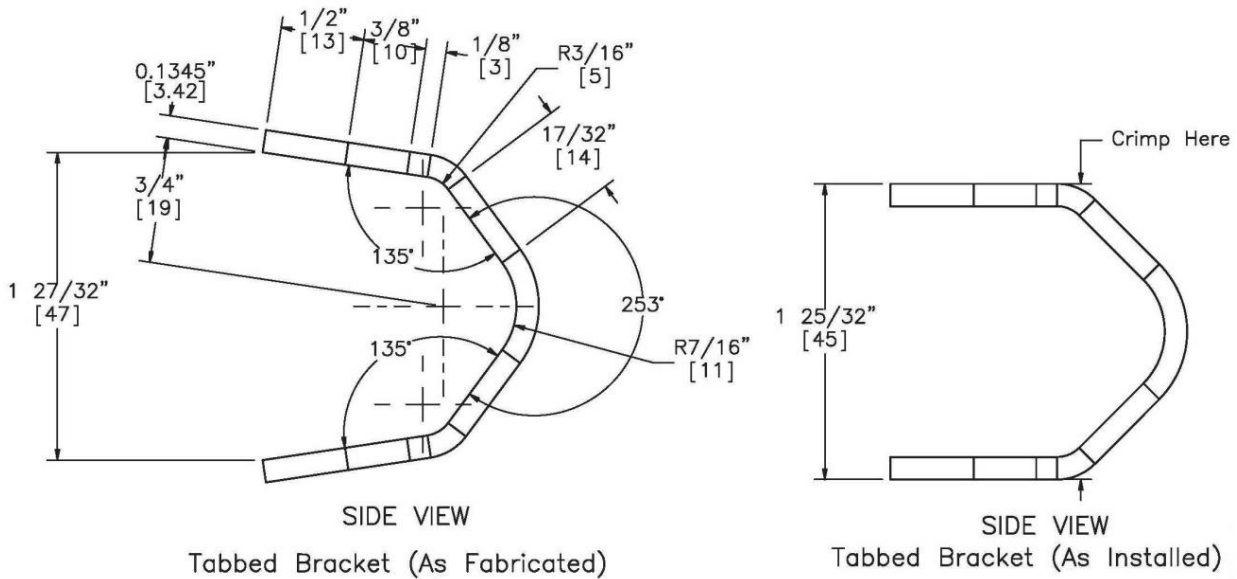


Figure 158. Side Views of Tabbed Bracket Version 1—Before and After Installation

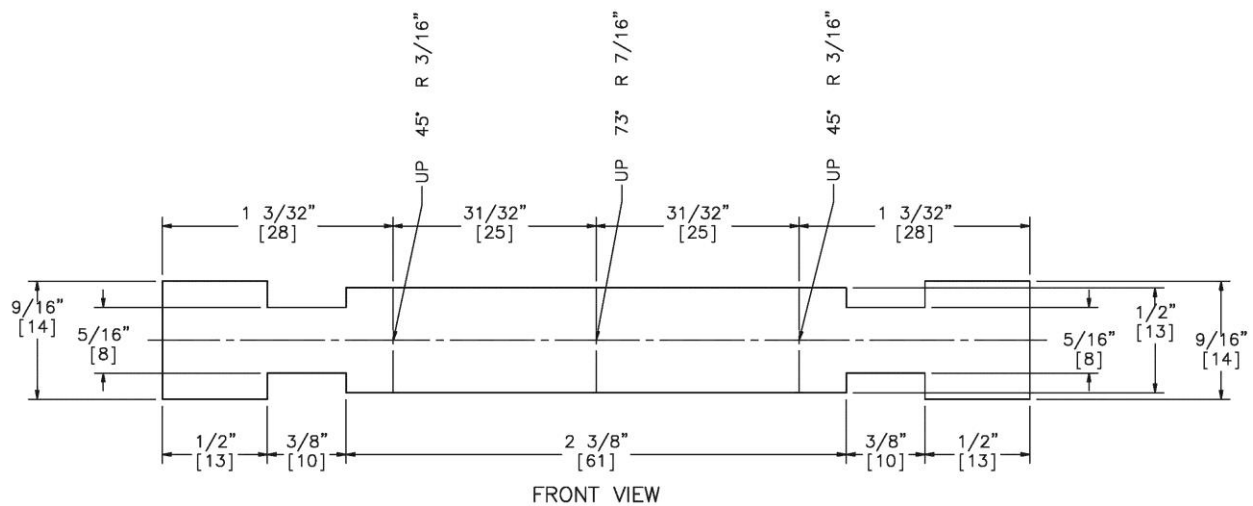


Figure 159. Flat Pattern for Tabbed Bracket Version 1

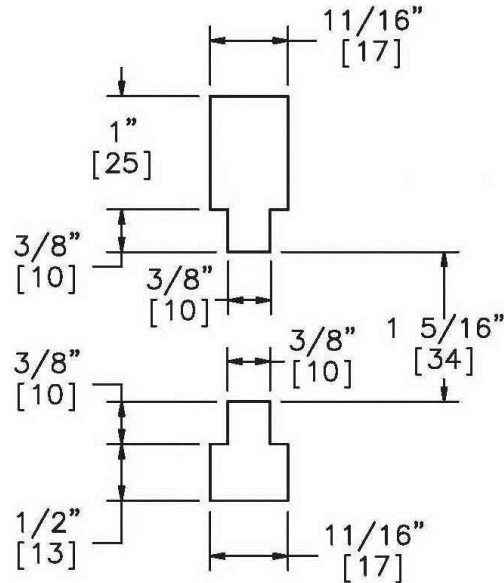


Figure 160. Tabbed Bracket Version 1 Keyway

Tabbed bracket Version 2 was fabricated from 11-gauge, grade 50 sheet steel. Using the design equations, the predicted lateral and vertical capacities were 6.28 kips (27.9 kN) and 225 lb (1.00 kN), respectively. Side views of the Version 2 bracket are shown in Figure 161. A flat pattern of the tabbed bracket is shown in Figure 162. The keyway corresponding to the Version 2 bracket is shown in Figure 163.

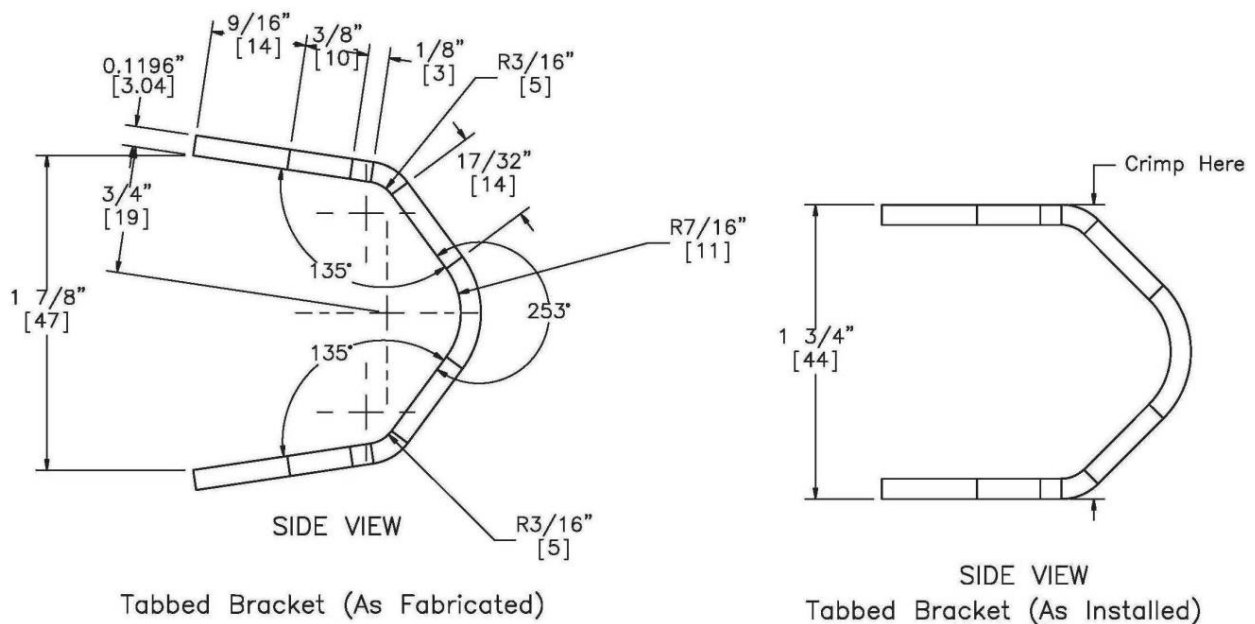


Figure 161. Side Views of Tabbed Bracket Version 2—Before and After Installation

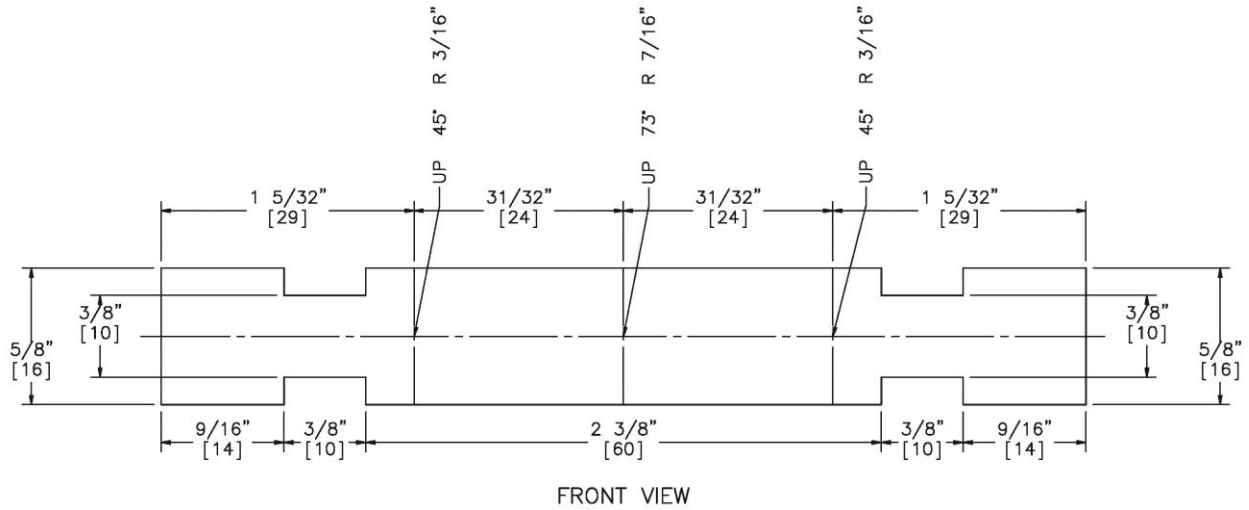


Figure 162. Flat Pattern of Tabbed Bracket Version 2

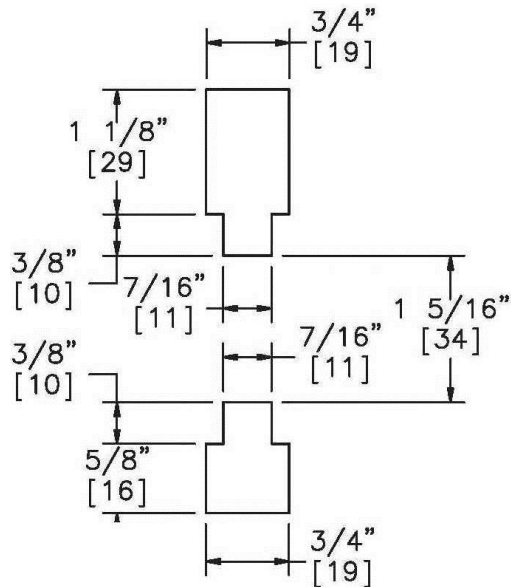


Figure 163. Tabbed Bracket Version 2 Keyway

The expected release loads for the crimp-in-place tabbed brackets from Round 1 are shown in Table 7.

Table 7. Expected Release Loads for Round 1 Crimp-In-Place Tabbed Brackets

Tabbed Bracket	Expected Lateral Release Load kips (kN)		Expected Vertical Release Load kips (kN)
	Failure Location 1	Failure Location 2	
Version 1	7.77 (34.5)	5.88 (26.2)	0.22 (1.0)
Version 2	7.77 (34.5)	6.28 (27.9)	0.22 (1.0)

11 DYNAMIC COMPONENT TESTS—CRIMP-IN-PLACE TABBED BRACKETS, ROUND 1

11.1 Results

In addition to keyway bolts, several variations of a tabbed bracket configuration were tested and evaluated. The tabbed bracket concepts were similar to the keyway bolts, in that they also used a keyway to catch or allow for free release of the cable-to-post attachment, depending on the orientation of the load—lateral or vertical. All of the tabbed brackets were fabricated from hot-rolled, ASTM A1011, HSLA Grade 50 sheet steel. The tabbed bracket thickness, cross-section width, method of attachment, and the mounting post section were varied for the Round 1 tests. The same setup and procedures used to test the keyway bolts was also used to test the tabbed brackets. Three rounds of design modifications, component testing, and evaluation were made to the tabbed brackets. Eight dynamic component tests (test nos. HTTPB-1 through HTTPB-8) were performed in the first round and are presented Chapters 10 and 11. Ten dynamic component tests (test nos. HTTPB-9 through HTTPB-16, including test nos. HTTPB-9R and HTTPB-12R) were performed in the second round, which are discussed later in Chapters 12 and 13. Twenty-four dynamic component tests (test nos. HTTPB-17 through HTTPB-40) were performed in the third round, which are discussed later in Chapters 14 and 15. Each individual concept was tested twice in its vertical orientation and twice in its lateral orientation in order to determine the structural capacities and cable release behaviors. For the sake of convenience, the consolidated drawing sets for all three rounds of dynamic component testing on tabbed brackets is shown in Figures 164 through 203. The test matrix and results for the first round of tests on the crimp-in-place tabbed brackets are summarized in Table 8.

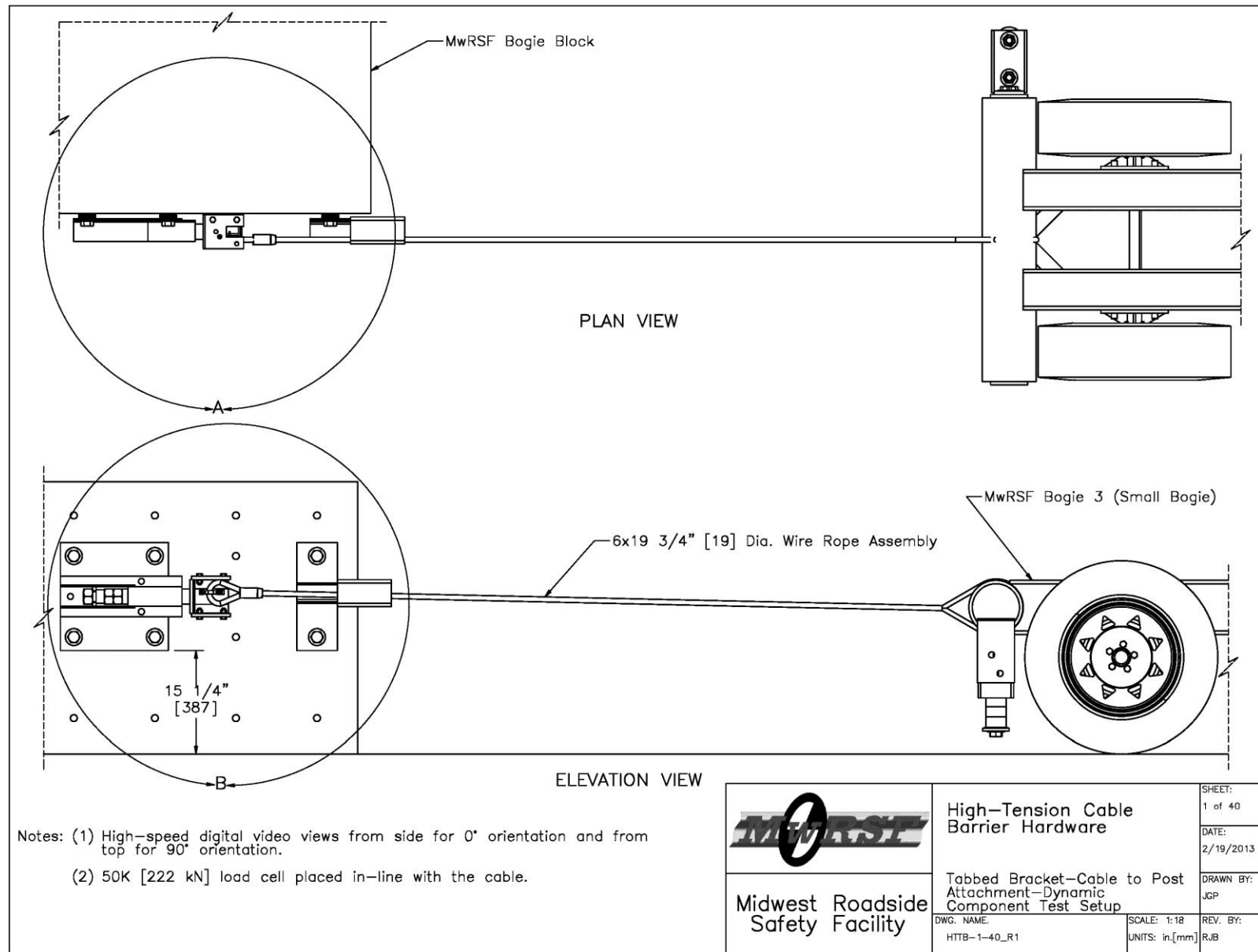


Figure 164. Bogie Test Setup, Test Nos. HTTP-1 through HTTP-40

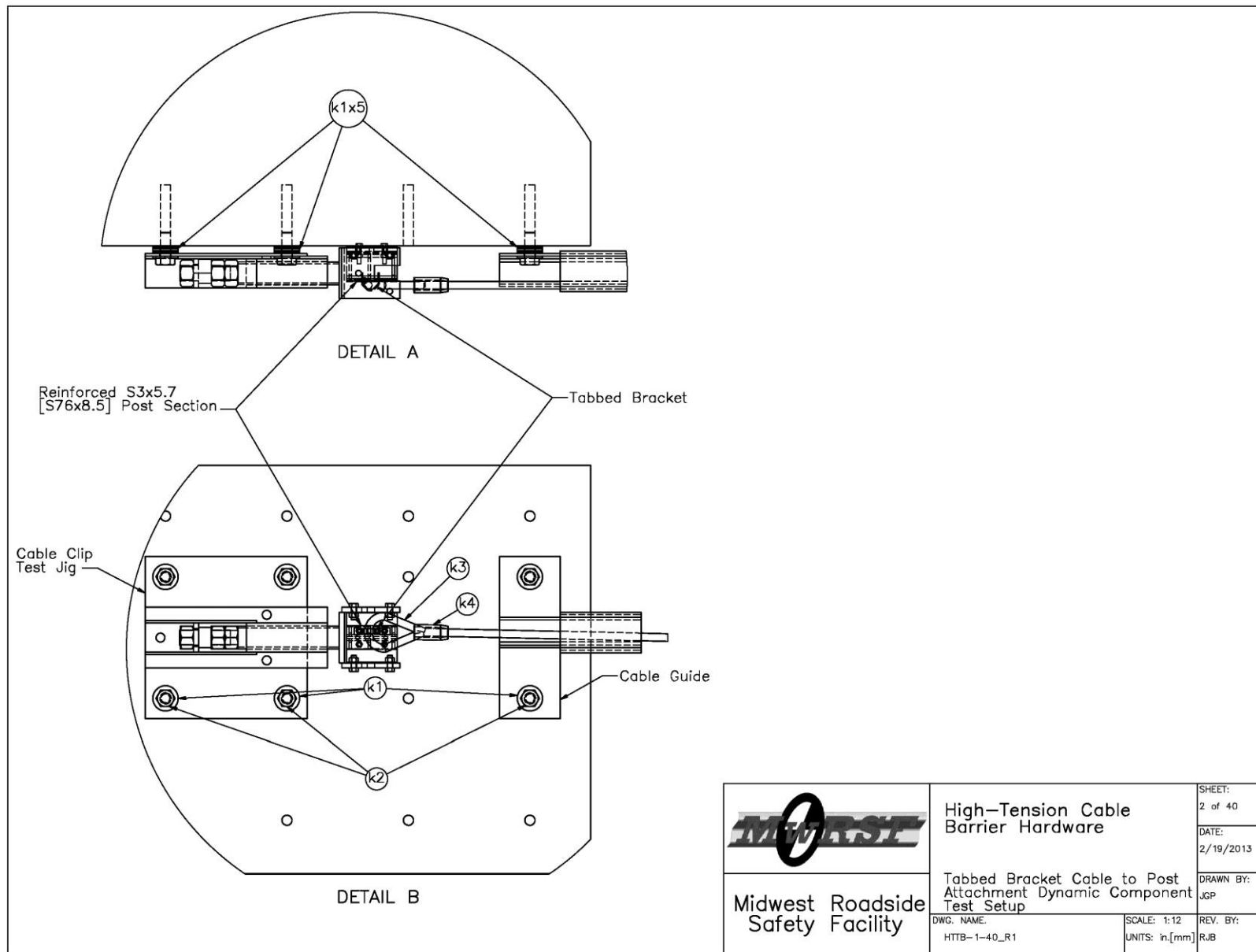


Figure 165. Test Jig Details, Test Nos. HTTPB-1 through HTTPB-40

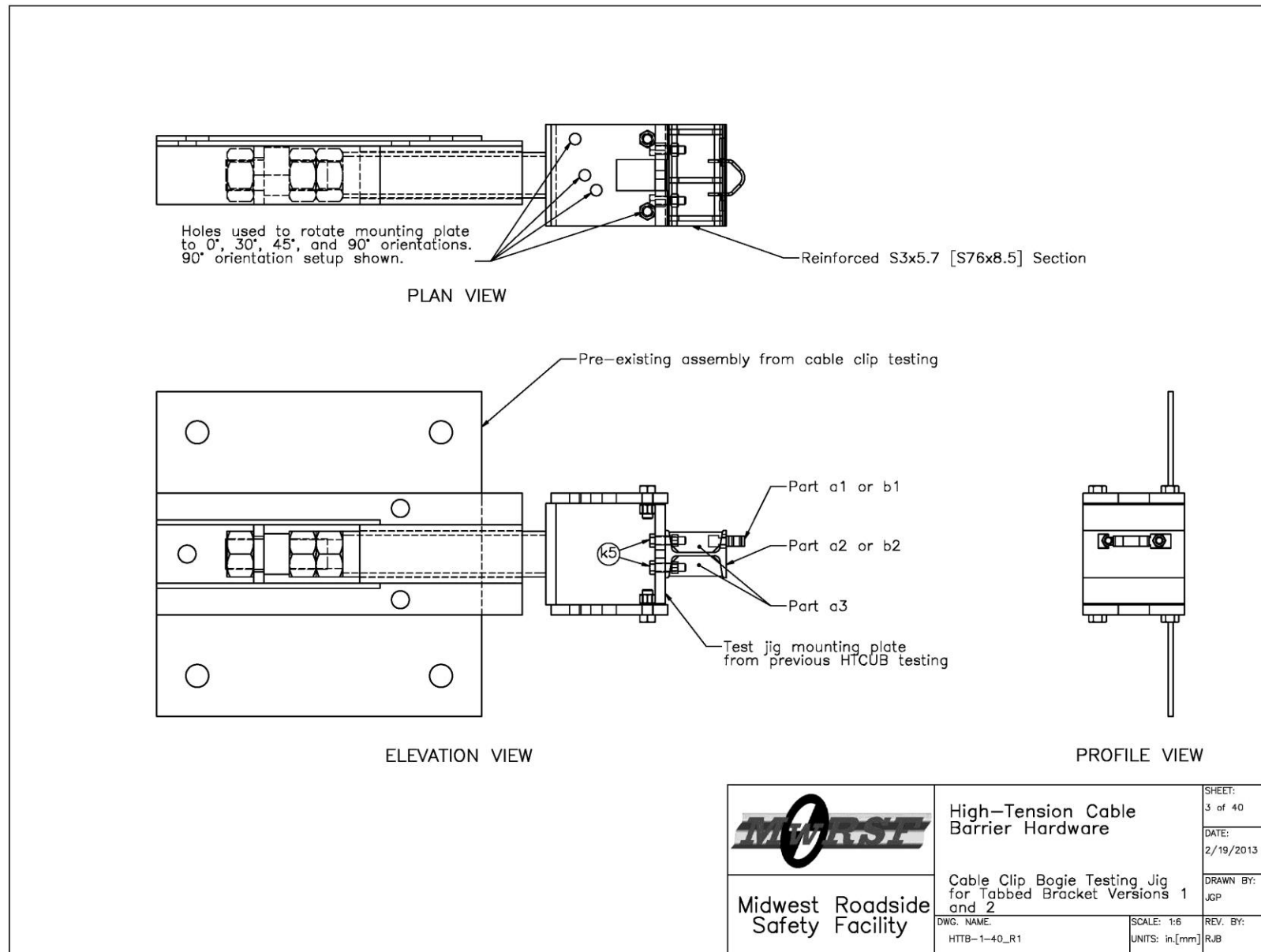


Figure 166. Test Jig Setup for Tabbed Bracket Versions 1 and 2, Test Nos. HTTPB-1 through HTTPB-40

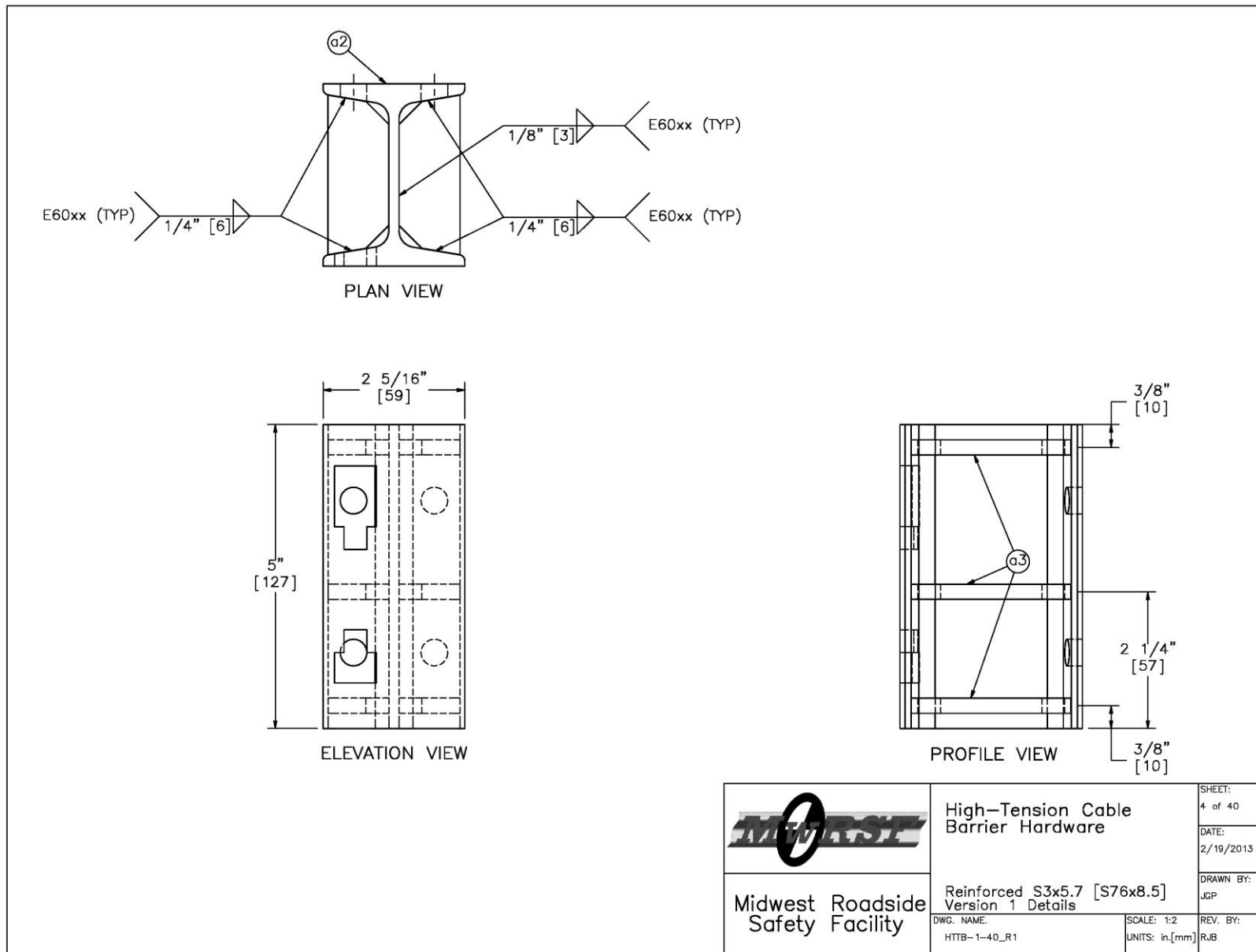


Figure 167. Reinforced S3x5.7 (S76x8.5) Section Version 1 Details, Test Nos. HTTB-1 through HTTB-40

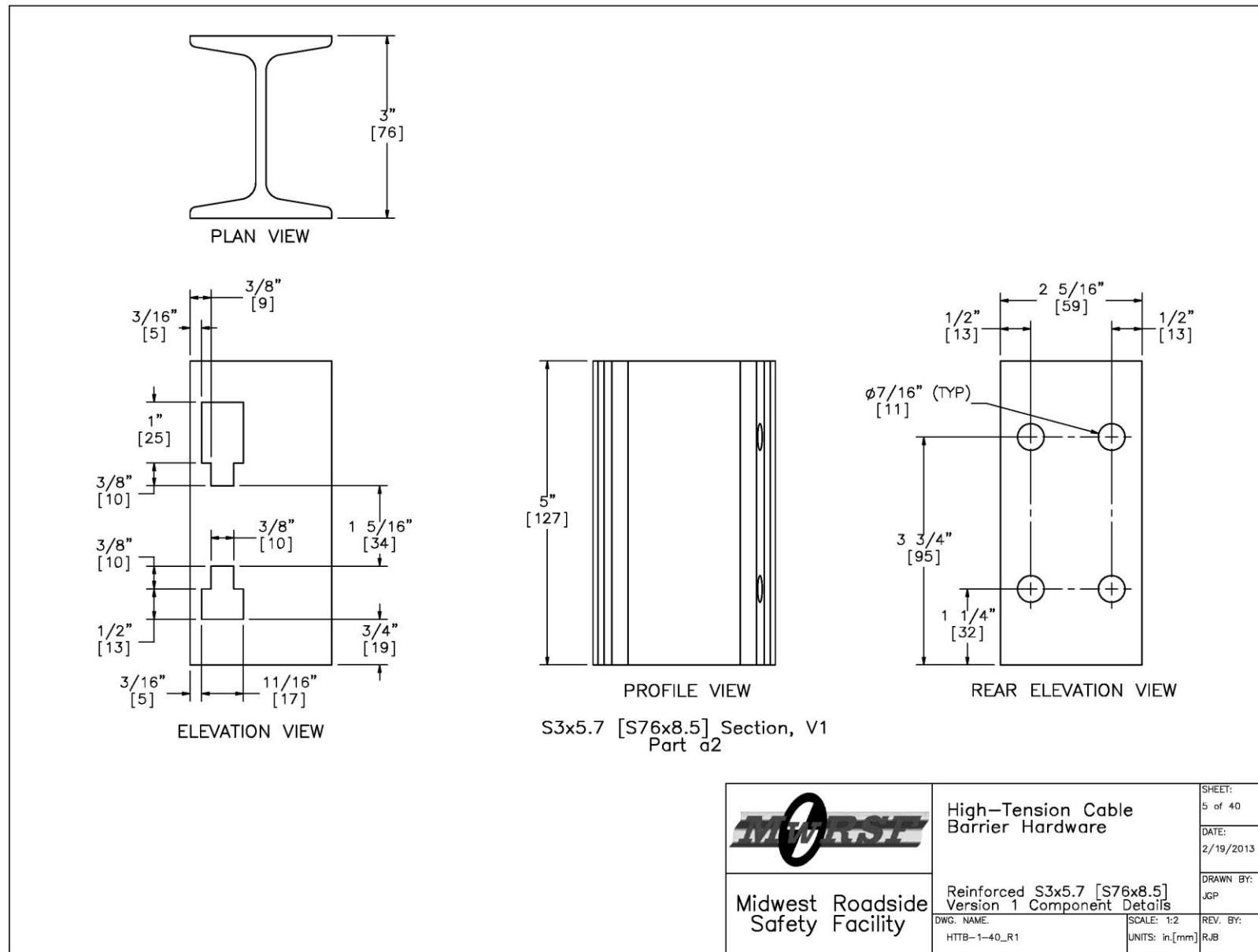


Figure 168. Reinforced S3x5.7 (S76x8.5) Section Version 1 Details, Test Nos. HTTB-1 through HTTB-40

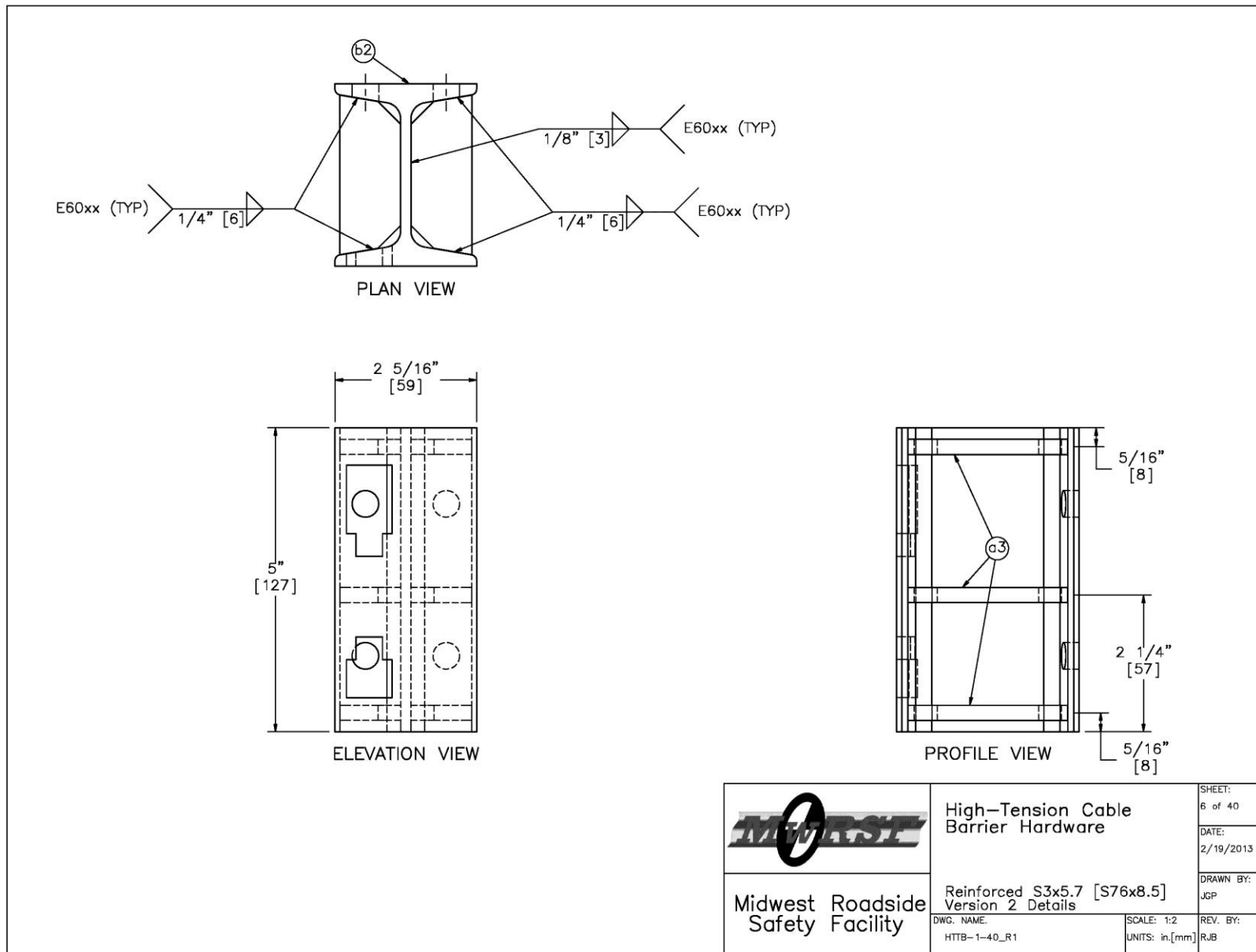


Figure 169. Reinforced S3x5.7 (S76x8.5) Section Version 2 Details, Test Nos. HTTB-1 through HTTB-40

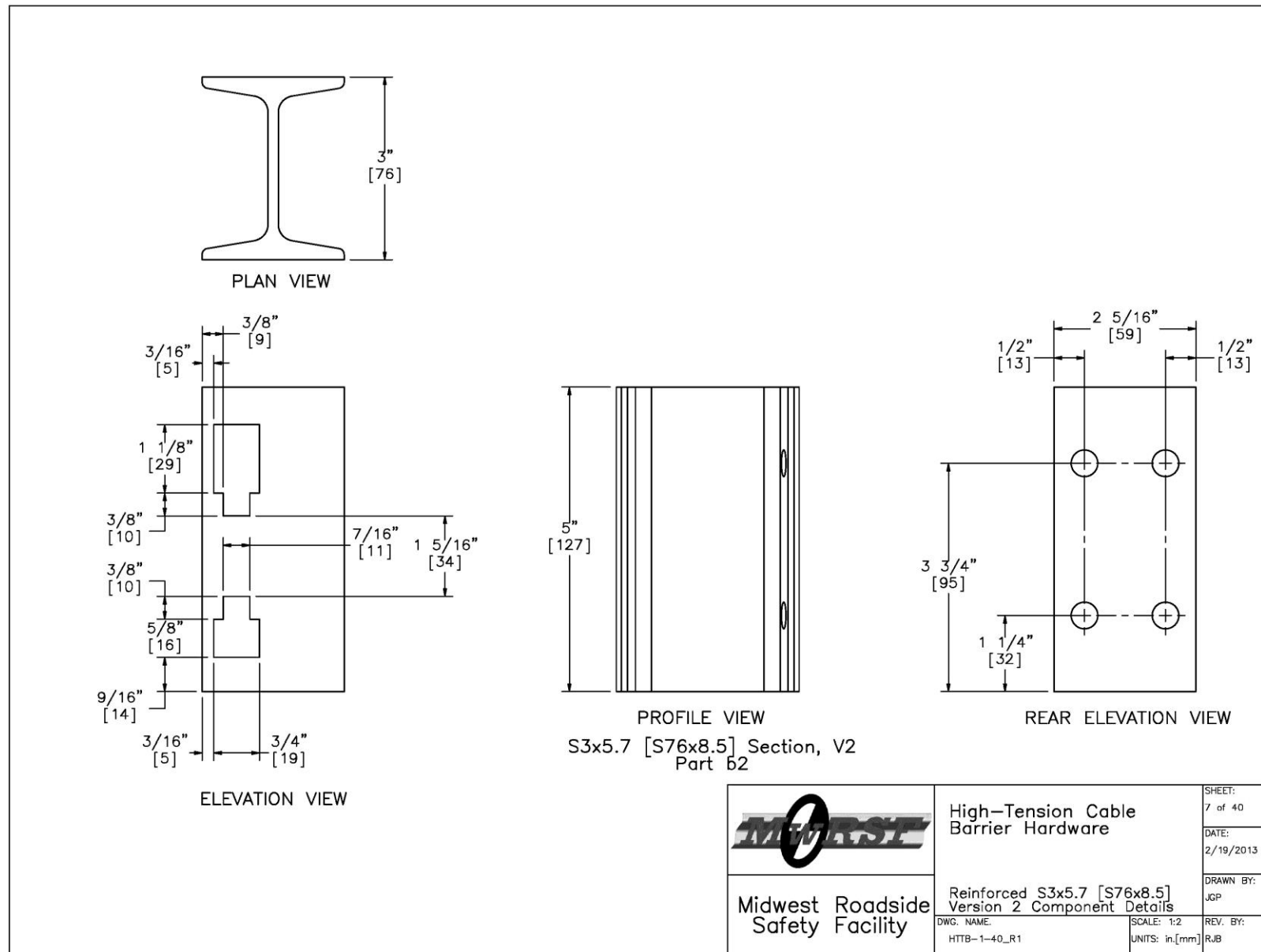


Figure 170. Reinforced S3x5.7 (S76x8.5) Section Version 2 Details, Test Nos. HTTB-1 through HTTB-40

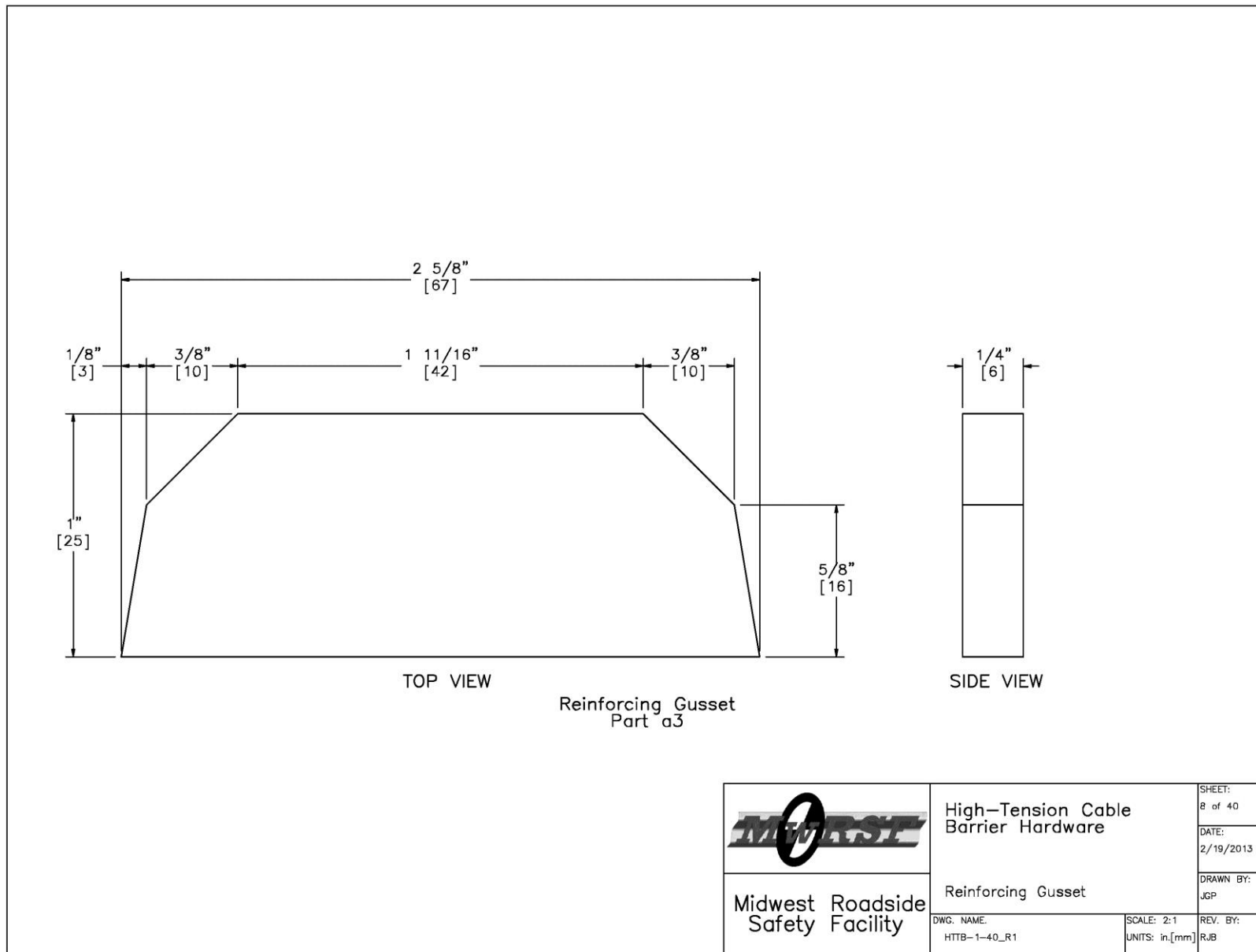


Figure 171. Reinforcing Gusset Details, Test Nos. HTTB-1 through HTTB-40

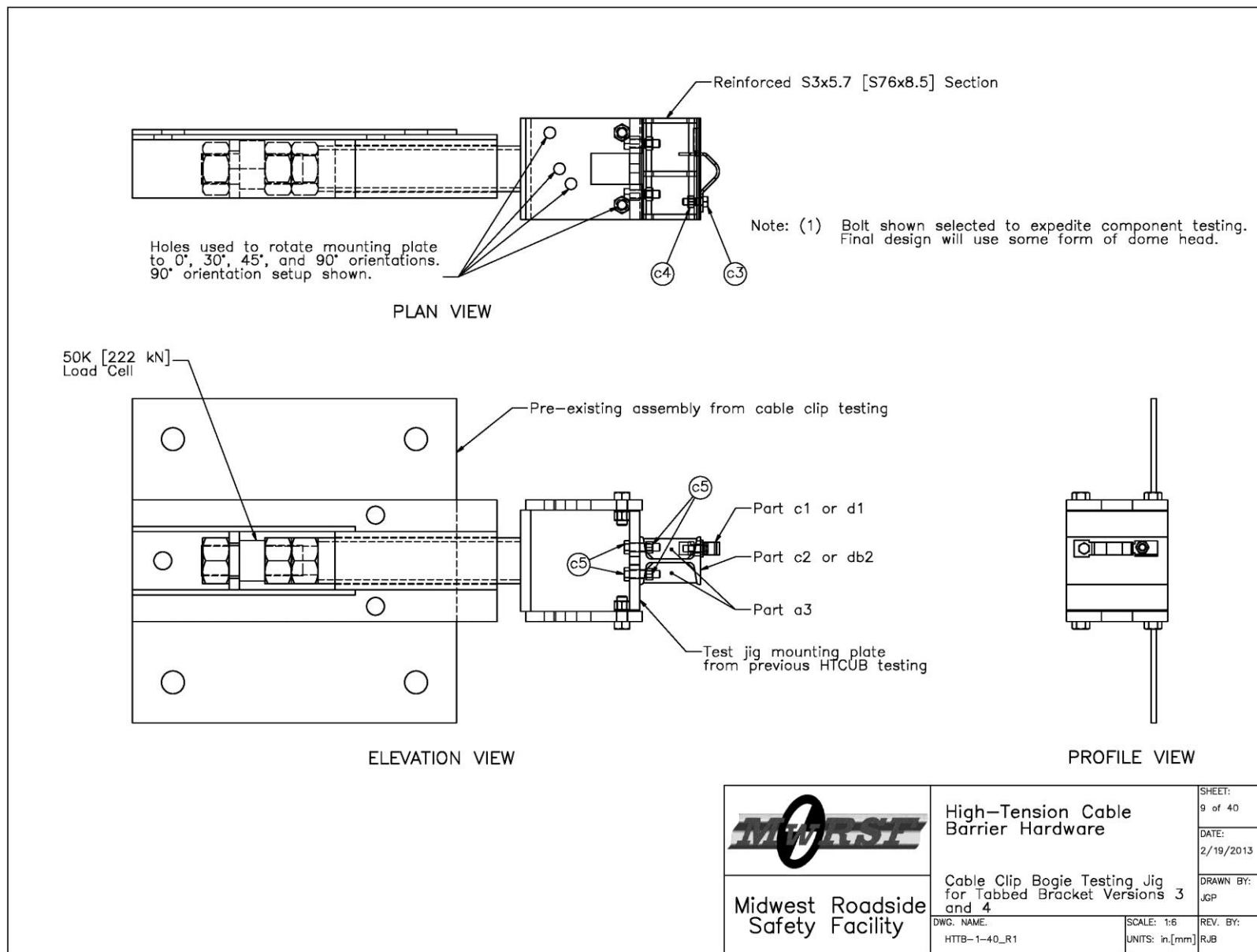


Figure 172. Test Jig Setup for Tabbed Bracket Versions 3 and 4, Test Nos. HTTB-1 through HTTB-40

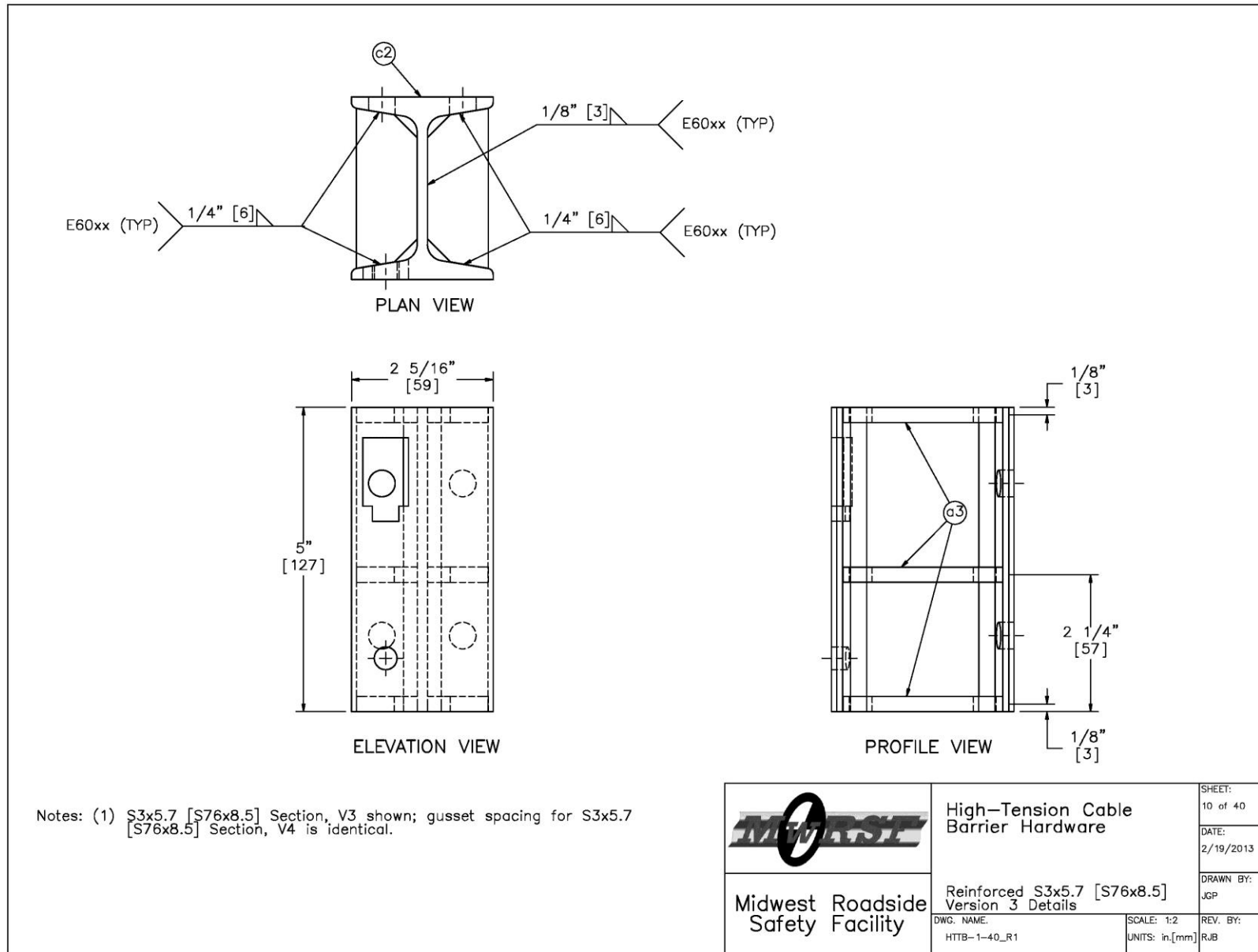


Figure 173. Reinforced S3x5.7 (S76x8.5) Section Version 3 Details, Test Nos. HTTB-1 through HTTB-40

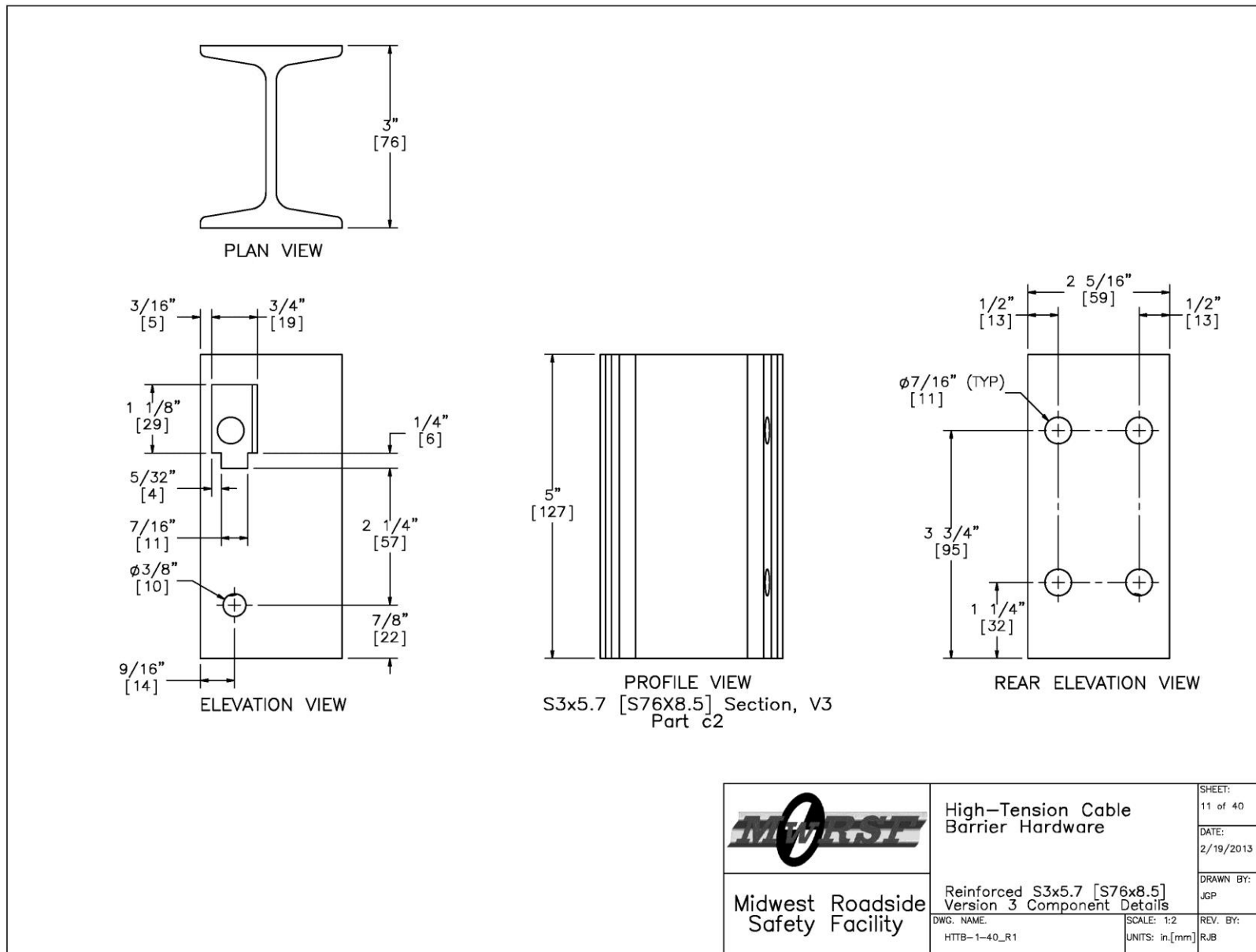


Figure 174. Reinforced S3x5.7 (S76x8.5) Section Version 3 Details, Test Nos. HTTB-1 through HTTB-40

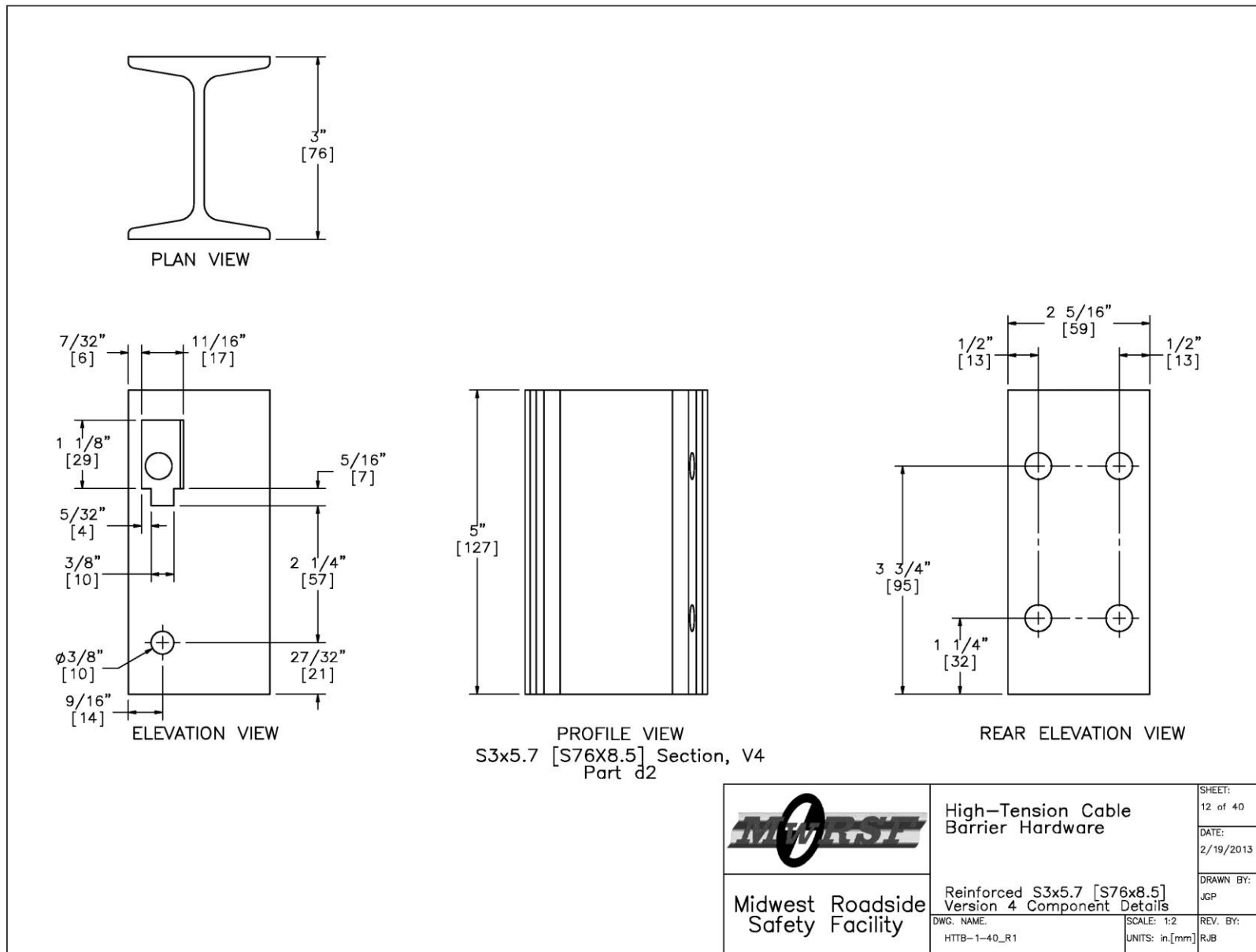


Figure 175. Reinforced S3x5.7 (S76x8.5) Section Version 4 Details, Test Nos. HTTB-1 through HTTB-40

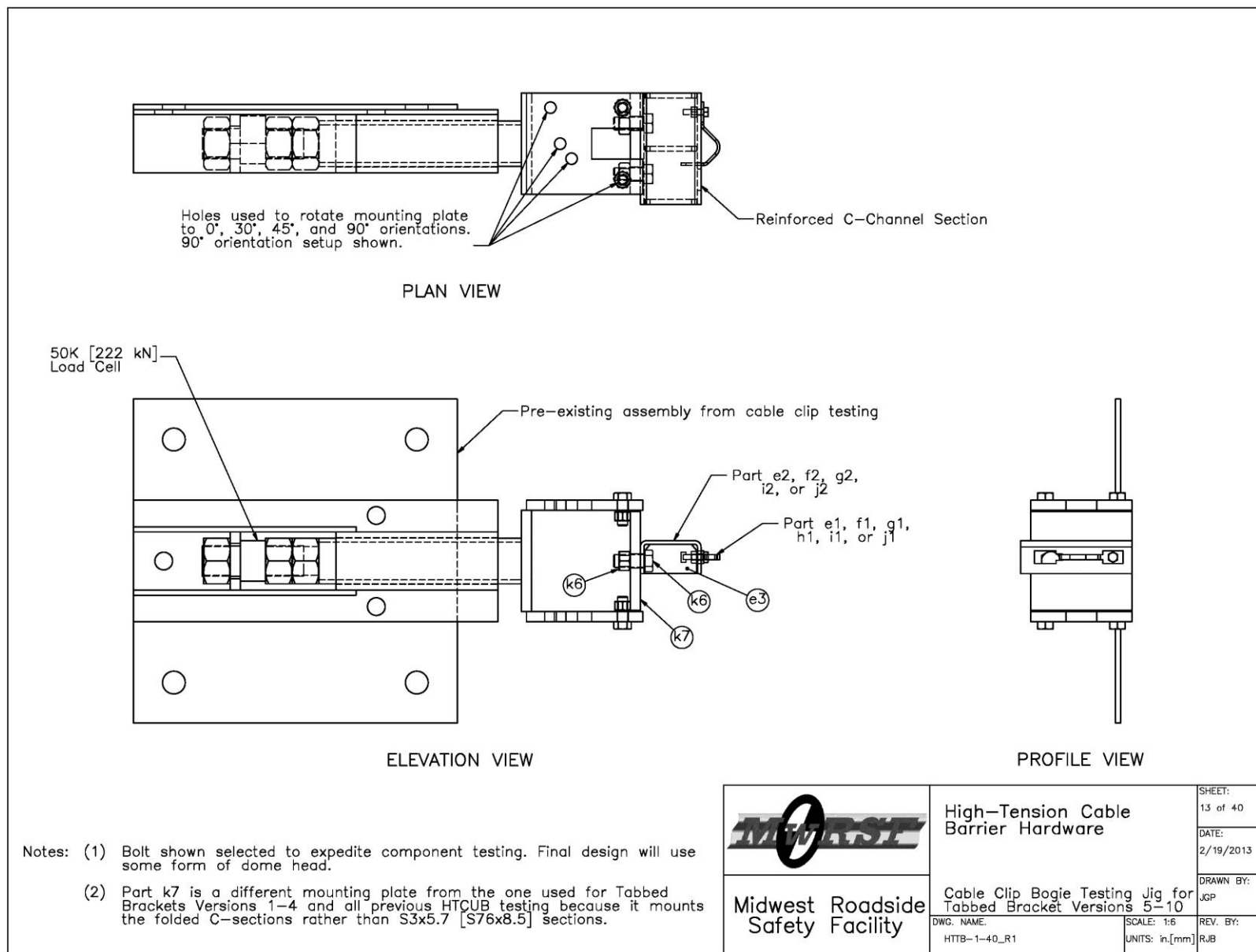


Figure 176. Test Jig Setup for Tabbed Bracket Version 5 through 10, Test Nos. HTTB-1 through HTTB-40

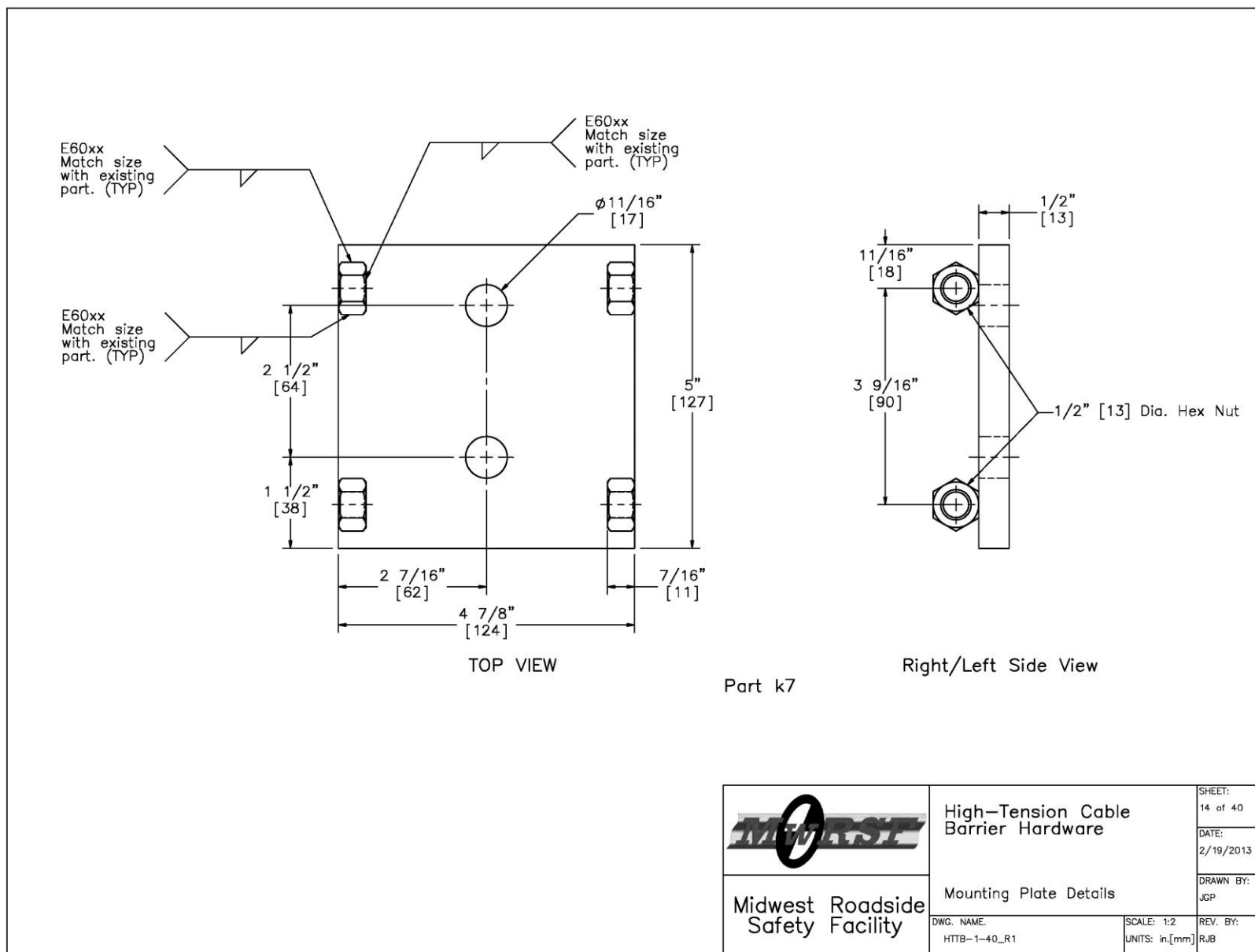


Figure 177. Mounting Plate Details, Test Nos. HTTB-1 through HTTB-40

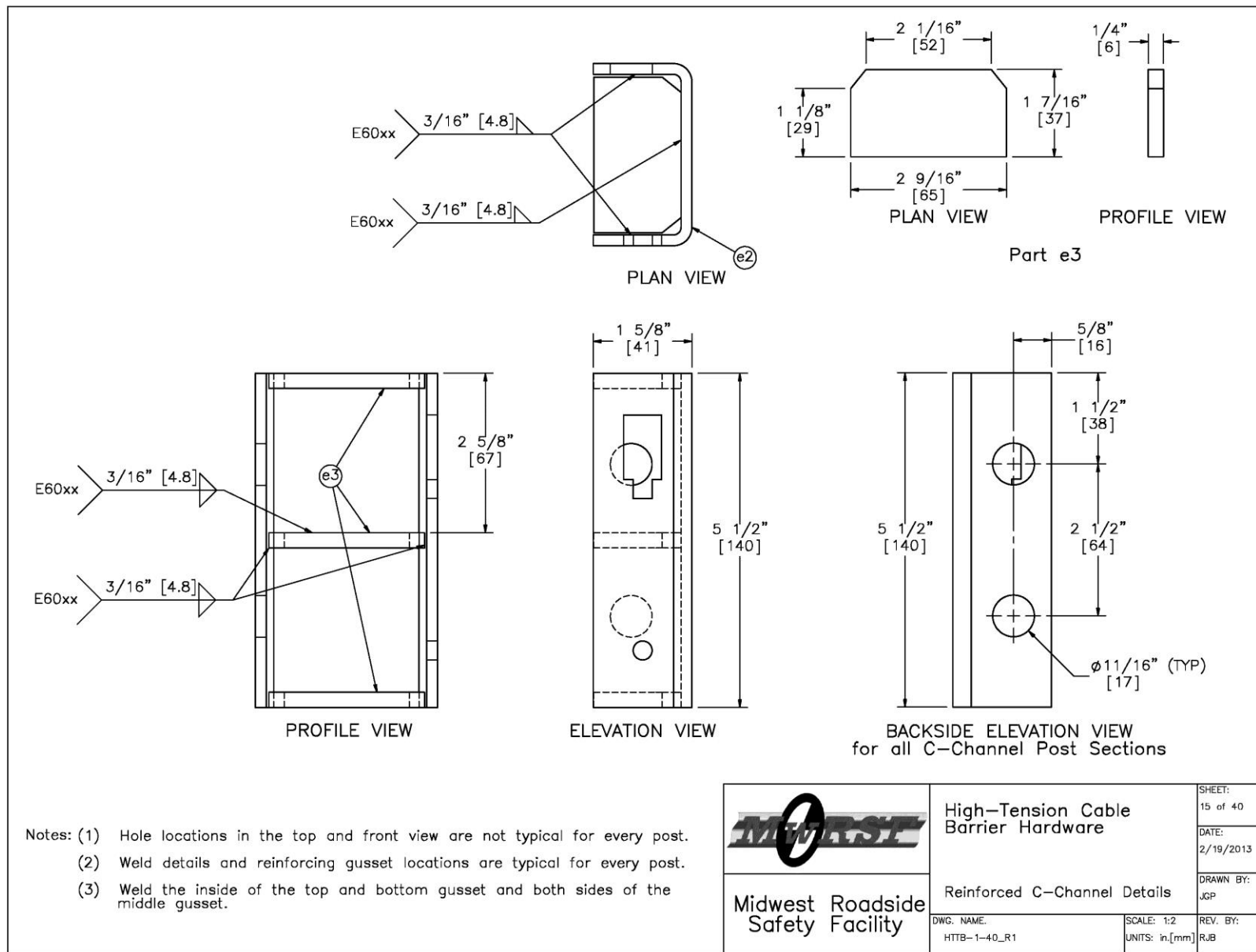


Figure 178. Reinforced C-Section Details, Test Nos. HTTB-1 through HTTB-40

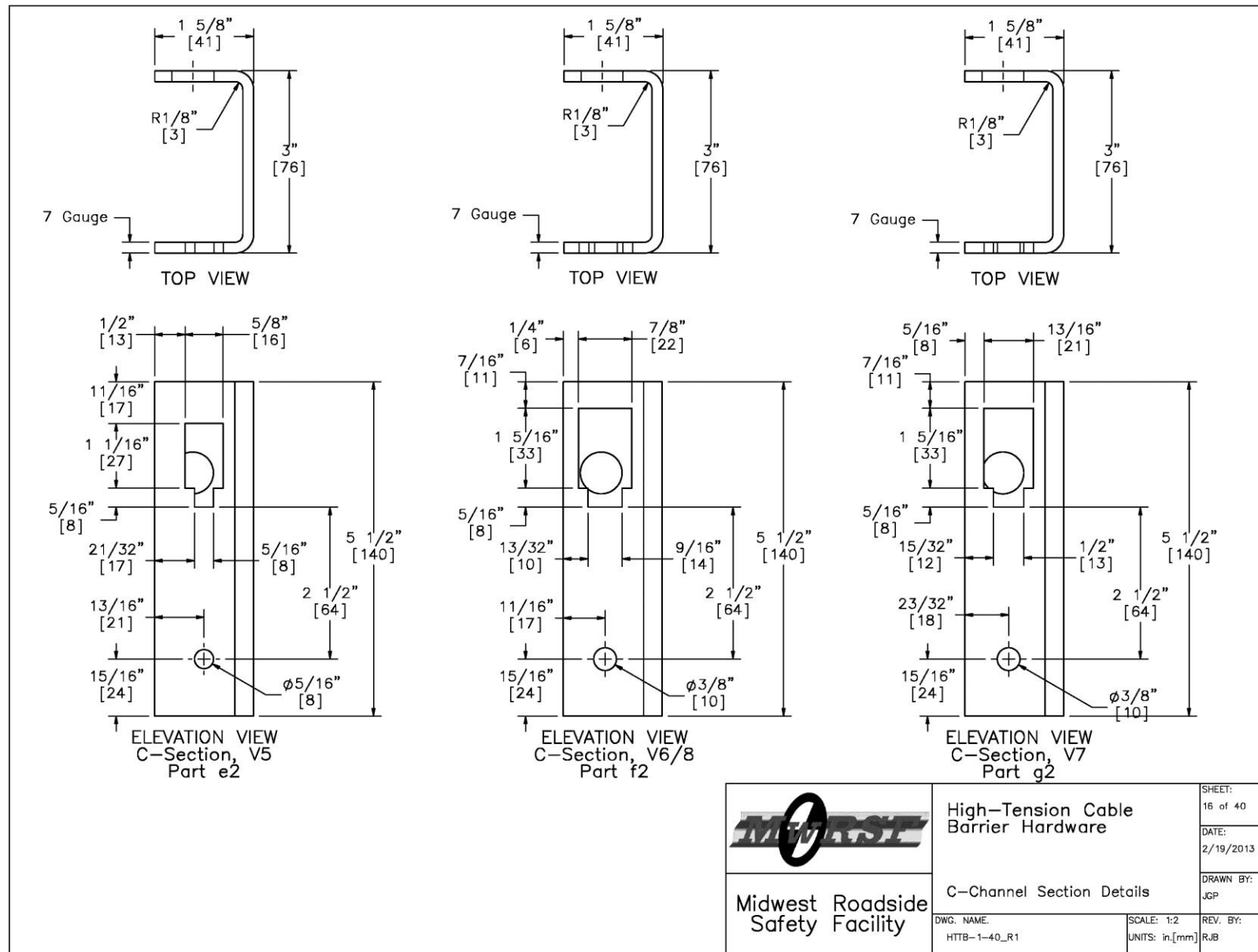


Figure 179. C-Section Details, Test Nos. HTTB-1 through HTTB-40

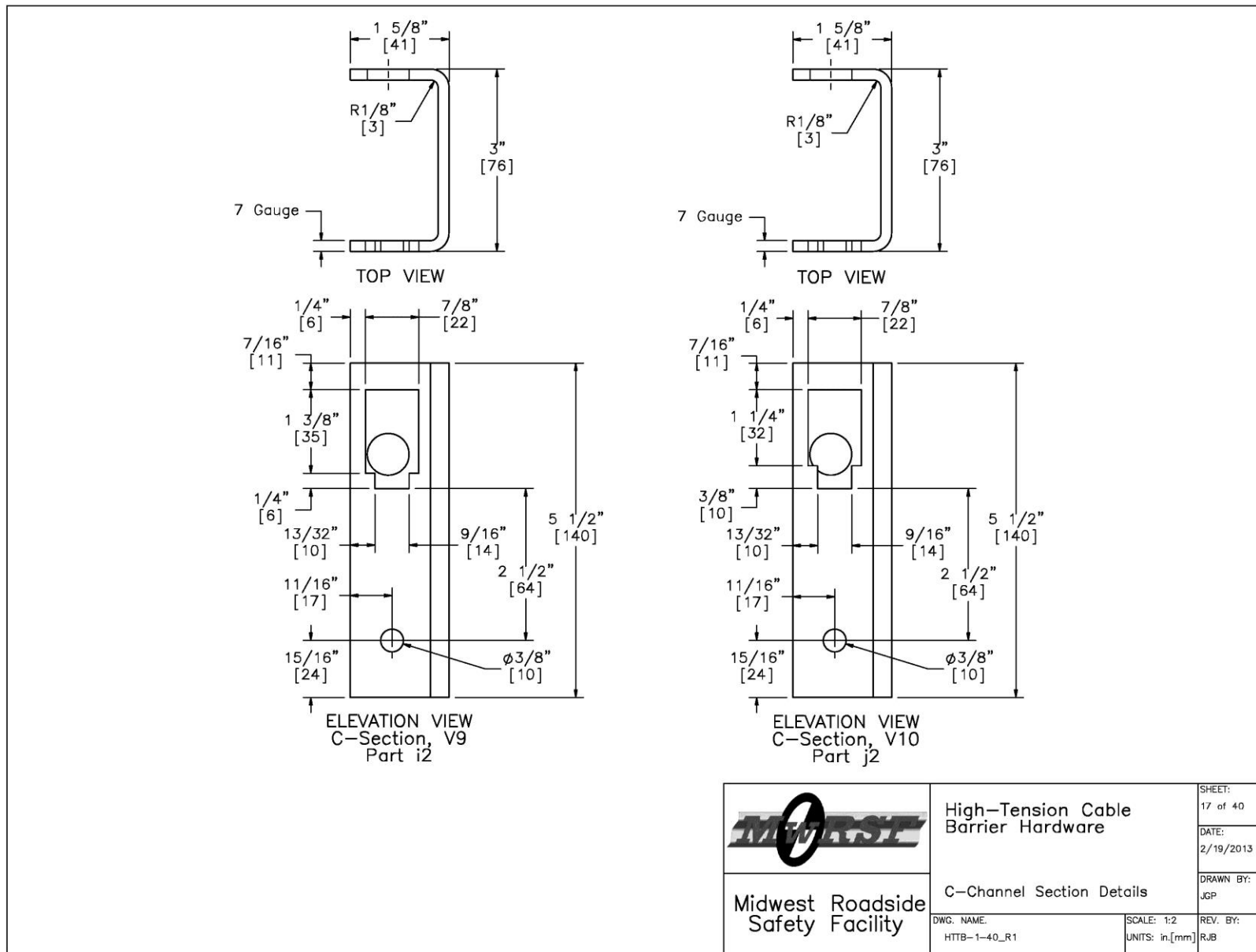


Figure 180. C-Section Details, Test Nos. HTTB-1 through HTTB-40

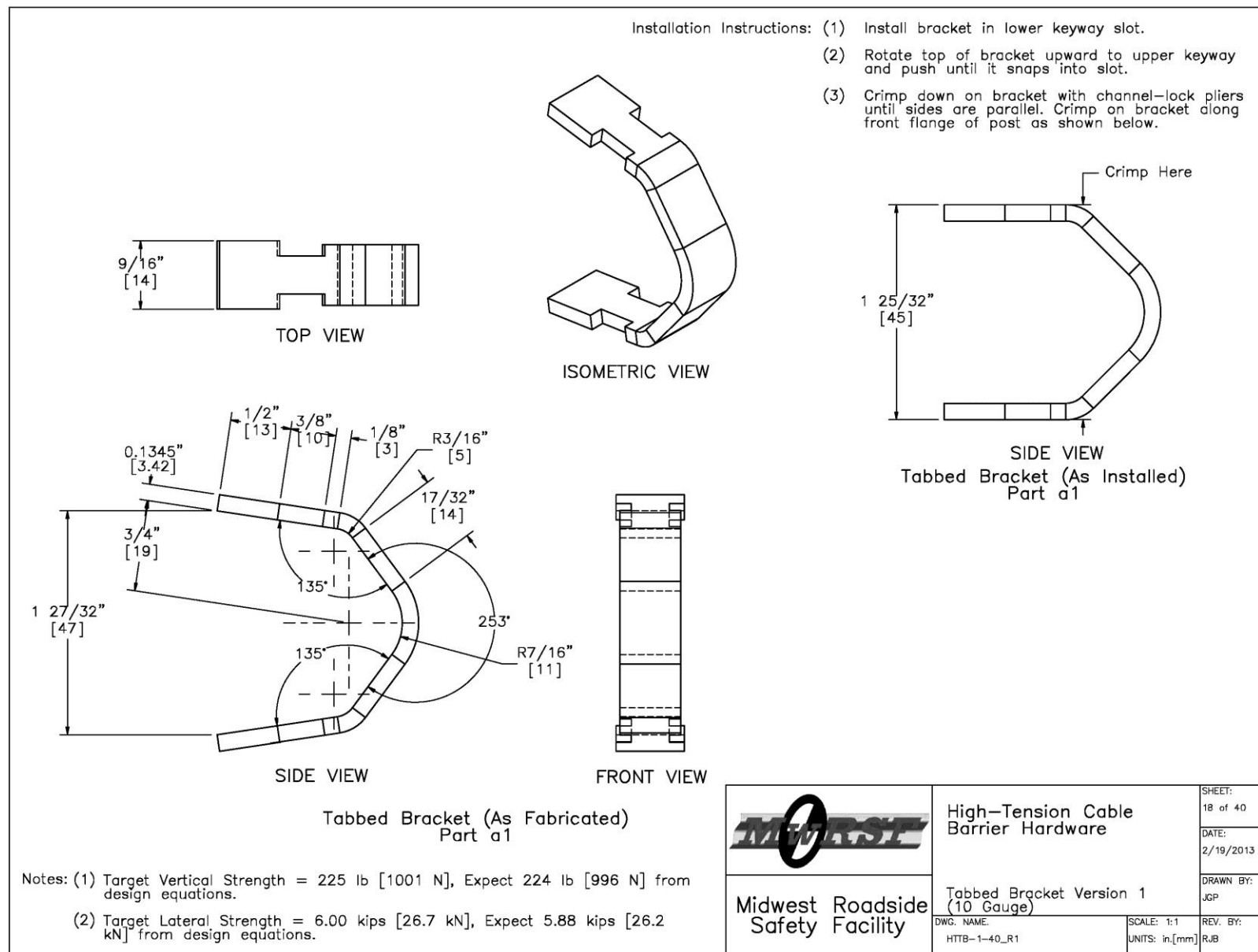


Figure 181. Tabbed Bracket Version 1, Test Nos. HTTB-1 through HTTB-40

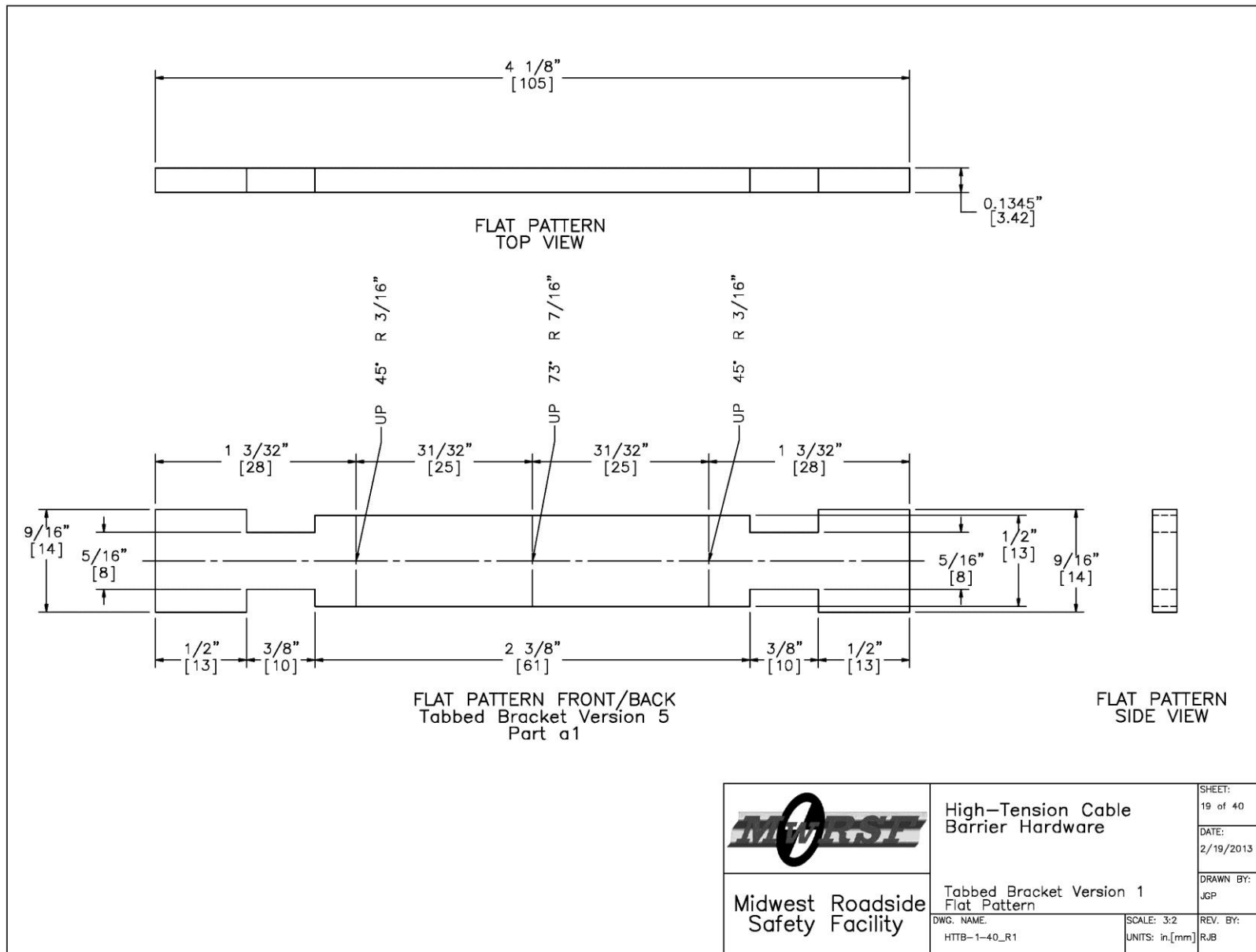


Figure 182. Version 1 Flat Pattern, Test Nos. HTTB-1 through HTTB-40

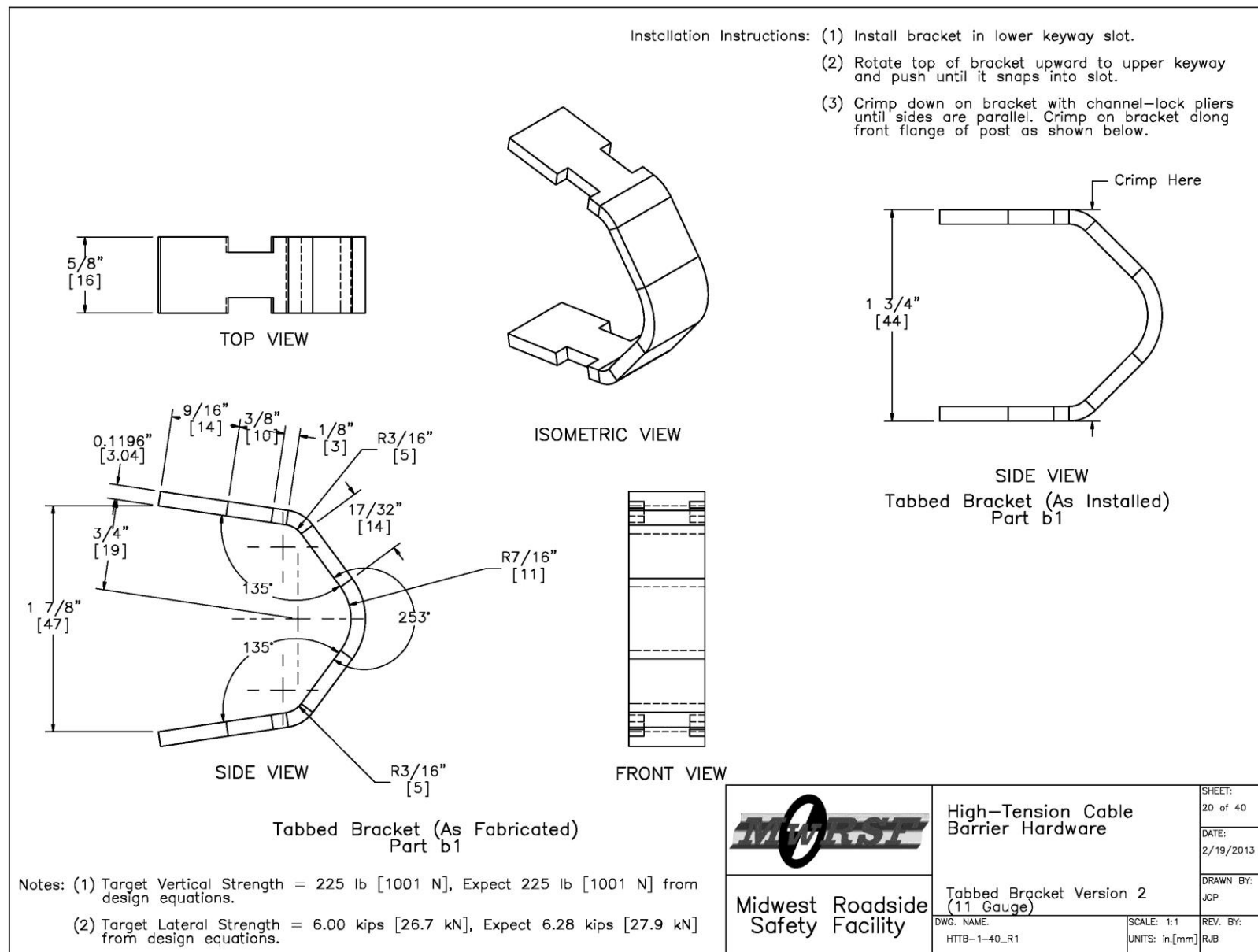


Figure 183. Tabbed Bracket Version 2, Test Nos. HTTB-1 through HTTB-40

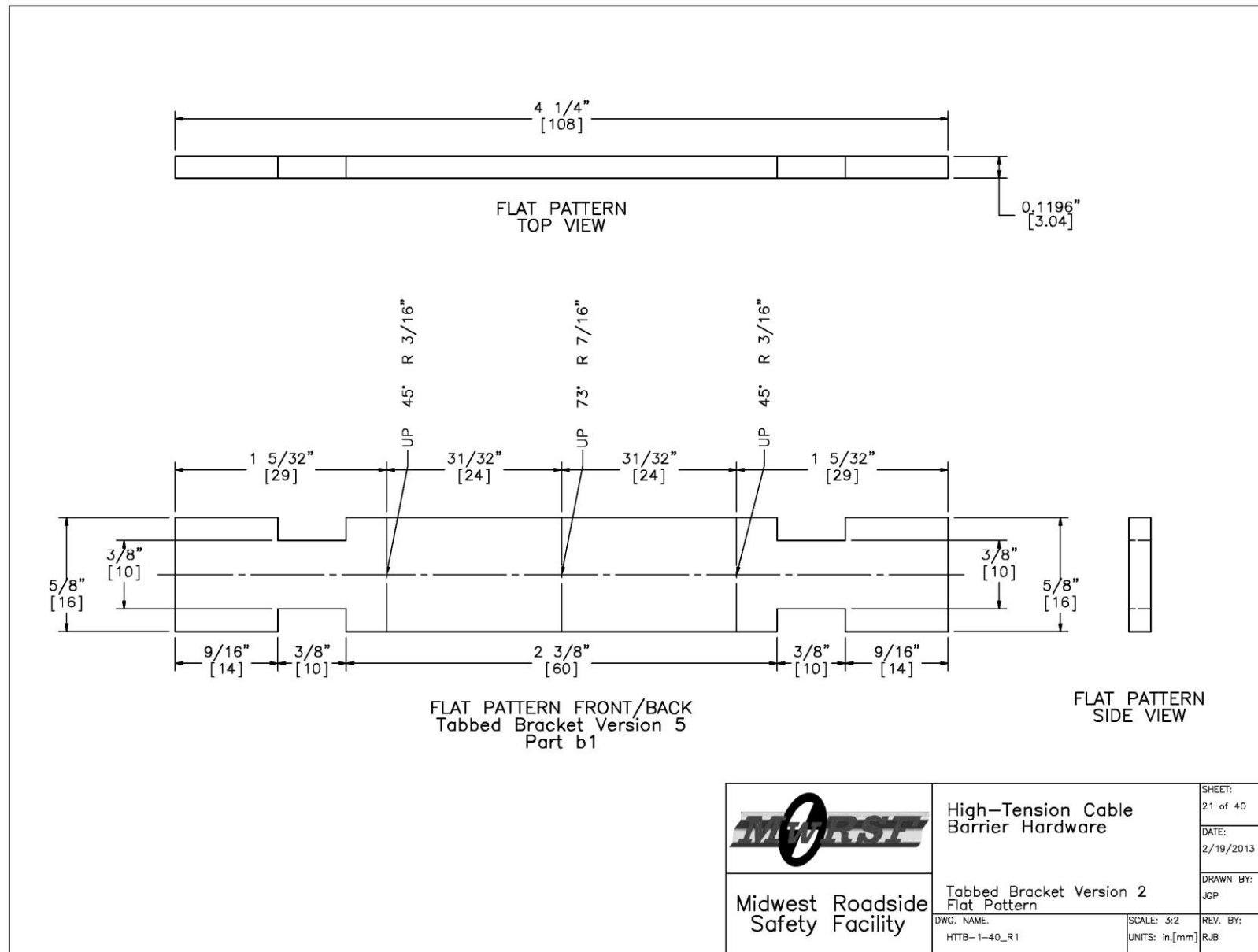


Figure 184. Version 2 Flat Pattern, Test Nos. HTTB-1 through HTTB-40

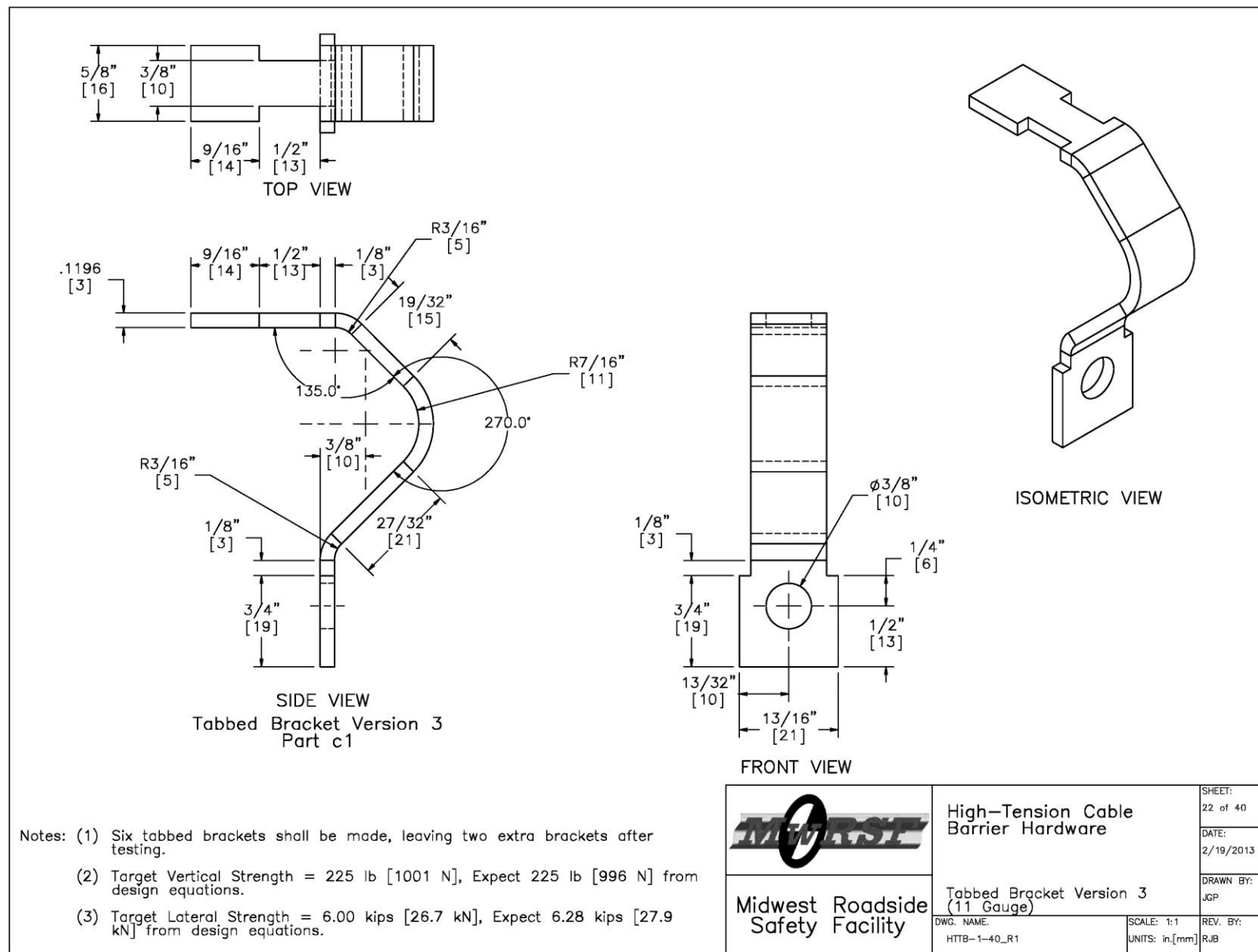


Figure 185. Tabbed Bracket Version 3, Test Nos. HTTB-1 through HTTB-40

Figure 186. Version 3 Flat Pattern, Test Nos. HTTB-1 through HTTB-40

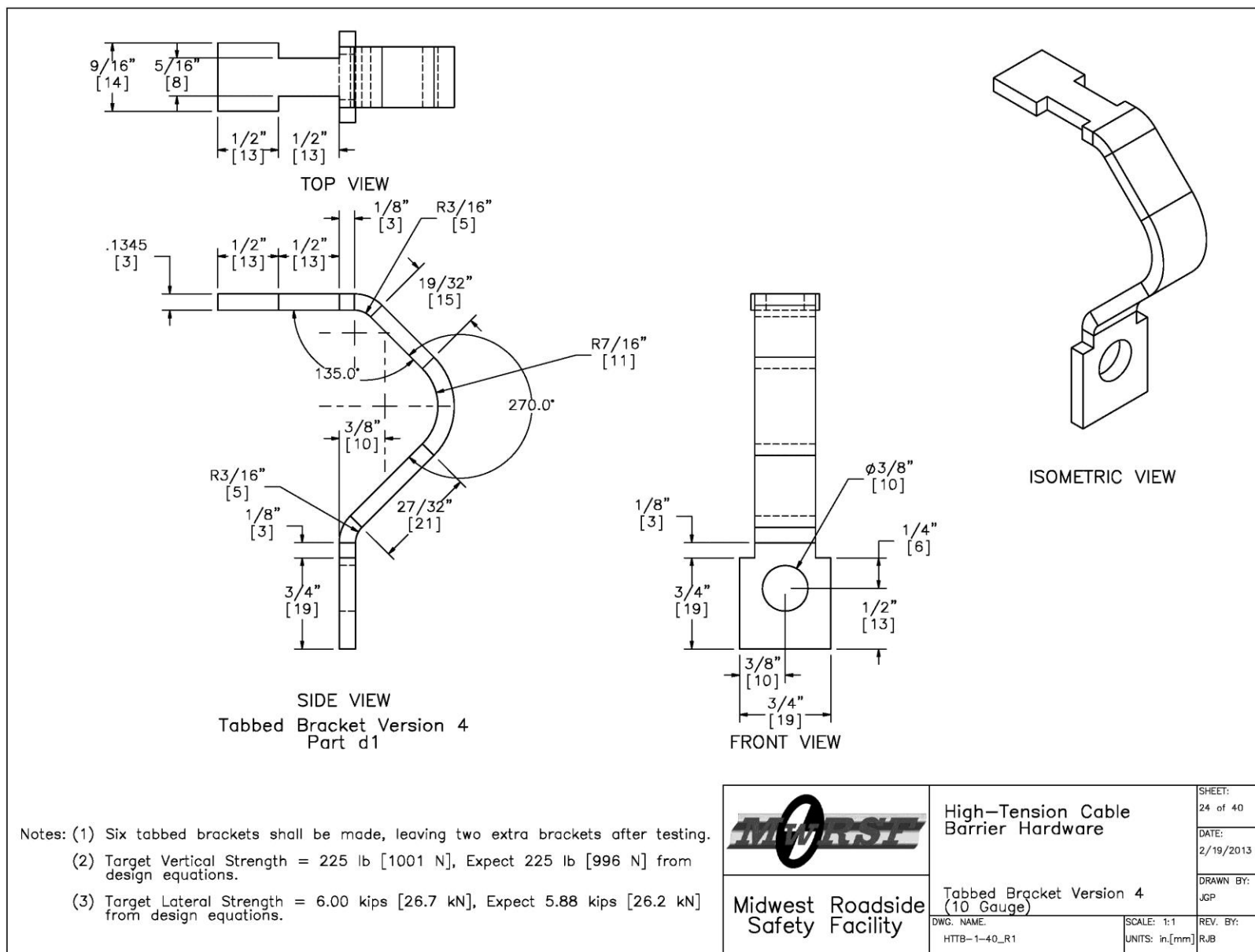


Figure 187. Tabbed Bracket Version 4, Test Nos. HTTB-1 through HTTB-40

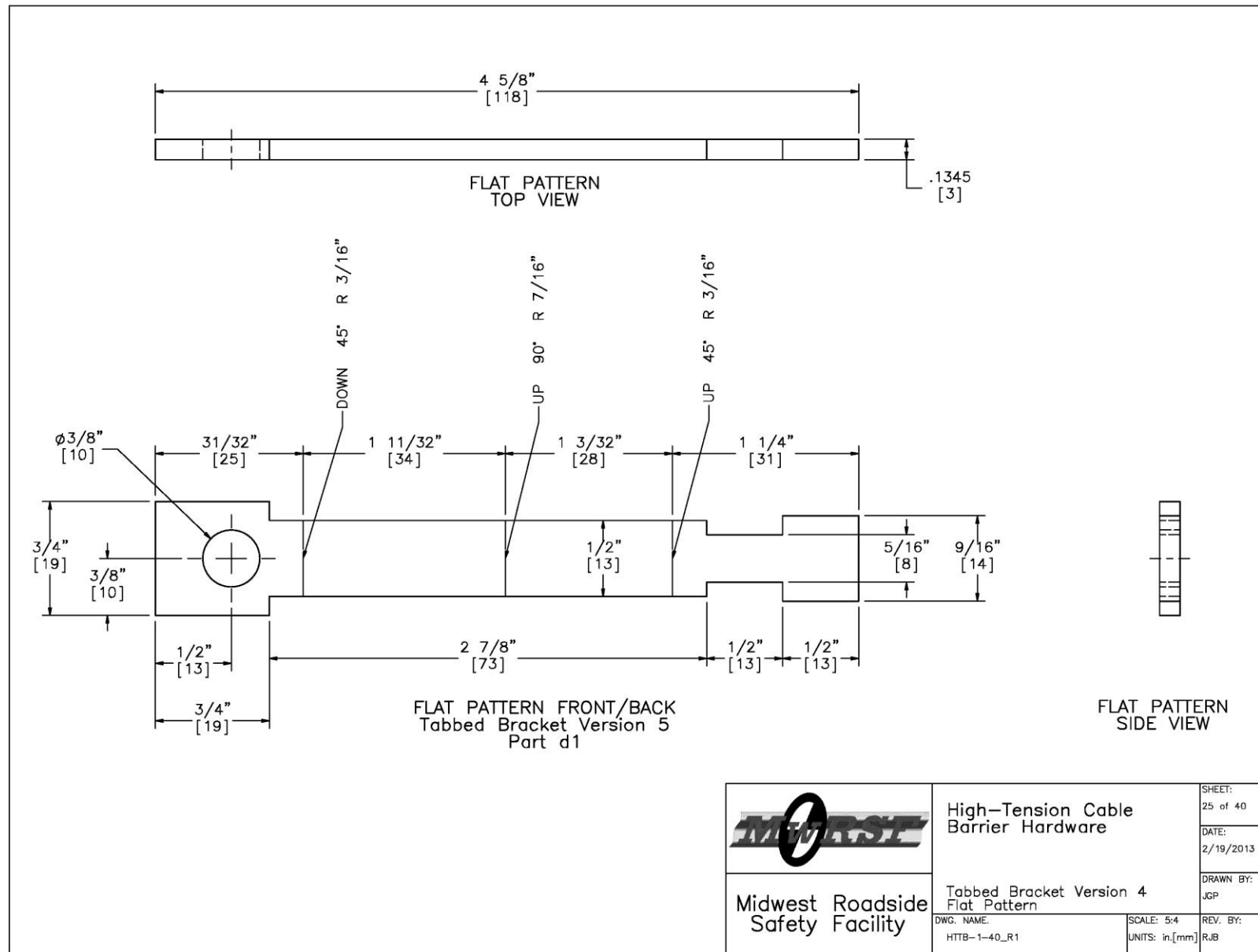


Figure 188. Version 4 Flat Pattern, Test Nos. HTTB-1 through HTTB-40

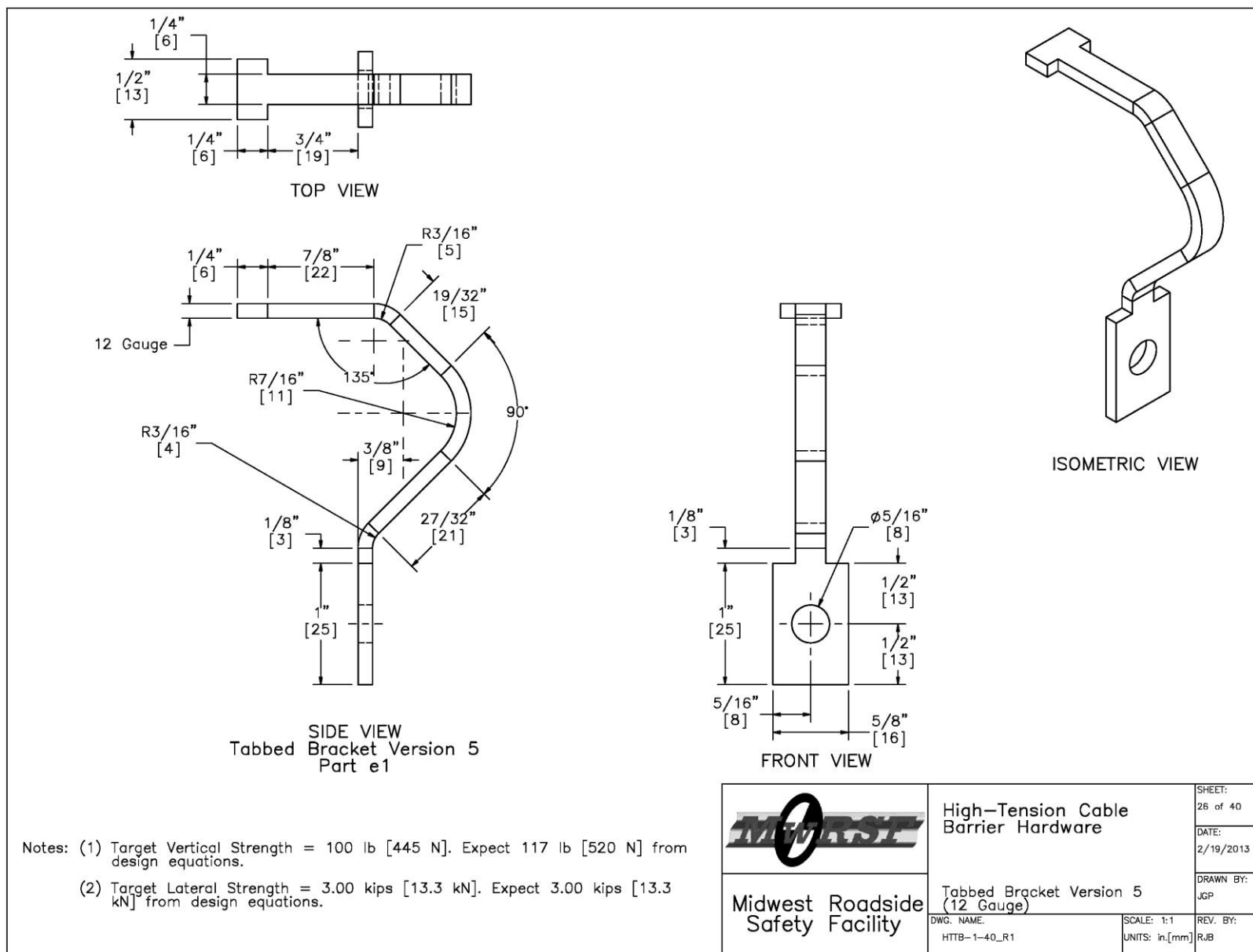
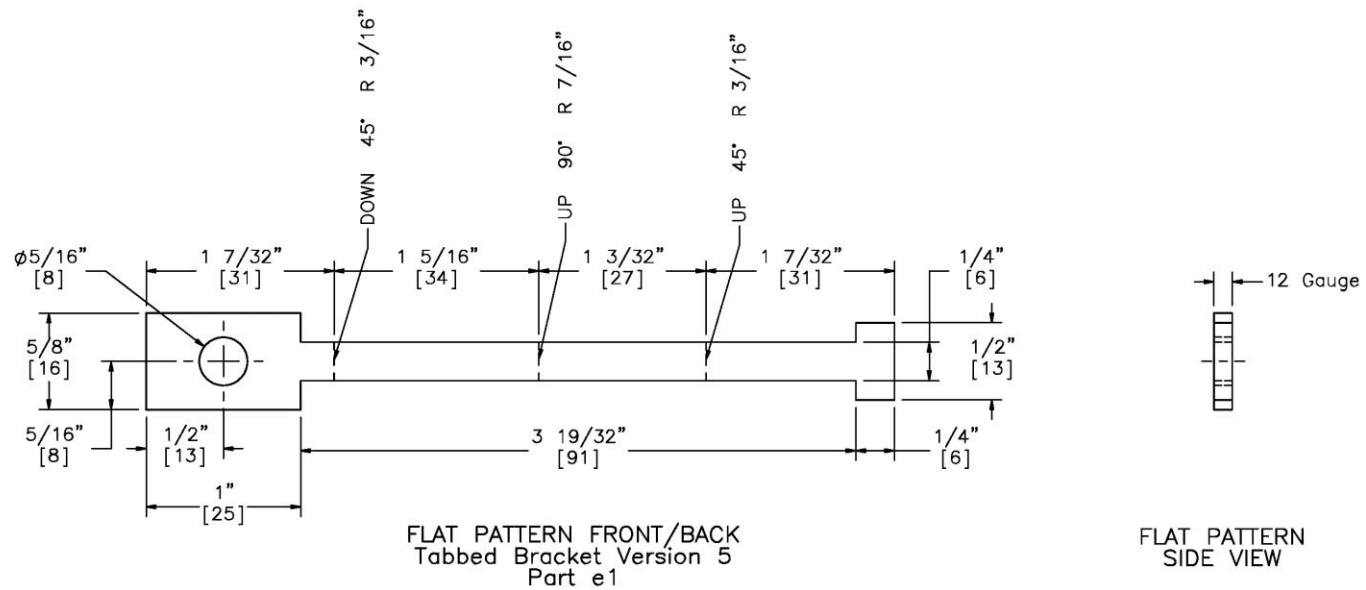


Figure 189. Tabbed Bracket Version 5, Test Nos. HTTB-1 through HTTB-40




	High-Tension Cable Barrier Hardware		SHEET: 27 of 40
	Tabbed Bracket Version 5 Flat Pattern		DATE: 2/19/2013
Midwest Roadside Safety Facility	DWG. NAME: HTTB-1-40_R1	SCALE: 1:1 UNITS: in.[mm]	DRAWN BY: JGP
		REV. BY: RJB	

Figure 190. Version 5 Flat Pattern, Test Nos. HTTB-1 through HTTB-40

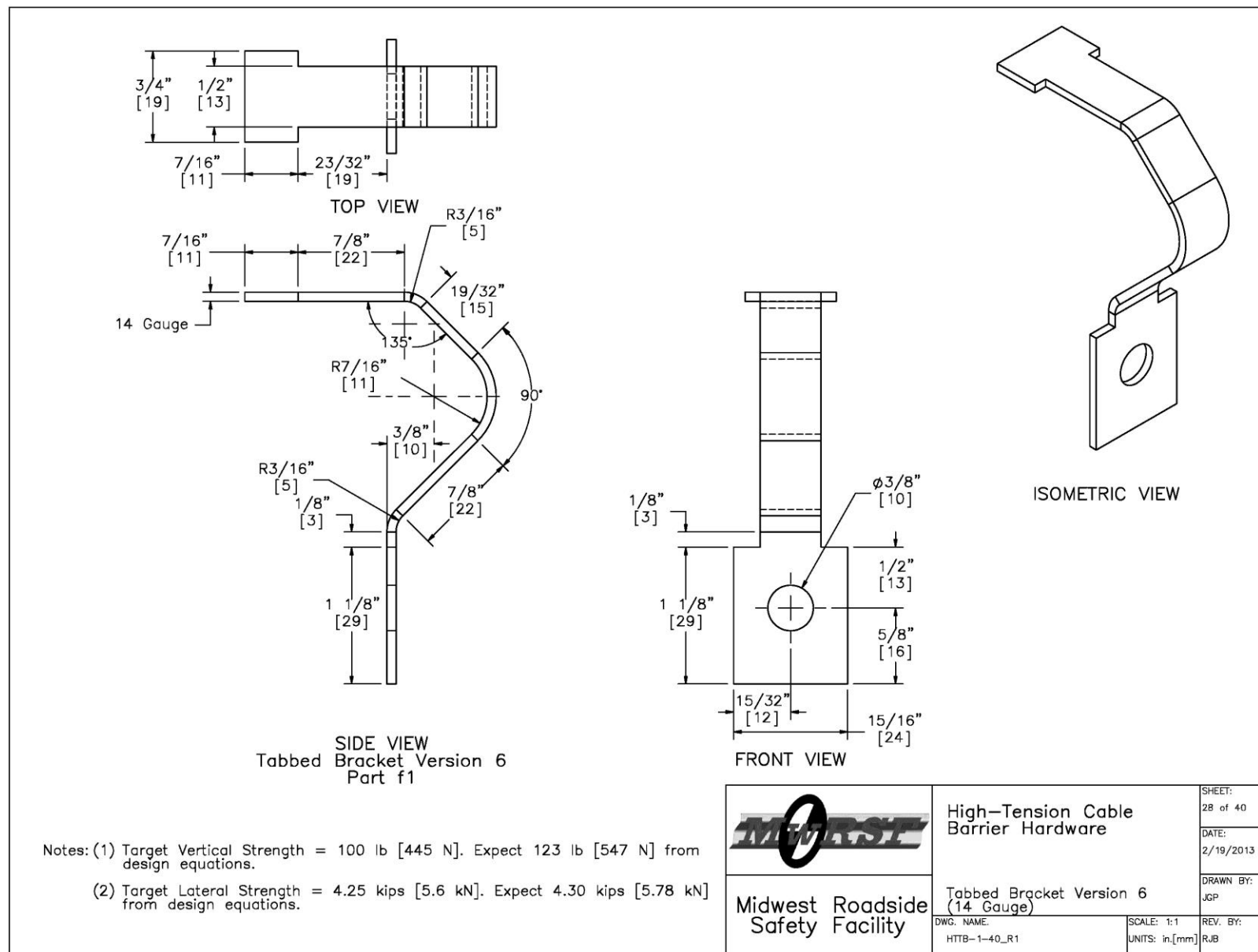


Figure 191. Tabbed Bracket Version 6, Test Nos. HTTPB-1 through HTTPB-40

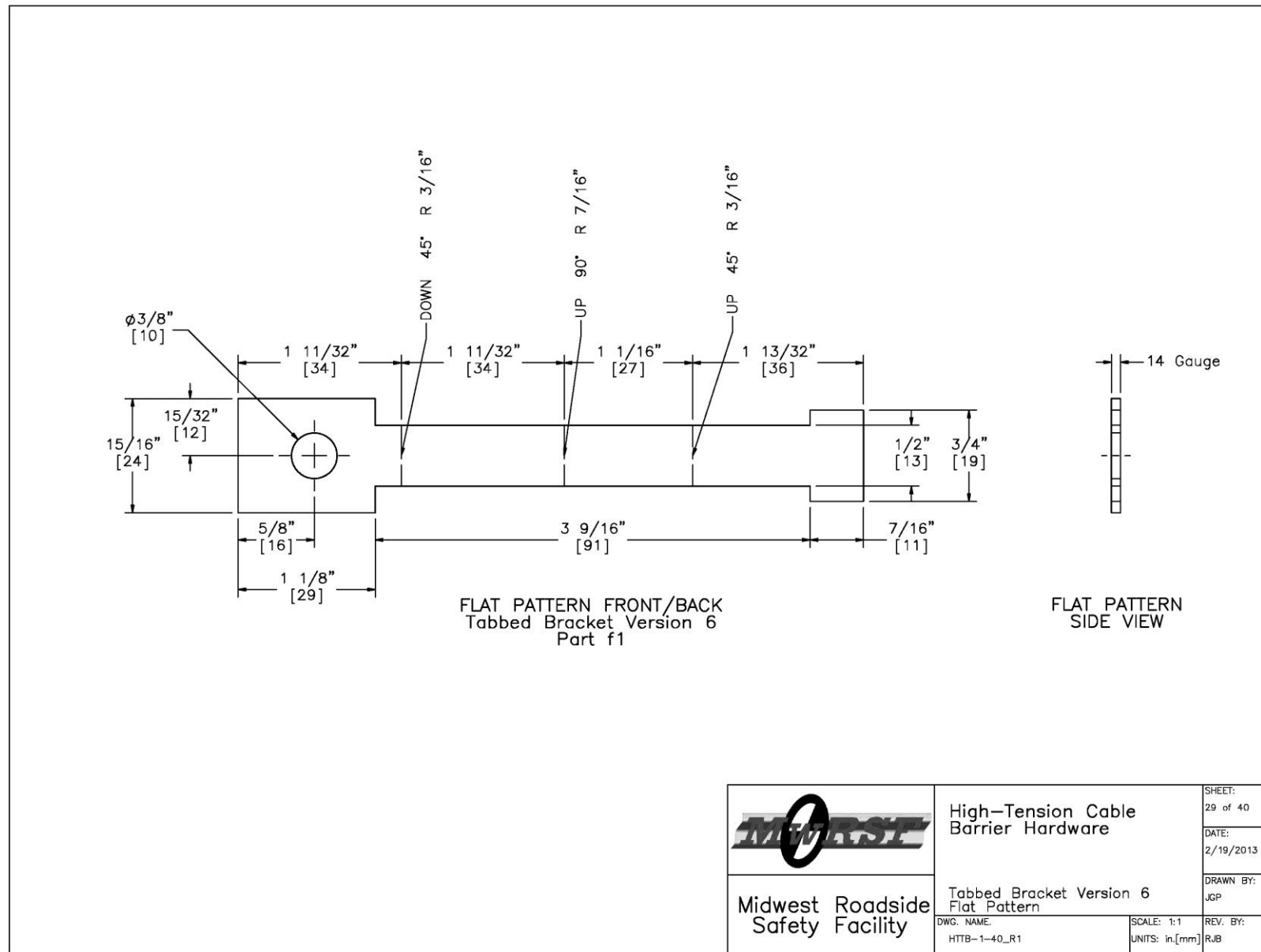


Figure 192. Version 6 Flat Pattern, Test Nos. HTTB-1 through HTTB-40

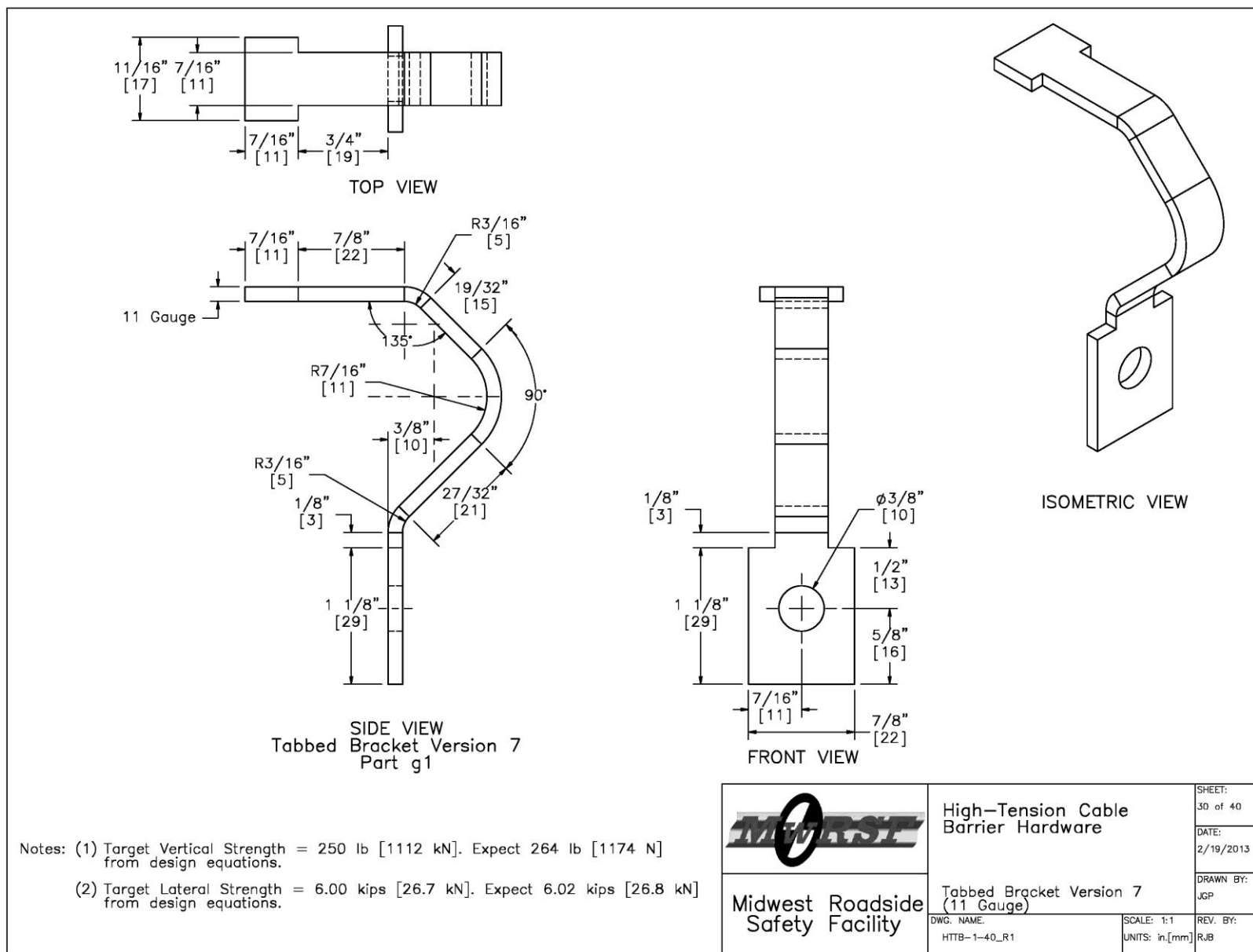
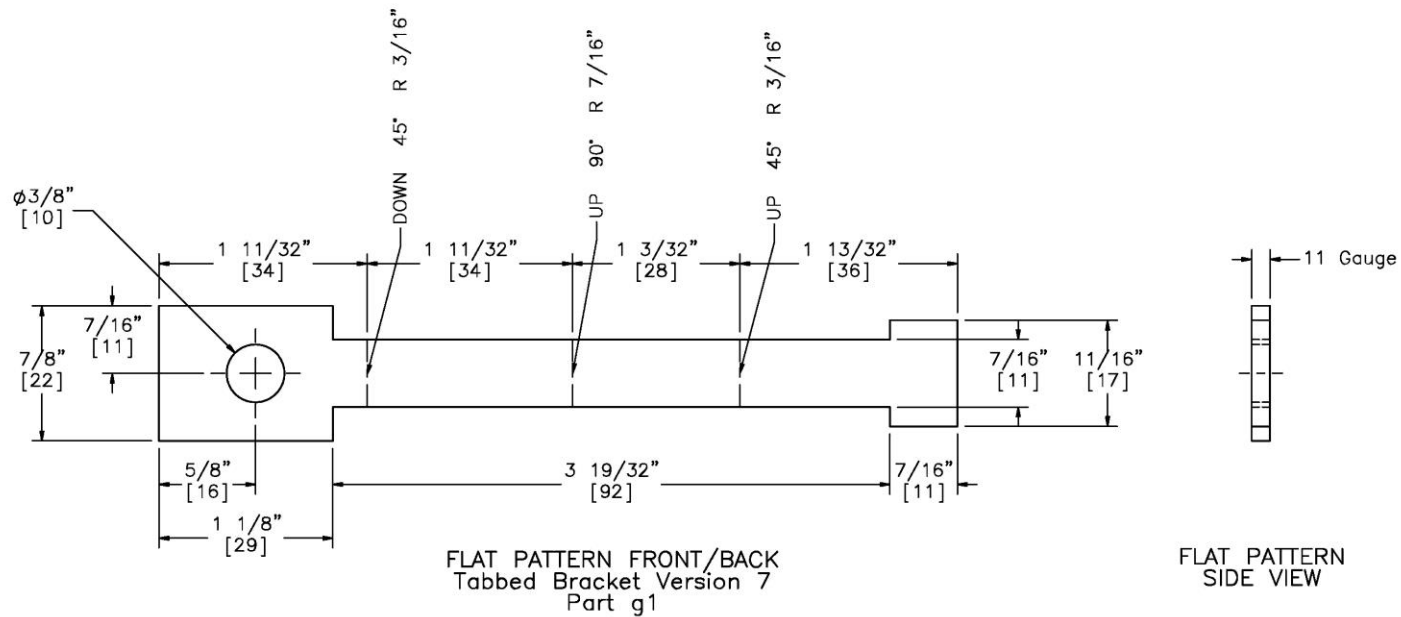


Figure 193. Tabbed Bracket Version 7, Test Nos. HTTB-1 through HTTB-40




	High-Tension Cable Barrier Hardware		SHEET: 31 of 40
	Tabbed Bracket Version 7 Flat Pattern		DATE: 2/19/2013
Midwest Roadside Safety Facility	DWG. NAME: HTTB-1-40_R1	SCALE: 1:1 UNITS: in.[mm]	DRAWN BY: JGP
			REV. BY: RJB

Figure 194. Version 7 Flat Pattern, Test Nos. HTTB-1 through HTTB-40

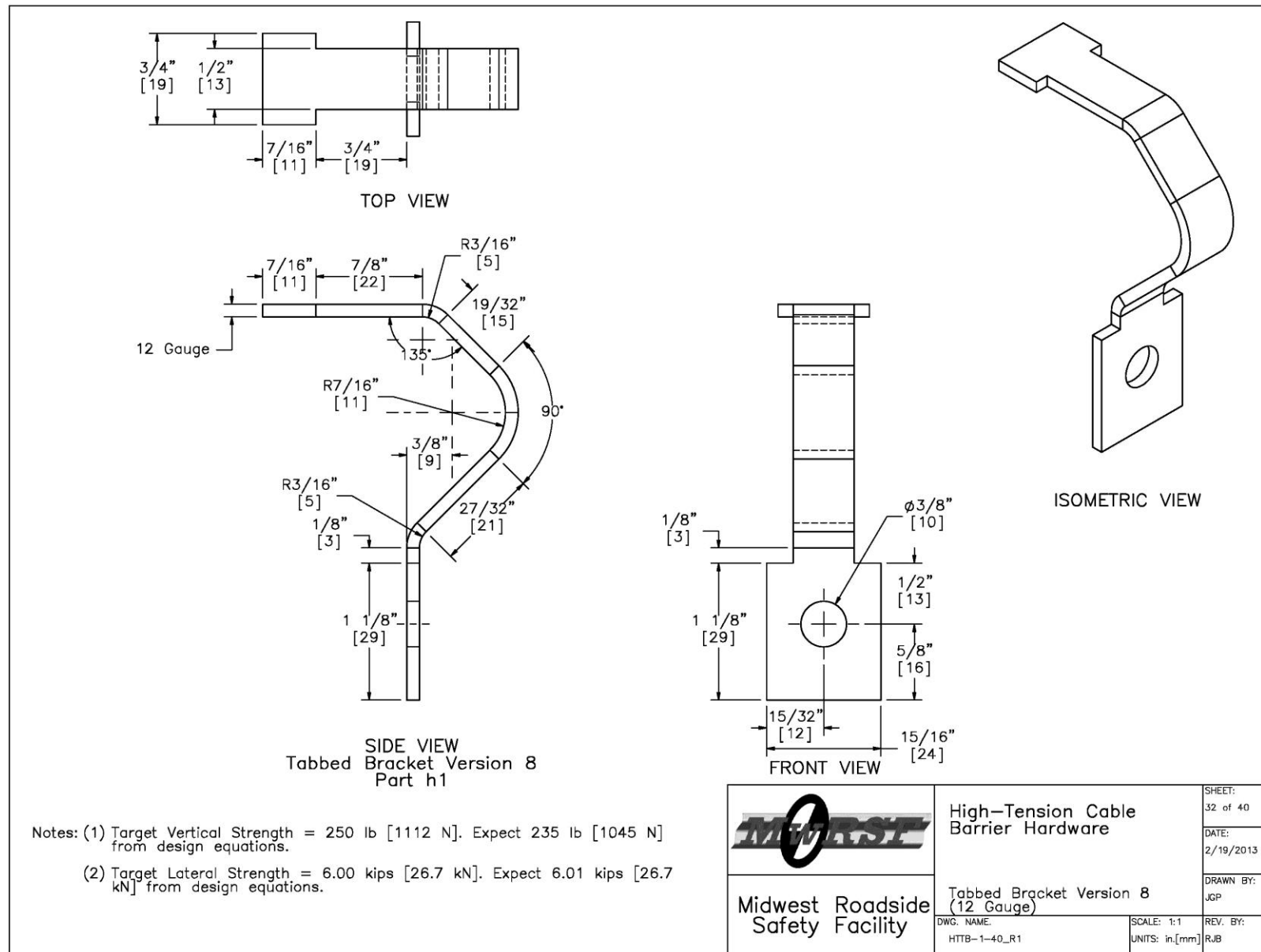


Figure 195. Tabbed Bracket Version 8, Test Nos. HTTB-1 through HTTB-40

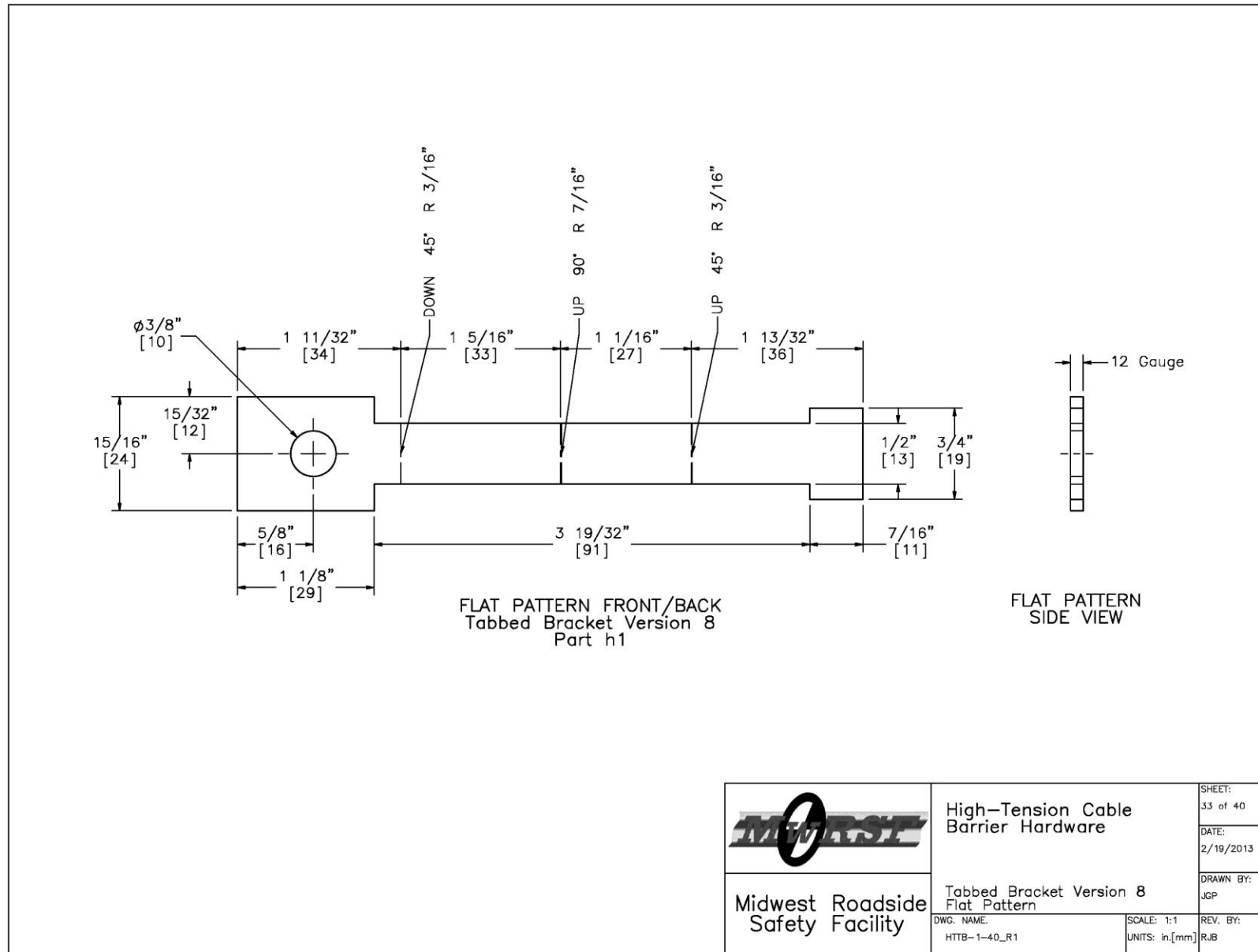


Figure 196. Version 8 Flat Pattern, Test Nos. HTTB-1 through HTTB-40

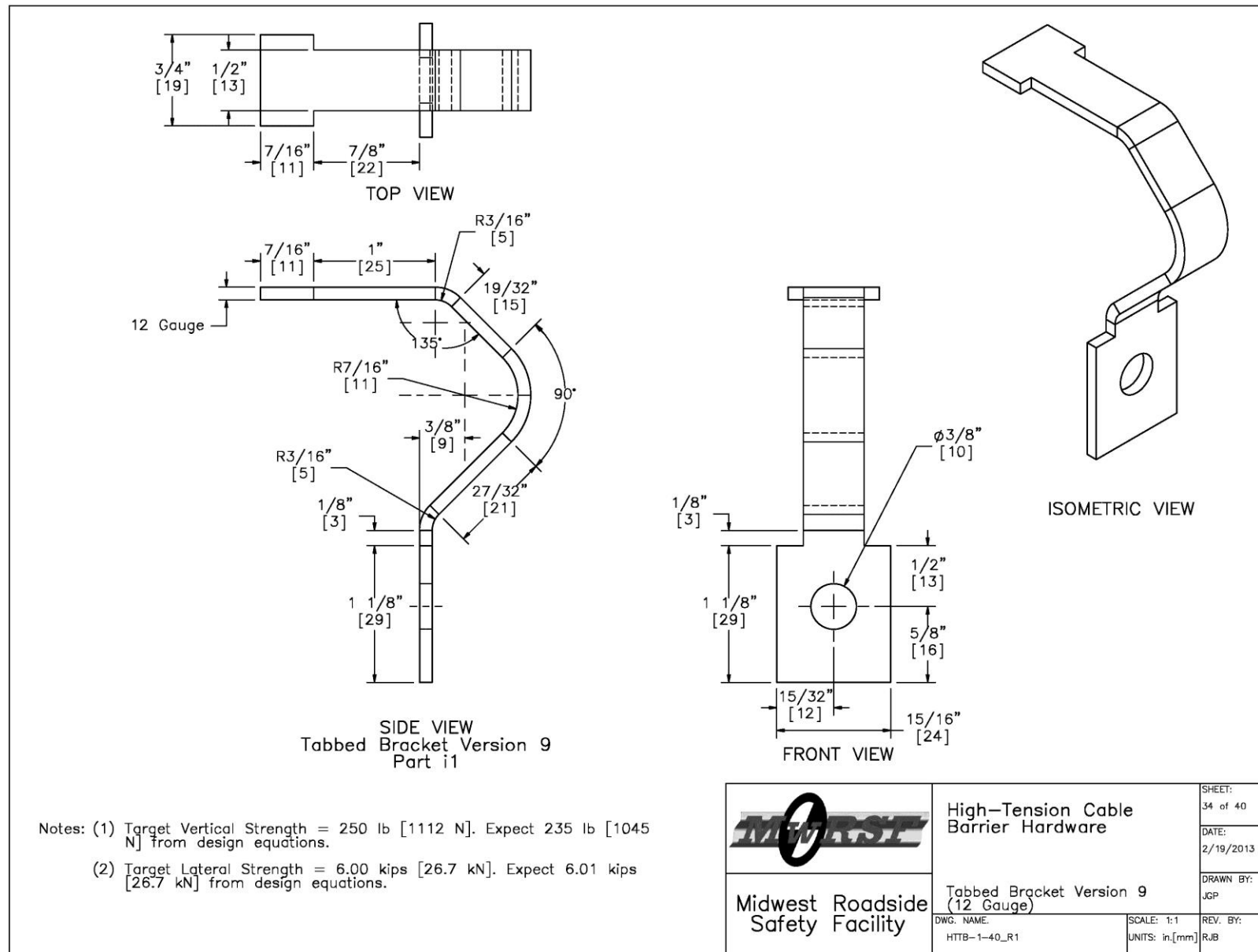


Figure 197. Tabbed Bracket Version 9, Test Nos. HTTB-1 through HTTB-40

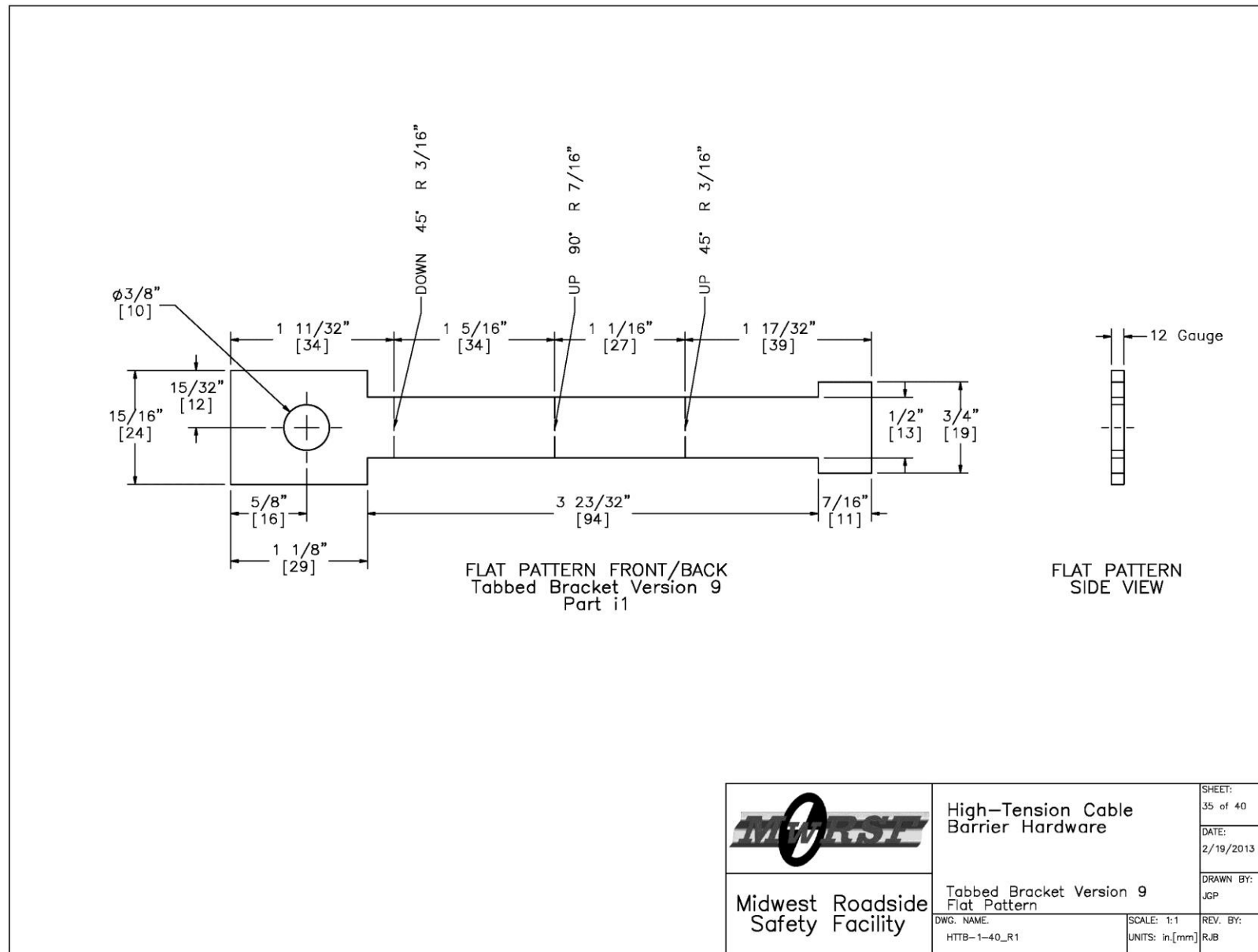


Figure 198. Version 9 Flat Pattern, Test Nos. HTTB-1 through HTTB-40

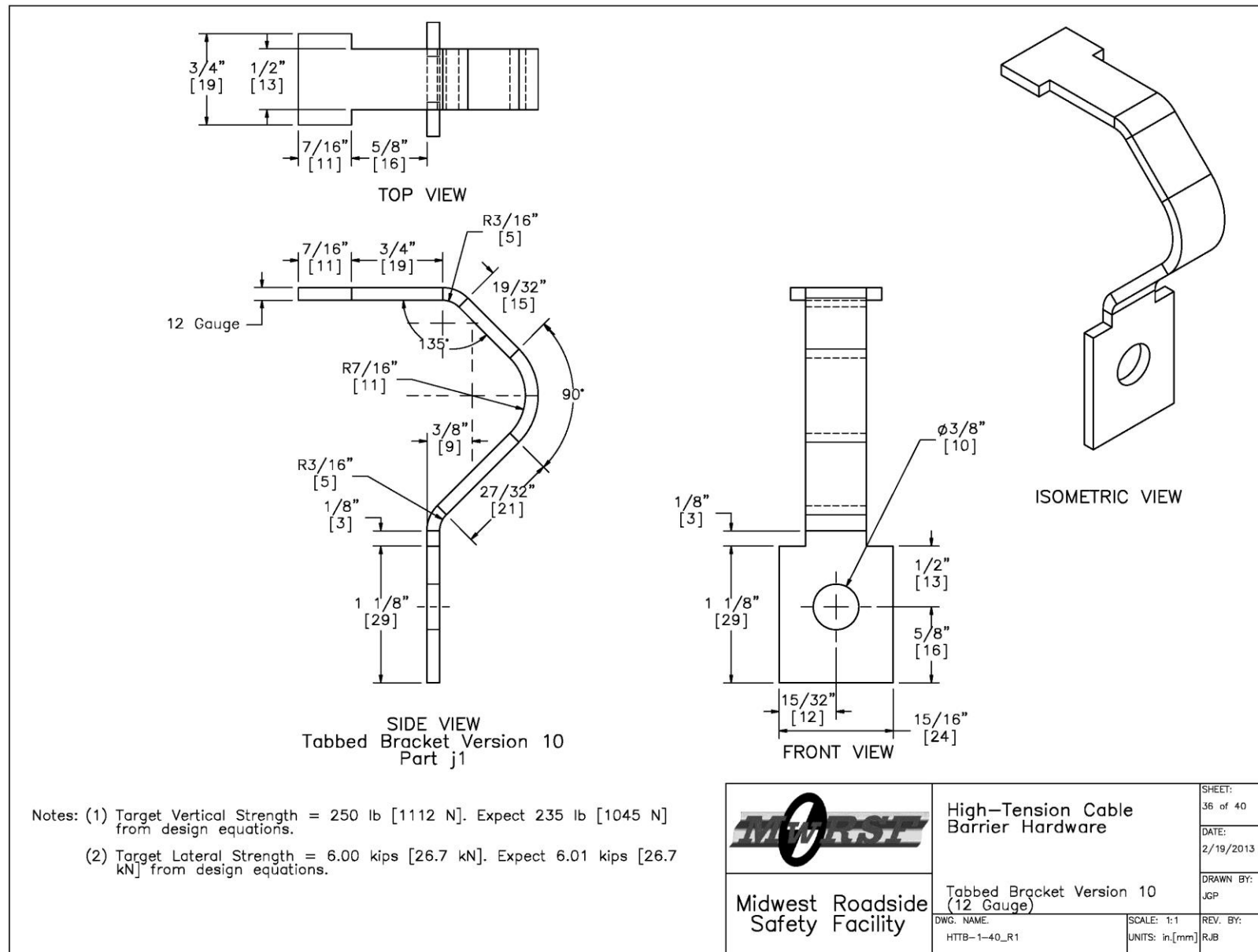
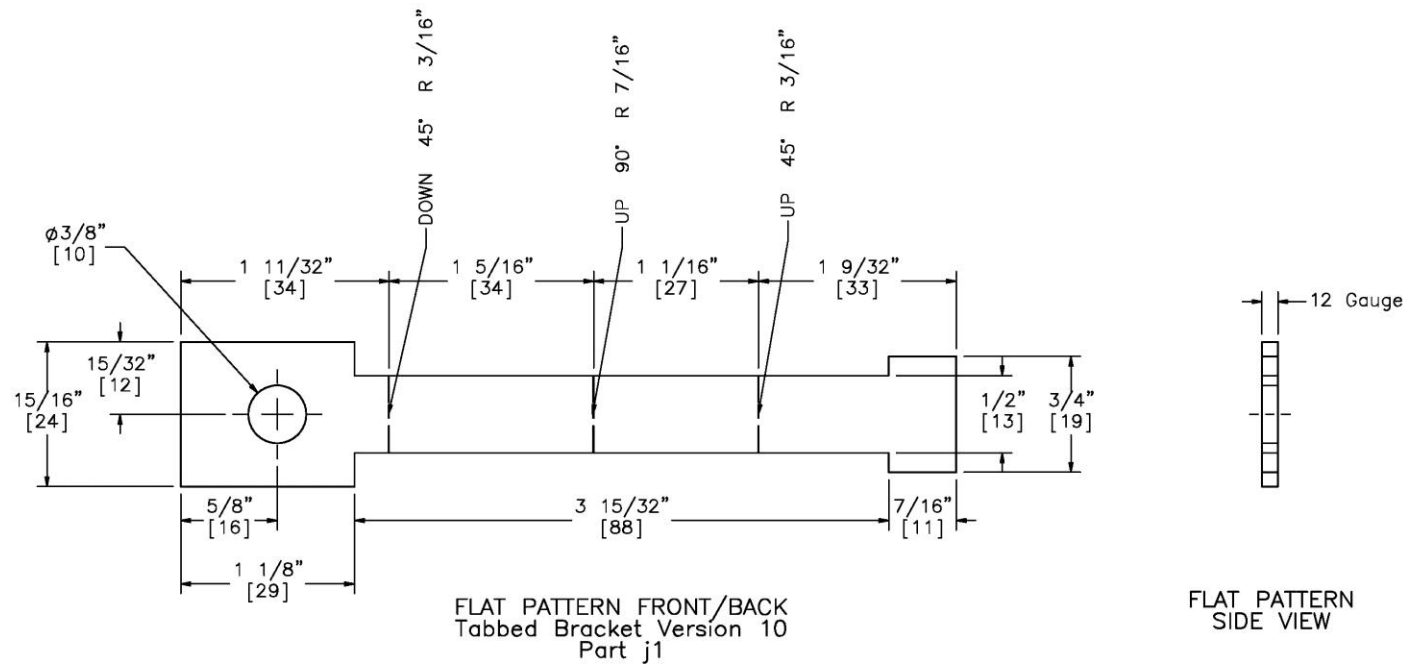


Figure 199. Tabbed Bracket Version 10, Test Nos. HTTB-1 through HTTB-40




	High-Tension Cable Barrier Hardware		SHEET: 37 of 40
	Tabbed Bracket Version 10 Flat Pattern		DATE: 2/19/2013
Midwest Roadside Safety Facility	DWG. NAME: HTTB-1-40_R1	SCALE: 1:1 UNITS: in.[mm]	DRAWN BY: JGP
			REV. BY: RJB

Figure 200. Version 10 Flat Pattern, Test Nos. HTTB-1 through HTTB-40


Bogie Test Matrix						
Test Qty	Tabbed Bracket	Variation	Orientation deg.	Load Direction	Post Section	Expected Strength (lb)
2	Version 1	Crimp-In-Place	0	Vertical	S3x5.7 [S76x8.5] Section, V1	224
2	Version 1	Crimp-In-Place	90	Lateral	S3x5.7 [S76x8.5] Section, V1	5,880
2	Version 2	Crimp-In-Place	0	Vertical	S3x5.7 [S76x8.5] Section, V2	225
2	Version 2	Crimp-In-Place	90	Lateral	S3x5.7 [S76x8.5] Section, V2	6,280
2	Version 3	Bolted	0	Vertical	S3x5.7 [S76x8.5] Section, V3	225
2	Version 3	Bolted	90	Lateral	S3x5.7 [S76x8.5] Section, V3	6,280
2	Version 4	Bolted	0	Vertical	S3x5.7 [S76x8.5] Section, V4	224
2	Version 4	Bolted	90	Lateral	S3x5.7 [S76x8.5] Section, V4	5,880
2	Version 5	Bolted	0	Vertical	C-Section, V5	117
2	Version 5	Bolted	90	Lateral	C-Section, V5	3,000
2	Version 6	Bolted	0	Vertical	C-Section, V6/8	123
2	Version 6	Bolted	90	Lateral	C-Section, V6/8	4,300
2	Version 7	Bolted	0	Vertical	C-Section, V7	264
2	Version 7	Bolted	90	Lateral	C-Section, V7	6,020
2	Version 8	Bolted	0	Vertical	C-Section, V6/8	235
2	Version 8	Bolted	90	Lateral	C-Section, V6/8	6,010
2	Version 9	Bolted	90	Lateral	C-Section, V9	6,010
2	Version 10	Bolted	0	Vertical	C-Section, V10	235
2	Version 10	Bolted	90	Lateral	C-Section, V10	6,010
<p>Notes: (1) The expected strength equations for Tabbed Bracket Versions 5–10 were slightly modified from those of Versions 1–4. This was in response to the observed lateral release loads in Versions 4 and 4 being lower by a factor of approximately 5/6.</p> <p>(2) Tabbed Bracket Version 9 was not tested in the vertical direction.</p>						
 <p>Midwest Roadside Safety Facility</p>					<p>High-Tension Cable Barrier Hardware</p> <p>Bogie Testing Matrix</p> <p>DWG. NAME: HTTB-1-40_R1</p> <p>SCALE: NONE UNITS: in.[mm]</p>	<p>SHEET: 38 of 40</p> <p>DATE: 2/19/2013</p> <p>DRAWN BY: JGP</p> <p>REV. BY: RJB</p>

Figure 201. Bogie Test Matrix, Test Nos. HTTB-1 through HTTB-40


Version 1			
Item No.	Qty	Description	Material Specification
a1	4	Tabbed Bracket Version 1, Crimp-In-Place	10-Gauge Hot-Rolled ASTM A1011 HSLA Grade 50
a2	1	S3x5.7 [S76x8.5] Section, V1	ASTM A572 GR50-07, ASTM A709 GR50-09A, ASTM A992-06A
a3	6	2 5/8"x1"x1/4" [67x25x6] Gusset	ASTM A36
Version 2			
Item No.	Qty	Description	Material Specification
b1	4	Tabbed Bracket Version 2, Crimp-In-Place	11-Gauge Hot-Rolled ASTM A1011 HSLA Grade 50
b2	1	S3x5.7 [S76x8.5] Section, V2	ASTM A572 GR50-07, ASTM A709 GR50-09A, ASTM A992-06A
a3	6	2 5/8"x1"x1/4" [67x25x6] Gusset	ASTM A36
Version 3			
Item No.	Qty	Description	Material Specification
c1	4	Tabbed Bracket Version 3, Bolted	11-Gauge Hot-Rolled ASTM A1011 HSLA Grade 50
c2	1	S3x5.7 [S76x8.5] Section, V3	ASTM A572 GR50-07, ASTM A709 GR50-09A, ASTM A992-06A
a3	6	2 5/8"x1"x1/4" [67x25x6] Gusset	ASTM A36
c3	4	5/16" [8] Dia. UNC, 1" Long Hex Cap Screw	SAE Grade 5
c4	4	5/16" [8] Dia. Heavy Hex Nut	ASTM A563 DH Galv.
Version 4			
Item No.	Qty	Description	Material Specification
d1	4	Tabbed Bracket Version 4, Bolted	10-Gauge Hot-Rolled ASTM A1011 HSLA Grade 50
d2	1	S3x5.7 [S76x8.5] Section, V4	ASTM A572 GR50-07, ASTM A709 GR50-09A, ASTM A992-06A
a3	6	2 5/8"x1"x1/4" [67x25x6] Gusset	ASTM A36
c3	4	5/16" [8] Dia. UNC, 1" Long Hex Cap Screw	SAE Grade 5
c4	4	5/16" [8] Dia. Heavy Hex Nut	ASTM A563 DH Galv.
Version 5			
Item No.	Qty	Description	Material Specification
e1	4	Tabbed Bracket Version 5, Bolted	12-Gauge Hot-Rolled ASTM A1011 HSLA Grade 50
e2	1	3"x1 5/8" [76x41] C-section, V5	7-Gauge Hot-Rolled ASTM A1011 HSLA Grade 50
e3	3	2 9/16"x1 7/16"x1/4" [67x25x6] Gusset	ASTM A36
e4	4	1/4" [6] Dia. UNC, 1" Long Hex Cap Screw	SAE Grade 5
Version 6			
Item No.	Qty	Description	Material Specification
f1	4	Tabbed Bracket Version 6, Bolted	14-Gauge Hot-Rolled ASTM A1011 HSLA Grade 50
f2	1	3"x1 5/8" [76x41] C-section, V6/8	7-Gauge Hot-Rolled ASTM A1011 HSLA Grade 50
e3	3	2 9/16"x1 7/16"x1/4" [67x25x6] Gusset	ASTM A36
c3	4	5/16" [8] Dia. UNC, 1" Long Hex Cap Screw	SAE Grade 5
c4	4	5/16" [8] Dia. Heavy Hex Nut	ASTM A563 DH Galv.
			High-Tension Cable Barrier Hardware
			Bill of Materials
Midwest Roadside Safety Facility			DWG. NAME: HTTB-1-40_R1 SCALE: NONE UNITS: in.[mm]
			SHEET: 39 of 40 DATE: 2/19/2013 DRAWN BY: JGP REV. BY: RJB

Figure 202. Bill of Materials, Test Nos. HTTB-1 through HTTB-40


Version 7			
Item No.	Qty	Description	Material Specification
g1	4	Tabbed Bracket Version 7, Bolted	11-Gauge Hot-Rolled ASTM A1011 HSLA Grade 50
g2	1	3"x1 5/8" [76x41] C-section, V7	7-Gauge Hot-Rolled ASTM A1011 HSLA Grade 50
e3	3	2 9/16"x1 7/16"x1/4" [67x25x6] Gusset	ASTM A36
c3	4	5/16" [8] Dia. UNC, 1" Long Hex Cap Screw	SAE Grade 5
c4	4	5/16" [8] Dia. Heavy Hex Nut	ASTM A563 DH Galv.
Version 8			
Item No.	Qty	Description	Material Specification
h1	4	Tabbed Bracket Version 8, Bolted	12-Gauge Hot-Rolled ASTM A1011 HSLA Grade 50
c3	4	5/16" [8] Dia. UNC, 1" Long Hex Cap Screw	SAE Grade 5
c4	4	5/16" [8] Dia. Heavy Hex Nut	ASTM A563 DH Galv.
Version 9			
Item No.	Qty	Description	Material Specification
i1	4	Tabbed Bracket Version 9, Bolted	12-Gauge Hot-Rolled ASTM A1011 HSLA Grade 50
i2	1	3"x1 5/8" [76x41] C-section, V9	7-Gauge Hot-Rolled ASTM A1011 HSLA Grade 50
e3	3	2 9/16"x1 7/16"x1/4" [67x25x6] Gusset	ASTM A36
c3	4	5/16" [8] Dia. UNC, 1" Long Hex Cap Screw	SAE Grade 5
c4	4	5/16" [8] Dia. Heavy Hex Nut	ASTM A563 DH Galv.
Version 10			
Item No.	Qty	Description	Material Specification
j1	4	Tabbed Bracket Version 10, Bolted	12-Gauge Hot-Rolled ASTM A1011 HSLA Grade 50
j2	1	3"x1 5/8" [76x41] C-section, V10	7-Gauge Hot-Rolled ASTM A1011 HSLA Grade 50
e3	3	2 9/16"x1 7/16"x1/4" [67x25x6] Gusset	ASTM A36
c3	4	5/16" [8] Dia. UNC, 1" Long Hex Cap Screw	SAE Grade 5
c4	4	5/16" [8] Dia. Heavy Hex Nut	ASTM A563 DH Galv.
Cable Clip Test Jig Setup			
Item No.	Qty	Description	Material Specification
k1	36	1" [25] Dia. Hardened Round Washer	ASTM F436
k2	6	1" [25] Dia. UNC, 2 1/2" [64] Long Heavy Hex Bolt	ASTM A307
k3	1	3/4" [19] Dia. 6x19 Wire Rope	—
k4	1	3/4" [19] Mechanical Splice	—
k5	4	3/8" [10] Dia. UNC, 1 1/2" [38] Long Hex Bolt and Nut	Bolt ASTM A307, Nut ASTM A563
k6	2	5/8" [16] Dia. UNC, 1 1/2" [38] Long Hex Bolt and Nut	Bolt ASTM A307, Nut ASTM A563
k7	1	4 7/8"x5"x1/4" [124x127x6] Mounting Plate with 4 welded Hex Nuts	ASTM A36
—	1	Cable Clip Bogie Test Jig (Pre-existing in Field)	—
—	1	Cable Guide (Pre-existing in Field)	—
Notes: (1) Tabbed Bracket Version 8 used the same reinforced C-section as Version 6. (2) Extra quantities of each tabbed bracket were on hand in case of the need for a test to be re-run. (3) Mounting plate (part k7) was different than previously used in cable clip testing. The old mounting plate was used with the S3x5.7 [S75x8.5] post sections. Part k7 was to be used with the C-sections.			<div>  <p>High-Tension Cable Barrier Hardware</p> <p>Bill of Materials</p> <p>DWG. NAME: HTTP-1-40_R1</p> <p>SCALE: NONE</p> <p>UNITS: in.[mm]</p> <p>REV. BY: RJB</p> </div> <div> <p>SHEET: 40 of 40</p> <p>DATE: 2/19/2013</p> <p>DRAWN BY: JGP</p> </div>

Figure 203. Bill of Materials, Test Nos. HTTP-1 through HTTP-40

Table 8 Summary of Dynamic Component Testing on Crimp-In-Place Tabbed Brackets, Round 1

Test No.	Load Direction	Tabbed Bracket	Gauge	Post Section	Expected Strength, kips (kN)	Release Load, kips (kN)	Test Result
HTTB-1	Lateral	Version 1, Crimp-In-Place, a1	10	S3x5.7 (S76x8.5) Section, V1, a2	5.88 (26.2)	5.87 (26.1)	Fracture through the bottom neck (Failure Location 2)
HTTB-2	Lateral	Version 1, Crimp-In-Place, a1	10	S3x5.7 (S76x8.5) Section, V1, a2	5.88 (26.2)	5.99 (26.6)	Fracture through the bottom neck (Failure Location 2)
HTTB-3	Lateral	Version 2, Crimp-In-Place, b1	11	S3x5.7 (S76x8.5) Section, V2, b2	6.28 (27.9)	6.40 (28.5)	Fracture through the bottom neck (Failure Location 2)
HTTB-4	Lateral	Version 2, Crimp-In-Place, b1	11	S3x5.7 (S76x8.5) Section, V2, b2	6.28 (27.9)	6.71 (29.8)	Fracture through the bottom neck (Failure Location 2)
HTTB-5	Vertical	Version 1, Crimp-In-Place, a1	10	S3x5.7 (S76x8.5) Section, V1, a2	0.22 (1.0)	2.87 (12.8)	Release through keyway, tabs scraped along inside of flange
HTTB-6	Vertical	Version 1, Crimp-In-Place, a1	10	S3x5.7 (S76x8.5) Section, V1, a2	0.22 (1.0)	2.80 (12.5)	Release through keyway, tabs scraped along inside of flange
HTTB-7	Vertical	Version 2, Crimp-In-Place, b1	11	S3x5.7 (S76x8.5) Section, V2, b2	0.22 (1.0)	1.43 (6.36)	Release through keyway, tabs scraped along inside of flange, snag load = 0.55 kips (2.4 kN)
HTTB-8	Vertical	Version 2, Crimp-In-Place, b1	11	S3x5.7 (S76x8.5) Section, V2, b2	0.22 (1.0)	1.20 (5.34)	Release through keyway, tabs scraped along inside of flange, snag load = 0.62 kips (2.7 kN)

11.1.1 Test No. HTTB-1 (TB V1, Crimp, Lateral)

For test no. HTTB-1, the cable pulled on the 10-gauge, grade 50 steel, crimp-in-place, tabbed bracket Version 1 at an angle of 90 degrees, perpendicular to the front face of the flange, thus imparting a lateral load. The post consisted of a 5-in. (127-mm) long, steel S3x5.7 (S76x8.5) section. The tabbed bracket was inserted into the top and bottom keyways and crimped into place with channel lock pliers. As the cable pulled on the tabbed bracket, the top and bottom tabs were caught in the narrow parts of their respective keyways. The cable continued to pull on the bracket until it fractured through the bottom neck (failure location 2). The peak load was 5.87 kips (26.1 kN). The force versus time plot is shown in Figure 204. Pre- and post-test photographs are shown in Figure 205. Sequential photographs are shown in Figure 206.

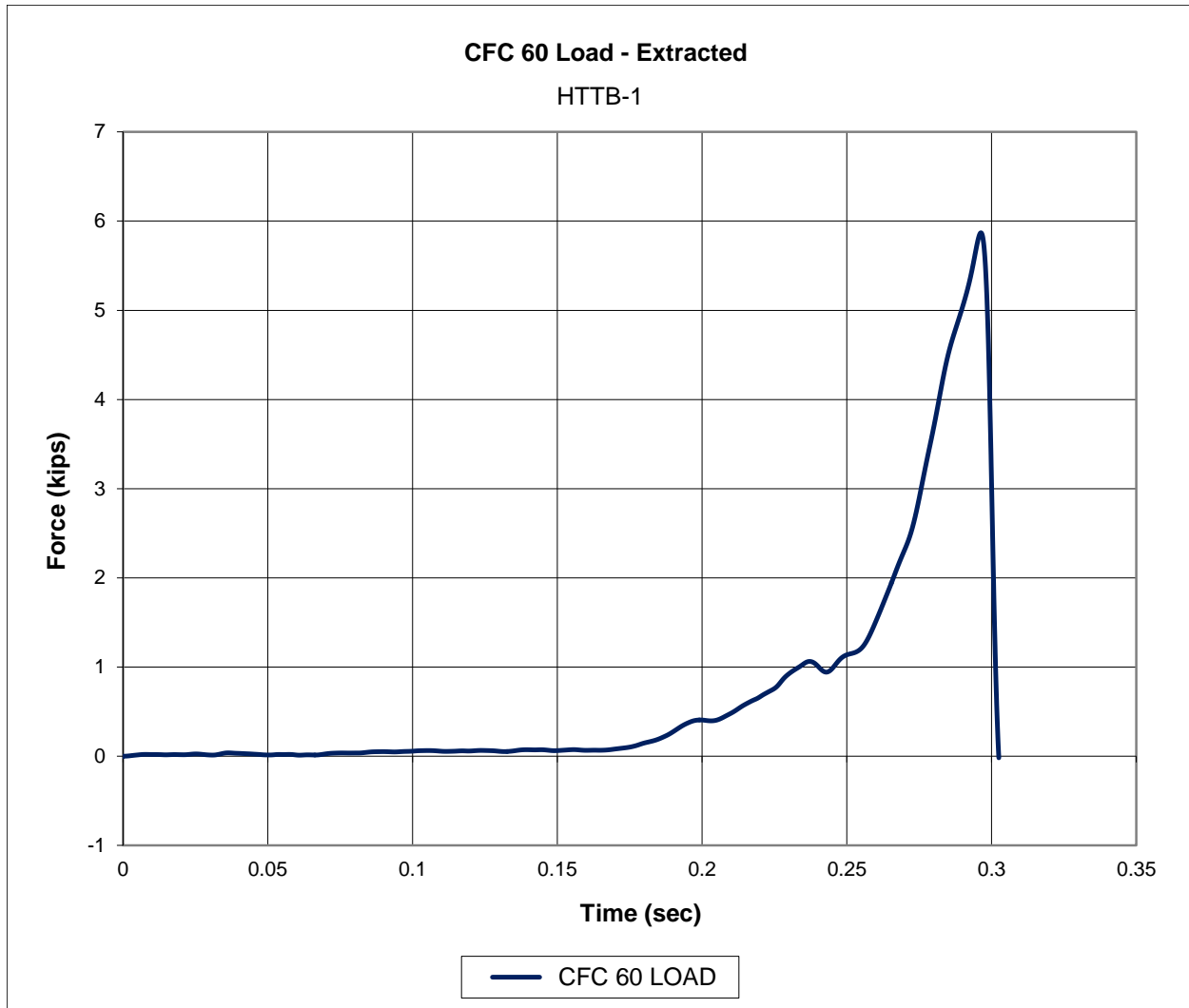


Figure 204. Force-Time Data, Test No. HTTB-1



Figure 205. Pre-Test and Post-Test Photographs, Test No. HTTPB-1

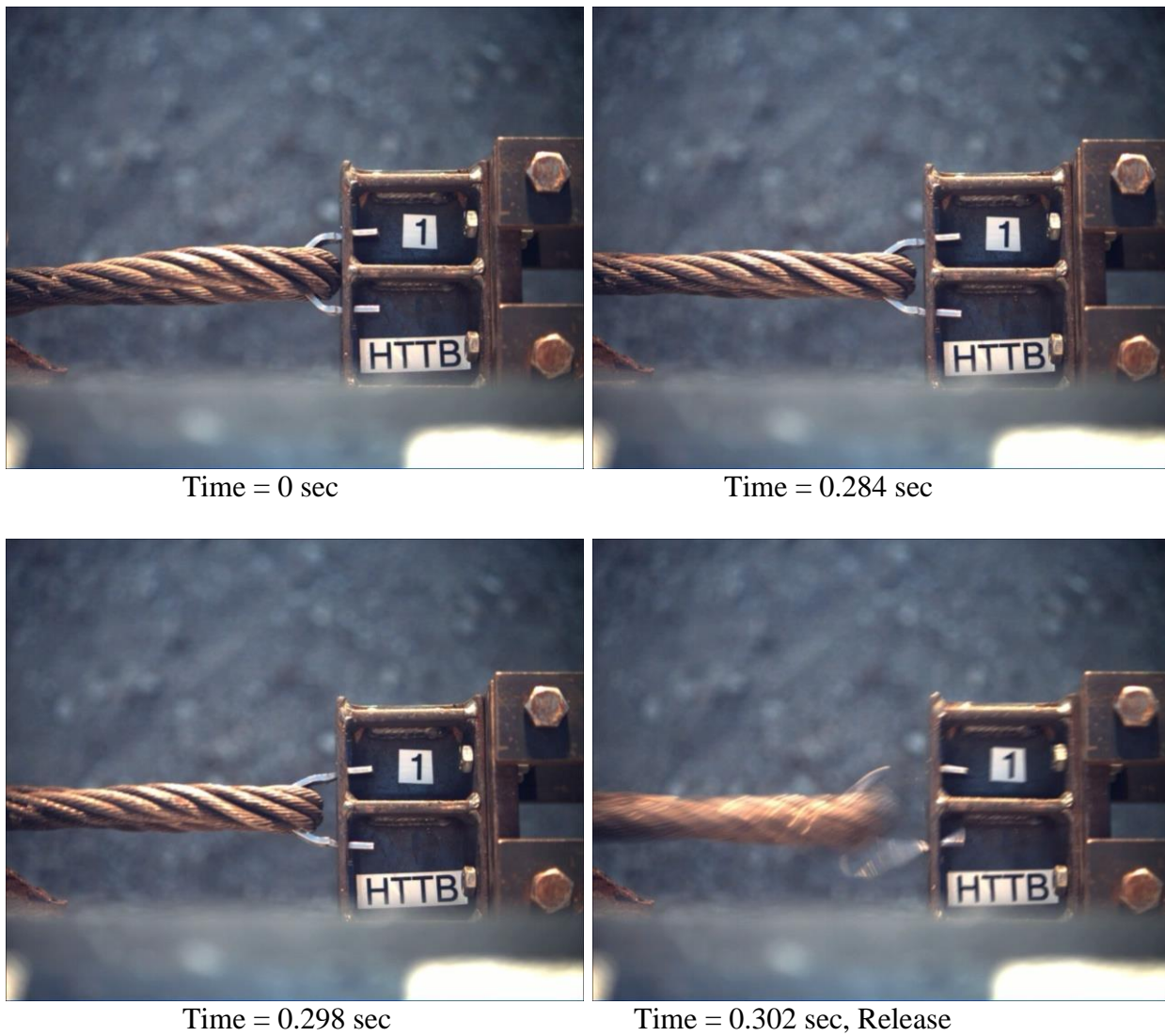


Figure 206. Sequential Photographs, Test No. HTTPB-1

11.1.2 Test No. HTTB-2 (TB V1, Crimp, Lateral)

For test no. HTTB-2, the cable pulled on the 10-gauge, grade 50 steel, crimp-in-place, tabbed bracket Version 1 at an angle of 90 degrees, perpendicular to the front face of the flange, thus imparting a lateral load. The post consisted of a 5-in. (127-mm) long, steel S3x5.7 (S76x8.5) section. The tabbed bracket was inserted into the top and bottom keyholes and crimped into place with channel lock pliers. As the cable pulled on the tabbed bracket, the top and bottom tabs were caught in the narrow parts of their respective keyways. The cable continued to pull on the bracket until it fractured through the bottom neck (failure location 2). The peak load was 5.99 kips (26.6 kN). The force versus time plot is shown in Figure 207. Pre- and post-test photographs are shown in Figure 208. Sequential photographs are shown in Figure 209.

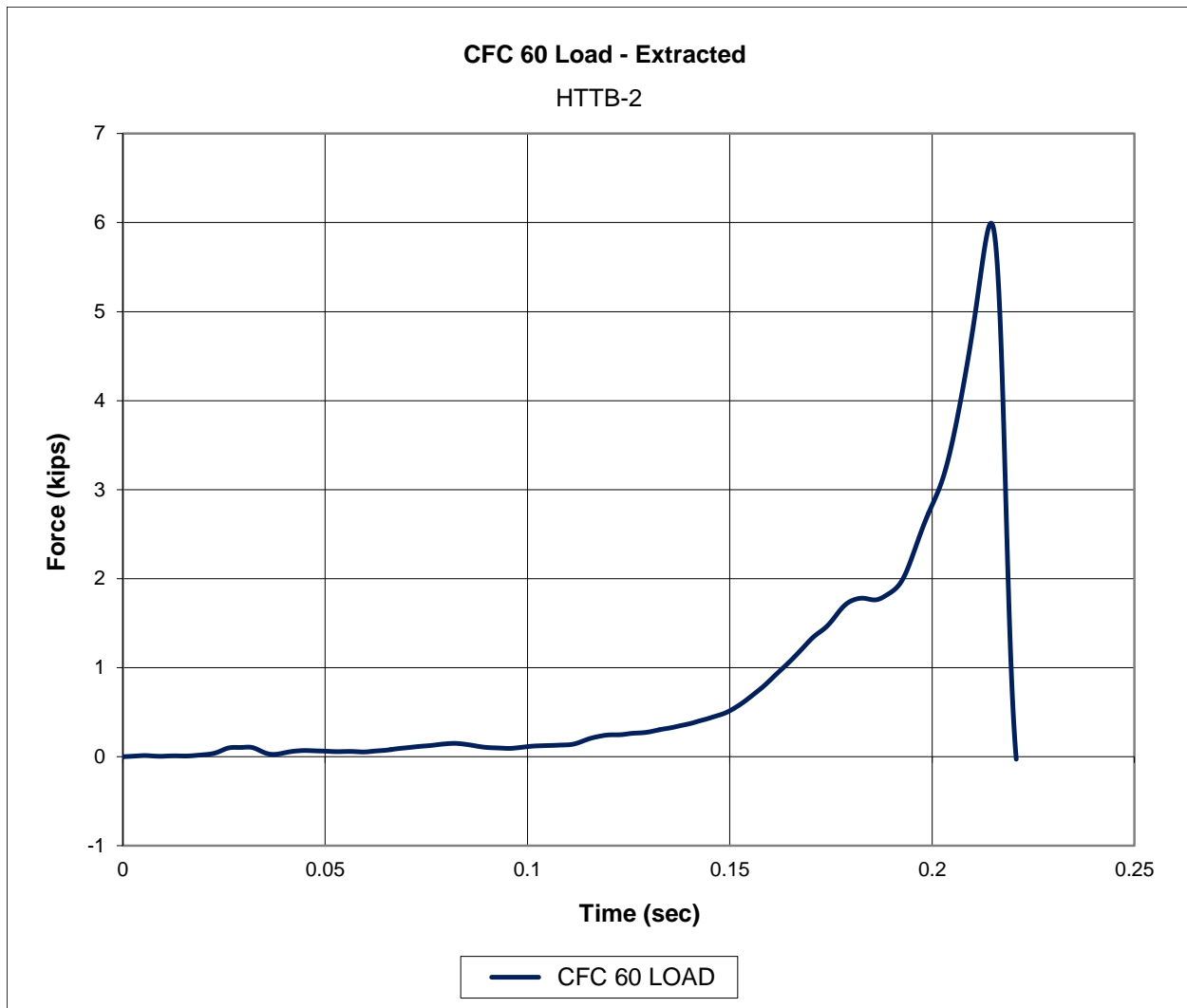


Figure 207. Force-Time Data, Test No. HTTB-2

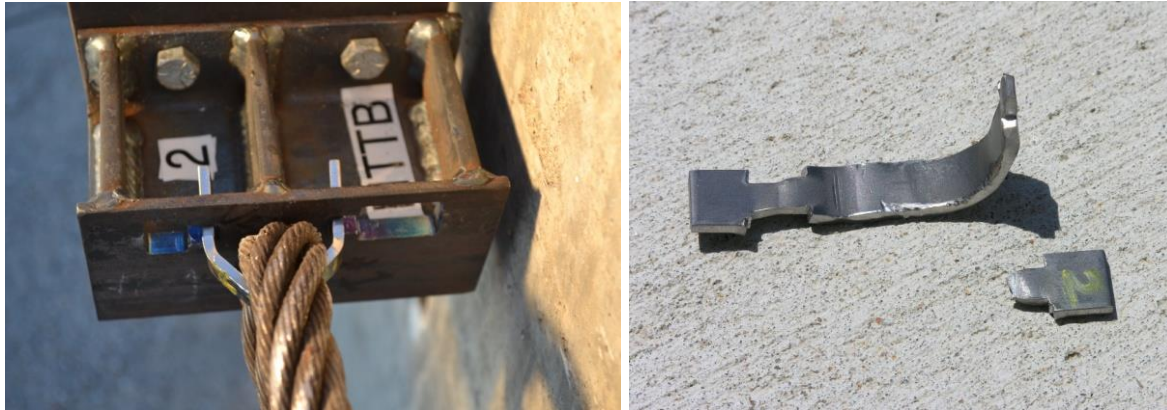


Figure 208. Pre-Test and Post-Test Photographs, Test No. HTTPB-2

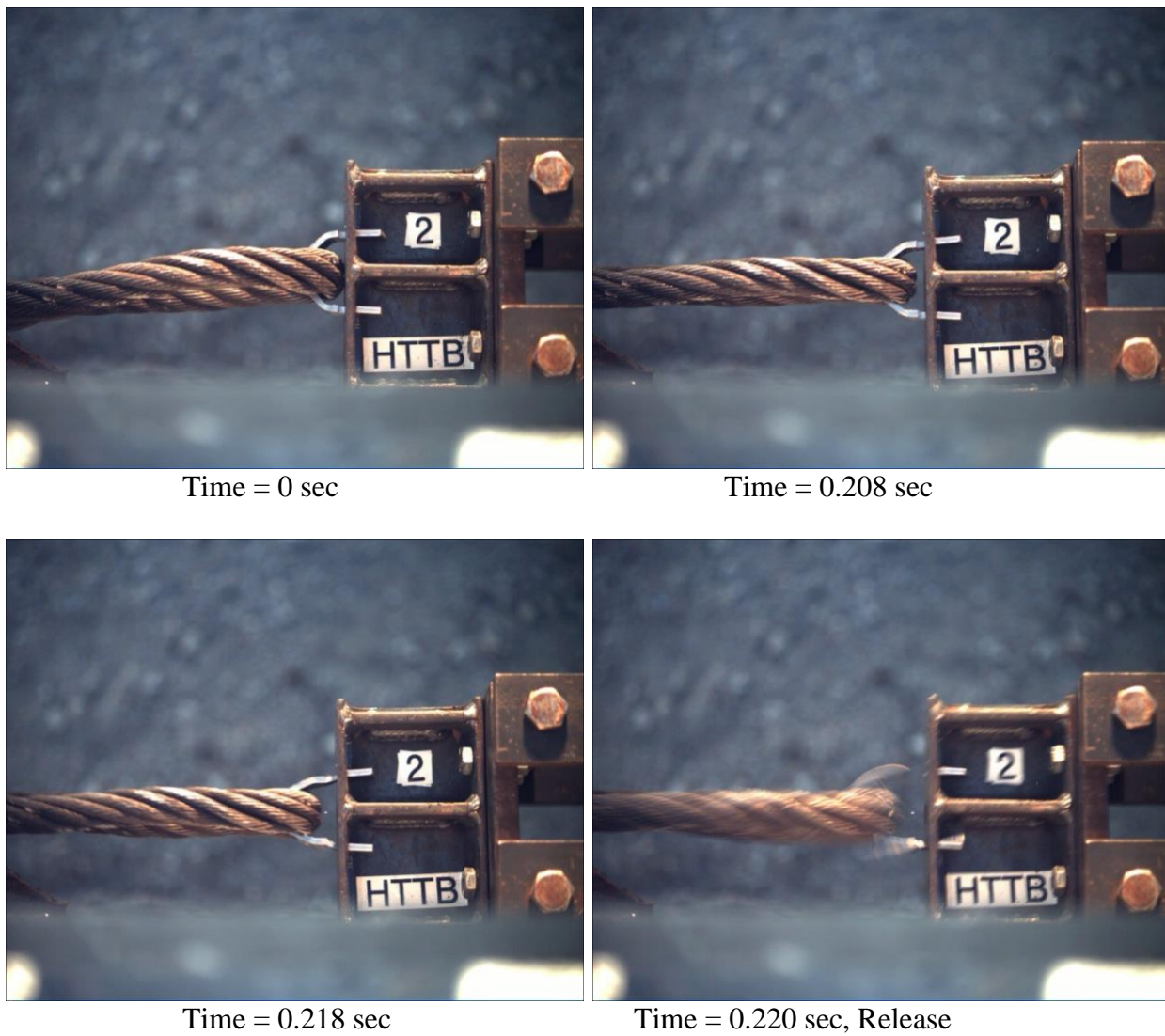


Figure 209. Sequential Photographs, Test No. HTTPB-2

11.1.3 Test No. HTTB-3 (TB V2, Crimp, Lateral)

For test no. HTTB-3, the cable pulled on the 11-gauge, grade 50 steel, crimp-in-place, tabbed bracket Version 2 at an angle of 90 degrees, perpendicular to the front face of the flange, thus imparting a lateral load. The post consisted of a 5-in. (127-mm) long, steel S3x5.7 (S76x8.5) section. The tabbed bracket was inserted into the top and bottom keyways and crimped into place with channel lock pliers. As the cable pulled on the tabbed bracket, the top and bottom tabs were caught in the narrow parts of their respective keyways. The cable continued to pull on the bracket until it fractured through the bottom neck (failure location 2). The peak load was 6.40 kips (28.5 kN). The force versus time plot is shown in Figure 210. Pre- and post-test photographs are shown in Figure 211. Sequential photographs are shown in Figure 212.

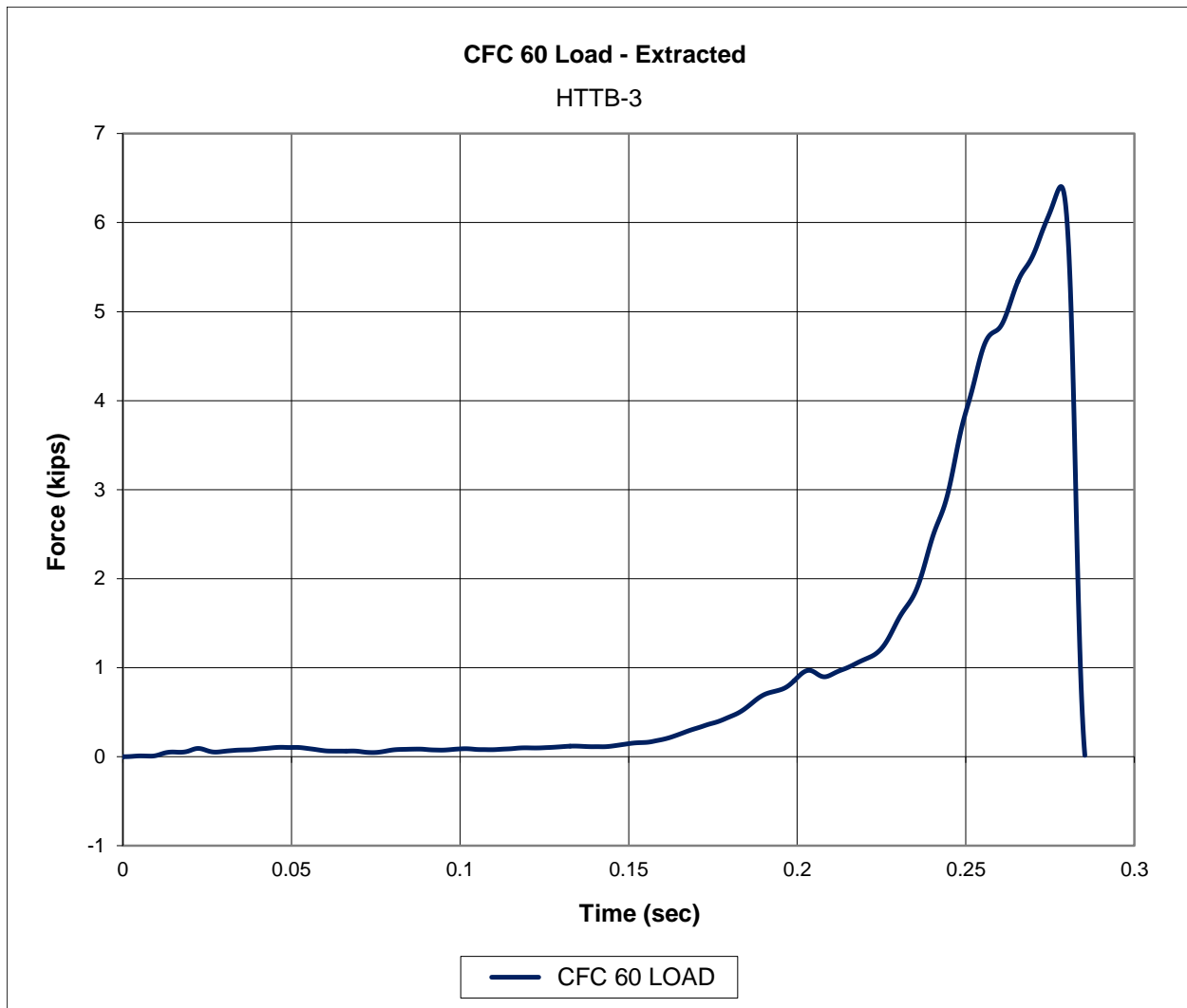
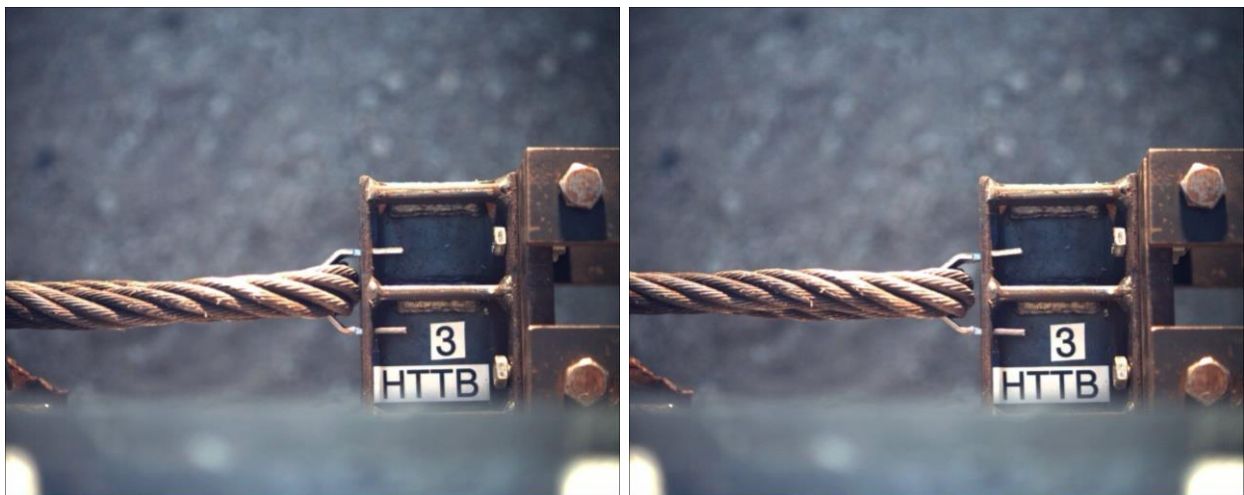


Figure 210. Force-Time Data, Test No. HTTB-3

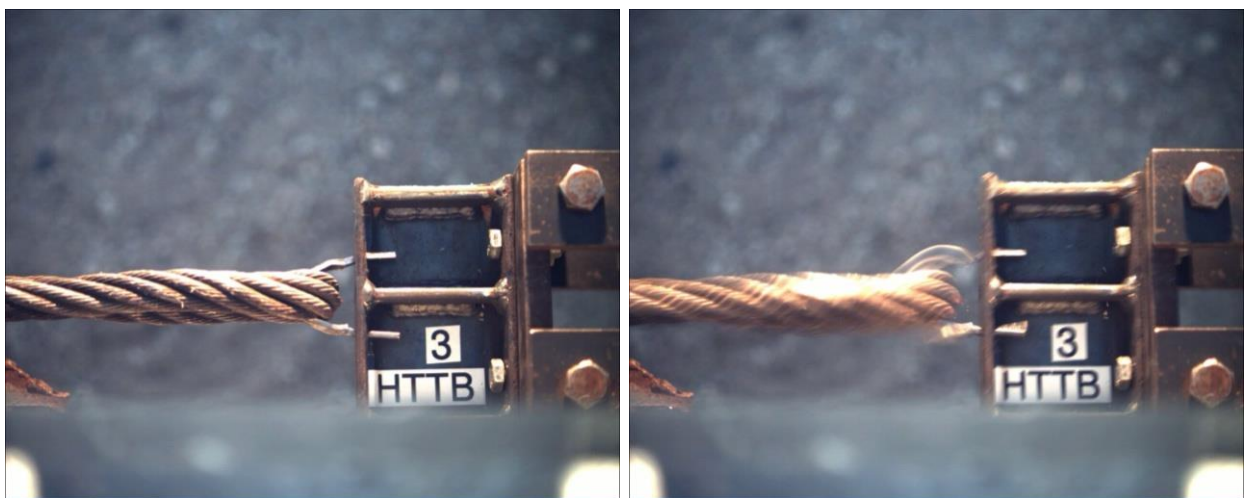


Figure 211. Pre-Test and Post-Test Photographs, Test No. HTTPB-3



Time = 0 sec

Time = 0.250 sec



Time = 0.282 sec

Time = 0.286 sec, Release

Figure 212. Sequential Photographs, Test No. HTTPB-3

11.1.4 Test No. HTTB-4 (TB V2, Crimp, Lateral)

For test no. HTTB-4, the cable pulled on the 11-gauge, grade 50 steel, crimp-in-place, tabbed bracket Version 2 at an angle of 90 degrees, perpendicular to the front face of the flange, thus imparting a lateral load. The post consisted of a 5-in. (127-mm) long, steel S3x5.7 (S76x8.5) section. The tabbed bracket was inserted into the top and bottom keyways and crimped into place with channel lock pliers. As the cable pulled on the tabbed bracket, the top and bottom tabs were caught in the narrow parts of their respective keyways. The cable continued to pull on the bracket until it fractured through the bottom neck (failure location 2). The peak load was 6.71 kips (29.8 kN). The force versus time plot is shown in Figure 213. Pre- and post-test photographs are shown in Figure 214. Sequential photographs are shown in Figure 215.

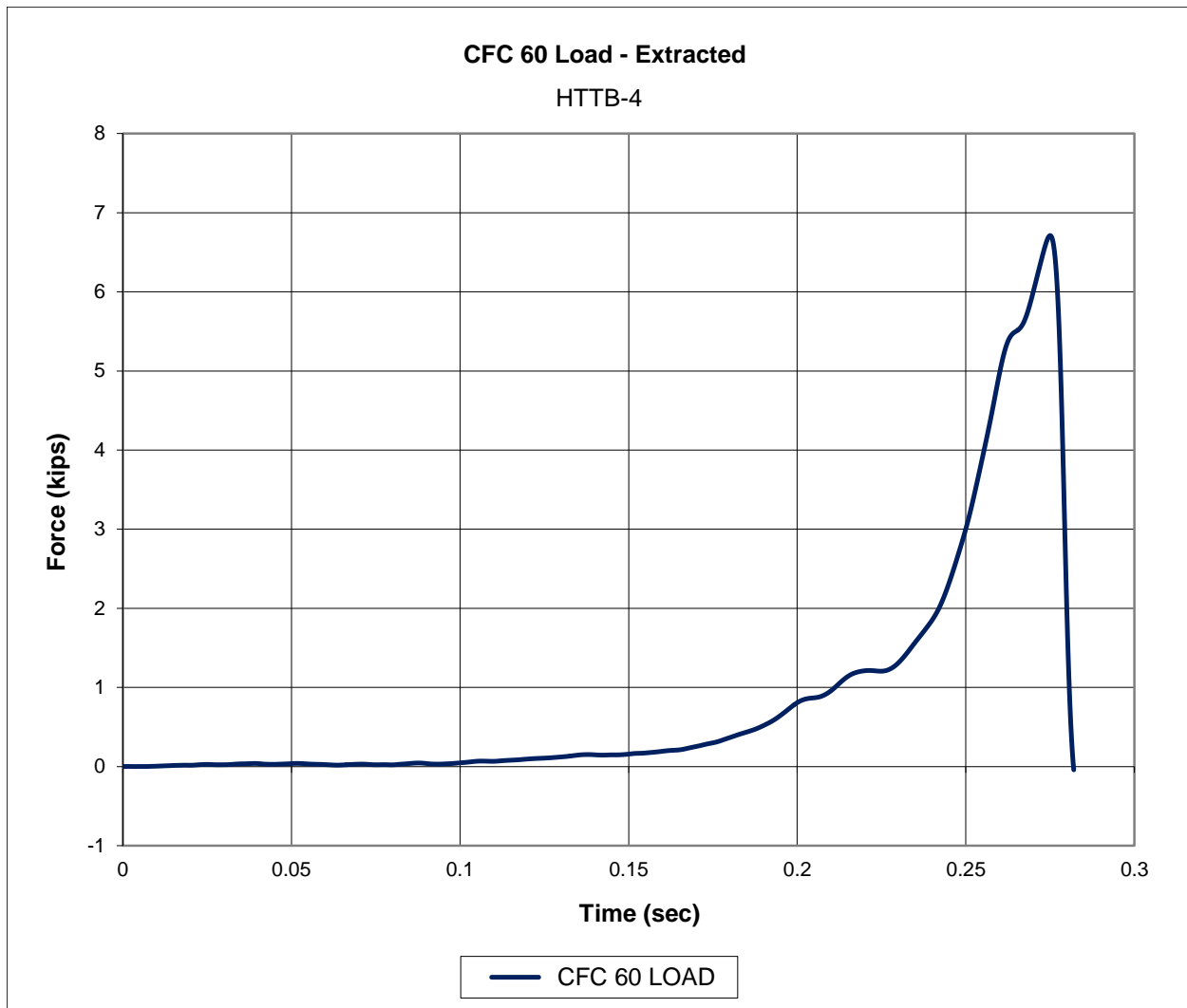


Figure 213. Force-Time Data, Test No. HTTB-4



Figure 214. Pre-Test and Post-Test Photographs, Test No. HTTPB-4

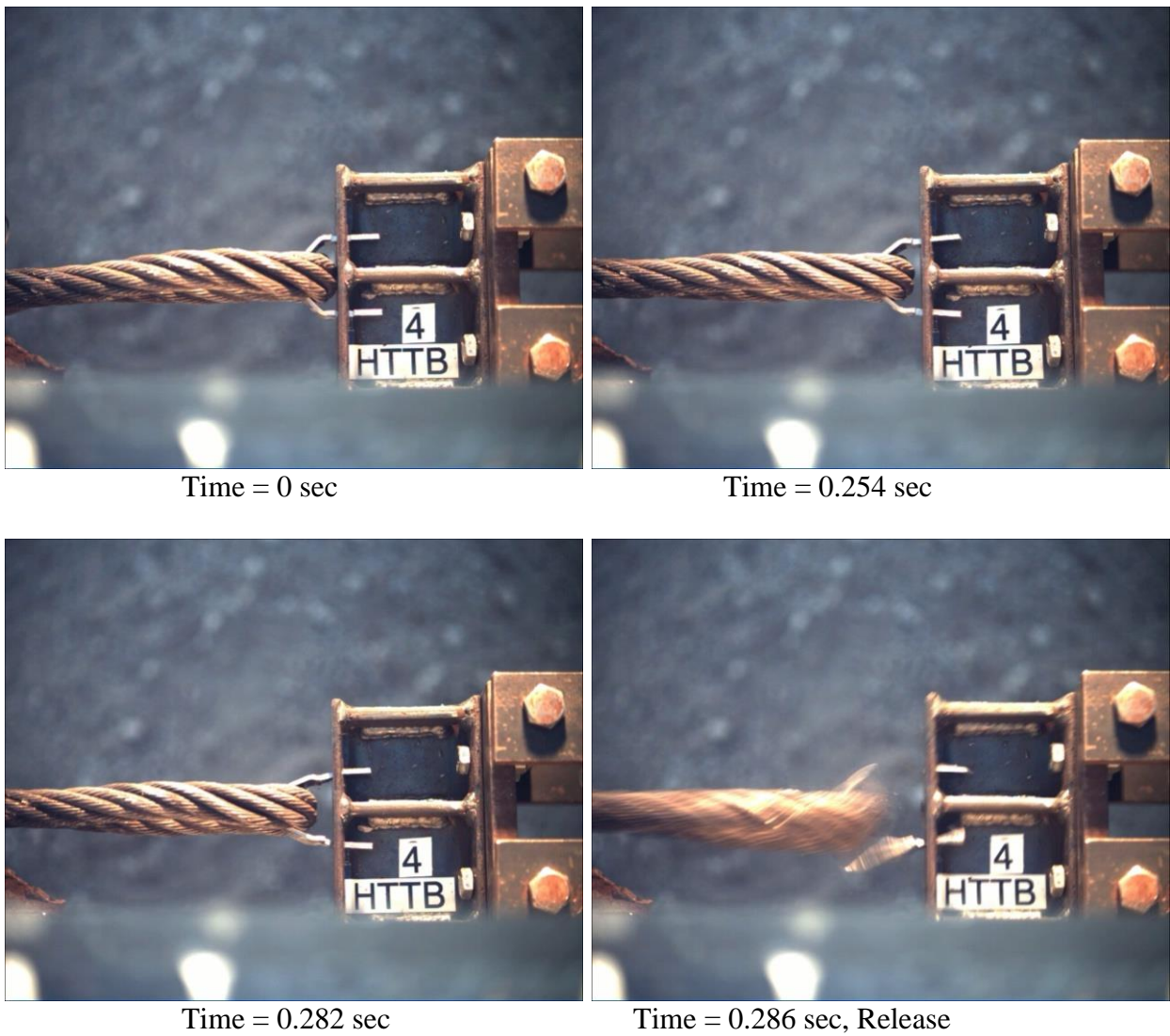


Figure 215. Sequential Photographs, Test No. HTTPB-4

11.1.5 Test No. HTTB-5 (TB V1, Crimp, Vertical)

For test no. HTTB-5, the cable pulled on the 10-gauge, grade 50 steel, crimp-in-place, tabbed bracket Version 1 at an angle of 0 degrees, parallel to the front face of the flange, thus imparting a vertical load. The post consisted of a 5-in. (127-mm) long, steel S3x5.7 (S76x8.5) section. The tabbed bracket was inserted into the top and bottom keyways and crimped into place with channel lock pliers. As the cable began to pull on the tabbed bracket, the bottom tab became caught in the top of its keyway. It was apparent from the way that the bracket began to deform that there was significant rotational freedom about the bottom end. Rather than bending about the middle of the bracket, as was expected, the top half of the bracket wrapped around the cable like a hook. Then, the head was pulled upward while scraping against the backside surface of the keyway. When the head finally cleared the narrow part of its keyway, the top half of the bracket began to rapidly straighten out. Subsequently, the head struck the top of the keyway before finally releasing. A peak load of 2.87 kips (12.8 kN) occurred as the head scraped against the backside surface of the keyway, just before slipping out. The force versus time plot is shown in Figure 216. Pre- and post-test photographs are shown in Figure 217. Sequential photographs are shown in Figure 218.

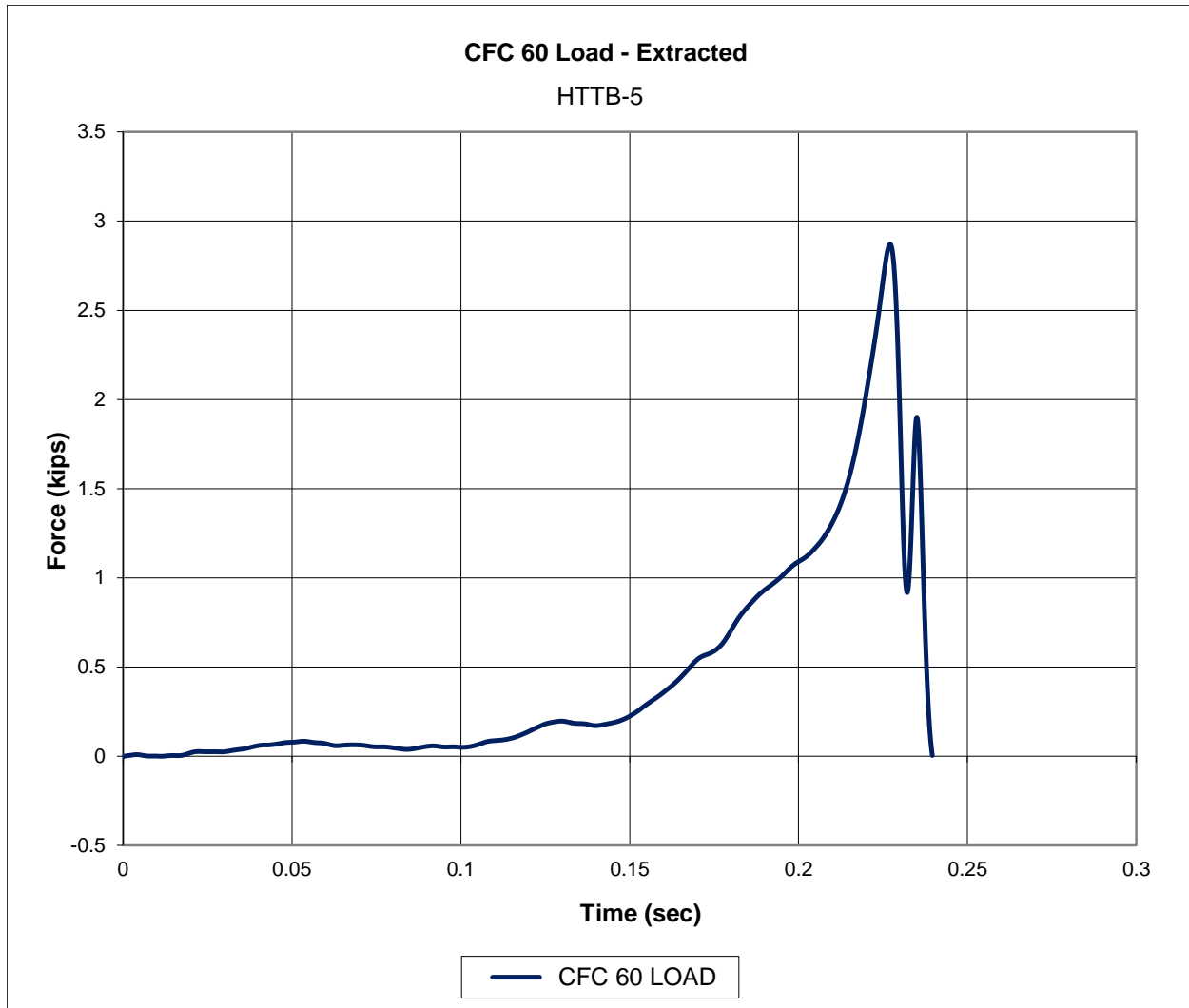
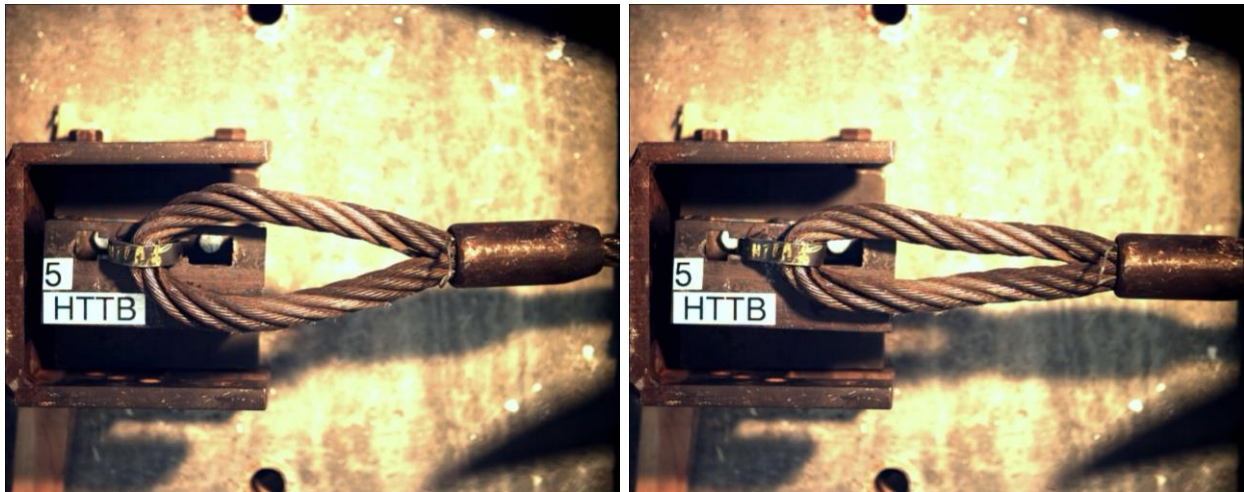


Figure 216. Force-Time Data, Test No. HTTB-5

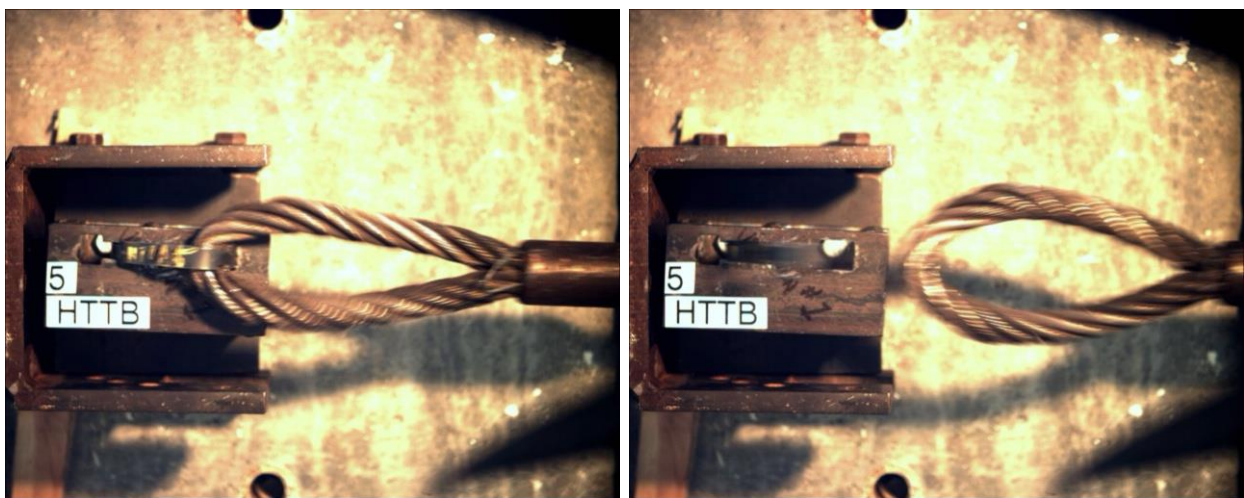


Figure 217. Pre-Test and Post-Test Photographs, Test No. HTTPB-5



Time = 0 sec

Time = 0.228 sec



Time = 0.234 sec

Time = 0.240 sec, Release

Figure 218. Sequential Photographs, Test No. HTTPB-5

11.1.6 Test No. HTTB-6 (TB V1, Crimp, Vertical)

For test no. HTTB-6, the cable pulled on the 10-gauge, grade 50 steel, crimp-in-place, tabbed bracket Version 1 at an angle of 0 degrees, parallel to the front face of the flange, thus imparting a vertical load. The post consisted of a 5-in. (127-mm) long, steel S3x5.7 (S76x8.5) section. The tabbed bracket was inserted into the top and bottom keyways and crimped into place with channel lock pliers. As the cable began to pull on the tabbed bracket, the bottom tab became caught in the top of its keyway. There appeared to be significant rotational freedom about the bottom end. The head scraped against the backside surface of the keyway as the top half of the bracket was dragged upward by the cable. As the cable continued to pull, the top half of the bracket appeared to wrap around the cable, although not as distinctly as in test no. HTTB-5. After the head finally slipped out of the narrow part of the keyway, the tab was able to rotate out of the wider part of the keyway, thus releasing the cable. A peak load of 2.80 kips (12.5 kN) occurred as the head scraped against the backside surface of the keyway, just before slipping out. The force versus time plot is shown in Figure 219. Pre- and post-test photographs are shown in Figure 220. Sequential photographs are shown in Figure 221.

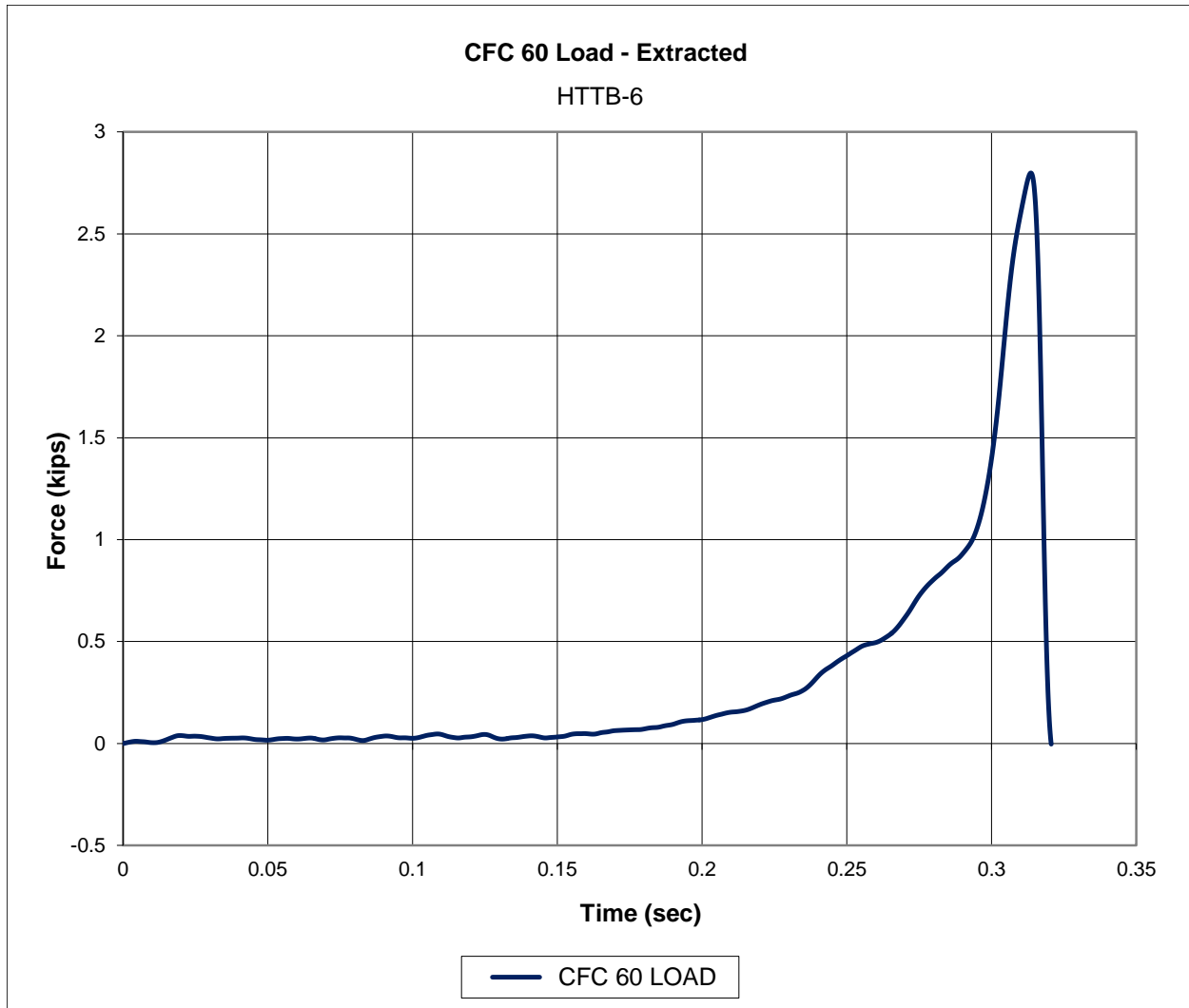


Figure 219. Force-Time Data, Test No. HTTB-6



Figure 220. Pre-Test and Post-Test Photographs, Test No. HTTPB-6

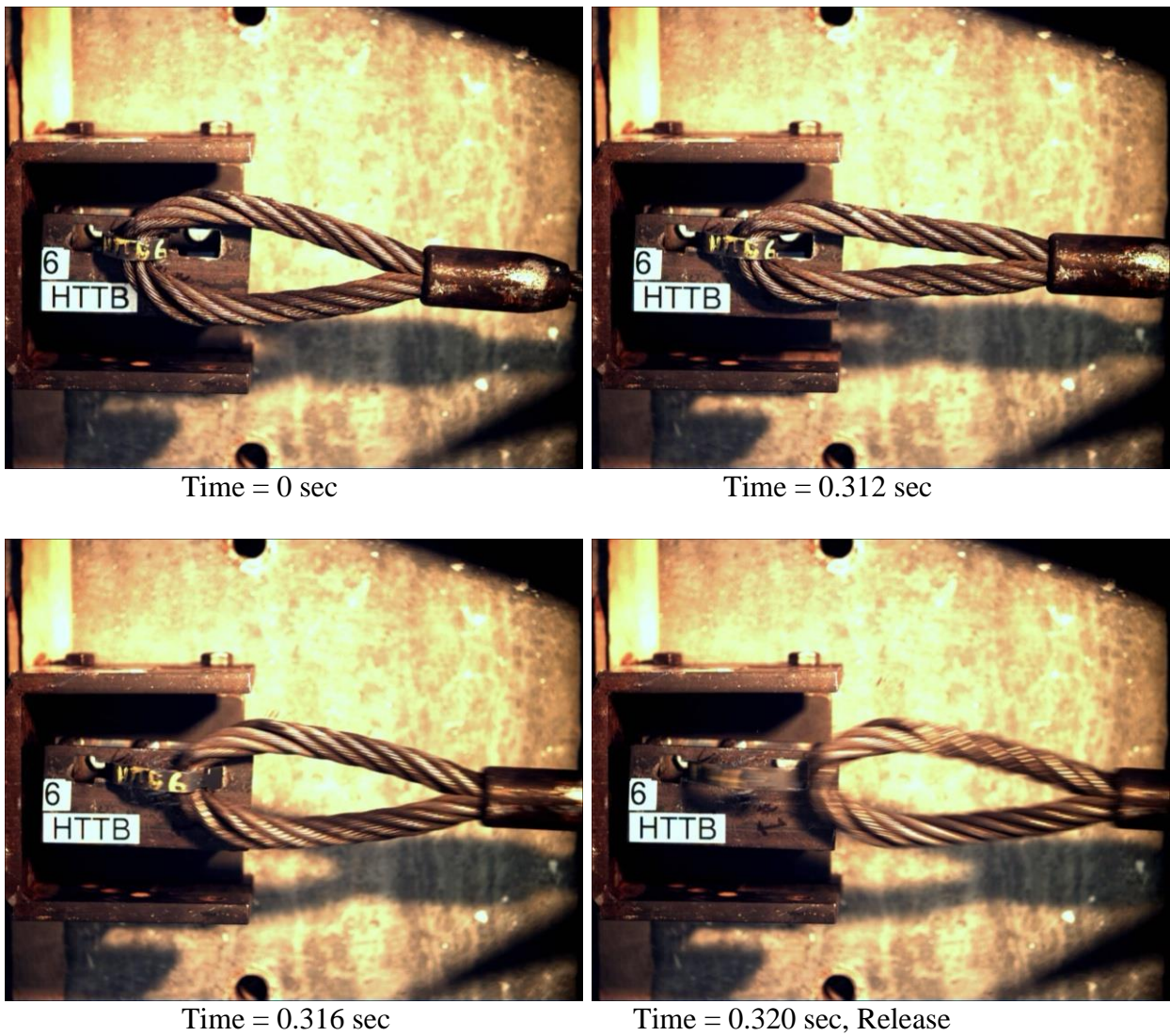


Figure 221. Sequential Photographs, Test No. HTTPB-6

11.1.7 Test No. HTTB-7 (TB V2, Crimp, Vertical)

For test no. HTTB-7, the cable pulled on the 11-gauge, grade 50 steel, crimp-in-place, tabbed bracket Version 2 at an angle of 0 degrees, parallel to the front face of the flange, thus imparting a vertical load. The post consisted of a 5-in. (127-mm) long, steel S3x5.7 (S76x8.5) section. The tabbed bracket was inserted into the top and bottom keyways and crimped into place with channel lock pliers. As the cable began to pull on the tabbed bracket, the bottom tab became caught in the top of its keyway. There appeared to be significant rotational freedom about the bottom end. The head scraped against the backside surface of the keyway as the top half of the bracket was pulled upward by the cable. The top half of the bracket did not wrap around the cable at all, as it seemed to do in test nos. HTTB-5 and HTTB-6. After the head finally slipped out of the narrow part of the keyway, the tab was able to rotate out of the wider part of the keyway. A peak load of 1.43 kips (6.36 kN) occurred as the head scraped against the backside surface of the keyway, just before slipping out. After the tab cleared the keyway, the cable was briefly snagged on the head, exerting a snag load of 551 lb (2,450 N). The force versus time plot is shown in Figure 222. Pre- and post-test photographs are shown in Figure 223. Sequential photographs are shown in Figure 224.

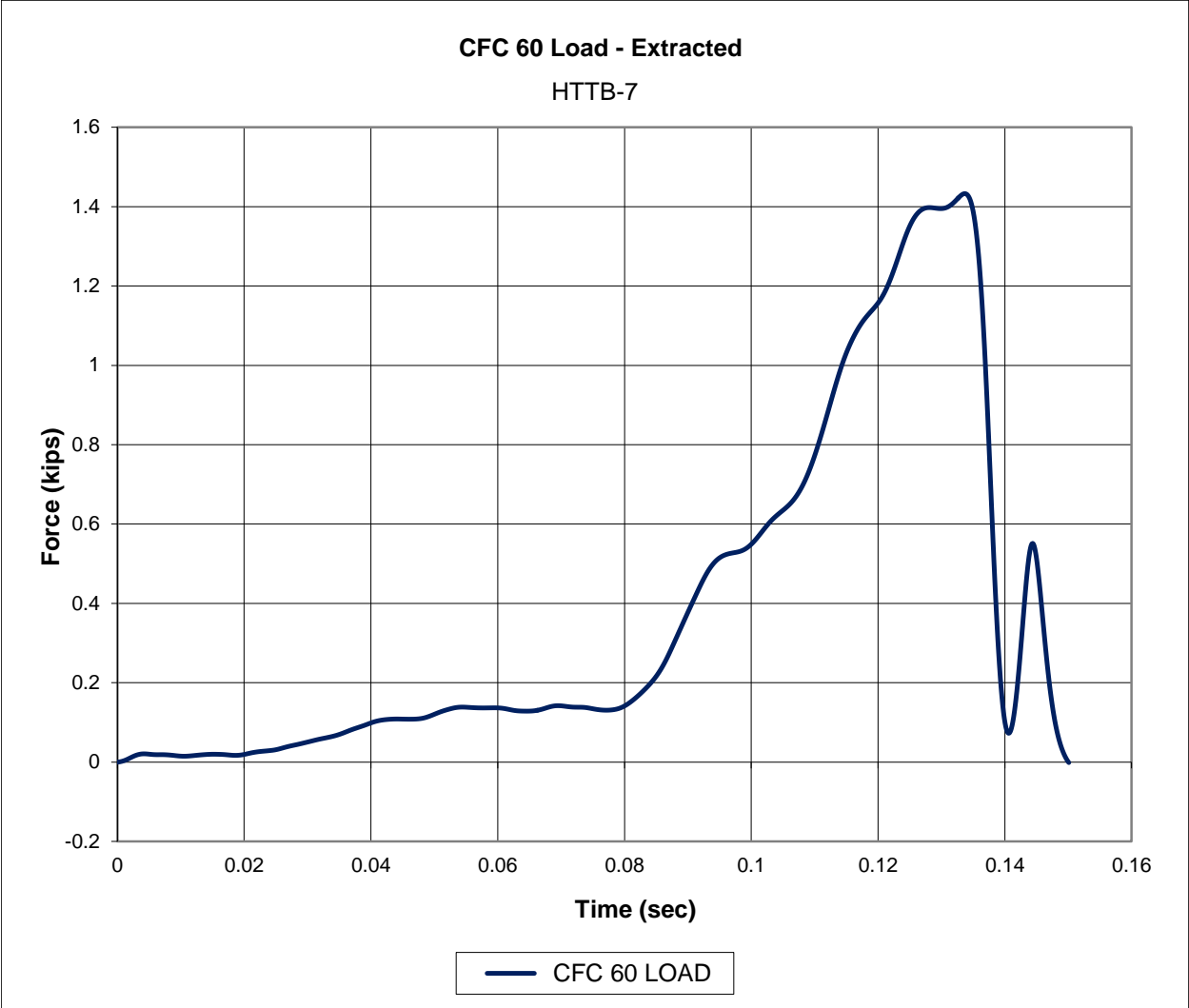


Figure 222. Force-Time Data, Test No. HTTB-7



Figure 223. Pre-Test and Post-Test Photographs, Test No. HTTPB-7

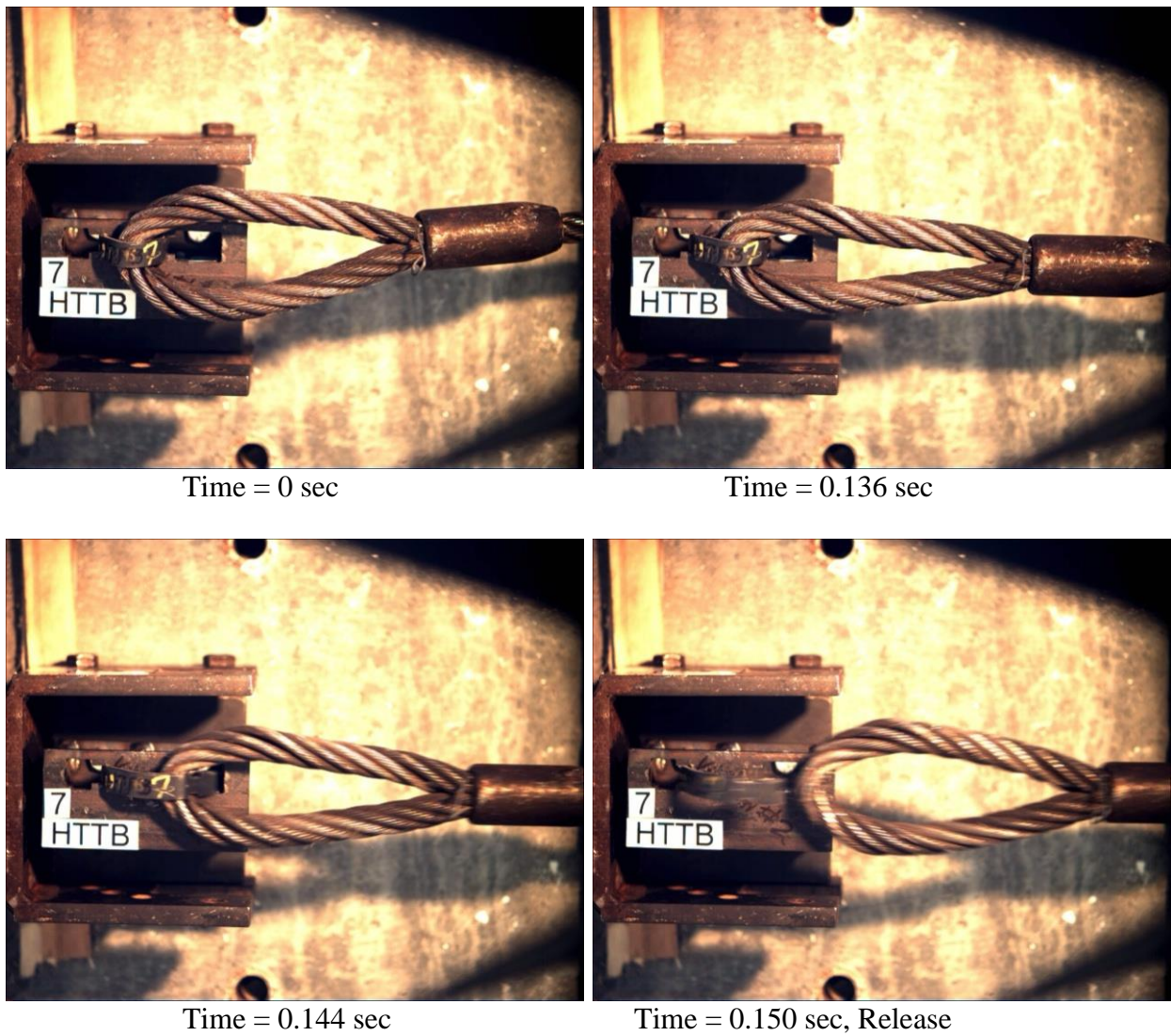


Figure 224. Sequential Photographs, Test No. HTTPB-7

11.1.8 Test No. HTTB-8 (TB V2, Crimp, Vertical)

For test no. HTTB-8, the cable pulled on the 11-gauge, grade 50 steel, crimp-in-place, tabbed bracket Version 2 at an angle of 0 degrees, parallel to the front face of the flange, thus imparting a vertical load. The post consisted of a 5-in. (127-mm) long, steel S3x5.7 (S76x8.5) section. The tabbed bracket was inserted into the top and bottom keyways and crimped into place with channel lock pliers. As the cable began to pull on the tabbed bracket, the bottom tab became caught in the top of its keyway. There appeared to be significant rotational freedom about the bottom end. The head scraped against the backside surface of the keyway as the top half of the bracket was pulled upward by the cable. The top half of the bracket did not wrap around the cable at all, as it seemed to do in test nos. HTTB-5 and HTTB-6. After the head finally slipped out of the narrow part of the keyway, the tab was able to rotate out of the wider part of the keyway. A peak force of 1.20 kips (5.34 kN) occurred as the head scraped against the backside surface of the keyway, just before slipping out. After the head cleared the keyway, the cable was briefly snagged on the head, exerting a snag load of 615 lb (2,740 N). The force versus time plot is shown in Figure 225. Pre- and post-test photographs are shown in Figure 226. Sequential photographs are shown in Figure 227.

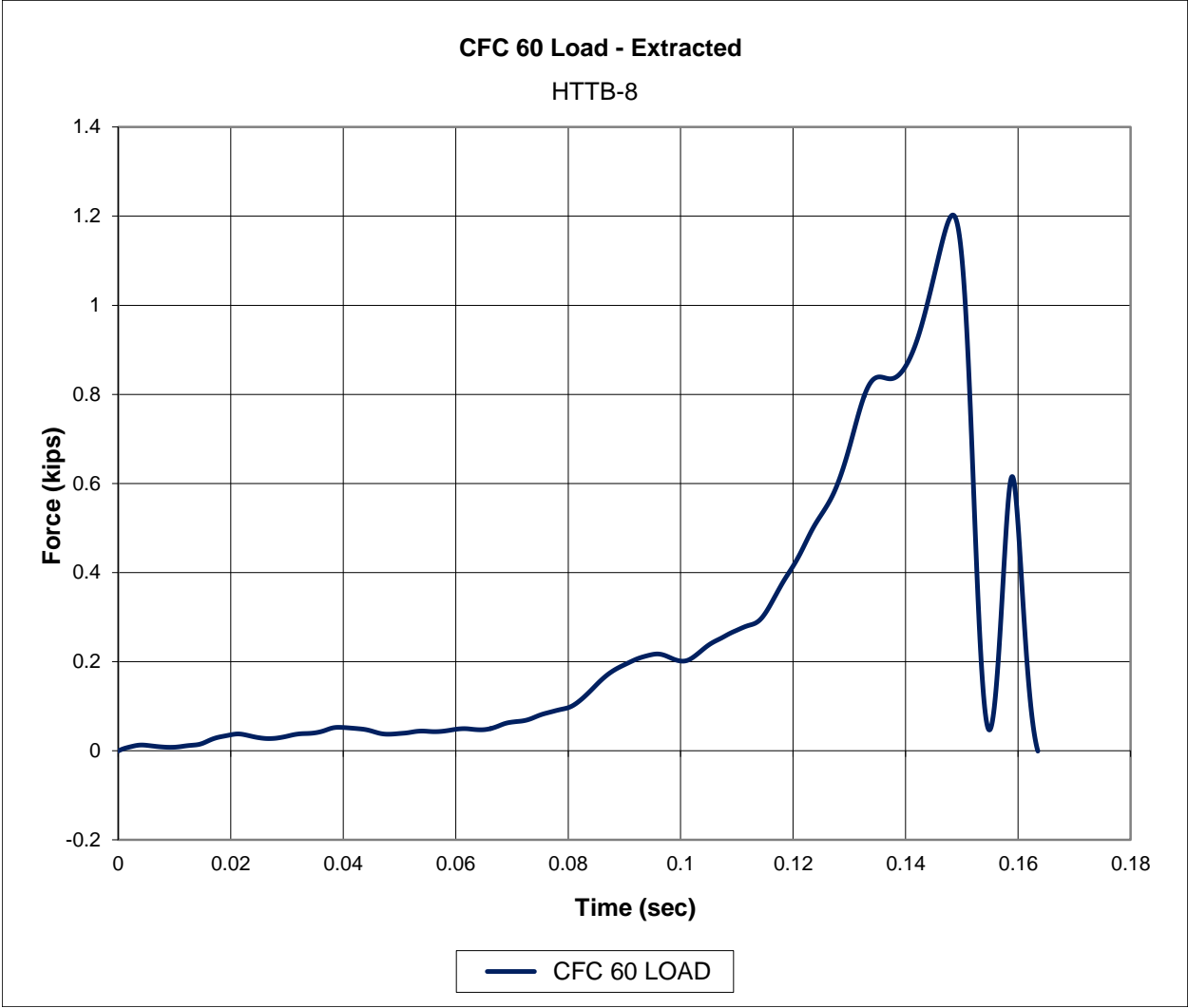


Figure 225. Force-Time Data, Test No. HTTB-8

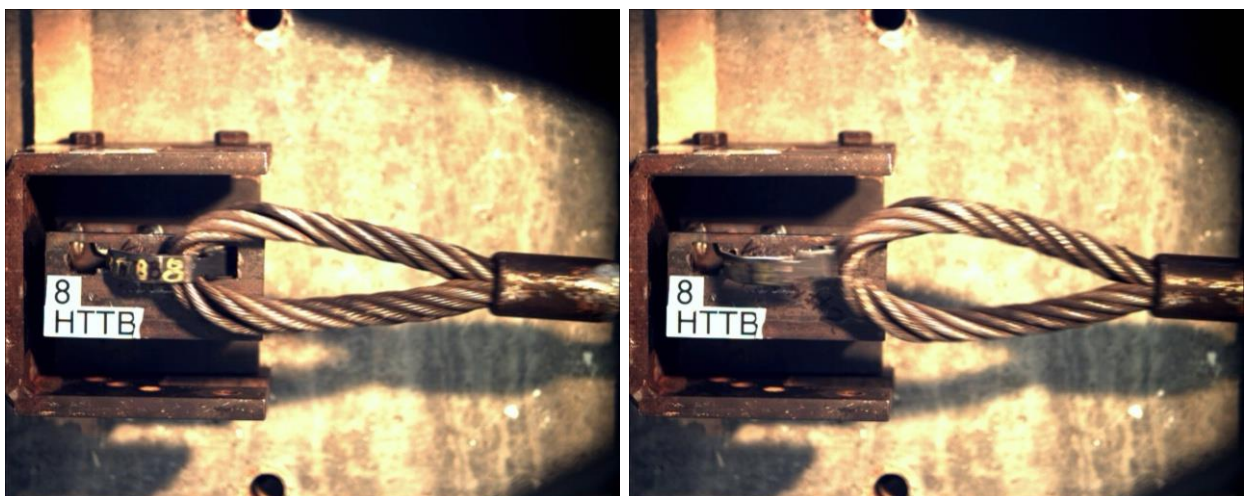


Figure 226. Pre-Test and Post-Test Photographs, Test No. HTTPB-8



Time = 0 sec

Time = 0.150 sec



Time = 0.158 sec

Time = 0.164 sec, Release

Figure 227. Sequential Photographs, Test No. HTTPB-8

11.2 Discussion

Eight dynamic component tests were performed in the first round of testing on tabbed brackets. Both versions of the tabbed brackets performed very well when pulled laterally. For tabbed bracket Version 1, the design equations predicted a lateral release load of 5.88 kips (26.2 kN), and the actual average lateral release load was 5.93 kips (26.4 kN). For tabbed bracket Version 2, the design equations predicted a lateral release load of 6.28 kips (27.9 kN), and the actual average lateral release load was 6.56 kips (29.2 kN).

Unfortunately, the crimp-in-place tabbed brackets provided vertical release loads that were deemed too high. For tabbed bracket Version 1, the design equations predicted a vertical release load of 224 lb (996 N), and the actual average vertical release load was 2.84 kips (12.6 kN). For tabbed bracket Version 2, the design equations predicted a vertical release load of 225 lb (1.00 kN), and the actual average vertical release load was 1.32 kips (5.87 kN). The high-speed video footage revealed tab scraping against the backside surface of the flange as the heads of the tabbed brackets were pulled upward by the cable.

The design equations did not account for the tab scraping. In the case of the keyway bolts, the tab-scraping problem was solved with the addition of a 1/4-in. (6-mm) shaft extension, thus creating additional clearance between the button head and the backside surface of the flange. However, a neck extension would not have worked with the crimp-in-place tabbed brackets; the crimp-in-place tabbed brackets were not fixed in place with the use of a bolt and nut. The space created by the extension would have been immediately lost as the bracket began to move upward.

In addition to the high vertical release loads, the crimp-in-place tabbed brackets were difficult to install. The brackets were crimped into place over the cable. However, it was difficult

to obtain a good grip with the channel lock pliers in this scenario. There is concern that these brackets may be improperly installed in the field. In addition, removal may also be cumbersome.

Due to the undesirable vertical release loads and difficult installation and removal of the crimp-in-place tabbed brackets, bolted tabbed brackets were considered for the next design iteration.

12 OVERVIEW OF BOLTED TABBED BRACKETS—ROUND 2

12.1 Introduction

Following the testing on the crimp-in-place, tabbed brackets, it was realized that future work was still needed. The research and development effort on the cable-to-post attachments for use with the bottom three cables was continued with the second round of design, testing, and evaluation for the tabbed brackets. Once again, the target lateral and vertical release loads were 6.00 kips (26.7 kN) and 225 lb (1.00 kN), respectively. The tabbed brackets that were developed in the second round were bolted to the front flange, rather than being crimped into place.

12.1.1 Dynamic Bogie Tests

All of the bolted tabbed brackets presented herein were tested using the same dynamic bogie testing setup and procedures described in Chapter 6. Different load orientations were used in order to determine the vertical and lateral release loads for each concept under dynamic loading conditions.

12.2 Bolted Tabbed Brackets

The bolted tabbed brackets consisted of three pieces—a non-symmetric tabbed bracket, a bolt, and a nut. While there were three parts versus two parts for the extended keyway bolt concept or common J bolts used in existing low-tension cable barriers, hardware installation was considered to be rather straight forward and easy. An installed bolted tabbed bracket is shown in Figure 228.



Figure 228. Installed Bolted Tabbed Bracket

12.2.1 Round 2 Design Equations

Equations were developed to guide the design process as well as to determine the actual dimensions of the prototype tabbed brackets. The dimensions, idealized load orientations, and assumed failure mechanisms and locations that were used in the development of the design equations, are shown in Figures 229 and 230.

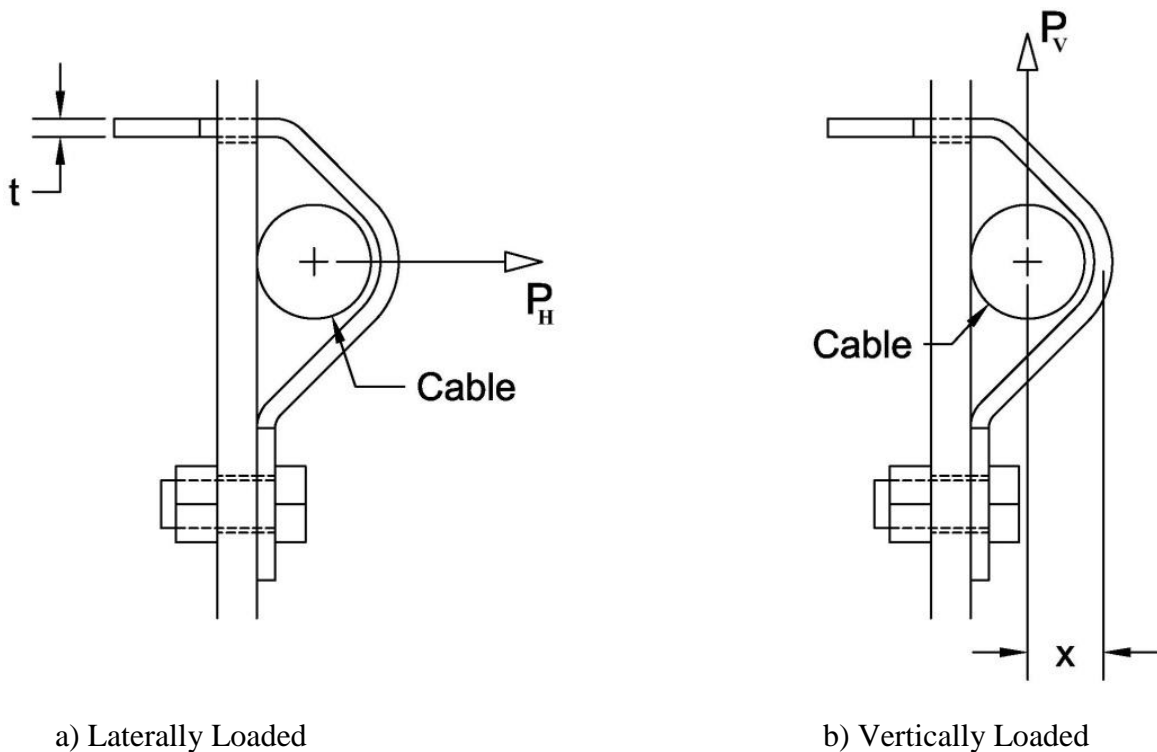


Figure 229. Bolted Tabbed Bracket—(a) Laterally Loaded and (b) Vertically Loaded

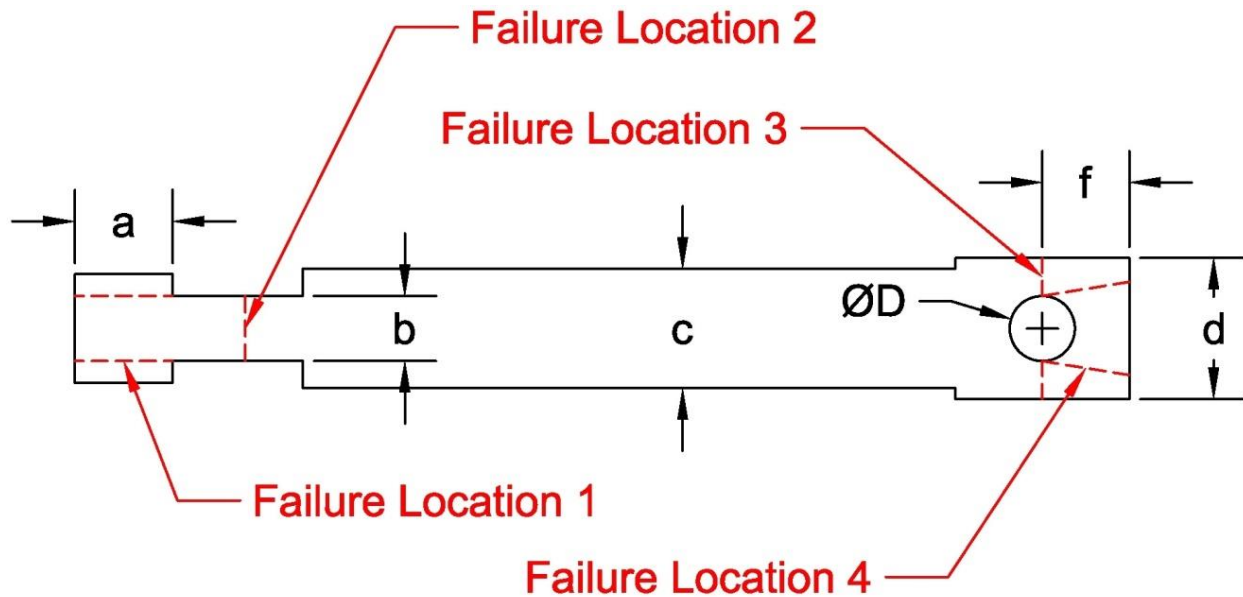


Figure 230. Dimensions and Failure Locations for Bolted Tabbed Bracket Design

For the lateral loading condition, as shown in Figure 229a, four failure locations were assumed in the bracket, as shown in Figure 231, thus resulting in four separate equations. It should be noted that dynamic magnification factors were not used in the second round of equations as they were not deemed necessary. One half of the horizontal load, P_H , was assumed to be distributed to each end of the tabbed bracket, as shown in Figure 231.



Figure 231. End Reactions for Use in the Design Equations

Failure location 1 was assumed to be a pure shear fracture. For pure shear, the shear yield strength is the tensile yield strength divided by the square root of three. This result corresponds to the maximum octahedral shear stress condition [75]. The same factor can be used with the ultimate tensile strength to obtain the ultimate shear strength. The lateral load needed to cause

failure at location 1 for two surfaces was calculated using Equation 12.1. The steps needed to derive the equation are also provided. The first step was to equate the end reaction with the available shear resistance.

$$\text{End Reaction} = \frac{P_{H_1}}{2} = A_1 \tau_u$$

Where A_1 = shear area for failure location 1 (two surfaces)
 τ_u ultimate shear strength

$$\frac{P_{H_1}}{2} = (2at) \frac{\sigma_u}{\sqrt{3}}$$

$$P_{H_1} = \frac{4}{\sqrt{3}} at \sigma_u \quad (12.1)$$

Where σ_u = ultimate tensile strength
a = length of head (see Figure 230)
t = thickness (see Figure 229a)

Failure location 2 was assumed to be a pure tensile fracture through the neck. The lateral load needed to cause failure at location 2 was calculated using Equation 12.2. The steps needed to derive the equation are also provided. The first step was to equate the end reaction with the available tensile resistance.

$$\text{End Reaction} = \frac{P_{H_2}}{2} = A_2 \sigma_u$$

Where A_2 = tensile area for failure location 2 (one surface)

$$\frac{P_{H_2}}{2} = (bt) \sigma_u$$

$$P_{H_2} = 2bt \sigma_u \quad (12.2)$$

Where σ_u = ultimate tensile strength
b = width of neck (see Figure 230)
t = thickness (see Figure 229a)

Failure location 3 was assumed to be a pure tensile fracture at the location of the bolt hole. It is common to use an additional width reduction of 1/16 in. (1.6 mm) for a bolt hole when

calculating the tensile area for such a fracture. The lateral load needed to cause failure at location 3 was calculated using Equation 12.3. The steps needed to derive the equation are also provided.

The first step was to equate the end reaction with the available tensile resistance.

$$\text{End Reaction} = \frac{P_{H_3}}{2} = A_3 \sigma_u$$

Where A_3 = tensile area for failure location 3

$$\frac{P_{H_3}}{2} = ((d - D - v)t)\sigma_u$$

$$P_{H_3} = 2(d - D - v)t\sigma_u = 2(d - d_b - \mu)t\sigma_u \quad (12.3)$$

Where d = width of bottom tab (see Figure 230)
 D = diameter of hole (see Figure 230)
 v = width reduction when using hole diameter = 1/16 in. (1.6 mm)
 d_b = diameter of bolt
 μ = width reduction when using bolt diameter = 1/8 in. (3.2 mm)

Failure location 4 was assumed to be a bearing and/or tearing failure at the bolt hole. Equation J3-6a from the American Institute of Steel Construction (AISC) *Specification for Structural Steel Buildings* [76] was used as a starting point.

$$R_n = 1.2l_c t \sigma_u \leq 2.4d_b t \sigma_u \quad (\text{AISC Equation J3-6a})$$

Where l_c = clear distance, in the direction of the force, between the edge of the hole and the edge of the material
 t = thickness of the connected material
 d_b = diameter of the bolt
 σ_u = ultimate tensile strength

The left side of the inequality is the tearing strength, and the right side is the bearing strength.

Equation 12.4, which gives the applied load, P_H , needed to cause tearing failure, was derived by equating the end reaction to the tearing strength.

$$\begin{aligned} \text{End Reaction} &= \frac{P_{H_4}}{2} = 1.2l_c t \sigma_u = 1.2\left(f - \frac{D}{2}\right)t\sigma_u \\ P_{H_4} &= 2.4\left(f - \frac{D}{2}\right)t\sigma_u = 2.4\left(f - \frac{d_b + v}{2}\right)t\sigma_u \end{aligned} \quad (12.4)$$

Where f = distance from the center of the bolt hole to the bottom edge of the bolted tabbed bracket (see Figure 230)
 D = diameter of the bolt hole (see Figure 230)
 d_b = diameter of the bolt
 v = 1/16 in. (1.6 mm)
 t = thickness of the connected material
 σ_u = ultimate tensile strength

The bearing strength only considers the diameter of the bolt and the thickness of the material. Only two different sizes of bolt were considered—1/4 in. (6 mm) and 5/16 in. (8 mm). Assuming an ultimate tensile strength of 70 ksi (483 MPa), the bearing strengths were calculated for the range of steel thicknesses that were being considered and are shown in Table 9.

Table 9 Calculated Bearing Strengths with $\sigma_u = 70$ ksi (483 MPa)

Steel Gauge	t, in. (mm)	Bearing Strength, kips (kN) = $2.4d_b t \sigma_u$	
		For $d_b = 1/4$ in. (6 mm)	For $d_b = 5/16$ in. (8 mm)
14	0.0747 (1.8974)	3.14 (14.0)	3.92 (17.4)
13	0.0897 (2.2784)	3.77 (16.8)	4.71 (20.9)
12	0.1046 (2.6568)	4.39 (19.5)	5.49 (24.4)
11	0.1196 (3.0378)	5.02 (22.3)	6.28 (27.9)
10	0.1345 (3.4163)	5.65 (25.1)	7.06 (31.4)

The minimum bearing strength was 3.14 kips (14.0 kN). According to the assumed load distribution, the total lateral load, P_H , based on a bearing capacity of 3.14 kips (14.0 kN) at the bolt hole of one end, would be 6.28 kips (27.9 kN), which was greater than the target lateral release load of 6.00 kips (26.7 kN). Thus, the bearing strength was effectively ignored during the design process.

The expected lateral release load for a particular bolted tabbed bracket was the minimum load calculated from Equations 12.1 through 12.4.

The vertical release load was assumed to occur in pure, plastic bending. As noted previously, no dynamic magnification factor was used in the second round equations. The

moment arm, x , was measured between the center of the cable and the mid-plane of the outer bracket, as shown in Figure 229b. The vertical release load for the cable was calculated using Equation 12.5. The steps used to derive the equation are also provided below.

$$P_V x = M_P$$

Where x = moment arm (see Figure 229b)
 M_P = plastic moment

$$P_V = \frac{M_P}{x} = \frac{Z \sigma_y}{x} = \frac{\frac{ct^2}{4} \sigma_y}{x} = \frac{ct^2 \sigma_y}{4x} \quad (12.5)$$

Where Z = plastic section modulus where bending occurs
 σ_y = yield strength
 c = cross-sectional width where bending occurs (see Figure 230)
 t = thickness (see Figure 229a)

When calculating the shear and tensile capacities of the Round 1 tabbed brackets, the steel strengths were 50 ksi (345 MPa) for the yield strength and 70 ksi (483 MPa) for the ultimate tensile strength. The actual strengths can be found on the material testing reports, as provided in Appendix E.

12.2.2 Dimensions and Structural Capacities

Tabbed bracket Versions 3 and 4 were tested in the second round. Tabbed bracket Version 3 was fabricated from 11-gauge, grade 50 sheet steel. Using the design equations, the predicted lateral and vertical capacities were 6.28 kips (27.9 kN) and 225 lb (1.00 kN), respectively. A side view of tabbed bracket Version 3 is shown in Figure 232. A flat pattern of the tabbed bracket is shown in Figure 233. The keyway corresponding to tabbed bracket Version 3 is shown in Figure 234.

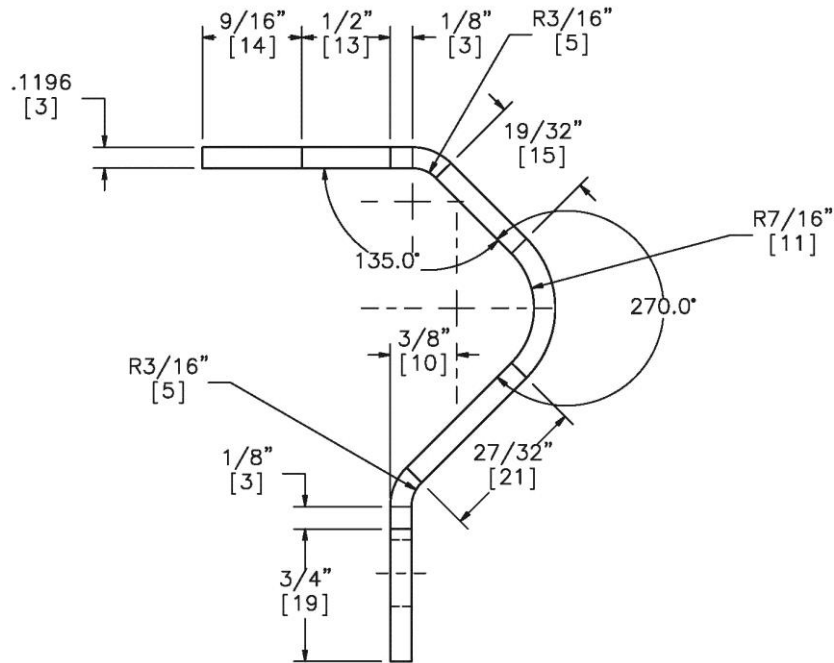


Figure 232. Side View of Tabbed Bracket Version 3

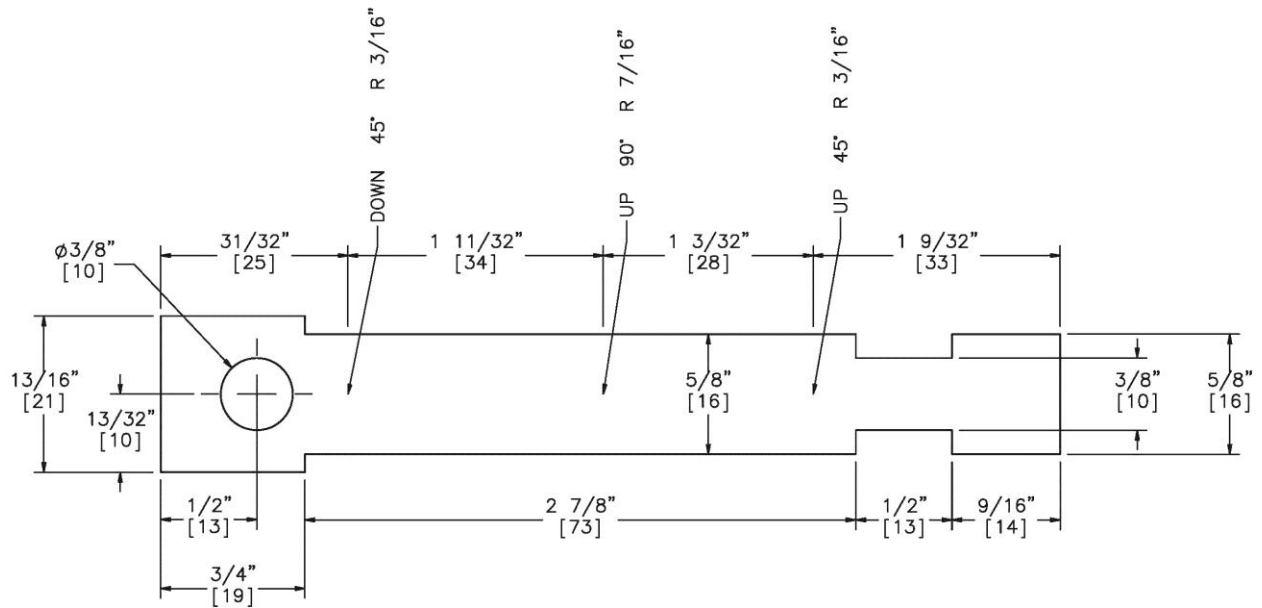


Figure 233. Flat Pattern of Tabbed Bracket Version 3

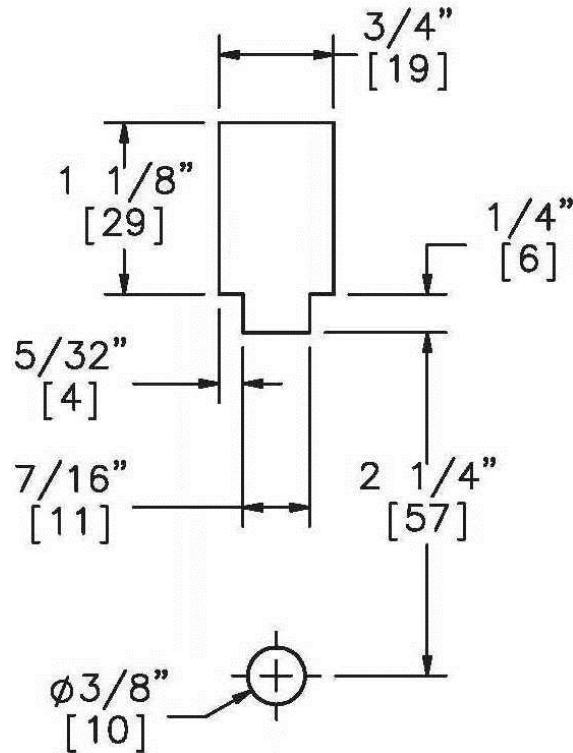


Figure 234. Tabbed Bracket Version 3 Keyway

Tabbed bracket Version 4 was fabricated from 10-gauge, grade 50 sheet steel. Using the design equations, the predicted lateral and vertical capacities were 5.88 kips (26.2 kN) and 224 lb (996 N), respectively. A side view of tabbed bracket Version 4 is shown in Figure 235. A flat pattern of the tabbed bracket is shown in Figure 236. The keyway corresponding to tabbed bracket Version 4 is shown in Figure 237.

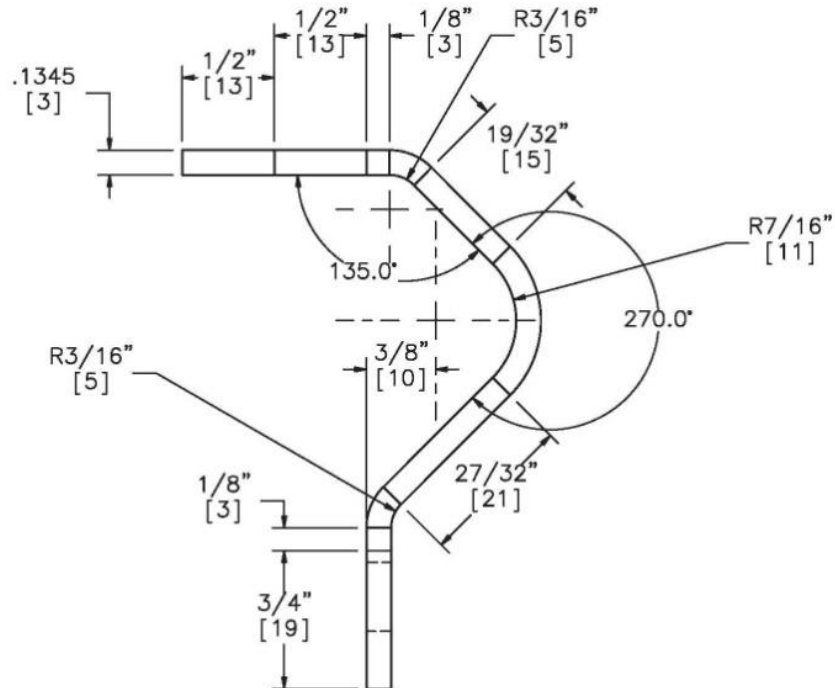


Figure 235. Side View of Tabbed Bracket Version 4

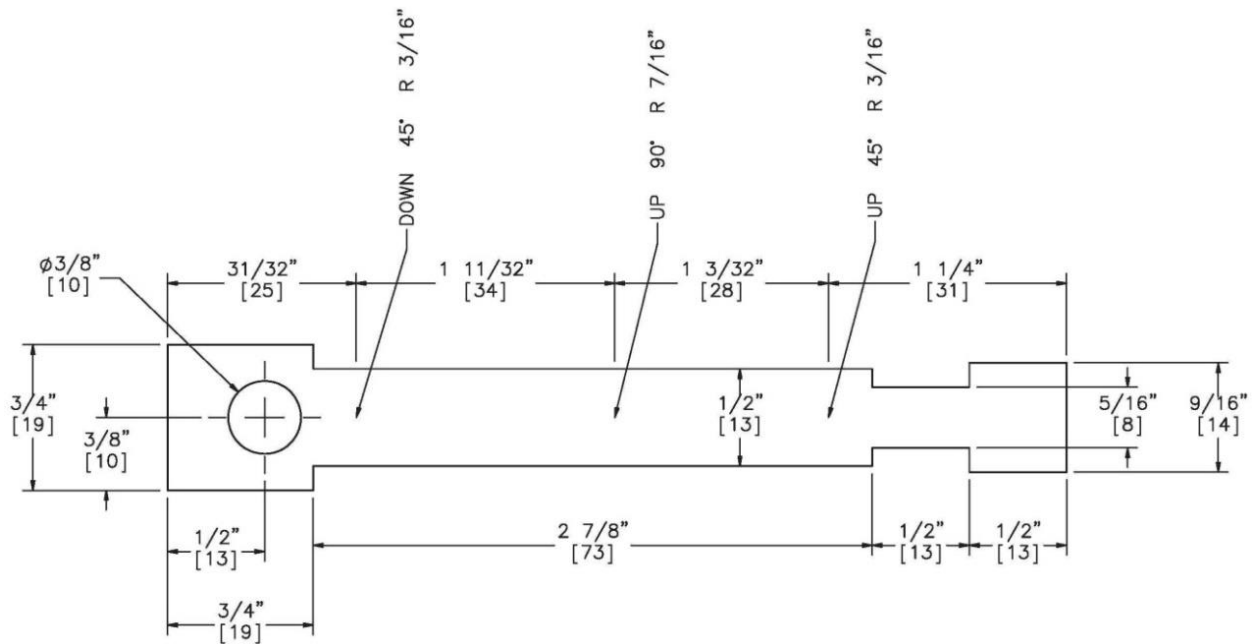


Figure 236. Flat Pattern of Tabbed Bracket Version 4

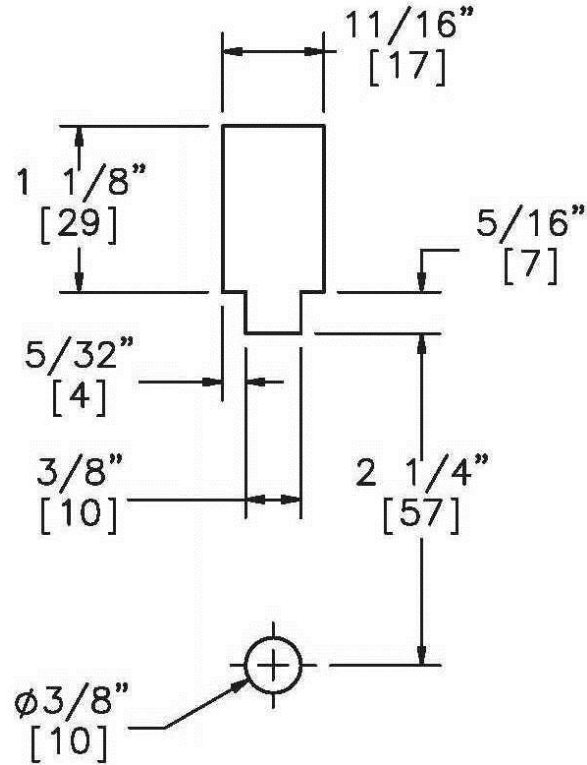


Figure 237. Tabbed Bracket Version 4 Keyway

The expected release loads for the bolted tabbed brackets from Round 2 are shown in Table 10.

Table 10. Expected Release Loads for Round 2 Bolted Tabbed Brackets

Tabbed Bracket	Expected Lateral Release Load kips (kN)				Expected Vertical Release Load kips (kN)
	Failure Location 1	Failure Location 2	Failure Location 3	Failure Location 4	
Version 3	7.77 (34.5)	6.28 (27.9)	6.28 (27.9)	6.28 (27.9)	0.22 (1.0)
Version 4	7.77 (34.5)	5.88 (26.2)	5.88 (26.2)	7.06 (31.4)	0.22 (1.0)

13 DYNAMIC COMPONENT TESTS—TABBED BRACKETS, ROUND 2

13.1 Results

All of the tabbed brackets were fabricated from hot-rolled, ASTM A1011, HSLA Grade 50 sheet steel. The tabbed bracket thickness, cross-section width, method of attachment, and the mounting post section were varied for the Round 2 tests. The same setup and procedures used to test the keyway bolts was also used to test the tabbed brackets. Three rounds of design modifications, component testing, and evaluation were made to the tabbed brackets. Eight dynamic component tests (test nos. HTTB-1 through HTTB-8) were performed in the first round, as discussed in Chapters 10 and 11. Ten dynamic component tests (test nos. HTTB-9 through HTTB-16, including test nos. HTTB-9R and HTTB-12R) were performed in the second round and are presented in Chapters 12 and 13. Twenty-four dynamic component tests (test nos. HTTB-17 through HTTB-40) were performed in the third round, which are discussed later in Chapters 14 and 15. Each individual concept was tested twice in its vertical orientation and twice in its lateral orientation in order to determine the structural capacities and cable release behaviors. For the sake of convenience, the consolidated drawing sets for all three rounds of dynamic component testing on tabbed brackets is shown in Figures 164 through 203, as provided in Chapter 11. The test matrix and results for the second round of tests on the bolted tabbed brackets are summarized in Table 11.

Table 11. Summary of Dynamic Component Testing on Bolted Tabbed Brackets, Round 2

Test No.	Load Direction	Tabbed Bracket	Gauge	Post Section	Expected Strength, kips (kN)	Release Load, kips (kN)	Test Result
HTTB-9	Vertical	Version 3, Bolted, c1	11	S3x5.7 (S76x8.5) Section, V3, c2	0.22 (1.0)	NA	No load cell data, heads scraped along the inside of the flange before the head released through the keyway
HTTB-9R	Vertical	Version 3, Bolted, c1	11	S3x5.7 (S76x8.5) Section, V3, c2	0.22 (1.0)	0.79 (3.5)	Tabs scraped along the inside of the flange before the head released through the keyway, snag load = 0.53 kips (2.4 kN)
HTTB-10	Vertical	Version 3, Bolted, c1	11	S3x5.7 (S76x8.5) Section, V3, c2	0.22 (1.0)	0.76 (3.4)	Tabs scraped along the inside of the flange before the head released through the keyway, snag load = 0.46 kips (2.1 kN)
HTTB-11	Lateral	Version 3, Bolted, c1	11	S3x5.7 (S76x8.5) Section, V3, c2	6.28 (27.9)	5.14 (22.9)	Fracture through the neck (Failure Location 2)
HTTB-12	Lateral	Version 3, Bolted, c1	11	S3x5.7 (S76x8.5) Section, V3, c2	6.28 (27.9)	2.38 (10.6)	No high-speed video, Tabs caught in narrow part of keyway initially, but slipped out, no fracture
HTTB-12R	Lateral	Version 3, Bolted, c1	11	S3x5.7 (S76x8.5) Section, V3, c2	6.28 (27.9)	5.21 (23.2)	Fracture through the neck (Failure Location 2)
HTTB-13	Vertical	Version 4, Bolted, d1	10	S3x5.7 (S76x8.5) Section, V4, d2	0.22 (1.0)	0.90 (4.0)	Tabs scraped along the inside of the flange before the head released through the keyway, snag load = 0.52 kips (2.3 kN)

Table 11. Summary of Dynamic Component Testing on Bolted Tabbed Brackets, Round 2 (Continued)

Test No.	Load Direction	Tabbed Bracket	Gauge	Post Section	Expected Strength, kips (kN)	Release Load, kips (kN)	Test Result
HTTB-14	Vertical	Version 4, Bolted, d1	10	S3x5.7 (S76x8.5) Section, V4, d2	0.22 (1.0)	0.99 (4.4)	No high-speed video, tabs scraped along the inside of the flange before the head released through the keyway, snag load = 0.63 kips (2.8 kN)
HTTB-15	Lateral	Version 4, Bolted, d1	10	S3x5.7 (S76x8.5) Section, V4, d2	5.88 (26.2)	4.45 (19.8)	Fracture through the neck (Failure Location 2)
HTTB-16	Lateral	Version 4, Bolted, d1	10	S3x5.7 (S76x8.5) Section, V4, d2	5.88 (26.2)	4.69 (20.9)	Fracture through the neck (Failure Location 2)

13.1.1 Test No. HTTB-9 (TB V3, Bolted, Vertical)

For test no. HTTB-9, the cable pulled on the 11-gauge, grade 50 steel, bolted tabbed bracket Version 3 at an angle of 0 degrees, parallel to the front face of the flange, thus imparting a vertical load. The post consisted of a 5-in. (127-mm) long, steel S3x5.7 (S76x8.5) section. The top end of the tabbed bracket rested in the narrow part of the keyway, while the bottom end was secured to the flange with a 5/16-in. (8-mm), grade 5, hex cap screw and nut. The bracket began to bend upward as the cable began to pull on it. As it moved upward, the head scraped against the backside surface of the front flange until it cleared the narrow part of the keyway. After the head cleared the narrow part of the keyway, the top end was able to rotate out, thus releasing the cable. Due to technical difficulties, no force-time data was recorded, but the high-speed video proved to be very useful. Pre- and post-test photographs are shown in Figure 238. Sequential photographs are shown in Figure 239.

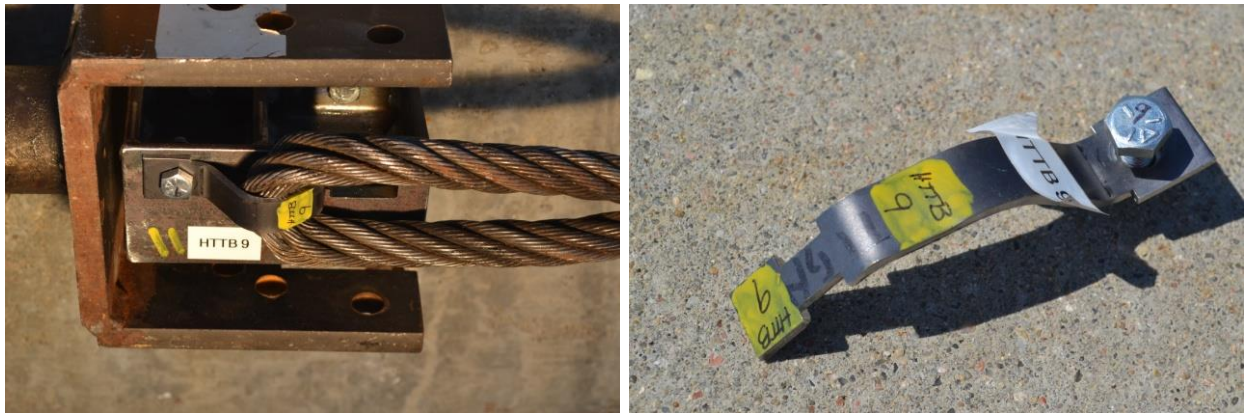
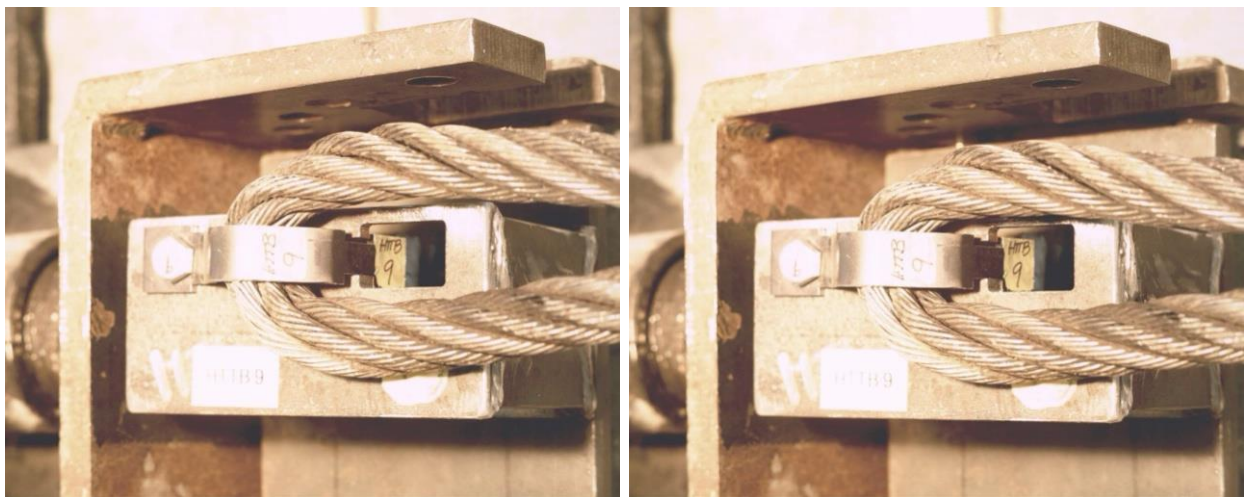
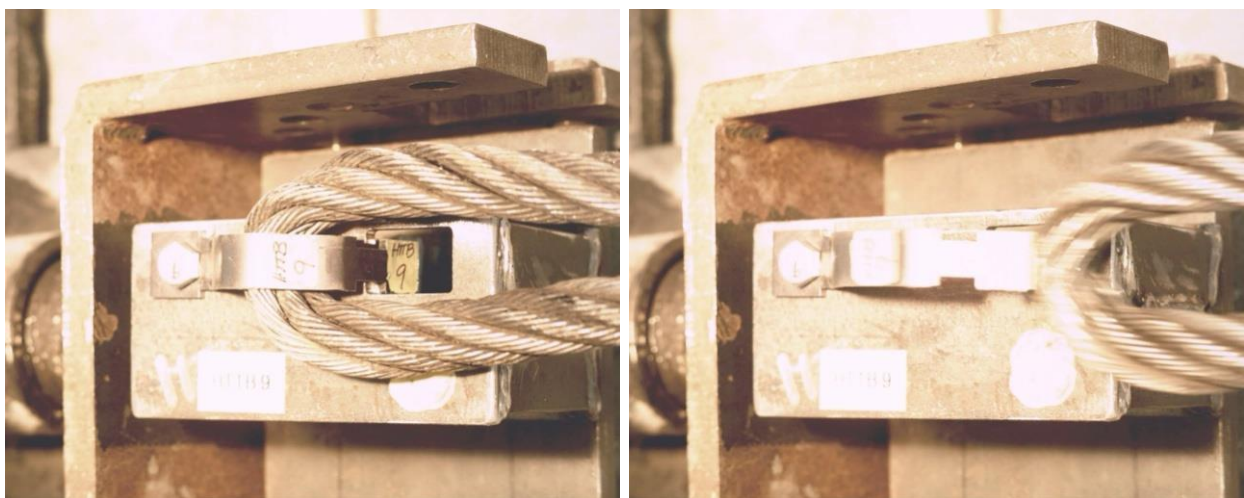


Figure 238. Pre-Test and Post-Test Photographs, Test No. HTTPB-9



Time = 0 sec

Time = 0.134 sec



Time = 0.168 sec

Time = 0.200 sec, Release

Figure 239. Sequential Photographs, Test No. HTTPB-9

13.1.2 Test No. HTTB-9R (TB V3, Bolted, Vertical)

Since no force-time data was collected for test no. HTTB-9, test no. HTTB-9R was performed as a replacement test. For the repeated test, the cable pulled on the 11-gauge, grade 50 steel, bolted tabbed bracket Version 3 at an angle of 0 degrees, parallel to the front face of the flange, thus imparting a vertical load. The post consisted of a 5-in. (127-mm) long, steel S3x5.7 (S76x8.5) section. The top end of the tabbed bracket rested in the keyway, while the bottom end was secured to the flange with a 5/16-in. (8-mm), grade 5, hex cap screw and nut. The bracket began to bend upward as the cable began to pull on it. As it moved upward, the head scraped against the backside surface of the front flange until it cleared the narrow part of the keyway. After the head cleared the narrow part of the keyway, the top end was able to rotate out. A peak force of 790 lb (3.51 kN) occurred as the head scraped against the backside surface of the keyway, just before slipping out. After the head cleared the keyway, the cable was briefly snagged on the head, exerting a snag load of 528 lb (2.35 kN). The force versus time plot is shown in Figure 240. Pre- and post-test photographs are shown in Figure 241. Sequential photographs are shown in Figure 242.

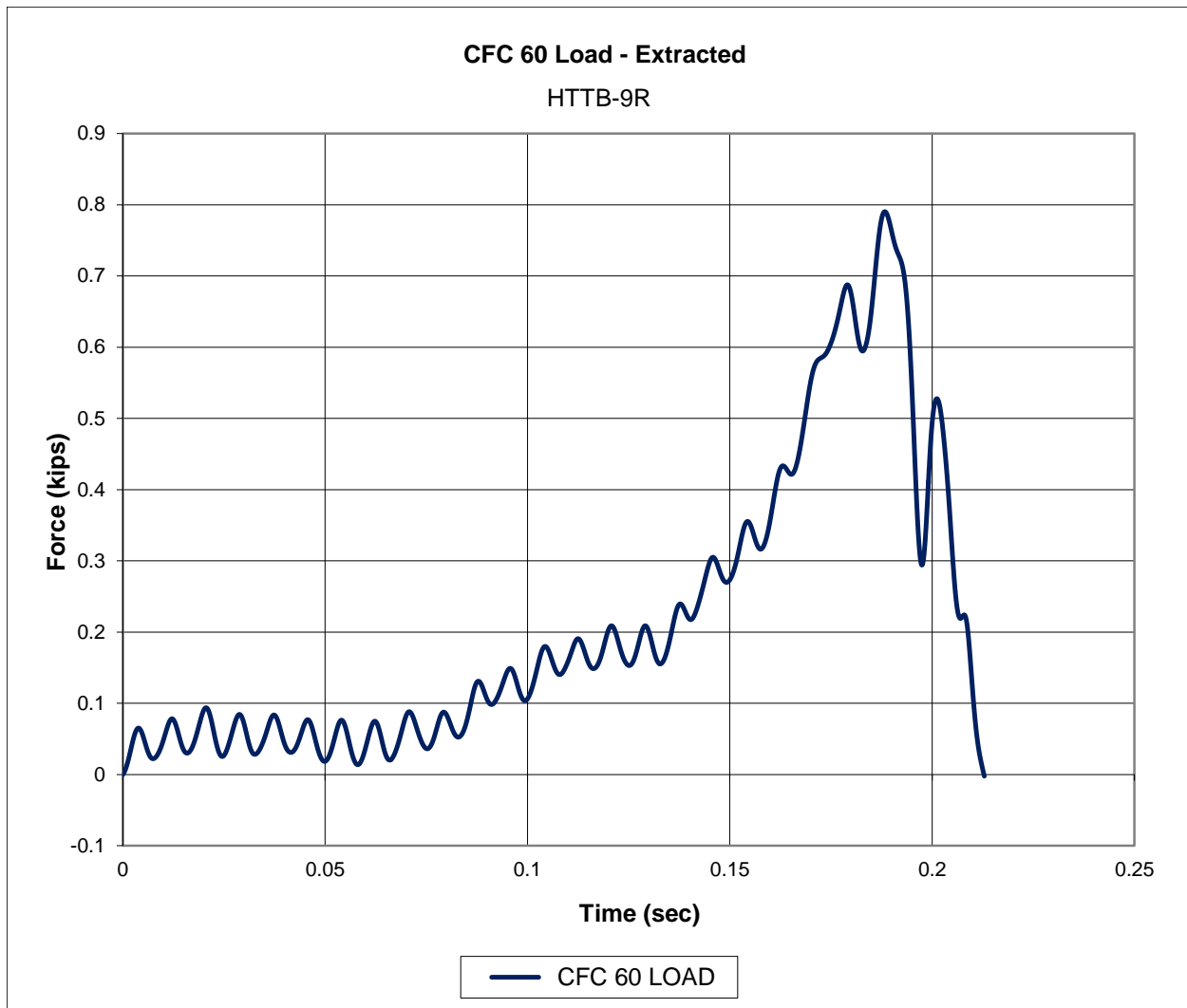


Figure 240. Force-Time Data, Test No. HTTB-9R

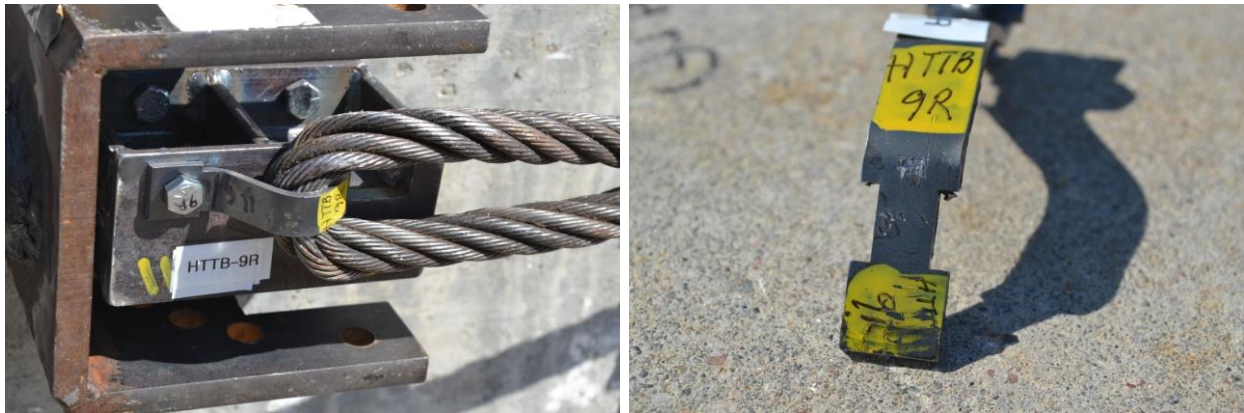


Figure 241. Pre-Test and Post-Test Photographs, Test No. HTTB-9R



Time = 0 sec

Time = 0.182 sec



Time = 0.198 sec

Time = 0.212 sec, Release

Figure 242. Sequential Photographs, Test No. HTTB-9R

13.1.3 Test No. HTTB-10 (TB V3, Bolted, Vertical)

For test no. HTTB-10, the cable pulled on the 11-gauge, grade 50 steel, bolted tabbed bracket Version 3 at an angle of 0 degrees, parallel to the front face of the flange, thus imparting a vertical load. The post consisted of a 5-in. (127-mm) long, steel S3x5.7 (S76x8.5) section. The top end of the tabbed bracket rested in the keyway, while the bottom end was secured to the flange with a 5/16-in. (8-mm), grade 5, hex cap screw and nut. The bracket began to bend upward as the cable began to pull on it. As it moved upward, the head scraped against the backside surface of the front flange until it cleared the narrow part of the keyway. After the head cleared the narrow part of the keyway, the top end was able to rotate out. A peak force of 760 lb (3.38 kN) occurred as the head scraped against the backside surface of the keyway, just before slipping out. After the head cleared the keyway, the cable was briefly snagged on the head, exerting a snag load of 462 lb (2.06 kN). The force versus time plot is shown in Figure 243. Pre- and post-test photographs are shown in Figure 244. Sequential photographs are shown in Figure 245.

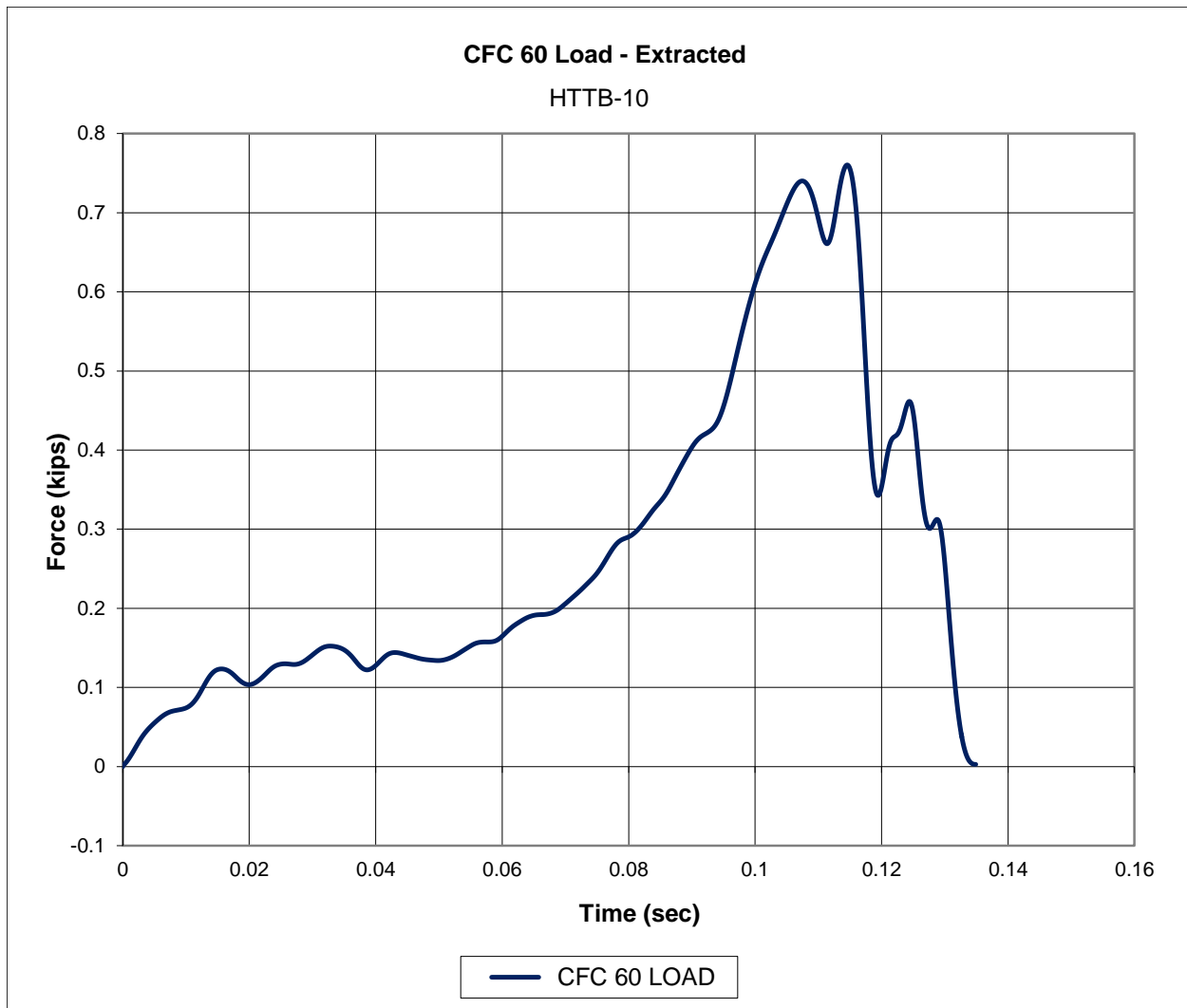


Figure 243. Force-Time Data, Test No. HTTB-10



Figure 244. Pre-Test and Post-Test Photographs, Test No. HTTPB-10



Time = 0 sec

Time = 0.116 sec



Time = 0.122 sec

Time = 0.134 sec, Release

Figure 245. Sequential Photographs, Test No. HTTPB-10

13.1.4 Test No. HTTB-11 (TB V3, Bolted, Lateral)

For test no. HTTB-11, the cable pulled on the 11-gauge, grade 50 steel, bolted tabbed bracket Version 3 at an angle of 90 degrees, perpendicular to the front face of the flange, thus imparting a lateral load. The post consisted of a 5-in. (127-mm) long, steel S3x5.7 (S76x8.5) section. The top end of the tabbed bracket rested in the keyway, while the bottom end was secured to the flange with a 5/16-in. (8-mm), grade 5, hex cap screw and nut. As the cable began to pull on the bracket, the head became caught in the narrow part of the keyway. The cable continued to pull until the bracket fractured through the neck (failure location 2). A peak force of 5.14 kips (22.9 kN) occurred as the head was pulled against the inside of the keyway, just before fracture. The force versus time plot is shown in Figure 246. Pre- and post-test photographs are shown in Figure 247. Sequential photographs are shown in Figure 248.

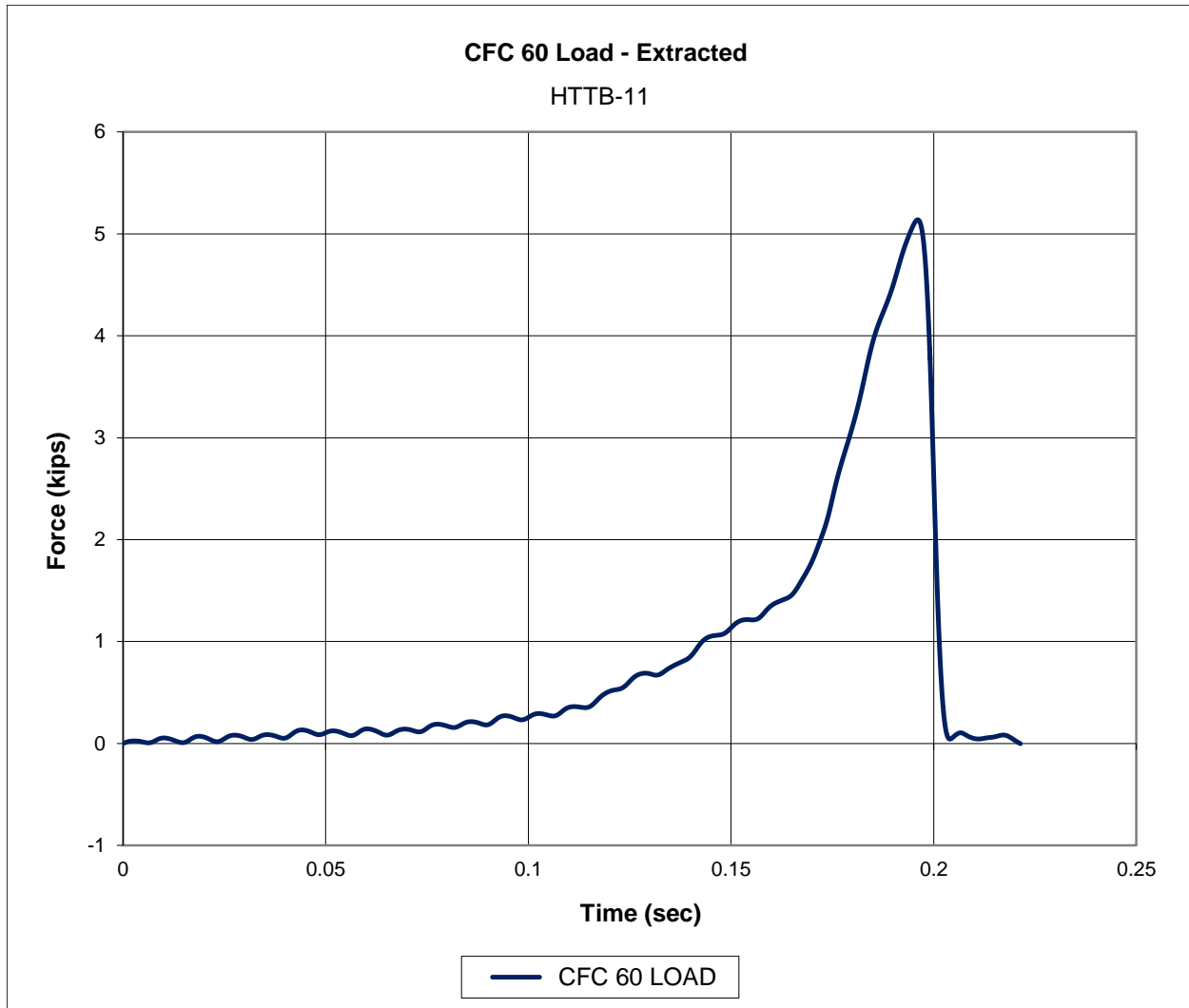
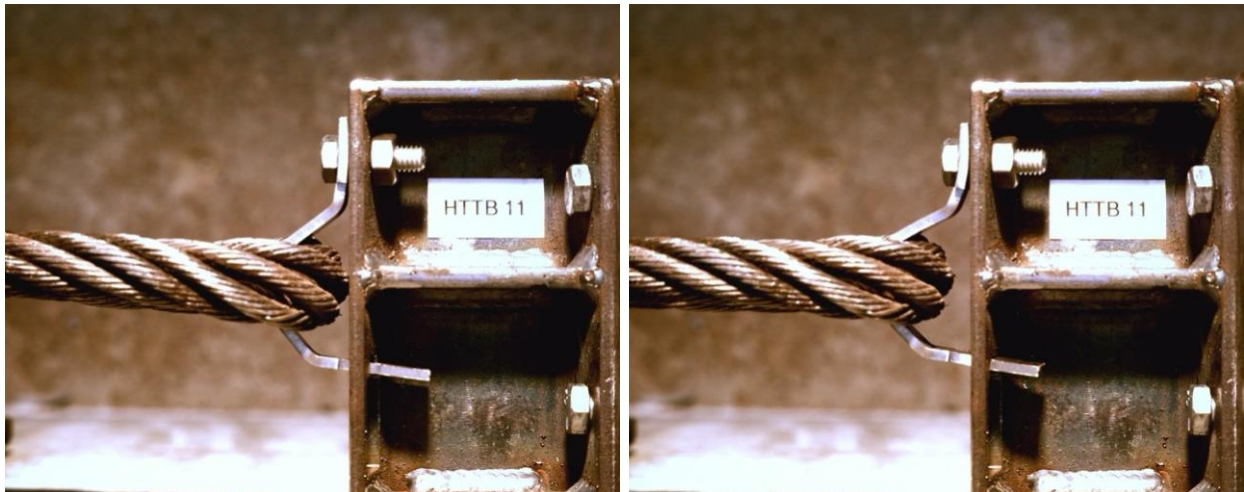


Figure 246. Force-Time Data, Test No. HTTB-11

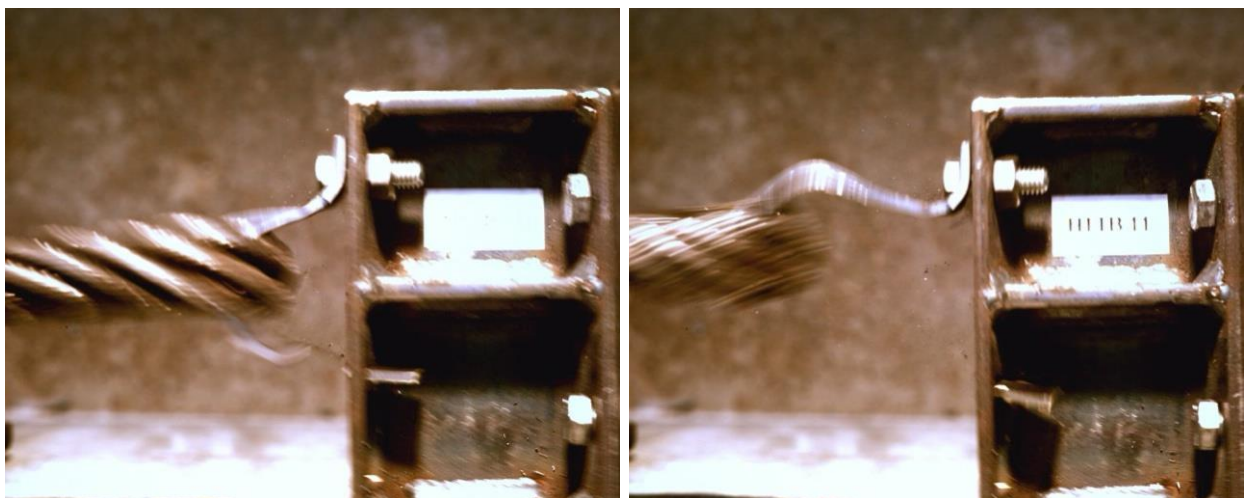


Figure 247. Pre-Test and Post-Test Photographs, Test No. HTTB-11



Time = 0 sec

Time = 0.190 sec



Time = 0.216 sec

Time = 0.220 sec, Release

Figure 248. Sequential Photographs, Test No. HTTB-11

13.1.5 Test No. HTTB-12 (TB V3, Bolted, Lateral)

For test no. HTTB-12, the cable pulled on the 11-gauge, grade 50 steel, bolted tabbed bracket Version 3 at an angle of 90 degrees, perpendicular to the front face of the flange, thus imparting a lateral load. The post consisted of a 5-in. (127-mm) long, steel S3x5.7 (S76x8.5) section. The top end of the tabbed bracket rested in the keyway, while the bottom end was secured to the flange with a 5/16-in. (8-mm), grade 5, hex cap screw and nut. As the cable began to pull on the bracket, the head became caught in the narrow part of the keyway. As the cable continued to pull on the bracket, the head began to slip out of the keyway until it was eventually free. No fracture had occurred. A peak force of 2.38 kips (10.6 kN) occurred as the head was pulled against the inside of the keyway, before slipping out. There was no high-speed video for this test, but the standard-speed video was useful nonetheless. The force versus time plot is shown in Figure 249. Pre- and post-test photographs are shown in Figure 250. Sequential photographs are shown in Figure 251.

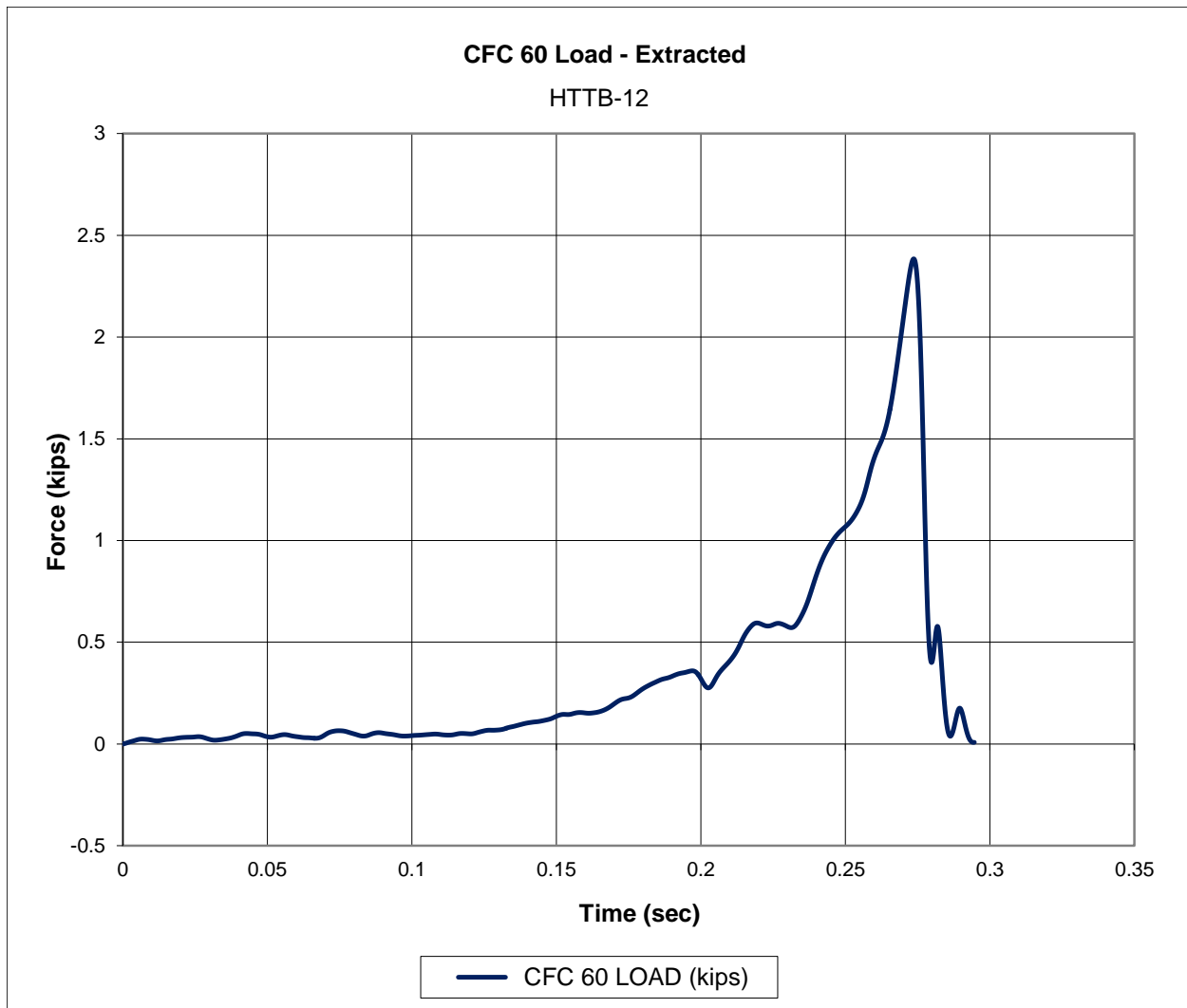


Figure 249. Force-Time Data, Test No. HTTB-12



Figure 250. Pre-Test and Post-Test Photographs, Test No. HTTB-12

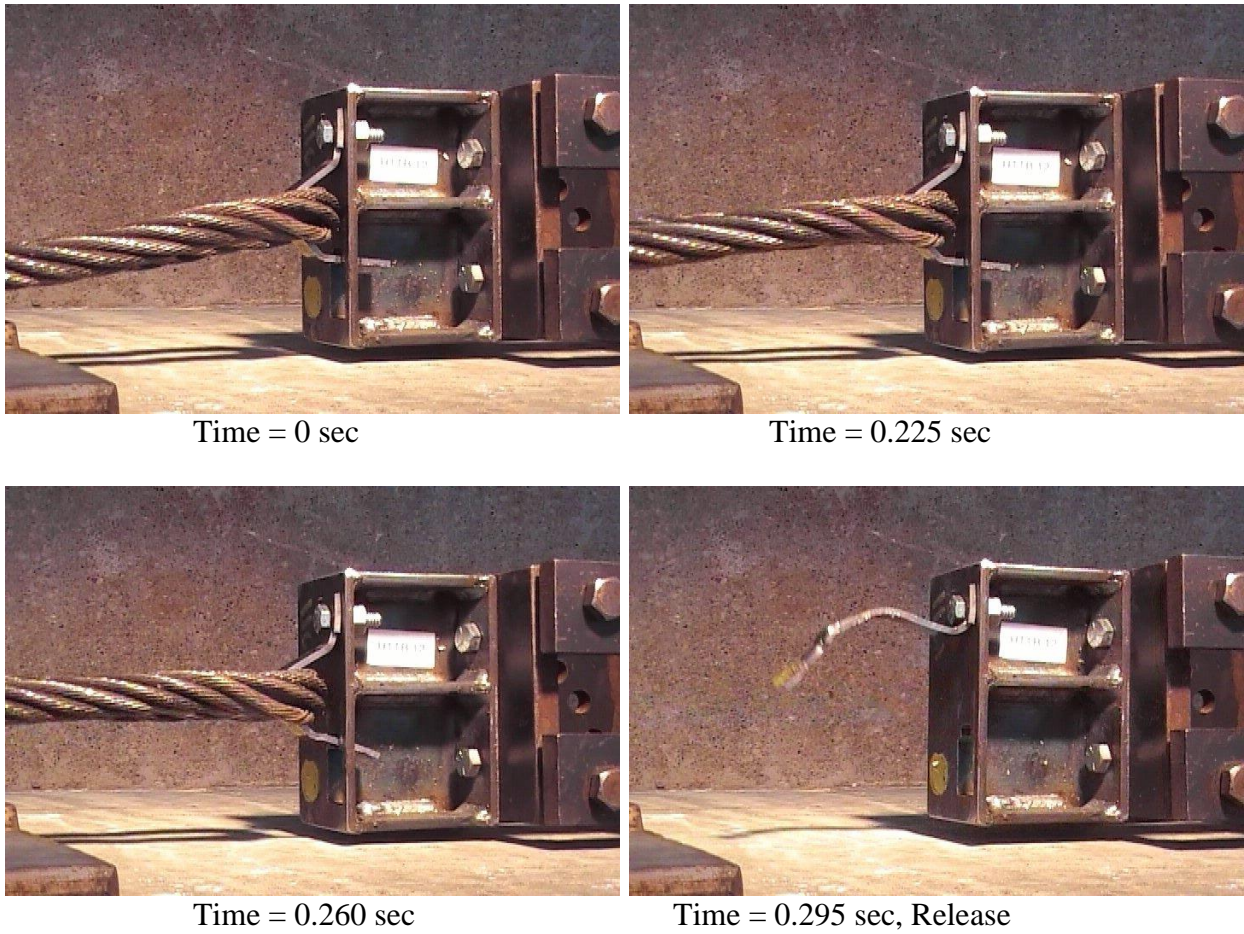


Figure 251. Sequential Photographs, Test No. HTTB-12

13.1.6 Test No. HTTB-12R (TB V3, Bolted, Lateral)

For test no. HTTB-12R, the cable pulled on the 11-gauge, grade 50 steel, bolted tabbed bracket Version 3 at an angle of 90 degrees, perpendicular to the front face of the flange, thus imparting a lateral load. The post consisted of a 5-in. (127-mm) long, steel S3x5.7 (S76x8.5) section. The previous test (test no. HTTB-12) exposed a fabrication flaw in the tabbed bracket. When installed, the top end of the bracket did not rest against the bottom of the slot, but it was angled slightly upward. Because of this slight upward angle, there was less contact area between the tabs and the inside of the keyway. Thus, the head slipped out of the keyway in test no. HTTB-12, rather than becoming caught in the keyway when pulled laterally. For this reason, the bracket was bent slightly to correct the flaw, as shown in Figure 252. The top end of the tabbed bracket rested in the keyway, while the bottom end was secured to the flange with a 5/16-in. (8-mm), grade 5, hex cap screw and nut. As the cable began to pull on the bracket, the head became caught in the narrow part of the keyway. The cable continued to pull until the bracket fractured through the neck (failure location 2). A peak force of 5.21 kips (23.2 kN) occurred as the head was pulled against the inside of the keyway, just before fracture. The force versus time plot is shown in Figure 253. Pre- and post-test photographs are shown in Figure 254. Sequential photographs are shown in Figure 255.

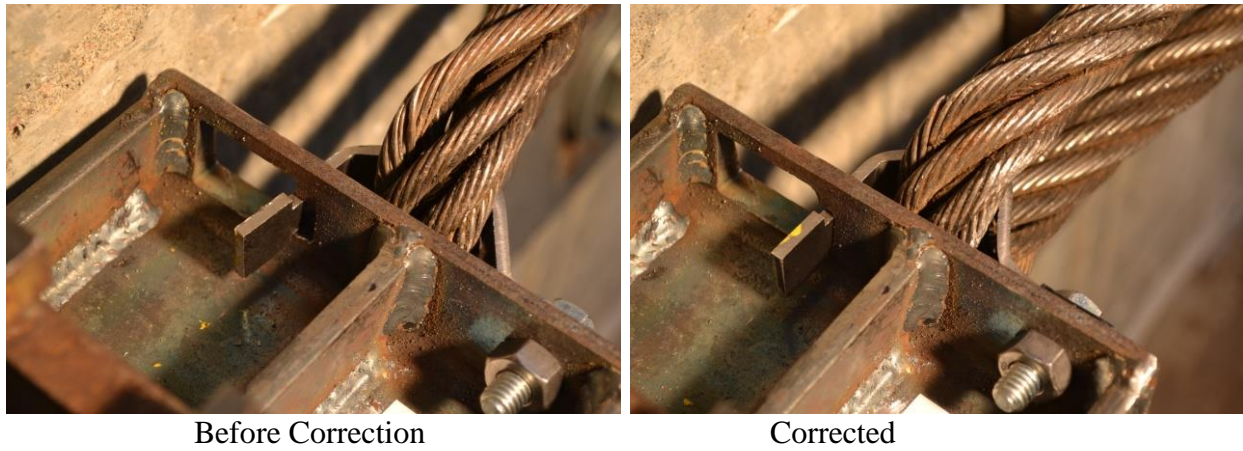


Figure 252. Correction of a Fabrication Flaw

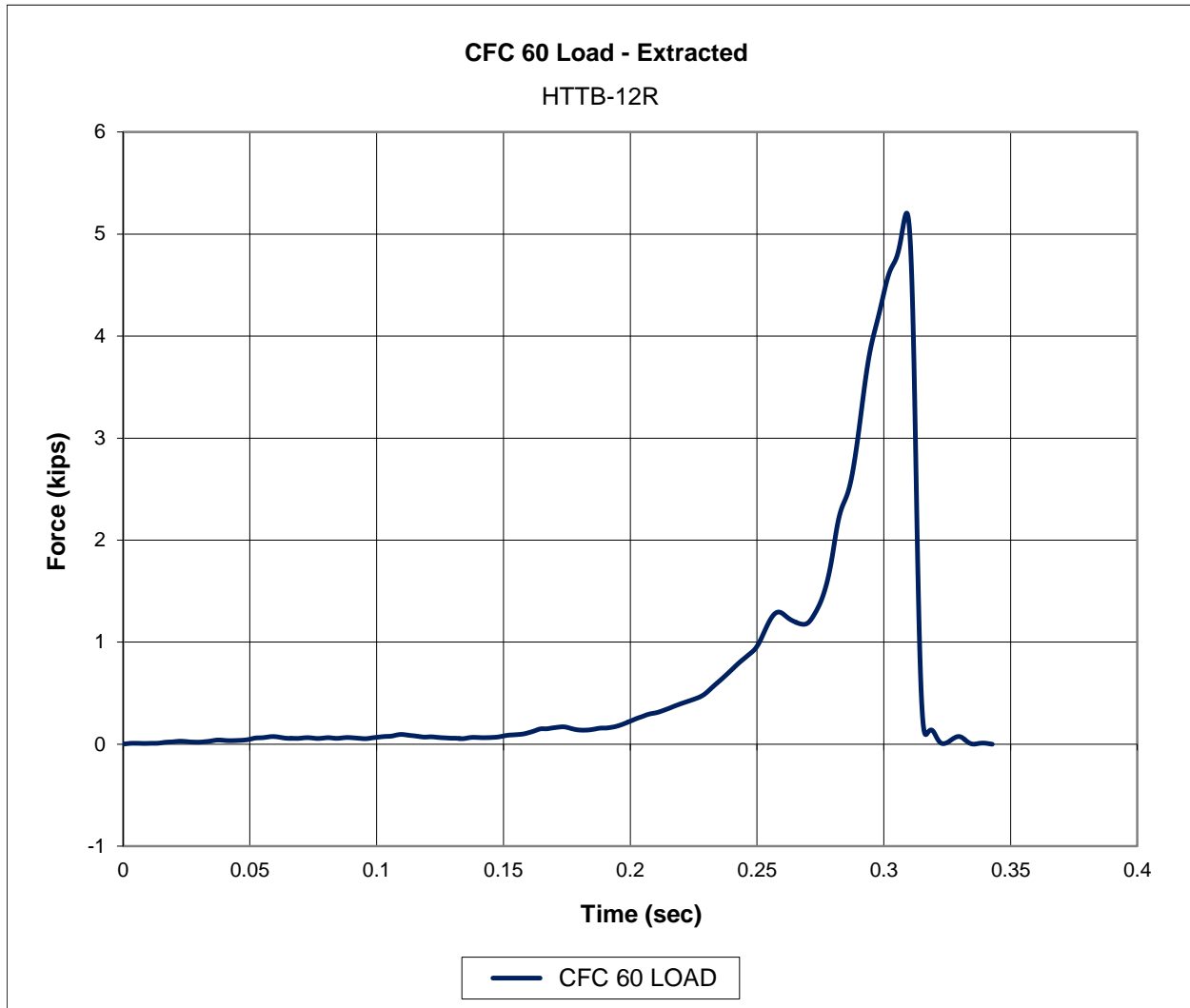


Figure 253. Force-Time Data, Test No. HTTB-12R



Figure 254. Pre-Test and Post-Test Photographs, Test No. HTTB-12R

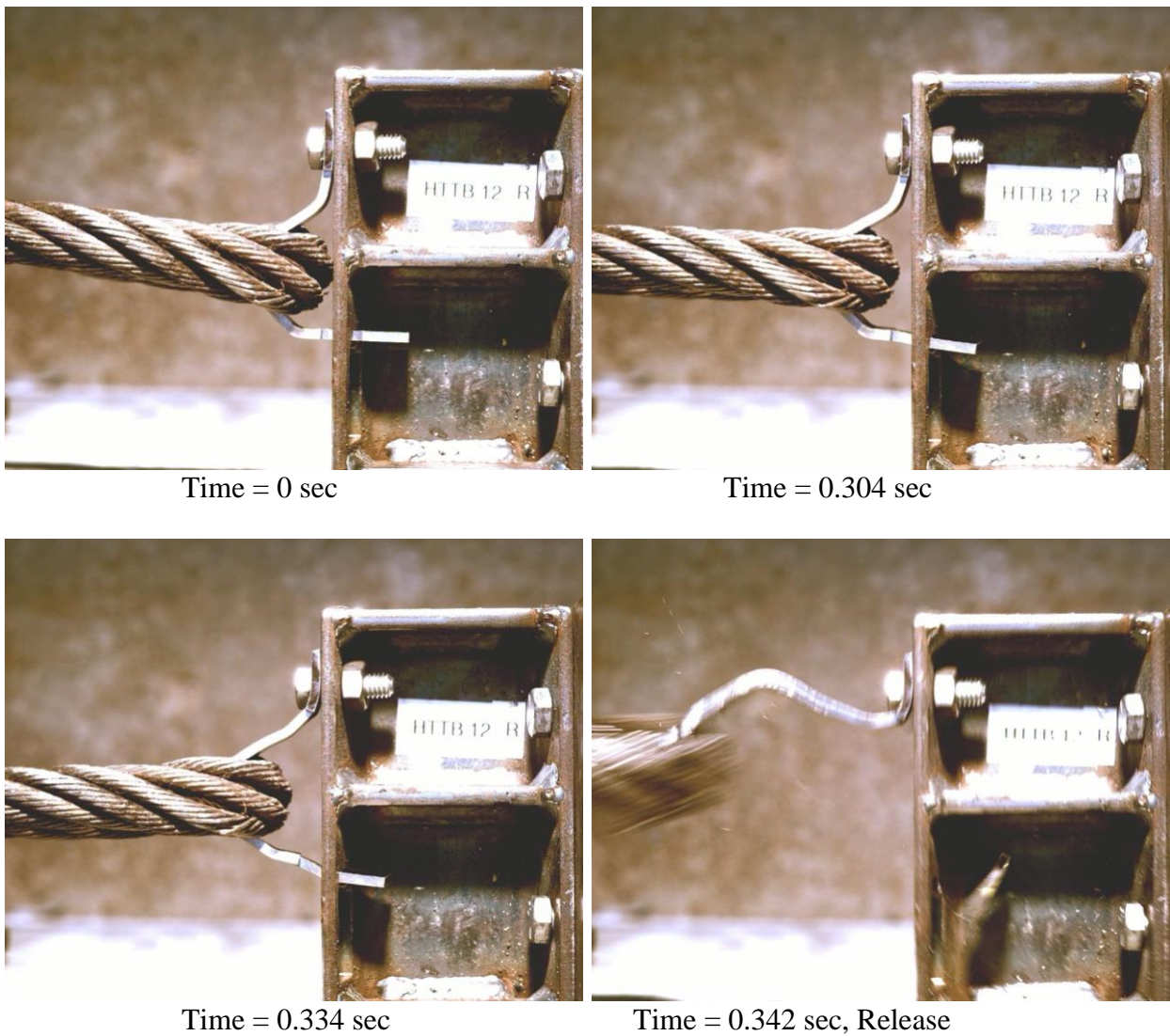


Figure 255. Sequential Photographs, Test No. HTTB-12R

13.1.7 Test No. HTTB-13 (TB V4, Bolted, Vertical)

For test no. HTTB-13, the cable pulled on the 10-gauge, grade 50 steel, bolted tabbed bracket Version 4 at an angle of 0 degrees, parallel to the front face of the flange, thus imparting a vertical load. The post consisted of a 5-in. (127-mm) long, steel S3x5.7 (S76x8.5) section. The bracket had to be bent in order to correct the fabrication flaw discovered in test no. HTTB-12. The top end of the tabbed bracket rested in the keyway, while the bottom end was secured to the flange with a 5/16-in. (8-mm), grade 5, hex cap screw and nut. The bracket began to bend upward as the cable began to pull on it. As it moved upward, the head scraped against the backside surface of the front flange until it cleared the narrow part of the keyway. After the head cleared the narrow part of the keyway, the top end was able to rotate out. A peak force of 899 lb (4.00 kN) occurred as the head scraped against the backside surface of the keyway, just before slipping out. After the head cleared the keyway, the cable was briefly snagged on the head, exerting a snag load of 515 lb (2.29 kN). The force versus time plot is shown in Figure 256. Pre- and post-test photographs are shown in Figure 257. Sequential photographs are shown in Figure 258.

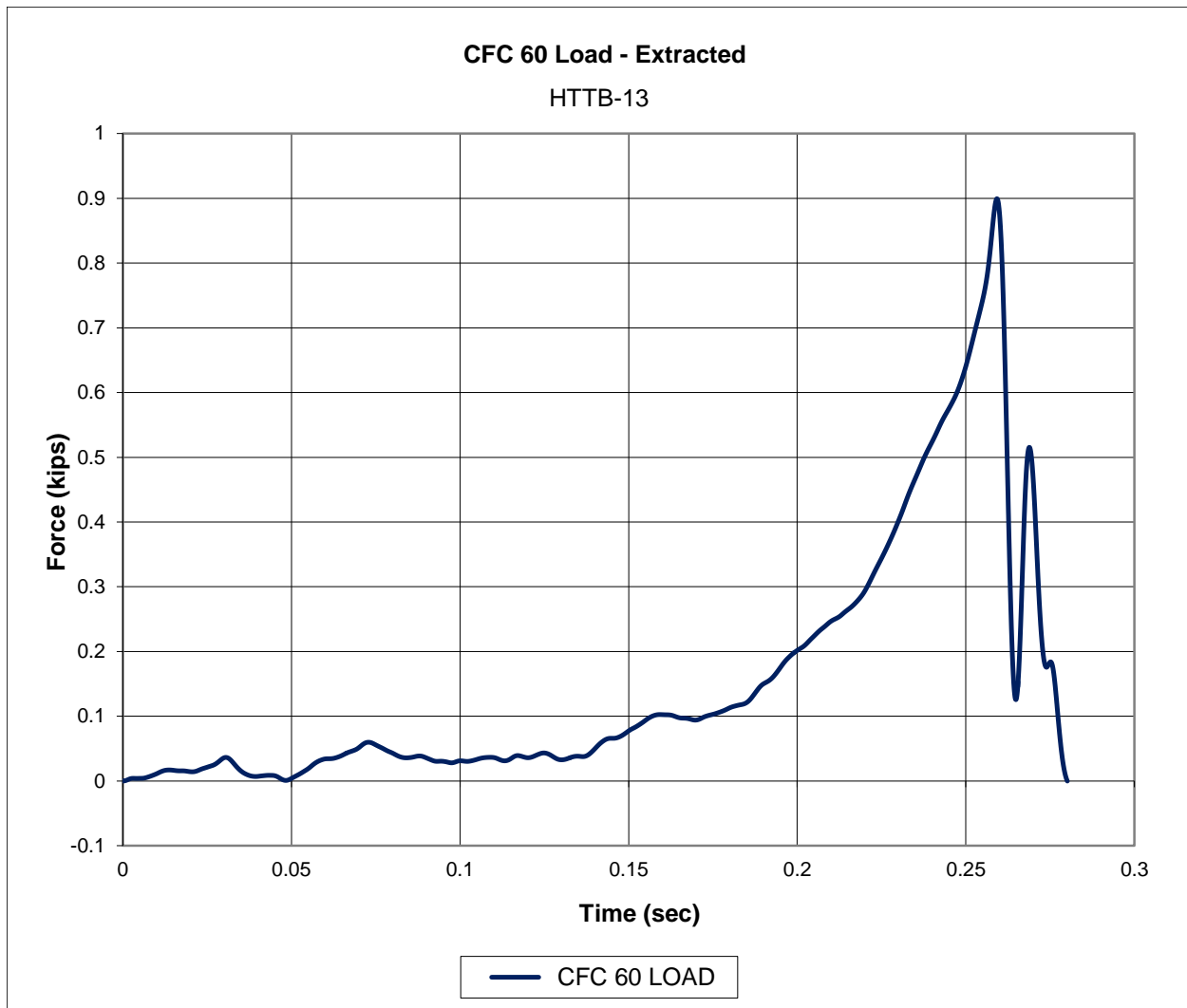
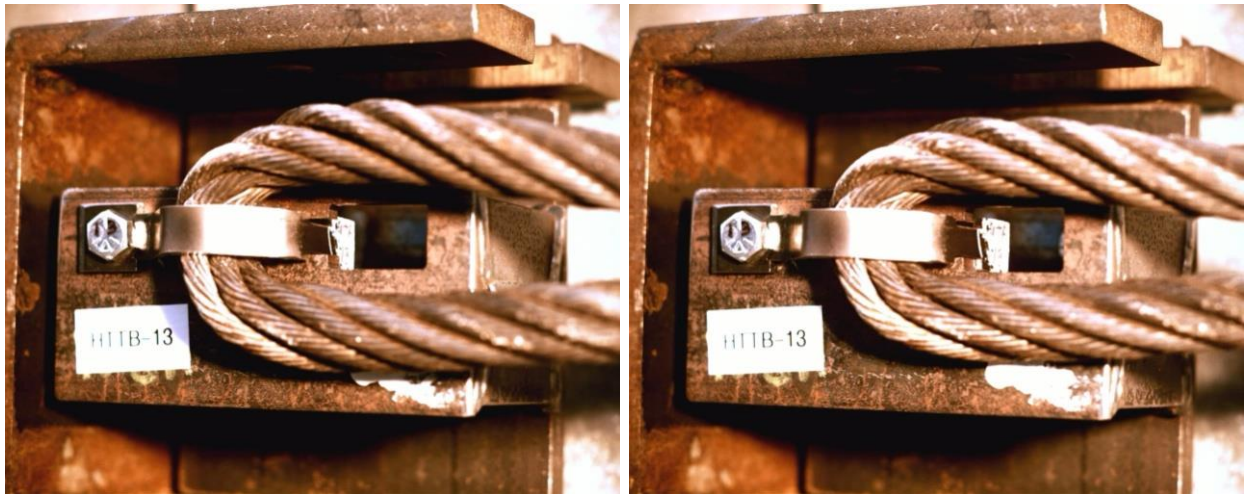


Figure 256. Force-Time Data, Test No. HTTB-13

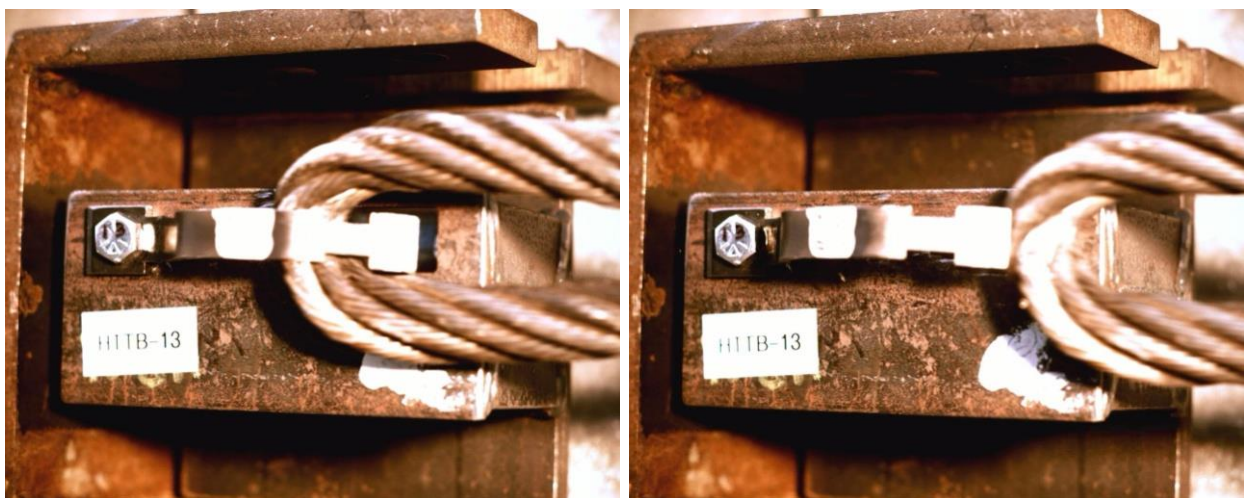


Figure 257. Pre-Test and Post-Test Photographs, Test No. HTTPB-13



Time = 0 sec

Time = 0.258 sec



Time = 0.270 sec

Time = 0.280 sec, Release

Figure 258. Sequential Photographs, Test No. HTTPB-13

13.1.8 Test No. HTTB-14 (TB V4, Bolted, Vertical)

For test no. HTTB-14, the cable pulled on the 10-gauge, grade 50 steel, bolted tabbed bracket Version 4 at an angle of 0 degrees, parallel to the front face of the flange, thus imparting a vertical load. The post consisted of a 5-in. (127-mm) long, steel S3x5.7 (S76x8.5) section. The bracket had to be bent in order to correct the fabrication flaw discovered in test no. HTTB-12. The top end of the tabbed bracket rested in the keyway, while the bottom end was secured to the flange with a 5/16-in. (8-mm), grade 5, hex cap screw and nut. The bracket began to bend upward as the cable began to pull on it. As it moved upward, the head scraped against the backside surface of the front flange until it cleared the narrow part of the keyway. After the head cleared the narrow part of the keyway, the top end was able to rotate out. A peak force of 989 lb (4.40 kN) occurred as the head scraped against the backside surface of the keyway, just before slipping out. After the head cleared the keyway, the cable was briefly snagged on the head, exerting a snag load of 627 lb (2.79 kN). There was no high-speed video for this test, but the standard-speed video was useful nonetheless. The force versus time plot is shown in Figure 259. Pre- and post-test photographs are shown in Figure 260. Sequential photographs are shown in Figure 261.

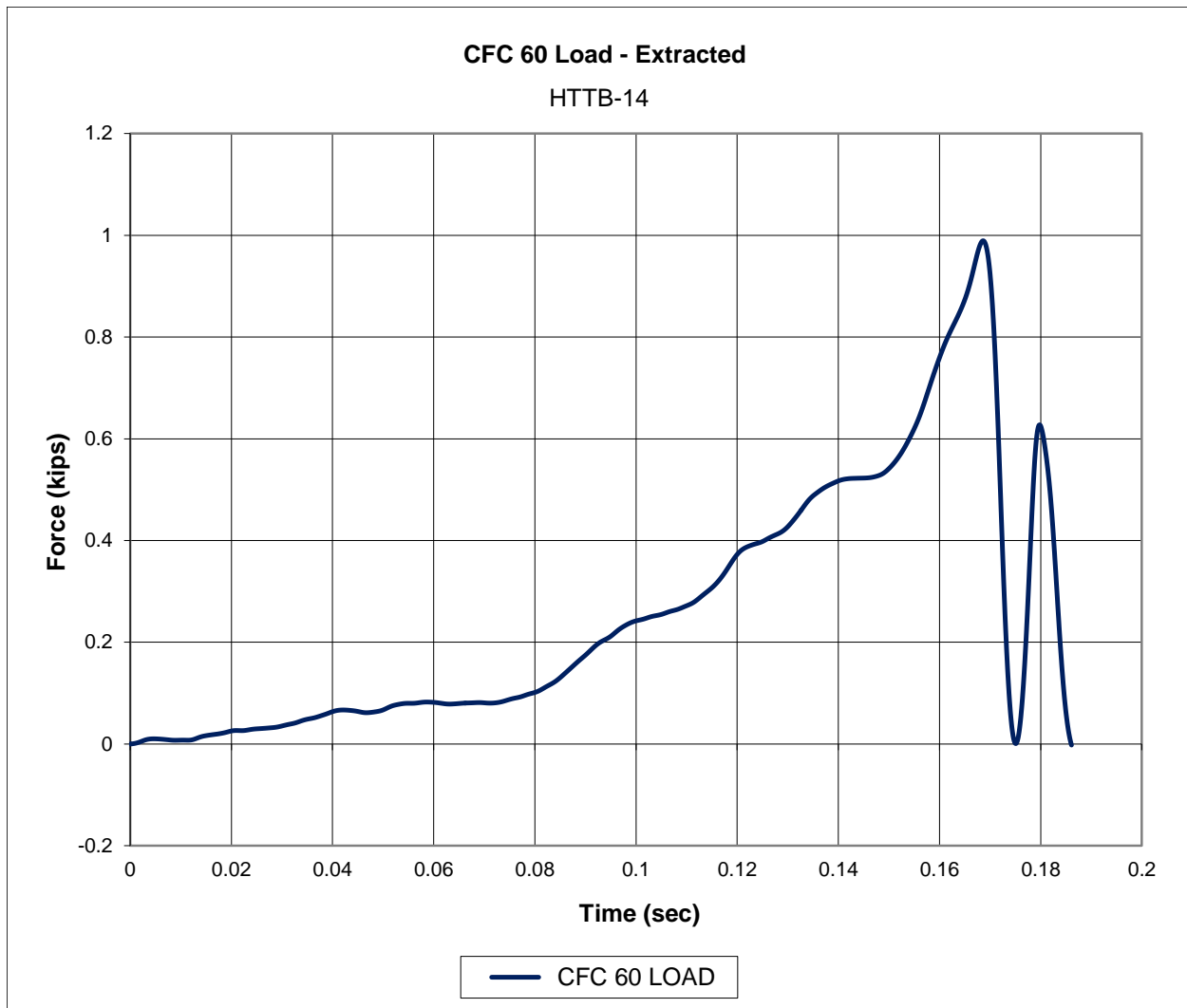


Figure 259. Force-Time Data, Test No. HTTB-14

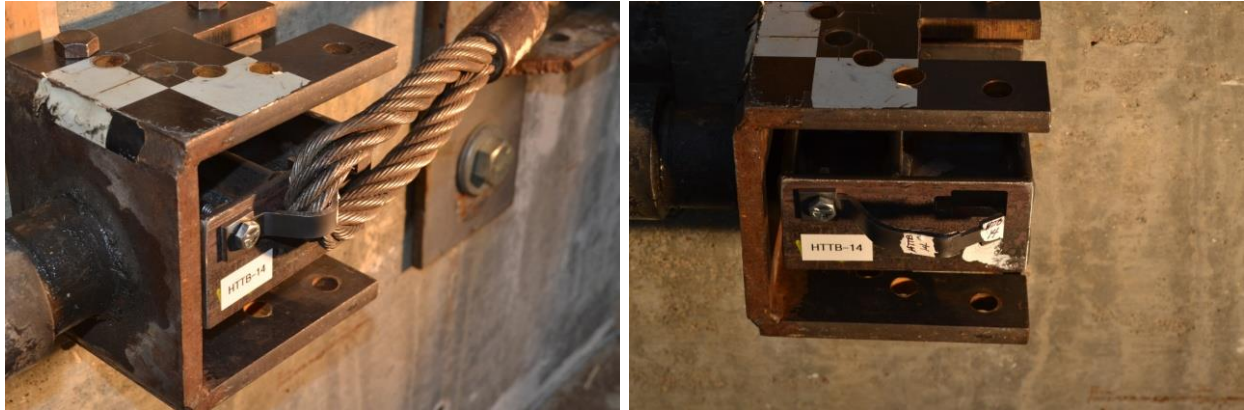


Figure 260. Pre-Test and Post-Test Photographs, Test No. HTTB-14

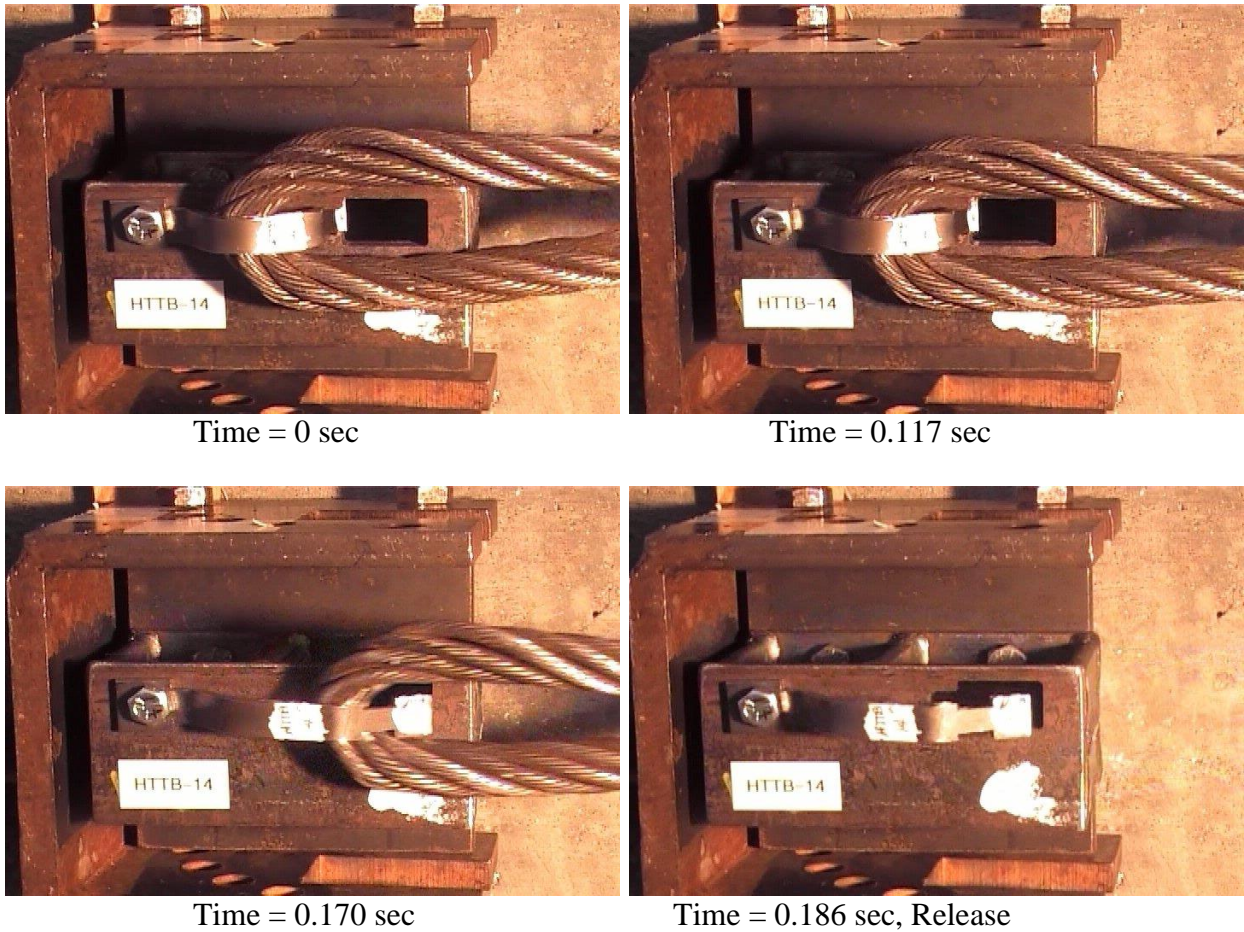


Figure 261. Sequential Photographs, Test No. HTTB-14

13.1.9 Test No. HTTB-15 (TB V4, Bolted, Lateral)

For test no. HTTB-15, the cable pulled on the 10-gauge, grade 50 steel, bolted tabbed bracket Version 4 at an angle of 90 degrees, perpendicular to the front face of the flange, thus imparting a lateral load. The post consisted of a 5-in. (127-mm) long, steel S3x5.7 (S76x8.5) section. The bracket had to be bent in order to correct the fabrication flaw discovered in test no. HTTB-12. The top end of the tabbed bracket rested in the keyway, while the bottom end was secured to the flange with a 5/16-in. (8-mm), grade 5, hex cap screw and nut. As the cable began to pull on the bracket, the head became caught in the narrow part of the keyway. The cable continued to pull until the bracket fractured through the neck (failure location 2). A peak load of 4.45 kips (19.8 kN) occurred as the head was pulled against the inside of the keyway, just before fracture. The force versus time plot is shown in Figure 262. Pre- and post-test photographs are shown in Figure 263. Sequential photographs are shown in Figure 264.

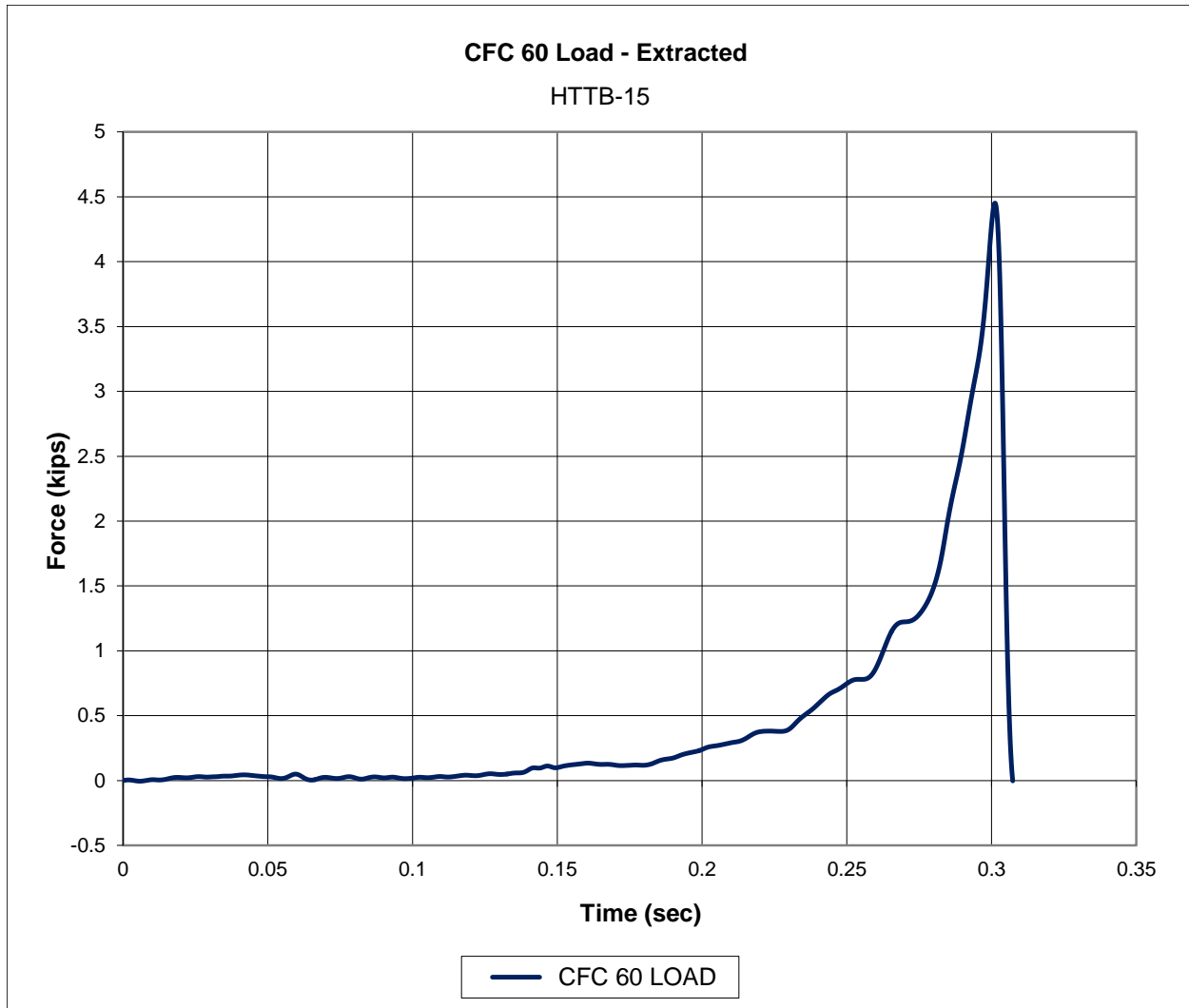


Figure 262. Force-Time Data, Test No. HTTB-15

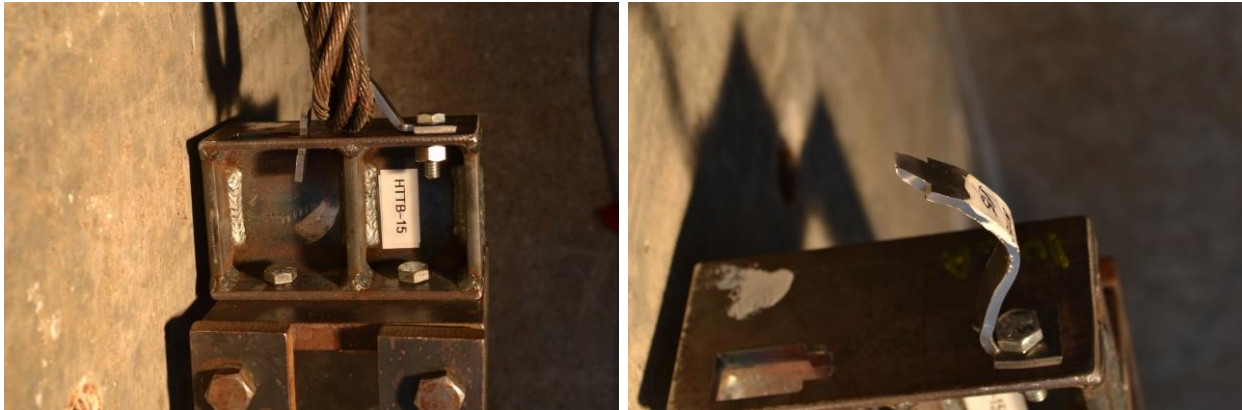


Figure 263. Pre-Test and Post-Test Photographs, Test No. HTTPB-15

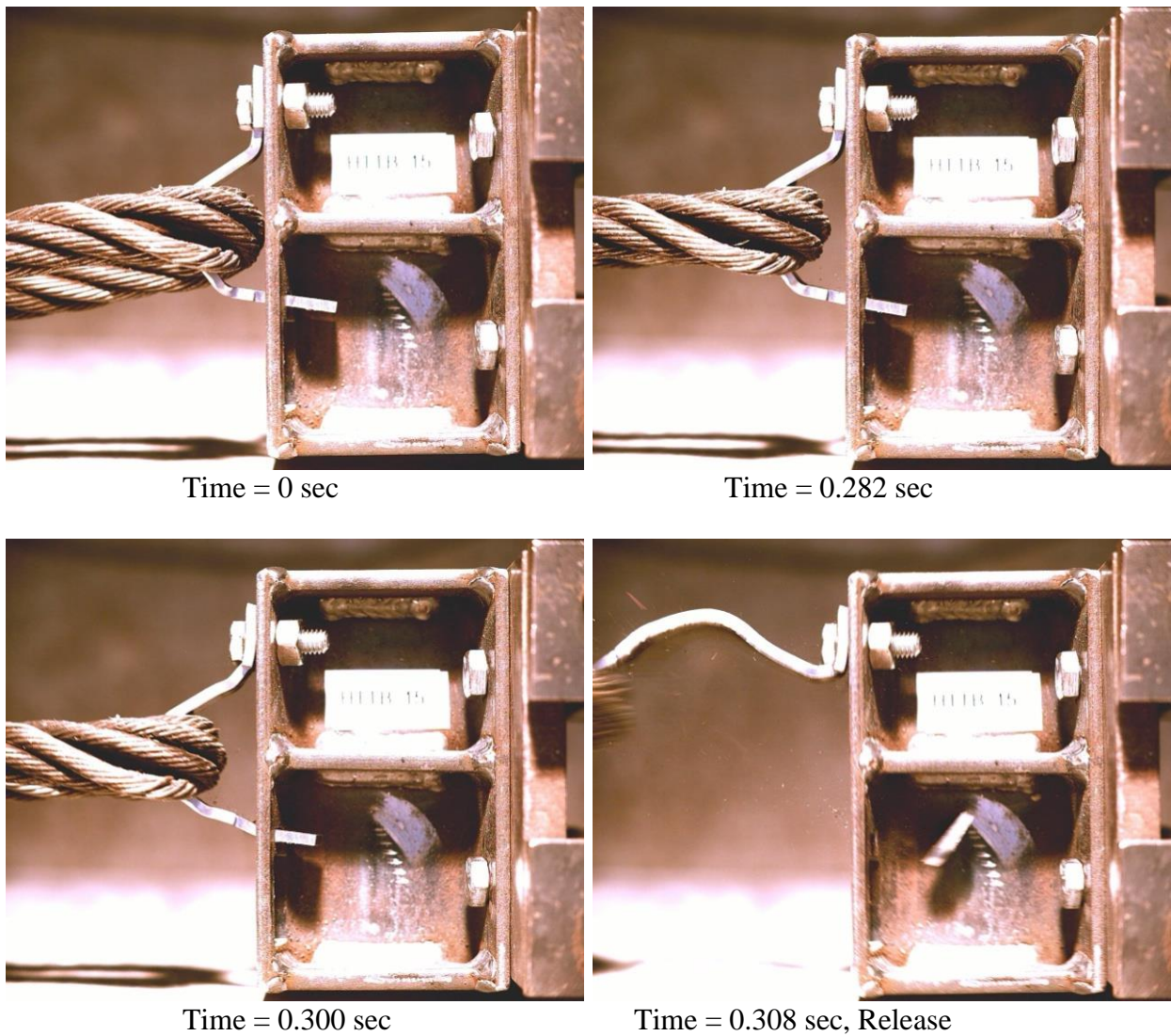


Figure 264. Sequential Photographs, Test No. HTTPB-15

13.1.10 Test No. HTTB-16 (TB V4, Bolted, Lateral)

For test no. HTTB-16, the cable pulled on the 10-gauge, grade 50 steel, bolted tabbed bracket Version 4 at an angle of 90 degrees, perpendicular to the front face of the flange, thus imparting a lateral load. The post consisted of a 5-in. (127-mm) long, steel S3x5.7 (S76x8.5) section. The bracket had to be bent in order to correct the fabrication flaw discovered in test no. HTTB-12. The top end of the tabbed bracket rested in the keyway, while the bottom end was secured to the flange with a 5/16-in. (8-mm), grade 5, hex cap screw and nut. As the cable began to pull on the bracket, the head became caught in the narrow part of the keyway. The cable continued to pull until the bracket fractured through the neck (failure location 2). A peak force of 4.69 kips (20.9 kN) occurred as the head was pulled against the inside of the keyway, just before fracture. The force versus time plot is shown in Figure 265. Pre- and post-test photographs are shown in Figure 266. Sequential photographs are shown in Figure 267.

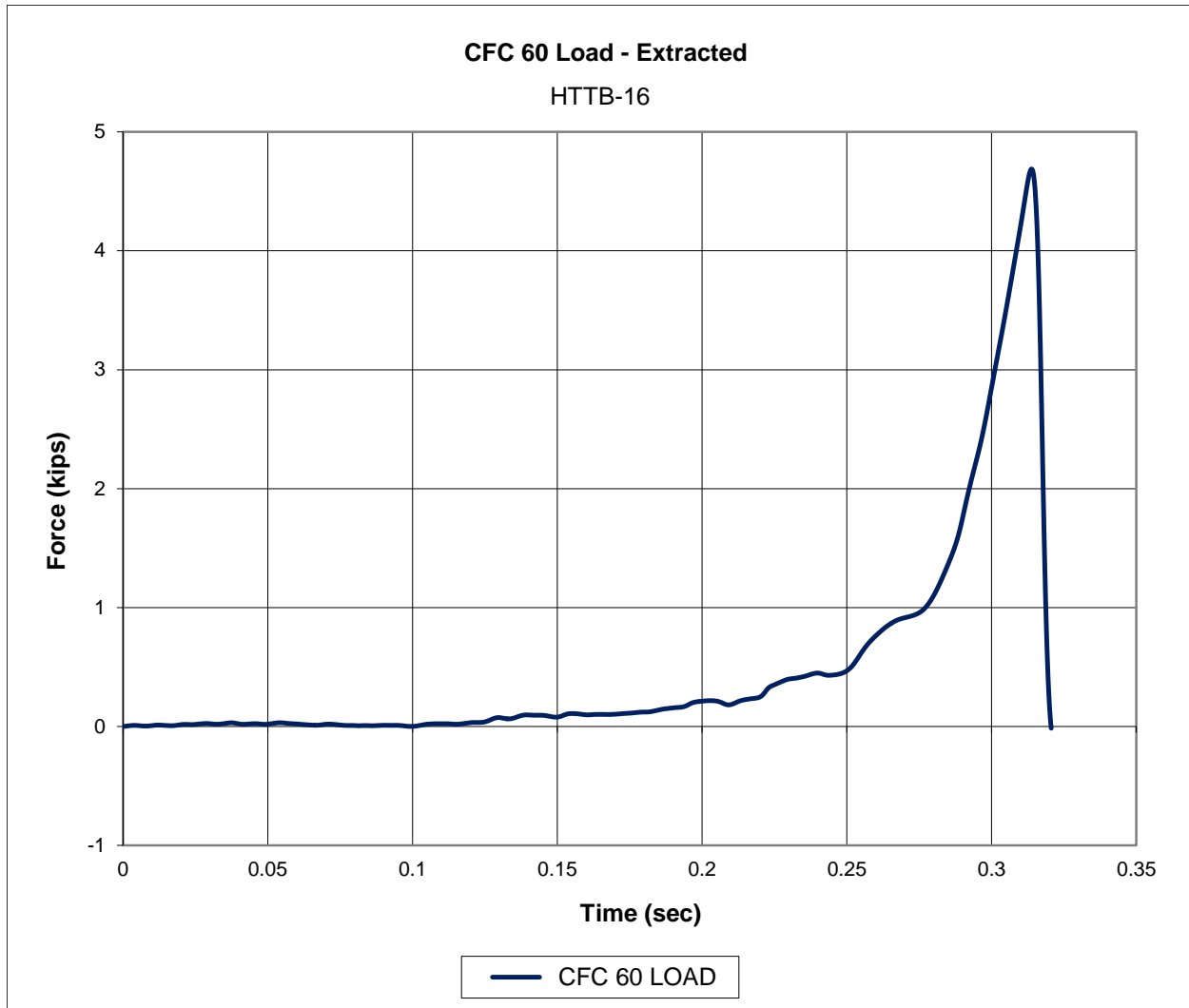


Figure 265. Force-Time Data, Test No. HTTB-16

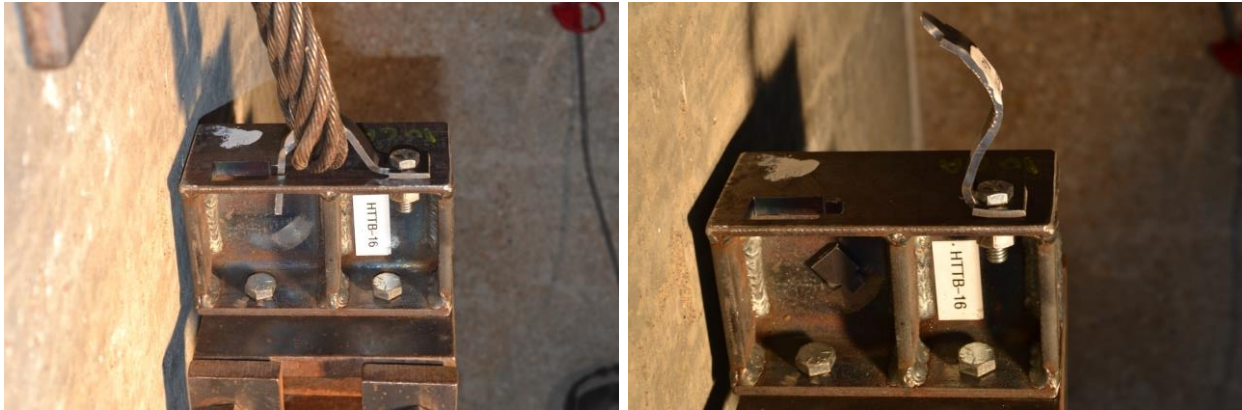


Figure 266. Pre-Test and Post-Test Photographs, Test No. HTTPB-16

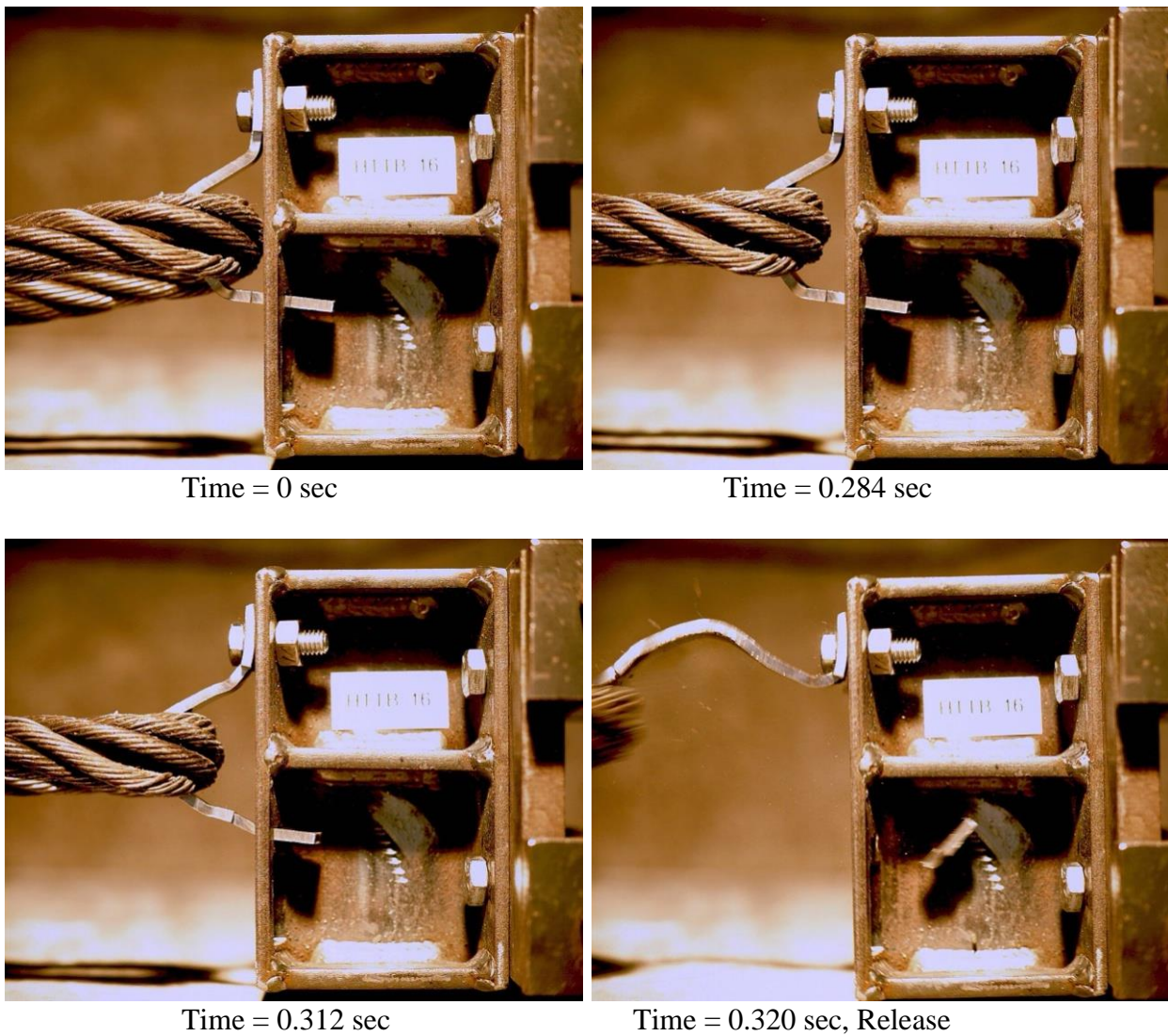


Figure 267. Sequential Photographs, Test No. HTTPB-16

13.2 Discussion

Ten dynamic component tests were performed in the second round of tests on bolted tabbed brackets. A fabrication flaw was detected that affected the lateral release behavior of the bolted tabbed bracket in test no. HTTB-12. When the tabbed bracket was pulled laterally, its head was briefly caught in the narrow, lower slot of the keyway. However, it eventually slipped out and released the cable before the full fracture load was developed. Upon inspection, it became apparent that the tabbed bracket was not properly seated. The head should have been resting against the bottom of the keyway, but it was not. The flaw was subsequently corrected, and the full fracture load was developed for all of the subsequent lateral pull tests.

Once the fabrication flaw was corrected, both versions performed consistently when pulled laterally. For the bolted tabbed bracket Version 3, the design equations predicted a lateral release load of 6.28 kips (27.9 kN), and the actual average lateral release load was 5.18 kips (23.0 kN). For the bolted tabbed bracket Version 4, the design equations predicted a lateral release load of 5.88 kips (26.2 kN), and the actual average lateral release load was 4.57 kips (20.3 kN). The actual lateral release loads were lower than the loads predicted by the design equations by a factor of approximately 5/6.

The Round 2 vertical release loads of the bolted tabbed brackets were significantly lower than those observed for the crimp-in-place tabbed brackets in Round 1 testing. However, they were still three to four and a half times higher than the loads predicted by the design equations. For the bolted tabbed bracket Version 3, the design equations predicted a vertical release load of 225 lb (1.00 kN), and the actual average vertical release load was 775 lb (3.45 kN). For tabbed bracket Version 4, the design equations predicted a vertical release load of 224 lb (996 N), and the actual average vertical release load was 944 lb (4.20 kN). Once again, the high-speed video revealed tab scraping against the inside of the flange as a factor. However, the tab scraping

observed with the Round 2 bolted tabbed brackets appeared to be less severe than the tab scraping observed with the Round 1 crimp-in-place tabbed brackets. Thus, it was determined that in order to significantly reduce the vertical release loads, not only would tab scraping need to be eliminated, but the bending stiffness would also need to be reduced. For Round 3, the vertical release load equations would be modified by a dynamic magnification factor of 1.5.

14 OVERVIEW OF BOLTED TABBED BRACKETS—ROUND 3

14.1 Introduction

The effort to design cable-to-post attachments for the bottom three cables was continued with the third (final) round of tabbed bracket design, testing, and evaluation. Six different versions of bolted tabbed brackets were created. As stated previously, the original targets for the lateral and vertical release loads were 6.00 kips (26.7 kN) and 225 lb (1.00 kN), respectively. However, those targets were not strictly followed for all of the tabbed brackets that were designed in this round, as will be discussed in subsection 14.2.2.

14.1.1 Dynamic Bogie Tests

All of the bolted tabbed brackets presented in this chapter were tested according to the dynamic bogie testing setup and procedures described in Chapter 6. Different load orientations were used in order to determine the vertical and lateral release loads for each concept under dynamic loading conditions.

14.2 Bolted Tabbed Bracket Design Modifications

There were three main differences between the bolted tabbed brackets in the second and third rounds. First, the shaft of the tabbed brackets was extended, similar to the extended keyway bolts. This change created space between the tabs and the back of the flange in an effort to eliminate tab scraping. Second, the shaft had a uniform width between the head and the bottom end where the bolt was fastened. This change was made to reduce as much as possible the plastic section for bending. Third, with one exception, different sheet steel thicknesses were used. An example of one of the tabbed brackets from Round 3 is shown in Figure 268.

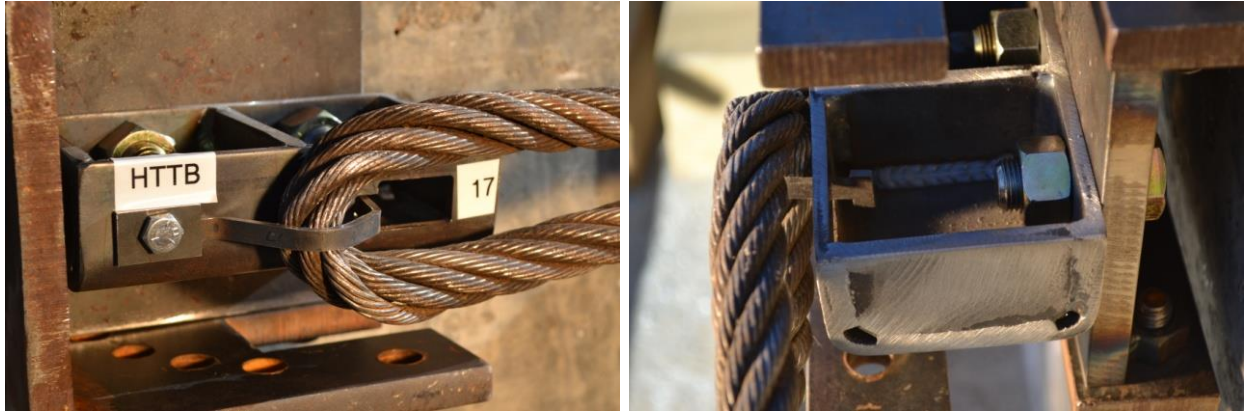


Figure 268. Round 3 Bolted Tabbed Bracket

14.2.1 Round 3 Design Equations

Equations were developed to guide the design process as well as to determine the dimensions of the prototype tabbed brackets. The dimensions, idealized load orientations, and assumed failure locations that were used in the development of the design equations, are shown in Figures 269 and 270.

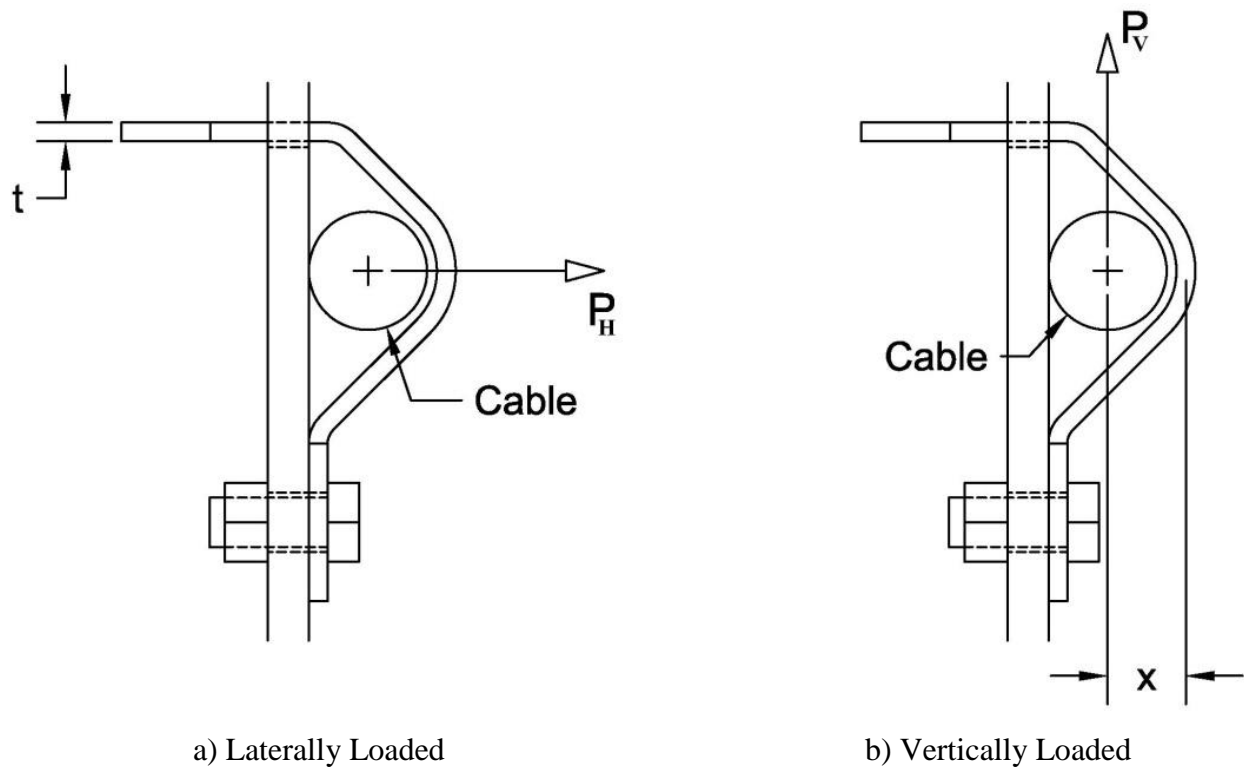


Figure 269. Bolted Tabbed Bracket—(a) Laterally Loaded and (b) Vertically Loaded

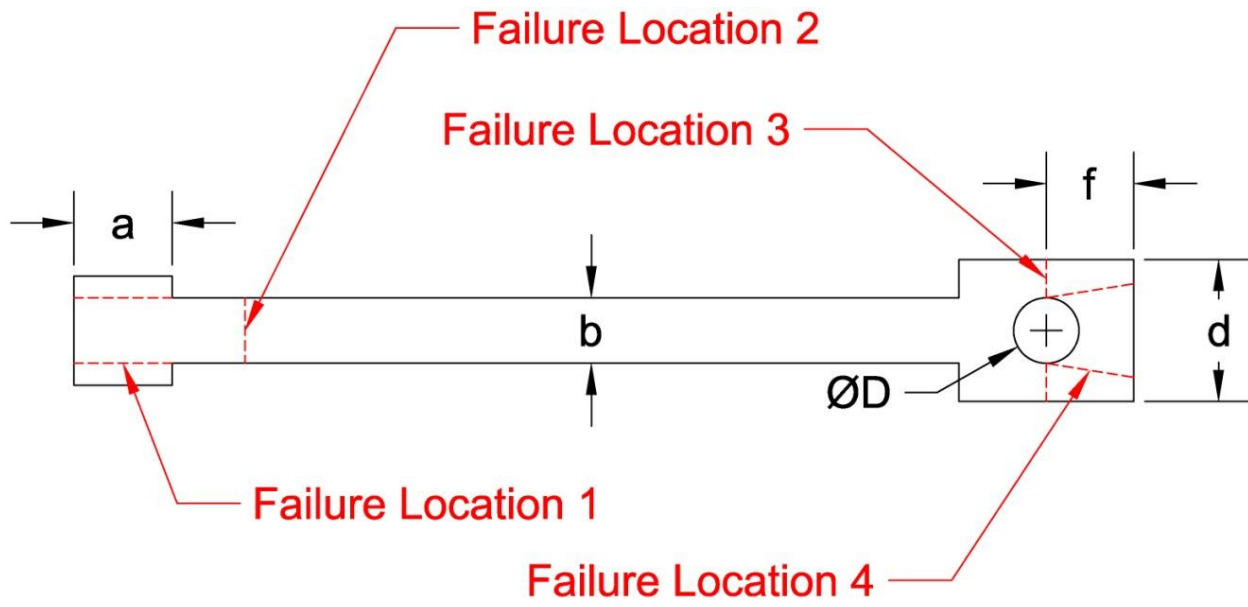


Figure 270. Dimensions and Failure Locations for Bolted Tabbed Bracket

The Round-1 design equations, which are discussed in Chapter 10, predicted the lateral release loads of the crimp-in-place tabbed brackets very well. Thus, the Round-2 equations, which are discussed in Chapter 12, were derived in a similar manner. However, the observed lateral loads for the second round were lower than the predicted loads by a factor of approximately 5/6. This error was probably due to the differing end conditions and the actual load distribution being different than what was assumed. The crimp-in-place tabbed brackets in the first round were symmetrical and assumed to have simply-supported end conditions. However, the lower bolted end of the tabbed brackets in Round 2 was partially fixed, thus resulting in the applied load, P_H , not being distributed evenly between the two ends, as the Round-2 equations had assumed. Thus, it seemed most prudent to modify the round-2 equations with a correction factor rather than derive new equations based on different theoretical end conditions and other sources of error.

As noted previously in Chapter 12, failure location 1 was assumed to be a pure shear fracture. In the second round of tabbed bracket tests, the lateral load needed to cause failure at location 1 was calculated using Equation 12.1.

$$P_{H_1} = \frac{4}{\sqrt{3}} at\sigma_u \quad (12.1)$$

For Round 3, the right side of Equation 12.1 was multiplied by a factor of 5/6 to account for the difference in the predicted versus observed lateral loads from the bolted tabbed brackets of Round 2, thus resulting in Equation 14.1.

$$P_{H_1} = \left(\frac{5}{6}\right) \frac{4}{\sqrt{3}} at\sigma_u = \frac{10}{3\sqrt{3}} at\sigma_u \quad (14.1)$$

Where σ_u = ultimate tensile strength
a = length of head (see Figure 270)
t = thickness (see Figure 269a)

As noted previously in Chapter 12, failure location 2 was assumed to be a pure tensile fracture through the neck. For the Round 2 tabbed bracket tests, the lateral load needed to cause failure at location 2 was calculated using Equation 12.2.

$$P_{H_2} = 2bt\sigma_u \quad (12.2)$$

For Round 3, the right side of Equation 12.2 was multiplied by a factor of 5/6 to account for the difference in the predicted versus observed lateral loads from the bolted tabbed brackets of Round 2, thus resulting in Equation 14.2.

$$P_{H_2} = \left(\frac{5}{6}\right) 2bt\sigma_u = \frac{5}{3} bt\sigma_u \quad (14.2)$$

Where σ_u = ultimate tensile strength
b = width of neck (see Figure 270)
t = thickness (see Figure 269a)

As noted previously in Chapter 12, failure location 3 was assumed to be a pure tensile fracture at the location of the bolt hole. For the Round 2 tabbed bracket tests, the lateral load needed to cause failure at location 3 was calculated using Equation 12.3.

$$P_{H_3} = 2(d - D - v)t\sigma_u = 2(d - d_b - \mu)t\sigma_u \quad (12.3)$$

For Round 3, the right side of Equation 12.3 was multiplied by a factor of 5/6 to account for the difference in the predicted versus observed lateral loads from the bolted tabbed brackets of Round 2, thus resulting in Equation 14.3.

$$P_{H_3} = \left(\frac{5}{6}\right) 2(d - D - v)t\sigma_u = \left(\frac{5}{6}\right) 2(d - d_b - \mu)t\sigma_u$$

$$P_{H_3} = \frac{5}{3}(d - D - v)t\sigma_u = \frac{5}{3}(d - d_b - \mu)t\sigma_u \quad (14.3)$$

Where d = width of bottom tab (see Figure 270)
 D = diameter of hole (see Figure 270)
 v = width reduction when using hole diameter = 1/16 in. (1.6 mm)
 d_b = diameter of the bolt
 μ = width reduction when using bolt diameter = 1/8 in. (3.2 mm)
 t = thickness (see Figure 269a)
 σ_u = ultimate tensile strength

As noted previously in Chapter 12, failure location 4 was assumed to be a tearing failure at the bolt hole. For the Round 2 tabbed bracket tests, the lateral load needed to cause failure at location 4 was calculated using Equation 12.4.

$$P_{H_4} = 2.4 \left(f - \frac{D}{2} \right) t\sigma_u = 2.4 \left(f - \frac{d_b + v}{2} \right) t\sigma_u \quad (12.4)$$

For Round 3, the right side of Equation 12.4 was multiplied by a factor of 5/6 to account for the difference in the predicted versus observed lateral loads from the bolted tabbed brackets of Round 2, thus resulting in Equation 14.4.

$$P_{H_4} = \left(\frac{5}{6}\right) 2.4 \left(f - \frac{D}{2} \right) t\sigma_u = \left(\frac{5}{6}\right) 2.4 \left(f - \frac{d_b + v}{2} \right) t\sigma_u$$

$$P_{H_4} = 2 \left(f - \frac{D}{2} \right) t \sigma_u = 2 \left(f - \frac{d_b + v}{2} \right) t \sigma_u \quad (14.4)$$

Where f = distance from the center of the bolt hole to the bottom edge of the bolted tabbed bracket (see Figure 270)
 D = diameter of the bolt hole (see Figure 270)
 d_b = diameter of the bolt
 v = 1/16 in. (1.6 mm)
 t = thickness (see Figure 269a)
 σ_u = ultimate tensile strength

The vertical release was assumed to occur in pure bending. For the third round, a dynamic magnification factor of 1.5 was incorporated into the equation for the vertical release load. This factor was not used in previous rounds. The moment arm, x , was measured between the center of the cable and the mid-plane of the outer bracket, as shown in Figure 269b. The vertical load needed to release the cable was calculated using Equation 14.5.

$$P_V = \frac{1.5M_P}{x} = \frac{1.5Z\sigma_y}{x} = \frac{1.5\left(\frac{bt^2}{4}\right)\sigma_y}{x} = \frac{3bt^2\sigma_y}{8x} \quad (14.5)$$

Where M_P = plastic moment
 x = moment arm (see Figure 269b)
 Z = plastic section modulus where bending occurs
 σ_y = yield strength
 b = cross-sectional width where bending occurs (see Figure 270)
 t = thickness (see Figure 269a)

When calculating the shear and tensile capacities of the Round 3 tabbed brackets, the steel strengths were 56 ksi (386 MPa) for the yield strength and 69 ksi (476 MPa) for the ultimate tensile strength. The actual strengths can be found on the material testing reports, as provided in Appendix E.

14.2.2 Dimensions and Structural Capacities

Tabbed bracket Version 5 was fabricated from 12-gauge, grade 50 sheet steel. Using the design equations, the predicted lateral and vertical capacities were 3.00 kips (13.3 kN) and 117 lb (520 N), respectively. A side view of tabbed bracket Version 5 is shown in Figure 271. A flat

pattern of the tabbed bracket is shown in Figure 272. The keyway corresponding to tabbed bracket Version 5 is shown in Figure 273.

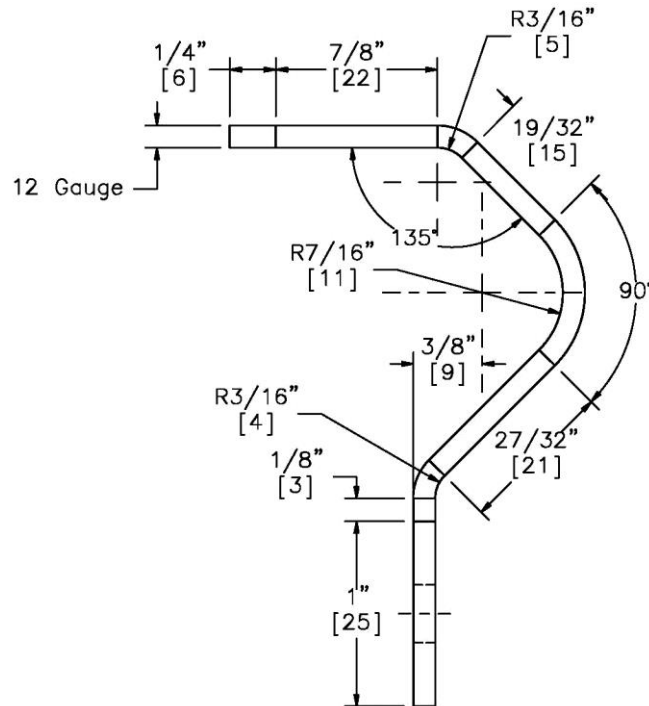


Figure 271. Side View of Tabbed Bracket Version 5

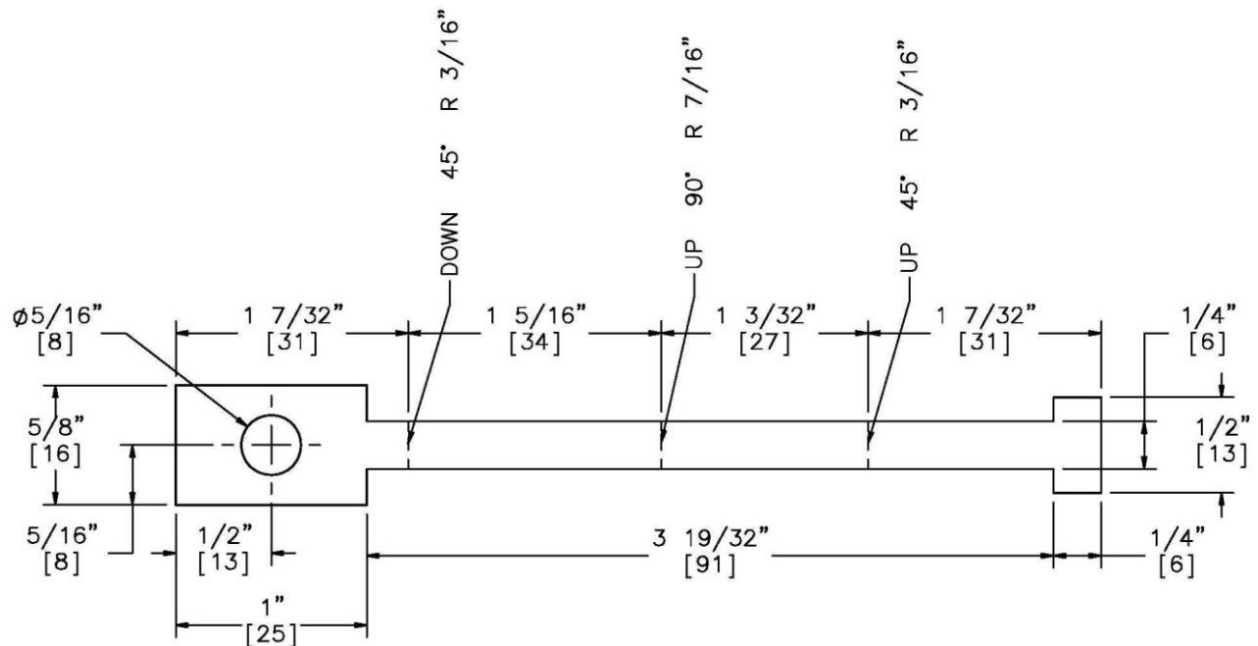


Figure 272. Flat Pattern of Tabbed Bracket Version 5

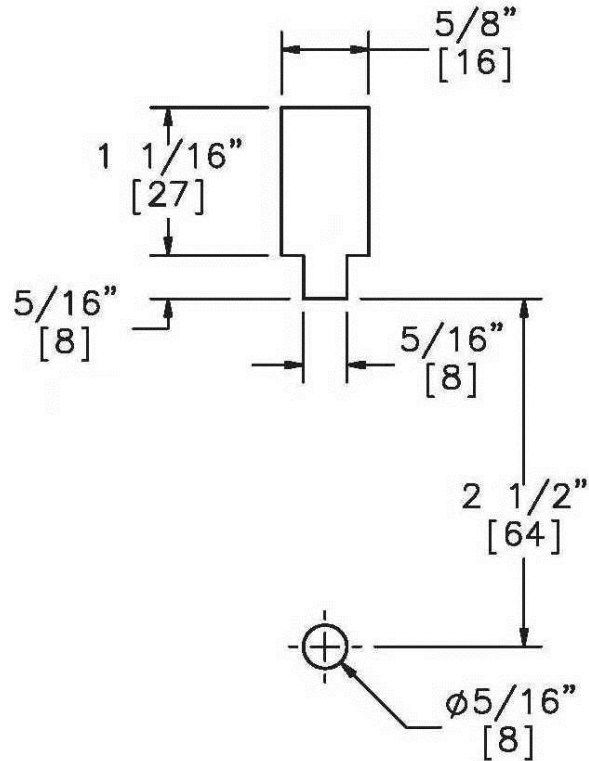


Figure 273. Tabbed Bracket Version 5 Keyway

Tabbed bracket Version 6 was fabricated from 14-gauge, grade 50 sheet steel. Using the design equations, the predicted lateral and vertical capacities were 4.30 kips (19.1 kN) and 123 lb (547 N), respectively. A side view of tabbed bracket Version 6 is shown in Figure 274. A flat pattern of the tabbed bracket is shown in Figure 275. The keyway corresponding to tabbed bracket Version 6 is shown in Figure 276.

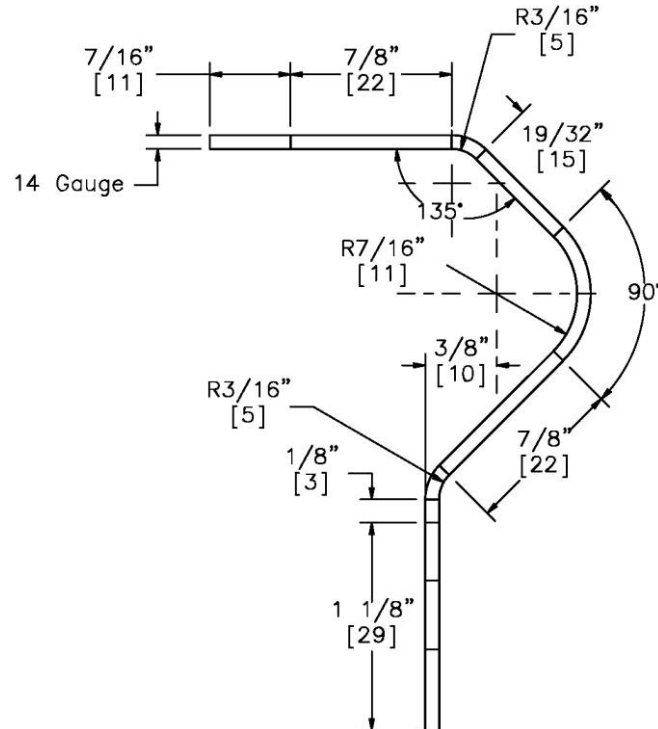


Figure 274. Side View of Tabbed Bracket Version 6

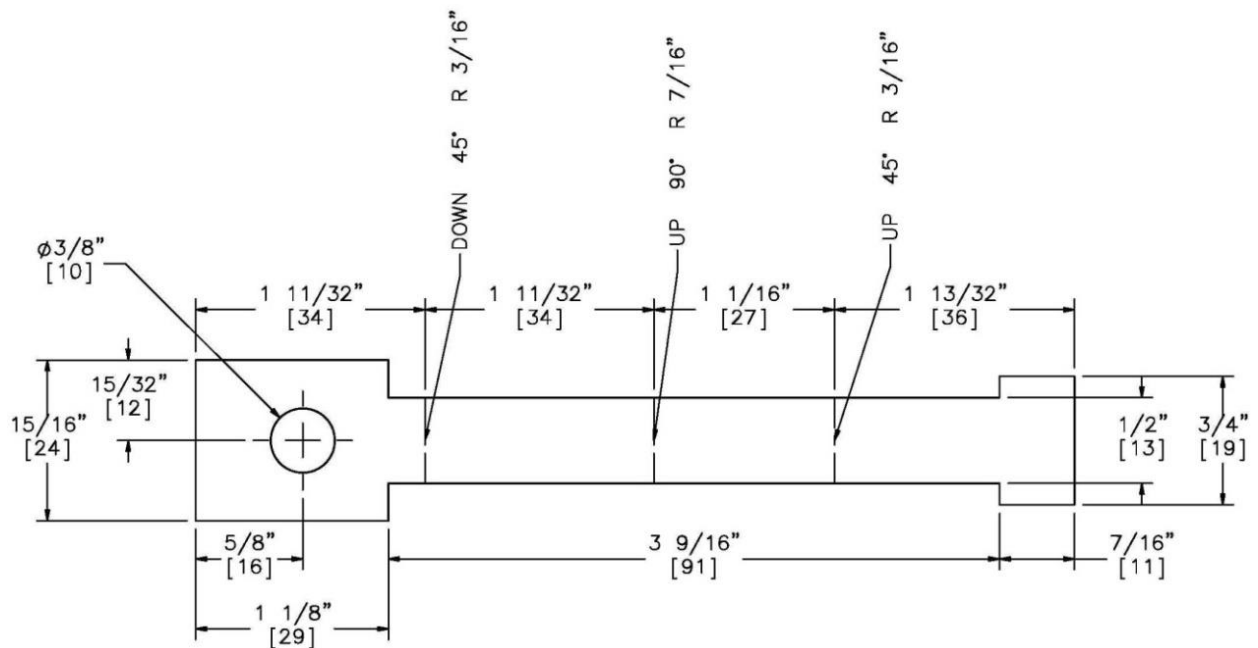


Figure 275. Flat Pattern of Tabbed Bracket Version 6

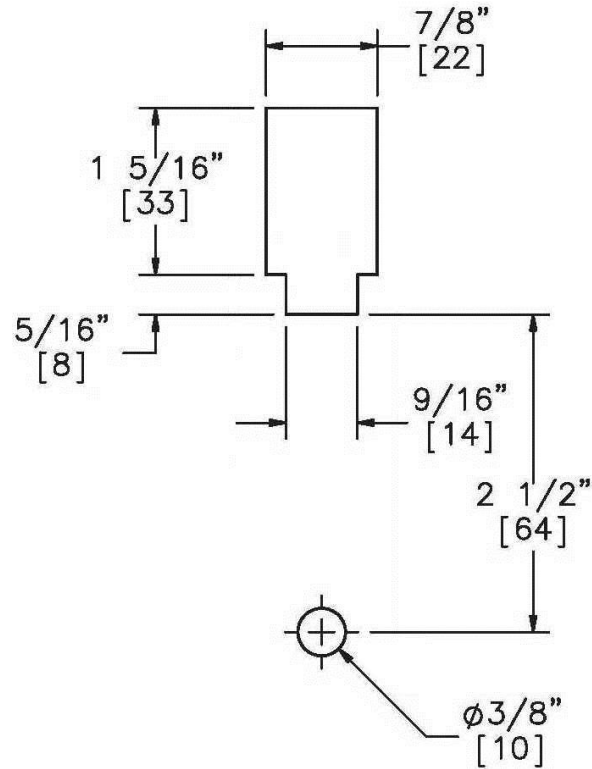


Figure 276. Tabbed Bracket Version 6 Keyway

Tabbed bracket Version 7 was fabricated from 11-gauge, grade 50 sheet steel. Using the design equations, the predicted lateral and vertical capacities were 6.02 kips (26.8 kN) and 264 lb (1.17 kN) respectively. A side view of tabbed bracket Version 7 is shown in Figure 277. A flat pattern of the tabbed bracket is shown in Figure 278. The keyway corresponding to Version 7 is shown in Figure 279.

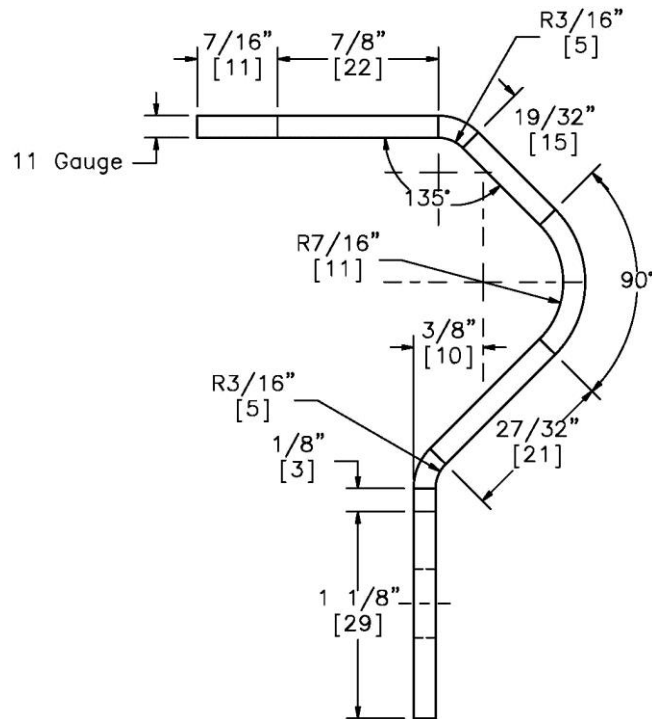


Figure 277. Side View of Tabbed Bracket Version 7

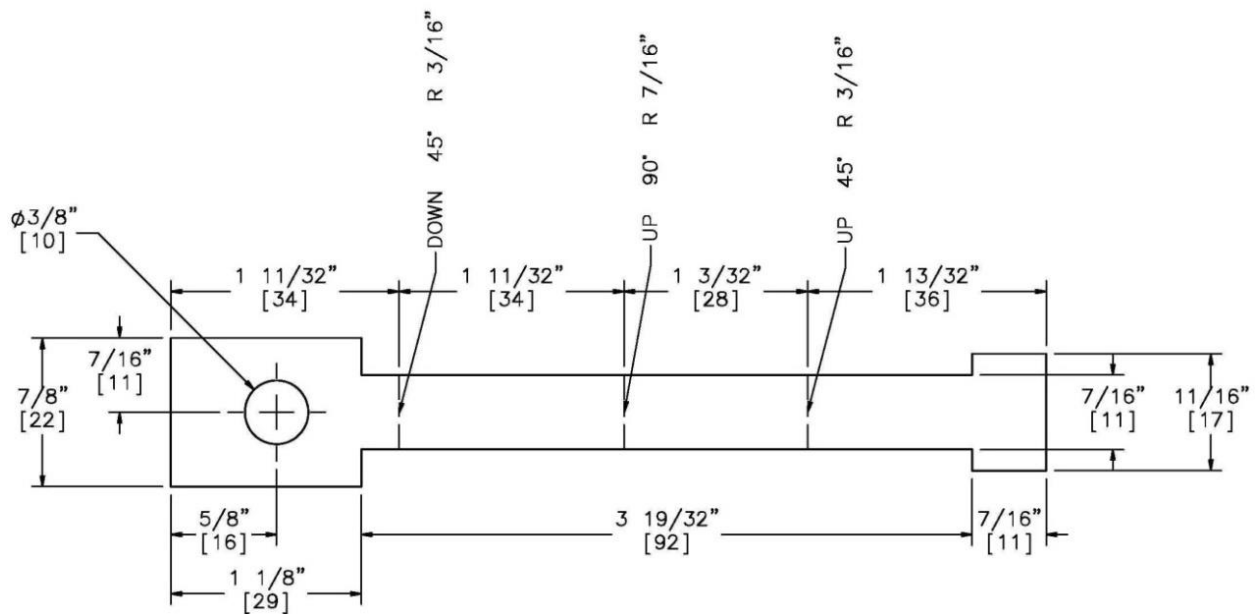


Figure 278. Flat Pattern of Tabbed Bracket Version 7

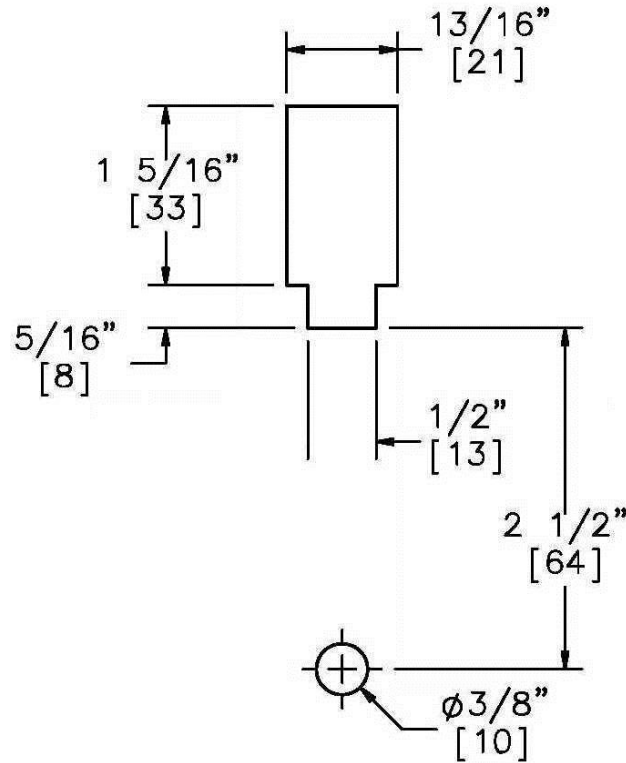


Figure 279. Tabbed Bracket Version 7 Keyway

Tabbed bracket Version 8 was fabricated from 12-gauge, grade 50 sheet steel. Using the design equations, the predicted lateral and vertical capacities were 6.01 kips (26.7 kN) and 235 lb (1.05 kN), respectively. A side view of tabbed bracket Version 8 is shown in Figure 280. A flat pattern of the tabbed bracket is shown in Figure 281. The keyway corresponding to tabbed bracket Version 8 is shown in Figure 282.

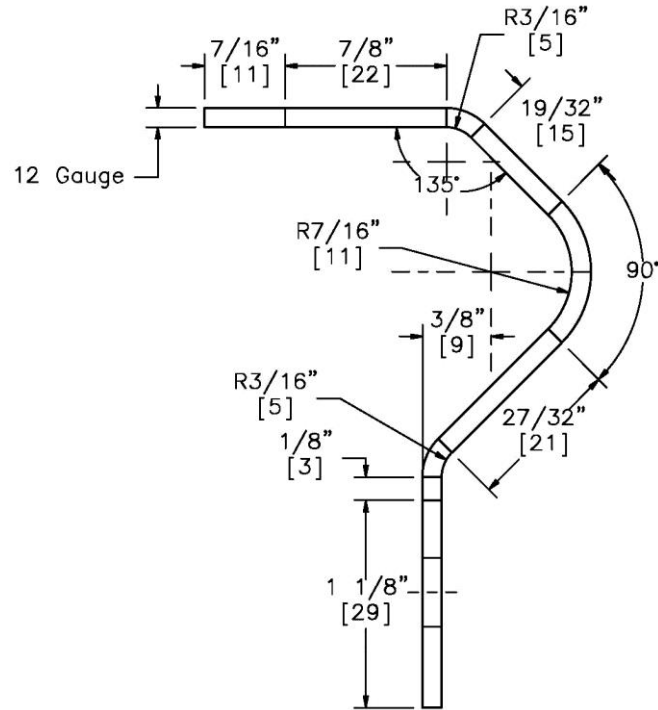


Figure 280. Side View of Tabbed Bracket Version 8

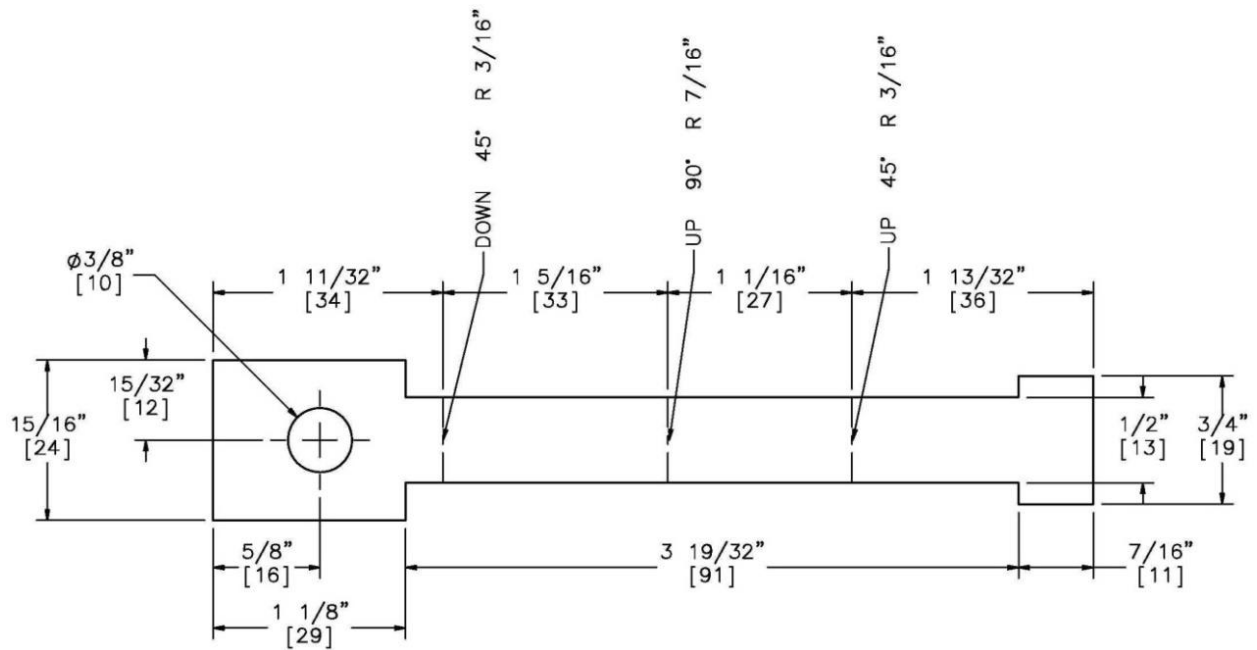


Figure 281. Flat Pattern of Tabbed Bracket Version 8

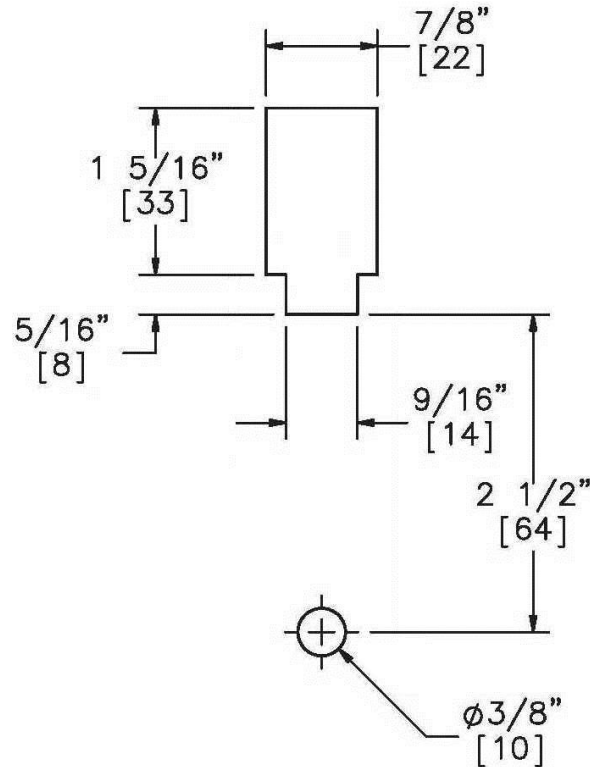


Figure 282. Tabbed Bracket Version 8 Keyway

Tabbed bracket Versions 9 and 10 were very similar to Version 8. Similar to Version 8, Versions 9 and 10 were fabricated from 12-gauge steel. In fact and according to the design equations, they were supposed to have the same vertical and lateral release loads as Version 8. The only differences were in the length of the neck and the depth of the narrow part of the keyway. If the length of the neck was too long in relation to the depth of the narrow part of the keyway, the head would not catch in the keyway when the bracket was pulled laterally. If the length of the neck was too short in relation to the depth of the narrow part of the keyway, there would be tab scraping against the back of the flange when the bracket was pulled vertically. This scraping behavior was clearly seen in the development and testing of the extended keyway bolts, as described in Chapter 5.

The neck of tabbed bracket Version 9 was 1/8 in. (3.2 mm) longer, and the narrow part of the keyway was 1/16 in. (1.6 mm) shallower than those of tabbed bracket Version 8. This

configuration increased the risk of the head slipping through the keyway—rather than catching in it—when the bracket was pulled laterally, but it also increased the likelihood of the head releasing through the keyway freely when the bracket was pulled vertically. A side view of tabbed bracket Version 9 is shown in Figure 283. A flat pattern of the tabbed bracket is shown in Figure 284. The keyway which corresponds to Version 9 is shown in Figure 285.

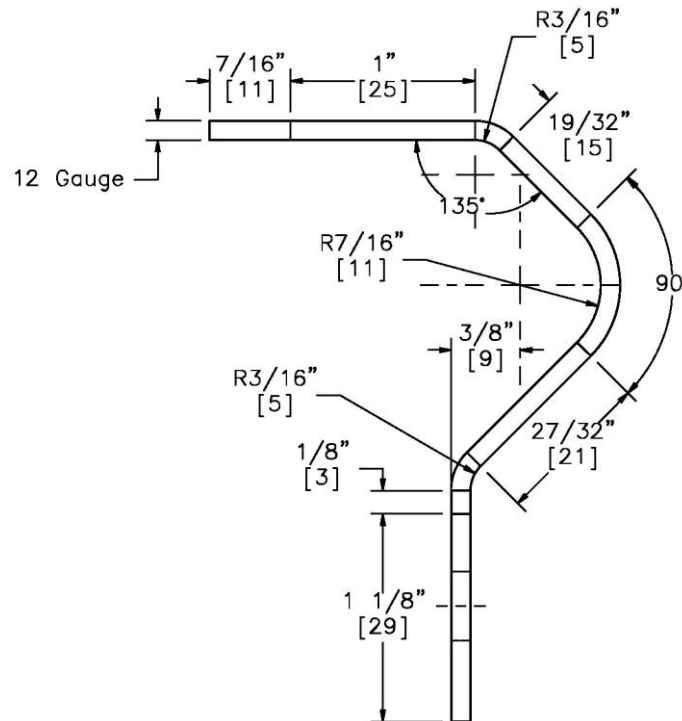


Figure 283. Side View of Tabbed Bracket Version 9

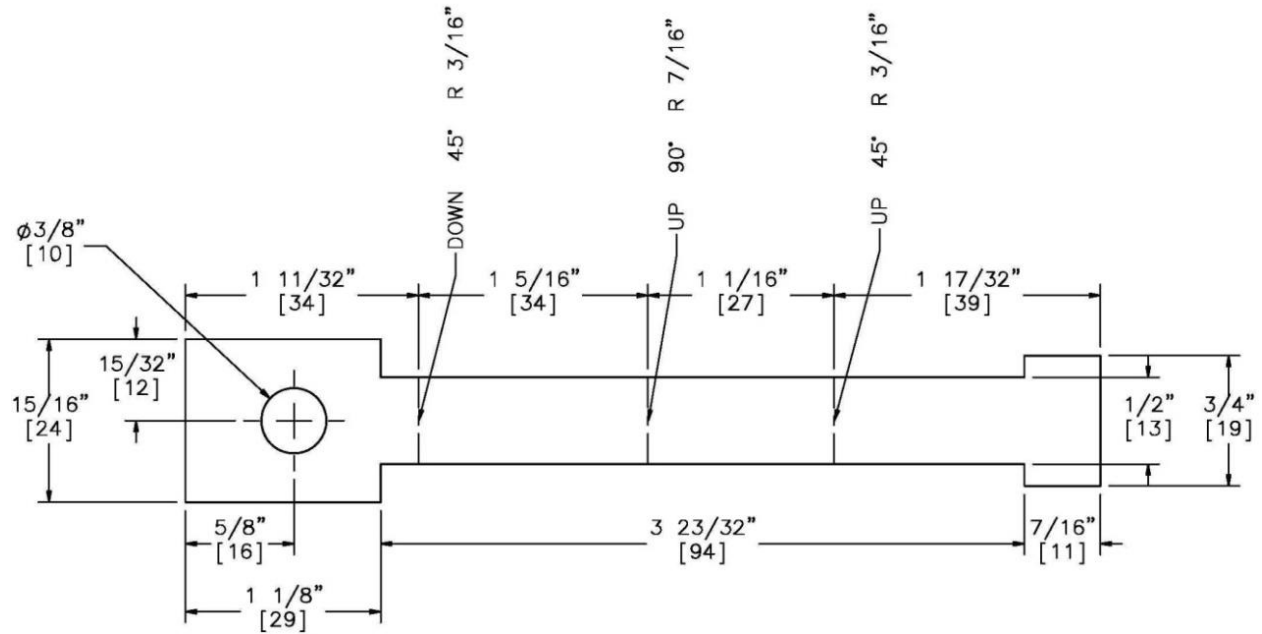


Figure 284. Flat Pattern of Tabbed Bracket Version 9

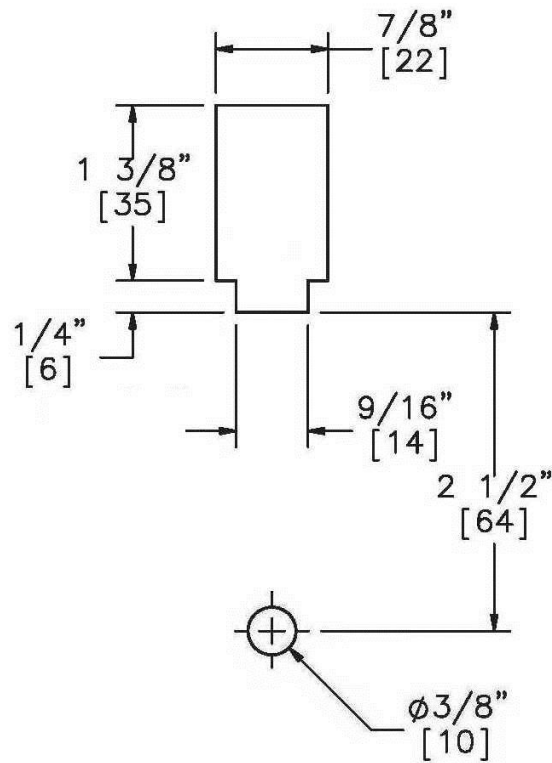


Figure 285. Tabbed Bracket Version 9 Keyway

The neck of tabbed bracket Version 10 was 1/8 in. (3.2 mm) shorter, and the narrow part of the keyway was 1/16 in. (1.6 mm) deeper than those of tabbed bracket Version 8. This configuration increased the likelihood that the head would catch in the keyway when the bracket was pulled laterally, but it also increased the risk of tab scraping against the back of the flange when the bracket was pulled vertically. A side view of tabbed bracket Version 10 is shown in Figure 286. A flat pattern of the tabbed bracket is shown in Figure 287. The keyway which corresponds to Version 10 is shown in Figure 288.

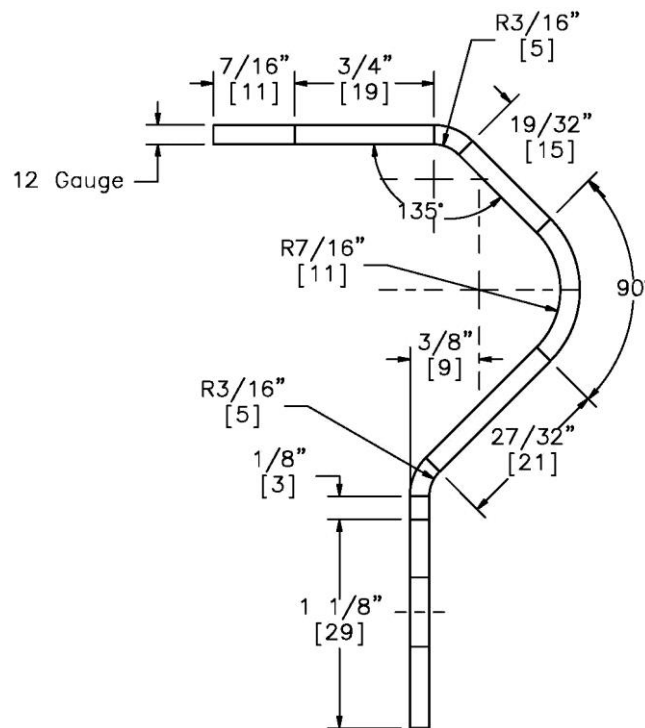


Figure 286. Side View of Tabbed Bracket Version 10

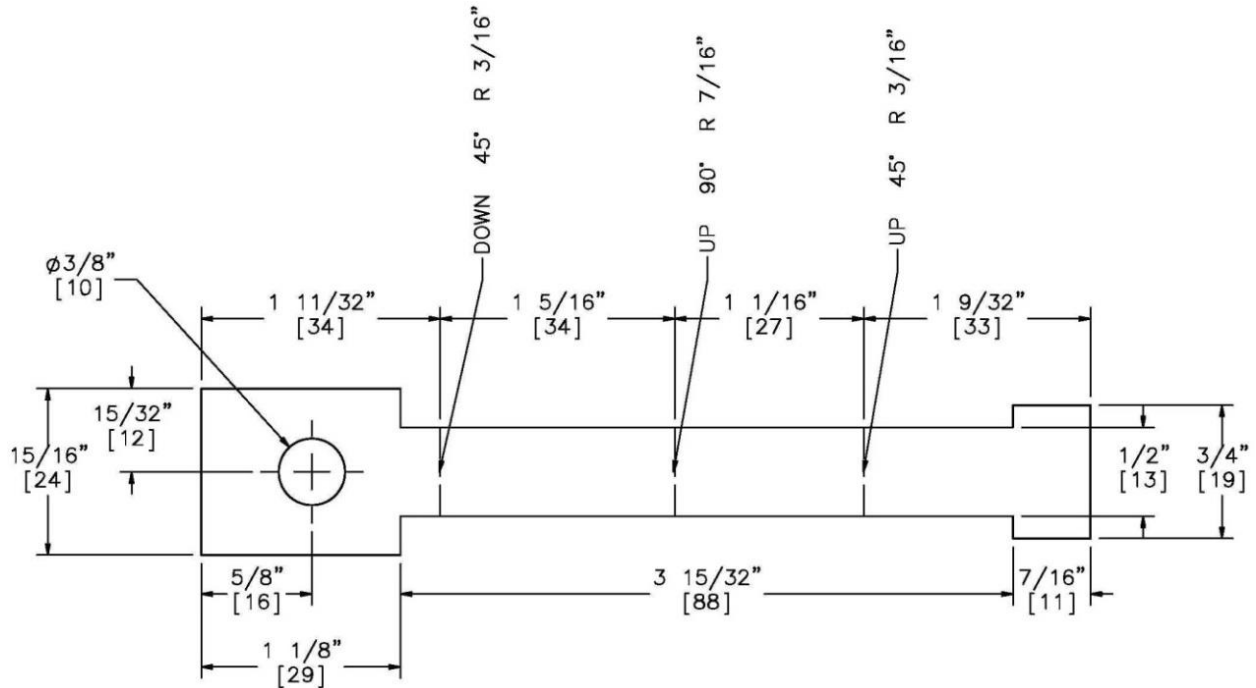


Figure 287. Flat Pattern of Tabbed Bracket Version 10

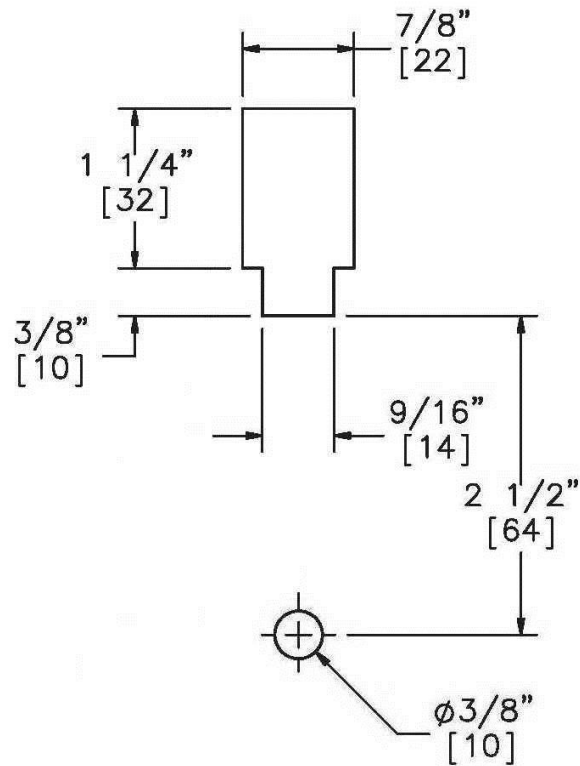


Figure 288. Tabbed Bracket Version 10 Keyway

The expected release loads for the bolted tabbed brackets from Round 3 are shown in Table 12.

Table 12. Expected Release Loads for Round 3 Bolted Tabbed Brackets

Tabbed Bracket	Expected Lateral Release Load kips (kN)				Expected Vertical Release Load kips (kN)
	Failure Location 1	Failure Location 2	Failure Location 3	Failure Location 4	
Version 5	3.47 (15.4)	3.01 (13.4)	3.01 (13.4)	4.51 (20.1)	0.12 (0.53)
Version 6	4.34 (19.3)	4.30 (19.1)	4.30 (19.1)	4.51 (20.1)	0.12 (0.53)
Version 7	6.95 (30.9)	6.02 (26.8)	6.02 (26.8)	7.22 (32.1)	0.26 (1.2)
Version 8	6.08 (27.0)	6.01 (26.7)	6.01 (26.7)	6.32 (28.1)	0.24 (1.1)
Version 9	6.08 (27.0)	6.01 (26.7)	6.01 (26.7)	6.32 (28.1)	0.24 (1.1)
Version 10	6.08 (27.0)	6.01 (26.7)	6.01 (26.7)	6.32 (28.1)	0.24 (1.1)

15 DYNAMIC COMPONENT TESTS—TABBED BRACKETS, ROUND 3

15.1 Results

All of the tabbed brackets were fabricated from hot-rolled, ASTM A1011, HSLA Grade 50 sheet steel. The tabbed bracket thickness, cross-section width, method of attachment, and the mounting post section were varied for the Round 3 tests. The same setup and procedures used to test the keyway bolts was also used to test the tabbed brackets. Three rounds of design modifications, component testing, and evaluation were made to the tabbed brackets. Eight dynamic component tests (test nos. HTTB-1 through HTTB-8) were performed in the first round, as discussed in Chapters 10 and 11. Ten dynamic component tests (test nos. HTTB-9 through HTTB-16, including test nos. HTTB-9R and HTTB-12R) were performed in the second round, as discussed in Chapters 12 and 13. Twenty-four dynamic component tests (test nos. HTTB-17 through HTTB-40) were performed in the third round and are presented in Chapters 14 and 15. Each individual concept was tested twice in its vertical orientation and twice in its lateral orientation in order to determine the structural capacities and cable release behaviors. For the sake of convenience, the consolidated drawing sets for all three rounds of dynamic component testing on tabbed brackets is shown in Figures 164 through 203, as provided in Chapter 11. The test matrix and results for the third round of tests on the bolted tabbed brackets are summarized in Table 13.

Table 13. Summary of Dynamic Component Testing on Bolted Tabbed Brackets, Round 3

Test No.	Load Direction	Tabbed Bracket	Gauge	Post Section	Expected Strength, kips (kN)	Release Load, kips (kN)	Test Result
HTTB-17	Vertical	Version 5, Bolted, e1	12	C-section, V5, e2	0.12 (0.53)	0.12 (0.53)	Free release through keyway, snag load = 0.13 kips (0.57 kN)
HTTB-18	Vertical	Version 5, Bolted, e1	12	C-section, V5, e2	0.12 (0.53)	0.15 (0.67)	Release through keyway, small amount of contact between tab and side of keyway, snag load = 0.10 kips (0.46 kN)
HTTB-19	Vertical	Version 8, Bolted, h1	12	C-section, V6/8, f2	0.24 (1.1)	0.24 (1.1)	Free release through keyway, snag load = 0.41 kips (1.8 kN)
HTTB-20	Vertical	Version 8, Bolted, h1	12	C-section, V6/8, f2	0.24 (1.1)	0.28 (1.2)	Free release through keyway, snag load = 0.36 kips (1.6 kN)
HTTB-21	Lateral	Version 8, Bolted, h1	12	C-section, V6/8, f2	6.01 (26.7)	5.71 (25.4)	No high-speed video, tabs caught in narrow part of keyway, tabs sheared off (Failure Location 1), cracking at bolt hole (Failure Location 3)
HTTB-22	Lateral	Version 8, Bolted, h1	12	C-section, V6/8, f2	6.01 (26.7)	5.59 (24.9)	Tabs caught in narrow part of keyway, tabs sheared off and bent (resembles Failure Location 1), yielding at bolt hole
HTTB-23	Lateral	Version 5, Bolted, e1	12	C-section, V5, e2	3.00 (13.3)	3.06 (13.6)	Tabs caught in narrow part of keyway, fracture through narrow part of bracket (Failure Location 2)
HTTB-24	Lateral	Version 5, Bolted, e1	12	C-section, V5, e2	3.00 (13.3)	2.97 (13.2)	Tabs caught in narrow part of keyway, fracture through narrow part of bracket (Failure Location 2)
HTTB-25	Lateral	Version 6, Bolted, f1	14	C-section, V6/8, f2	4.30 (19.1)	3.50 (15.6)	Tabs caught in narrow part of keyway, Cracks formed and tabs bent inward (resembles Failure Location 1)

Table 13. Summary of Dynamic Component Testing on Bolted Tabbed Brackets, Round 3 (Continued)

Test No.	Load Direction	Tabbed Bracket	Gauge	Post Section	Expected Strength kips (kN)	Release Load kips (kN)	Test Result
HTTB-26	Lateral	Version 6, Bolted, f1	14	C-section, V6/8, f2	4.30 (19.1)	3.44 (15.3)	Tabs caught in narrow part of keyway, Cracks formed and tabs bent inward (resembles Failure Location 1)
HTTB-27	Lateral	Version 7, Bolted, g1	11	C-section, V7, g2	6.02 (26.8)	4.04 (18.0)	Tabs caught in narrow part of keyway, corner of one tab sheared off and head twisted and slipped through narrow part of the keyway
HTTB-28	Lateral	Version 7, Bolted, g1	11	C-section, V7, g2	6.02 (26.8)	4.88 (21.7)	Tabs caught in narrow part of keyway, corner of one tab sheared off and head twisted and slipped through narrow part of the keyway
HTTB-29	Lateral	Version 9, Bolted, i1	12	C-section, V9, i2	6.01 (26.7)	0.77 (3.4)	Tabs failed to catch in narrow part of keyway, free release through keyway
HTTB-30	Lateral	Version 9, Bolted, i1	12	C-section, V9, i2	6.01 (26.7)	0.44 (2.0)	Tabs failed to catch in narrow part of keyway, free release through keyway
HTTB-31	Lateral	Version 10, Bolted, j1	12	C-section, V10, j2	6.01 (26.7)	6.03 (26.8)	Tabs caught in narrow part of keyway, fracture at bolt hole (Failure Location 3)
HTTB-32	Lateral	Version 10, Bolted, j1	12	C-section, V10, j2	6.01 (26.7)	6.17 (27.4)	Tabs caught in narrow part of keyway, fracture through narrow part of bracket (Failure Location 2), cracking at bolt hole (Failure Location 3)
HTTB-33	Vertical	Version 6, Bolted, f1	14	C-section, V6/8, f2	0.12 (0.53)	NA	Load cell data unusable, edge of tab snagged on side of keyway as it released through the keyway
HTTB-34	Vertical	Version 6, Bolted, f1	14	C-section, V6/8, f2	0.12 (0.53)	NA	Load cell data unusable, edge of tab snagged on side of keyway as it released through the keyway

Table 13. Summary of Dynamic Component Testing on Bolted Tabbed Brackets, Round 3 (Continued)

Test No.	Load Direction	Tabbed Bracket	Gauge	Post Section	Expected Strength, kips (kN)	Release Load, kips (kN)	Test Result
HTTB-35	Vertical	Version 7, Bolted, g1	11	C-section, V7, g2	0.26 (1.2)	0.46 (2.0)	Edge of tab snagged on side of keyway as the head released through, cable snag load = 0.47 kips (2.1 kN)
HTTB-36	Vertical	Version 7, Bolted, g1	11	C-section, V7, g2	0.26 (1.2)	0.31 (1.4)	Edge of tab rubbed against side of keyway as the head released through, snag load = 0.65 kips (2.9 kN)
HTTB-37	Vertical	Version 10, Bolted, j1	12	C-section, V10, j2	0.24 (1.1)	0.42 (1.9)	Edge of tab rubbed against side of keyway as the head released through, snag load = 0.53 kips (2.4 kN)
HTTB-38	Vertical	Version 10, Bolted, j1	12	C-section, V10, j2	0.24 (1.1)	0.27 (1.2)	Edge of tab rubbed against side of keyway as the head released through, snag load = 0.46 kips (2.0 kN)
HTTB-39	Vertical	Version 6, Bolted, f1	14	C-section, V6/8, f2	0.12 (0.53)	0.12 (0.53)	Edge of tab rubbed against side of keyway as the head released through, snag load = 0.20 kips (0.91 kN)
HTTB-40	Vertical	Version 6, Bolted, f1	14	C-section, V6/8, f2	0.12 (0.53)	NA	Load cell data unusable, no high-speed video

15.1.1 Test No. HTTB-17 (TB V5, Bolted, Vertical)

For test no. HTTB-17, the cable pulled on the 12-gauge, grade 50 steel, bolted tabbed bracket Version 5 at an angle of 0 degrees, parallel to the front face of the flange, thus imparting a vertical load. The post consisted of a 5-½-in. (140-mm) long, folded C-section, fabricated from 7-gauge, grade 50 sheet steel. The top end of the tabbed bracket rested in the keyway, while the bottom end was secured to the flange with a ¼-in. (6-mm), grade 5, hex cap screw and nut. The bracket began to bend as the cable began to pull on it. As the bracket bent, the head rotated out of the keyway freely with a maximum release load of 122 lb (543 N). A peak load of 128 lb (569 N) occurred as the cable became snagged on the head, after the tab had already cleared the keyway. The force versus time plot is shown in Figure 289. Pre- and post-test photographs are shown in Figure 290. Sequential photographs are shown in Figure 291.

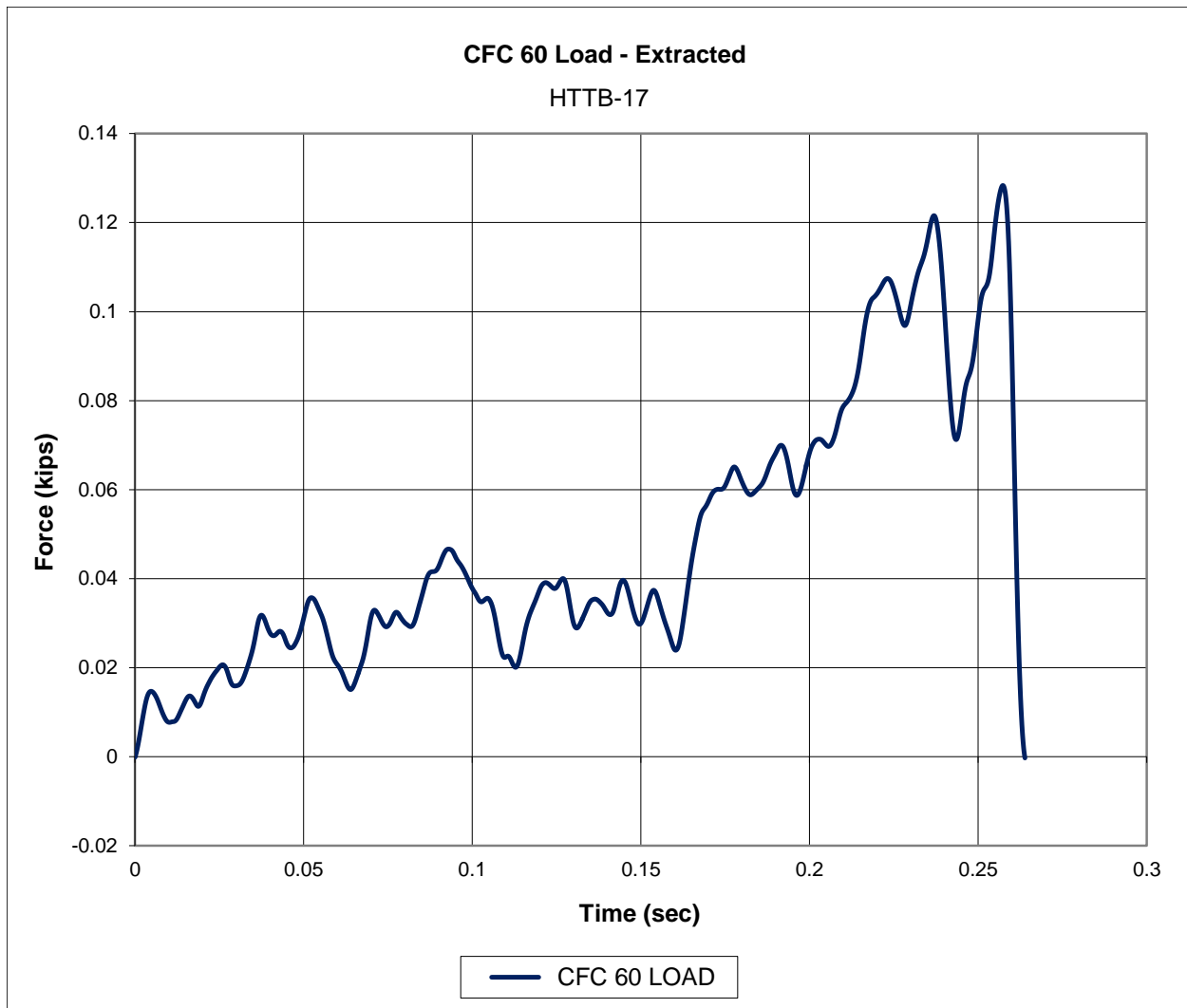


Figure 289. Force-Time Data, Test No. HTTB-17

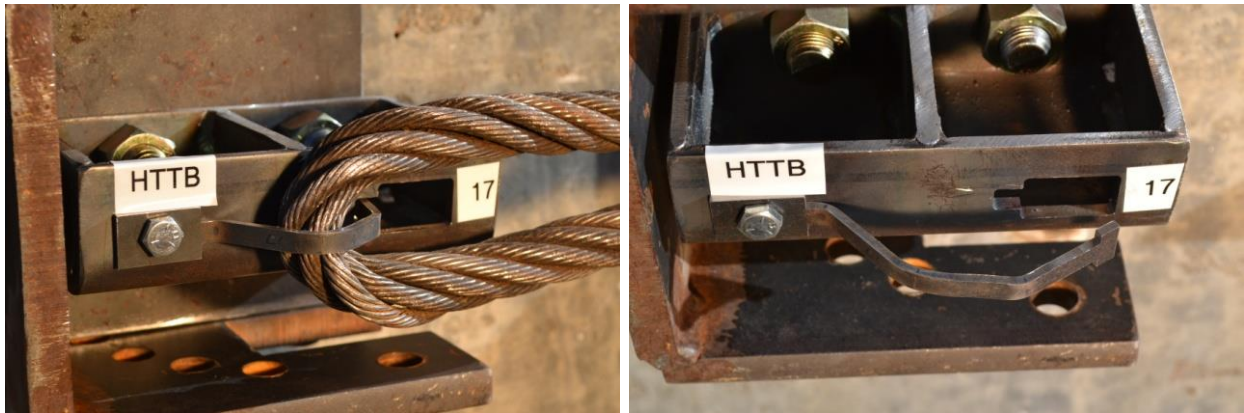


Figure 290. Pre-Test and Post-Test Photographs, Test No. HTTPB-17

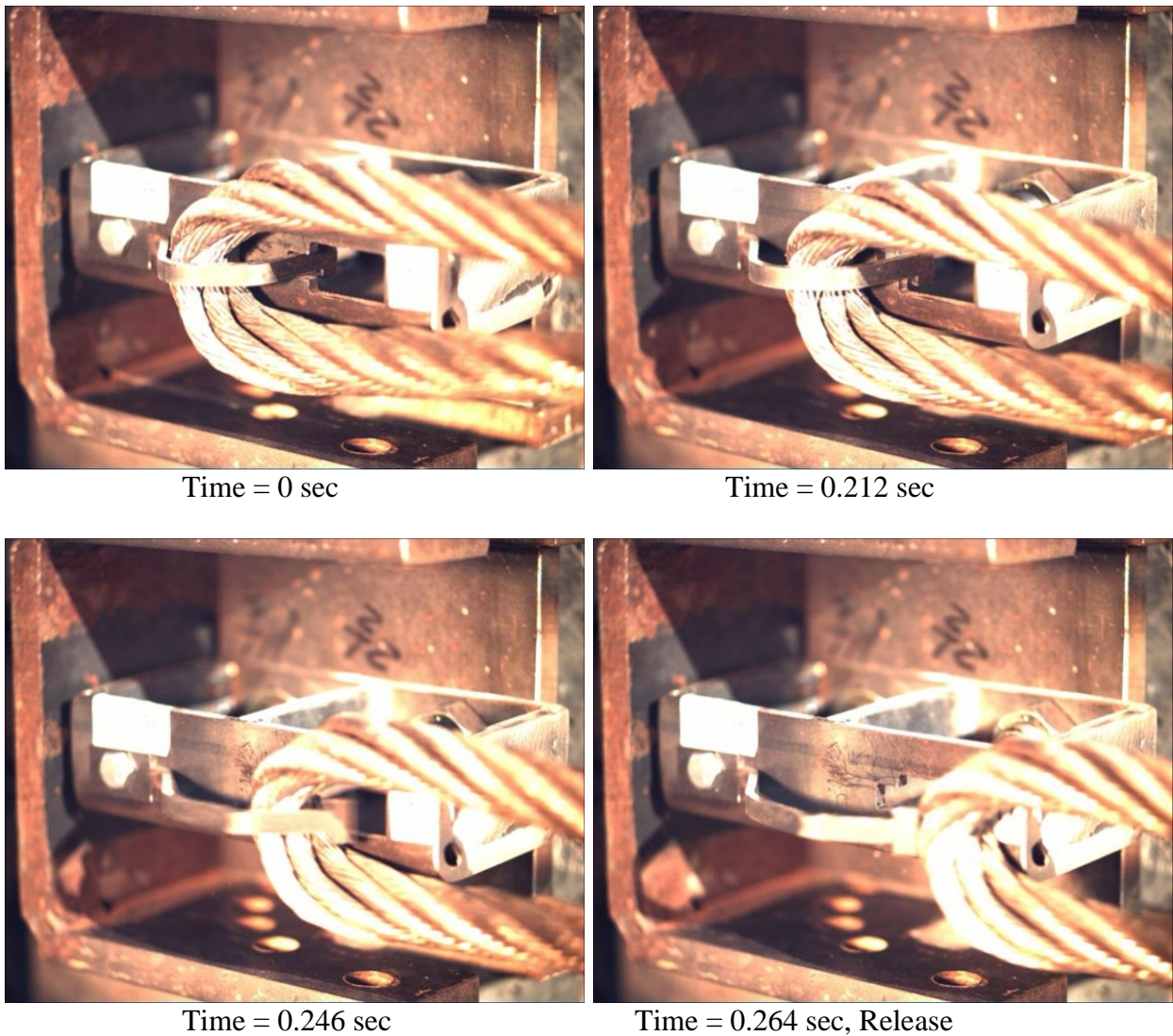


Figure 291. Sequential Photographs, Test No. HTTPB-17

15.1.2 Test No. HTTB-18 (TB V5, Bolted, Vertical)

For test no. HTTB-18, the cable pulled on the 12-gauge, grade 50 steel, bolted tabbed bracket Version 5 at an angle of 0 degrees, parallel to the front face of the flange, thus imparting a vertical load. The post consisted of a 5-½-in. (140-mm) long, folded C-section, fabricated from 7-gauge, grade 50 sheet steel. The top end of the tabbed bracket rested in the keyway, while the bottom end was secured to the flange with a ¼-in. (6-mm), grade 5, hex cap screw and nut. The bracket began to bend as the cable began to pull on it. As the bracket bent, the head rotated out of the keyway. There was a small amount of contact between the tab and the side of the keyway before the head rotated through completely. A peak load of 148 lb (658 N) occurred as the bracket bent and the head rotated out of the keyway. A small snag load of 103 lb (458 N) occurred after the head cleared the keyway. The force versus time plot is shown in Figure 292. Pre- and post-test photographs are shown in Figure 293. Sequential photographs are shown in Figure 294.

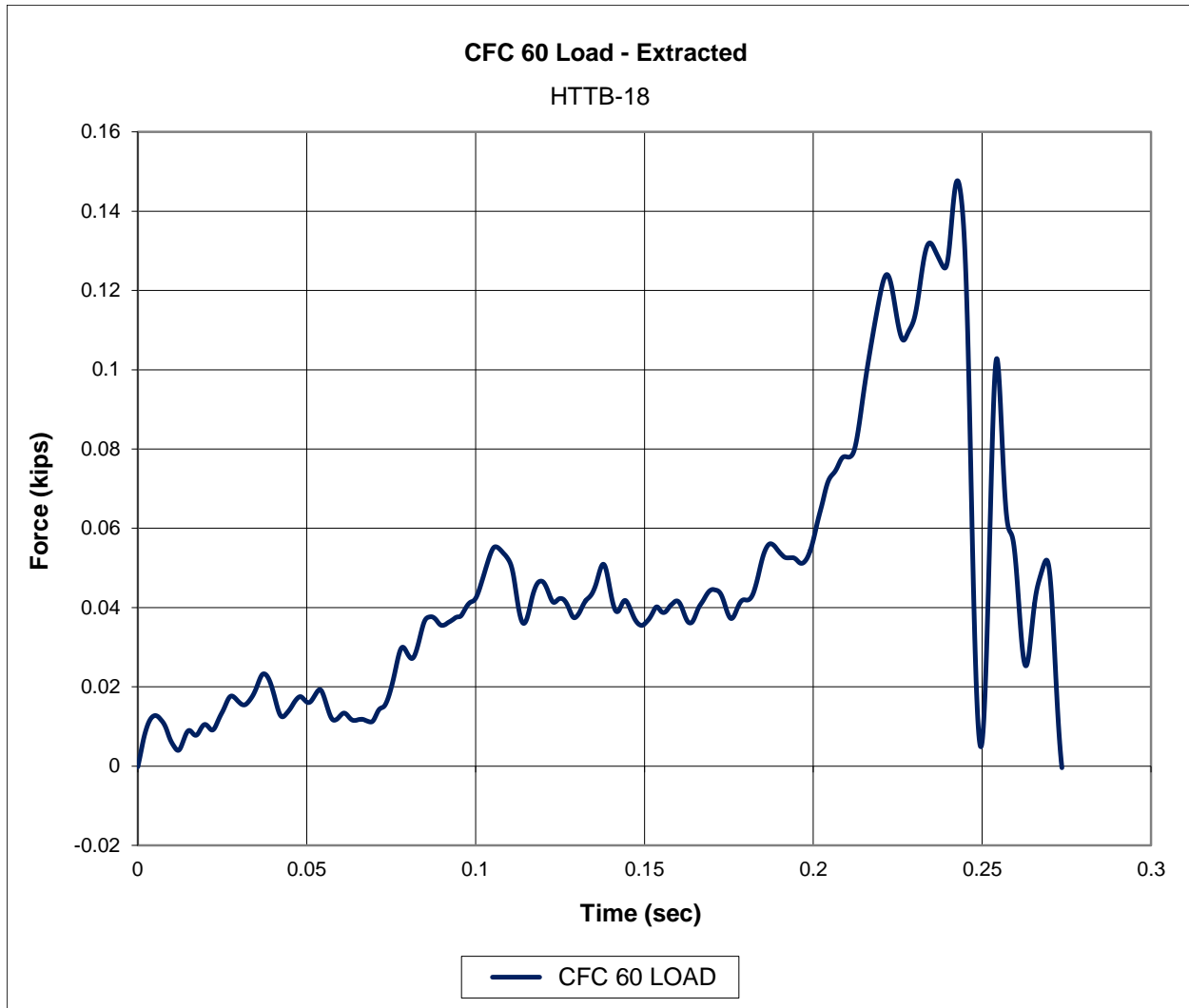


Figure 292. Force-Time Data, Test No. HTTB-18

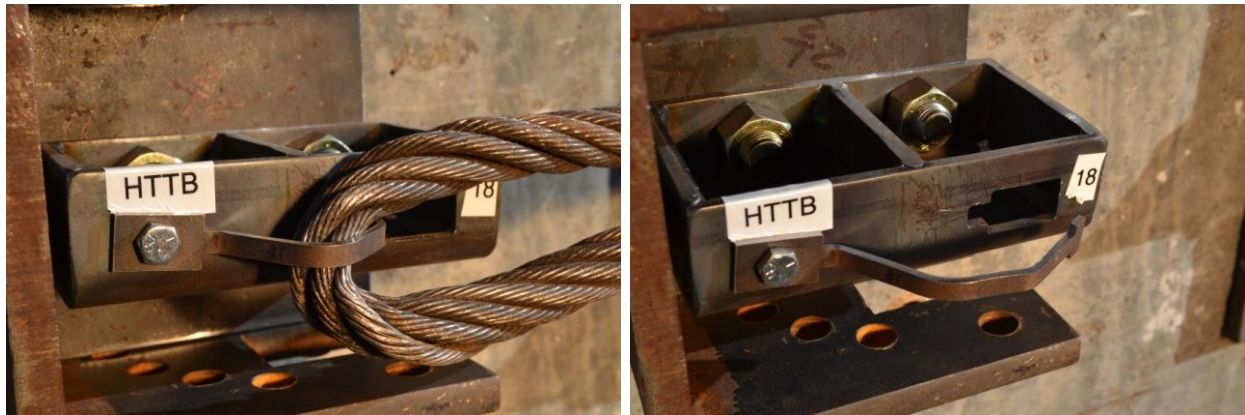


Figure 293. Pre-Test and Post-Test Photographs, Test No. HTTPB-18

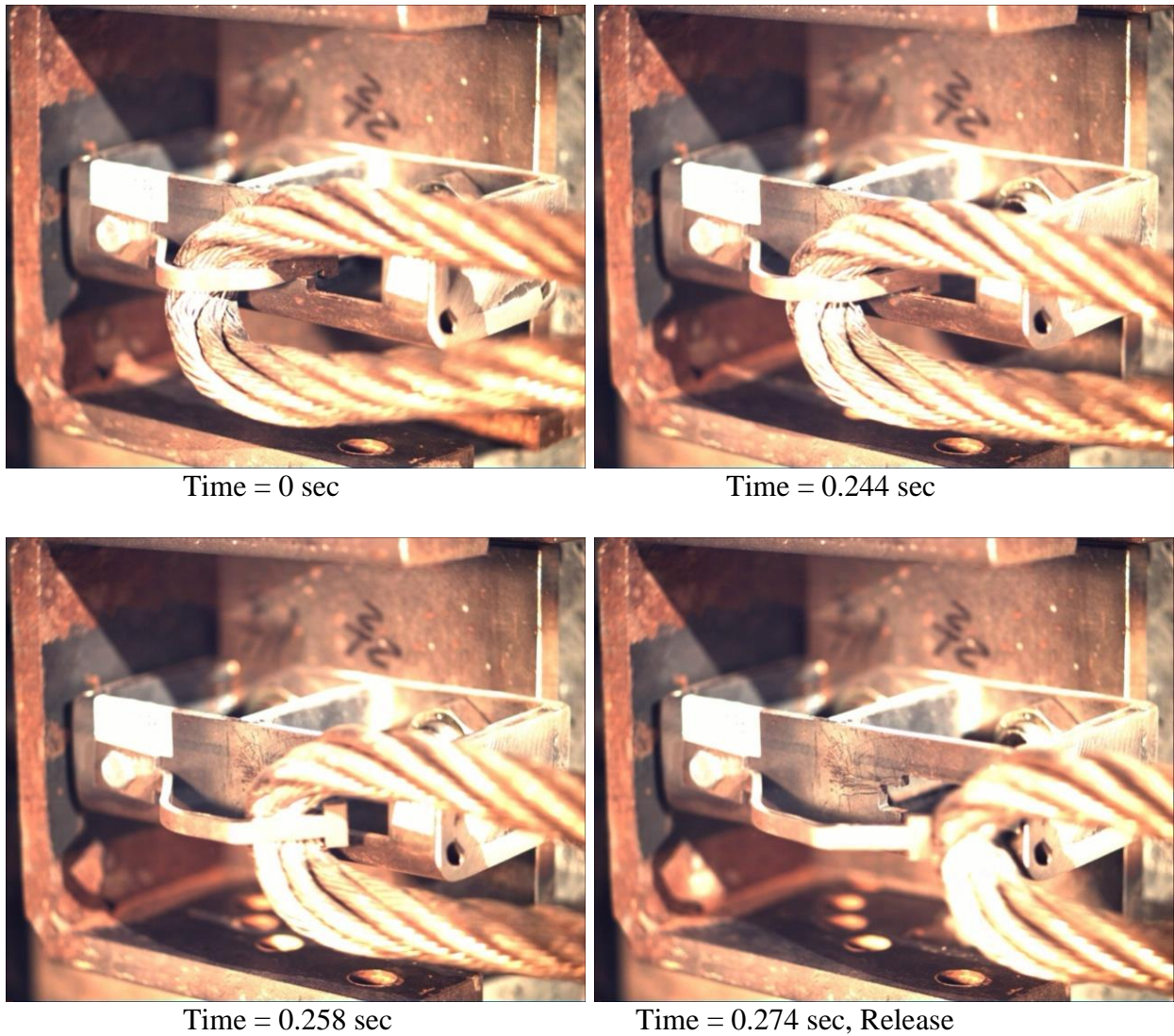


Figure 294. Sequential Photographs, Test No. HTTPB-18

15.1.3 Test No. HTTB-19 (TB V5, Bolted, Vertical)

For test no. HTTB-19, the cable pulled on the 12-gauge, grade 50 steel, bolted tabbed bracket Version 8 at an angle of 0 degrees, parallel to the front face of the flange, thus imparting a vertical load. The post consisted of a 5-½-in. (140-mm) long, folded C-section, fabricated from 7-gauge, grade 50 sheet steel. The top end of the tabbed bracket rested in the keyway, while the bottom end was secured to the flange with a 5/16-in. (8-mm), grade 5, hex cap screw and nut. The bracket began to bend as the cable began to pull on it. As the bracket bent, the head rotated out of the keyway freely with a maximum release load of 239 lb (1.06 kN). A peak load of 406 lb (1.81 kN) occurred as the cable became snagged on the head, after it had already cleared the keyway. The force versus time plot is shown in Figure 295. Pre- and post-test photographs are shown in Figure 296. Sequential photographs are shown in Figure 297.

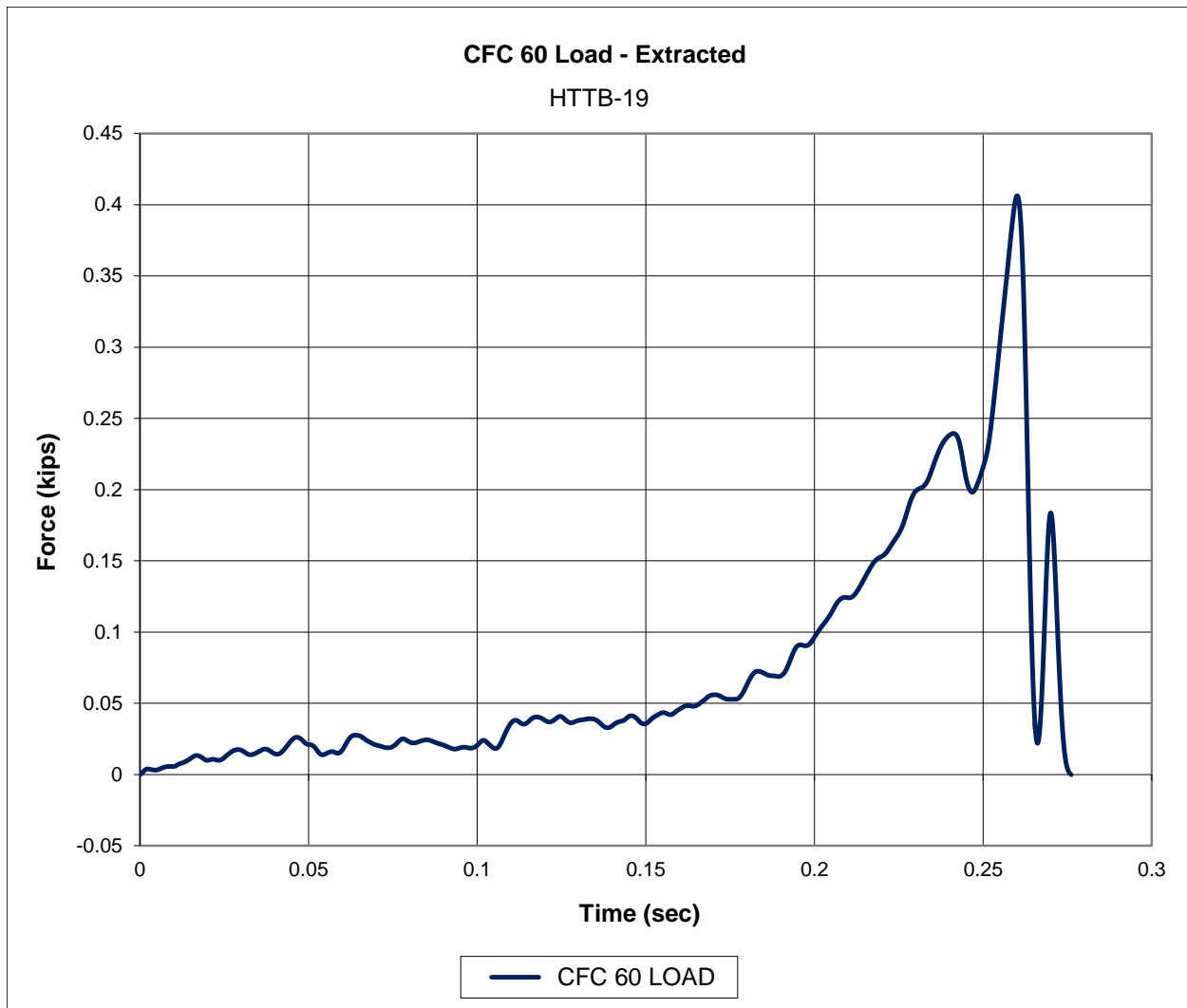


Figure 295. Force-Time Data, Test No. HTTB-19

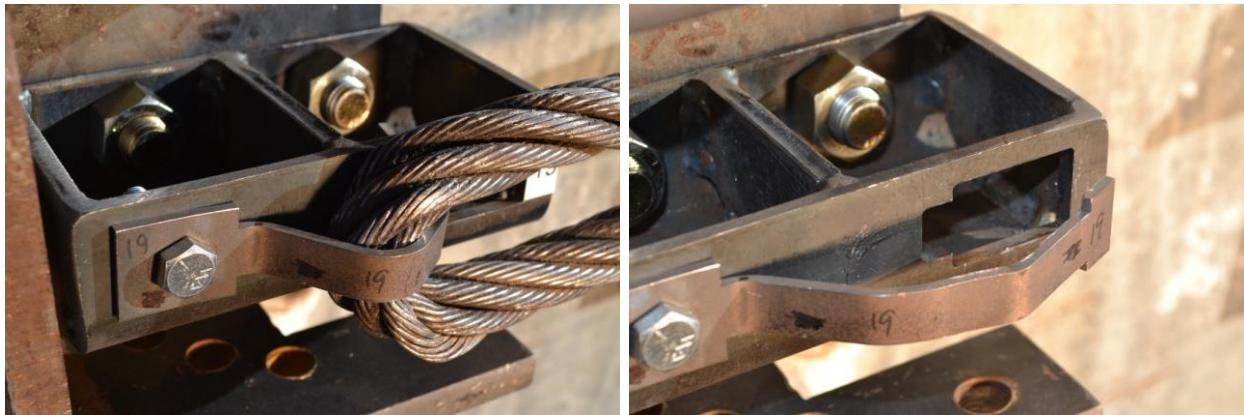


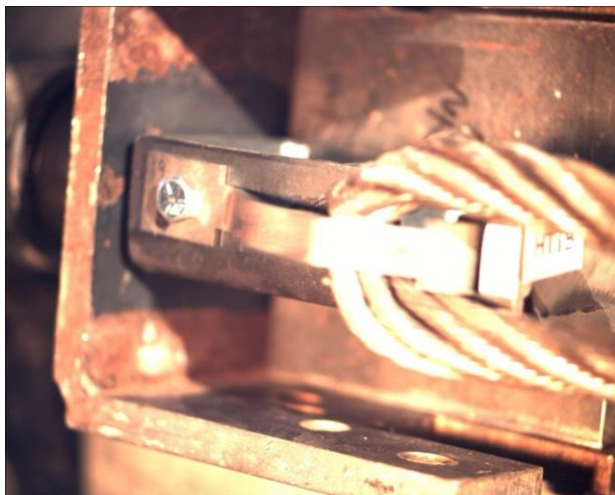
Figure 296. Pre-Test and Post-Test Photographs, Test No. HTTPB-19



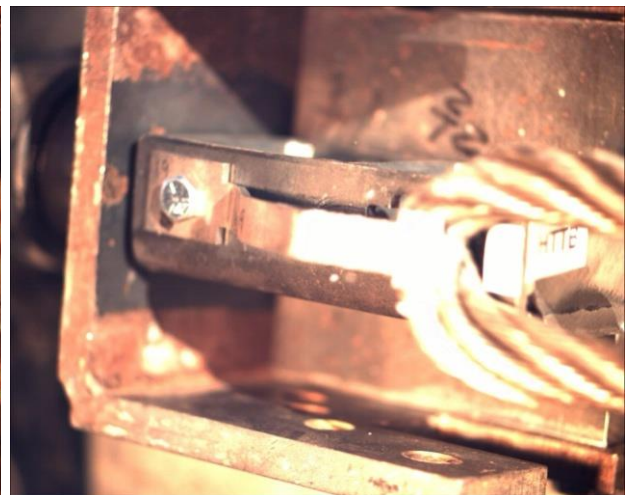
Time = 0 sec



Time = 0.242 sec



Time = 0.260 sec



Time = 0.270 sec, Release

Figure 297. Sequential Photographs, Test No. HTTPB-19

15.1.4 Test No. HTTB-20 (TB V8, Bolted, Vertical)

For test no. HTTB-20, the cable pulled on the 12-gauge, grade 50 steel, bolted tabbed bracket Version 8 at an angle of 0 degrees, parallel to the front face of the flange, thus imparting a vertical load. The post consisted of a 5-½-in. (140-mm) long, folded C-section, fabricated from 7-gauge, grade 50 sheet steel. The top end of the tabbed bracket rested in the keyway, while the bottom end was secured to the flange with a 5/16-in. (8-mm), grade 5, hex cap screw and nut. The bracket began to bend as the cable began to pull on it. As the bracket bent, the head rotated out of the keyway freely with a maximum release load of 283 lb (1.26 kN). A peak load of 362 lb (1.61 kN) occurred as the cable became snagged on the head, after it had already cleared the keyway. The force versus time plot is shown in Figure 298. Pre- and post-test photographs are shown in Figure 299. Sequential photographs are shown in Figure 300.

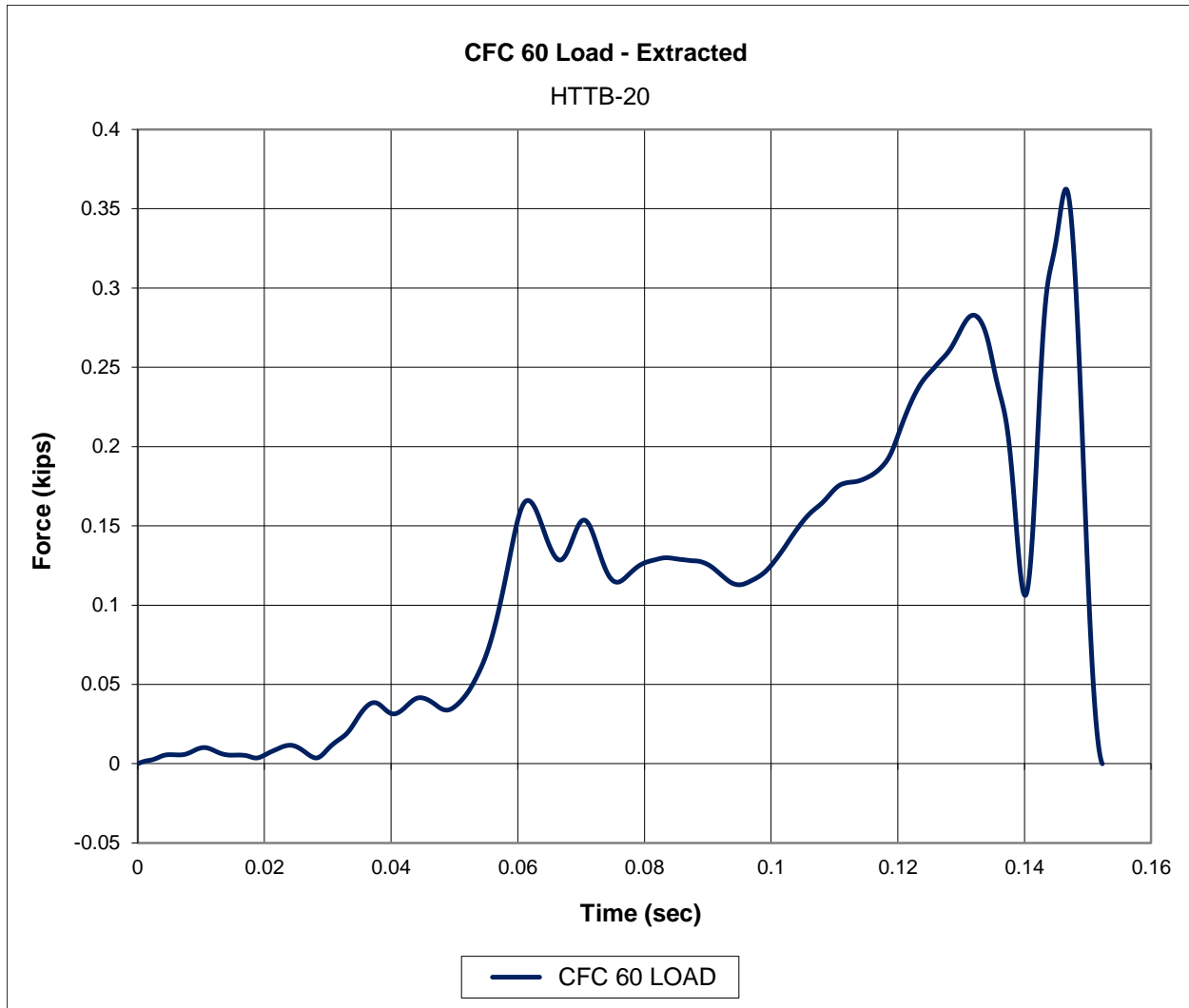


Figure 298. Force-Time Data, Test No. HTTB-20

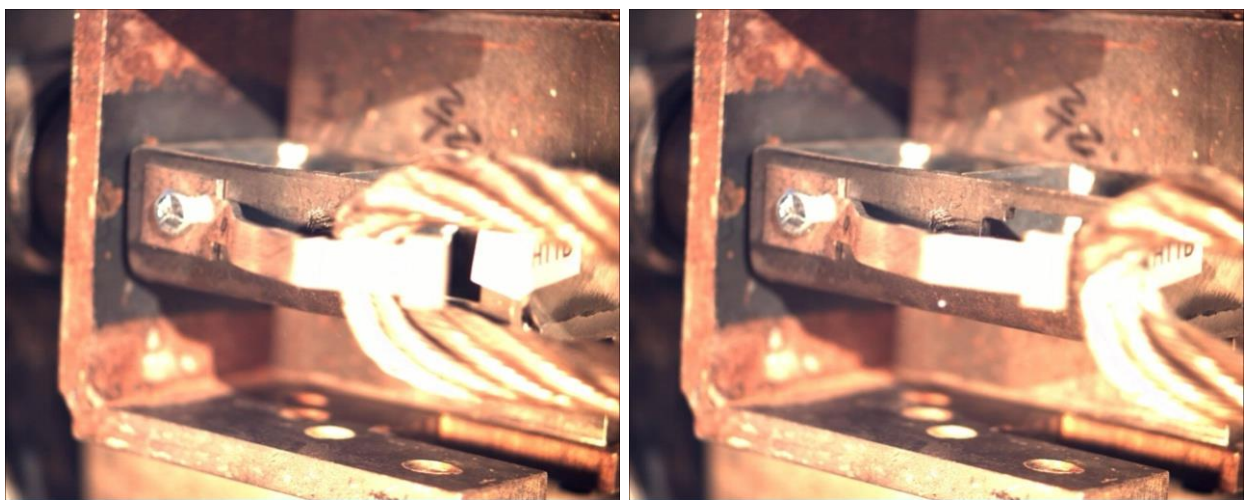


Figure 299. Pre-Test and Post-Test Photographs, Test No. HTTPB-20



Time = 0 sec

Time = 0.132 sec



Time = 0.140 sec

Time = 0.152 sec, Release

Figure 300. Sequential Photographs, Test No. HTTPB-20

15.1.5 Test No. HTTB-21 (TB V8, Bolted, Lateral)

For test no. HTTB-21, the cable pulled on the 12-gauge, grade 50 steel, bolted tabbed bracket Version 8 at an angle of 90 degrees, perpendicular to the front face of the flange, thus imparting a lateral load. The post consisted of a 5-½-in. (140-mm) long, folded C-section, fabricated from 7-gauge, grade 50 sheet steel. The top end of the tabbed bracket rested in the keyway, while the bottom end was secured to the flange with a 5/16-in. (8-mm), grade 5, hex cap screw and nut. As the cable began to pull on the bracket, the head became caught in the narrow part of the keyway. The cable continued to pull until the tabs were sheared off (failure location 1). There was also significant cracking at the location of the bolt hole, indicating that tensile fracture (failure location 3) was imminent at that location. A peak load of 5.71 kips (25.4 kN) occurred as the head was pulled against the inside of the keyway, just before shear failure. Due to technical difficulties, there was no high-speed video, but the standard speed video was useful nonetheless. The force versus time plot is shown in Figure 301. Pre- and post-test photographs are shown in Figure 302. Sequential photographs are shown in Figure 303.

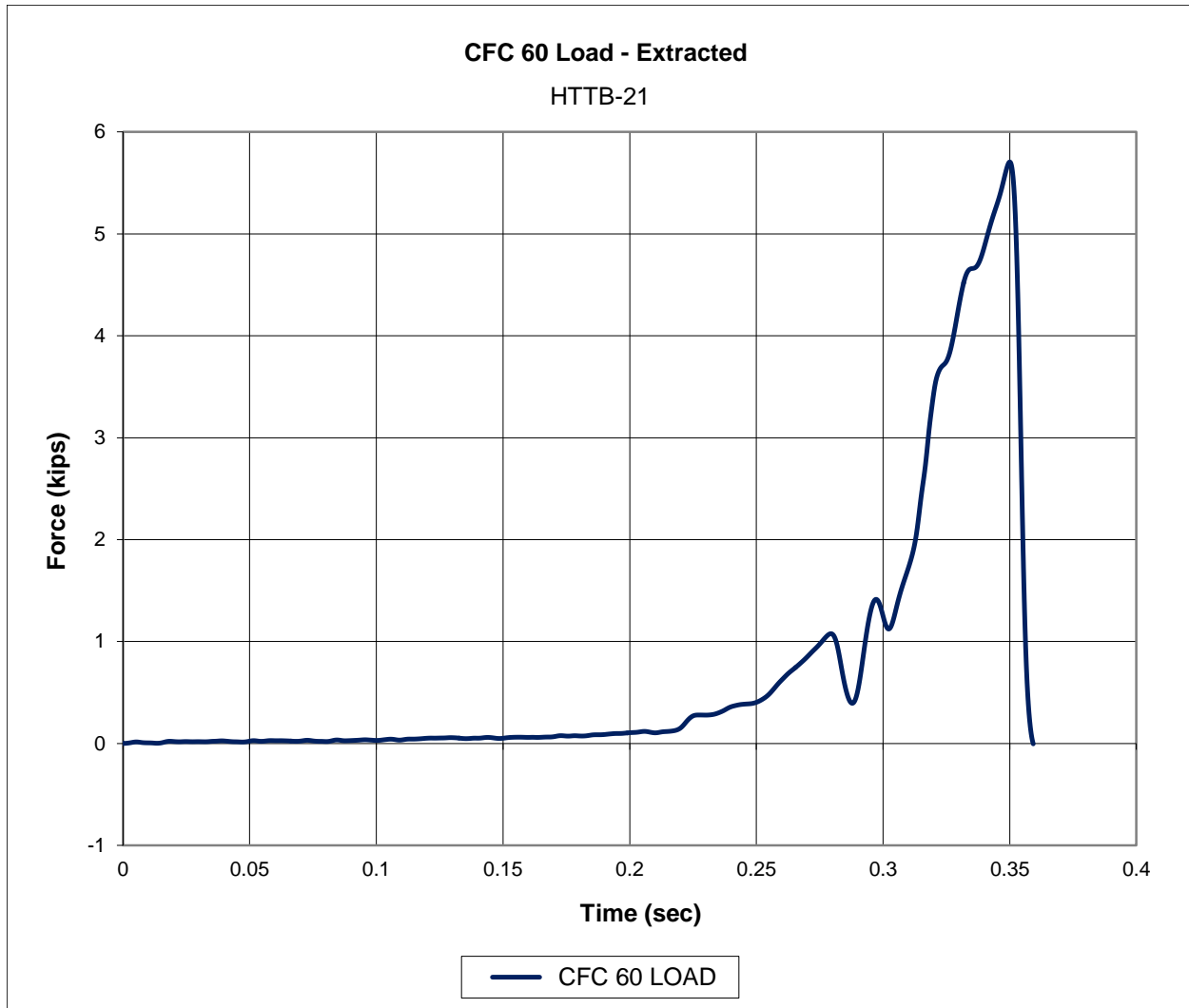


Figure 301. Force-Time Data, Test No. HTTB-21



Figure 302. Pre-Test and Post-Test Photographs, Test No. HTTPB-21

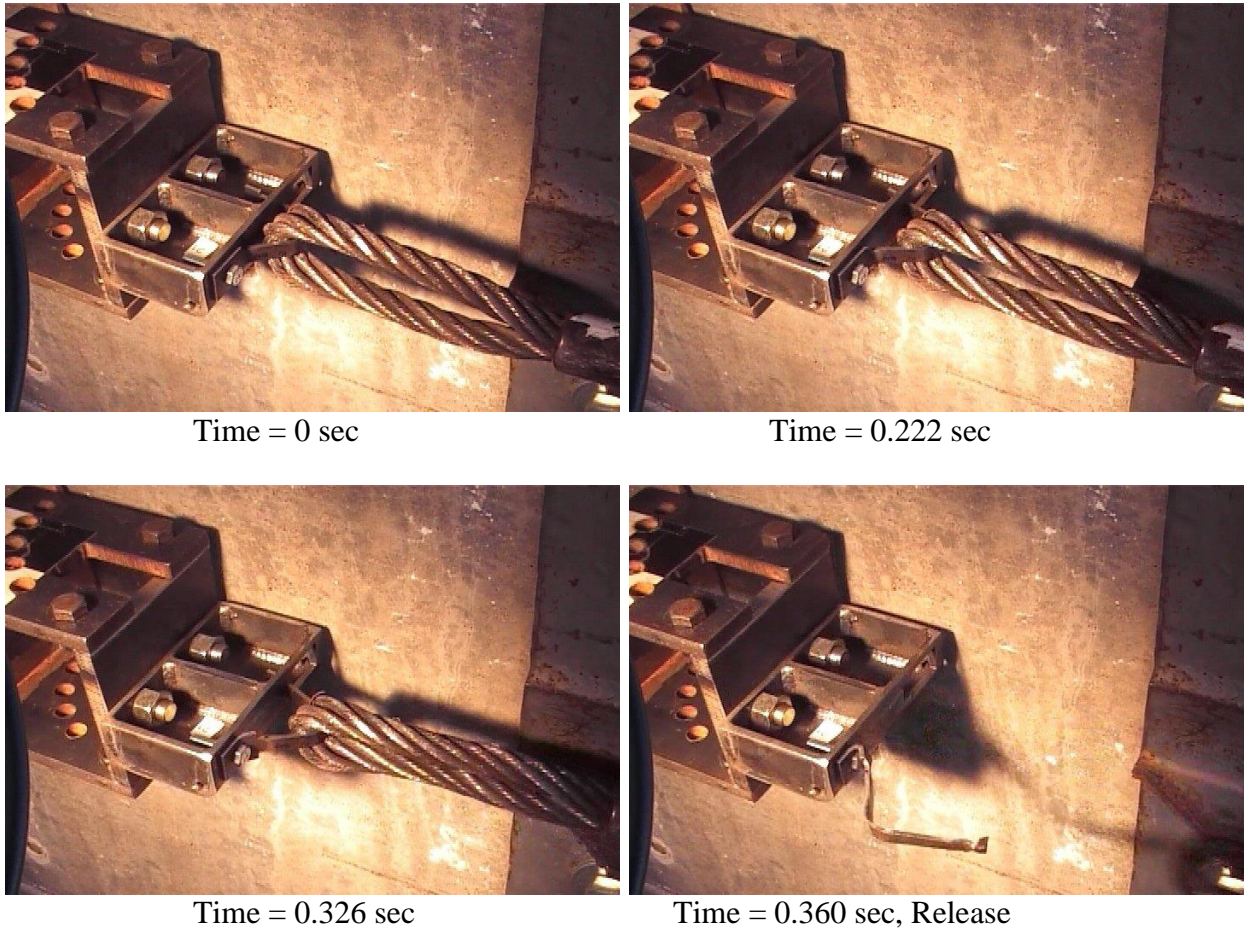


Figure 303. Sequential Photographs, Test No. HTTPB-21

15.1.6 Test No. HTTB-22 (TB V8, Bolted, Lateral)

For test no. HTTB-22, the cable pulled on the 12-gauge, grade 50 steel, bolted tabbed bracket Version 8 at an angle of 90 degrees, perpendicular to the front face of the flange, thus imparting a lateral load. The post consisted of a 5-½-in. (140-mm) long, folded C-section, fabricated from 7-gauge, grade 50 sheet steel. The top end of the tabbed bracket rested in the keyway, while the bottom end was secured to the flange with a 5/16-in. (8-mm), grade 5, hex cap screw and nut. As the cable began to pull on the bracket, the head became caught in the narrow part of the keyway. The cable continued to pull until cracks began to form along the shear planes of the tabs. As the cracks grew, the entire head bent out of plane, until slipping through the keyway (failure location 1). There was also yielding of the steel at the location of the bolt hole, indicating that tensile fracture (failure location 3) was imminent at that location. A peak load of 5.59 kips (24.9 kN) occurred as the head was pulled against the inside of the keyway, just before shear failure. The force versus time plot is shown in Figure 304. Pre- and post-test photographs are shown in Figure 305. Sequential photographs are shown in Figure 306.

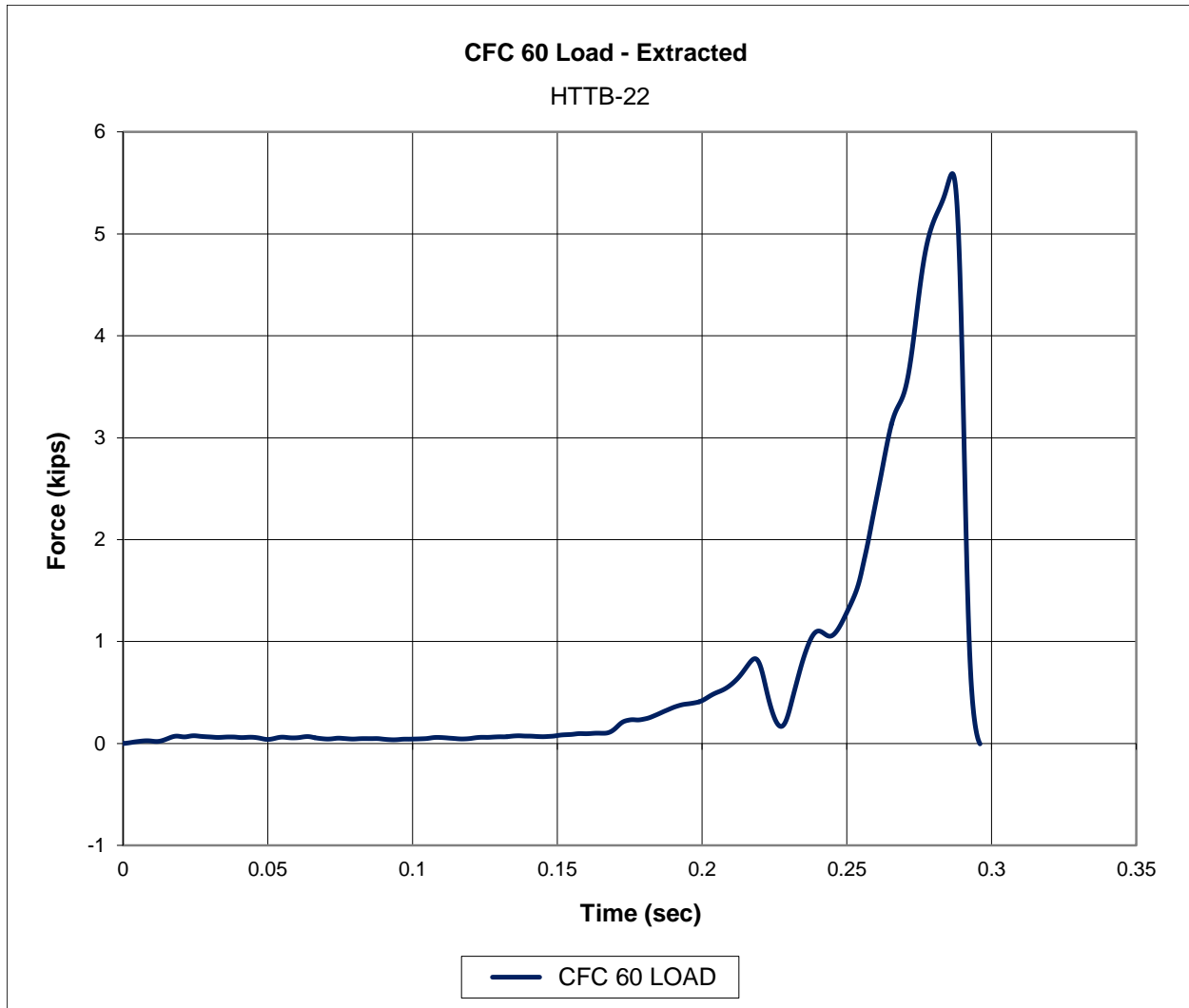


Figure 304. Force-Time Data, Test No. HTTB-22

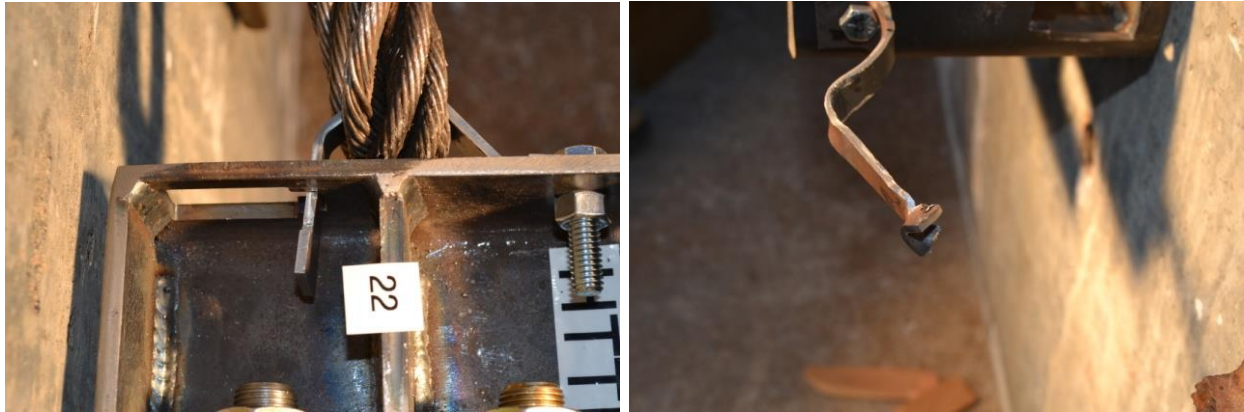
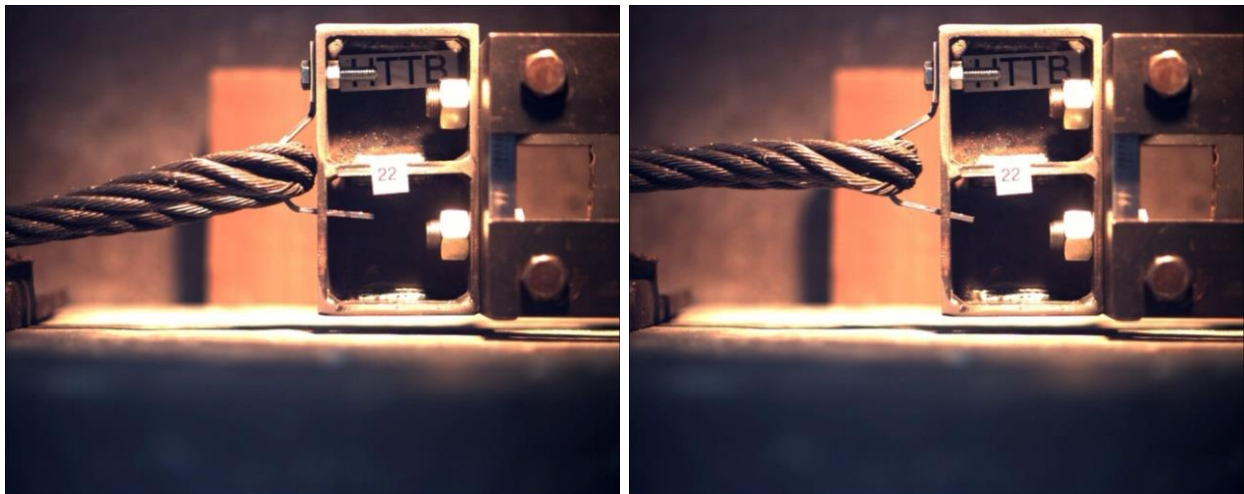
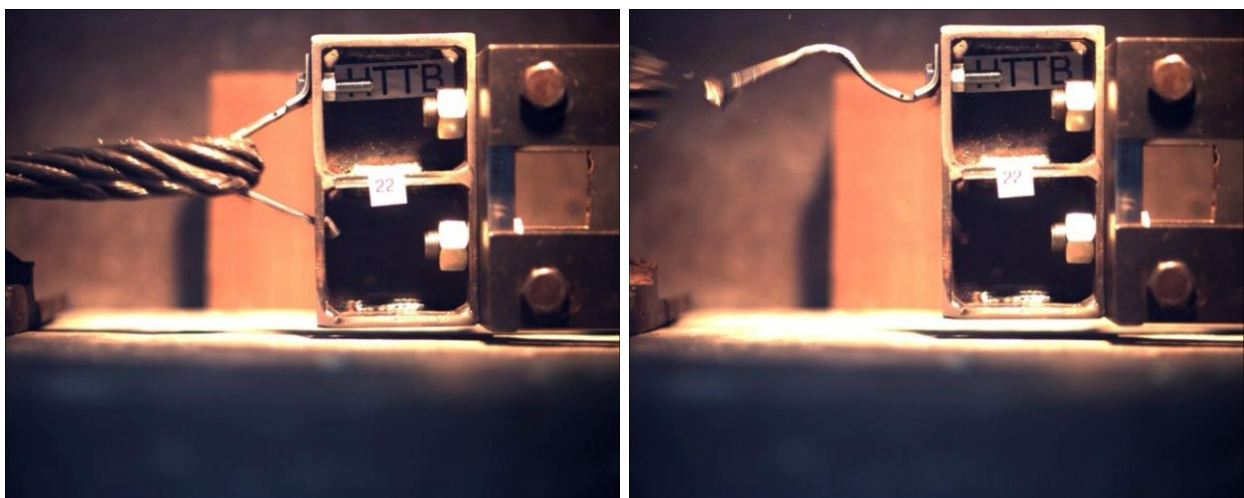


Figure 305. Pre-Test and Post-Test Photographs, Test No. HTTPB-22



Time = 0 sec

Time = 0.188 sec



Time = 0.286 sec

Time = 0.296 sec, Release

Figure 306. Sequential Photographs, Test No. HTTPB-22

15.1.7 Test No. HTTB-23 (TB V5, Bolted, Lateral)

For test no. HTTB-23, the cable pulled on the 12-gauge, grade 50 steel, bolted tabbed bracket Version 5 at an angle of 90 degrees, perpendicular to the front face of the flange, thus imparting a lateral load. The post consisted of a 5-½-in. (140-mm) long, folded C-section, fabricated from 7-gauge, grade 50 sheet steel. The top end of the tabbed bracket rested in the keyway, while the bottom end was secured to the flange with a ¼-in. (6-mm), grade 5, hex cap screw and nut. As the cable began to pull on the bracket, the head became caught in the narrow part of the keyway. The cable continued to pull until fracture occurred through the narrow part of the bracket (failure location 2). A peak load of 3.06 kips (13.6 kN) occurred as the head was pulled against the inside of the keyway, just before fracture. The force versus time plot is shown in Figure 307. Pre- and post-test photographs are shown in Figure 308. Sequential photographs are shown in Figure 309.

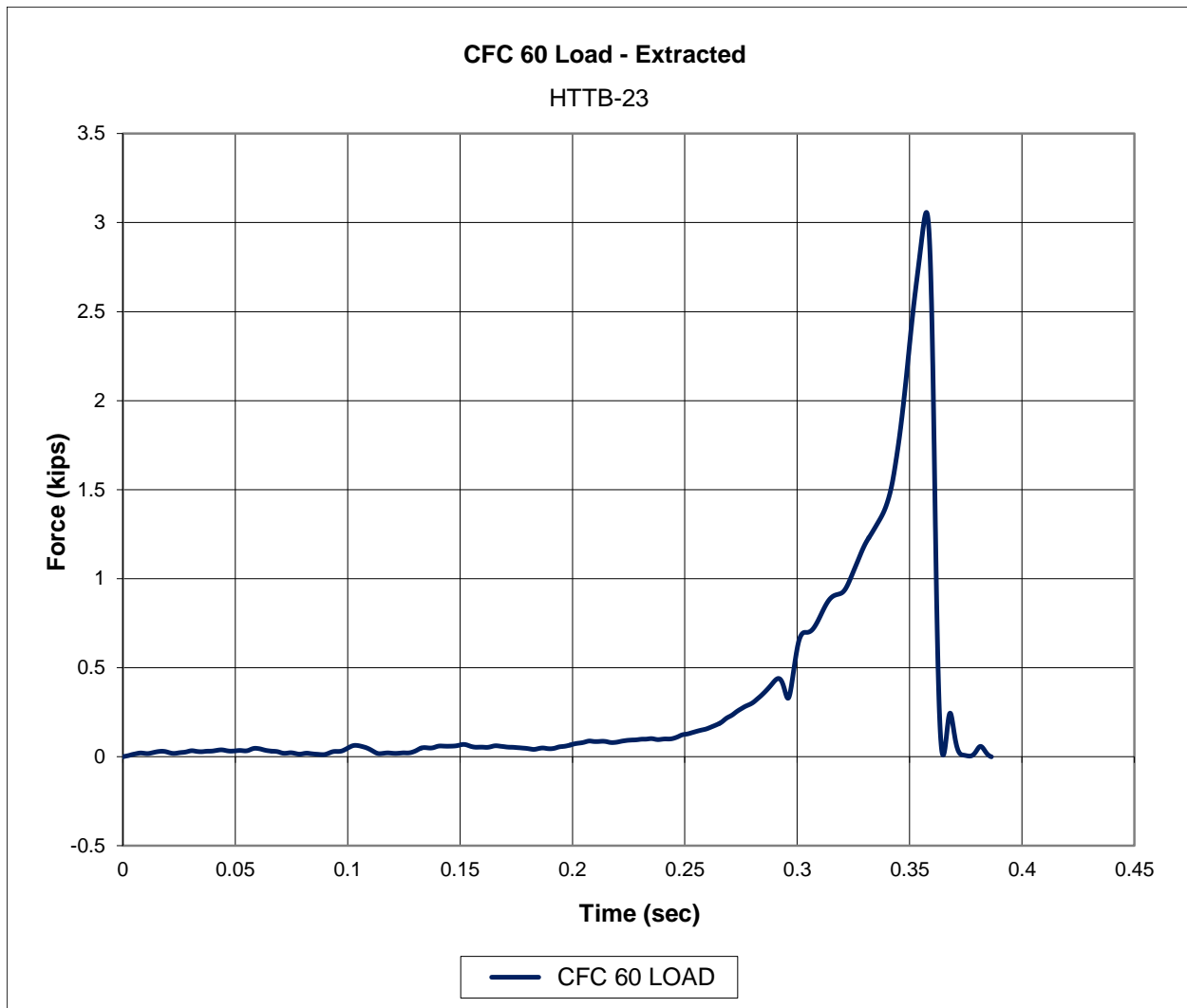


Figure 307. Force-Time Data, Test No. HTTB-23

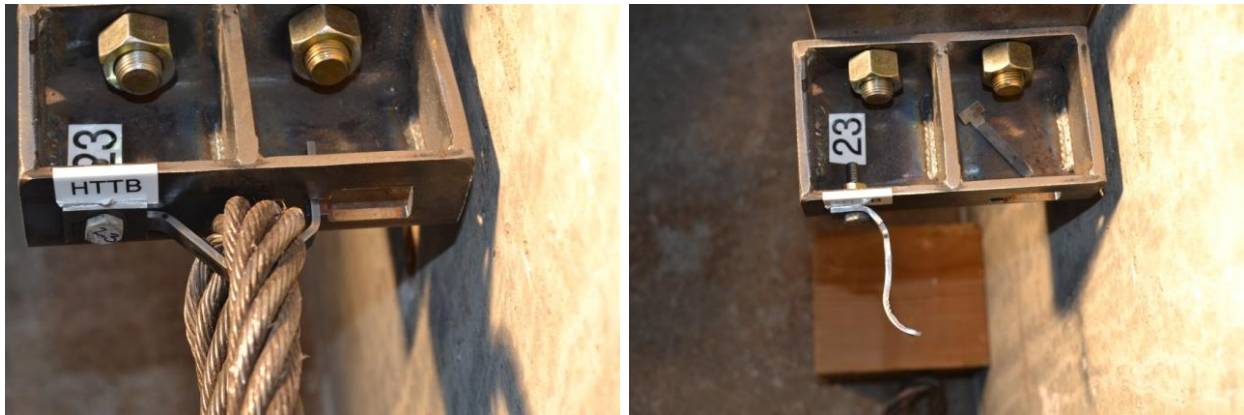
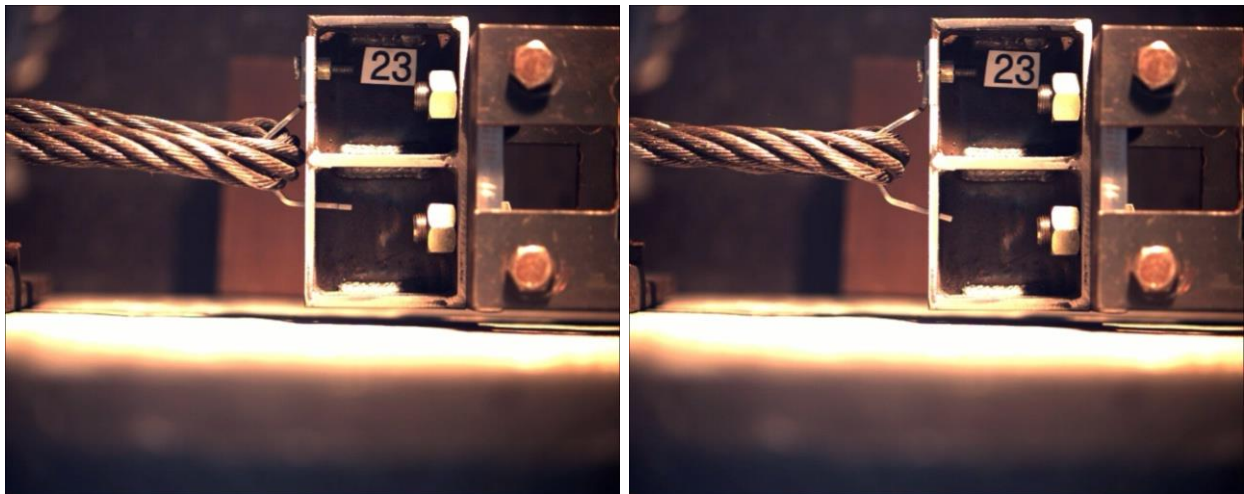
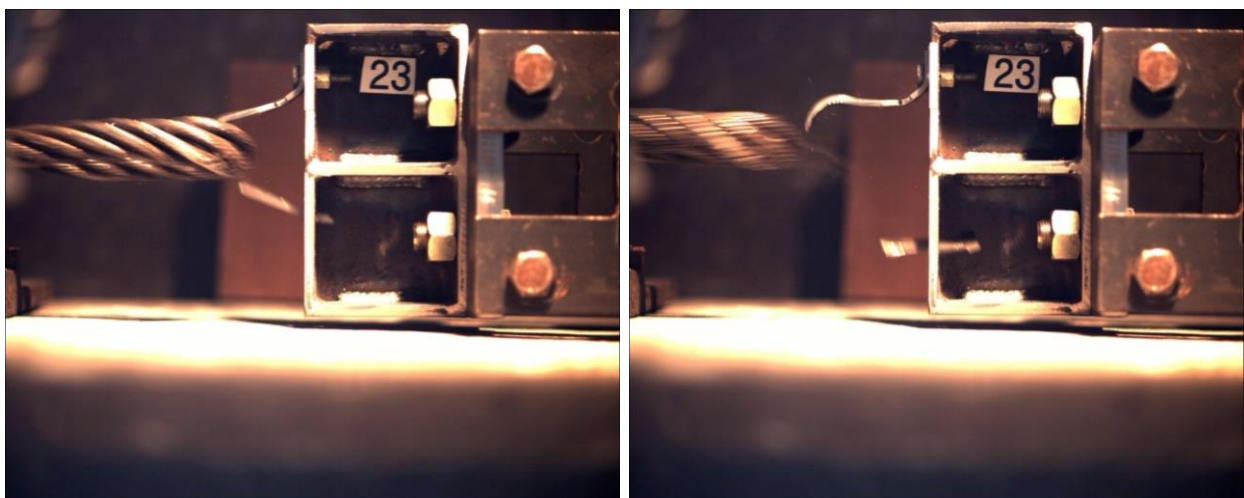


Figure 308. Pre-Test and Post-Test Photographs, Test No. HTTPB-23



Time = 0 sec

Time = 0.302 sec



Time = 0.380 sec

Time = 0.386 sec, Release

Figure 309. Sequential Photographs, Test No. HTTPB-23

15.1.8 Test No. HTTB-24 (TB V5, Bolted, Lateral)

For test no. HTTB-24, the cable pulled on the 12-gauge, grade 50 steel, bolted tabbed bracket Version 5 at an angle of 90 degrees, perpendicular to the front face of the flange, thus imparting a lateral load. The post consisted of a 5-½-in. (140-mm) long, folded C-section, fabricated from 7-gauge, grade 50 sheet steel. The top end of the tabbed bracket rested in the keyway, while the bottom end was secured to the flange with a ¼-in. (6-mm), grade 5, hex cap screw and nut. As the cable began to pull on the bracket, the head became caught in the narrow part of the keyway. The cable continued to pull until fracture occurred through the narrow part of the bracket (failure location 2). A peak load of 2.97 kips (13.2 kN) occurred as the head was pulled against the inside of the keyway, just before fracture. The force versus time plot is shown in Figure 310. Pre- and post-test photographs are shown in Figure 311. Sequential photographs are shown in Figure 312.

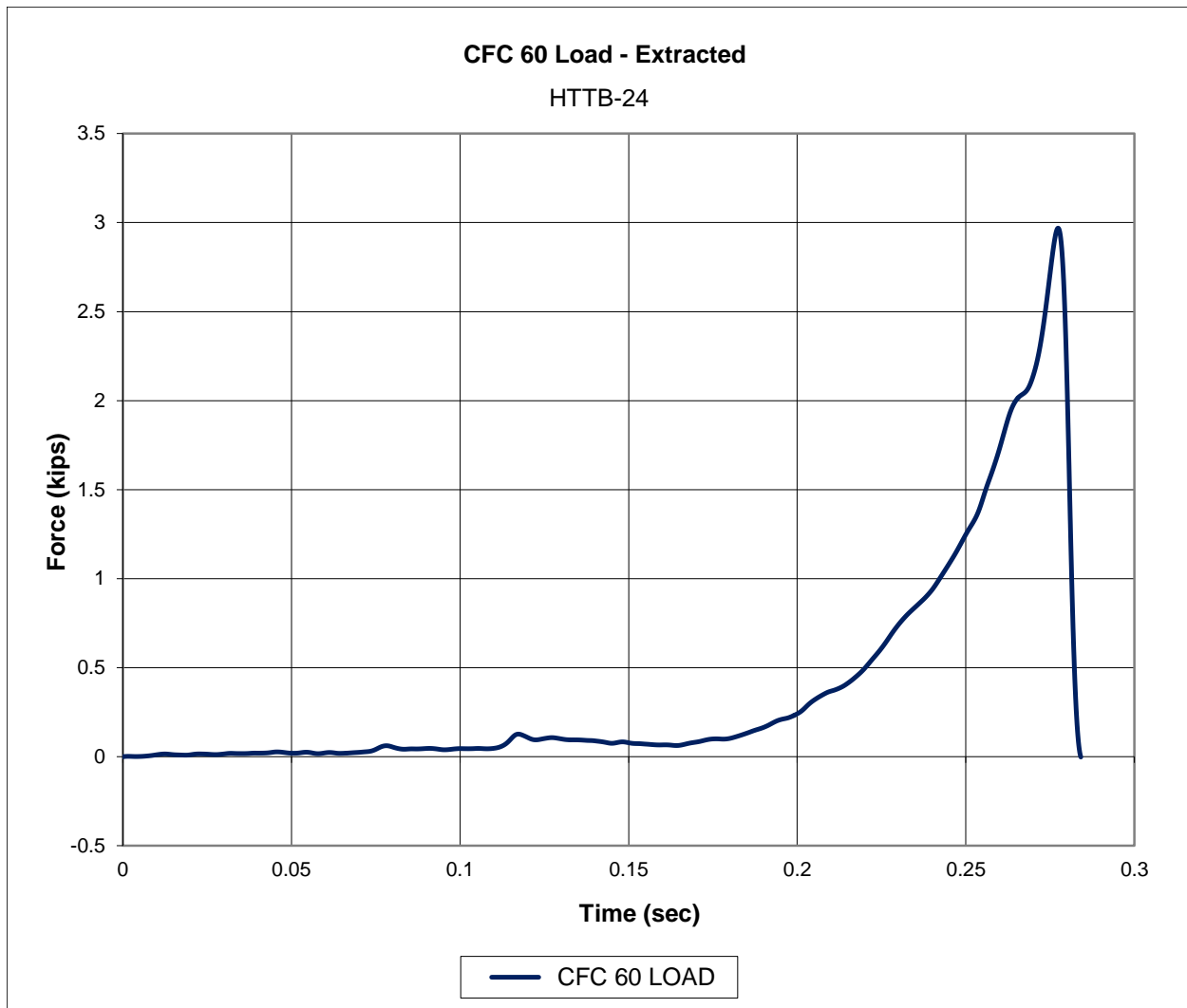
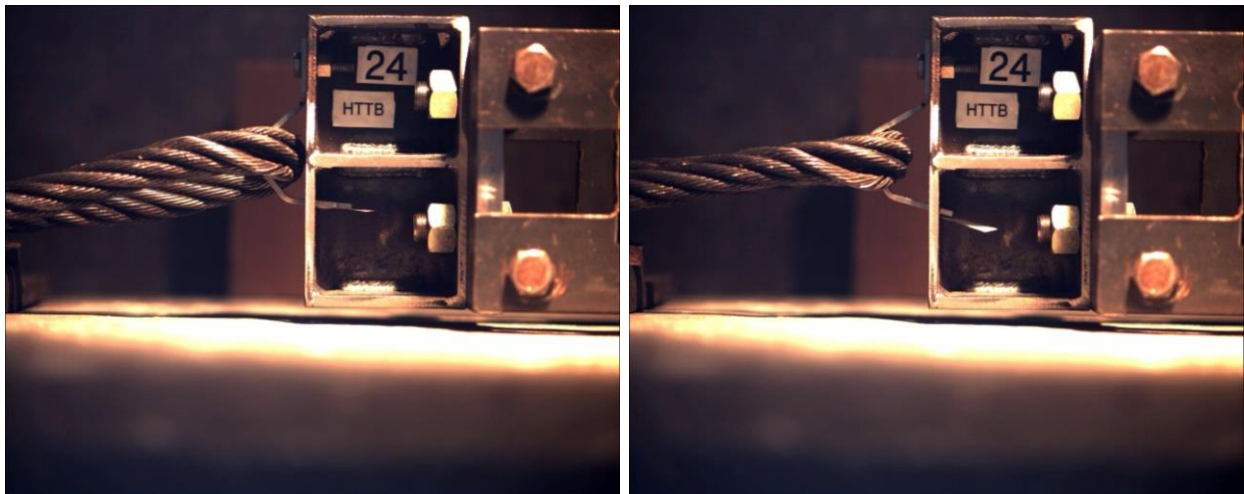


Figure 310. Force-Time Data, Test No. HTTB-24

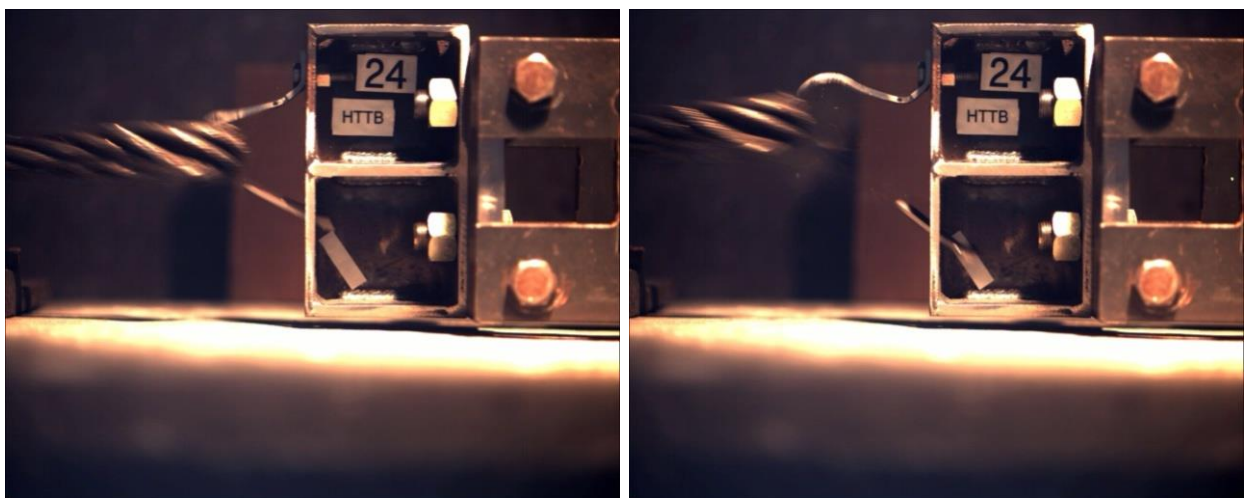


Figure 311. Pre-Test and Post-Test Photographs, Test No. HTTPB-24



Time = 0 sec

Time = 0.114 sec



Time = 0.280 sec

Time = 0.284 sec, Release

Figure 312. Sequential Photographs, Test No. HTTPB-24

15.1.9 Test No. HTTB-25 (TB V6, Bolted, Lateral)

For test no. HTTB-25, the cable pulled on the 14-gauge, grade 50 steel, bolted tabbed bracket Version 6 at an angle of 90 degrees, perpendicular to the front face of the flange, thus imparting a lateral load. The post consisted of a 5-½-in. (140-mm) long, folded C-section, fabricated from 7-gauge, grade 50 sheet steel. The top end of the tabbed bracket rested in the keyway, while the bottom end was secured to the flange with a 5/16-in. (8-mm), grade 5, hex cap screw and nut. As the cable began to pull on the bracket, the head became caught in the narrow part of the keyway. The cable continued to pull until cracks began to form along the shear planes of the tabs. As the cracks grew, the entire head bent out of plane, until slipping through the keyway (failure location 1). There was also yielding of the steel at the location of the bolt hole, indicating that tensile fracture (failure location 3) was imminent at that location. A peak load of 3.50 kips (15.6 kN) occurred as the head was pulled against the inside of the keyway, just before shear failure. The force versus time plot is shown in Figure 313. Pre- and post-test photographs are shown in Figure 314. Sequential photographs are shown in Figure 315.

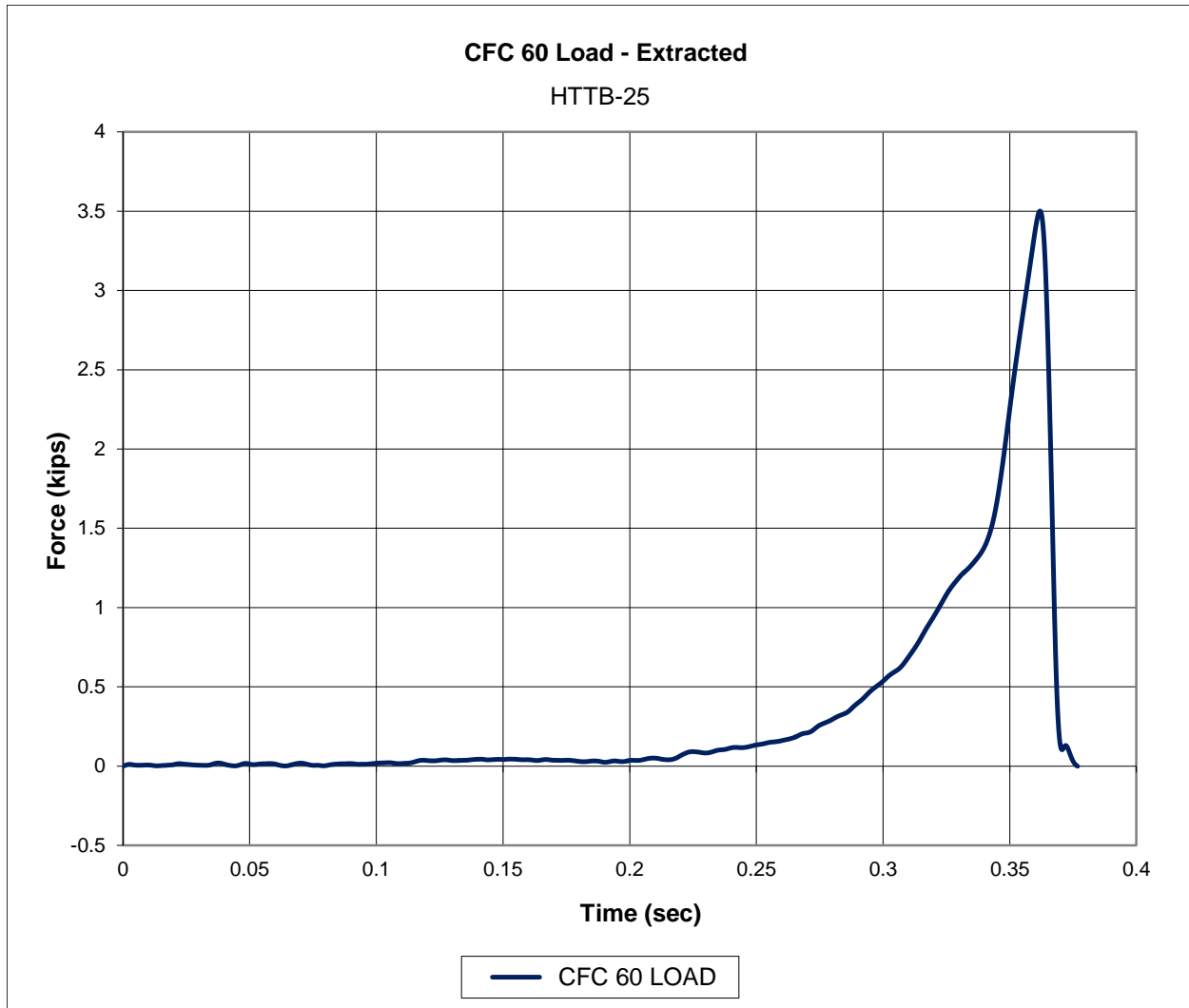


Figure 313. Force-Time Data, Test No. HTTB-25



Figure 314. Pre-Test and Post-Test Photographs, Test No. HTTB-25

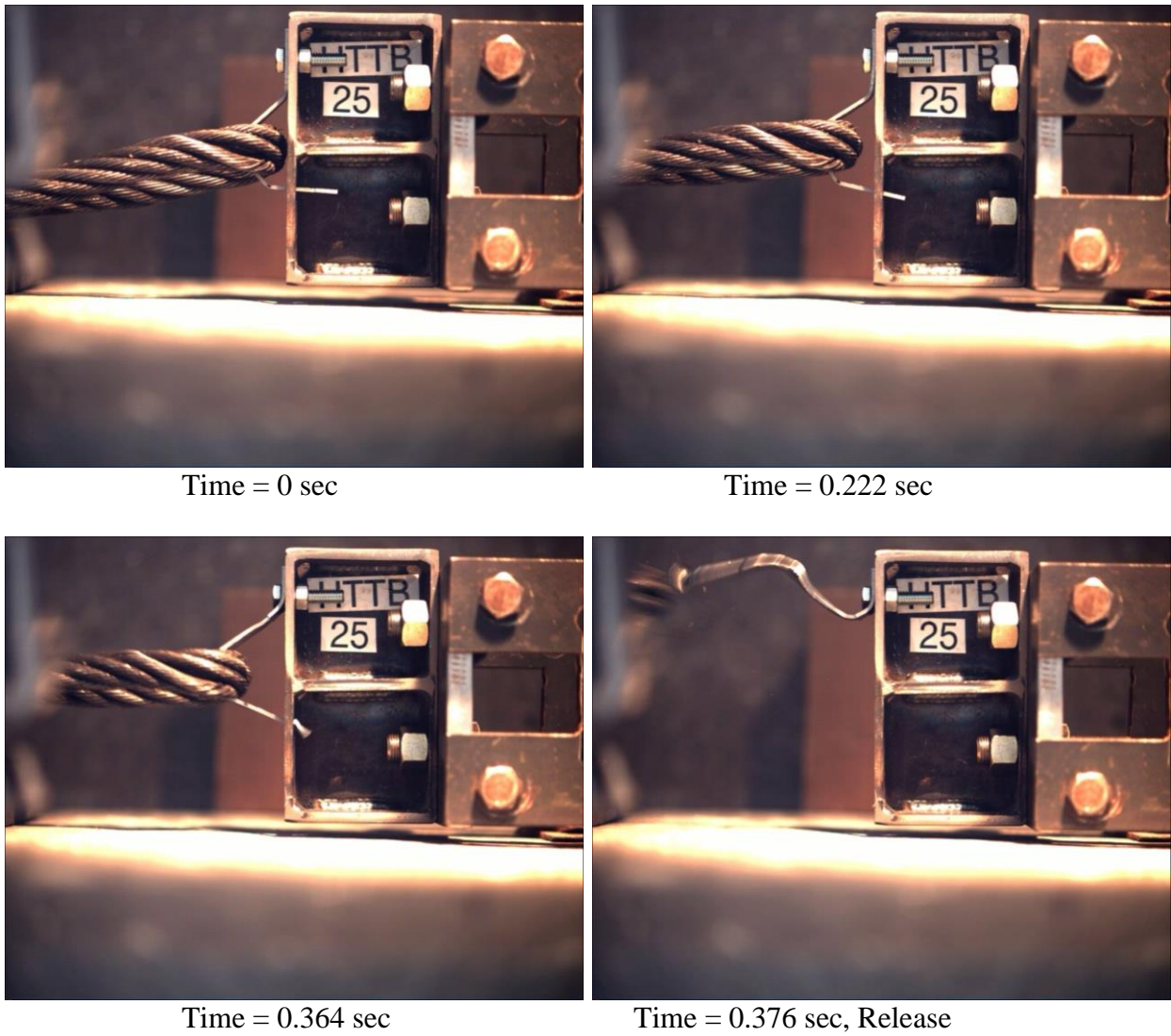


Figure 315. Sequential Photographs, Test No. HTTB-25

15.1.10 Test No. HTTB-26 (TB V6, Bolted, Lateral)

For test no. HTTB-26, the cable pulled on the 14-gauge, grade 50 steel, bolted tabbed bracket Version 6 at an angle of 90 degrees, perpendicular to the front face of the flange, thus imparting a lateral load. The post consisted of a 5-½-in. (140-mm) long, folded C-section, fabricated from 7-gauge, grade 50 sheet steel. The top end of the tabbed bracket rested in the keyway, while the bottom end was secured to the flange with a 5/16-in. (8-mm), grade 5, hex cap screw and nut. As the cable began to pull on the bracket, the head became caught in the narrow part of the keyway. The cable continued to pull until cracks began to form along the shear planes of the tabs. As the cracks grew, the entire head bent out of plane, until slipping through the keyway (failure location 1). There was also yielding of the steel at the location of the bolt hole, indicating that tensile fracture (failure location 3) was imminent at that location. A peak load of 3.44 kips (15.3 kN) occurred as the head was pulled against the inside of the keyway, just before shear failure. The force versus time plot is shown in Figure 316. Pre- and post-test photographs are shown in Figure 317. Sequential photographs are shown in Figure 318.

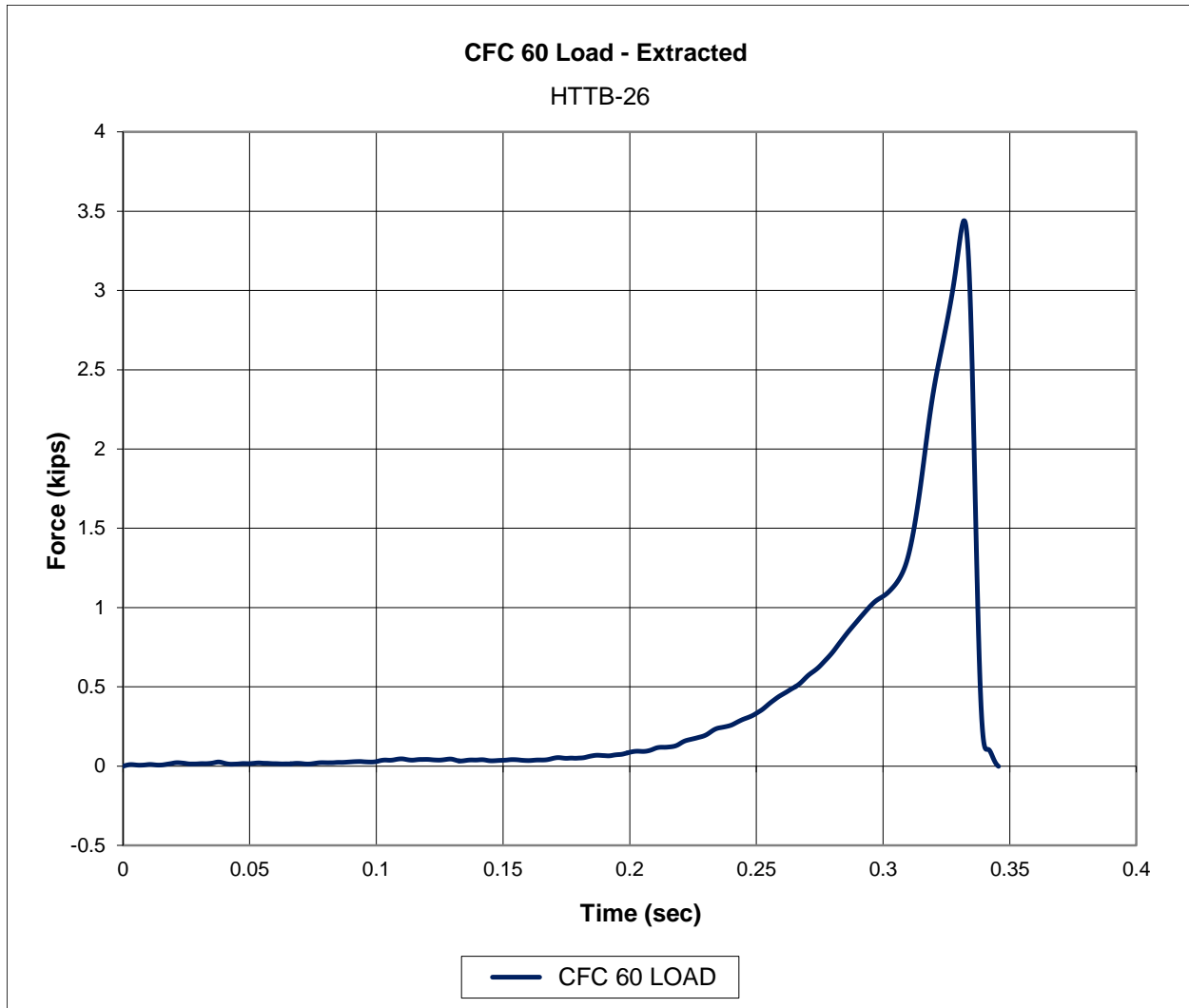
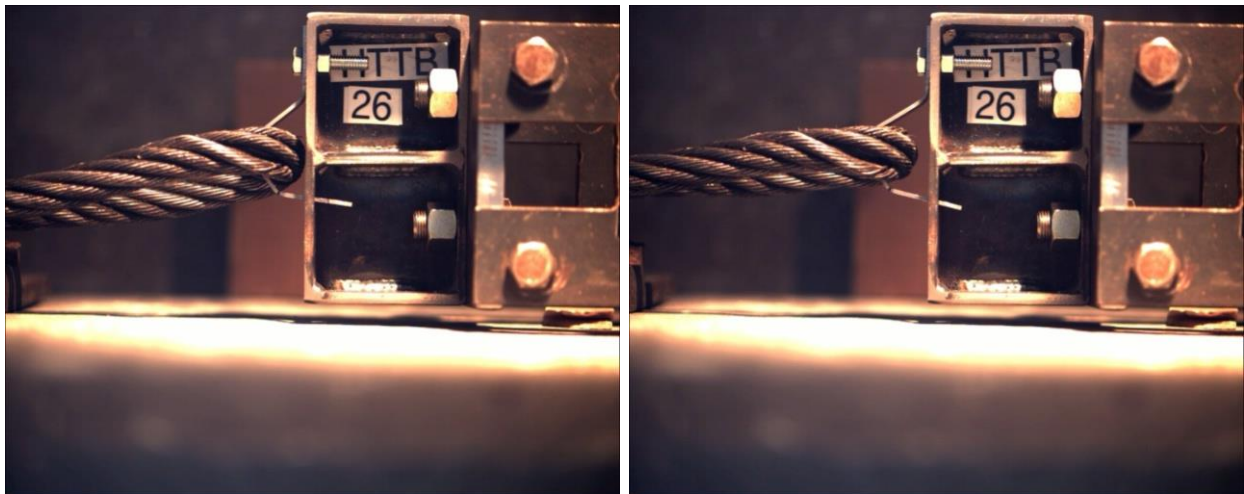


Figure 316. Force-Time Data, Test No. HTTB-26

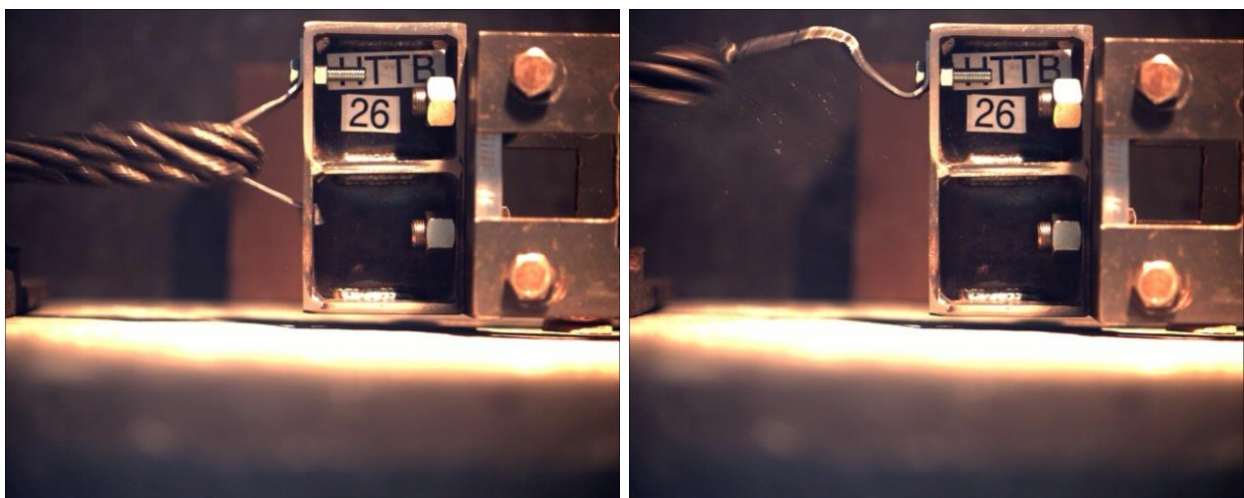


Figure 317. Pre-Test and Post-Test Photographs, Test No. HTTPB-26



Time = 0 sec

Time = 0.200 sec



Time = 0.336 sec

Time = 0.346 sec, Release

Figure 318. Sequential Photographs, Test No. HTTPB-26

15.1.11 Test No. HTTB-27 (TB V7, Bolted, Lateral)

For test no. HTTB-27, the cable pulled on the 11-gauge, grade 50 steel, bolted tabbed bracket Version 7 at an angle of 90 degrees, perpendicular to the front face of the flange, thus imparting a lateral load. The post consisted of a 5-½-in. (140-mm) long, folded C-section, fabricated from 7-gauge, grade 50 sheet steel. The top end of the tabbed bracket rested in the keyway, while the bottom end was secured to the flange with a 5/16-in. (8-mm), grade 5, hex cap screw and nut. As the cable began to pull on the bracket, the head became caught in the narrow part of the keyway. The cable continued to pull until the corner of one of the tabs sheared off. As this happened, the bracket began to twist, allowing the head to slip through the narrow part of the keyway. This type of failure was not anticipated. A peak load of 4.04 kips (18.0 kN) occurred as the head was pulled against the inside of the keyway, just before the corner of the one tab sheared off. The force versus time plot is shown in Figure 319. Pre- and post-test photographs are shown in Figure 320. Sequential photographs are shown in Figure 321.

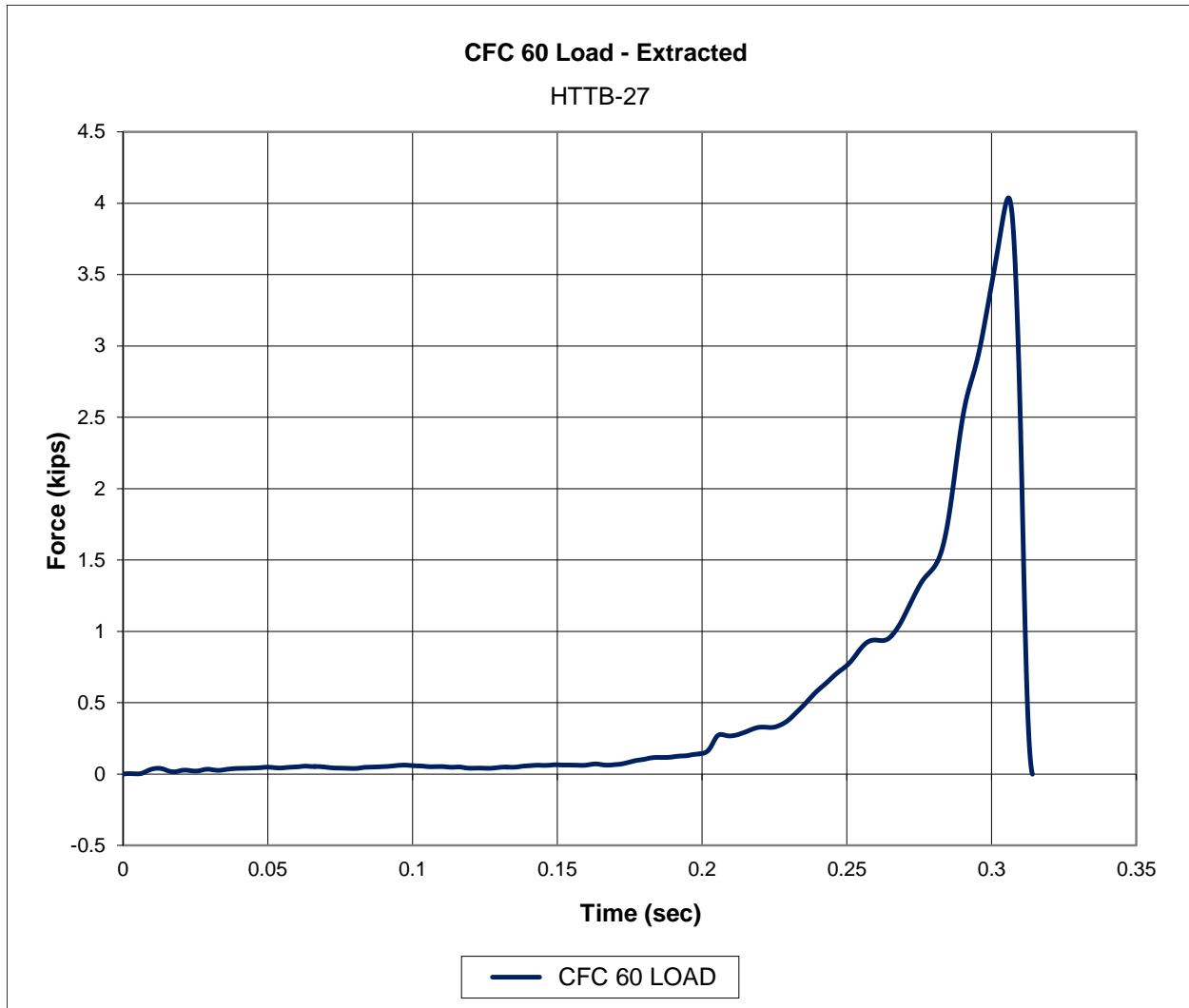


Figure 319. Force-Time Data, Test No. HTTB-27



Figure 320. Pre-Test and Post-Test Photographs, Test No. HTTPB-27

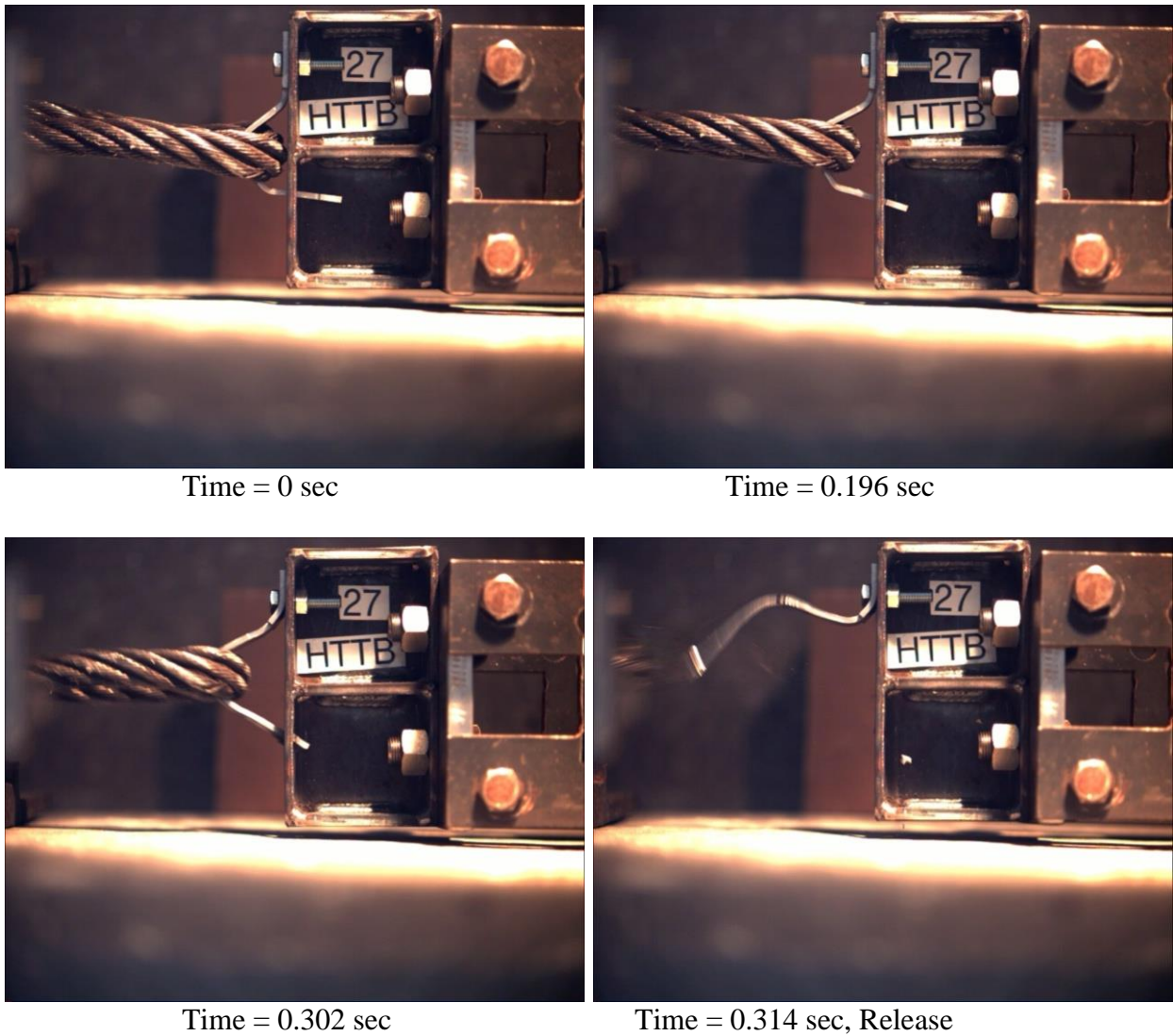


Figure 321. Sequential Photographs, Test No. HTTPB-27

15.1.12 Test No. HTTB-28 (TB V7, Bolted, Lateral)

For test no. HTTB-28, the cable pulled on the 11-gauge, grade 50 steel, bolted tabbed bracket Version 7 at an angle of 90 degrees, perpendicular to the front face of the flange, thus imparting a lateral load. The post consisted of a 5-½-in. (140-mm) long, folded C-section, fabricated from 7-gauge, grade 50 sheet steel. The top end of the tabbed bracket rested in the keyway, while the bottom end was secured to the flange with a 5/16-in. (8-mm), grade 5, hex cap screw and nut. As the cable began to pull on the bracket, the head became caught in the narrow part of the keyway. The cable continued to pull until the corner of one of the tabs sheared off. As this happened, the bracket began to twist, allowing the head to slip through the narrow part of the keyway. This type of failure was not anticipated. A peak load of 4.88 kips (21.7 kN) occurred as the head was pulled against the inside of the keyway, just before the corner of the one tab sheared off. The force versus time plot is shown in Figure 322. Pre- and post-test photographs are shown in Figure 323. Sequential photographs are shown in Figure 324.

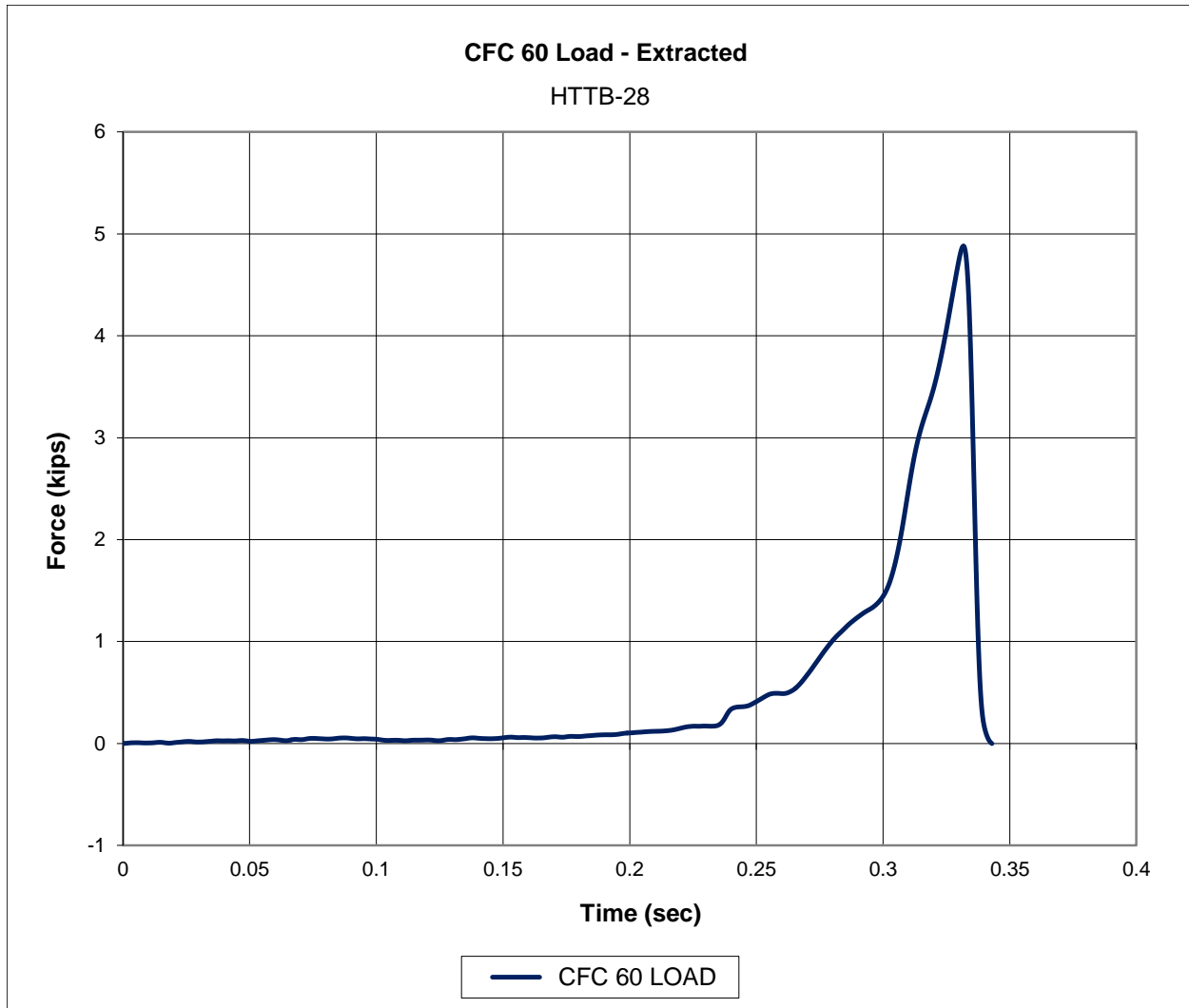


Figure 322. Force-Time Data, Test No. HTTB-28



Figure 323. Pre-Test and Post-Test Photographs, Test No. HTTPB-28

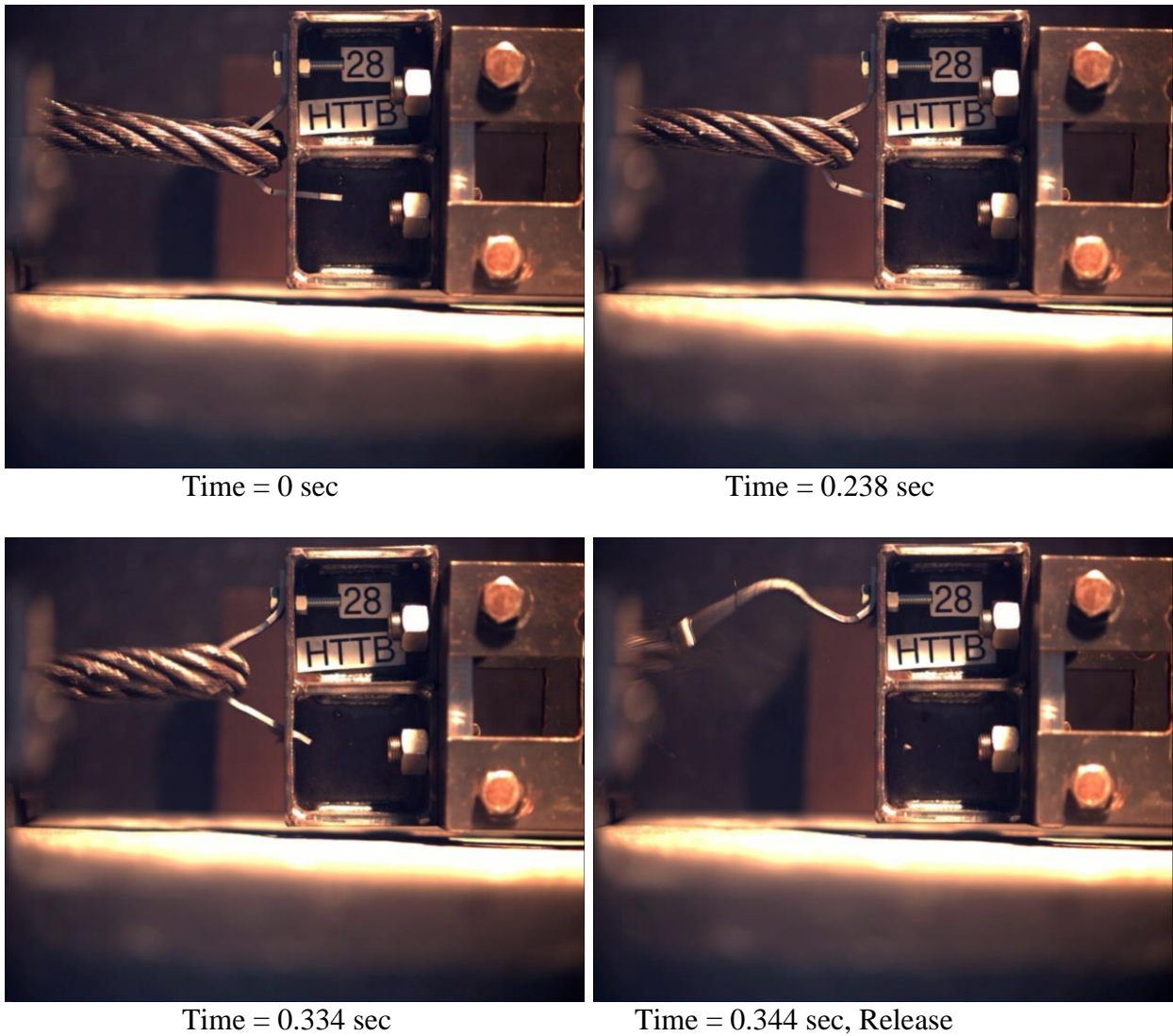


Figure 324. Sequential Photographs, Test No. HTTPB-28

15.1.13 Test No. HTTB-29 (TB V9, Bolted, Lateral)

For test no. HTTB-29, the cable pulled on the 12-gauge, grade 50 steel, bolted tabbed bracket Version 9 at an angle of 90 degrees, perpendicular to the front face of the flange, thus imparting a lateral load. The post consisted of a 5-½-in. (140-mm) long, folded C-section, fabricated from 7-gauge, grade 50 sheet steel. The top end of the tabbed bracket rested in the keyway, while the bottom end was secured to the flange with a 5/16-in. (8-mm), grade 5, hex cap screw and nut. As the cable began to pull on the bracket, the head was not caught in the narrow part of the keyway. Instead of becoming caught in the narrow part of the keyway, the head released through the wide part freely. A peak load of 768 lb (3.42 kN) occurred as the bracket bent straight out by the cable. The force versus time plot is shown in Figure 325. Pre- and post-test photographs are shown in Figure 326. Sequential photographs are shown in Figure 327.

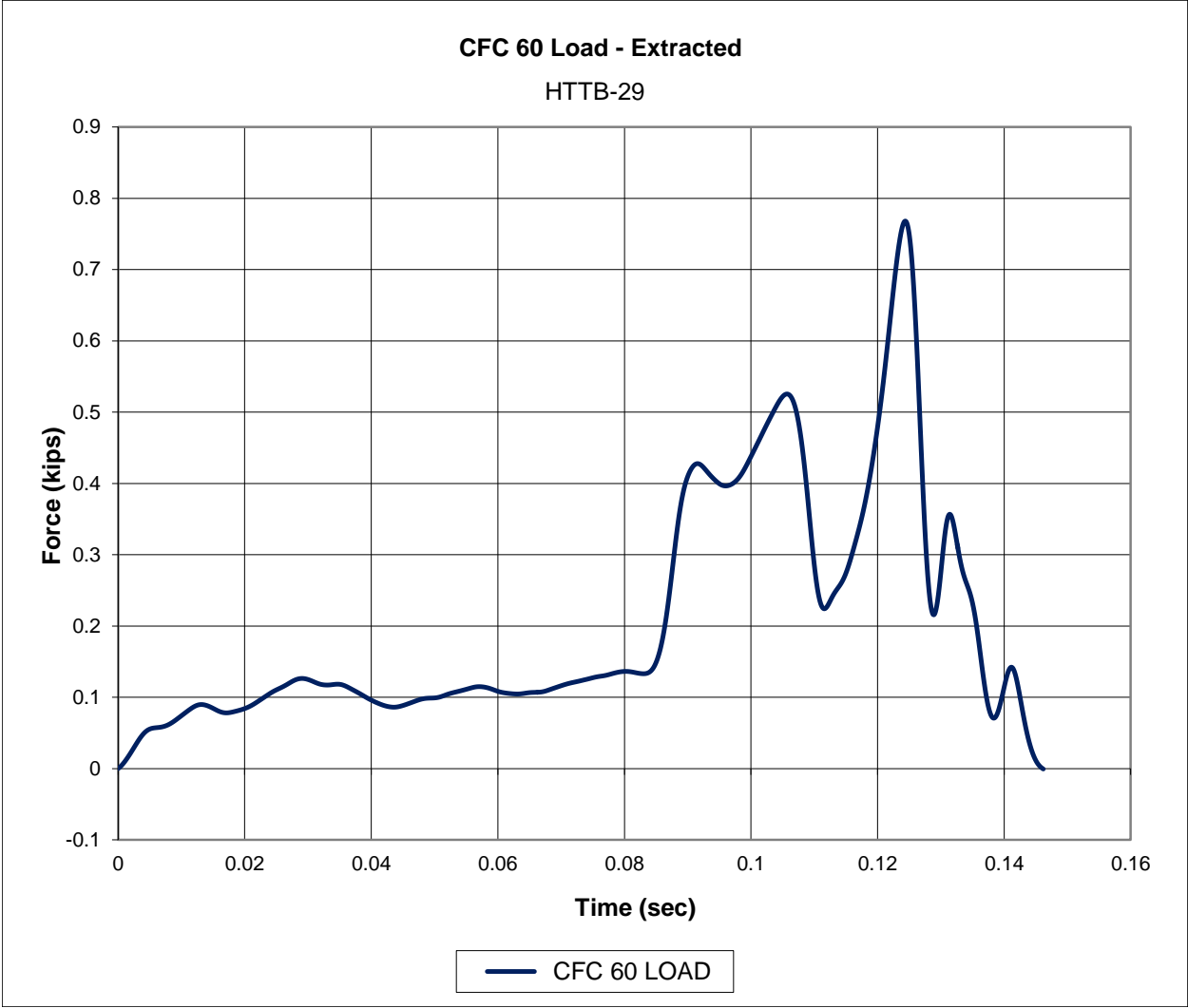


Figure 325. Force-Time Data, Test No. HTTB-29



Figure 326. Pre-Test and Post-Test Photographs, Test No. HTTPB-29

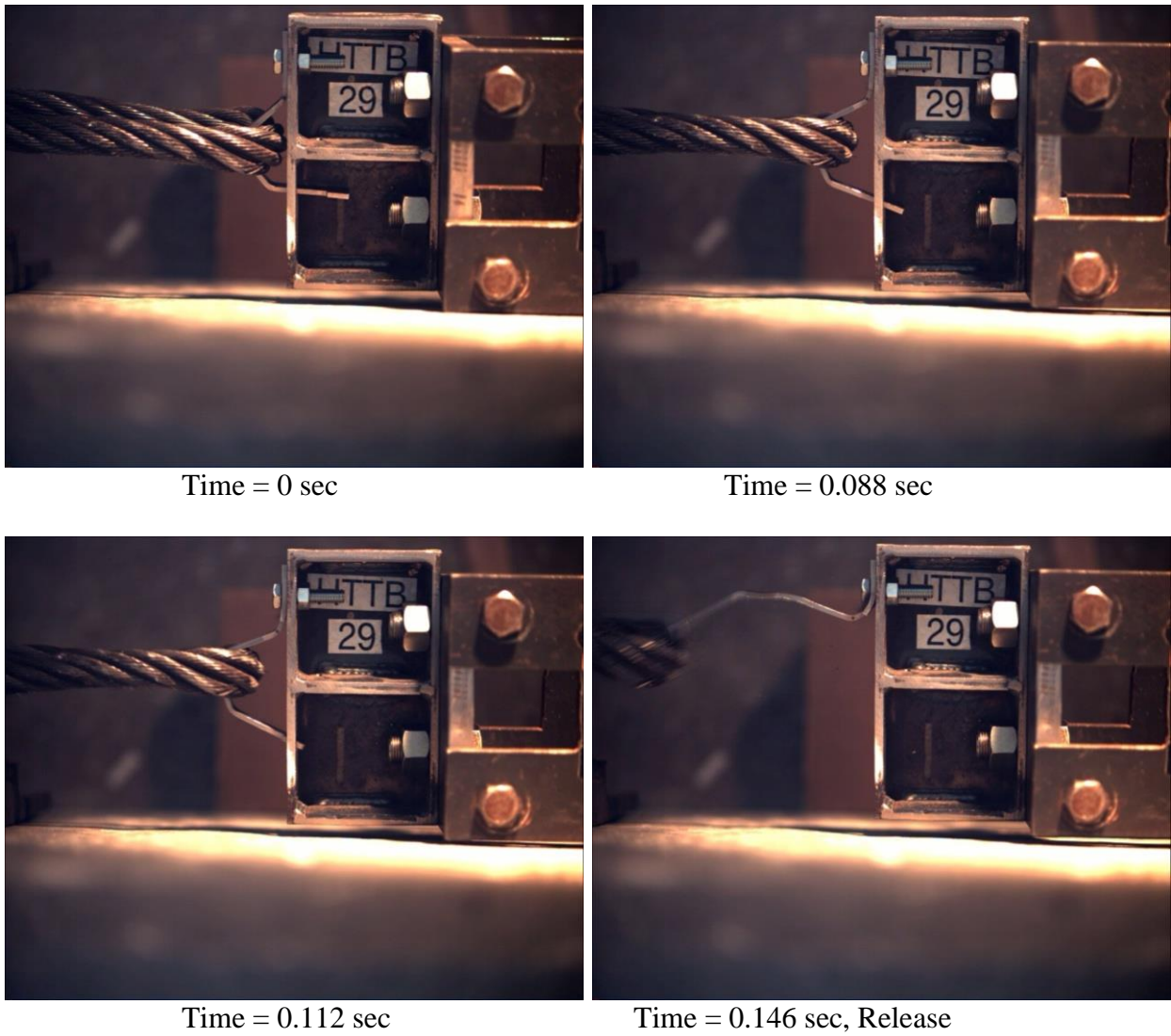


Figure 327. Sequential Photographs, Test No. HTTPB-29

15.1.14 Test No. HTTB-30 (TB V9, Bolted, Lateral)

For test no. HTTB-30, the cable pulled on the 12-gauge, grade 50 steel, bolted tabbed bracket Version 9 at an angle of 90 degrees, perpendicular to the front face of the flange, thus imparting a lateral load. The post consisted of a 5-½-in. (140-mm) long, folded C-section, fabricated from 7-gauge, grade 50 sheet steel. The top end of the tabbed bracket rested in the keyway, while the bottom end was secured to the flange with a 5/16-in. (8-mm), grade 5, hex cap screw and nut. As the cable began to pull on the bracket, the head was not caught in the narrow part of the keyway. Instead of becoming caught in the narrow part of the keyway, the head released through the wide part freely. A peak load of 437 lb (1.94 kN) occurred as the bracket bent straight out by the cable. The force versus time plot is shown in Figure 328. Pre- and post-test photographs are shown in Figure 329. Sequential photographs are shown in Figure 330.

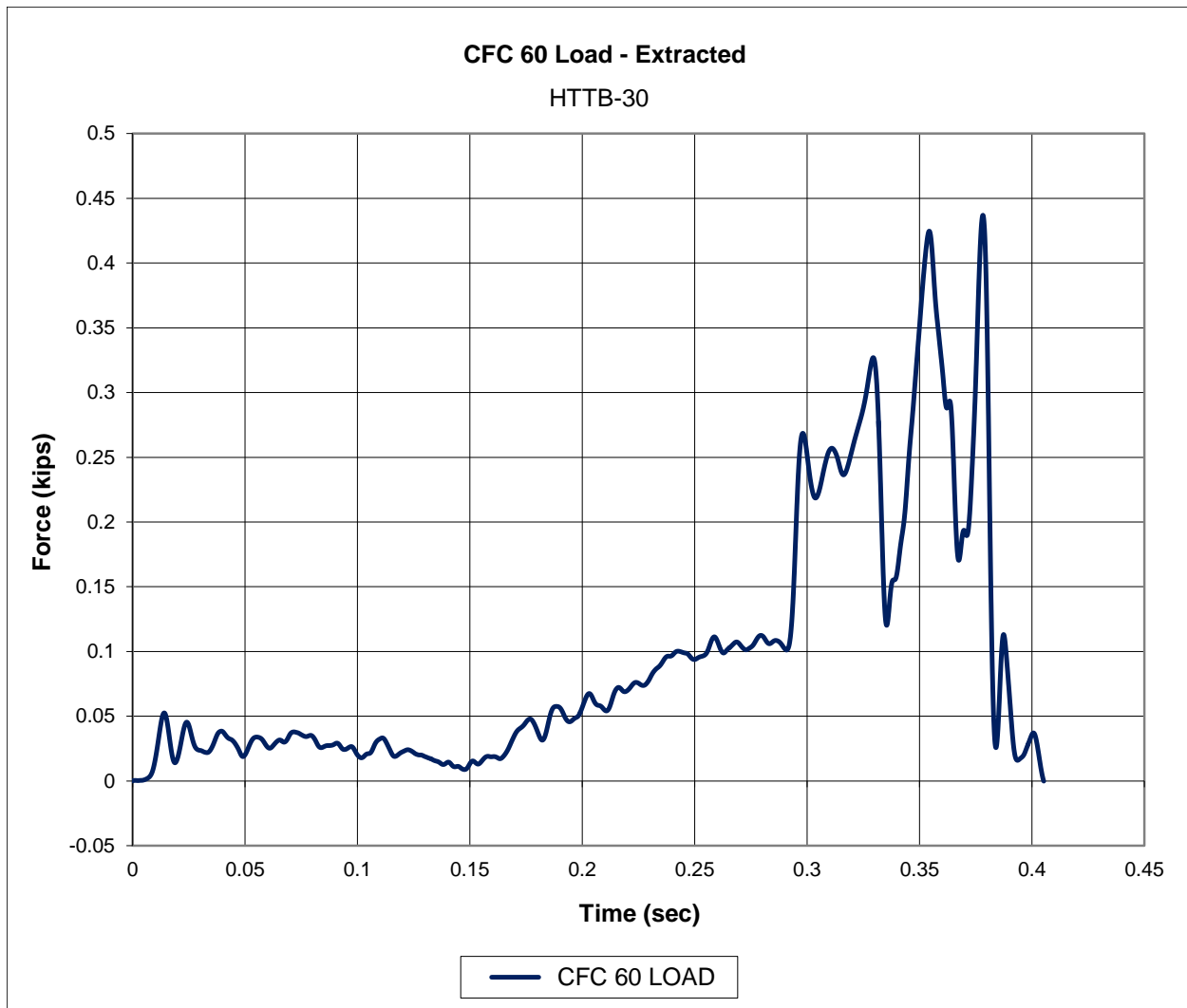


Figure 328. Force-Time Data, Test No. HTTB-30



Figure 329. Pre-Test and Post-Test Photographs, Test No. HTTB-30

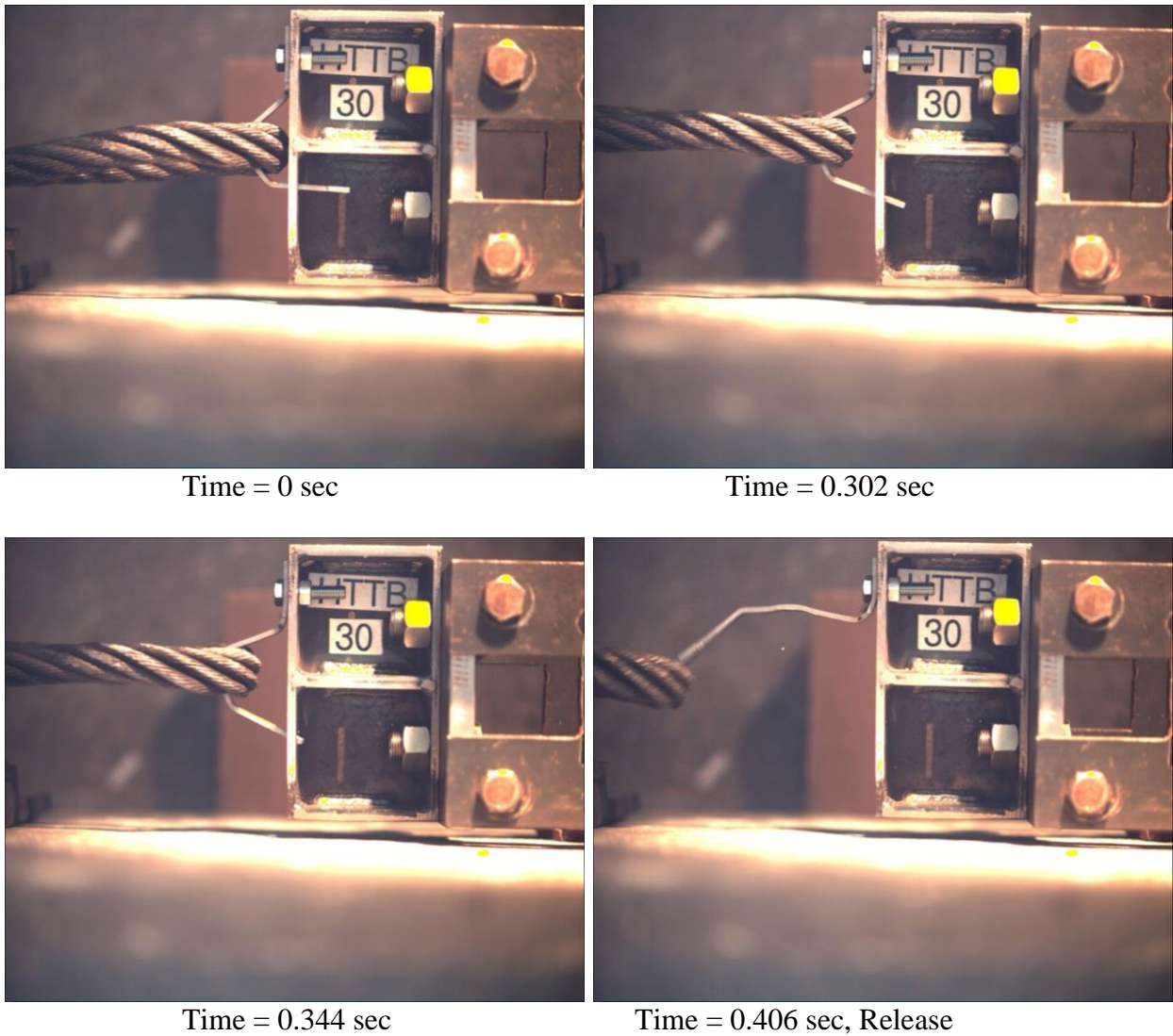


Figure 330. Sequential Photographs, Test No. HTTB-30

15.1.15 Test No. HTTB-31 (TB V10, Bolted, Lateral)

For test no. HTTB-31, the cable pulled on the 12-gauge, grade 50 steel, bolted tabbed bracket Version 10 at an angle of 90 degrees, perpendicular to the front face of the flange, thus imparting a lateral load. The post consisted of a 5-½-in. (140-mm) long, folded C-section, fabricated from 7-gauge, grade 50 sheet steel. The top end of the tabbed bracket rested in the keyway, while the bottom end was secured to the flange with a ¼-in. (6-mm), grade 5, hex cap screw and nut. As the cable began to pull on the bracket, the head became caught in the narrow part of the keyway. The cable continued to pull until fracture occurred through the cross-section where the bolt hole was located (failure location 3). A peak load of 6.03 kips (26.8 kN) occurred as the head was pulled against the inside of the keyway, just before fracture. The force versus time plot is shown in Figure 331. Pre- and post-test photographs are shown in Figure 332. Sequential photographs are shown in Figure 333.

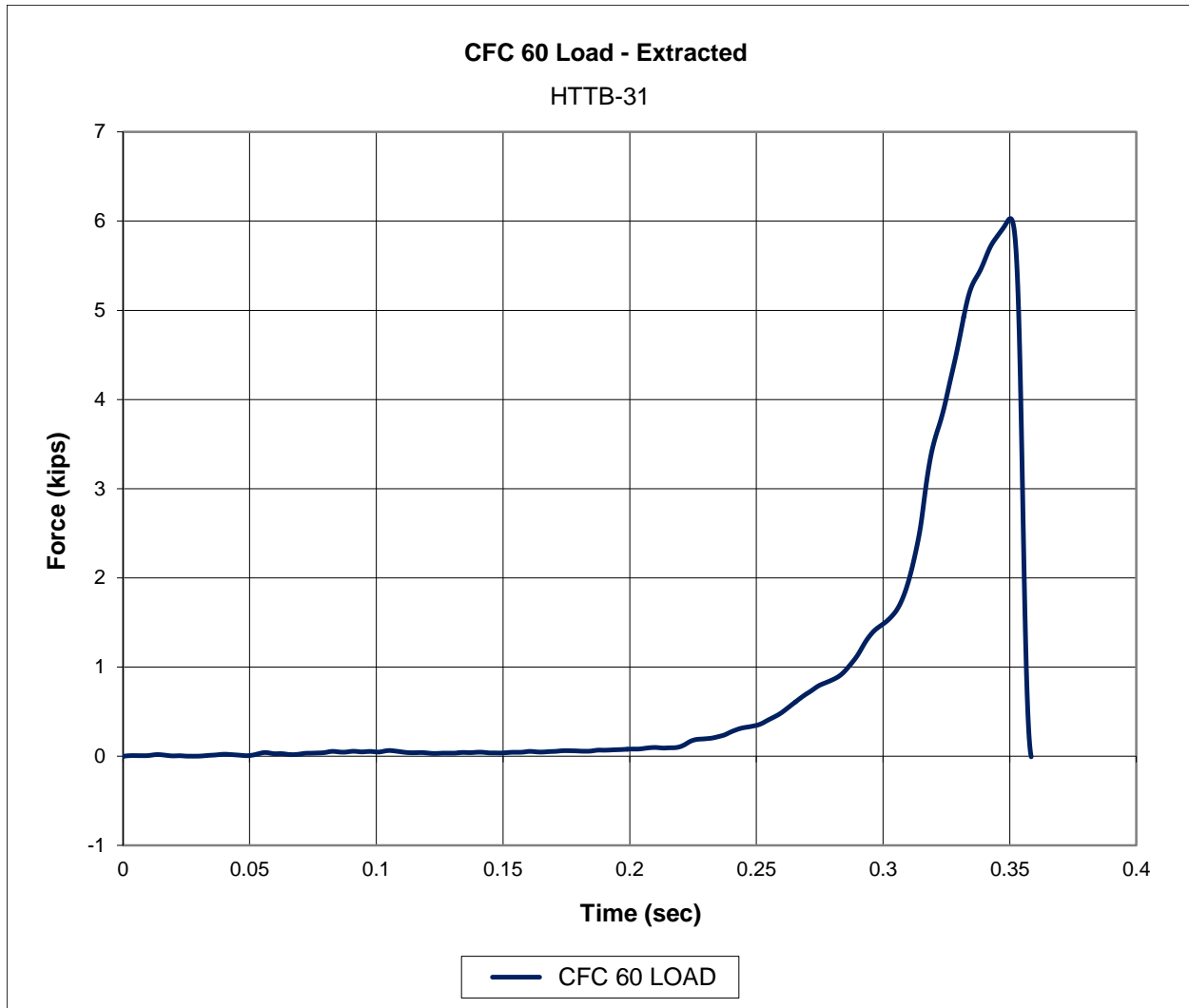


Figure 331. Force-Time Data, Test No. HTTB-31



Figure 332. Pre-Test and Post-Test Photographs, Test No. HTTB-31

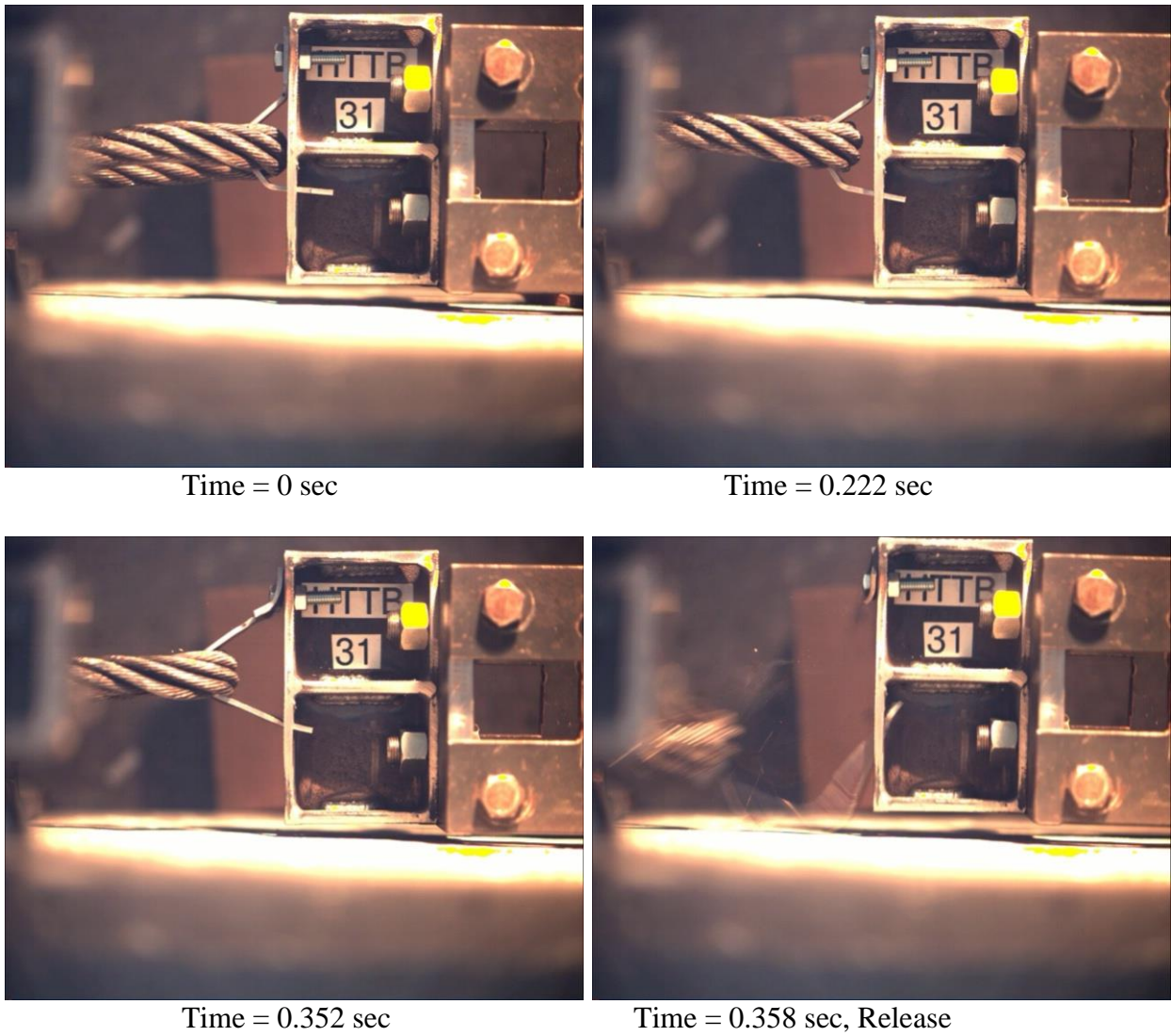


Figure 333. Sequential Photographs, Test No. HTTB-31

15.1.16 Test No. HTTB-32 (TB V10, Bolted, Lateral)

For test no. HTTB-32, the cable pulled on the 12-gauge, grade 50 steel, bolted tabbed bracket Version 10 at an angle of 90 degrees, perpendicular to the front face of the flange, thus imparting a lateral load. The post consisted of a 5-½-in. (140-mm) long, folded C-section, fabricated from 7-gauge, grade 50 sheet steel. The top end of the tabbed bracket rested in the keyway, while the bottom end was secured to the flange with a ¼-in. (6-mm), grade 5, hex cap screw and nut. As the cable began to pull on the bracket, the head became caught in the narrow part of the keyway. The cable continued to pull until fracture occurred through the narrow part of the bracket (failure location 2). There was also significant cracking of the cross-section at the location of the bolt hole, indicating that tensile fracture (failure location 3) was imminent at that location. A peak load of 6.17 kips (27.4 kN) occurred as the head was pulled against the inside of the keyway, just before fracture. Significant cracking occurred at the location of the bolt hole as well, indicating that tensile failure was imminent at that location. The force versus time plot is shown in Figure 334. Pre- and post-test photographs are shown in Figure 335. Sequential photographs are shown in Figure 336.

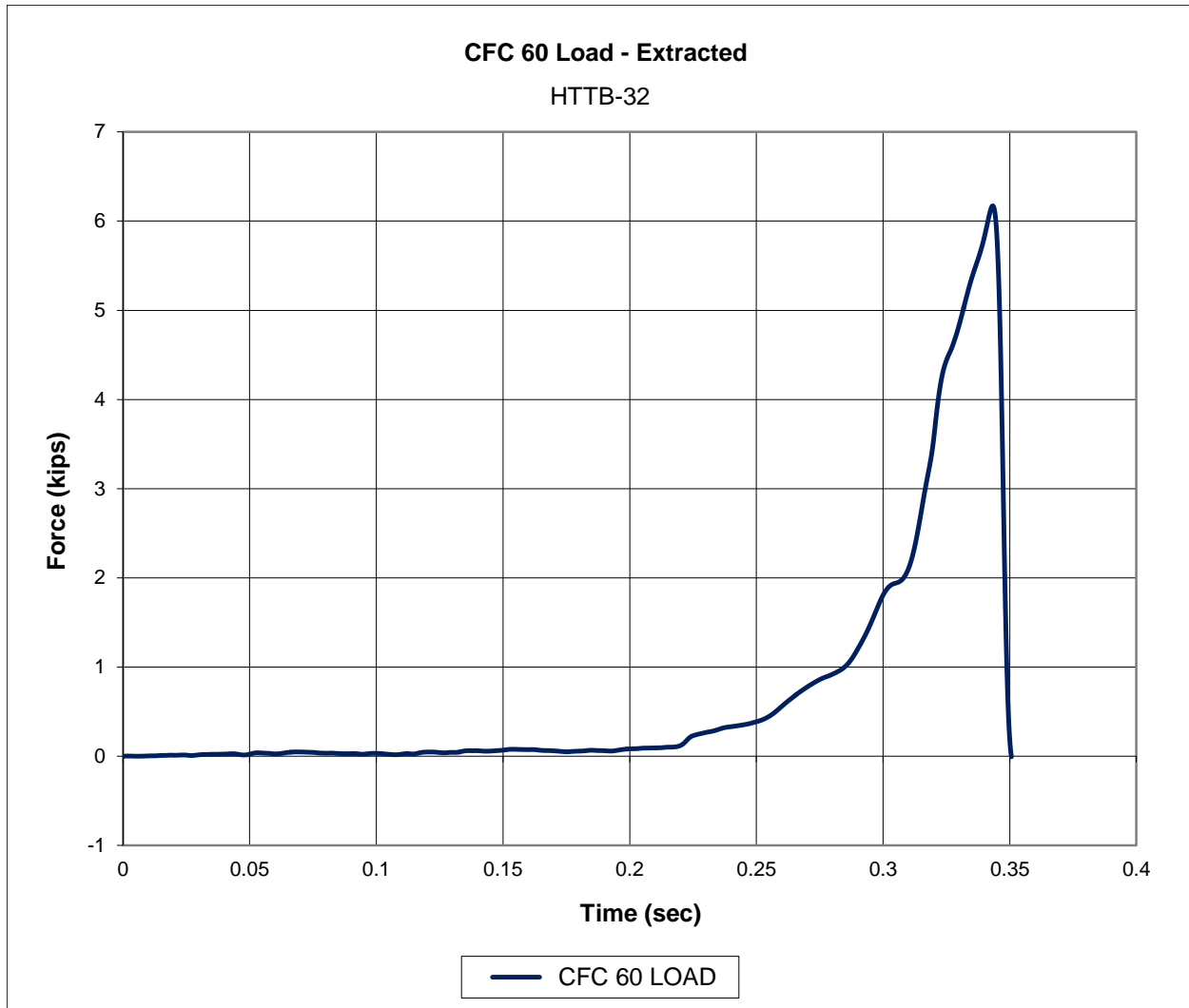


Figure 334. Force-Time Data, Test No. HTTB-32

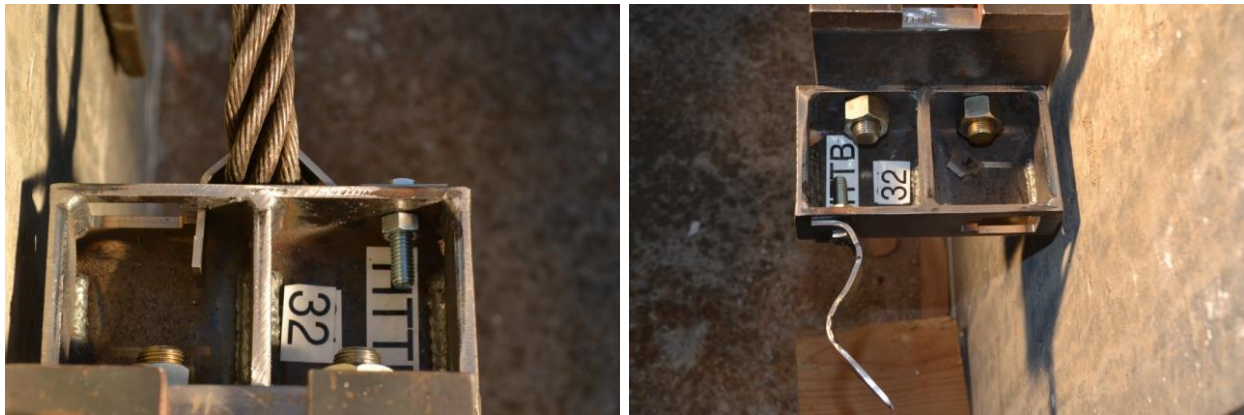
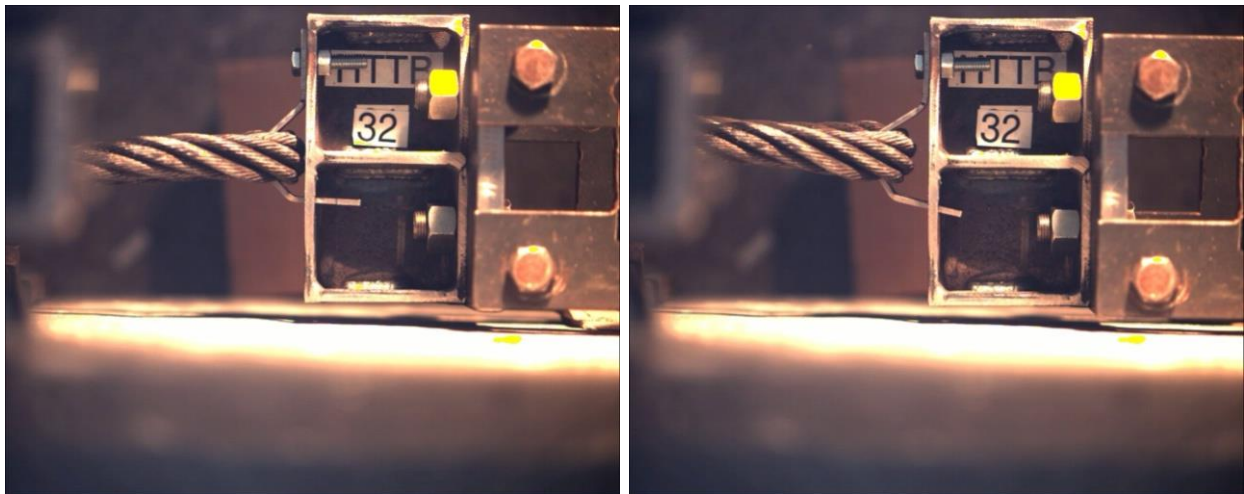
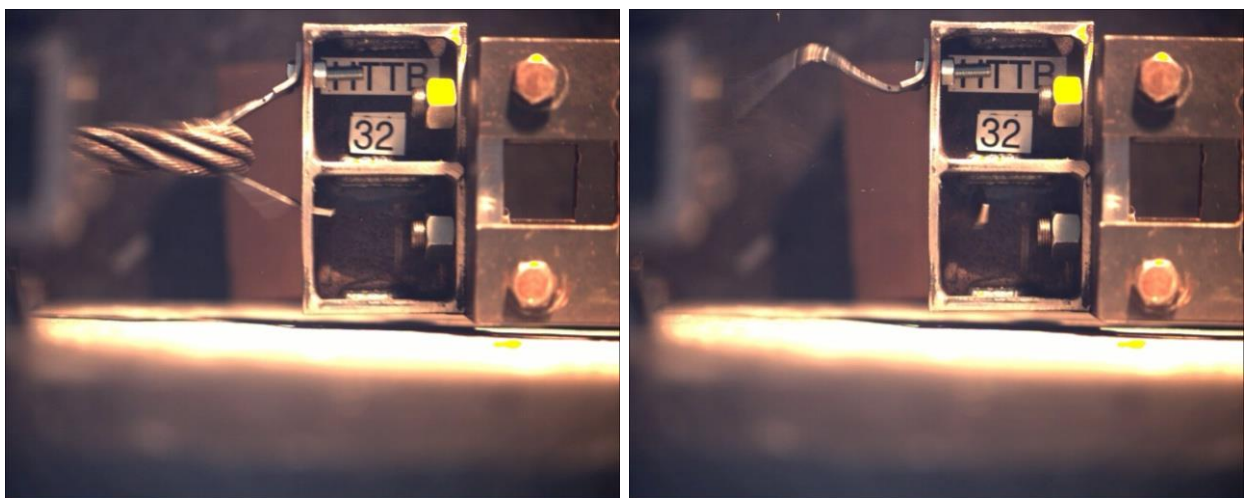


Figure 335. Pre-Test and Post-Test Photographs, Test No. HTTPB-32



Time = 0 sec

Time = 0.218 sec



Time = 0.342 sec

Time = 0.350 sec, Release

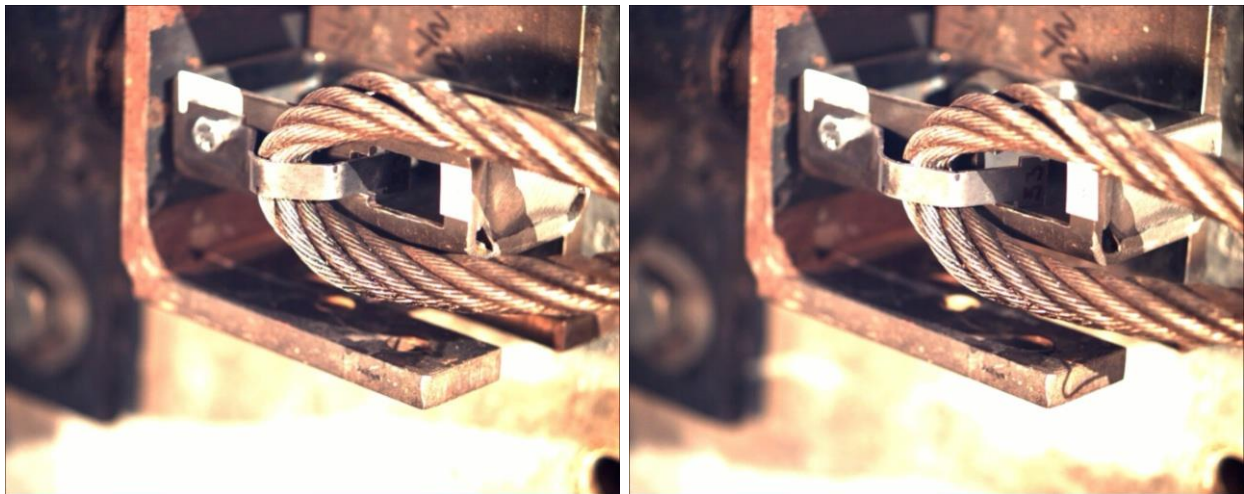
Figure 336. Sequential Photographs, Test No. HTTPB-32

15.1.17 Test No. HTTB-33 (TB V6, Bolted, Vertical)

For test no. HTTB-33, the cable pulled on the 14-gauge, grade 50 steel, bolted tabbed bracket Version 6 at an angle of 0 degrees, parallel to the front face of the flange, thus imparting a vertical load. The post consisted of a 5-½-in. (140-mm) long, folded C-section, fabricated from 7-gauge, grade 50 sheet steel. The top end of the tabbed bracket rested in the keyway, while the bottom end was secured to the flange with a 5/16-in. (8-mm), grade 5, hex cap screw and nut. The bracket began to bend as the cable began to pull on it. As the bracket bent, the edge of one of the tabs snagged the side of the keyway before the head finally released through it. The load cell data was not usable. Therefore, the peak forces were not known. Pre- and post-test photographs are shown in Figure 337. Sequential photographs are shown in Figure 338.

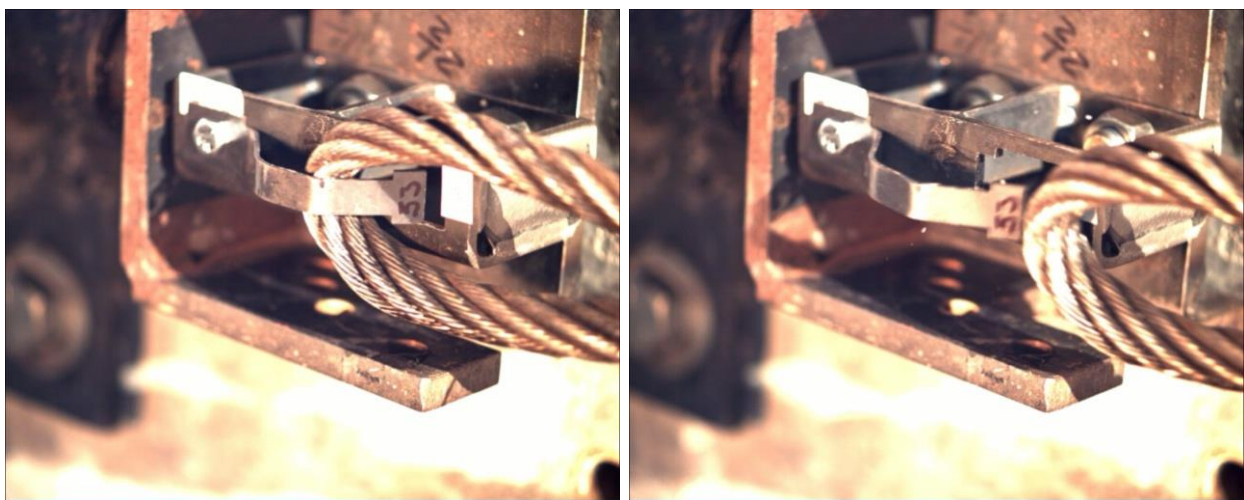


Figure 337. Pre-Test and Post-Test Photographs, Test No. HTTP-33



Time = 0 sec

Time = 0.178 sec



Time = 0.198 sec

Time = 0.218 sec, Release

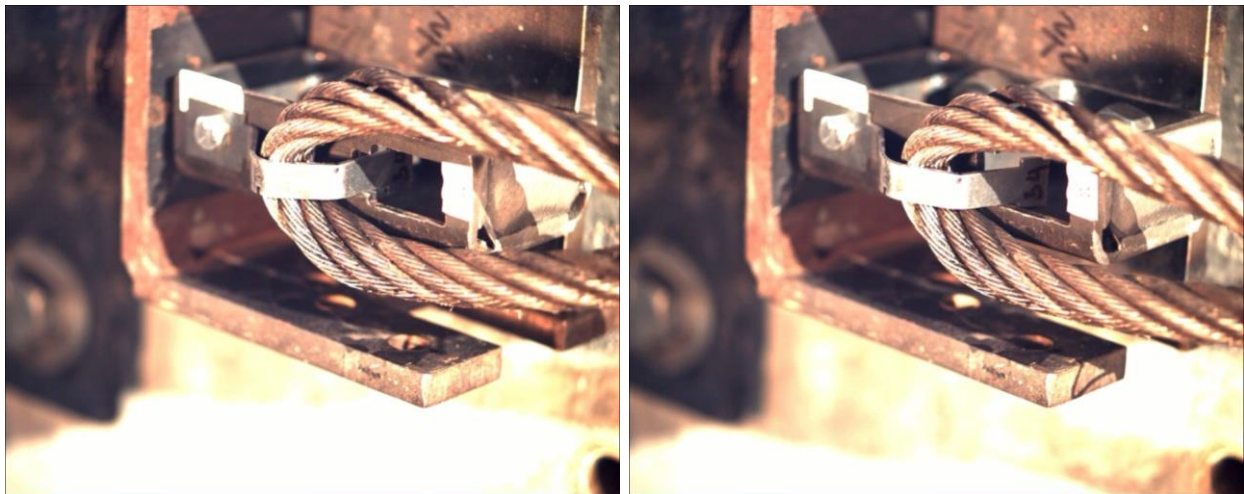
Figure 338. Sequential Photographs, Test No. HTTP-33

15.1.18 Test No. HTTB-34 (TB V6, Bolted, Vertical)

For test no. HTTB-34, the cable pulled on the 14-gauge, grade 50 steel, bolted tabbed bracket Version 6 at an angle of 0 degrees, parallel to the front face of the flange, thus imparting a vertical load. The post consisted of a 5-½-in. (140-mm) long, folded C-section, fabricated from 7-gauge, grade 50 sheet steel. The top end of the tabbed bracket rested in the keyway, while the bottom end was secured to the flange with a 5/16-in. (8-mm), grade 5, hex cap screw and nut. The bracket began to bend as the cable began to pull on it. As the bracket bent, the edge of one of the tabs snagged the side of the keyway before the head finally released through it. The load cell data was not usable. Therefore, the peak forces were not known. Pre- and post-test photographs are shown in Figure 339. Sequential photographs are shown in Figure 340.

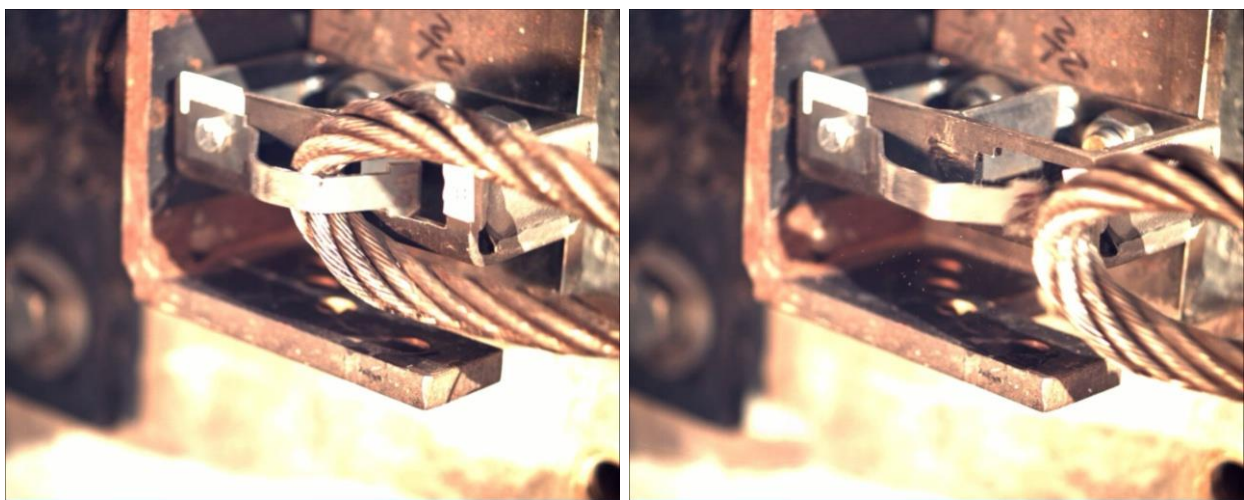


Figure 339. Pre-Test and Post-Test Photographs, Test No. HTTP-34



Time = 0 sec

Time = 0.144 sec



Time = 0.166 sec

Time = 0.190 sec, Release

Figure 340. Sequential Photographs, Test No. HTTP-34

15.1.19 Test No. HTTB-35 (TB V7, Bolted, Vertical)

For test no. HTTB-35, the cable pulled on the 11-gauge, grade 50 steel, bolted tabbed bracket Version 7 at an angle of 0 degrees, parallel to the front face of the flange, thus imparting a vertical load. The post consisted of a 5-½-in. (140-mm) long, folded C-section, fabricated from 7-gauge, grade 50 sheet steel. The top end of the tabbed bracket rested in the keyway, while the bottom end was secured to the flange with a 5/16-in. (8-mm), grade 5, hex cap screw and nut. The bracket began to bend as the cable began to pull on it. As the bracket bent, the edge of one of the tabs snagged the side of the keyway before the head finally released through it. A maximum release load of 464 lb (2.06 kN) occurred as the tab snagged the side of the keyway while the head was releasing through it. A snag load of 465 lb (2.07 kN) occurred after the head cleared the keyway and as the cable snagged on the tabs. The force versus time plot is shown in Figure 341. Pre- and post-test photographs are shown in Figure 342. Sequential photographs are shown in Figure 343.

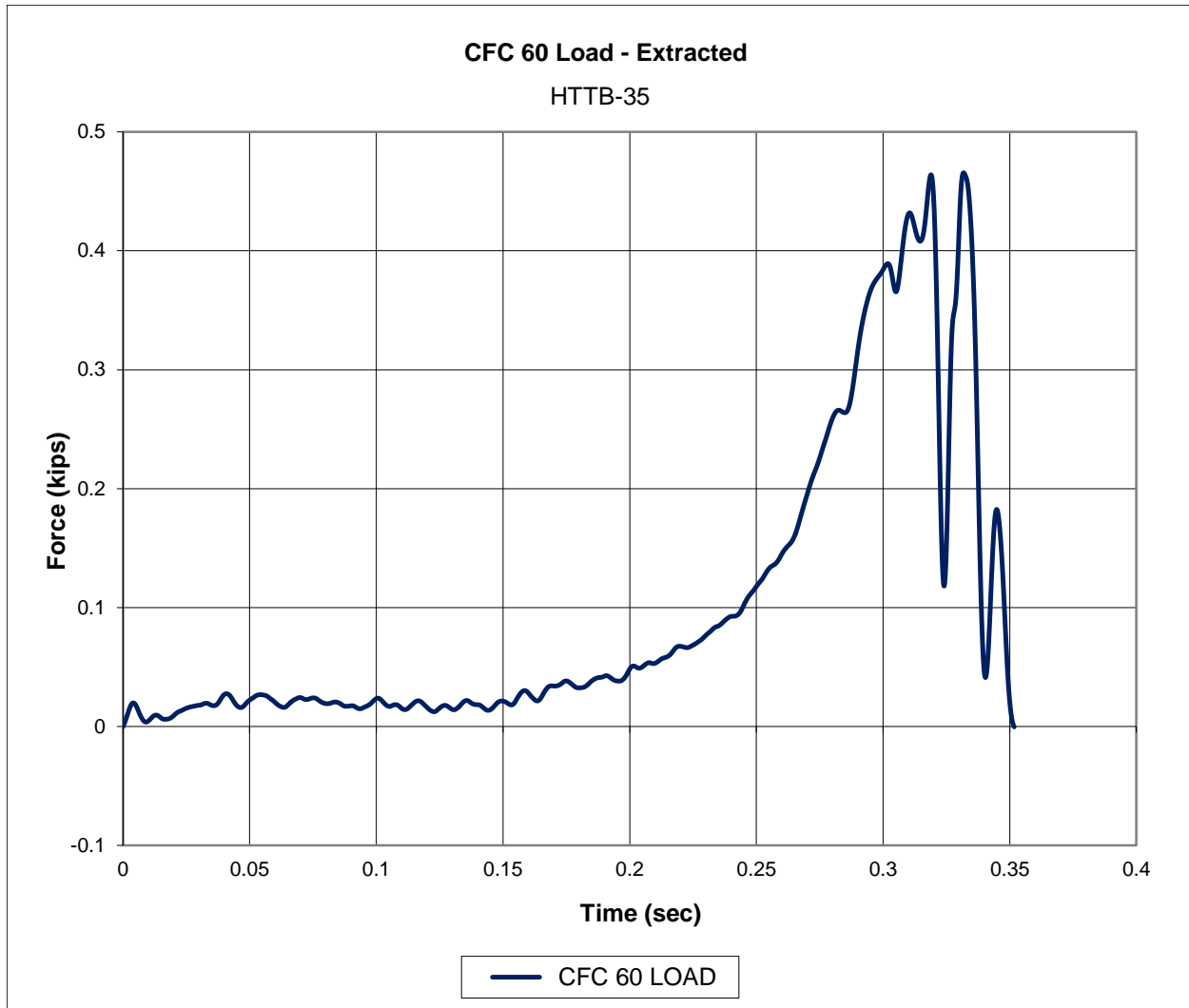


Figure 341. Force-Time Data, Test No. HTTB-35

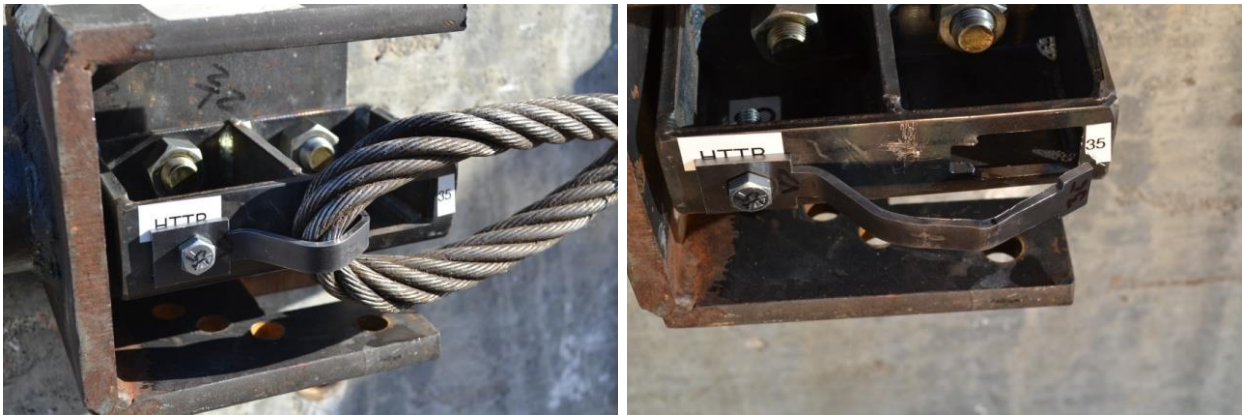
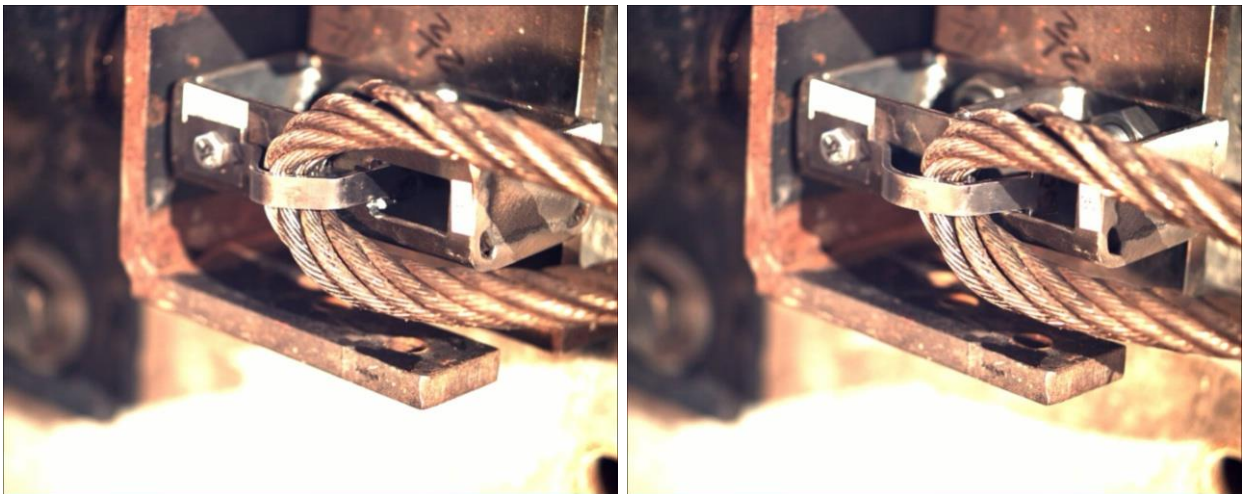
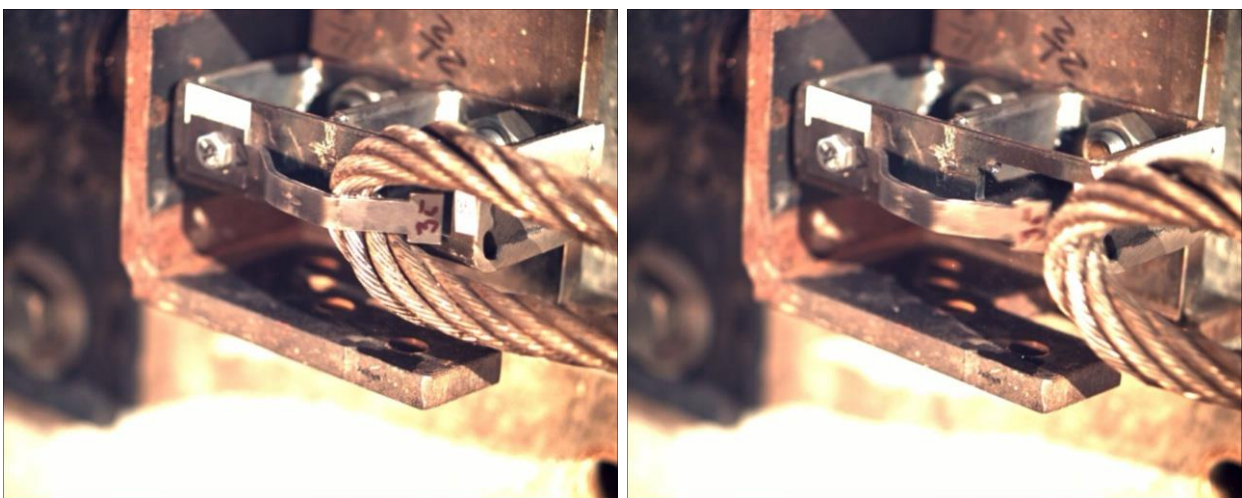


Figure 342. Pre-Test and Post-Test Photographs, Test No. HTTP-35



Time = 0 sec

Time = 0.312 sec



Time = 0.330 sec

Time = 0.352 sec, Release

Figure 343. Sequential Photographs, Test No. HTTP-35

15.1.20 Test No. HTTB-36 (TB V7, Bolted, Vertical)

For test no. HTTB-36, the cable pulled on the 11-gauge, grade 50 steel, bolted tabbed bracket Version 7 at an angle of 0 degrees, parallel to the front face of the flange, thus imparting a vertical load. The post consisted of a 5-½-in. (140-mm) long, folded C-section, fabricated from 7-gauge, grade 50 sheet steel. The top end of the tabbed bracket rested in the keyway, while the bottom end was secured to the flange with a 5/16-in. (8-mm), grade 5, hex cap screw and nut. The bracket began to bend as the cable began to pull on it. As the bracket bent, the edge of one of the tabs rubbed against—but was not snagged on—the side of the keyway. The head released through the keyway relatively freely. A maximum release load of 309 lb (1.37 kN) occurred as the bracket was bending and the head was releasing through the keyway. A snag load of 654 lb (2.91 kN) occurred after the head cleared the keyway and as the cable snagged on the tabs. The force versus time plot is shown in Figure 344. Pre- and post-test photographs are shown in Figure 345. Sequential photographs are shown in Figure 346.

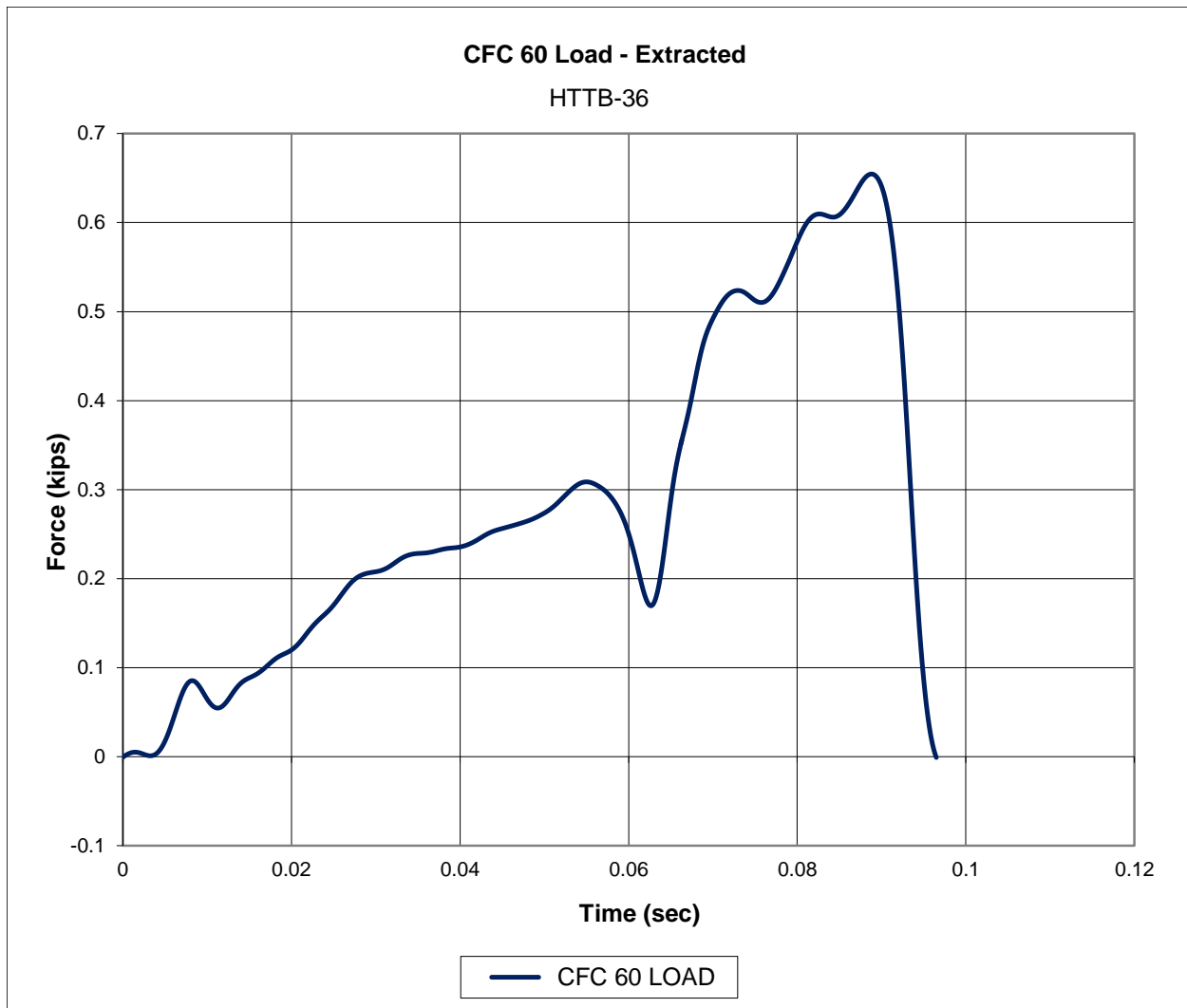
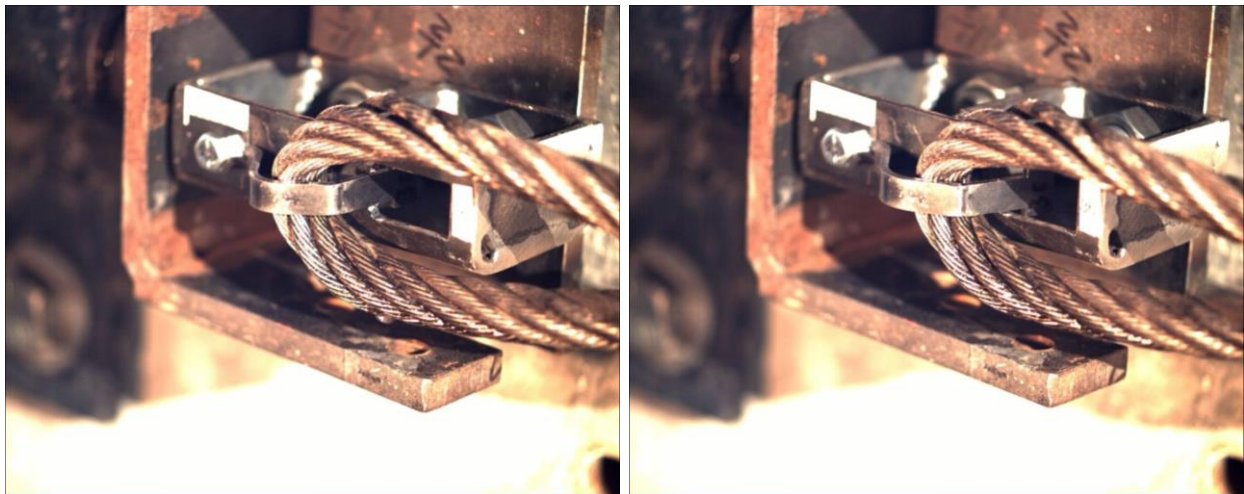


Figure 344. Force-Time Data, Test No. HTTB-36

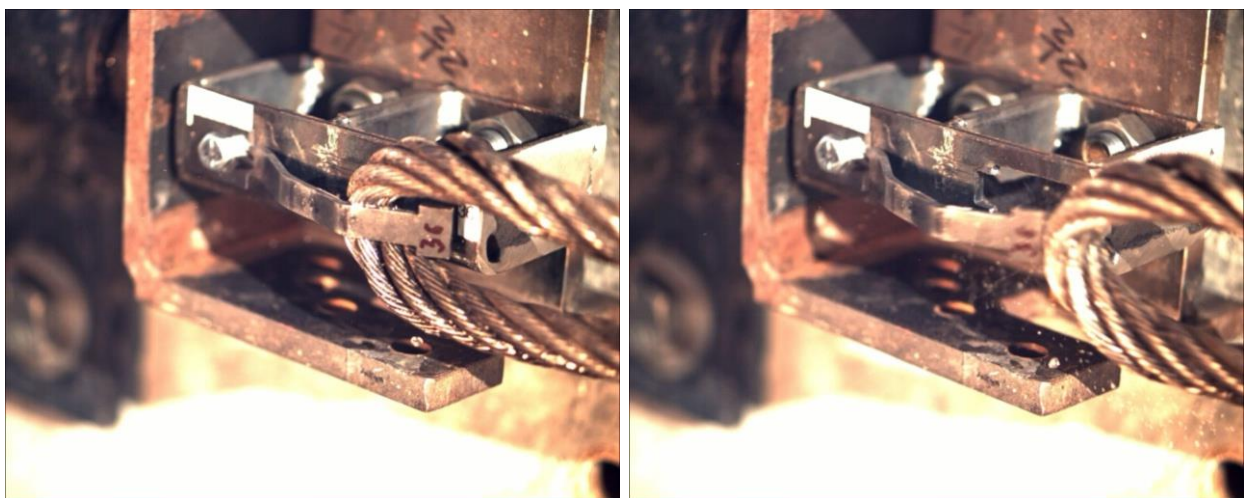


Figure 345. Pre-Test and Post-Test Photographs, Test No. HTTPB-36



Time = 0 sec

Time = 0.042 sec



Time = 0.080 sec

Time = 0.096 sec, Release

Figure 346. Sequential Photographs, Test No. HTTPB-36

15.1.21 Test No. HTTB-37 (TB V10, Bolted, Vertical)

For test no. HTTB-37, the cable pulled on the 12-gauge, grade 50 steel, bolted tabbed bracket Version 10 at an angle of 0 degrees, parallel to the front face of the flange, thus imparting a vertical load. The post consisted of a 5-1/2-in. (140-mm) long, folded C-section, fabricated from 7-gauge, grade 50 sheet steel. The top end of the tabbed bracket rested in the keyway, while the bottom end was secured to the flange with a 5/16-in. (8-mm), grade 5, hex cap screw and nut. The bracket began to bend as the cable began to pull on it. As the bracket bent, the edge of one of the tabs rubbed against—but was not snagged on—the side of the keyway. The head released through the keyway relatively freely. A maximum release load of 419 lb (1.86 kN) occurred as the bracket was bending and the head was releasing through the keyway. A snag load of 528 lb (2.35 kN) occurred after the head cleared the keyway and as the cable snagged on the tabs. The force versus time plot is shown in Figure 347. Pre- and post-test photographs are shown in Figure 348. Sequential photographs are shown in Figure 349.

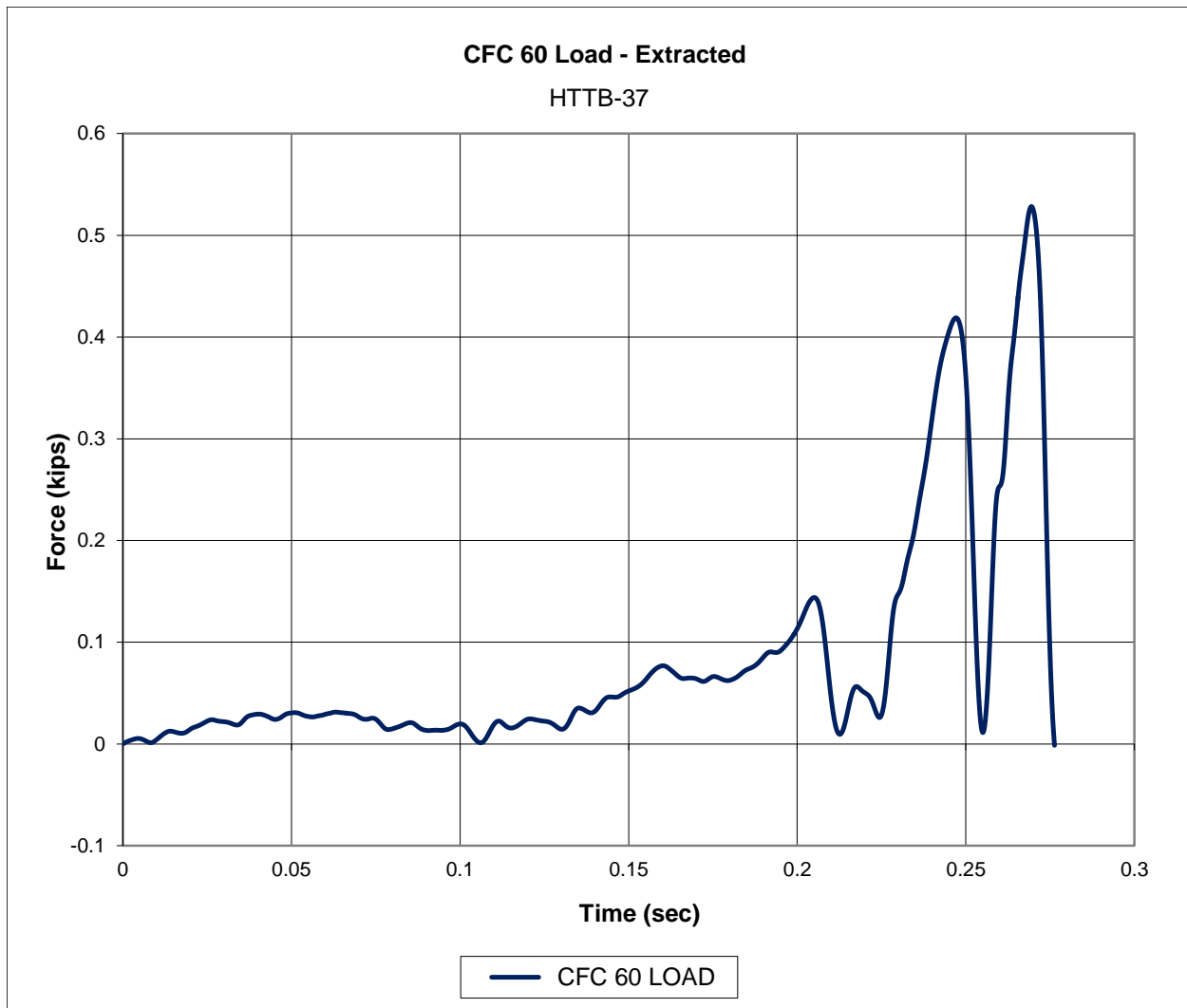


Figure 347. Force-Time Data, Test No. HTTB-37

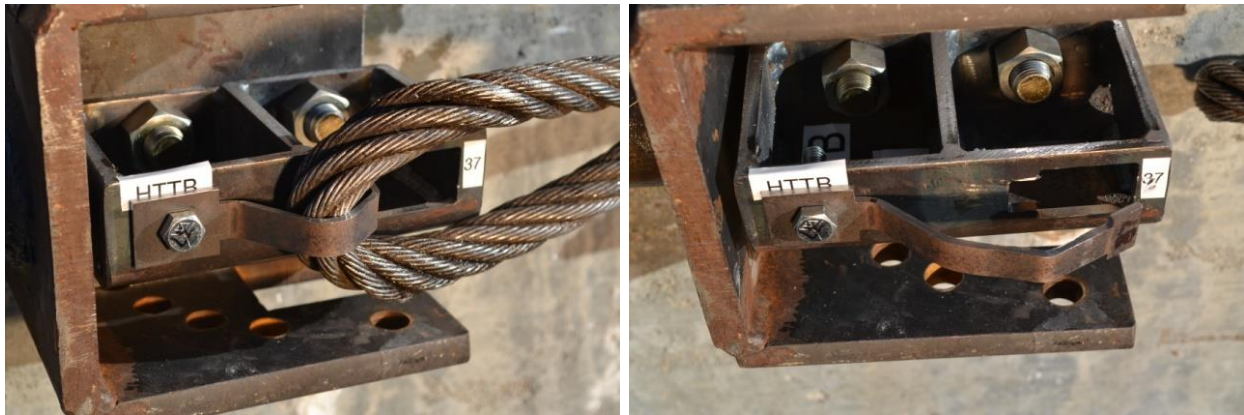
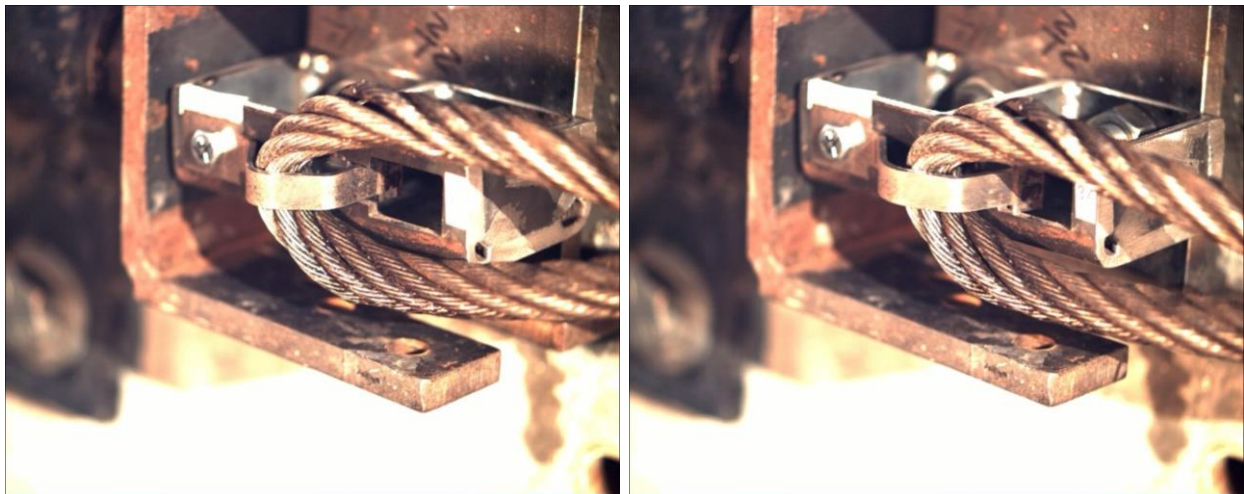
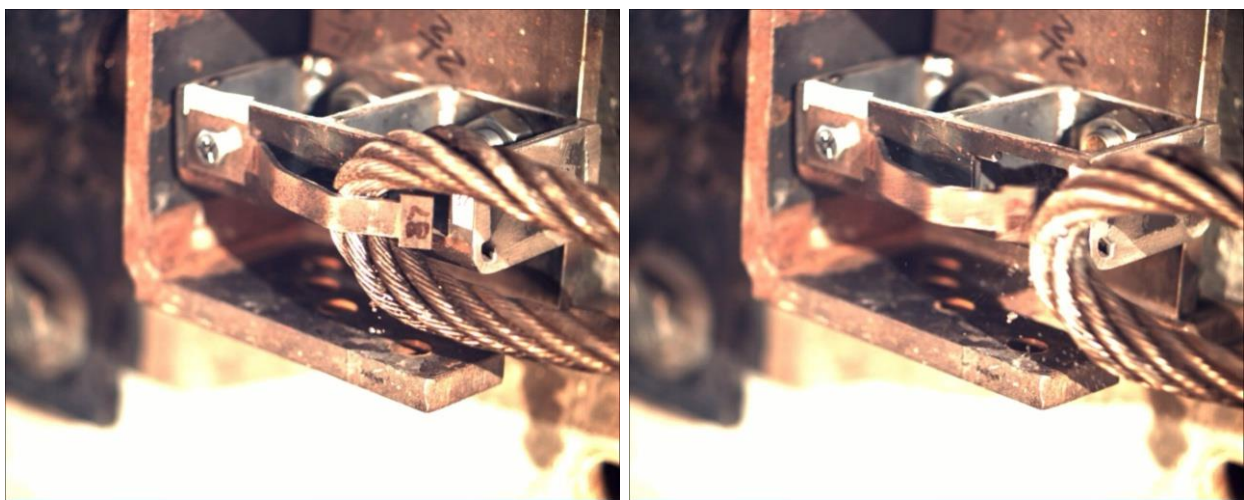


Figure 348. Pre-Test and Post-Test Photographs, Test No. HTTPB-37



Time = 0 sec

Time = 0.240 sec



Time = 0.260 sec

Time = 0.276 sec, Release

Figure 349. Sequential Photographs, Test No. HTTPB-37

15.1.22 Test No. HTTB-38 (TB V10, Bolted, Vertical)

For test no. HTTB-38, the cable pulled on the 12-gauge, grade 50 steel, bolted tabbed bracket Version 10 at an angle of 0 degrees, parallel to the front face of the flange, thus imparting a vertical load. The post consisted of a 5-1/2-in. (140-mm) long, folded C-section, fabricated from 7-gauge, grade 50 sheet steel. The top end of the tabbed bracket rested in the keyway, while the bottom end was secured to the flange with a 5/16-in. (8-mm), grade 5, hex cap screw and nut. The bracket began to bend as the cable began to pull on it. As the bracket bent, the edge of one of the tabs rubbed against—but was not snagged on—the side of the keyway. The head released through the keyway relatively freely. A maximum release load of 272 lb (1.21 kN) occurred as the bracket was bending and the head was releasing through the keyway. A snag load of 458 lb (2.04 kN) occurred after the head cleared the keyway, as the cable snagged on the tabs. The force versus time plot is shown in Figure 344. Pre- and post-test photographs are shown in Figure 345. Sequential photographs are shown in Figure 346.

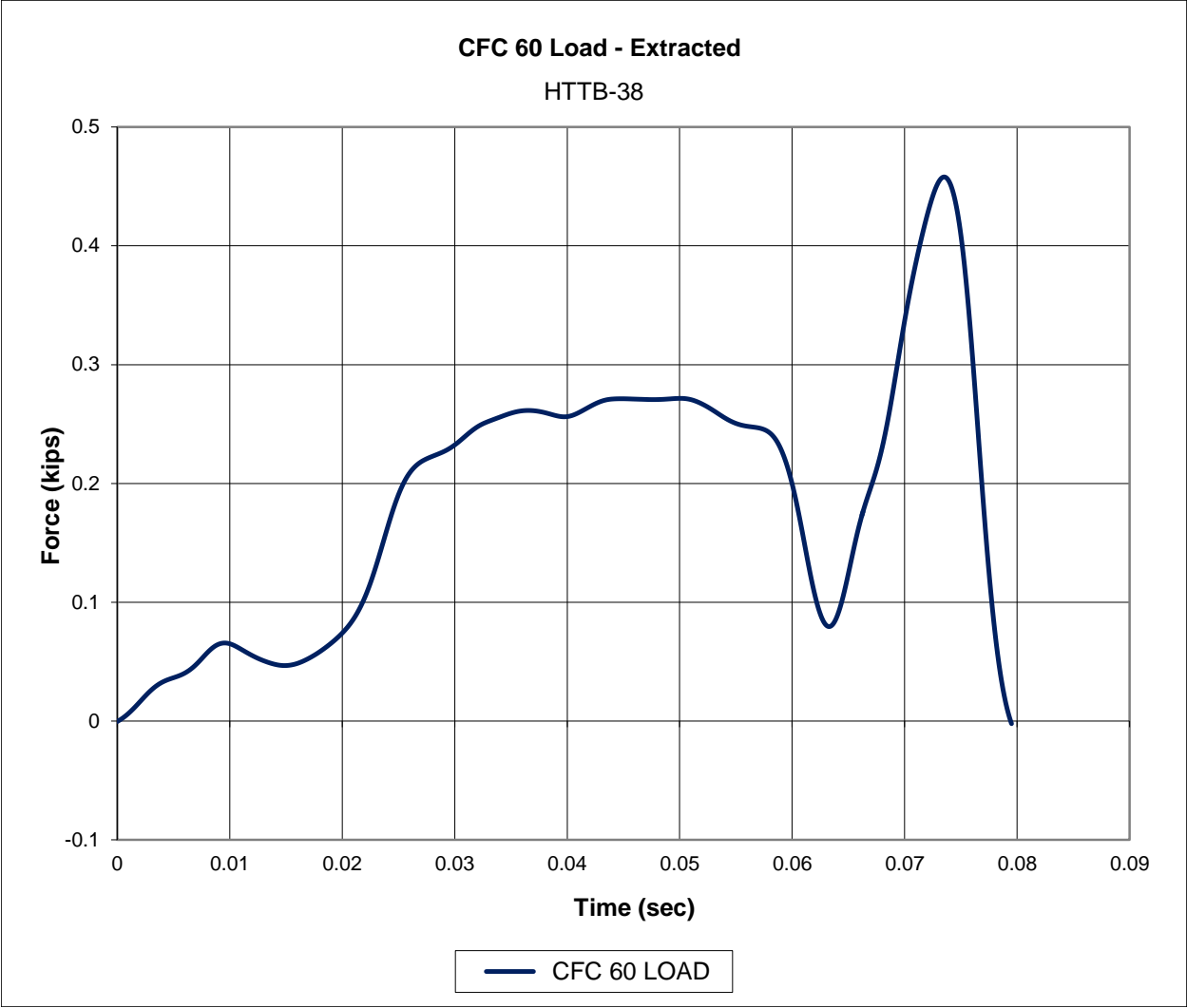
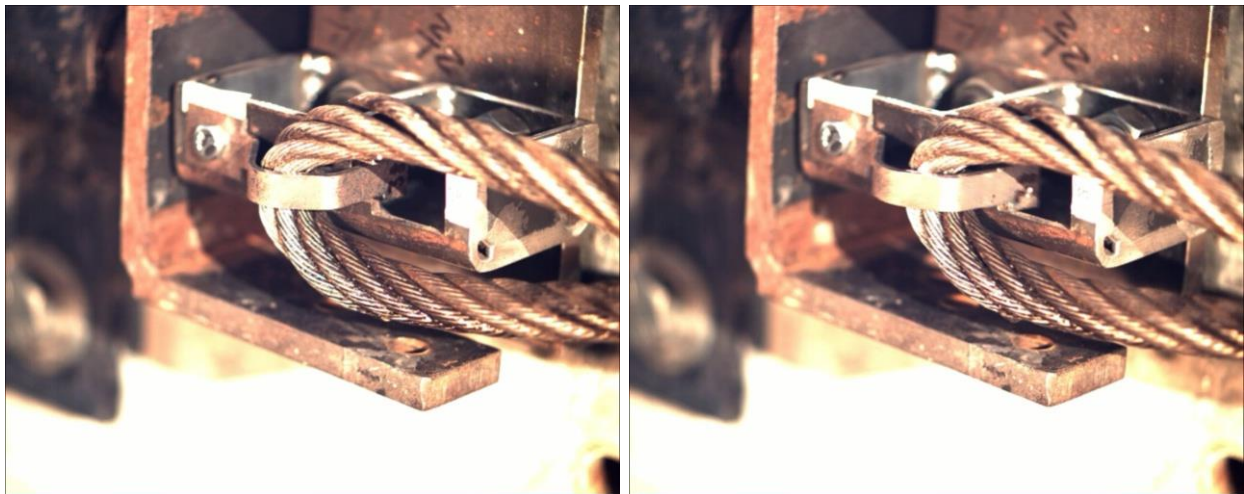


Figure 350. Force-Time Data, Test No. HTTB-38

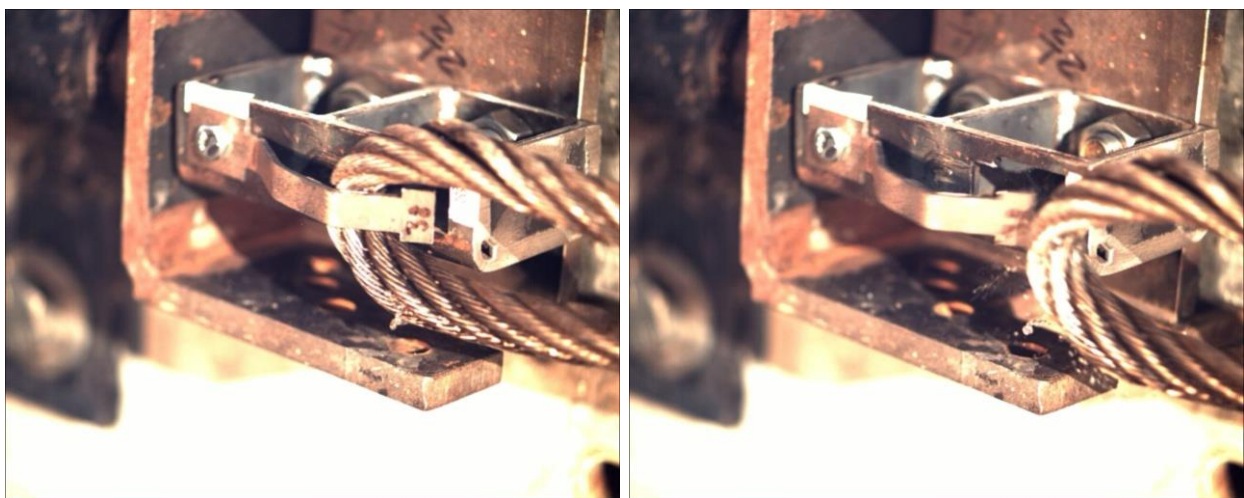


Figure 351. Pre-Test and Post-Test Photographs, Test No. HTTB-38



Time = 0 sec

Time = 0.052 sec



Time = 0.066 sec

Time = 0.080 sec, Release

Figure 352. Sequential Photographs, Test No. HTTB-38

15.1.23 Test No. HTTPB-39 (TB V6, Bolted, Vertical)

Test no. HTTPB-39 was a re-trial of test no. HTTPB-33; since, the data was not usable for that test. For test no. HTTPB-39, the cable pulled on the 14-gauge, grade 50 steel, bolted tabbed bracket Version 6 at an angle of 0 degrees, parallel to the front face of the flange, thus imparting a vertical load. The post consisted of a 5-½-in. (140-mm) long, folded C-section, fabricated from 7-gauge, grade 50 sheet steel. The top end of the tabbed bracket rested in the keyway, while the bottom end was secured to the flange with a 5/16-in. (8-mm), grade 5, hex cap screw and nut. The bracket began to bend as the cable began to pull on it. As the bracket bent, the edge of one of the tabs rubbed against—but was not snagged on—the side of the keyway. The head released through the keyway relatively freely. A maximum release load of 124 lb (552 N) occurred as the bracket was bending and the head was releasing through the keyway. A snag load of 204 lb (907 N) occurred after the head cleared the keyway, as the cable snagged on the tabs. The force versus time plot is shown in Figure 353. Pre- and post-test photographs are shown in Figure 354. Sequential photographs are shown in Figure 355.

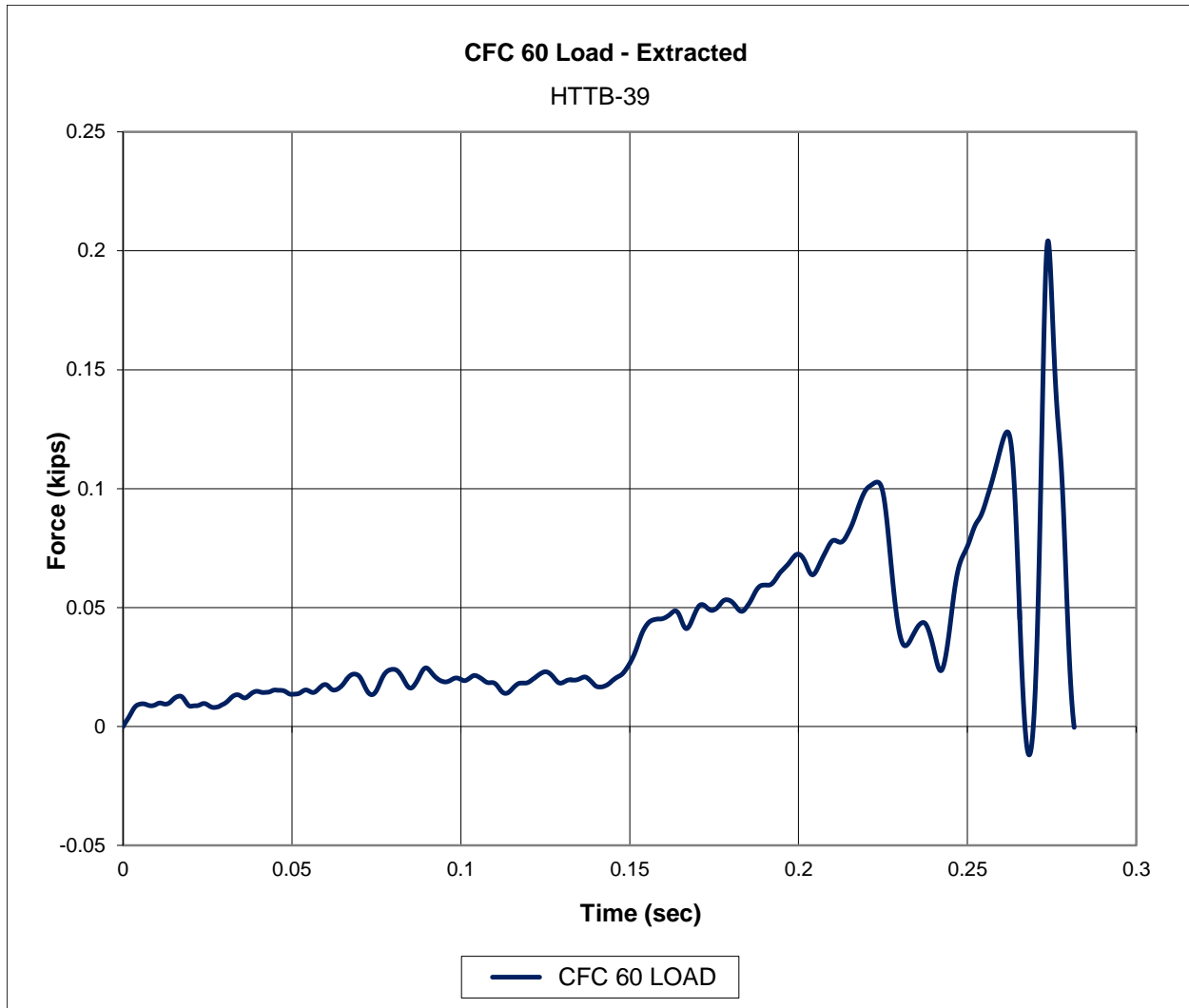
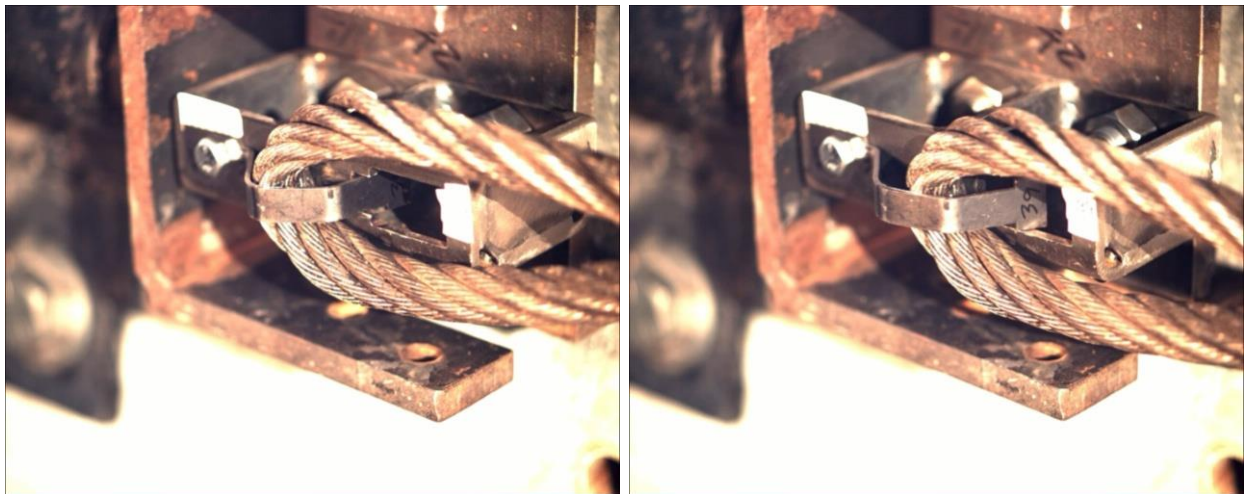


Figure 353. Force-Time Data, Test No. HTTB-39

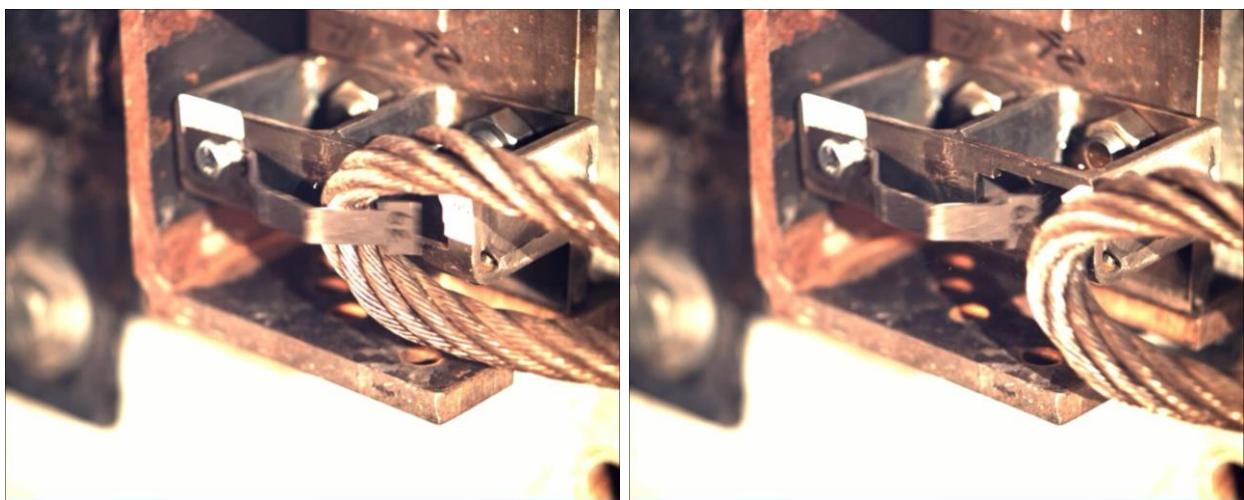


Figure 354. Pre-Test and Post-Test Photographs, Test No. HTTPB-39



Time = 0 sec

Time = 0.248 sec



Time = 0.262 sec

Time = 0.282 sec, Release

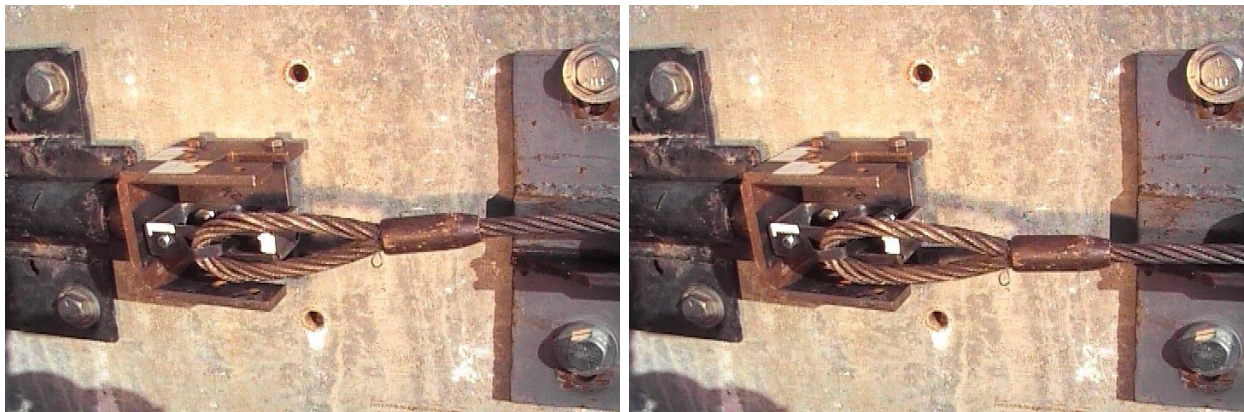
Figure 355. Sequential Photographs, Test No. HTTPB-39

15.1.24 Test No. HTTPB-40 (TB V6, Bolted, Vertical)

Test no. HTTPB-40 was a re-trial of test no. HTTPB-34; since, the data was not usable for that test. For test no. HTTPB-40, the cable pulled on the 14-gauge, grade 50 steel, bolted tabbed bracket Version 6 at an angle of 0 degrees, parallel to the front face of the flange, thus imparting a vertical load. The post consisted of a 5-½-in. (140-mm) long, folded C-section, fabricated from 7-gauge, grade 50 sheet steel. The head rested in the keyway, while the bottom end was secured to the flange with a 5/16-in. (8-mm), grade 5, hex cap screw and nut. Due to technical difficulties, there was no high-speed video for this test. From the standard speed video, it was clear that the head released through the keyway as the cable pulled on the bracket. The load cell data was not usable. Therefore, the peak loads were not known. Pre- and post-test photographs are shown in Figure 356. Sequential photographs are shown in Figure 357.

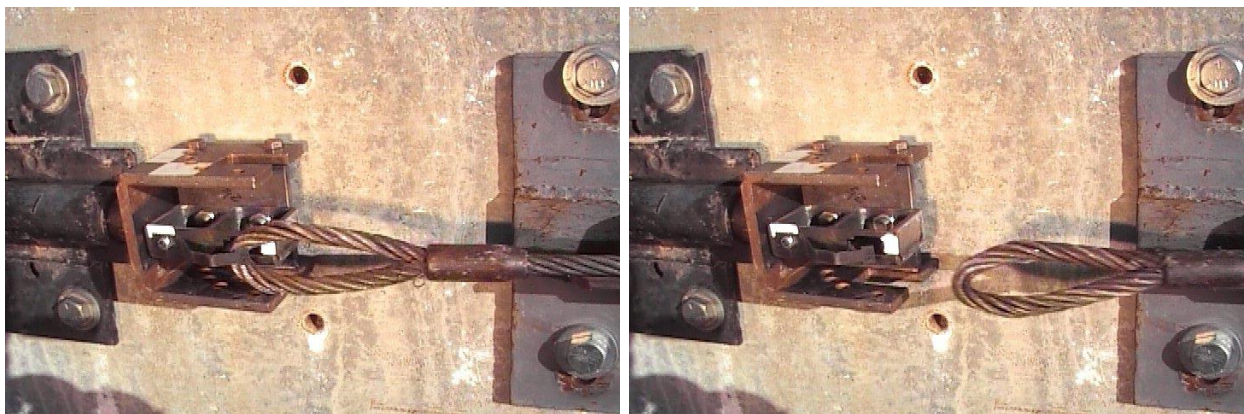


Figure 356. Pre-Test and Post-Test Photographs, Test No. HTTP-40



Time = 0 sec

Time = 0.172 sec



Time = 0.206 sec

Time = 0.240 sec, Release

Figure 357. Sequential Photographs, Test No. HTTP-40

15.2 Discussion

Twenty-four dynamic component tests were performed in Round 3. One of the main goals was to determine whether the bolted tabbed brackets exhibited ideal cable release behavior. When pulled laterally, the head was expected to become caught in the narrow part of the keyway, and the tabbed bracket was expected to fracture in some manner. When pulled vertically, the tabbed bracket was expected to bend upward, allowing the head to rotate up and out of the wider part of the keyway without scraping against the inside of the flange. With the exception of Versions 7 and 9, all of the bolted tabbed brackets in the third round of testing exhibited ideal behavior.

For both lateral pull tests on tabbed bracket Version 7 (test nos. HTTB-27 and HTTB-28), its head became caught in the narrow part of the keyway. However, as the cable continued to pull laterally, the head began to twist and slip through the narrow part of the keyway, shearing off the corner of one of the tabs. Ideally, both tabs would have been completely sheared off. The head-twisting did not allow the full fracture strength to be developed. This behavior was interesting, but due to the success of the other tabbed bracket versions in this round, it was not deemed worthy of further investigation.

For both lateral pull tests on tabbed bracket Version 9 (test nos. HTTB-29 and HTTB-30), the head failed to be captured in the narrow part of the keyway and instead freely released through the wider part of the keyway. Actually, this behavior was somewhat expected. For tabbed bracket Version 9, the narrow part of the keyway was shallower and the head extended farther past the inside of the flange than used in any other tabbed bracket. After observing this behavior, it was decided to not vertically test tabbed bracket Version 9.

For the bolted tabbed brackets that behaved ideally, the design equations predicted the lateral release loads very well, as shown in Table 14.

Table 14. Expected vs. Observed Lateral Release Loads for Ideal Bolted Tabbed Brackets

Tabbed Bracket Version	Test No. HTTB-	Lateral Release Load, kips (kN)					Actual Failure Location
		Expected at Failure Location				Observed	
		1	2	3	4		
5	23	3.47 (15.4)	3.01 (13.4)	3.01 (13.4)	4.51 (20.1)	3.06 (13.6)	2
	24	3.47 (15.4)	3.01 (13.4)	3.01 (13.4)	4.51 (20.1)	2.97 (13.2)	2
6	25	4.34 (19.3)	4.30 (19.1)	4.30 (19.1)	4.51 (20.1)	3.50 (15.6)	1
	26	4.34 (19.3)	4.30 (19.1)	4.30 (19.1)	4.51 (20.1)	3.44 (15.3)	1
8	21	6.08 (27.0)	6.01 (26.8)	6.01 (26.8)	6.32 (28.1)	5.71 (25.4)	1
	22	6.08 (27.0)	6.01 (26.8)	6.01 (26.8)	6.32 (28.1)	5.59 (24.9)	1
10	31	6.08 (27.0)	6.01 (26.8)	6.01 (26.8)	6.32 (28.1)	6.03 (26.8)	3
	32	6.08 (27.0)	6.01 (26.8)	6.01 (26.8)	6.32 (28.1)	6.17 (27.4)	2

*Red highlighted cells show the expected release load corresponding to the actual failure location.

*Blue highlighted cells show observed lateral release loads which were greater than or deemed “close enough” to the 6-kip (27-kN) target

The design equations worked especially well when fracture occurred at failure locations 2 or 3, both of which assumed pure tensile fracture. However, the design equations over-predicted the release loads for failure location 1, in which pure shear fracture was assumed. No conclusions were made about why the design equations over-predicted lateral capacity for failure location 1. However, it should be noted that the design equations did not account for stress concentrators at square corners, or bending and buckling of the tabbed bracket’s head, both of which seemed to contribute to the failure of tabbed bracket Versions 6 and 8.

It should be noted that the tabbed brackets that were tested and evaluated in previous rounds exhibited tab scraping against the inside of the flange when loaded vertically. However, all of the bolted tabbed brackets that were tested and evaluated in this round performed ideally

when pulled vertically. Thus, it was valid to compare the observed vertical release loads to the loads predicted by the design equations, as shown in Table 15. In general, the equations under-predicted the vertical release loads but not by a consistent margin.

Table 15. Expected vs. Observed Vertical Release Loads for Bolted Tabbed Brackets

Tabbed Bracket Version	Test No. HTTPB-	Vertical Release Load lb (kN)	
		Expected	Observed
5	17	117 (0.52)	122 (0.54)
	18	117 (0.52)	148 (0.66)
6	39	123 (0.55)	124 (0.55)
7	35	264 (1.17)	464 (2.06)
	36	264 (1.17)	309 (1.37)
8	19	235 (1.05)	239 (1.06)
	20	235 (1.05)	283 (1.26)
10	37	235 (1.05)	419 (1.86)
	38	235 (1.05)	272 (1.21)

*Blue highlighted cells show observed vertical release loads which were less than or deemed “close enough” to the 225-lb (1.00-kN) target

Following the Round 3 testing on the bolted tabbed brackets, it was concluded that no more design modifications or testing was needed. A sufficient number of brackets provided the desired cable release behavior for cable-to-post attachment for the bottom three cables. Thus, the final step in the design process was to select cable-to-post attachment hardware for the lower three cables, which is described in Chapter 16.

16 CABLE-TO-POST ATTACHMENT CONCLUSIONS

16.1 Summary of Design and Testing Efforts

The original keyway bolts, as used in full-scale test nos. 4CMB-4, 4CMB-5, and 4CMBLT-1, had lateral and vertical release loads of 8.00 kips (35.6 kN) and 1.18 kips (5.25 kN), respectively, according to results obtained during a prior dynamic component testing program [71].

As a result of the re-design and testing efforts discussed previously, much was learned and accomplished regarding the behavior of the cable-to-post attachments. For the continuation effort reported herein, a total of seventy dynamic component tests were performed on modified/extended keyway bolts as well as various types of tabbed brackets. These design prototypes, along with the corresponding lateral and vertical release loads, are summarized in Table 16. Two tests were performed on each concept and for each load orientation. Unless otherwise noted, the lateral and vertical release loads reported in Table 16 were the averages. In general, if the two tests did not provide similar results, the design was considered to be flawed where the behavior was deemed inconsistent.

Table 16. Summary of Design Concepts for Cable-to-Post Attachments

Design Concept	Material	Average Cable Release Loads, kips (kN)	
		Lateral	Vertical
Keyway Bolt in Original Dual-Width Keyway	ASTM A449	8.00 (35.6)	1.18 (5.25)
Keyway Bolt in Small Oversized Keyway	ASTM A449	¹ 1.14 (5.07)	0.48 (2.1)
Keyway Bolt in Small Oversized Keyway	AISI C1018	0.535 (2.38)	0.35 (1.6)
Keyway Bolt in Large Oversized Keyway	ASTM A449	1.03 (4.58)	0.45 (2.0)
Keyway Bolt in Large Oversized Keyway	AISI C1018	1.04 (4.63)	0.33 (1.5)
Modified Keyway Bolt in Large Oversized Keyway	AISI C1018	¹ 0.80 (3.6)	1.44 (6.41)
Extended Keyway Bolt in Original Dual-Width Keyway	AISI C1018	2.64 (11.7)	0.41 (1.8)
Extended Keyway Bolt in Modified Dual-Width Keyway	AISI C1018	² 6.47 (28.8)	0.49 (2.2)
Tabbed Bracket Version 1, Crimp-In-Place	Hot-Rolled ASTM A1011 HSLA Grade 50	5.93 (26.4)	2.84 (12.6)
Tabbed Bracket Version 2, Crimp-In-Place	Hot-Rolled ASTM A1011 HSLA Grade 50	6.56 (29.2)	1.32 (5.87)
Tabbed Bracket Version 3, Bolted	Hot-Rolled ASTM A1011 HSLA Grade 50	³ 5.18 (23.0)	0.78 (3.47)
Tabbed Bracket Version 4, Bolted	Hot-Rolled ASTM A1011 HSLA Grade 50	4.57 (20.3)	0.94 (4.2)
Tabbed Bracket Version 5, Bolted	Hot-Rolled ASTM A1011 HSLA Grade 50	3.02 (13.4)	0.14 (0.62)
Tabbed Bracket Version 6, Bolted	Hot-Rolled ASTM A1011 HSLA Grade 50	3.47 (15.4)	0.12 (0.53)
Tabbed Bracket Version 7, Bolted	Hot-Rolled ASTM A1011 HSLA Grade 50	4.46 (19.8)	0.39 (1.7)
Tabbed Bracket Version 8, Bolted	Hot-Rolled ASTM A1011 HSLA Grade 50	5.65 (25.1)	0.26 (1.2)
Tabbed Bracket Version 9, Bolted	Hot-Rolled ASTM A1011 HSLA Grade 50	0.60 (2.7)	Not Tested
Tabbed Bracket Version 10, Bolted	Hot-Rolled ASTM A1011 HSLA Grade 50	6.10 (27.1)	0.35 (1.6)

1. Single value—lower reported

2. The assumed lateral release load for bolt fracture through threads was reported

3. 3 tests total, 2.38-kip (10.6-kN) value disregarded due to fabrication flaw

The first part of the re-design effort, as described in Chapters 5 through 9, was to modify the existing cable-to-post attachments at the lower three cable locations in order to reduce the vertical release load to approximately 225 lb (1.00 kN), while maintaining a lateral release load of approximately 6.00 kips (26.7 kN). Thus, AISI C1018 extended keyway bolts were designed and tested, which provided lateral and vertical release loads of 6.47 kips (28.8 kN) and 486 lb (2.16 kN), respectively. This result was a significant improvement over the ASTM A449 keyway bolts, which provided a vertical release load of 1.18 kips. However, it was believed that the vertical cable release load could be further reduced, while still maintaining a lateral cable release load close to 6.00 kips (26.7 kN).

The second part of the re-design effort was to develop some completely new concepts. This effort resulted in several tabbed bracket designs, as described in Chapters 10 through 15. There were two main variations of the tabbed brackets—crimp-in-place and bolted which referenced the method of attachment to the post. The crimp-in-place variation was ultimately discarded in favor of the bolted variation. Subsequently, two rounds of design modifications and tests were used to evaluate the bolted tabbed brackets, which resulted in five different working versions.

16.2 Selection of Cable-to-Post Attachment

As noted above, the target lateral and vertical cable release loads were 6.00 kips (26.7 kN) and 225 lb (1.00 kN), respectively. These goals guided the design process, although they were not treated like rigid criteria to be met. After design equations had been developed, evaluated, and revised, there remained some additional concern by project team members regarding the potential for unpredictable cable release behavior, especially in the vertical direction, when installed in actual cable barrier systems. For this reason, some of the bolted

tabbed brackets were deliberately designed with significantly lower vertical and lateral cable release loads.

Bolted tabbed bracket Version 6 was deemed the best concept from those having lower target vertical and lateral cable release loads. Its lateral and vertical cable release loads were 3.47 kips (15.4 kN) and 124 lb (552 N), respectively. A vertical cable release load lower than the 225-lb (1.00-kN) target was considered to be beneficial. However, the trade-off was a lower lateral release load, which meant a reduced ability for the bracket to develop the full moment capacity of the post when loaded laterally.

Bolted tabbed bracket Version 8 had lateral and vertical cable release loads of 5.65 kips (25.1 kN) and 261 lb (1.16 kN), respectively, which was very close to the initial targeted values. Bolted tabbed bracket Version 10 was very similar to Version 8 in performance and design. It had lateral and vertical cable release loads of 6.10 kips (27.1 kN) and 346 lb (1.54 kN), respectively. Both Versions 8 and 10 were caught in their respective keyways when pulled laterally and released through freely when pulled vertically, which was the desired behavior. Bolted tabbed bracket Version 8 is shown next to keyway Version 8 in Figure 358.

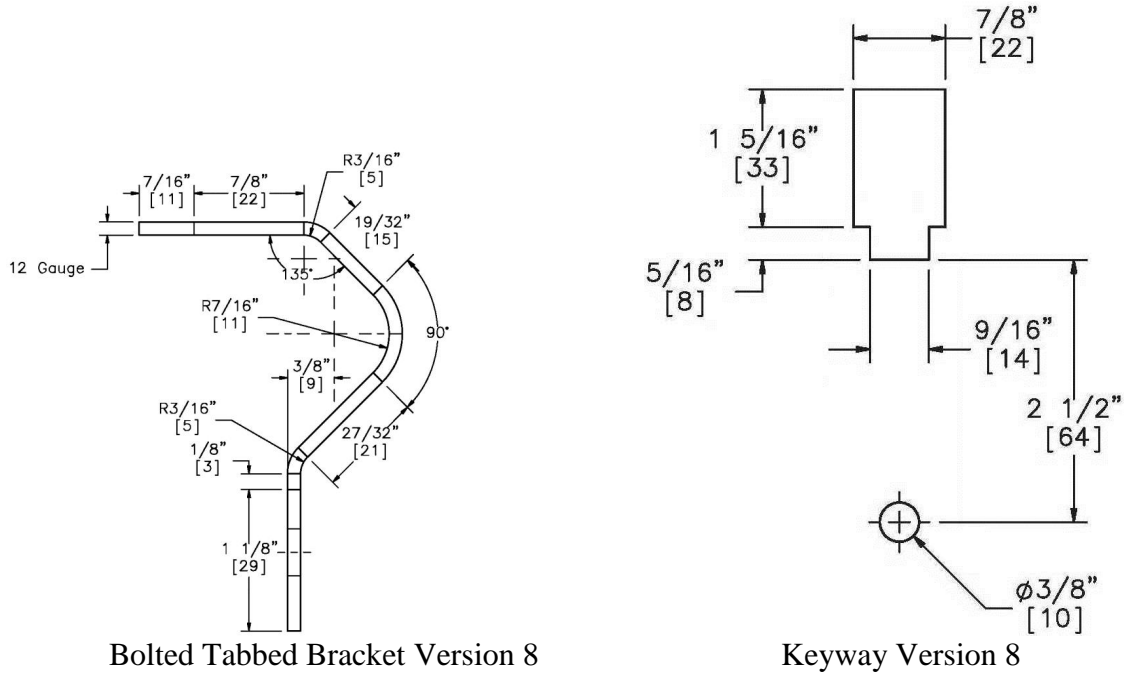


Figure 358. Bolted Tabbed Bracket Version 8 and Keyway Version 8

Bolted tabbed bracket Version 10 is shown next to keyway Version 10 in Figure 359.

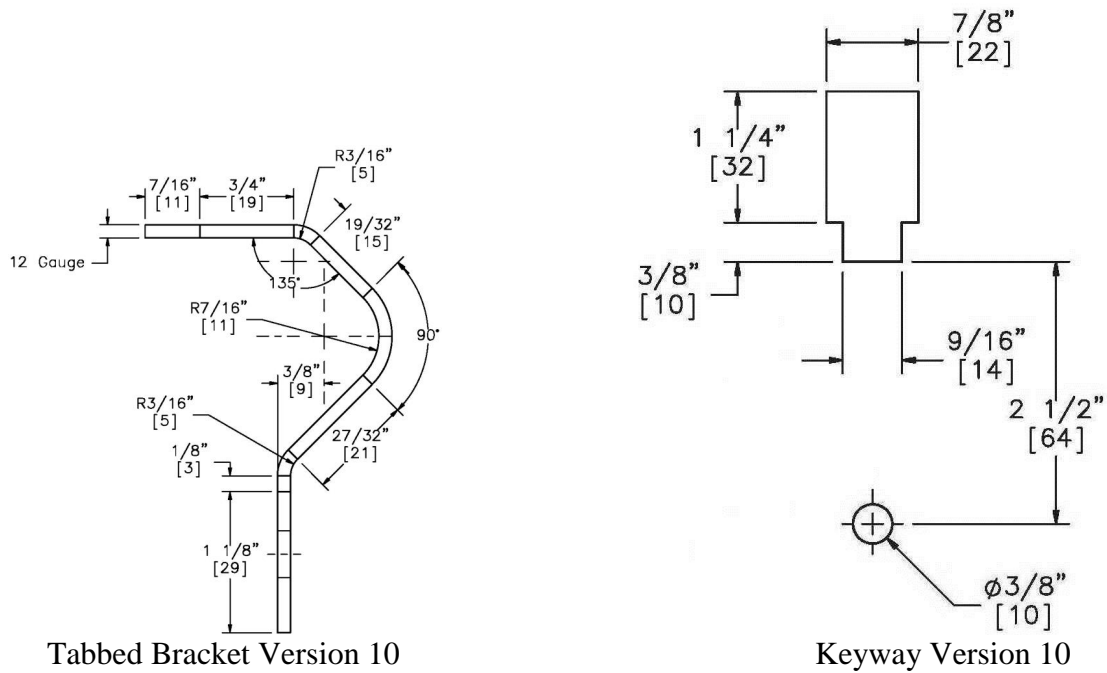


Figure 359. Bolted Tabbed Bracket Version 10 and Keyway Version 10

Either bolted tabbed bracket—Version 8 or 10—will fit into either keyway. The neck of bolted tabbed bracket Version 8 was longer than that of Version 10 by 1/8 in. (3.2 mm). The lower, narrow slot of keyway Version 8 was shallower than that of Version 10 by 1/16 in. (1.6 mm). Since bolted tabbed bracket Version 8 caught in its own keyway when pulled laterally, it is almost certain that bolted tabbed bracket Version 10 would also catch in keyway Version 8 when pulled laterally. Furthermore, since bolted tabbed bracket Version 10 released freely through its own keyway when pulled vertically, it is almost certain that it would also release freely through keyway Version 8 when pulled vertically. In fact, keyway Version 8 is probably better suited for bolted tabbed bracket Version 10. The vertical release load of bolted tabbed bracket Version 10, when used with keyway Version 8, would probably range between 261 lb (1.16 kN) and 346 lb (1.54 kN)—the vertical release loads of the two bolted tabbed brackets when used in their own keyways. Likewise, the lateral release load of that combination would probably range between 5.65 kips (25.1 kN) and 6.10 kips (27.1 kN)—the lateral release loads of the two bolted tabbed brackets when used in their own keyways.

Finally, the selection of a preferred cable-to-post attachment was between bolted tabbed bracket Version 8 and bolted tabbed bracket Version 10. The shorter neck of tabbed bracket Version 10 was ultimately more desirable; since, there would be additional clearance away from the backside surface of the flange. Ultimately, bolted tabbed bracket Version 10, in combination with keyway Version 8, was selected for the new cable-to-post attachment for the bottom three cables of the high-tension, 4-cable median barrier. However, it should be noted that the AISI C1018 extended keyway bolt may also provide acceptable behavior when used in high-tension, cable barrier systems.

17 TOP CABLE-TO-POST ATTACHMENT DETAILS

17.1 Introduction

A cable median barrier must be able to capture passenger vehicles, regardless of where impact occurs within the system. In full-scale crash test no. 4CMB-5, the pickup truck (2270P vehicle) impacted the system just upstream from a post. As the post was struck and rotated backward, the top cable was pulled down and allowed the vehicle to override the barrier system. To prevent this behavior, it was believed that the top cable-to-post attachment would need to restrain the cable under static loading conditions but allow cable release almost immediately when a post was struck by a vehicle.

Previously, the same cable-to-post attachment was used at all four cable locations. However, it was deemed necessary to utilize a weaker cable-to-post attachment for the top cable than used for the lower three cables. This concept was completely new and required a fresh start with new ideas. The new, top cable-to-post attachment would need to be relatively simple, easy to install, and have vertical and lateral cable release loads in the range of 100 to 200 lb (445 to 890 N). The new hardware would also need to be corrosion resistant. To begin this effort, it was decided initially to investigate the availability and use of small diameter, galvanized carbon steel, brass, and stainless steel round rods. It was believed that design prototypes could be fabricated rather easily, and their vertical release loads could be tested statically using a tensile testing machine. During the investigation of black and galvanized carbon steel rod or wire, it was realized that local vendors were unable to provide information about the material properties (i.e., yield, ultimate tensile strength, and ductility). However, brass and stainless steel round rods were found to be readily available in the sizes needed and with the material properties provided. Thus, only brass and stainless steel materials were considered for the formed cable-to-post attachments using bent rods or wire, although galvanized carbon steel rods remain a possibility for the future,

as long as they have similar material properties to the brass rods that were ultimately selected. In addition, commercially-available, stainless steel cable ties were also explored.

Several sizes of round rods or bars were acquired using brass and stainless steel materials with varying mechanical properties. The yield strength and tensile strength for each specimen (material and size) is summarized in Table 17.

Table 17. Round Rod or Bar Material-Type, Size, and Strength

Material	Diameter, in. (mm)	Yield Strength, ksi (MPa)	Tensile Strength, ksi (MPa)
C360 Brass	1/16 (1.6)	Not Provided on Mill Certificate	80 (552)
C360 Brass	3/32 (2.4)	Not Provided on Mill Certificate	73 (503)
C360 Brass	1/8 (3.2)	62 (427)	81 (558)
C360 Brass	3/16 (4.8)	63 (434)	68 (469)
C360 Brass	1/4 (6.4)	Not Provided on Mill Certificate	Not Provided on Mill Certificate
T-303 Stainless Steel	3/32 (2.4)	77 (531)	105 (724)
T-304 Stainless Steel	1/8 (3.2)	97 (669)	113 (779)
T-304 Stainless Steel	3/16 (4.8)	98 (676)	115 (793)
T-304 Stainless Steel	1/4 (6.4)	98 (676)	114 (786)

17.1.1 Static Tensile Testing

All of the prototype designs denoted in this chapter were later subjected to static tensile testing using the procedures and setup described in Chapter 18. The results from these static tests are presented and discussed in Chapter 19.

Forty-five static tests were conducted on the various designs, as detailed in the subsections that follow. There were two rounds of tests. Round 1 included web-inserted curved rods, squeeze-in-place curved rods, and HellermannTyton stainless steel cable ties. Round 2 included revised web-inserted curved rods and straight rods. A limited number of photographs of

the concepts are shown in this chapter. Detailed drawings were not made, but preliminary sketches were created and used for in-house fabrication, as depicted in Appendix D.

17.2 Top Cable-to-Post Attachment Design Concepts

17.2.1 Web-Inserted Curved Rods

The first concept consisted of web-inserted curved rods that were to be placed over the cable. Their lower, bent ends were to be inserted through pre-drilled or punched holes placed in the web. Once inserted, both ends would be bent upward as much as possible, thus securing the curved rod into place. Five variations were fabricated and tested. These five variations included: C360 brass rods with diameters of 1/16 in. (1.8 mm), 3/32 in. (2.4 mm), and 1/8 in. (3.2 mm); a T-303 stainless steel rod with a diameter of 3/32 in. (2.4 mm); and a T-304 stainless steel rod with a diameter of 1/8 in. (3.2 mm). An example of one of these variations is shown in Figure 360.

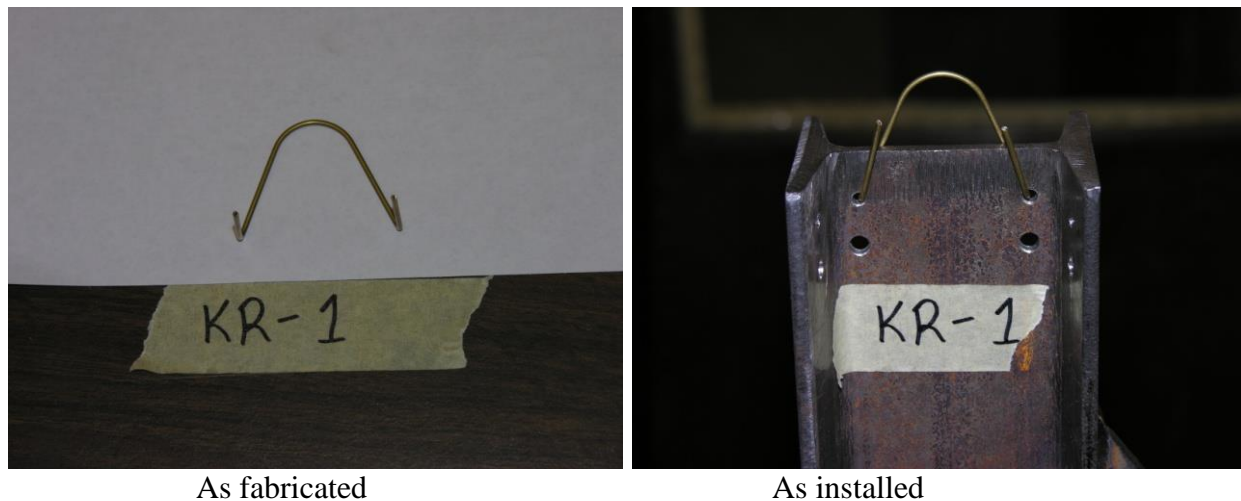


Figure 360. Web-Inserted Curved Rod Example

17.2.2 Revised Web-Inserted Curved Rods

Revised web-inserted curved rods were tested in the second round of static tests. There were two variations of revised web-inserted curved rods, both using a diameter of 1/8 in. (3.2

mm). One variation was fabricated from C360 brass, while the other variation used T-304 stainless steel. The revised prototypes were slightly different from the web-inserted curved rods utilized, as shown in Figure 361.

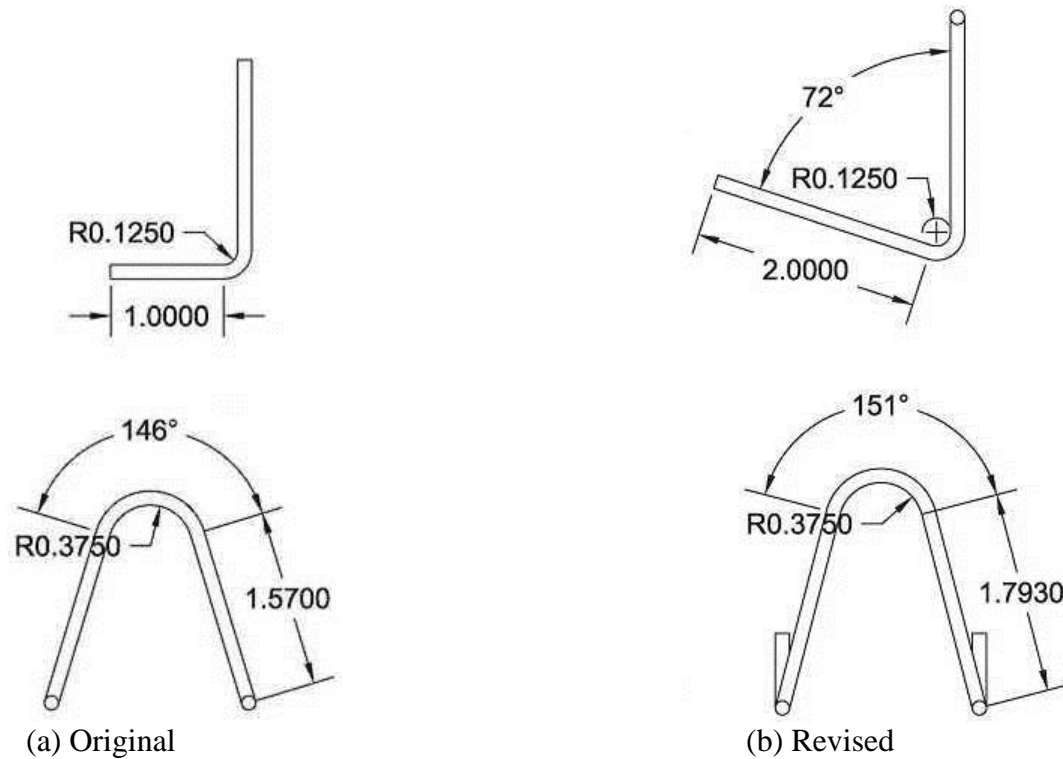


Figure 361. 1/8-in. (3.2-mm) Web-Inserted Curved Rod—(a) Original and (b) Revised

It should be noted that the original 1/8-in. (3.2-mm) web-inserted curved rods. The revised prototypes were lengthened, which made them easier to install and bend upward. Easy installation usually results in improved field installation.

17.2.3 Squeeze-In-Place Curved Rods

Squeeze-in-place curved rods were to be placed over the cable. Their lower ends were to be inserted through pre-drilled or punched holes placed in the flanges. To install the squeeze-in-place curved rods, the open end had to be squeezed together and properly positioned between the flanges with holes. Then, the open leg ends would be released and allowed to spring back into

the holes. Five different variations were fabricated and tested. These five variations included: C360 brass rods with diameters of 1/16 in. (1.8 mm), 3/32 in. (2.4 mm), and 1/8 in. (3.2 mm); a T-303 stainless steel rod with a diameter of 3/32 in.; and a T-304 stainless steel rod with a diameter of 1/8 in. (3.2 mm). An example of one of these variations is shown in Figure 362. The squeeze-in-place curved rods were relatively easy to install, even with a little practice. These prototypes could also be easily removed when squeezed together with almost no observable deformation.

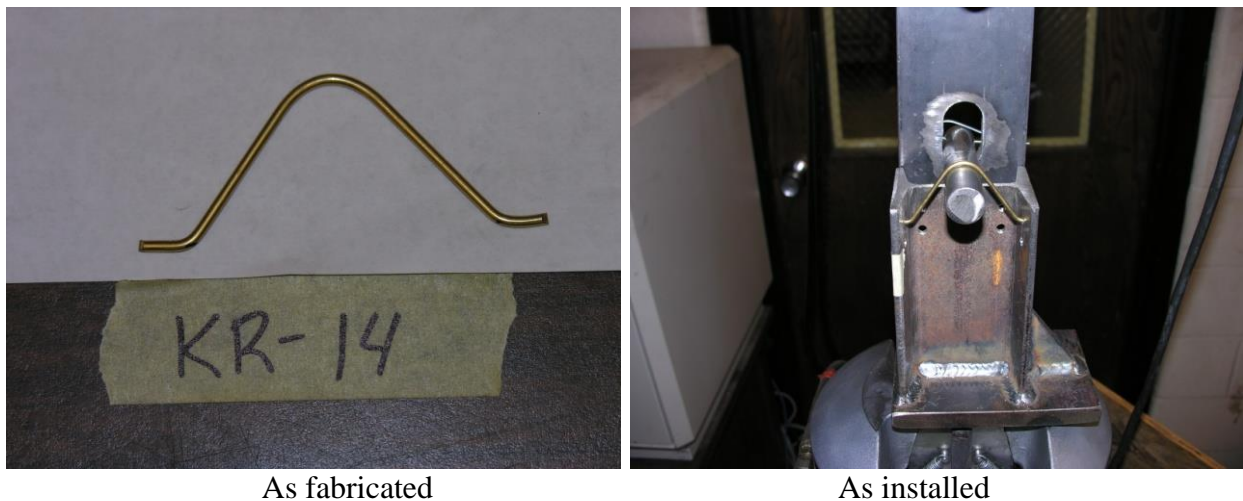


Figure 362. Squeeze-In-Place Curved Rod Example

17.2.4 HellermannTyton Stainless Steel Cable Ties

HellermannTyton stainless steel cable ties were configured to be looped through holes in the flanges and tightened over the cable. The cable ties were fabricated from 304 stainless steel. Two variations were acquired for later testing. The first variation was rated for a tensile force of 250 lb (1.11 kN). Its thickness and width were 0.012 in. (0.30 mm) and 0.31 in. (7.9 mm), respectively. The second variation was rated for a tensile force of 150 lb (667 N). Its thickness and width were 0.012 in. (0.30 mm) and 0.18 in. (4.6 mm), respectively. An example of one of

these variations is shown in Figure 363. These cable ties were installed by hand and had a self-locking, ball bearing mechanism. Installation of the cable tie was relatively easy.

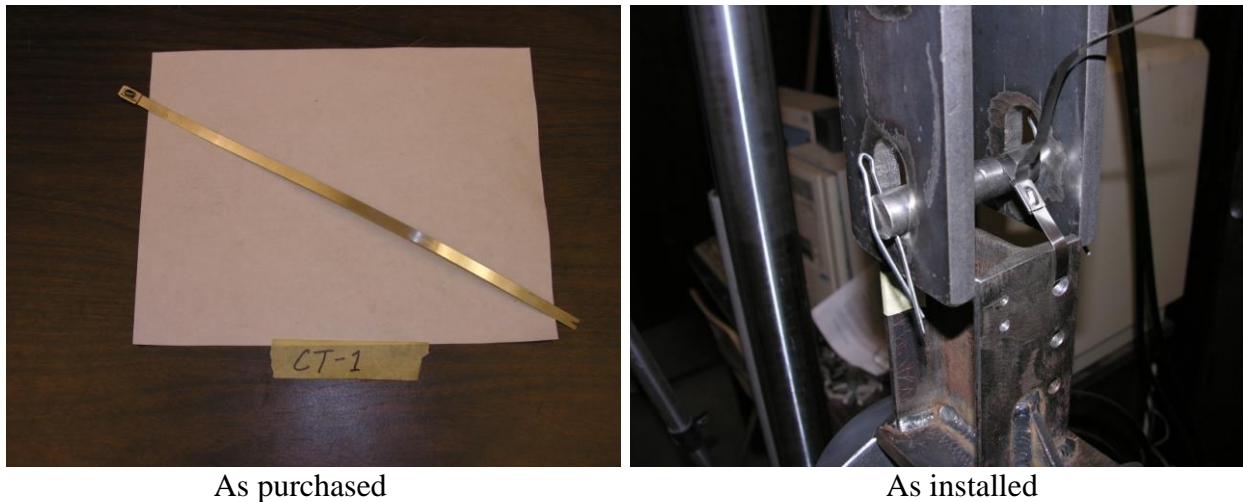


Figure 363. HellermannTyton Stainless Steel Cable Tie Example

17.2.5 Straight Rods

For the final design concept, a straight rod with bent ends was positioned over a cable which was placed in the bottom of a v-notch in the web. The straight rod with bent ends was inserted through a hole and slot in the flanges. Six different variations were fabricated and tested. These variations included C360 brass and T-304 stainless steel rods with diameters of 1/8 in. (3.2 mm), 3/16 in. (4.8 mm), and 1/4 in. (6.4 mm). An example of one of these variations is shown in Figure 364. For all of the concepts denoted in Chapter 17, the straight brass rods with bent ends were the easiest to install.



As fabricated



As Installed

Figure 364. Straight Rod Example

18 TOP CABLE-TO-POST ATTACHMENT STATIC TEST CONDITIONS

18.1 Purpose

The vertical cable release behavior of several top cable-to-post attachment concepts was evaluated with static tensile tests before considering dynamic bogie testing. These tests were used as a first step in the evaluation process. Their main advantage was that many static tests could be performed in a short time period and at a relatively low cost as compared to bogie testing. It was useful to observe deformations to the top cable-to-post attachments and determine vertical cable release loads. Next, engineering judgment could be used to select a concept which might perform well in a bogie test and eventually in a full-scale crash testing program.

18.2 Scope

Once again, forty-five static tensile tests were performed on the various top cable-to-post attachment concepts. These tests utilized a test jig, fixed within a tensile testing machine, to anchor the top cable-to-post attachments. For a given test, the top cable-to-post attachments were loaded at a constant displacement rate until they failed. The loads and displacements were recorded for each test.

18.3 Testing Facility

Static testing was performed at the University of Nebraska-Lincoln's Mechanical Engineering Materials Lab, located in the Walter Scott Engineering Center.

18.4 Equipment and Instrumentation

Several types of equipment and instrumentation were utilized for the static testing program, including an MTS 810 with a displacement transducer and a 20-kip (89-kN) load cell, a test jig, standard-speed digital video, and digital still cameras.

18.4.1 MTS 810

The Material Testing System (MTS) 810 was used to test the top cable-to-post attachment concepts under static loads. A 20-kip (89-kN) load cell measured the force placed on each attachment, while displacement transducers measured the corresponding deflection. Most tests were performed on the prototype hardware using a displacement rate of 0.2 in./min (5 mm/min). However, one concept used a displacement rate of 0.4 in./min (10 mm/min), while another used a displacement rate of 0.8 in./min (20 mm/min).

18.4.2 Test Jig

The test jig consisted of a top assembly and a bottom assembly. The bottom assembly was one piece, consisting of a section of S3x5.7 (S76x8.5) steel post, welded on the bottom to a ½-in. (13-mm) thick steel plate. On the bottom of that steel plate, another ½-in. (13-mm) thick steel plate was welded perpendicular to it, which allowed the bottom clamp of the MTS 810 to secure it.

The top assembly consisted of four pieces. The top-most piece consisted of a ½-in. (13-mm) thick steel plate, which allowed the top clamp of the MTS 810 to secure it, and a ¾-in. (19-mm) diameter steel bar was welded to its bottom. Two, identical, symmetric, ½-in. (13-mm) thick steel plates—one on each end—were hung from the steel bar of the top-most piece of the assembly. Each of these plates had two slots. The slots were used to hang the plates from the top-most piece and to provide a place to set the bottom-most piece. The bottom-most piece was a ¾-in. (19-mm) diameter steel bar, used to simulate the cable. A photograph of the test jig is shown in Figure 365.



Figure 365. Test Jig for Static Tests

18.4.3 Digital Photography

Digital photographs of the samples were taken before and after static testing. These were taken with a Nikon Coolpix 8800 digital camera. Video footage of the static tests was collected with a JVC digital video camera.

19 TOP CABLE-TO-POST ATTACHMENT STATIC TESTING RESULTS AND DISCUSSION

19.1 Results

Several top cable-to-post attachment concepts were fabricated, as described in detail in Chapter 17, for use in a static testing program. Forty-five static component tests were conducted. All of the tests were configured to pull vertically on the top cable-to-post attachments. The test results varied greatly, and there were some observed problems and/or errors. These problems were associated with operator error (not knowing how long the MTS machine would run until it timed out), or a lack of knowledge of the concept behavior behave when loaded (not knowing whether prototypes would release quickly or slowly, and how much deflection to expect). Despite these problems, much information was garnered.

As previously noted, the top cable-to-post attachments should provide relatively low lateral and vertical cable release strengths, say between 100 and 200 lb (445 and 890 N), to accommodate static loading conditions resulting from horizontal and vertical road alignments. However, the cable must be able to immediately release when the impacted post rotates backward and downward. It was also believed the vertical release behavior under static loading conditions would be indicative of cable release under real-world dynamic loading conditions. As noted previously, simple CAD details of the concepts can be found in Appendix D.

19.2 Web-Inserted Curved Rods

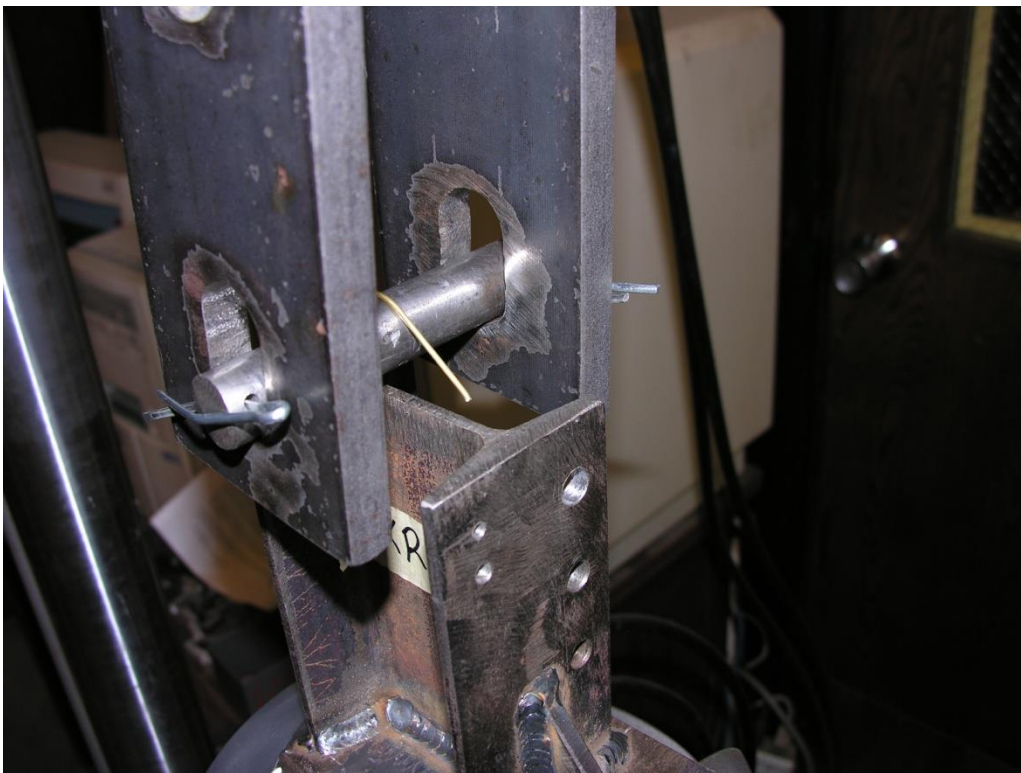
Web-inserted curved rod concepts were tested in test nos. KR-1 through KR-10. The test matrix and results are summarized in Table 18. Before and after photographs for one of the tests, as shown in Figure 366, are provided for a web-inserted curved rod.

Table 18. Test Matrix and Results for Web-Inserted Curved Rods

Test No.	Material	Diameter in. (mm)	Rate in./min (mm/min)	Peak Load lb (N)	Notes
KR-1	C360 Brass	1/16 (1.6)	0.2 (5)	6 (27)	Bent and fractured at hole
KR-2	C360 Brass	1/16 (1.6)	0.2 (5)	59 (262)	Bent and fractured at hole
KR-3	C360 Brass	3/32 (2.4)	0.2 (5)	185 (823)	Bent and fractured at hole
KR-4	C360 Brass	3/32 (2.4)	0.2 (5)	205 (910)	Bent and fractured at hole
KR-5	C360 Brass	1/8 (3.2)	0.2 (5)	275 (1,223)	Bent and fractured at hole
KR-6	C360 Brass	1/8 (3.2)	0.2 (5)	295 (1,314)	Bent and fractured at hole
KR-7	T-303 Stainless Steel	3/32 (2.4)	0.2 (5)	113 (502.6)	Bent and slipped out of holes
KR-8	T-303 Stainless Steel	3/32 (2.4)	0.2 (5)	138 (613)	Bent and slipped out of holes
KR-9	T-304 Stainless Steel	1/8 (3.2)	0.2 (5)	331 (1,472)	Bent and slipped out of holes
KR-10	T-304 Stainless Steel	1/8 (3.2)	0.2 (5)	362 (1,609)	Bent and slipped out of holes



Before



After

Figure 366. Example of Web-Inserted Curved Rod Test

19.2.1 Test Nos. KR-1 and KR-2 (Web, 1/16-in. Brass)

For test nos. KR-1 and KR-2, web-inserted curved rods, fabricated from 1/16-in. (1.6-mm) diameter, C360 brass, were vertically loaded at a displacement rate of 0.2 in./min (5 mm/min). In test no. KR-1, the rod fractured near one of the bolt holes, just as it was beginning to bend. The peak load for test no. KR-1 was 6 lb (27 N). In test no. KR-2, the rod began to bend and slip out of one of the holes before it finally fractured. The peak load for test no. KR-2 was 59.0 lb (262 N). The force versus displacement curve for test nos. KR-1 and KR-2 is shown in Figure 367. Pre- and post-test photographs are shown in Figures 368 and 369.

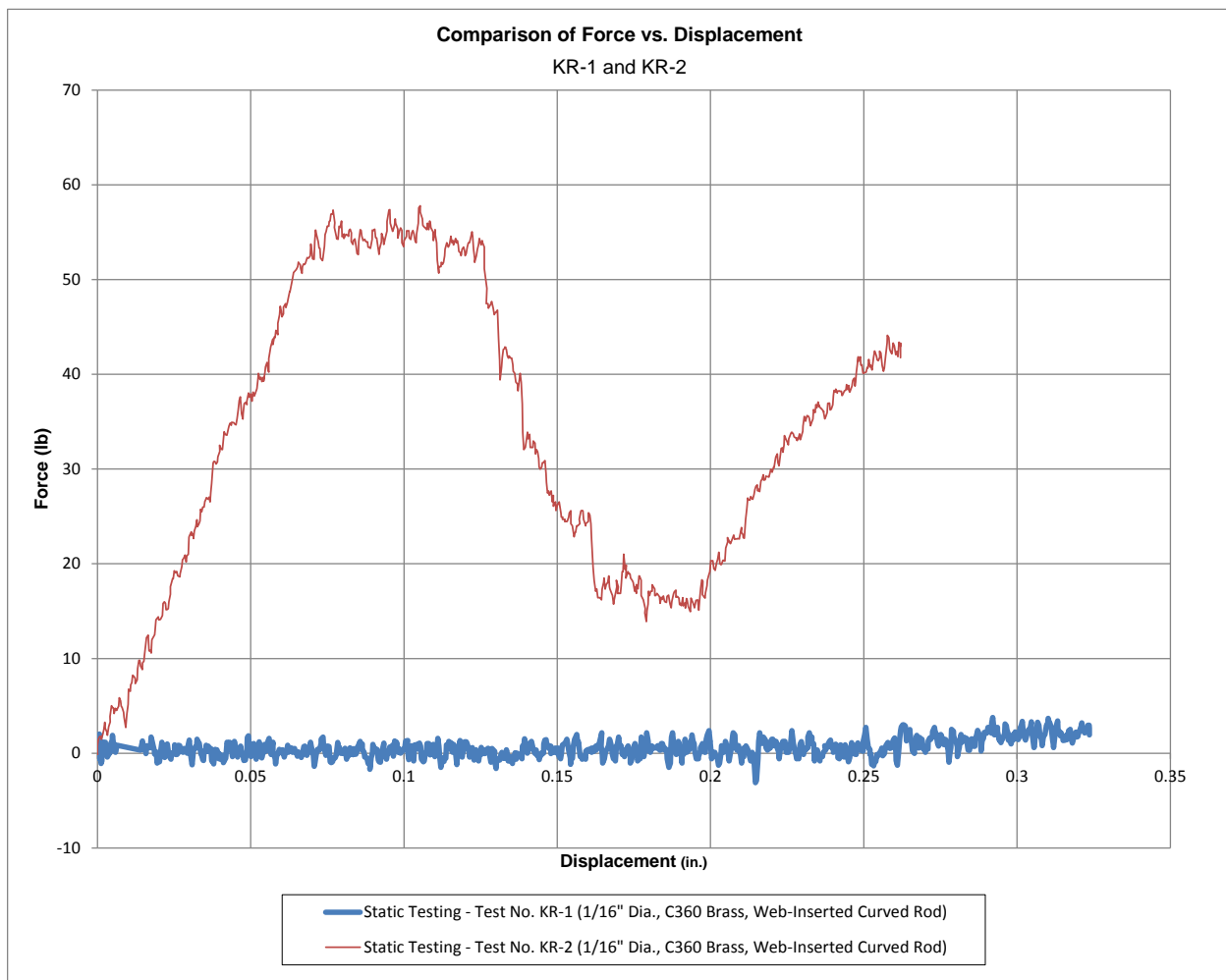


Figure 367. Force Versus Displacement, Test Nos. KR-1 and KR-2

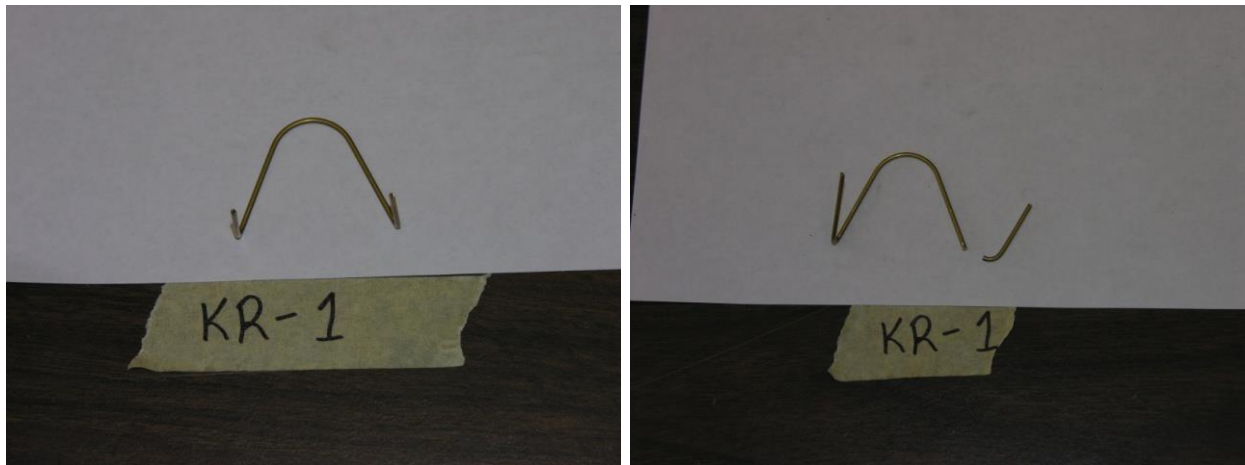


Figure 368. Pre-Test and Post-Test Photographs, Test No. KR-1

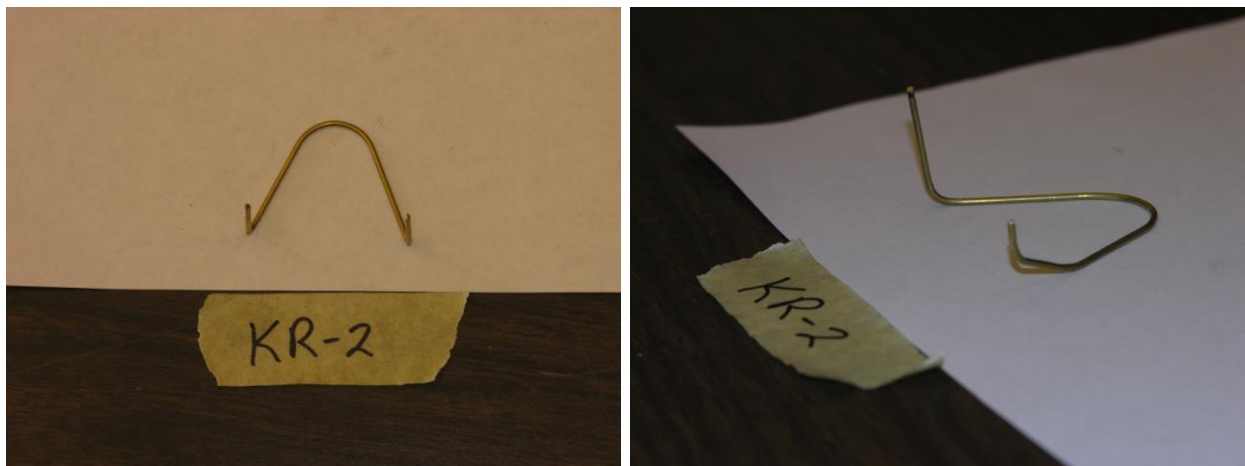


Figure 369. Pre-Test and Post-Test Photographs, Test No. KR-2

19.2.2 Test Nos. KR-3 and KR-4 (Web, 3/32-in. Brass)

For test nos. KR-3 and KR-4, web-inserted curved rods, fabricated from 3/32-in. (2.4-mm) diameter, C360 brass, were vertically loaded at a displacement rate of 0.2 in./min (5 mm/min). In both tests, the rods began to bend and slip out of one of the holes before finally fracturing. The peak loads for test nos. KR-3 and KR-4 were 185 lb (823 N) and 205 lb (910 N), respectively. The force versus displacement curve for test nos. KR-3 and KR-4 is shown in Figure 370. Pre- and post-test photographs are shown in Figures 371 and 372.

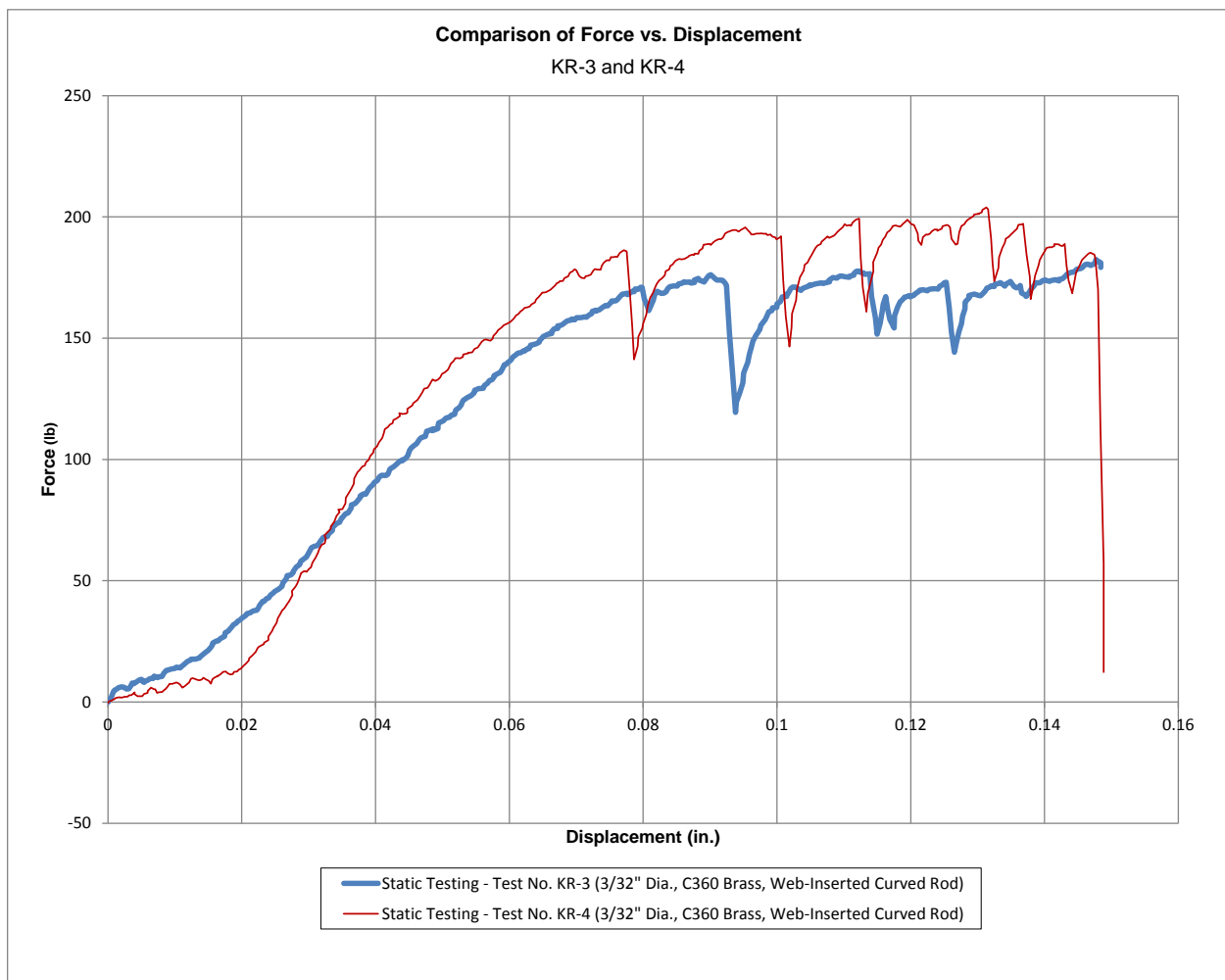


Figure 370. Force Versus Displacement, Test Nos. KR-3 and KR-4

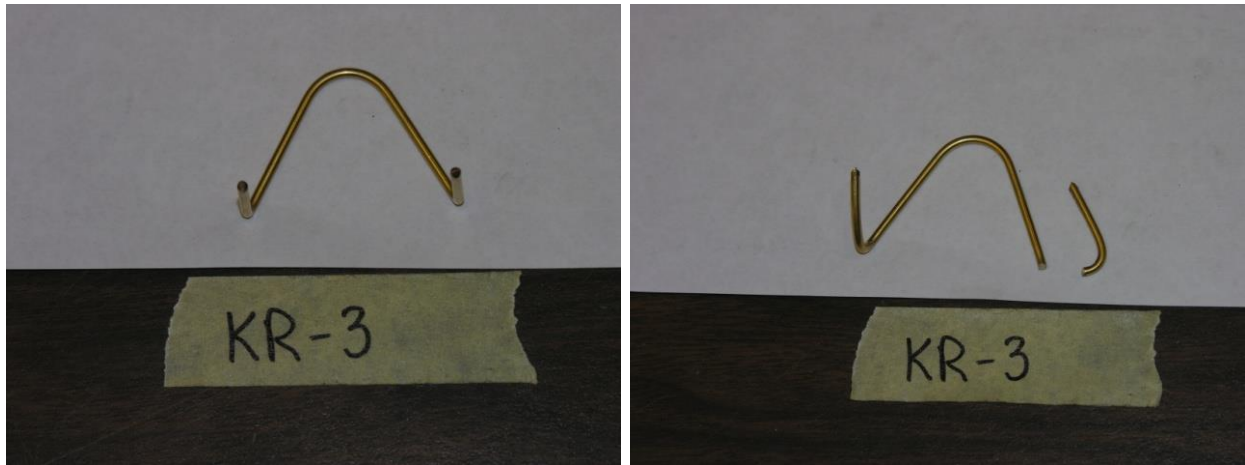


Figure 371. Pre-Test and Post-Test Photographs, Test No. KR-3

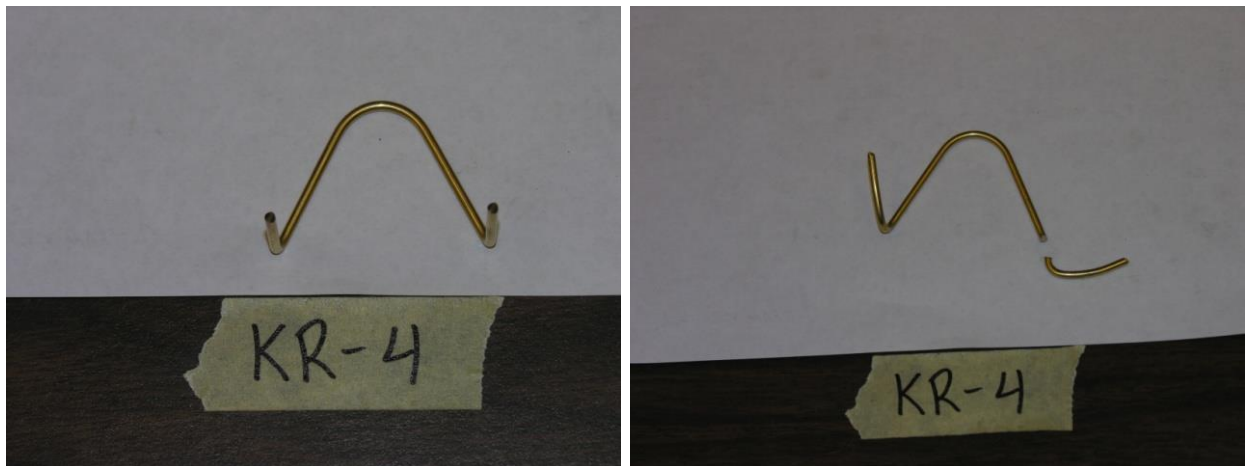


Figure 372. Pre-Test and Post-Test Photographs, Test No. KR-4

19.2.3 Test Nos. KR-5 and KR-6 (Web, 1/8-in. Brass)

For test nos. KR-5 and KR-6, web-inserted curved rods, fabricated from 1/8-in. (3.2-mm) diameter, C360 brass, were vertically loaded at a displacement rate of 0.2 in./min (5 mm/min). In both tests, the rods began to bend and slip out of one of the holes before finally fracturing. The peak loads for test nos. KR-5 and KR-6 were 275 lb (1,223 N) and 295 lb (1,314 N), respectively. The force versus displacement curve for test nos. KR-5 and KR-6 is shown in Figure 373. Pre- and post-test photographs are shown in Figures 374 and 375.

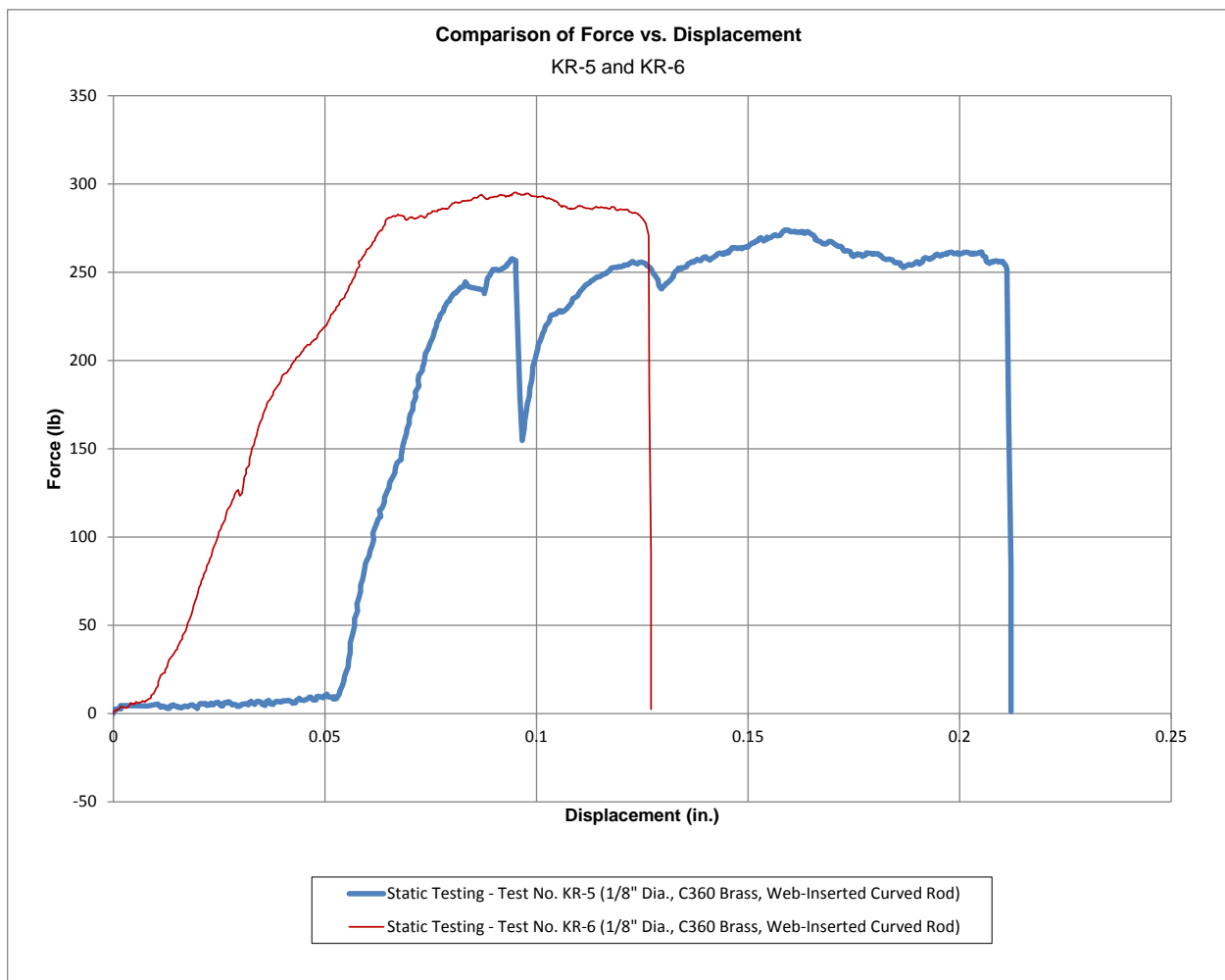


Figure 373. Force Versus Displacement, Test Nos. KR-5 and KR-6

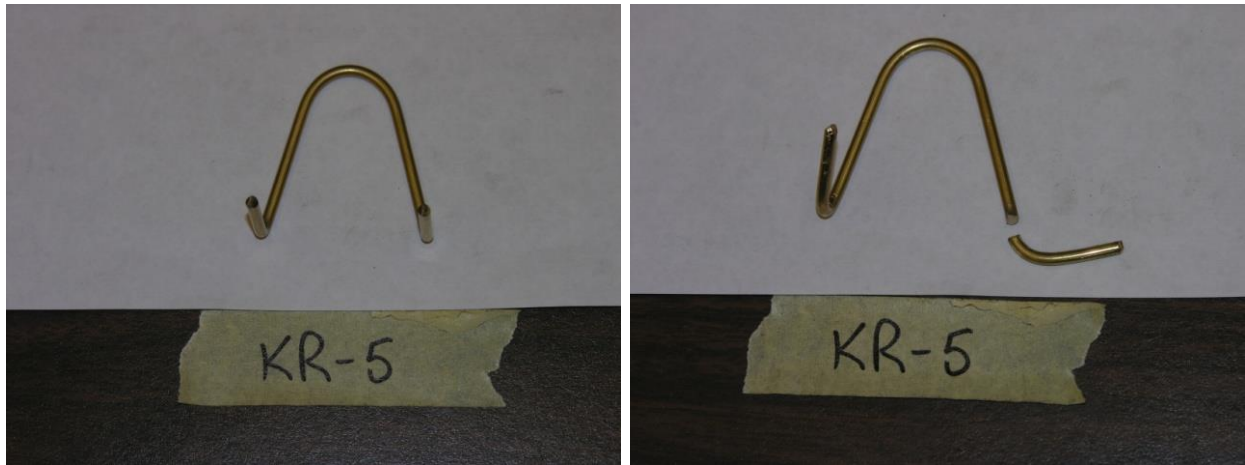


Figure 374. Pre-Test and Post-Test Photographs, Test No. KR-5

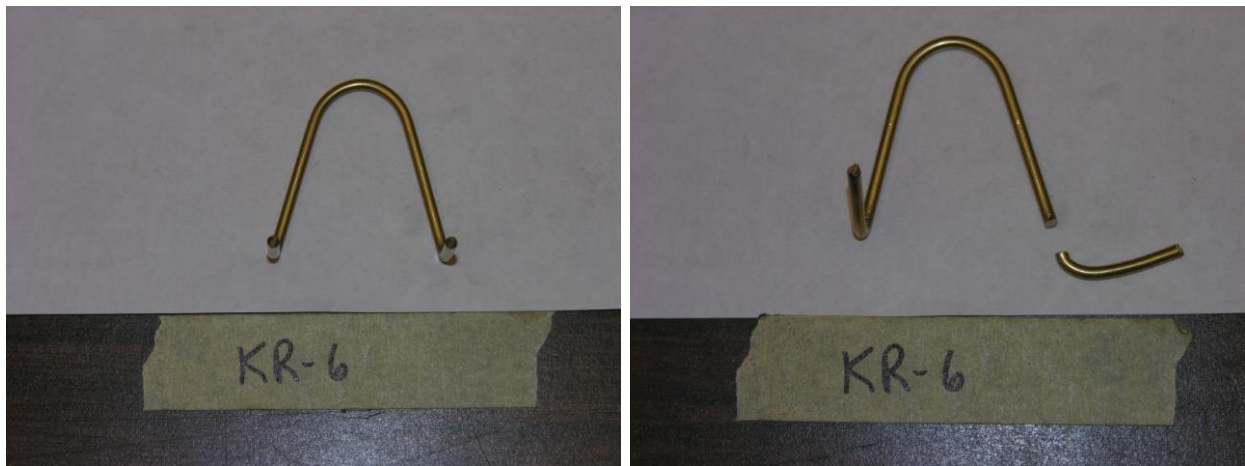


Figure 375. Pre-Test and Post-Test Photographs, Test No. KR-6

19.2.4 Test Nos. KR-7 and KR-8 (Web, 3/32-in. Stainless)

For test nos. KR-7 and KR-8, web-inserted curved rods, fabricated from 3/32-in. (2.4-mm) diameter, T-303 stainless steel, were vertically loaded at a displacement rate of 0.2 in./min (5 mm/min). In both tests, the rods began to bend, eventually slipping out of the holes. The peak loads for test nos. KR-7 and KR-8 were 113 lb (503 N) and 138 lb (613 N), respectively. The force versus displacement curve for test nos. KR-7 and KR-8 is shown in Figure 376. Pre- and post-test photographs are shown in Figures 377 and 378.

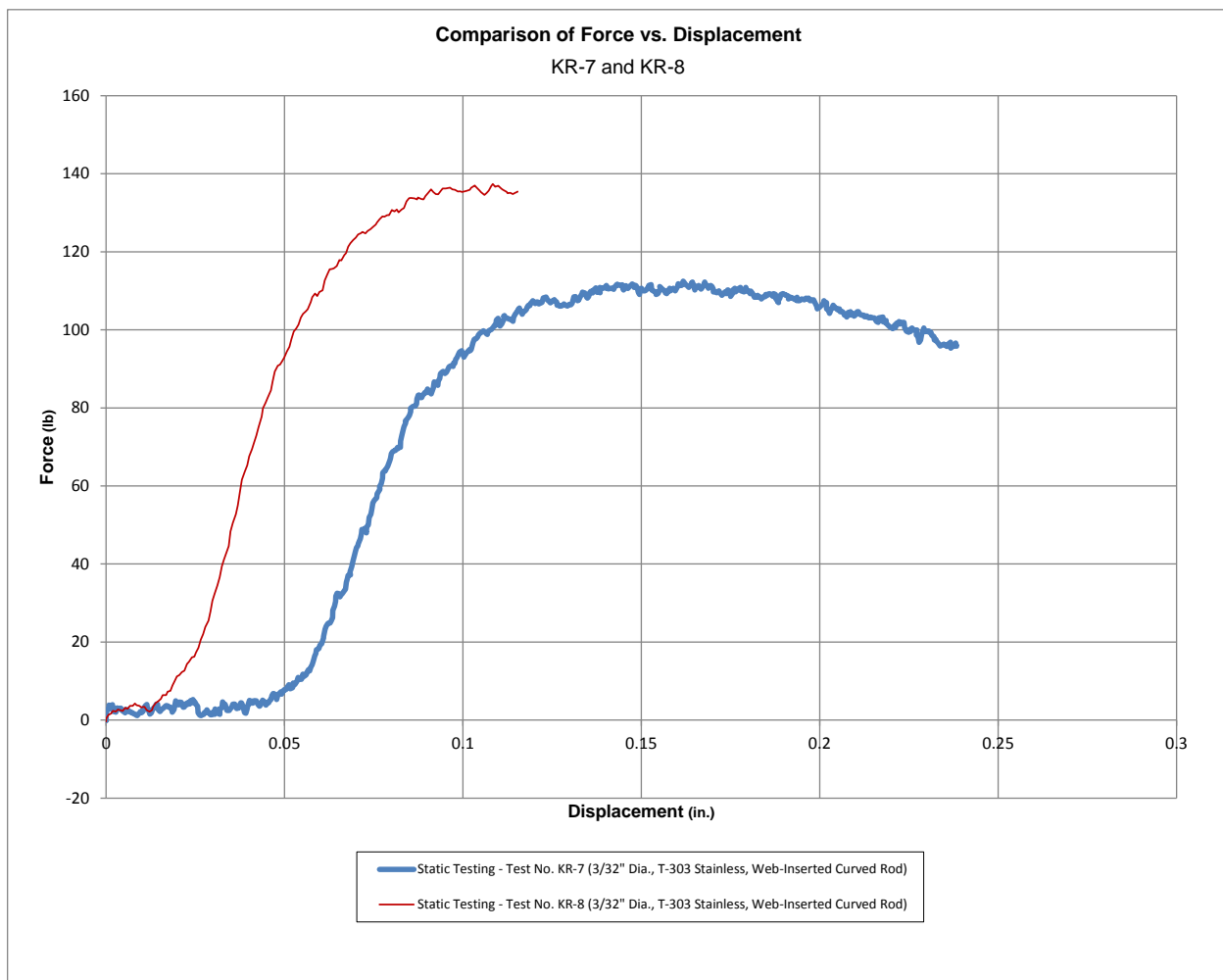


Figure 376. Force Versus Displacement, Test Nos. KR-7 and KR-8

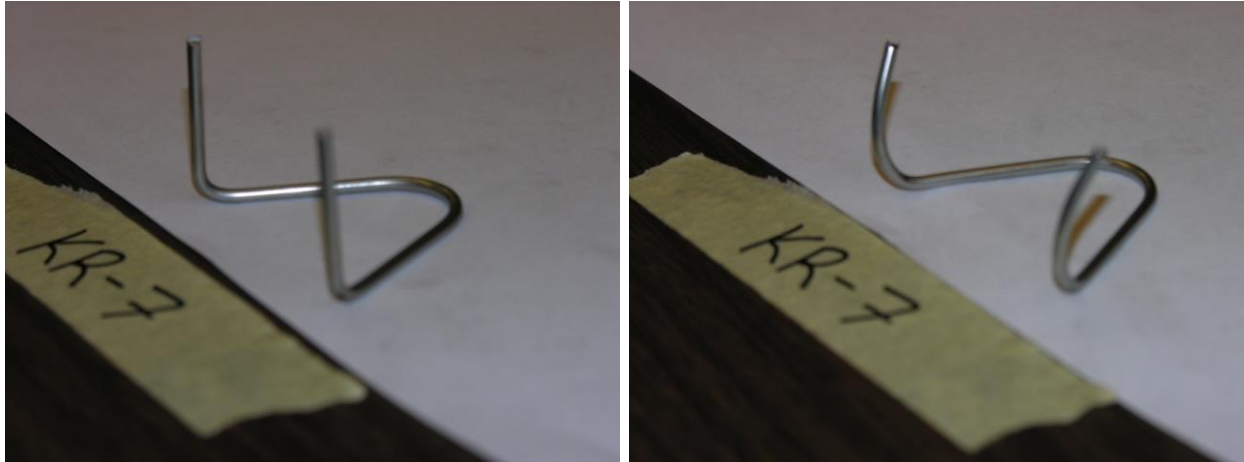


Figure 377. Pre-Test and Post-Test Photographs, Test No. KR-7

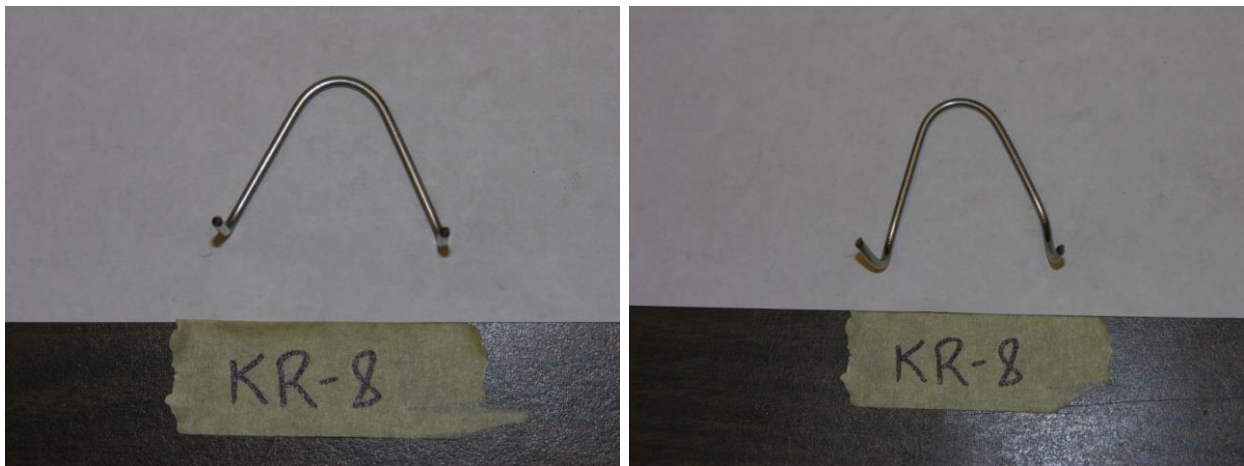


Figure 378. Pre-Test and Post-Test Photographs, Test No. KR-8

19.2.5 Test Nos. KR-9 and KR-10 (Web, 1/8-in. Stainless)

For test nos. KR-9 and KR-10, web-inserted curved rods, fabricated from 1/8-in. (3.2-mm) diameter, T-304 stainless steel, were vertically loaded at a displacement rate of 0.2 in./min (5 mm/min). In both tests, the rods began to bend, eventually slipping out of the holes. The peak loads for test nos. KR-9 and KR-10 were 331 lb (1,472 N) and 362 lb (1,609 N), respectively. The force versus displacement curve for test nos. KR-9 and KR-10 is shown in Figure 379. Pre- and post-test photographs are shown in Figures 380 and 381.

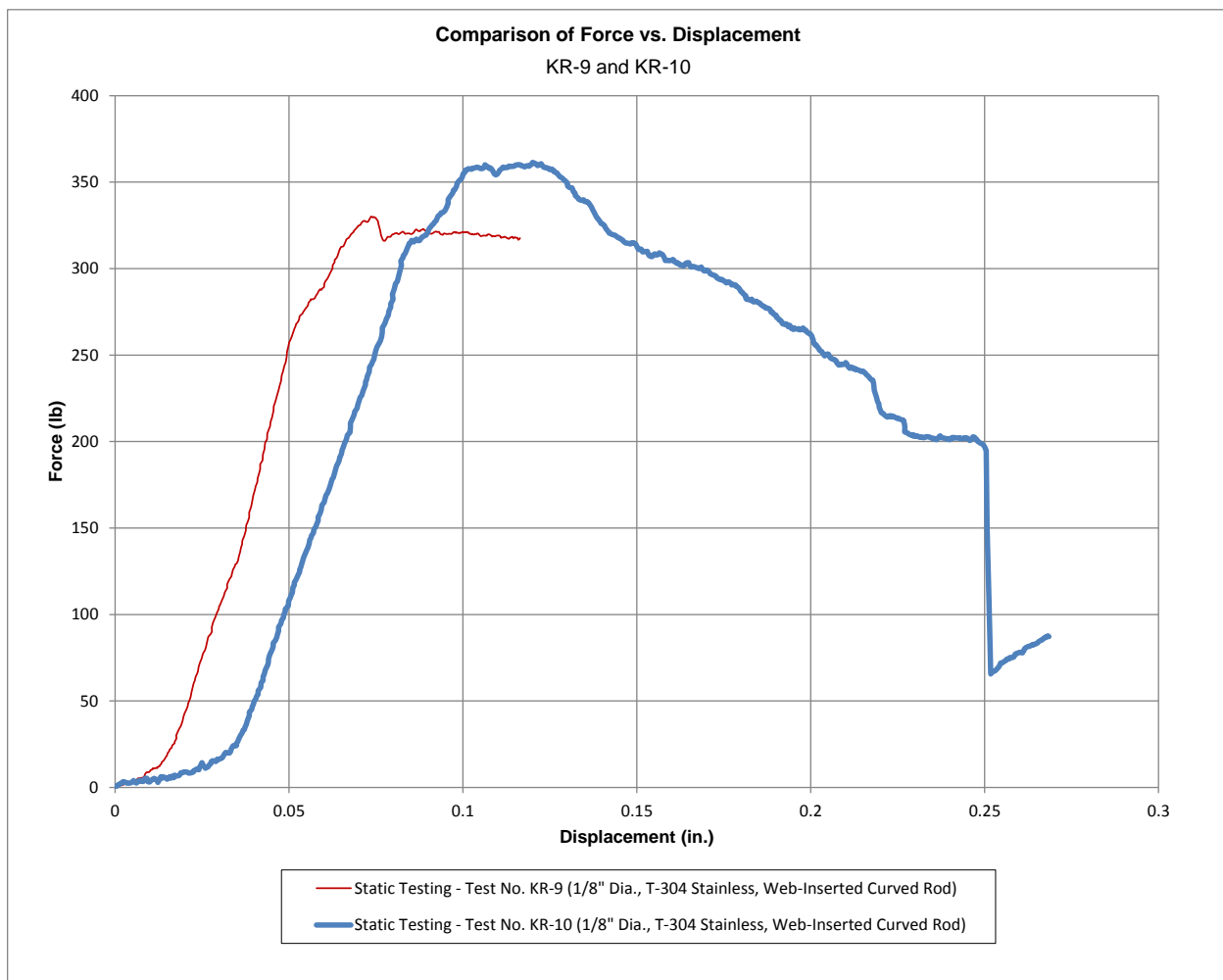


Figure 379. Force Versus Displacement, Test Nos. KR-9 and KR-10

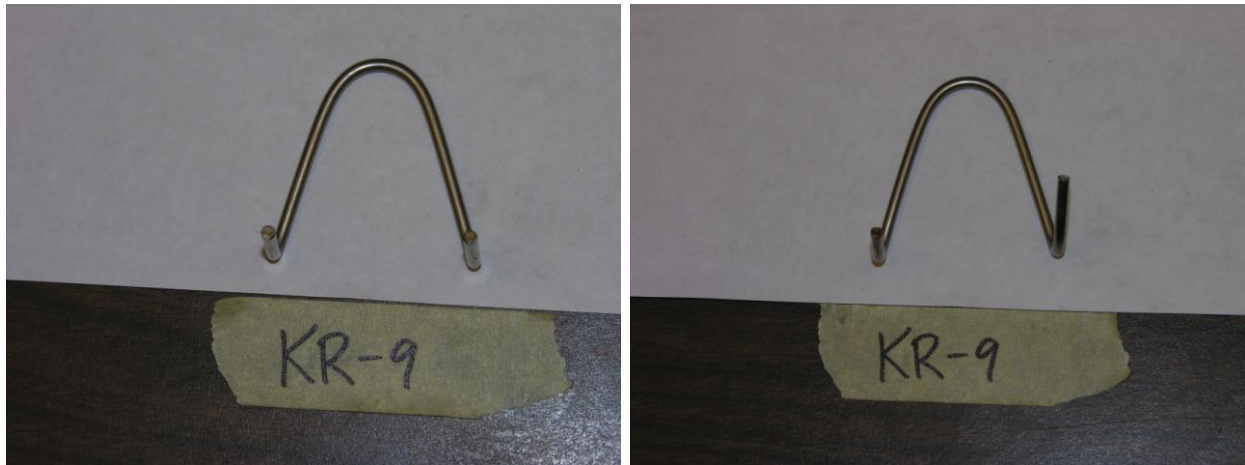


Figure 380. Pre-Test and Post-Test Photographs, Test No. KR-9

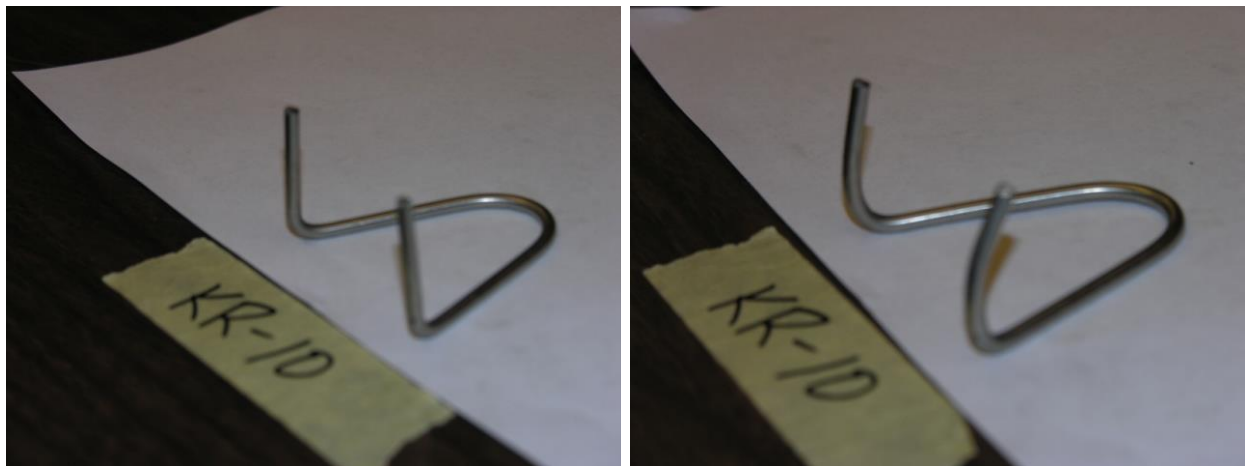


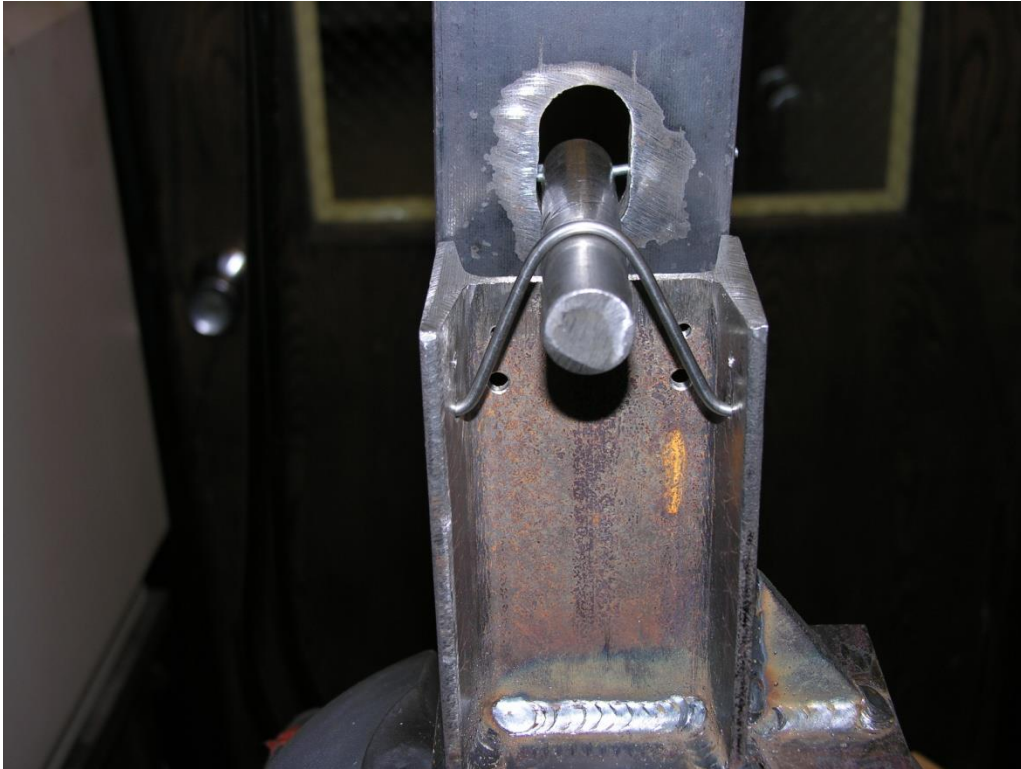
Figure 381. Pre-Test and Post-Test Photographs, Test No. KR-10

19.3 Squeeze-In-Place Curved Rods

Squeeze-in-place curved rod concepts were tested in test nos. KR-11 through KR-20. The test matrix and results are summarized in Table 19. Before and after photographs for one of the tests, as shown in Figure 382, are provided for a squeeze-in-place curved rod.

Table 19. Test Matrix and Results for Squeeze-In-Place Curved Rods

Test No.	Material	Diameter in. (mm)	Rate in./min (mm/min)	Peak Load lb (N)	Notes
KR-11	C360 Brass	1/16 (1.6)	0.2 (5)	8 (36)	Bent and slipped out of holes
KR-12	C360 Brass	1/16 (1.6)	0.2 (5)	11 (49)	Bent and slipped out of holes
KR-13	C360 Brass	3/32 (2.4)	0.2 (5)	31 (137)	Bent and slipped out of holes
KR-14	C360 Brass	3/32 (2.4)	0.2 (5)	37 (163)	Bent and slipped out of holes
KR-15	C360 Brass	1/8 (3.2)	0.2 (5)	58 (258)	Bent and slipped out of holes
KR-16	C360 Brass	1/8 (3.2)	0.2 (5)	62 (277)	Bent and slipped out of holes
KR-17	T-303 Stainless Steel	3/32 (2.4)	0.2 (5)	41 (183)	Bent and slipped out of holes
KR-18	T-303 Stainless Steel	3/32 (2.4)	0.2 (5)	42 (185)	Bent and slipped out of holes
KR-19	T-304 Stainless Steel	1/8 (3.2)	0.2 (5)	76 (336)	Bent and slipped out of holes
KR-20	T-304 Stainless Steel	1/8 (3.2)	0.2 (5)	71 (315)	Bent and slipped out of holes



Before



After

Figure 382. Example of Squeeze-In-Place Curved Rod Test

19.3.1 Test Nos. KR-11 and KR-12 (Squeeze, 1/16-in. Brass)

For test nos. KR-11 and KR-12, squeeze-in-place curved rods, fabricated from 1/16-in. (1.6-mm) diameter, C360 brass, were vertically loaded at a displacement rate of 0.2 in./min (5 mm/min). In both tests, as the rods were pulled upward, their ends slipped out of the holes in the flanges. The peak loads for test nos. KR-11 and KR-12 were 8 lb (36 N) and 11 lb (49 N), respectively. The force versus displacement curve for test nos. KR-11 and KR-12 is shown in Figure 383. Pre-test photographs are shown in Figures 384 and 385. There was no noticeable plastic deformation of the squeeze-in-place curved rods between the beginning and end states.

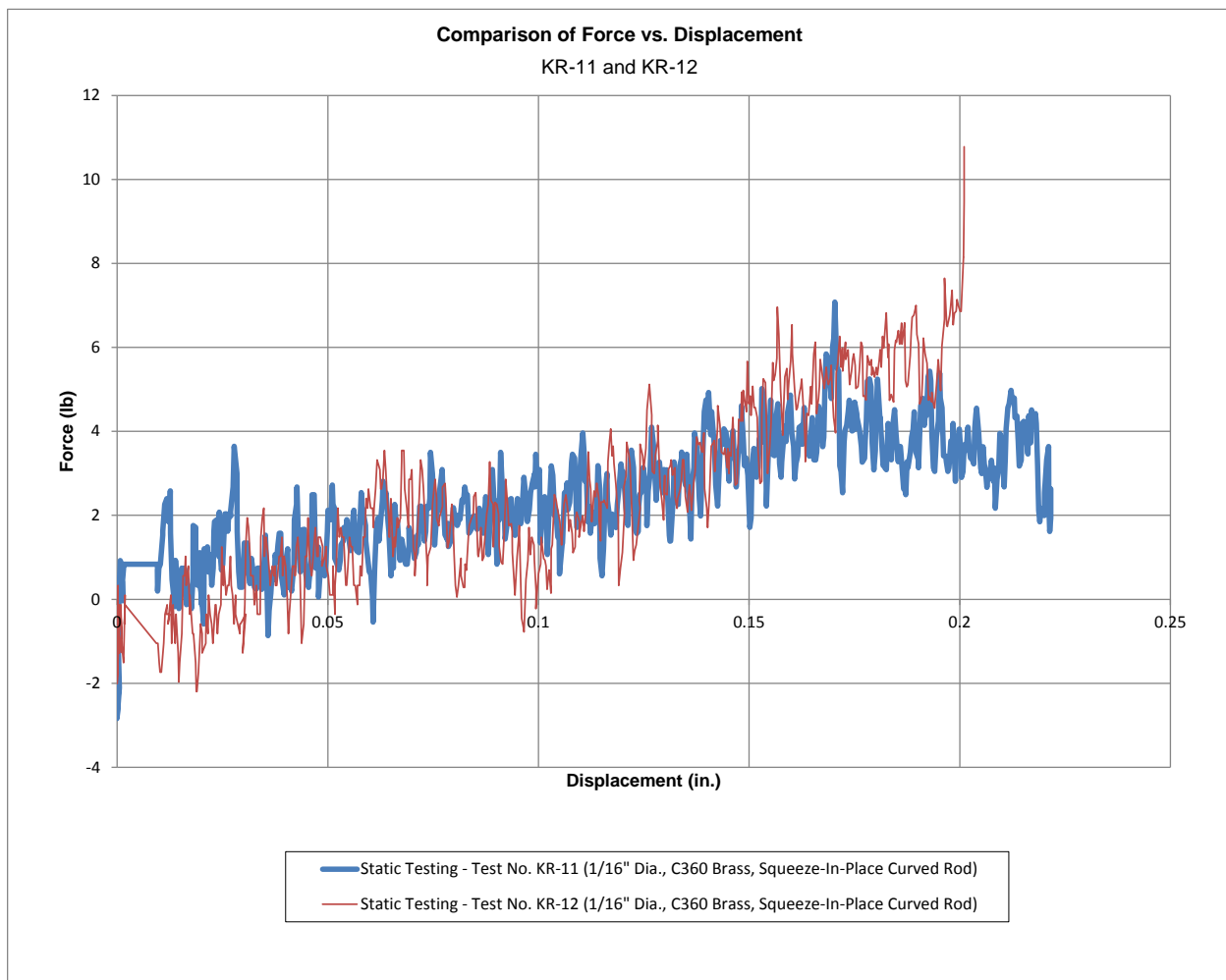


Figure 383. Force Versus Displacement, Test Nos. KR-11 and KR-12

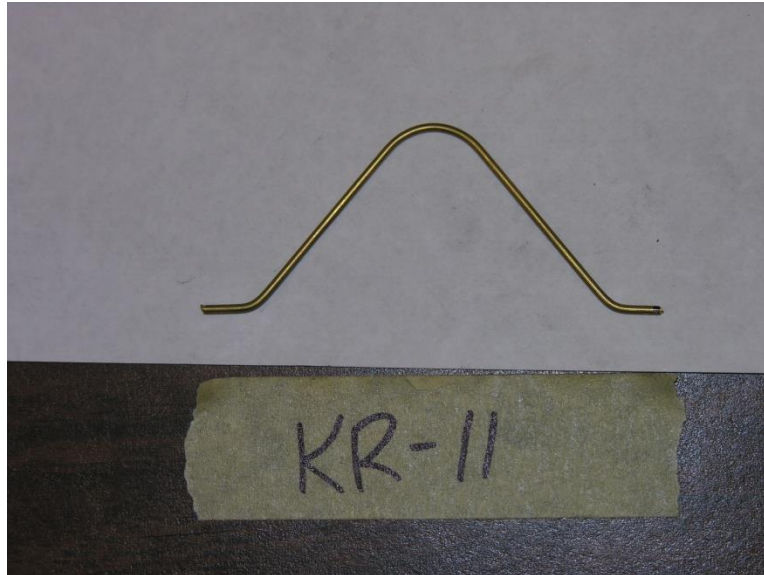


Figure 384. Pre-Test Photograph, Test No. KR-11

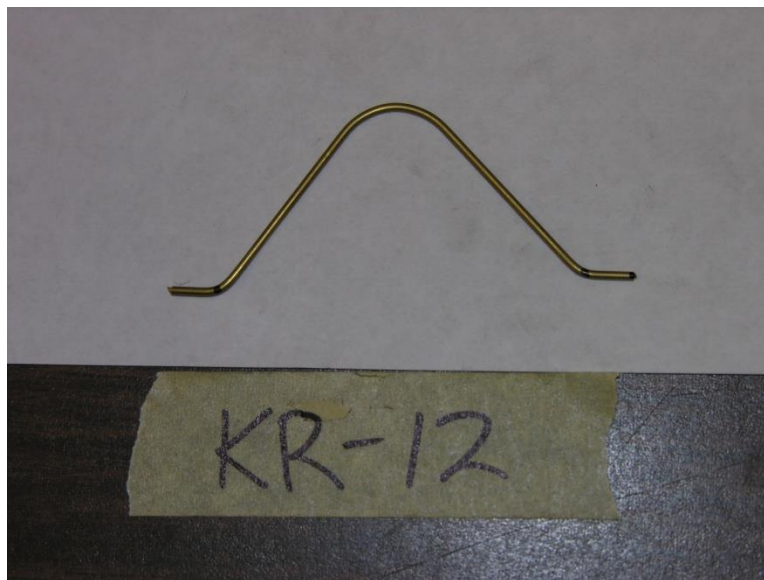


Figure 385. Pre-Test Photograph, Test No. KR-12

19.3.2 Test Nos. KR-13 and KR-14 (Squeeze, 3/32-in. Brass)

For test nos. KR-13 and KR-14, squeeze-in-place curved rods, fabricated from 3/32-in. (2.4-mm) diameter, C360 brass, were vertically loaded at a displacement rate of 0.2 in./min (5 mm/min). In both tests, as the rods were pulled upward, their ends slipped out of the holes in the flanges. The peak loads for test nos. KR-13 and KR-14 were 31 lb (137 N) and 37 lb (163 N), respectively. The force versus displacement curve for test nos. KR-13 and KR-14 is shown in Figure 386. Pre-test photographs are shown in Figures 387 and 388. There was no noticeable plastic deformation of the squeeze-in-place curved rods between the beginning and end states.

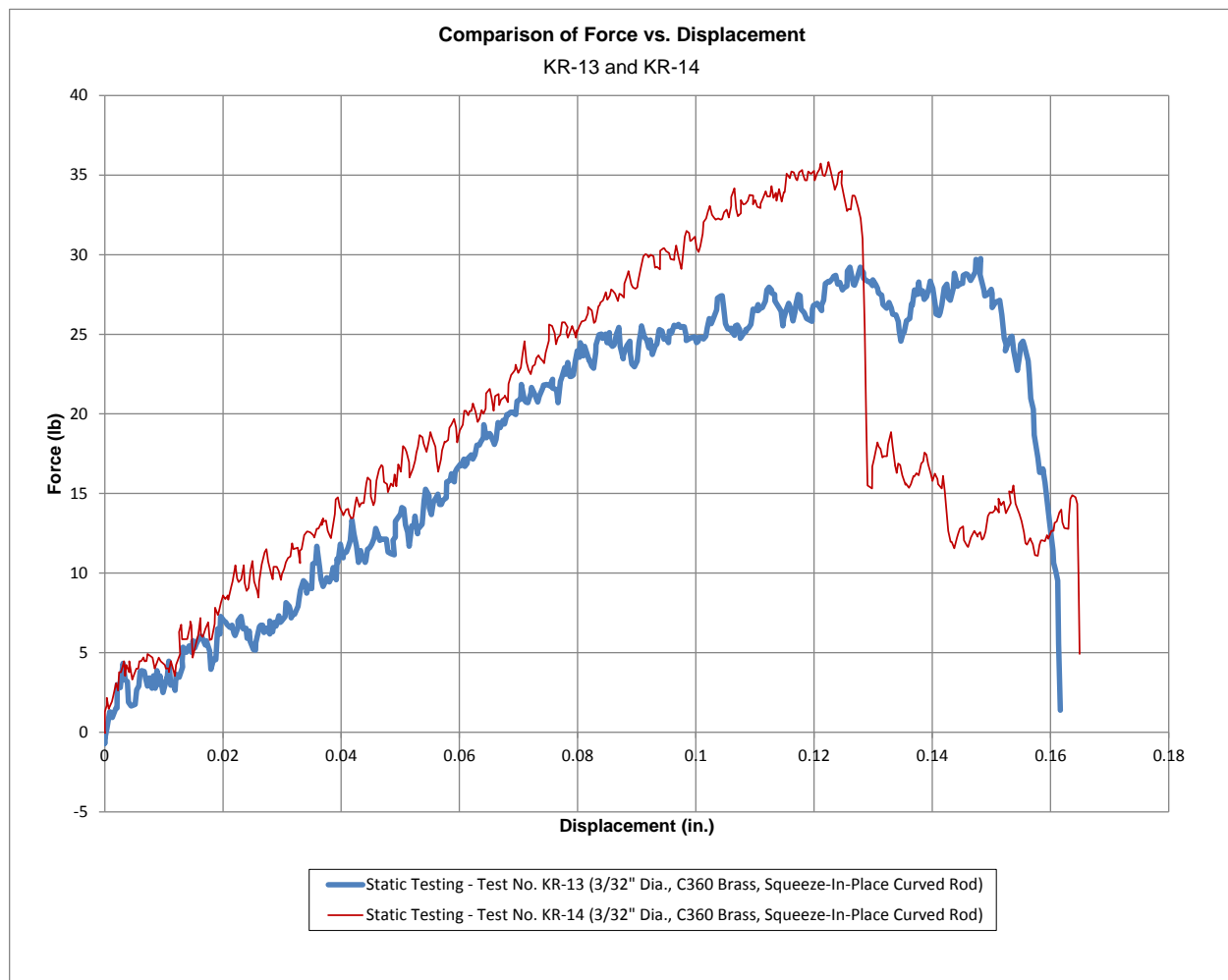


Figure 386. Force Versus Displacement, Test Nos. KR-13 and KR-14

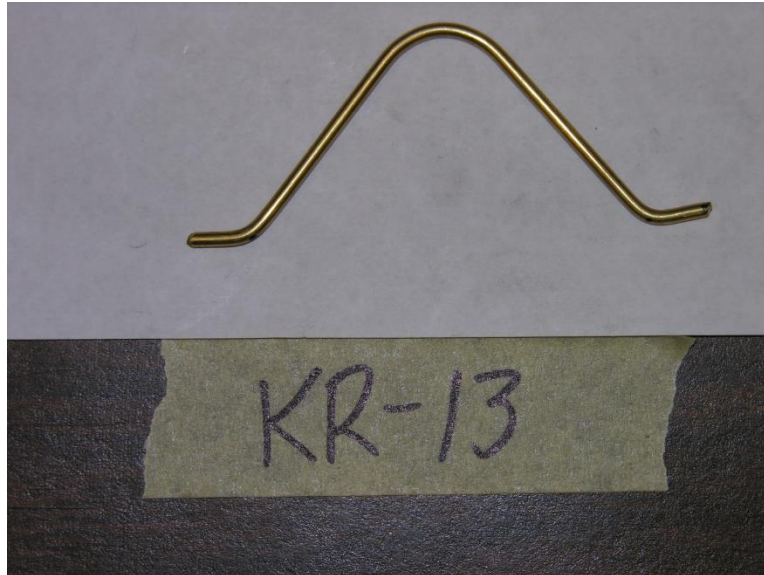


Figure 387. Pre-Test Photograph, Test No. KR-13

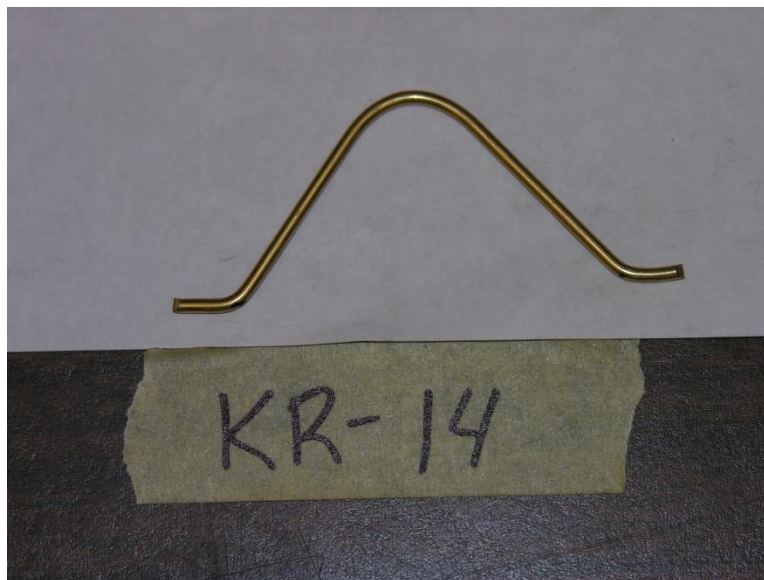


Figure 388. Pre-Test Photograph, Test No. KR-14

19.3.3 Test Nos. KR-15 and KR-16 (Squeeze, 1/8-in. Brass)

For test nos. KR-15 and KR-16, squeeze-in-place curved rods, fabricated from 1/8-in. (3.2-mm) diameter, C360 brass, were vertically loaded at a displacement rate of 0.2 in./min (5 mm/min). In both tests, as the rods were pulled upward, their ends slipped out of the holes in the flanges. The peak loads for test nos. KR-15 and KR-16 were 58 lb (258 N) and 62 lb (277 N), respectively. The force versus displacement curve for test nos. KR-15 and KR-16 is shown in Figure 389. Pre-test photographs are shown in Figures 390 and 391. There was no noticeable plastic deformation of the squeeze-in-place curved rods between the beginning and end states.

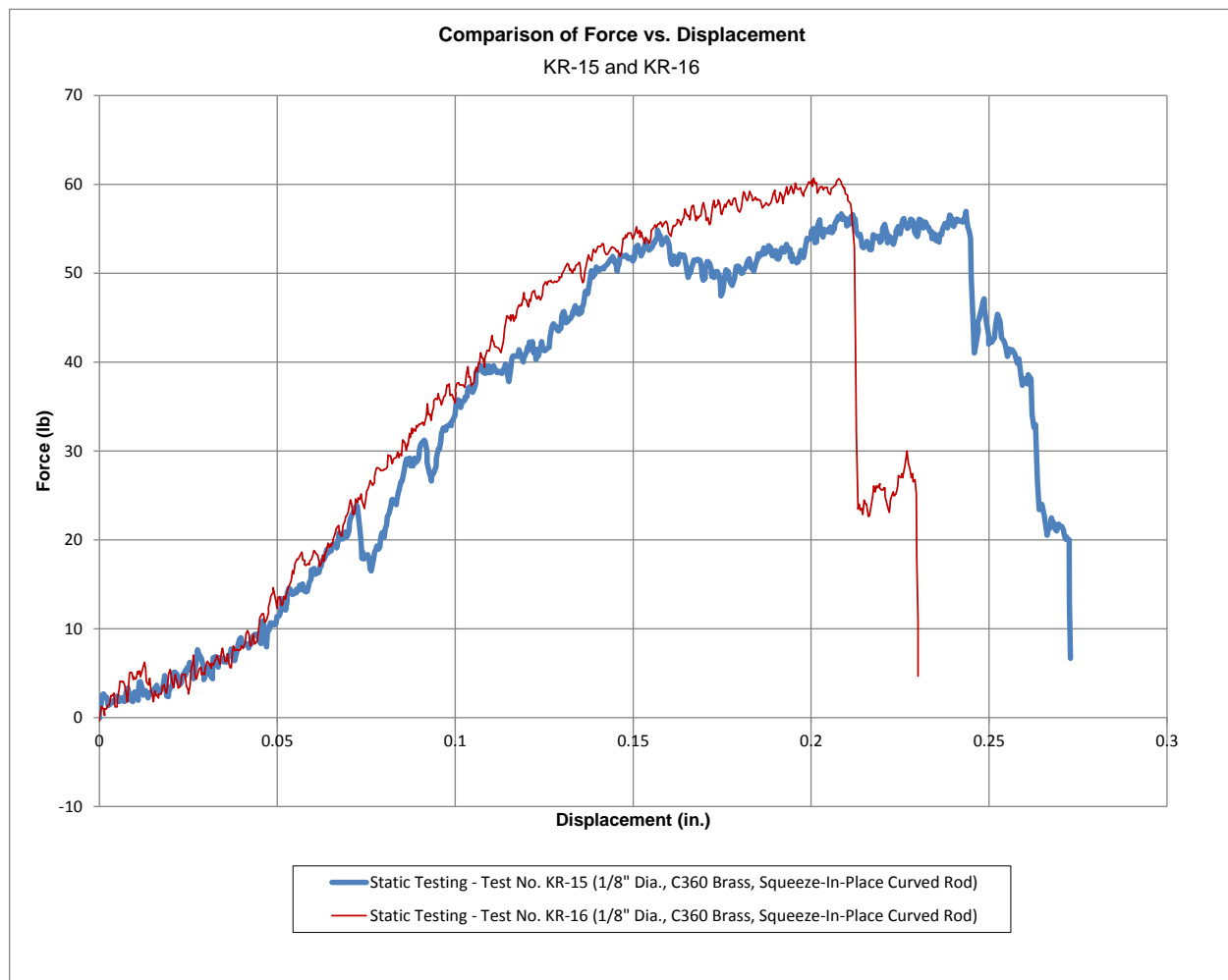


Figure 389. Force Versus Displacement, Test Nos. KR-15 and KR-16

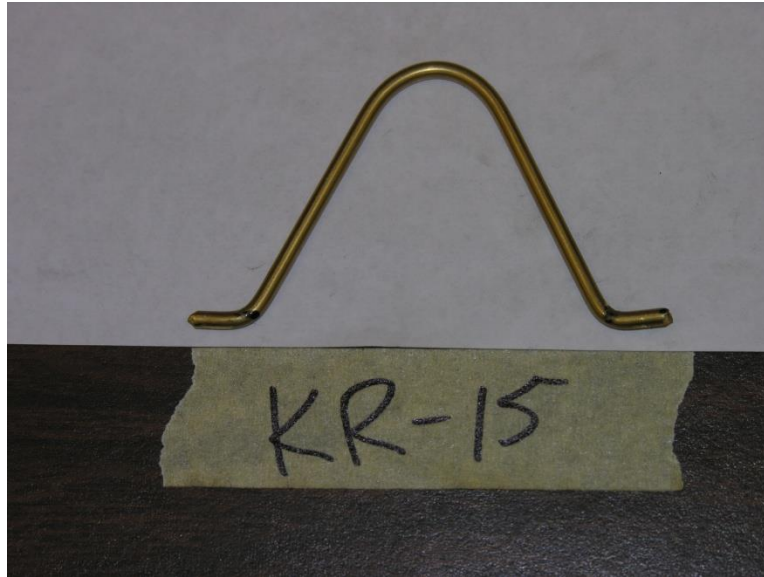


Figure 390. Pre-Test Photograph, Test No. KR-15



Figure 391. Pre-Test Photograph, Test No. KR-16

19.3.4 Test Nos. KR-17 and KR-18 (Squeeze, 3/32-in. Stainless)

For test nos. KR-17 and KR-18, squeeze-in-place curved rods, fabricated from 3/32-in. (2.4-mm) diameter, T-303 stainless steel, were vertically loaded at a displacement rate of 0.2 in./min (5 mm/min). In both tests, as the rods were pulled upward, their ends slipped out of the holes in the flanges. The peak loads for test nos. KR-17 and KR-18 were 41 lb (183 N) and 42 lb (185 N), respectively. The force versus displacement curve for test nos. KR-17 and KR-18 is shown in Figure 392. Pre-test photographs are shown in Figures 393 and 394. There was no noticeable plastic deformation of the squeeze-in-place curved rods between the beginning and end states.

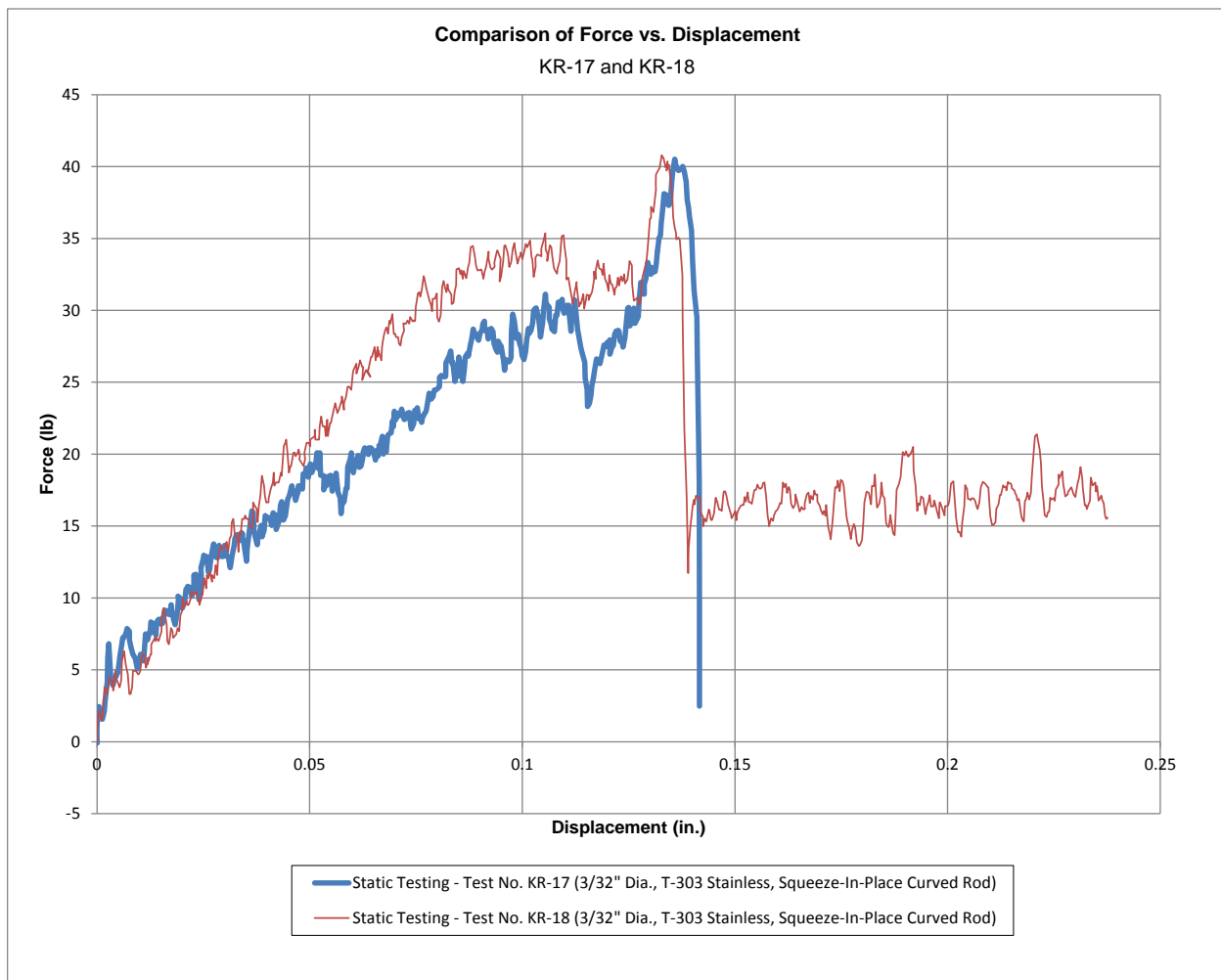


Figure 392. Force Versus Displacement, Test Nos. KR-17 and KR-18

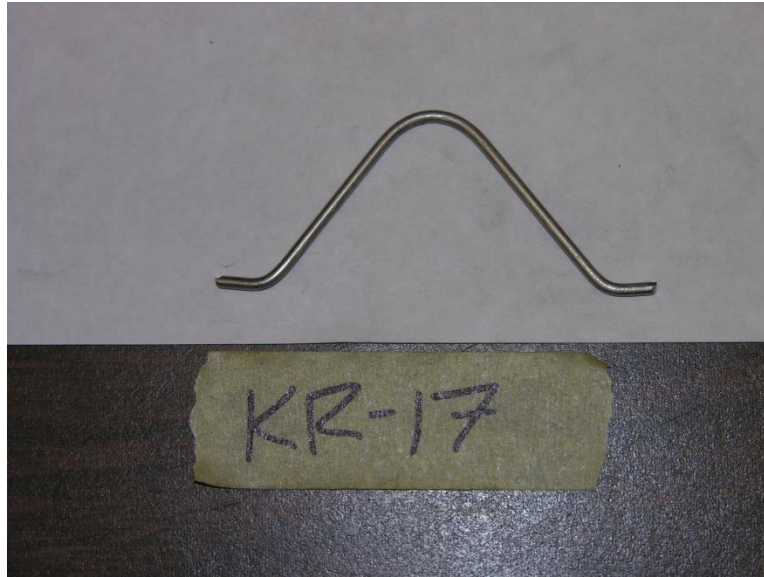


Figure 393. Pre-Test Photograph, Test No. KR-17

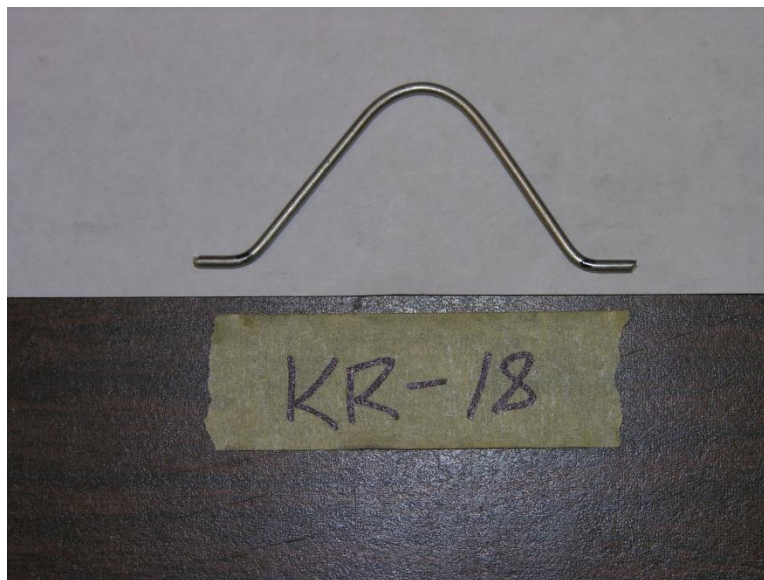


Figure 394. Pre-Test Photograph, Test No. KR-18

19.3.5 Test Nos. KR-19 and KR-20 (Squeeze, 1/8-in. Stainless)

For test nos. KR-19 and KR-20, squeeze-in-place curved rods, fabricated from 1/8-in. (3.2-mm) diameter, T-304 stainless steel, were vertically loaded at a displacement rate of 0.2 in./min (5 mm/min). In both tests, as the rods were pulled upward, their ends slipped out of the holes in the flanges. The peak loads for test nos. KR-19 and KR-20 were 76 lb (336 N) and 71 lb (315 N), respectively. The force versus displacement curve for test nos. KR-19 and KR-20 is shown in Figure 395. Pre-test photographs are shown in Figures 396 and 397. There was no noticeable plastic deformation of the squeeze-in-place curved rods between the beginning and end states.

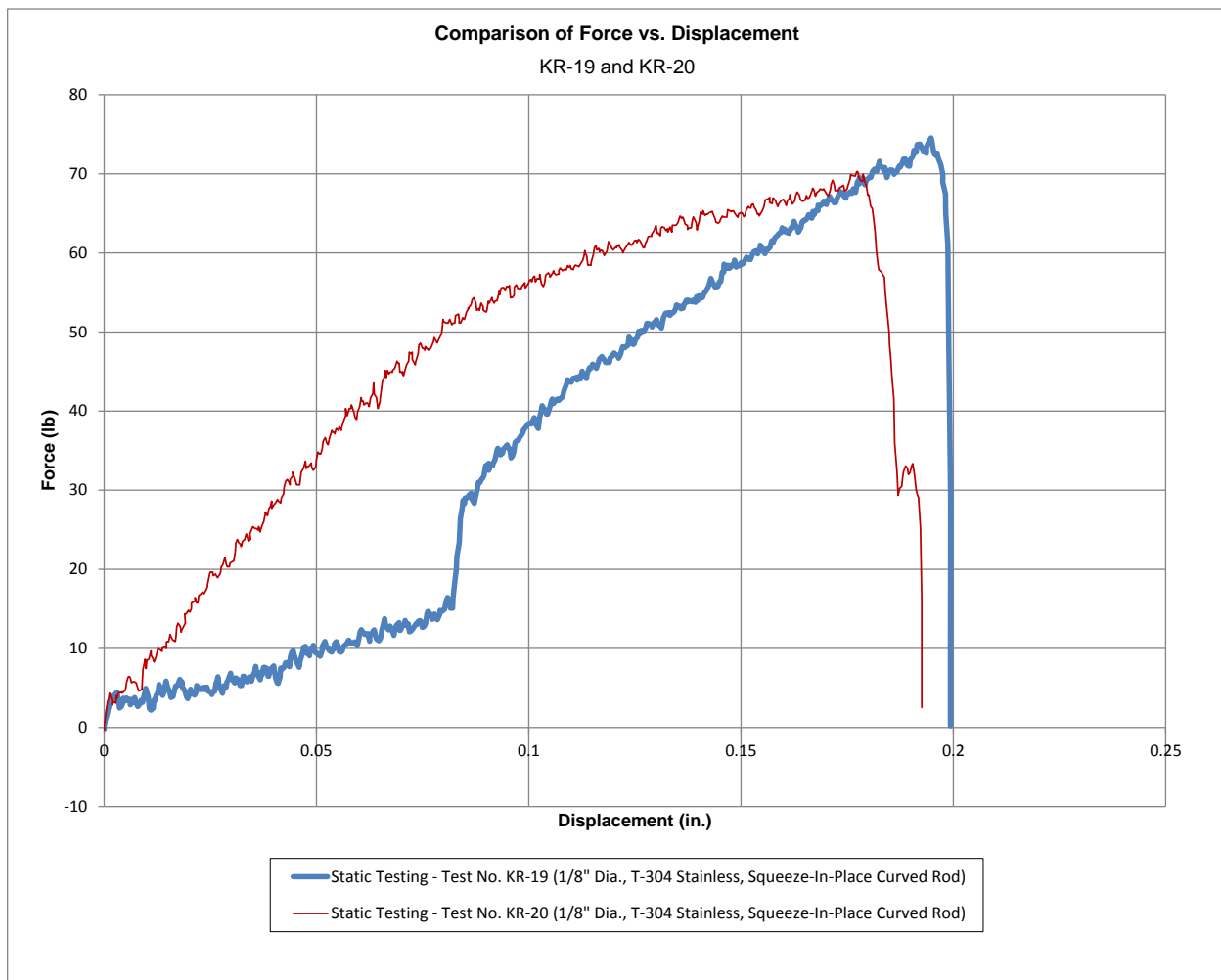


Figure 395. Force Versus Displacement, Test Nos. KR-19 and KR-20

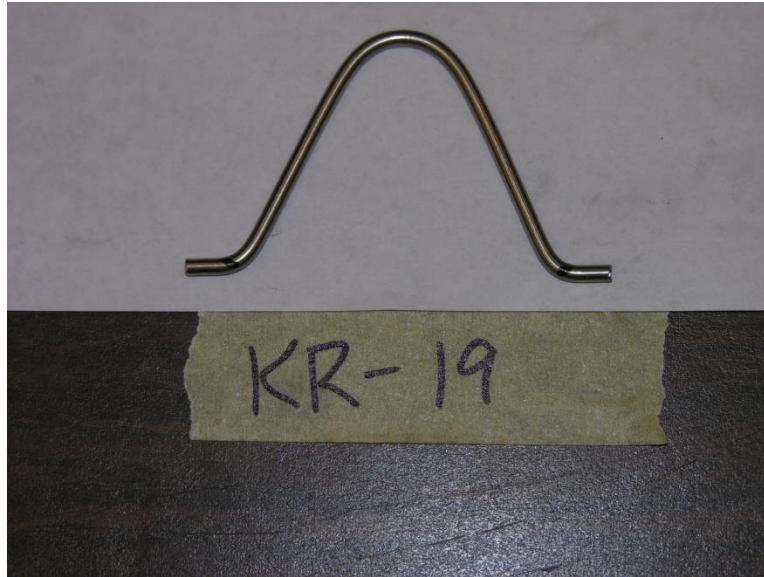


Figure 396. Pre-Test Photograph, Test No. KR-19

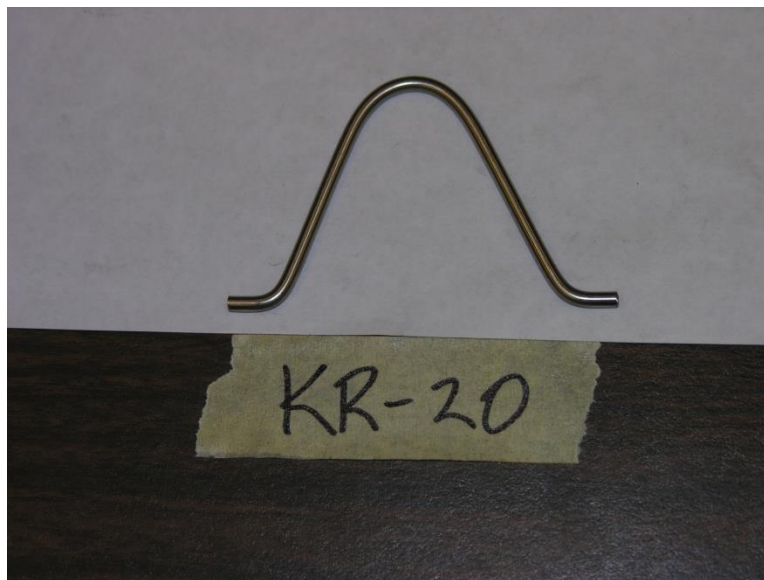


Figure 397. Pre-Test Photograph, Test No. KR-20

19.4 HellermannTyton Stainless Steel Cable Ties

HellermannTyton stainless steel cable ties were tested in test nos. TCT-1 through TCT-9. The test matrix and results are summarized in Table 20. Before and after photographs for one of the tests, as shown in Figure 398, are provided for a HellermannTyton stainless steel cable tie.

Table 20. Test Matrix and Results for HellermannTyton Stainless Steel Cable Ties

Test No.	Material	Cross-Section in. (mm)		Rate in./min (mm/min)	Peak Load lb (N)	Notes
		Width	Thickness			
TCT-4	Stainless Steel 304	0.31 (7.9)	0.012 (0.30)	0.4 (10)	353 (1,572)	Locking mechanism failure
TCT-6	Stainless Steel 304	0.31 (7.9)	0.012 (0.30)	0.4 (10)	349 (1,554)	Locking mechanism failure
TCT-7	Stainless Steel 304	0.31 (7.9)	0.012 (0.30)	0.4 (10)	274 (1,217)	Locking mechanism failure
TCT-8	Stainless Steel 304	0.18 (4.6)	0.012 (0.30)	0.4 (10)	133 (593)	Locking mechanism failure
TCT-9	Stainless Steel 304	0.18 (4.6)	0.012 (0.30)	0.4 (10)	182 (809)	Locking mechanism failure



Before



After

Figure 398. Example of HellermannTyton Stainless Steel Cable Tie Test

19.4.1 Tests that timed out

Test nos. TCT-1 through TCT-3 and TCT-5 all timed out before failure. This result occurred due in part to operator error. For some reason, the MTS did not run longer than 100 sec. Fortunately, several extra cable ties were available for use. Test nos. TCT-4, TCT-6, and TCT-7 used the same cable ties to successfully demonstrate component behavior.

19.4.2 Test Nos. TCT-4, TCT-6 and TCT-7 (Ties, 0.31-in.)

For test nos. TCT-4, TCT-6, and TCT-7, HellermannTyton cable ties, type MBT14HS, fabricated from 0.31-in. (7.9-mm) wide by 0.012-in. (0.30-mm) thick, stainless steel 304, were vertically loaded at a displacement rate of 0.4 in./min (10 mm/min). The locking mechanisms failed in all three tests. The peak loads for test nos. TCT-4, TCT-6, and TCT-7 were 353 lb (1,572 N), 349 lb (1,554 N), and 274 lb (1,217 N), respectively. The force versus displacement curve for test nos. TCT-4, TCT-6 and TCT-7 is shown in Figure 399. Pre- and post-test photographs are shown in Figures 400 through 402.

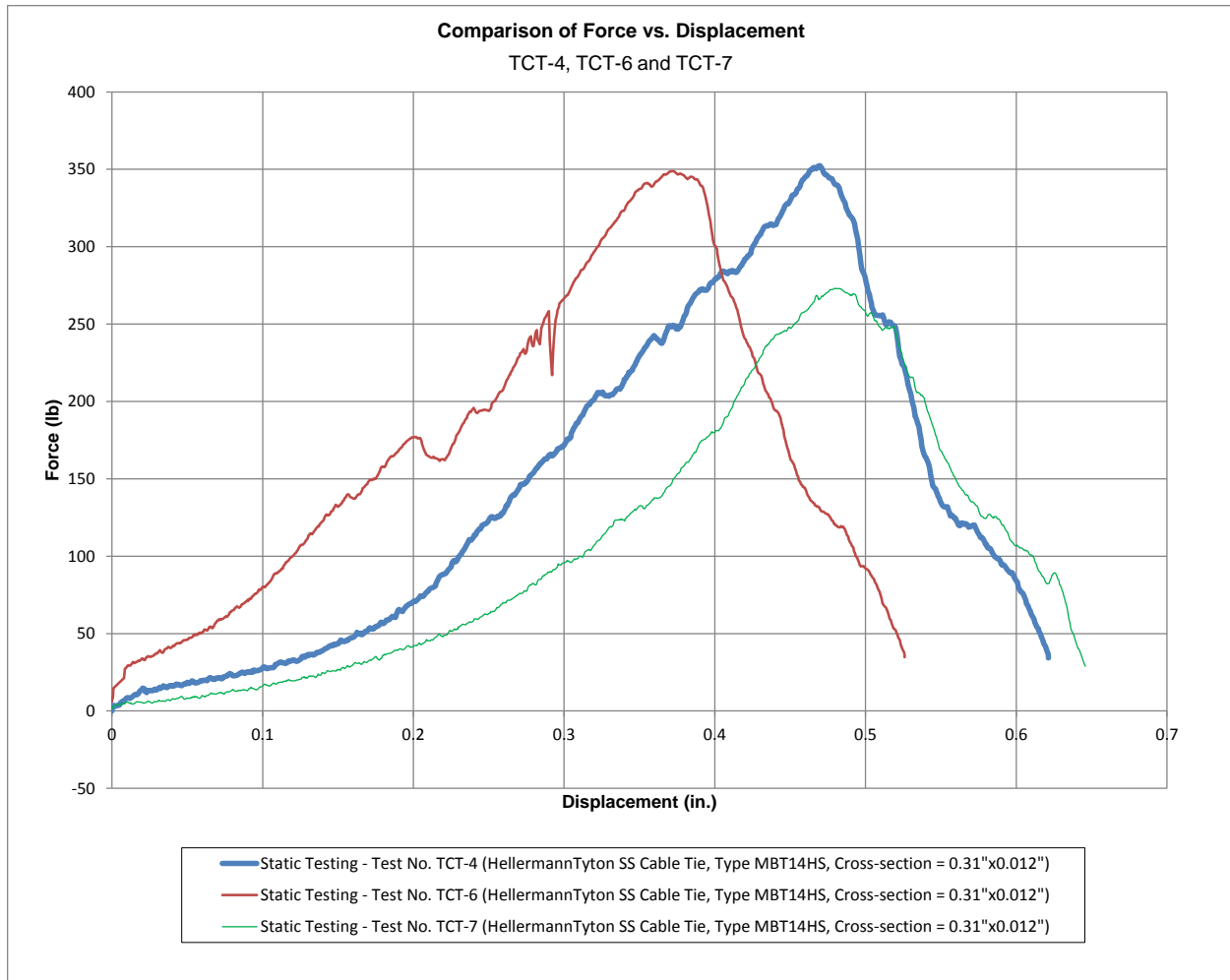


Figure 399. Force Versus Displacement, Test Nos. TCT-4, TCT-6 and TCT-7



Figure 400. Pre-Test and Post-Test Photographs, Test No. TCT-4



Figure 401. Pre-Test and Post-Test Photographs, Test No. TCT-6



Figure 402. Pre-Test and Post-Test Photographs, Test No. TCT-7

19.4.3 Test Nos. TCT-8 and TCT-9 (Ties, 0.18-in.)

For test nos. TCT-8 and TCT-9, HellermannTyton cable ties, type MBT14SS, fabricated from 0.18-in. (4.6-mm) wide by 0.012-in. (0.30-mm) thick, stainless steel 304, were vertically loaded at a displacement rate of 0.4 in./min (10 mm/min). The locking mechanisms failed in both tests. The peak loads for test nos. TCT-8 and TCT-9 were 133 lb (593 N) and 182 lb (809 N), respectively. The force versus displacement curve for test nos. TCT-8 and TCT-9 is shown in Figure 403. Pre- and post-test photographs are shown in Figures 404 and 405.

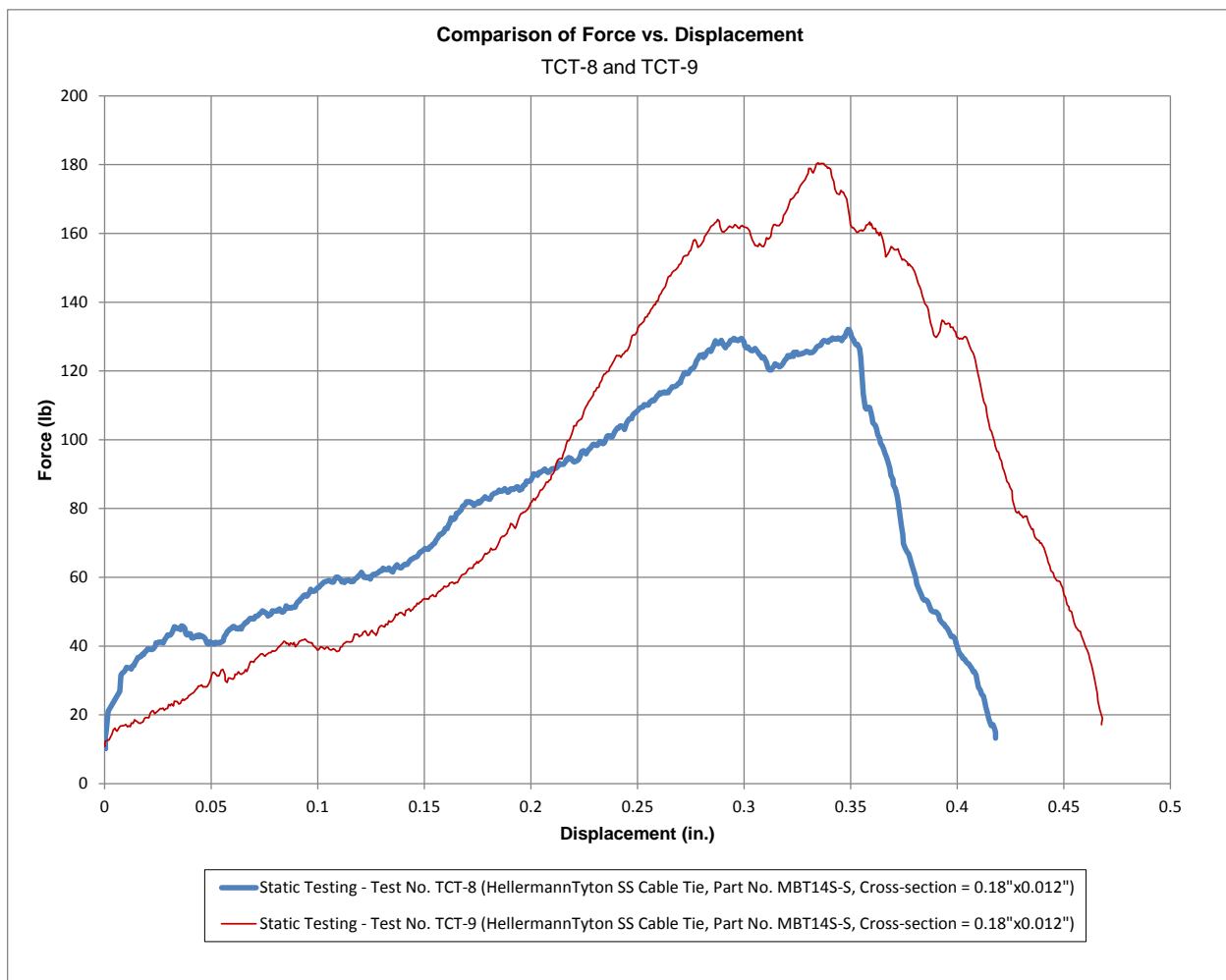


Figure 403. Force Versus Displacement, Test Nos. TCT-8 and TCT-9



Figure 404. Pre-Test and Post-Test Photographs, Test No. TCT-8

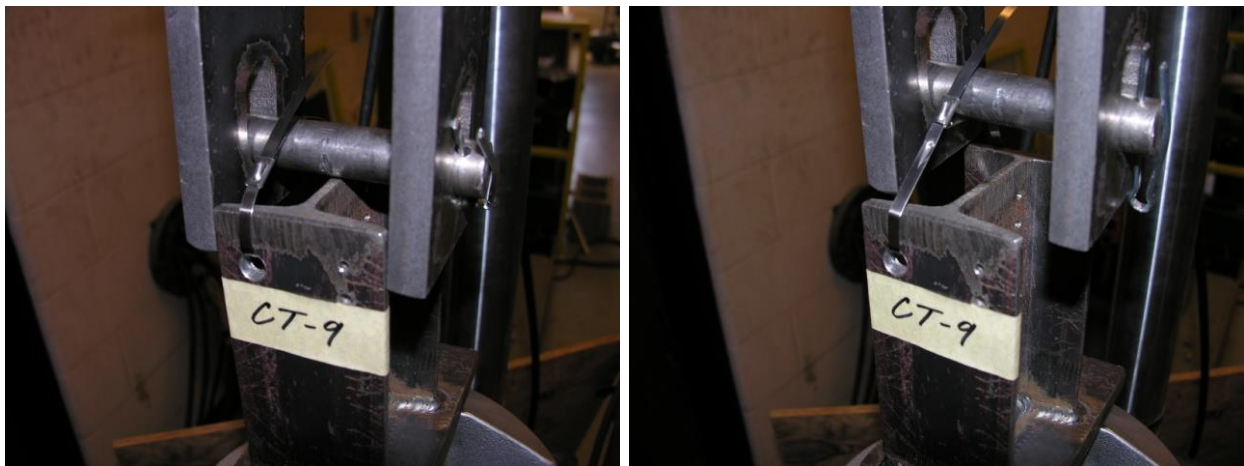


Figure 405. Pre-Test and Post-Test Photographs, Test No. TCT-9

19.5 Revised Web-Inserted Curved Rods

Revised web-inserted curved rod concepts were tested in test nos. KR-21 through KR-24. The test matrix and results are summarized in Table 21. Before and after photographs for one for the tests, as shown in Figure 406, are provided for a revised web-inserted curved rod.

Table 21. Test Matrix and Results for Revised Web-Inserted Curved Rods

Test No.	Material	Diameter in. (mm)	Rate in./min (mm/min)	Peak Load lb (N)	Notes
KR-21	C360 Brass	1/8 (3.2)	0.2 (5)	567 (2,520)	Bent and fractured at hole
KR-22	C360 Brass	1/8 (3.2)	0.2 (5)	545 (2,426)	Bent and fractured at hole
KR-23	T-304 Stainless Steel	1/8 (3.2)	0.2 (5)	799 (3,554)	Bent and slipped out of hole
KR-24	T-304 Stainless Steel	1/8 (3.2)	0.2 (5)	884 (3,930)	Bent and slipped out of hole



Before



After

Figure 406. Example Revised Web-Inserted Curved Rod Test

19.5.1 Test Nos. KR-21 and KR-22 (Rev. Web, 1/8-in. Brass)

For test nos. KR-21 and KR-22, revised web-inserted curved rods, fabricated from 1/8-in. (3.2-mm) diameter, C360 brass, were vertically loaded at a displacement rate of 0.2 in./min (5 mm/min). In both tests, the rods began to bend, before finally fracturing at the location of one of the holes. The peak loads for test nos. KR-21 and KR-22 were 567 lb (2,520 N) and 545 lb (2,462 N), respectively. The force versus displacement curve for test nos. KR-21 and KR-22 is shown in Figure 407. Pre- and post-test photographs are shown in Figures 408 and 409.

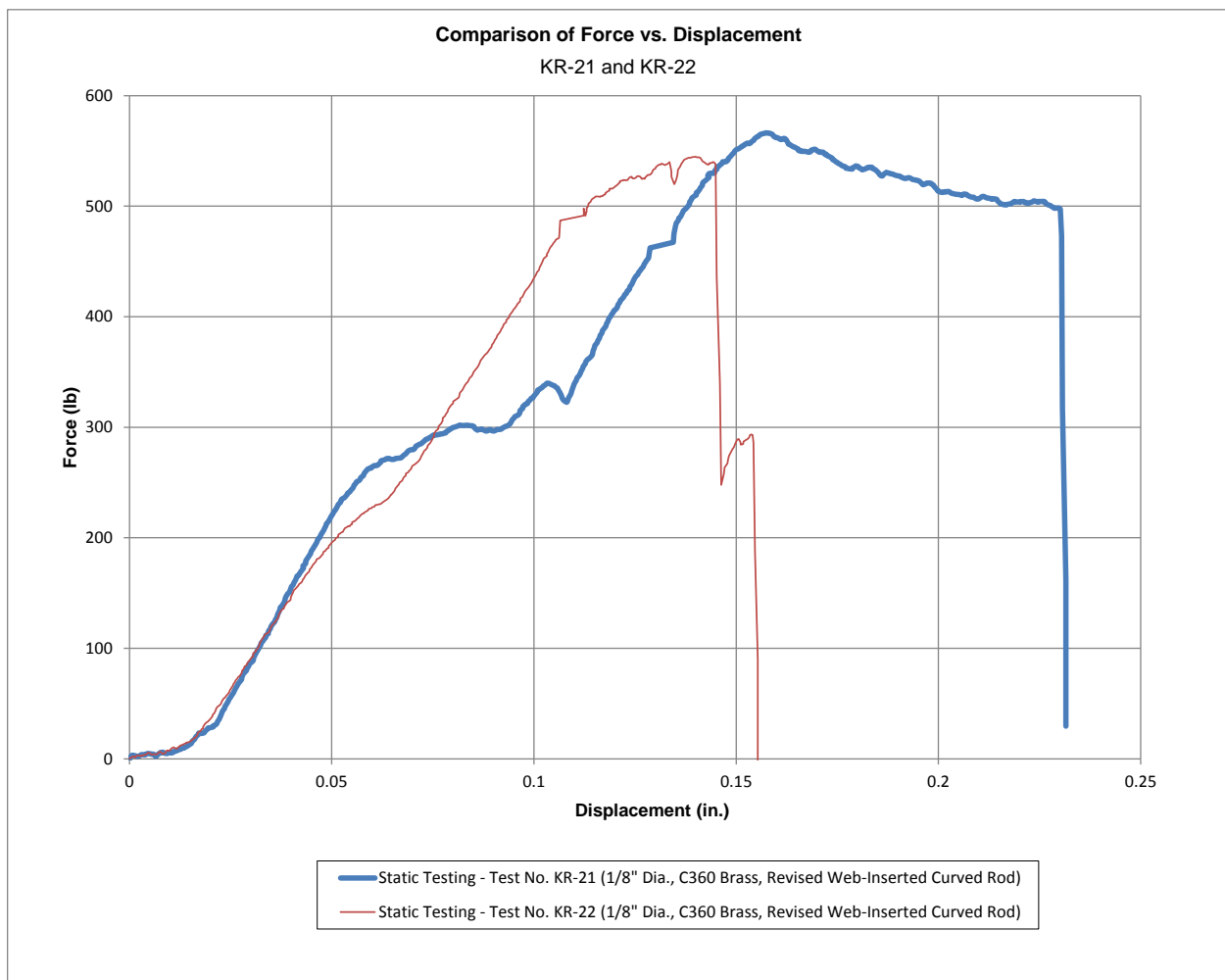


Figure 407. Force Versus Displacement, Test Nos. KR-21 and KR-22



Figure 408. Pre-Test and Post-Test Photographs, Test No. KR-21



Figure 409. Pre-Test and Post-Test Photographs, Test No. KR-22

19.5.2 Test Nos. KR-23 and KR-24 (Rev. Web, 1/8-in. Stainless)

For test nos. KR-23 and KR-24, revised web-inserted curved rods, fabricated from 1/8-in. (3.2-mm) diameter, T-304 stainless steel, were vertically loaded at a displacement rate of 0.2 in./min (5 mm/min). In both tests, the rods bent and eventually slipped out of the holes. The peak loads for test nos. KR-23 and KR-24 were 799 lb (3,554 N) and 884 lb (3,930 N), respectively. The force versus displacement curve for test nos. KR-23 and KR-24 is shown in Figure 410. Pre- and post-test photographs are shown in Figures 411 and 412.

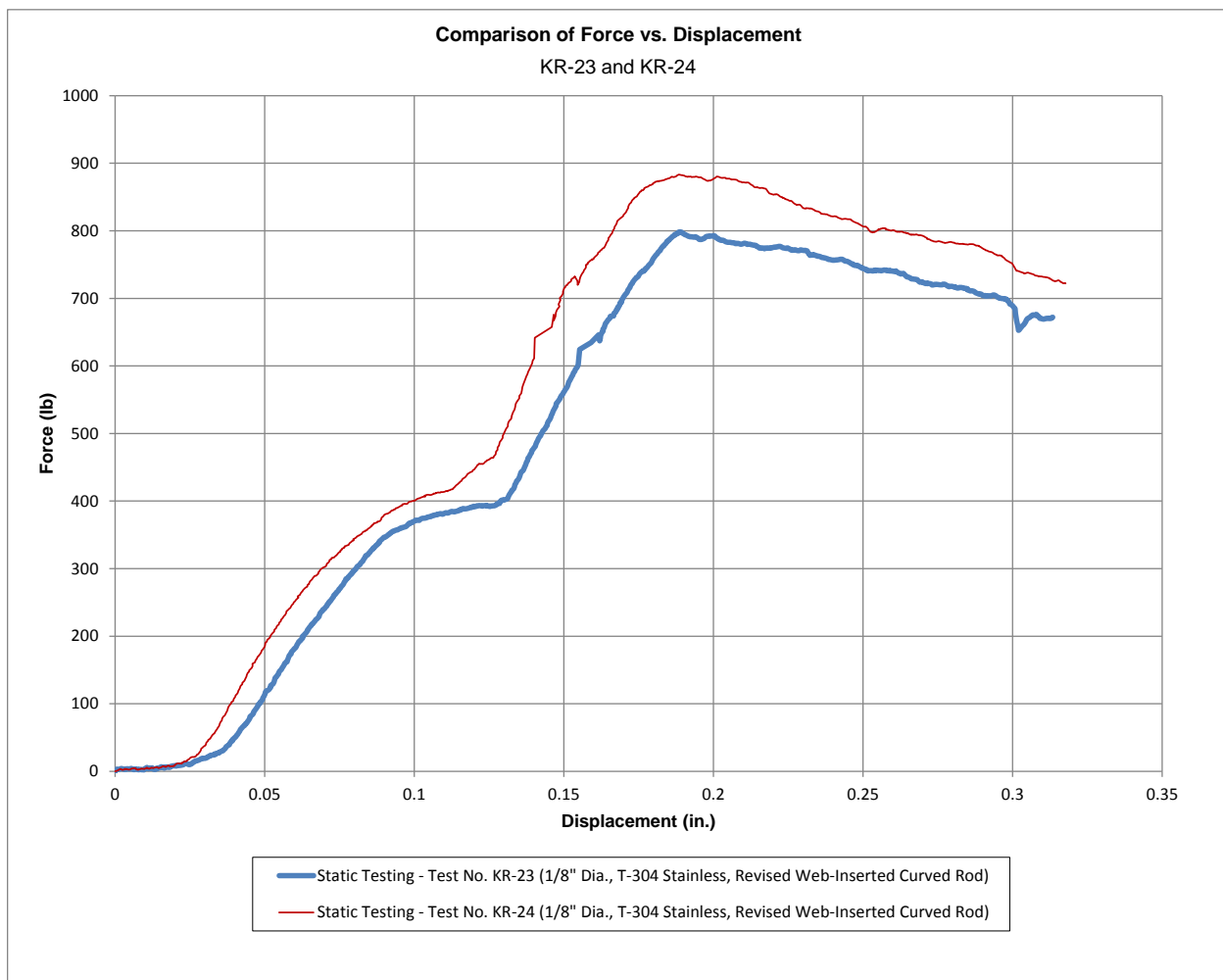


Figure 410. Force Versus Displacement, Test Nos. KR-23 and KR-24

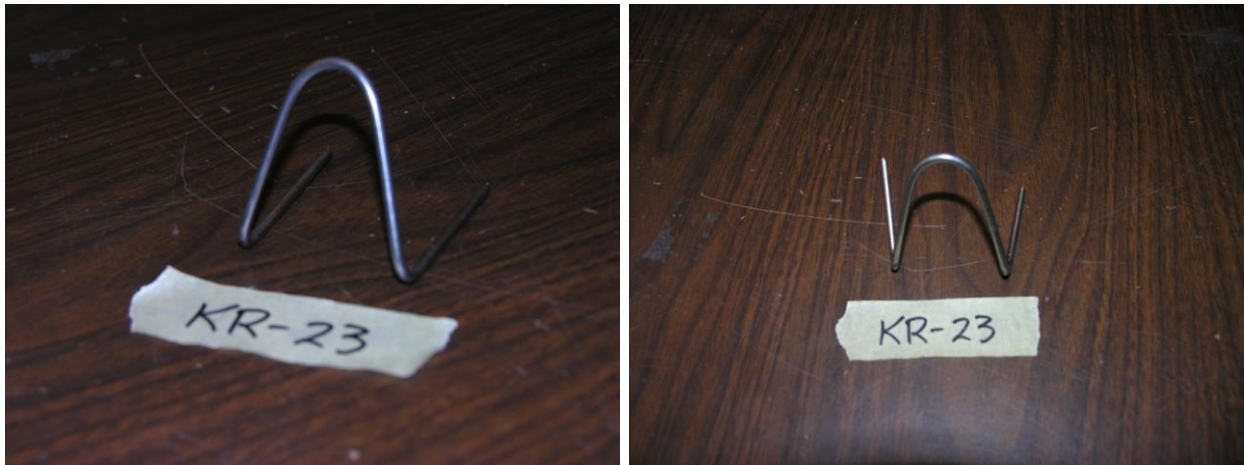


Figure 411. Pre-Test and Post-Test Photographs, Test No. KR-23

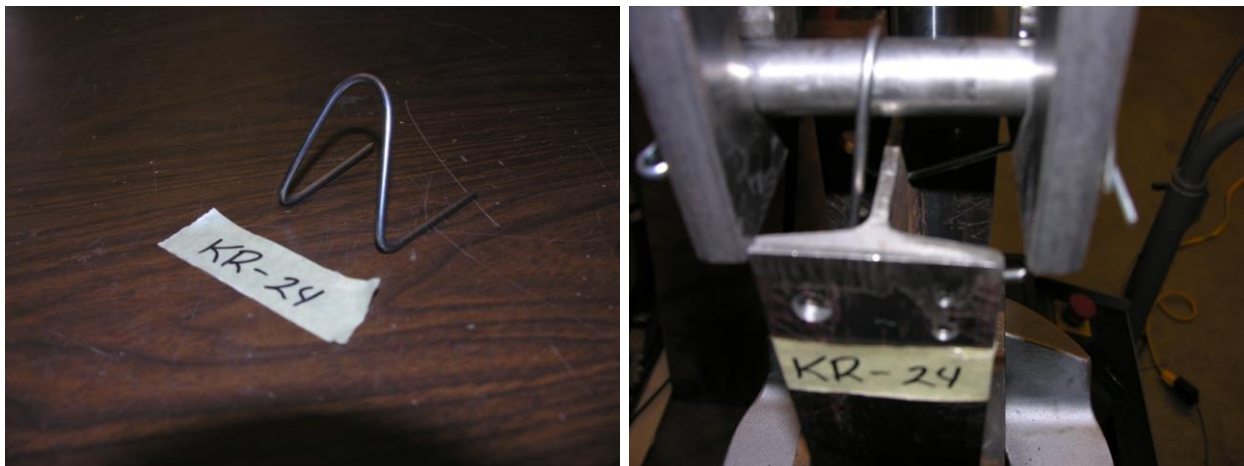


Figure 412. Pre-Test and Post-Test Photographs, Test No. KR-24

19.6 Straight Rods

Straight rod concepts were tested in test nos. KR-25 through KR-36. The test matrix and results are summarized in Table 22. Before and after photographs for one of the tests, as shown in Figure 413, are provided for a straight rod.

Table 22. Test Matrix and Results for Straight Rods

Test No.	Material	Diameter, in. (mm)	Rate, in./min (mm/min)	Peak Load, lb (N)	Notes
KR-25	C360 Brass	1/8 (3.2)	0.2 (5)	169 (753)	Timed out twice, slipped out on 3rd run
KR-26	C360 Brass	1/8 (3.2)	0.8 (20)	181 (806)	Bent and fractured at location of hole
KR-27	T-304 Stainless	1/8 (3.2)	0.8 (20)	360 (1,603)	Bent and slipped out of hole
KR-28	T-304 Stainless	1/8 (3.2)	0.8 (20)	412 (1,833)	Bent and slipped out of hole
KR-29	C360 Brass	3/16 (4.8)	0.8 (20)	732 (3,254)	Bent and fractured at location of hole
KR-30	C360 Brass	3/16 (4.8)	0.8 (20)	681 (3,030)	Bent and slipped out of hole
KR-31	T-304 Stainless	3/16 (4.8)	0.8 (20)	1,465 (6,517)	Bent and slipped out of hole, local yielding caused hole to warp
KR-32	T-304 Stainless	3/16 (4.8)	0.8 (20)	1,234 (5,489)	Bent and slipped out of hole, local yielding caused hole to warp
KR-33	C360 Brass	1/4 (6.4)	0.8 (20)	1,301 (5,787)	Bent and fractured at location of hole
KR-34	C360 Brass	1/4 (6.4)	0.8 (20)	1,313 (5,840)	Bent and fractured at location of hole
KR-35	T-304 Stainless	1/4 (6.4)	0.8 (20)	2,858 (12,710)	Bent and slipped out of hole, local yielding caused hole to warp
KR-36	T-304 Stainless	1/4 (6.4)	0.8 (20)	2,503 (11,130)	Bent and slipped out of hole, local yielding caused hole to warp



Before



After

Figure 413. Example of Straight Rod Test

19.6.1 Test No. KR-25 (Straight, 1/8-in. Brass)

For test no. KR-25, a straight rod, fabricated from 1/8-in. (3.2-mm) diameter, C360 brass, was vertically loaded at a displacement rate of 0.2 in./min (5 mm/min). The MTS timed out twice. On the third run, one end of the straight rod finally slipped out of the hole. The peak load for test no. KR-25 occurred in the second run and was 169 lb (753 N). The force versus displacement curve for test no. KR-25 is shown in Figure 414. Pre- and post-test photographs are shown in Figure 415.

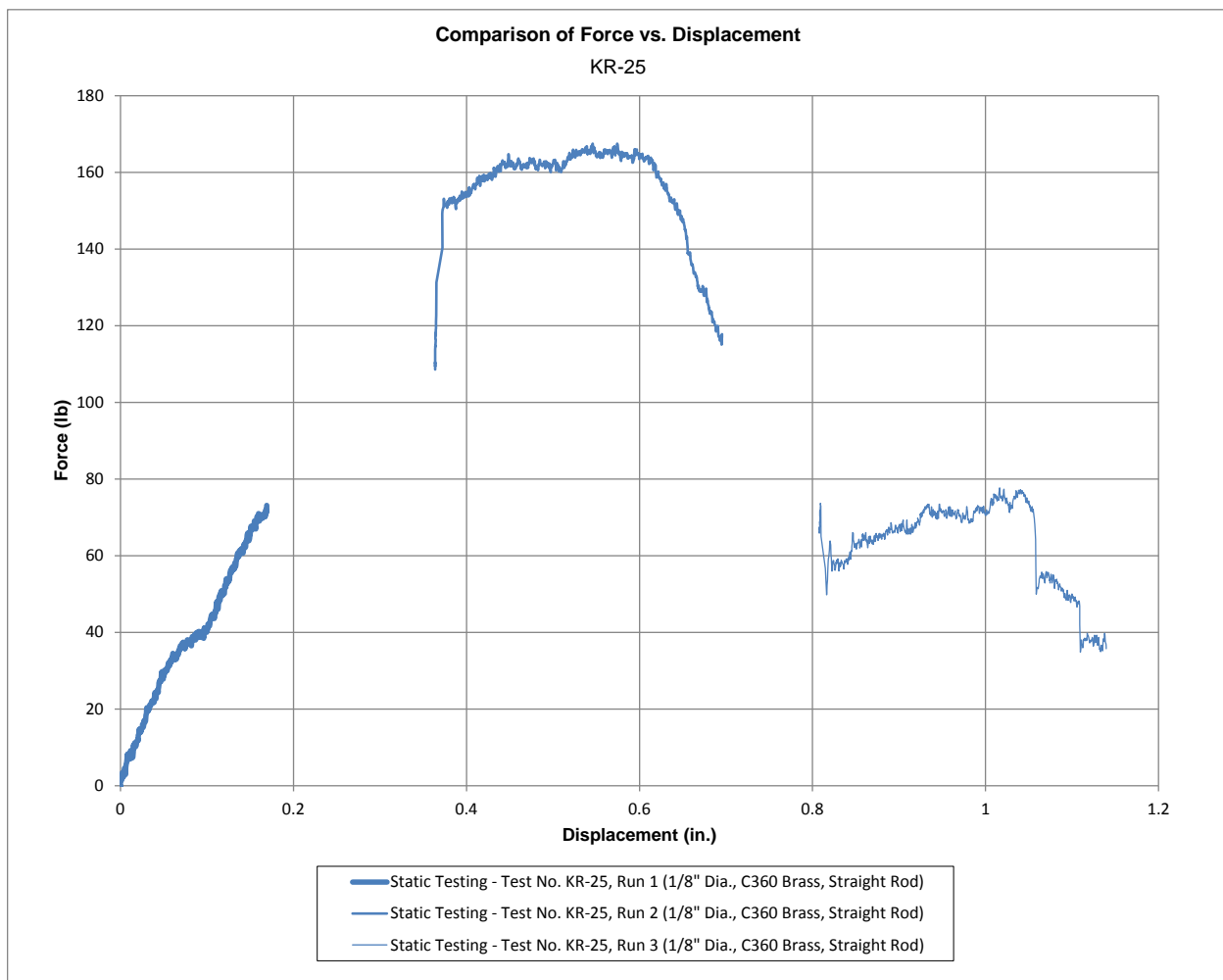


Figure 414. Force Versus Displacement, Test No. KR-25



Figure 415. Pre-Test and Post-Test Photographs, Test No. KR-25

19.6.2 Test No. KR-26 (Straight, 1/8-in. Brass)

For test no. KR-26, a straight rod, fabricated from 1/8-in. (3.2-mm) diameter, C360 brass, was vertically loaded at a displacement rate of 0.8 in./min (20 mm/min). The rod bent significantly before finally fracturing at a hole location. The peak load for test no. KR-26 was 181 lb (806 N). The force versus displacement curve for test no. KR-26 is shown in Figure 416. Pre- and post-test photographs are shown in Figure 417.

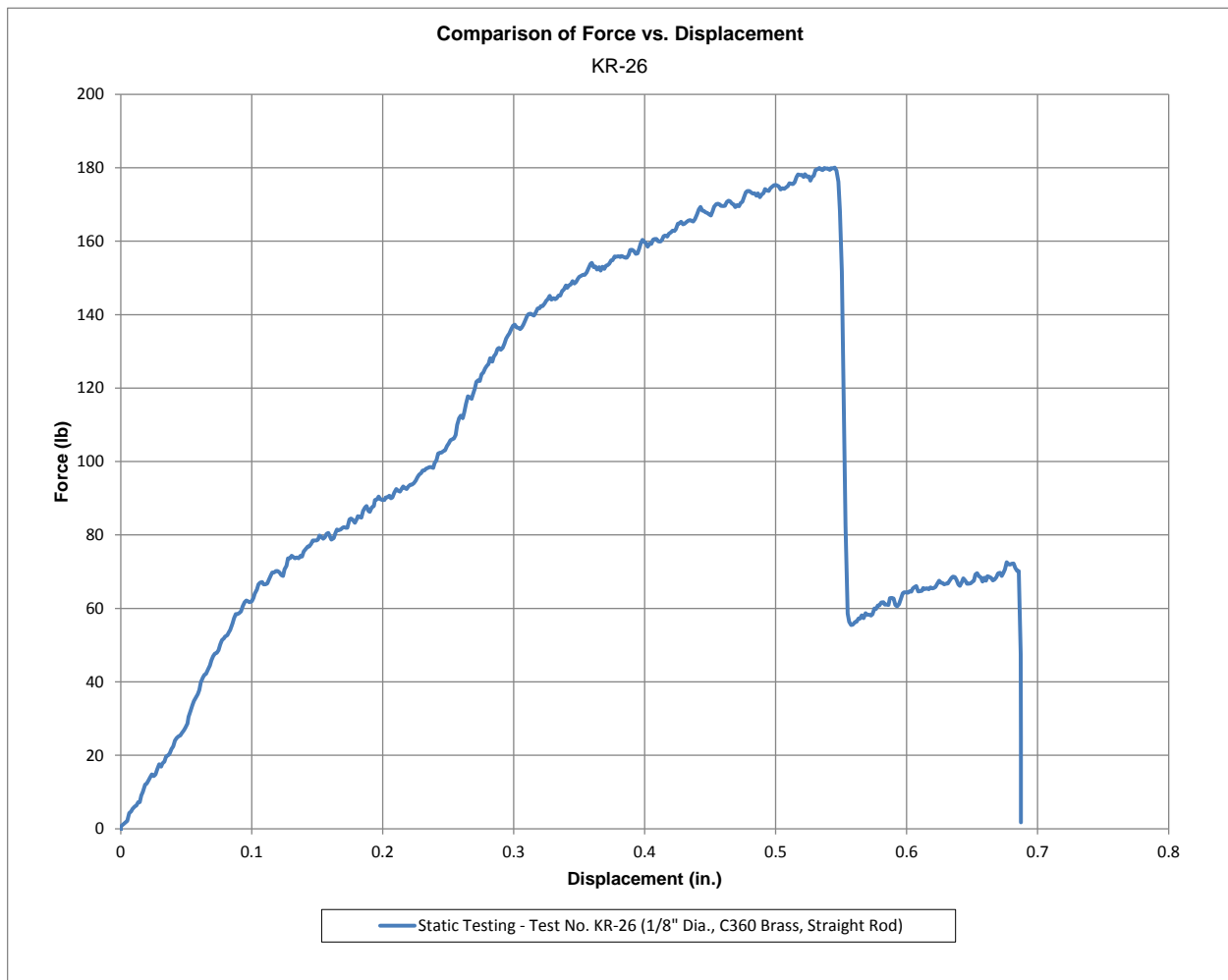


Figure 416. Force Versus Displacement, Test No. KR-26

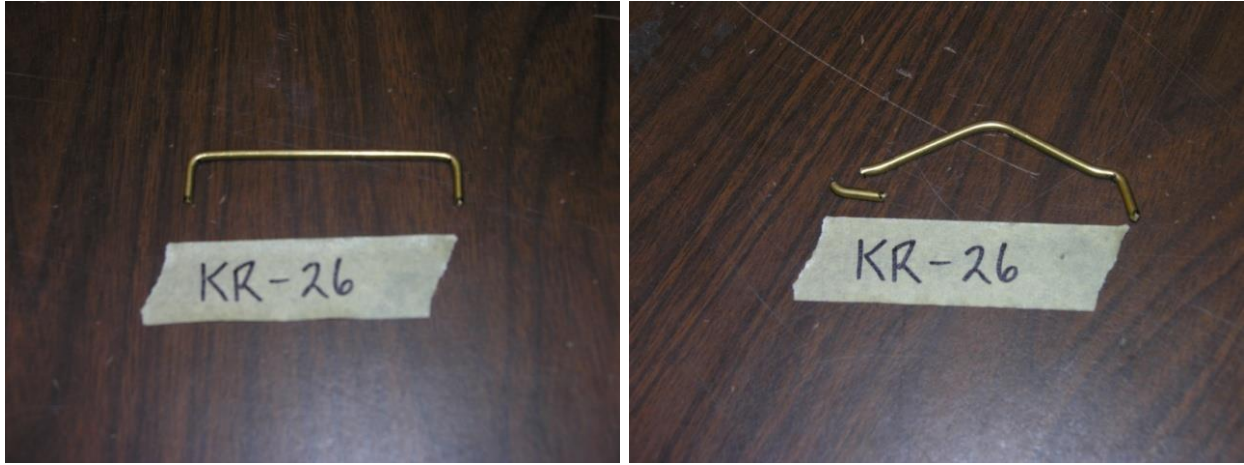


Figure 417. Pre-Test and Post-Test Photographs, Test No. KR-26

19.6.3 Test Nos. KR-27 and KR-28 (Straight, 1/8-in. Stainless)

For test nos. KR-27 and KR-28, straight rods, fabricated from 1/8-in. (3.2-mm) diameter, T-304 stainless steel, were vertically loaded at a displacement rate of 0.8 in./min (20 mm/min). In both tests, the rods bent significantly before one end finally slipped out of its hole. The peak loads for test nos. KR-27 and KR-28 were 360 lb (1,603 N) and 412 lb (1,833 N), respectively. The force versus displacement curve for test nos. KR-27 and KR-28 is shown in Figure 418. Pre- and post-test photographs are shown in Figures 419 and 420.

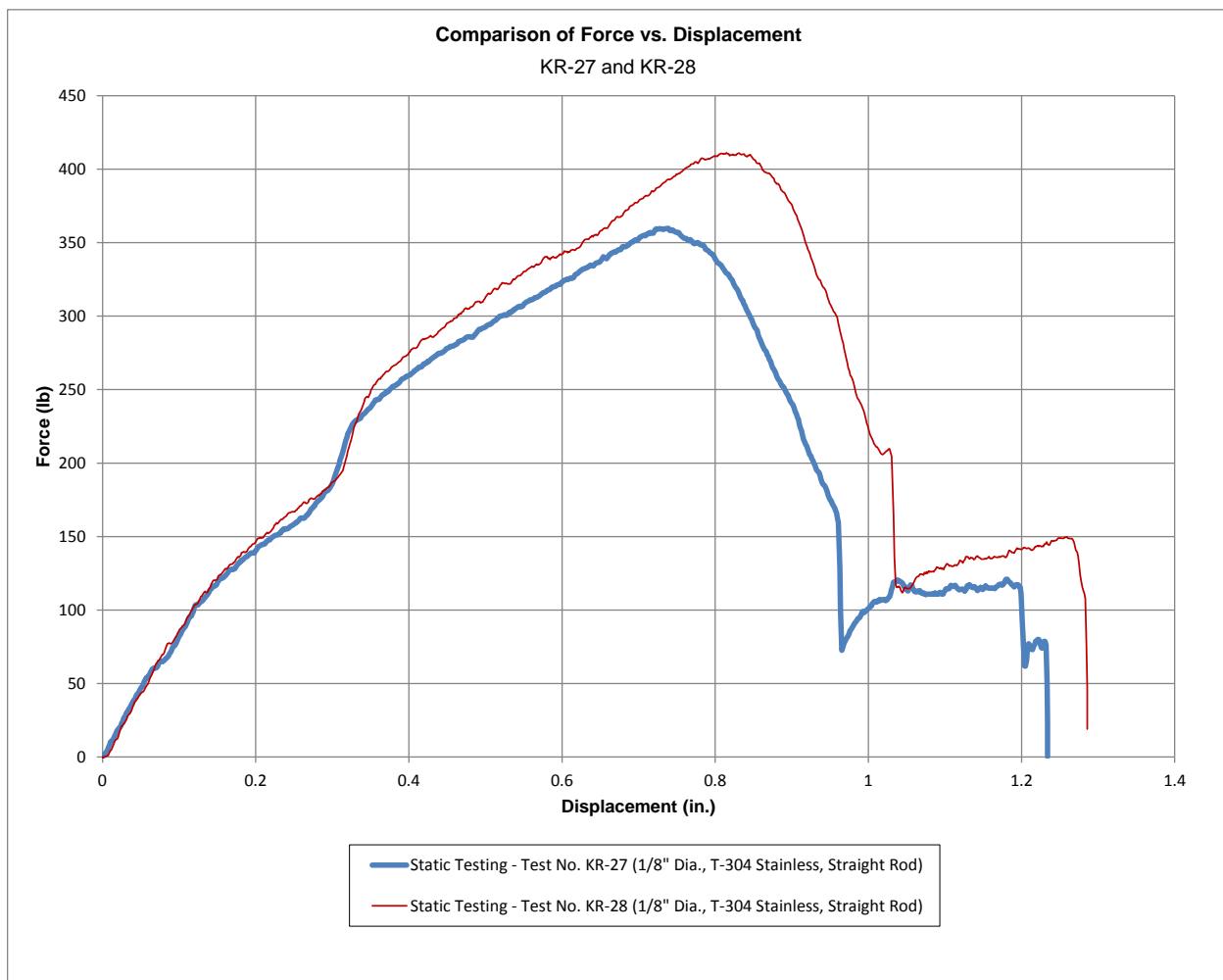


Figure 418. Force Versus Displacement, Test Nos. KR-27 and KR-28



Figure 419. Pre-Test and Post-Test Photographs, Test No. KR-27

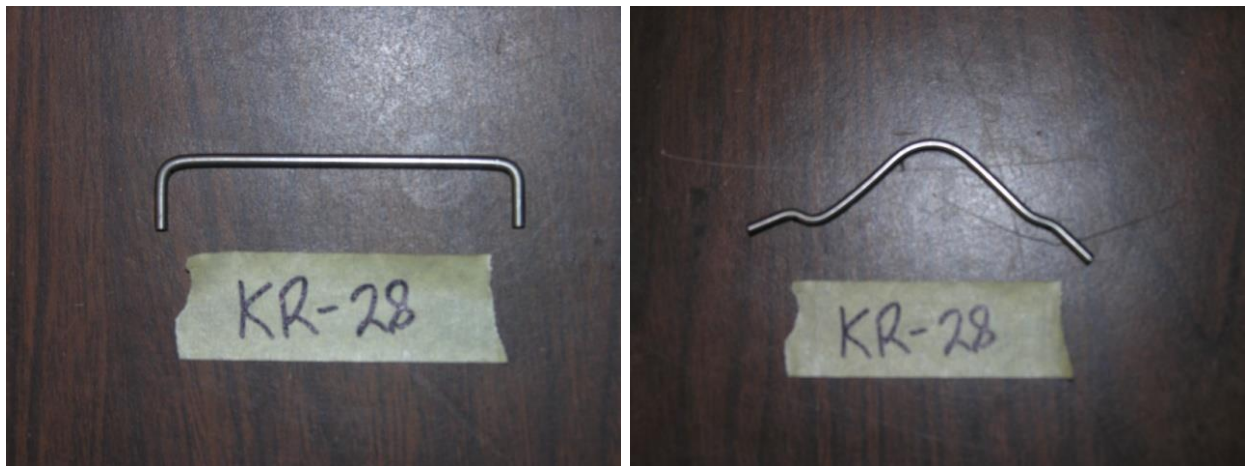


Figure 420. Pre-Test and Post-Test Photographs, Test No. KR-28

19.6.4 Test Nos. KR-29 and KR-30 (Straight, 3/16-in. Brass)

For test nos. KR-29 and KR-30, straight rods, fabricated from 3/16-in. (4.8-mm) diameter, C360 brass, were vertically loaded at a displacement rate of 0.8 in./min (20 mm/min). In test no. KR-29, the rod bent significantly before one end fractured at the location of its hole. In test no. KR-30, the rod bent significantly before one end finally slipped out of its hole. The peak loads for test nos. KR-29 and KR-30 were 732 lb (3,254 N) and 681 lb (3,030 N), respectively. The force versus displacement curve for test nos. KR-29 and KR-30 is shown in Figure 421. Pre- and post-test photographs are shown in Figures 422 and 423.

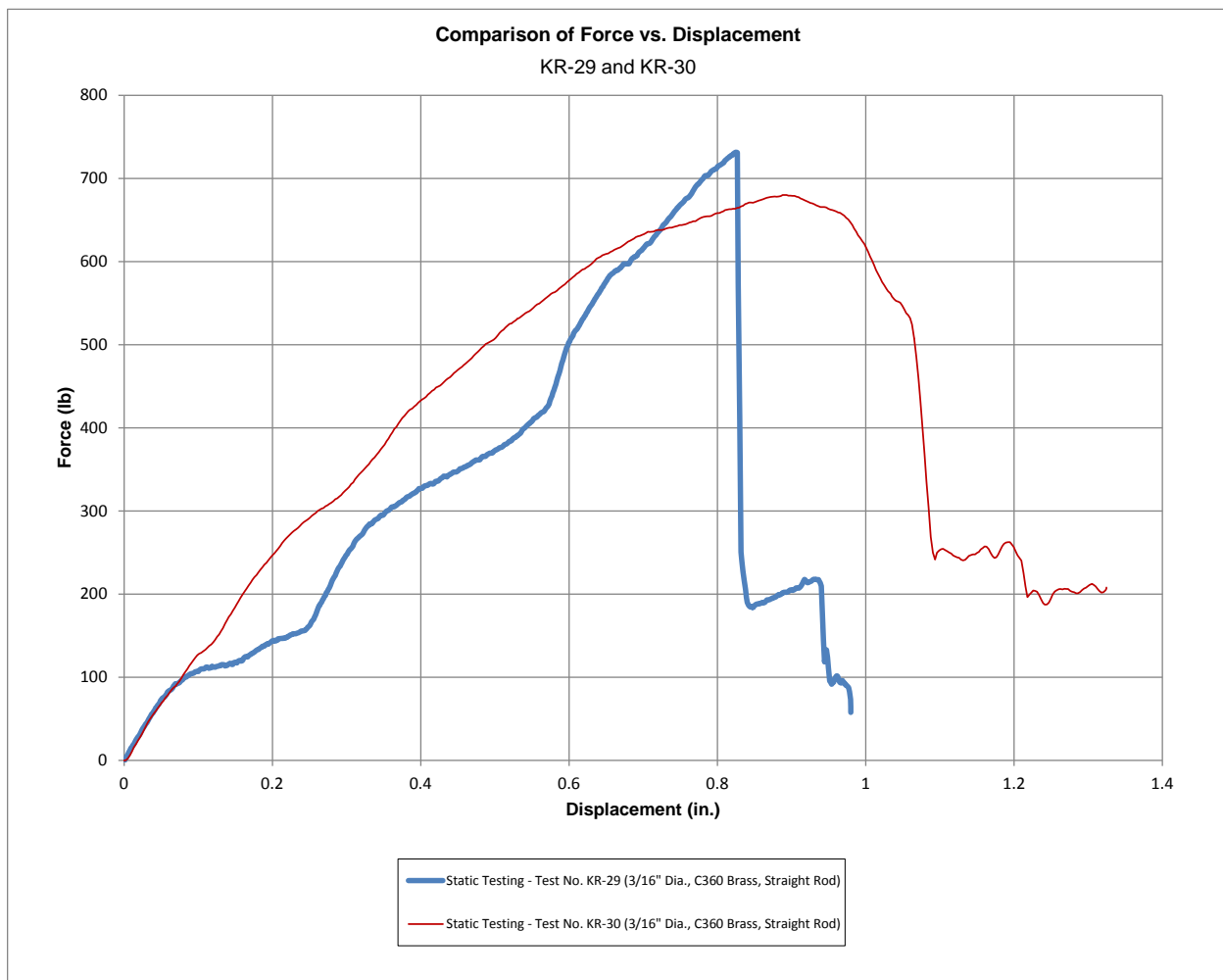


Figure 421. Force Versus Displacement, Test Nos. KR-29 and KR-30



Figure 422. Pre-Test and Post-Test Photographs, Test No. KR-29



Figure 423. Pre-Test and Post-Test Photographs, Test No. KR-30

19.6.5 Test Nos. KR-31 and KR-32 (Straight, 3/16-in. Stainless)

For test nos. KR-31 and KR-32, straight rods, fabricated from 3/16-in. (4.8-mm) diameter, T-304 stainless steel, were vertically loaded at a displacement rate of 0.8 in./min (20 mm/min). In both tests, the rods bent significantly before one end finally slipped out of its hole. There was also some local yielding of the flange around the holes. The peak loads for test nos. KR-31 and KR-32 were 1,465 lb (6,517 N) and 1,234 lb (5,489 N), respectively. The force versus displacement curve for test nos. KR-31 and KR-32 is shown in Figure 424. Pre- and post-test photographs are shown in Figures 425 and 426.

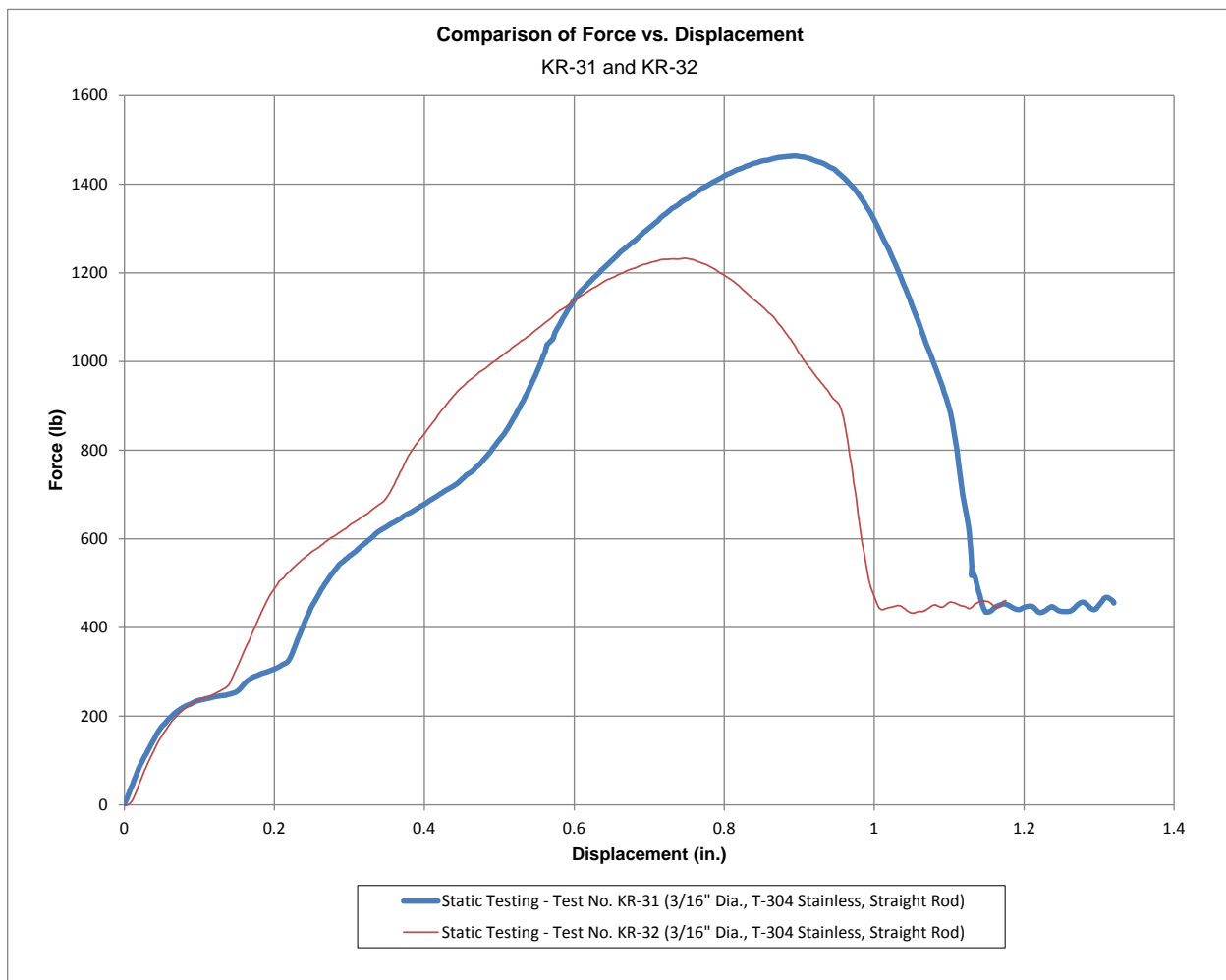


Figure 424. Force Versus Displacement, Test No. KR-31 and KR-32

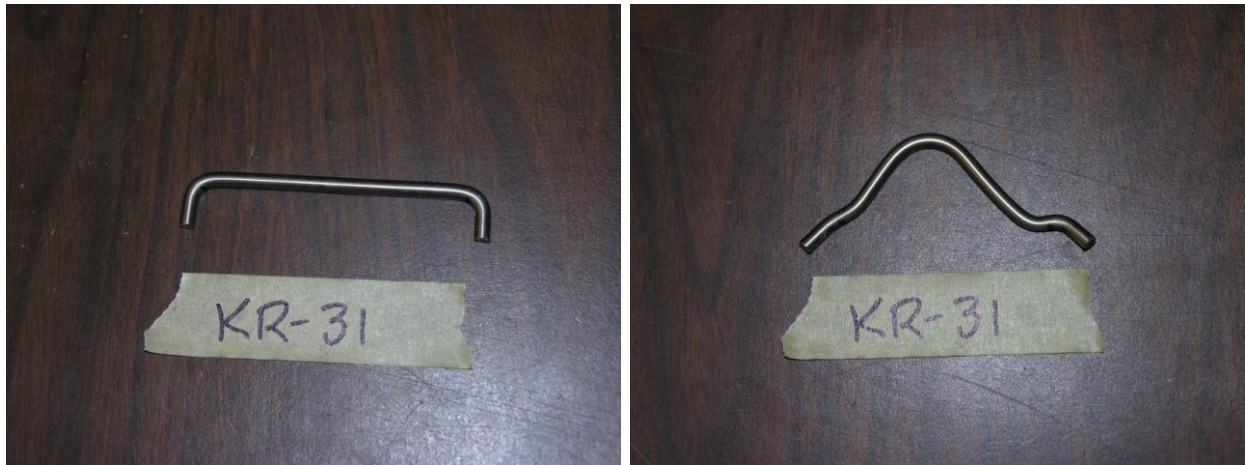


Figure 425. Pre-Test and Post-Test Photographs, Test No. KR-31



Figure 426. Pre-Test and Post-Test Photographs, Test No. KR-32

19.6.6 Test Nos. KR-33 and KR-34 (Straight, 1/4-in. Brass)

For test nos. KR-33 and KR-34, straight rods, fabricated from 1/4-in. (6.4-mm) diameter, C360 brass, were vertically loaded at a displacement rate of 0.8 in./min (20 mm/min). In both tests, the rods bent significantly before one end fractured at the location of its hole. There was also some local yielding of the flange around the holes. The peak loads for test nos. KR-33 and KR-34 were 1,301 lb (5,787 N) and 1,313 lb (5,840 N), respectively. The force versus displacement curve for test nos. KR-33 and KR-34 is shown in Figure 427. Pre- and post-test photographs are shown in Figures 428 and 429.

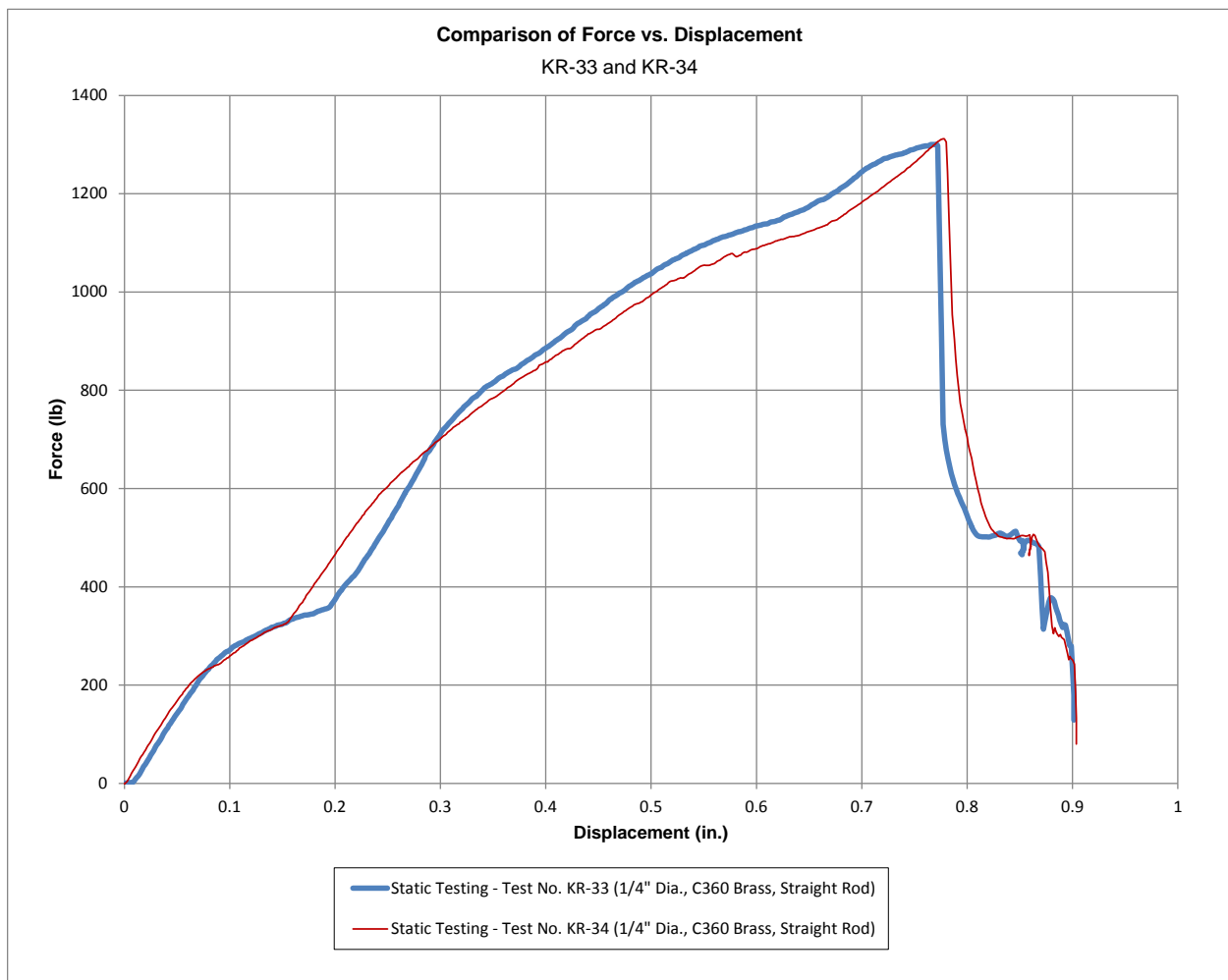


Figure 427. Force Versus Displacement, Test Nos. KR-33 and KR-34



Figure 428. Pre-Test and Post-Test Photographs, Test No. KR-33



Figure 429. Pre-Test and Post-Test Photographs, Test No. KR-34

19.6.7 Test Nos. KR-35 and KR-36 (Straight, 1/4-in. Stainless)

For test nos. KR-35 and KR-36, straight rods, fabricated from 1/4-in. (6.4-mm) diameter, T-304 stainless steel, were vertically loaded at a displacement rate of 0.8 in./min (20 mm/min). In both tests, the rods bent significantly before one end finally slipped out of its hole. There was also significant local yielding of the flange around the holes. The peak loads for test nos. KR-35 and KR-36 were 2,858 lb (12,710 N) and 2,503 lb (11,130 N), respectively. The force versus displacement curve for test nos. KR-35 and KR-36 is shown in Figure 430. Pre- and post-test photographs are shown in Figures 431 and 432.

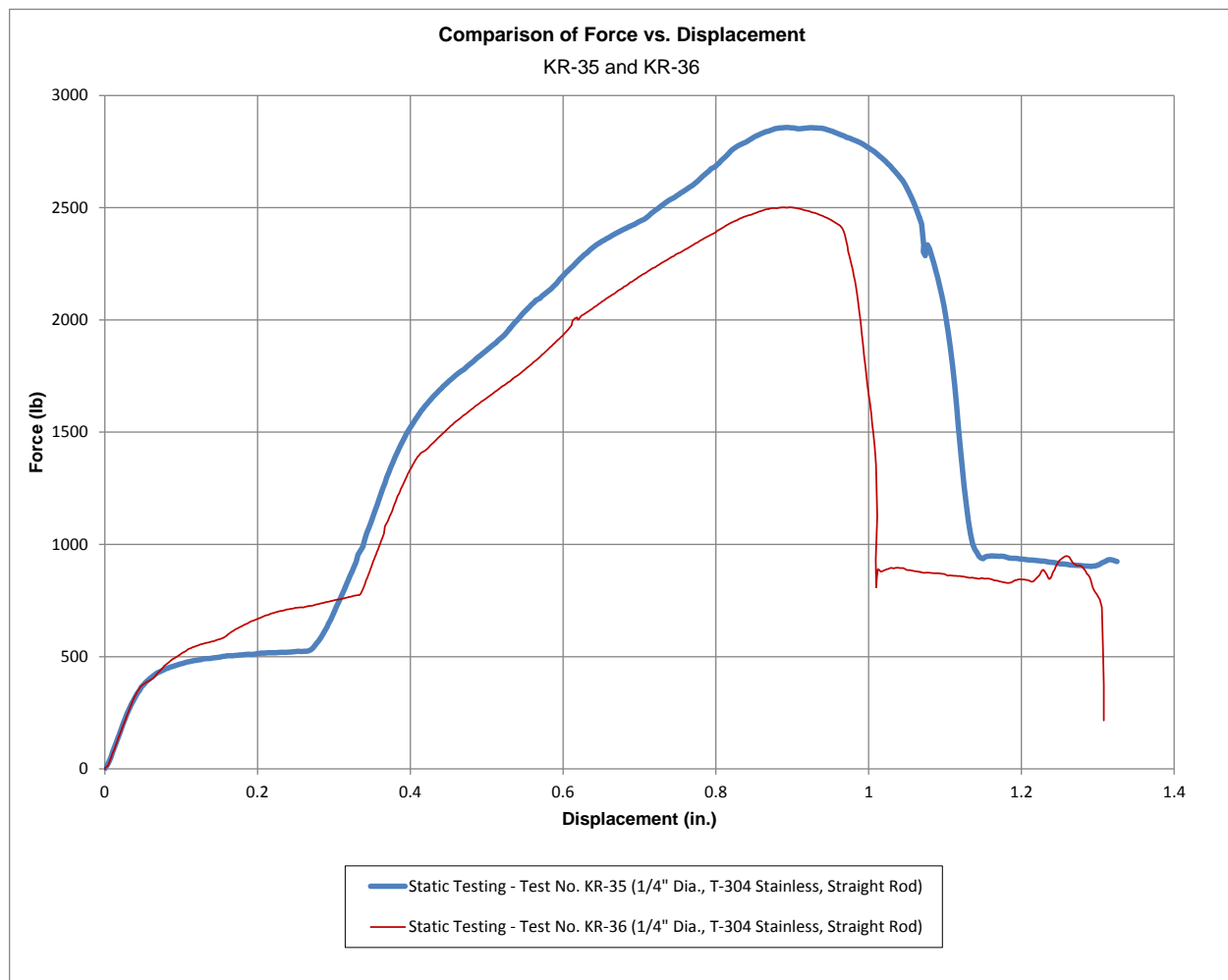


Figure 430. Force Versus Displacement, Test Nos. KR-35 and KR-36



Figure 431. Pre-Test and Post-Test Photographs, Test No. KR-35



Figure 432. Pre-Test and Post-Test Photographs, Test No. KR-36

19.7 Discussion

Forty-five static tensile tests were performed on twenty different prototype concepts for the top cable-to-post attachment. The average vertical release loads for each of the twenty concepts are summarized in Table 23.

Table 23. Average Vertical Release Loads for Top Cable-to-Post Attachments

Rod Concepts				
Concept		Diameter in. (mm)	Material	Average Vertical Release Load lb (N)
Web-Inserted Curved Rod		1/16 (1.6)	C360 Brass	32 (144)
Web-Inserted Curved Rod		3/32 (2.4)	C360 Brass	195 (866)
Web-Inserted Curved Rod		1/8 (3.2)	C360 Brass	285 (1,269)
Web-Inserted Curved Rod		3/32 (2.4)	T-303 Stainless Steel	126 (558)
Web-Inserted Curved Rod		1/8 (3.2)	T-304 Stainless Steel	346 (1,541)
Squeeze-In-Place Curved Rod		1/16 (1.6)	C360 Brass	10 (44)
Squeeze-In-Place Curved Rod		3/32 (2.4)	C360 Brass	34 (151)
Squeeze-In-Place Curved Rod		1/8 (3.2)	C360 Brass	60 (268)
Squeeze-In-Place Curved Rod		3/32 (2.4)	T-303 Stainless Steel	42 (184)
Squeeze-In-Place Curved Rod		1/8 (3.2)	T-304 Stainless Steel	73 (325)
Revised Web-Inserted Curved Rod		1/8 (3.2)	C360 Brass	556 (2,473)
Revised Web-Inserted Curved Rod		1/8 (3.2)	T-304 Stainless Steel	841 (3,742)
Straight Rod		1/8 (3.2)	C360 Brass	175 (779)
Straight Rod		1/8 (3.2)	T-304 Stainless Steel	386 (1,718)
Straight Rod		3/16 (4.8)	C360 Brass	706 (3,142)
Straight Rod		3/16 (4.8)	T-304 Stainless Steel	1,350 (6,003)
Straight Rod		1/4 (6.4)	C360 Brass	1,307 (5,814)
Straight Rod		1/4 (6.4)	T-304 Stainless Steel	2,681 (11,920)
HellermannTyton Cable Ties				
Type	Cross-Section in. (mm)		Material	Average Vertical Release Load lb (N)
	Width	Thickness		
MBT14HS	0.31 (7.9)	0.012 (0.30)	Stainless Steel 304	325 (1,447)
MBT14SS	0.18 (4.6)	0.012 (0.30)	Stainless Steel 304	157 (700.8)

*Blue highlighted cells show average vertical release loads in the target range

The static tests were used to determine which concepts were simple, easy to install, and which provided a vertical cable release load in the range of 100 to 200 lb (445 to 890 N). From the twenty different top cable-to-post attachment prototypes, four provided vertical cable release loads within the target range. These concepts included: the 3/32-in. (2.4-mm) diameter, C360 brass, web-inserted curved rod; the 3/32-in. (2.4-mm) diameter, T-303 stainless steel, web-inserted curved rod; the HellermannTyton stainless steel cable tie, type MBT14SS; and the 1/8-in. (3.2-mm) diameter, C360 brass, straight rod. Since the 1/8-in. (3.2-mm) diameter, C360 brass, straight rod was the simplest and easiest to install, it was chosen for additional dynamic testing and evaluation.

While the lateral release load was never actually measured for the straight rods, it was reasoned that the lateral cable release loads would be similar to the vertical release loads. This assumption was based on the fact that the cable would be placed in a 1V:1H sloped, web v-notch with the straight rod positioned over it. Therefore, if a purely lateral force were applied to the top cable, the reaction of the straight rod would be purely vertical, and the reaction of the sloped surface of the v-notch would be at a 45-degree angle, as shown in Figure 433.

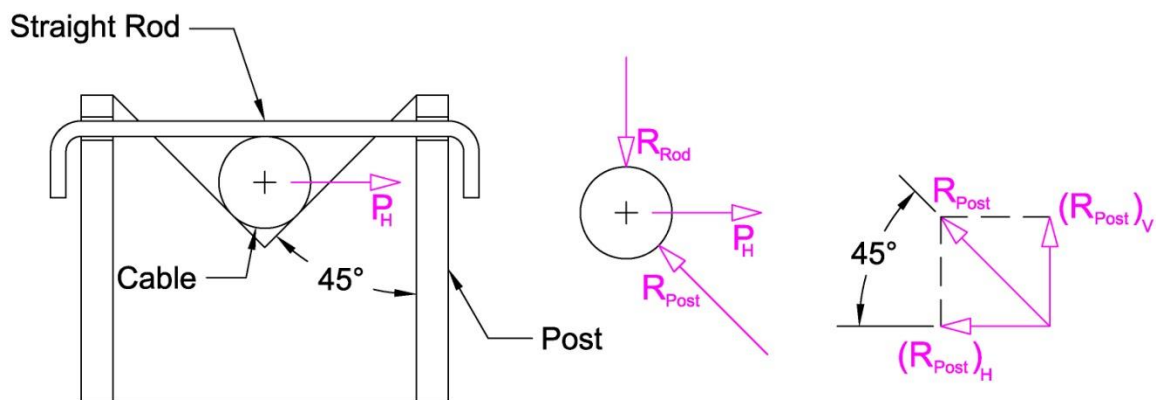


Figure 433. Lateral Resistance of the Straight Rod and V-Notch

For static equilibrium, the vertical reaction of the straight rod, R_{Rod} , must be equal in magnitude to the vertical component of the post reaction, $(R_{Post})_V$. Likewise, the applied horizontal force,

P_H , must be equal in magnitude to the horizontal component of the post reaction, $(R_{Post})_V$. Since the v-notch where the cable sits has 1V:1H slopes (i.e., makes a 45-degree angle), the vertical and horizontal components of the post reaction are equal in magnitude. Therefore, the vertical reaction of the straight rod is equal in magnitude to the applied lateral force.

Thus, the 1/8-in. (3.2-mm) diameter, C360 brass, straight rod with bent ends was to be subjected to dynamic bogie testing and evaluated to ensure that the cable would release when a post was struck by a surrogate vehicle. The bogie test setup and procedures are described in Chapter 20, and the test results are discussed in Chapter 21.

20 TOP CABLE-TO-POST ATTACHMENT—BOGIE IMPACT TEST CONDITIONS

20.1 Purpose

A bogie impact test on a scaled-down cable barrier system was deemed an excellent way to investigate and verify individual component behavior without the high costs associated with conducting a full-scale crash test. Thus, one such bogie impact test was performed to evaluate the prototype concept of a 1/8-in. (3.2-mm) diameter, C360 brass, straight rod with bent ends. The straight rods were installed as the top cable-to-post attachment for a series of S3x5.7 (S76x8.5) steel posts with an upper high-tension cable.

When the cable barrier system is impacted by a vehicle at a post, the top cable-to-post attachment must adequately and quickly release the cable, thus preventing that top cable from being pulled down with the rotating post. If the top cable is pulled down with the rotating post, it may not capture the vehicle, thus resulting in barrier override. Test no. HTTC-1 was performed to verify whether the 1/8-in. (3.2-mm) diameter, C360 brass, straight rods with bent ends would release the top cable immediately after the critical post was struck.

20.2 Test Setup and Details

The basic test setup consisted of five S3x5.7 (S76x8.5) steel posts, spaced at 16 ft (1.9 m) centers, with a tensioned cable mounted on top of all five posts. The cable, tensioned to 4,300 lb (19.1 kN), was placed in pre-cut v-notches on top of the line posts, and was anchored to cable terminals at both ends. Straight rods with bent ends, fabricated from 1/8-in. (3.2-mm) diameter, C360 brass were installed as top cable-to-post attachments at each post. The cable terminals were spaced 6 ft-10-5/8 in. (2.10 m) away from the line posts on both ends. The cable height was 40 in. (1016 mm) above the ground. For line post installation, an 8-in. (200-mm) diameter hole was cored into the concrete deck to a depth of 18 in. (457 mm). The post was installed in the hole, and the hole was filled with soil and compacted.

A 1,877-lb (851-kg) bogie vehicle impacted the barrier system at the center post at a speed of 49.4 mph (79.5 km/h) and at a 25-degree angle. The post was impacted at a height of 26-3/4 in. (673 mm) above the ground. The centerline of the bogie was aligned with the center of the post. The test would be considered a success if the cable quickly released away from the impacted post and the bogie went under it. The test would be considered a failure if it resulted in the cable itself being over-run by the bogie as a result of a failure to release away from the impacted post as it rotated backward and downward. Further, it would be undesirable for the cable to be pulled downward more than 2 in. (51 mm) before being released out of the notch. The drawing set for test no. HTTC-1 is shown in Figures 434 through 446.

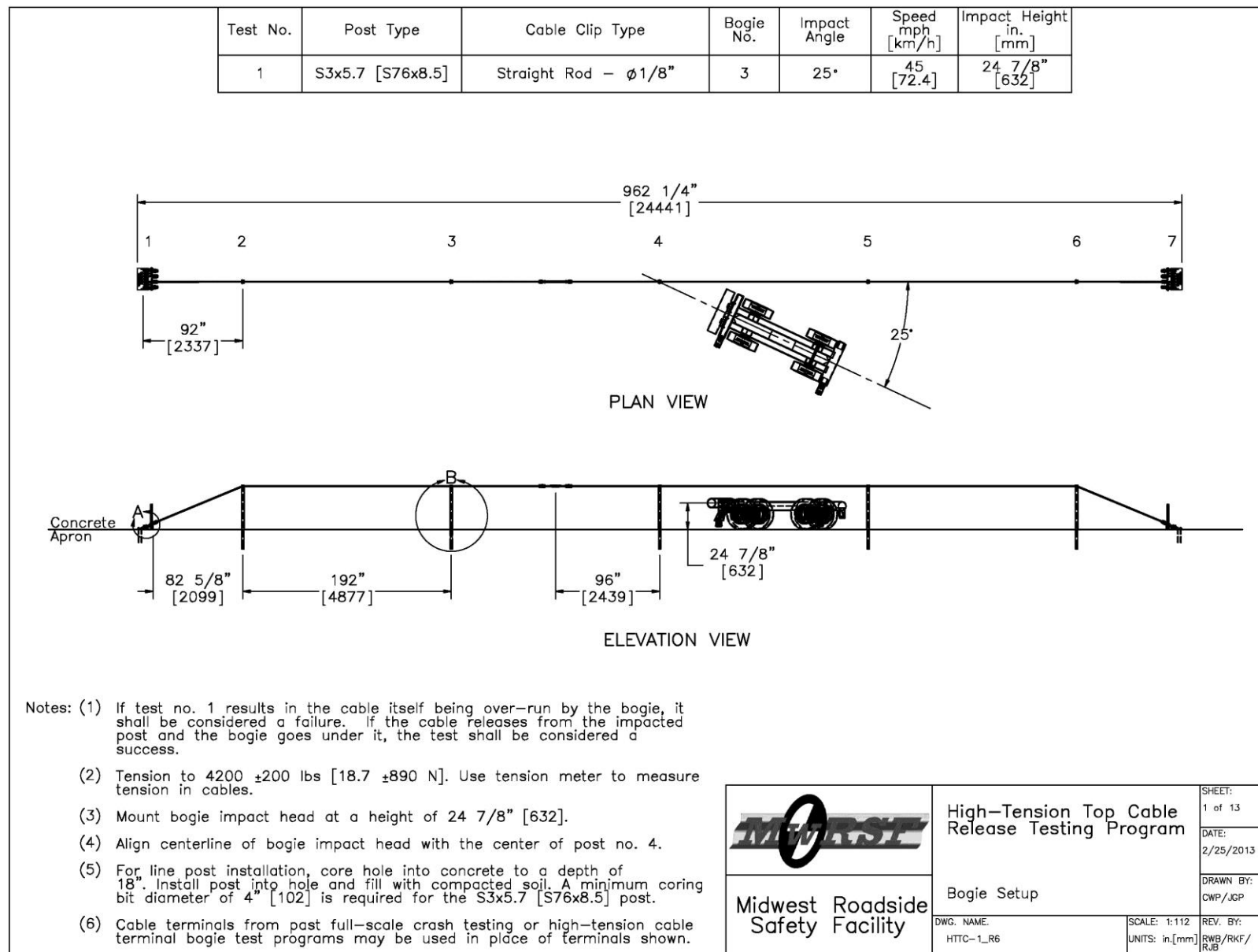


Figure 434. Bogie Test Setup, Test No. HTTC-1

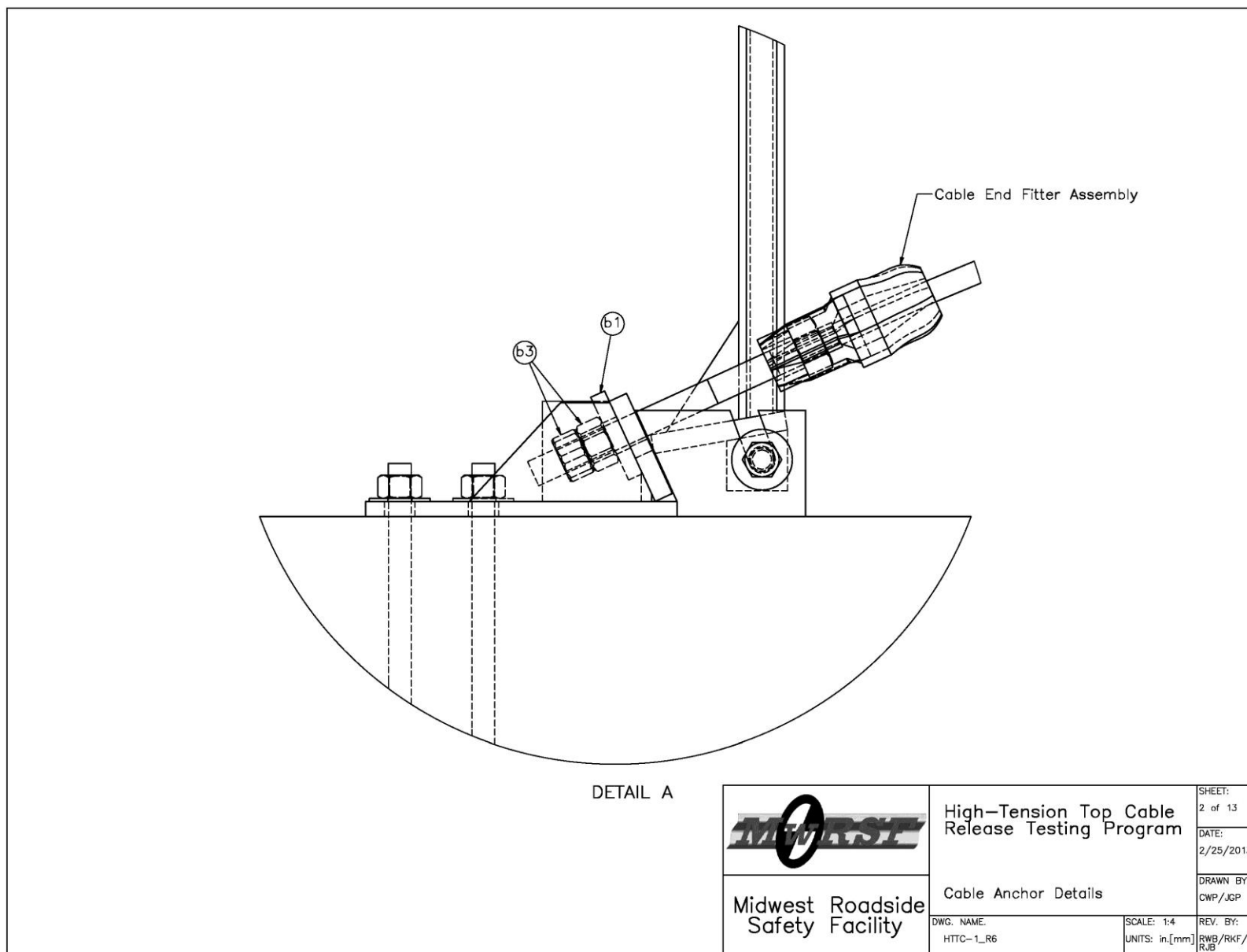


Figure 435. Cable Anchor Details, Test No. HTTC-1

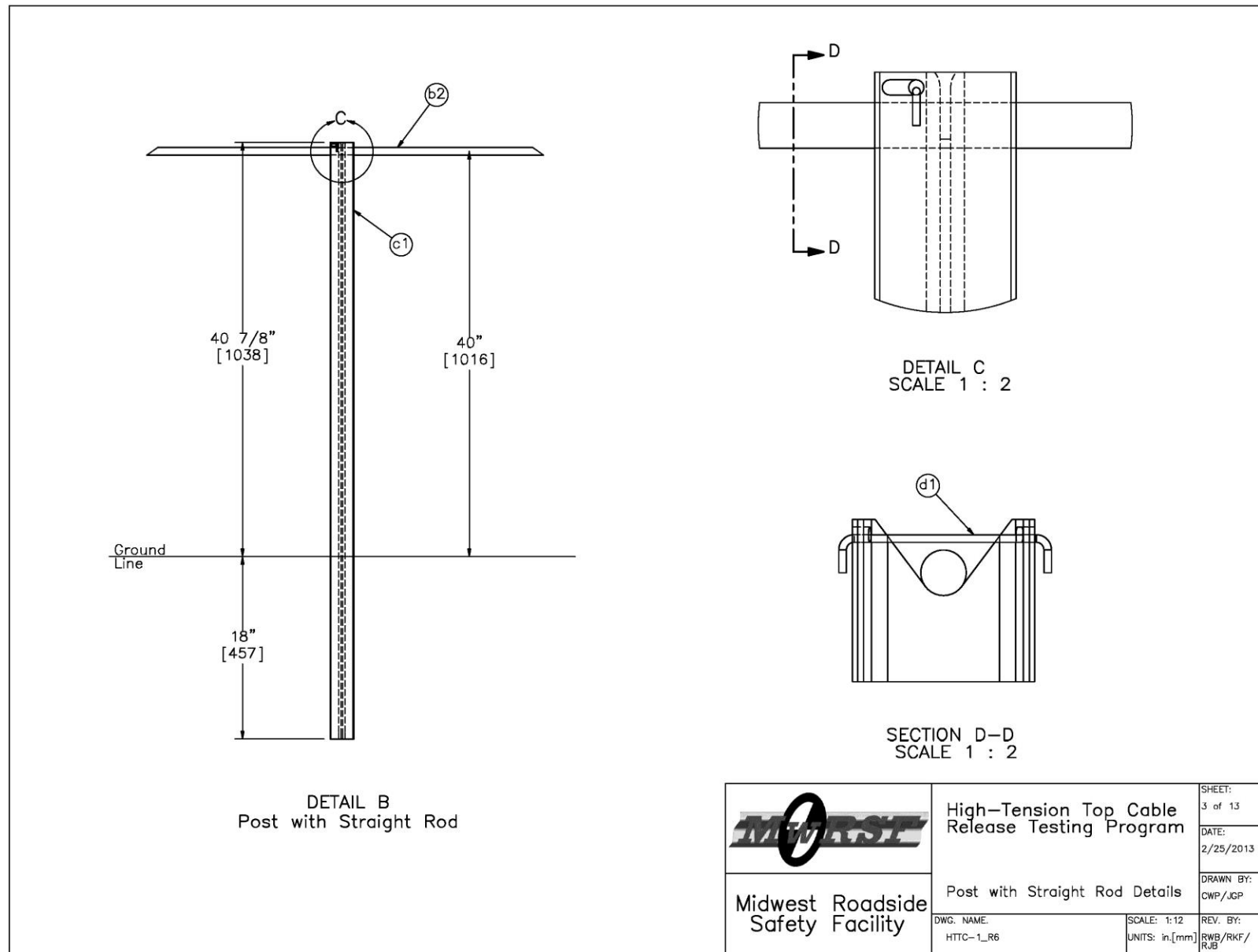


Figure 436. Post with Straight Rod Details, Test No. HTTC-1

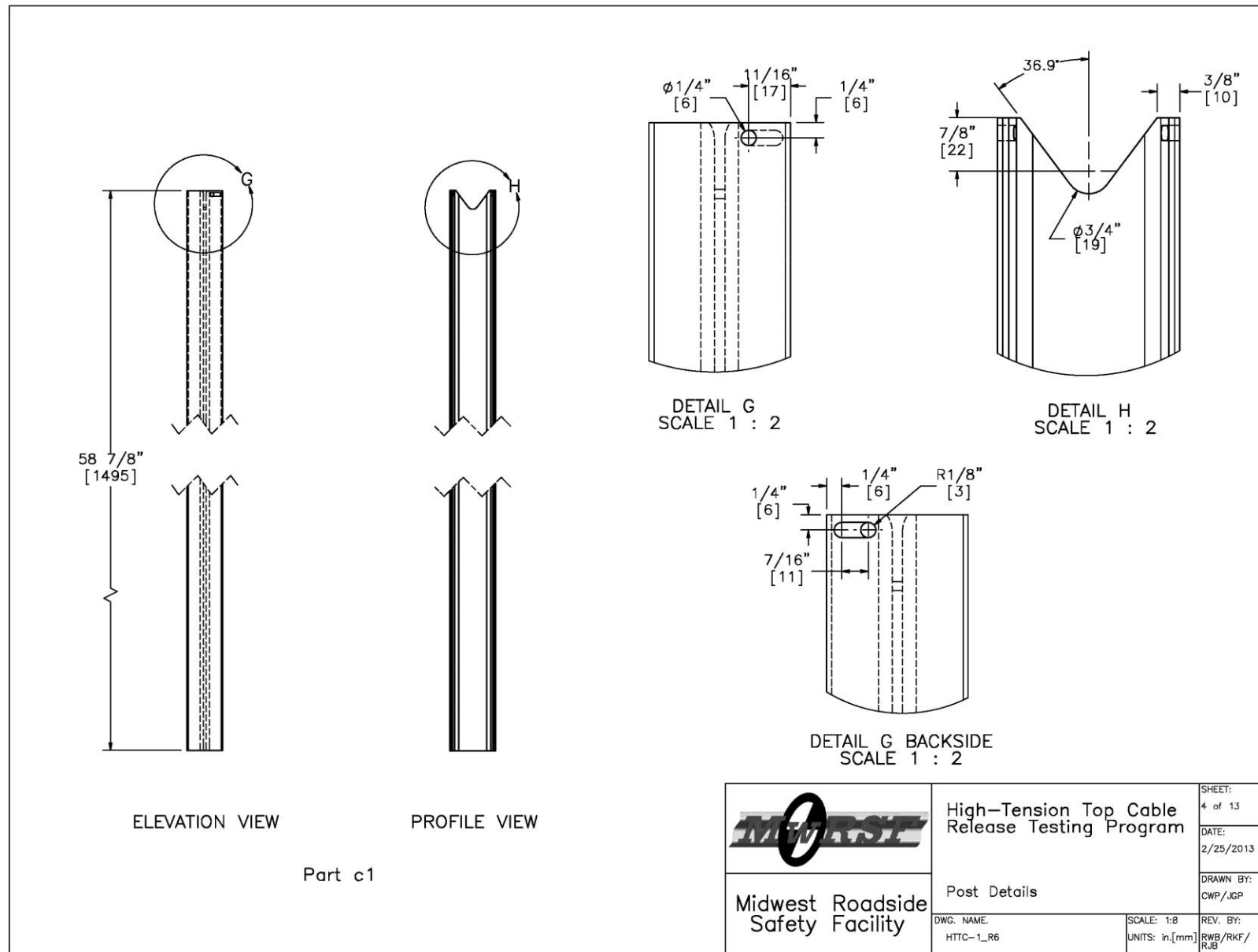


Figure 437. Post Details, Test No. HTTC-1

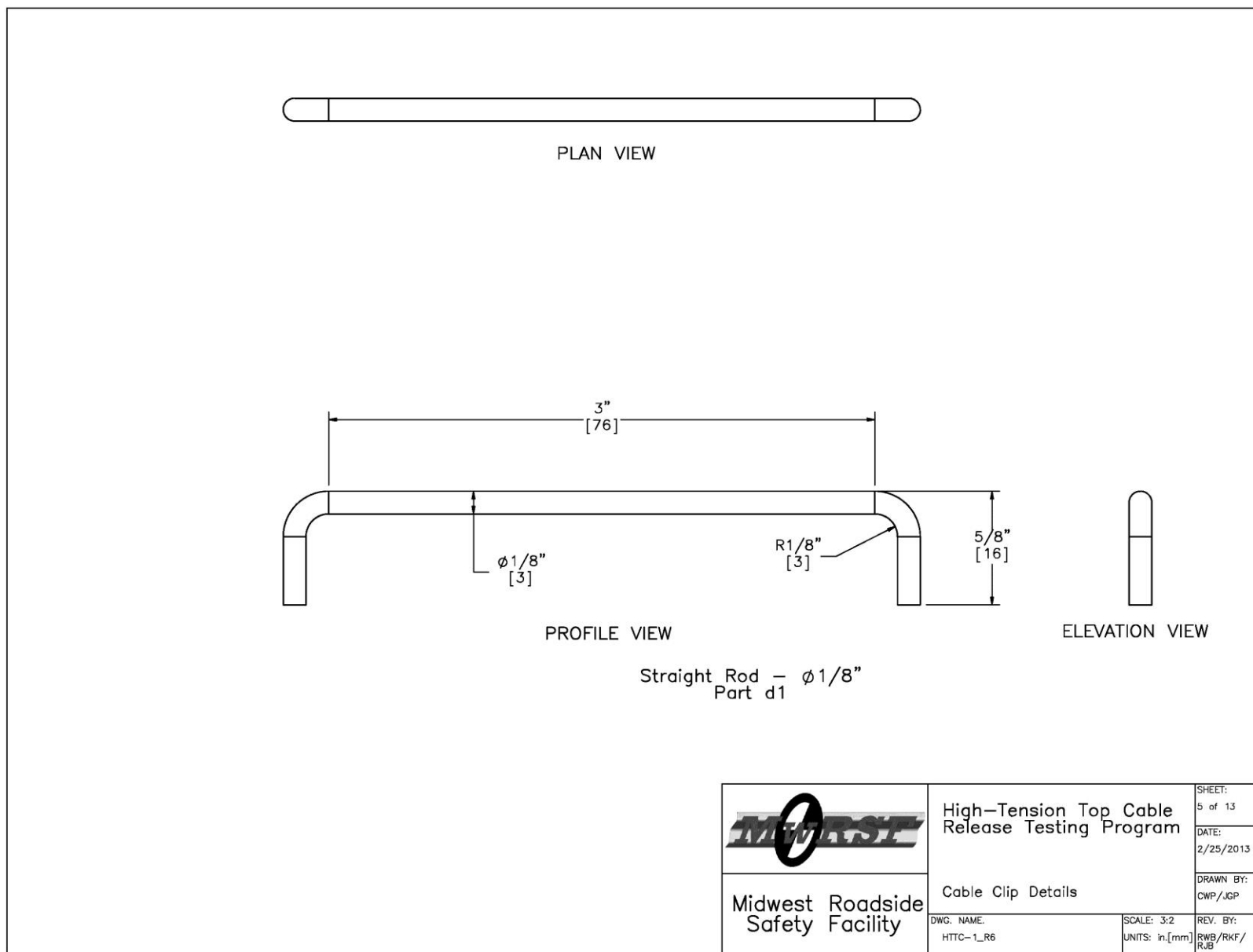


Figure 438. Straight Rod Details, Test No. HTTC-1

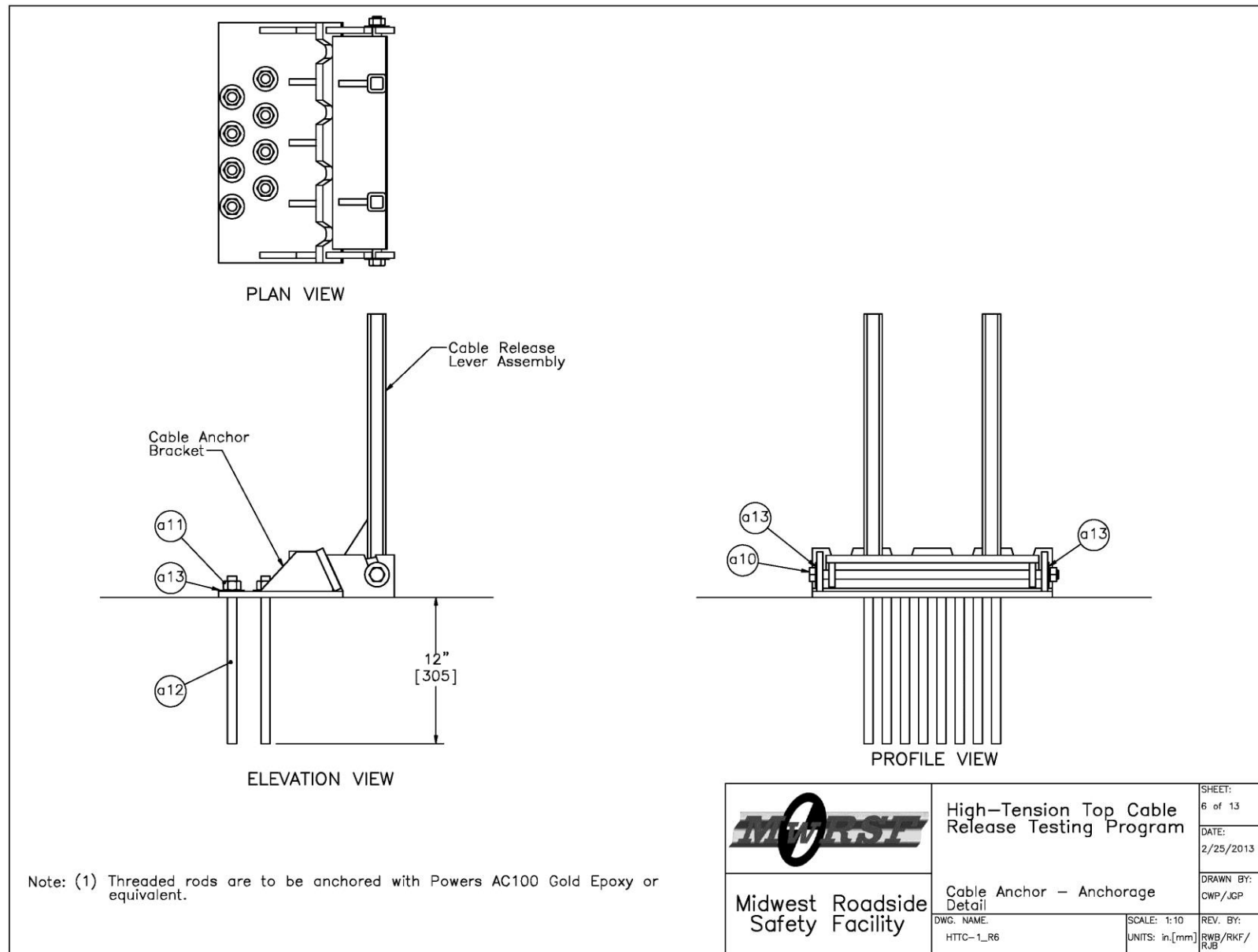


Figure 439. Anchorage Details, Test No. HTCC-1

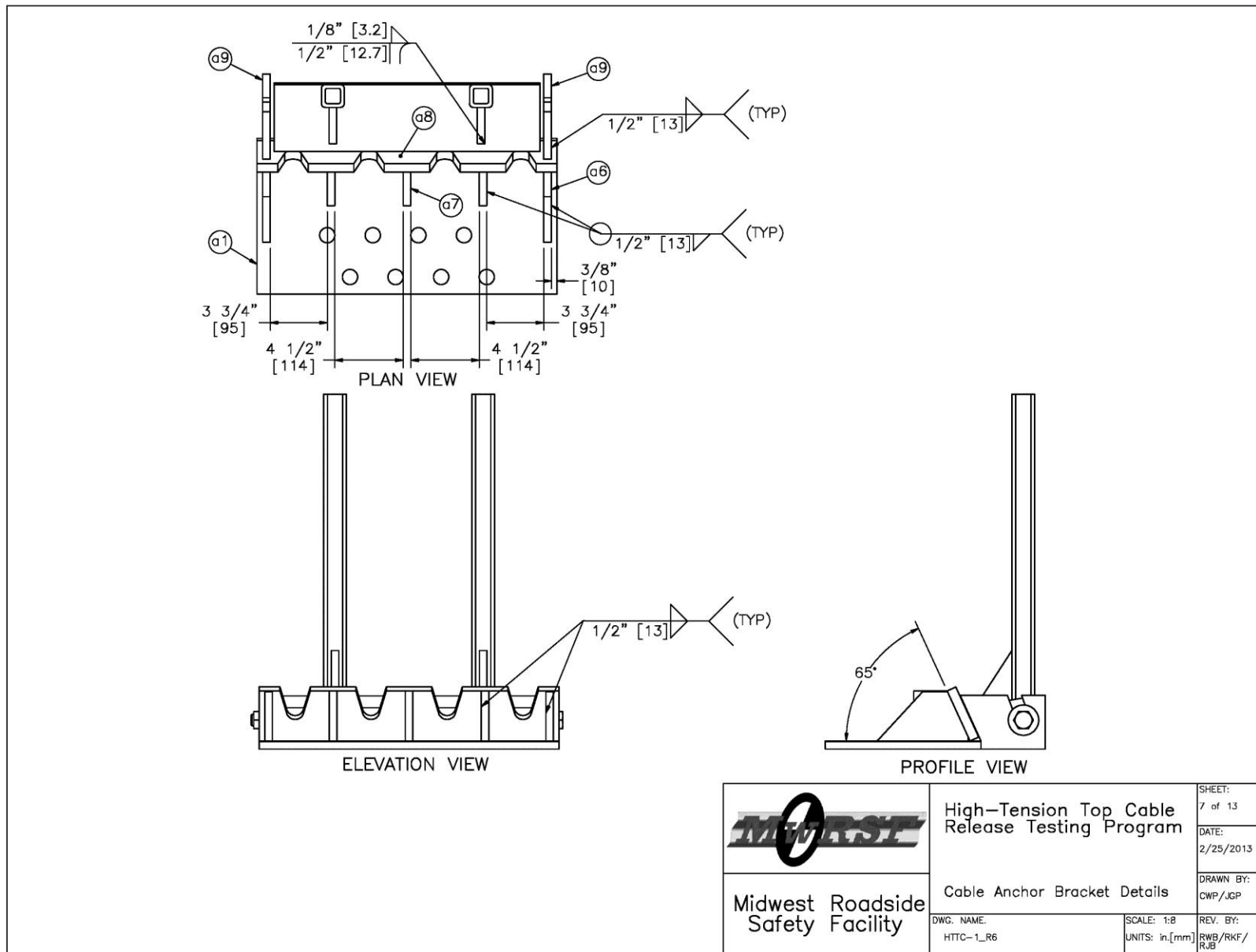


Figure 440. Cable Anchor Bracket Details, Test No. HTTC-1

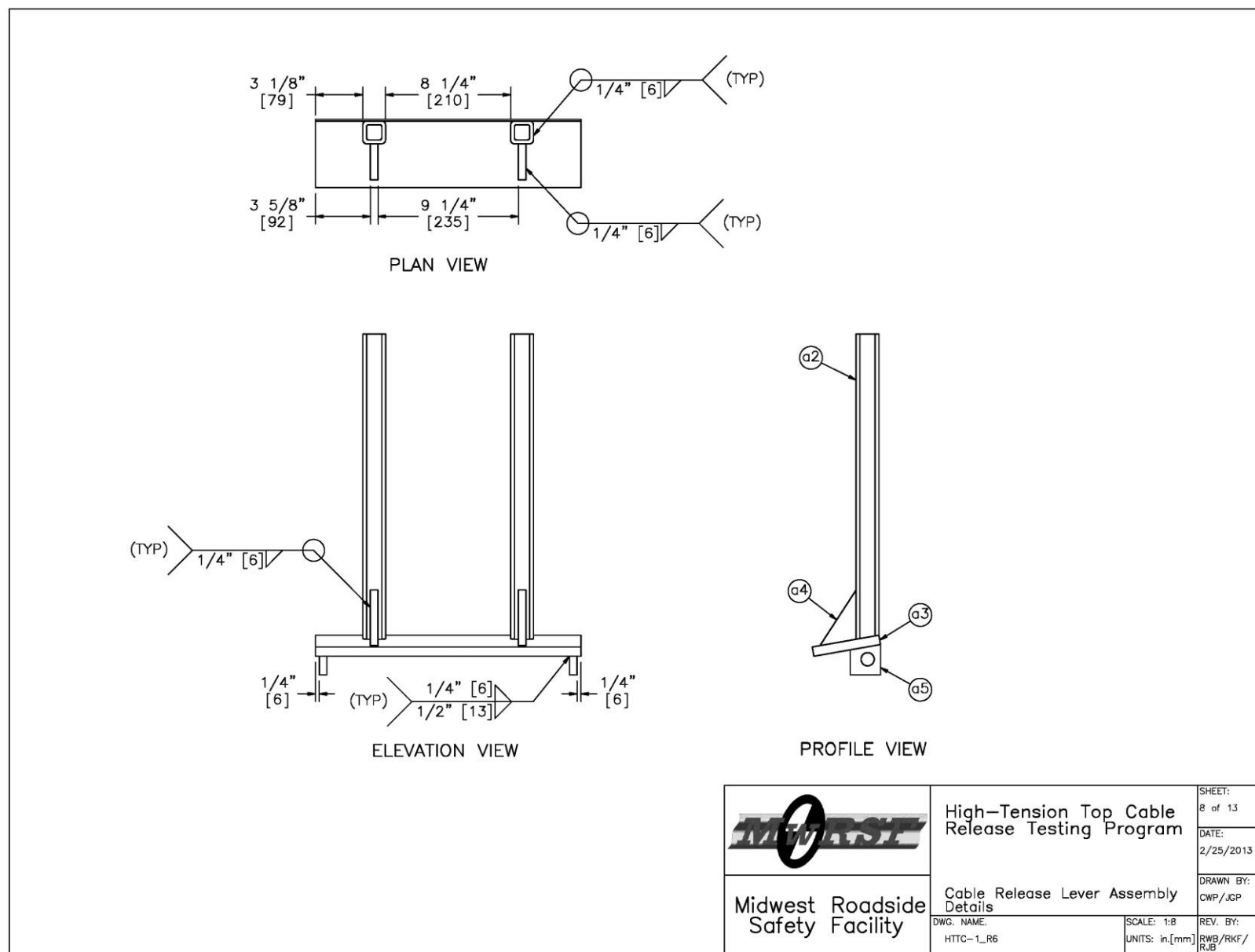


Figure 441. Cable Release Lever Assembly Details, Test No. HTTC-1

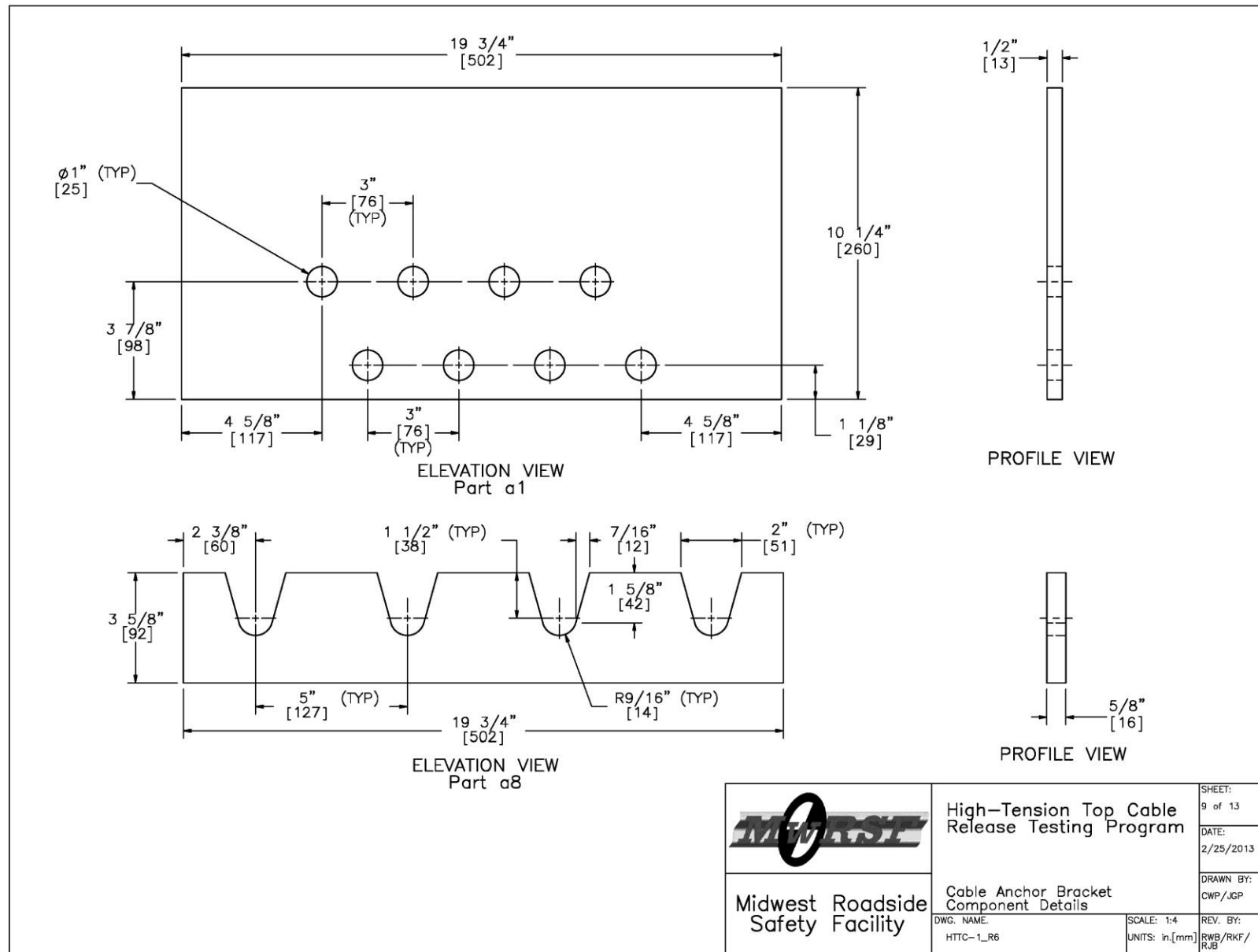


Figure 442. Cable Anchor Bracket Component Details, Test No. HTTC-1

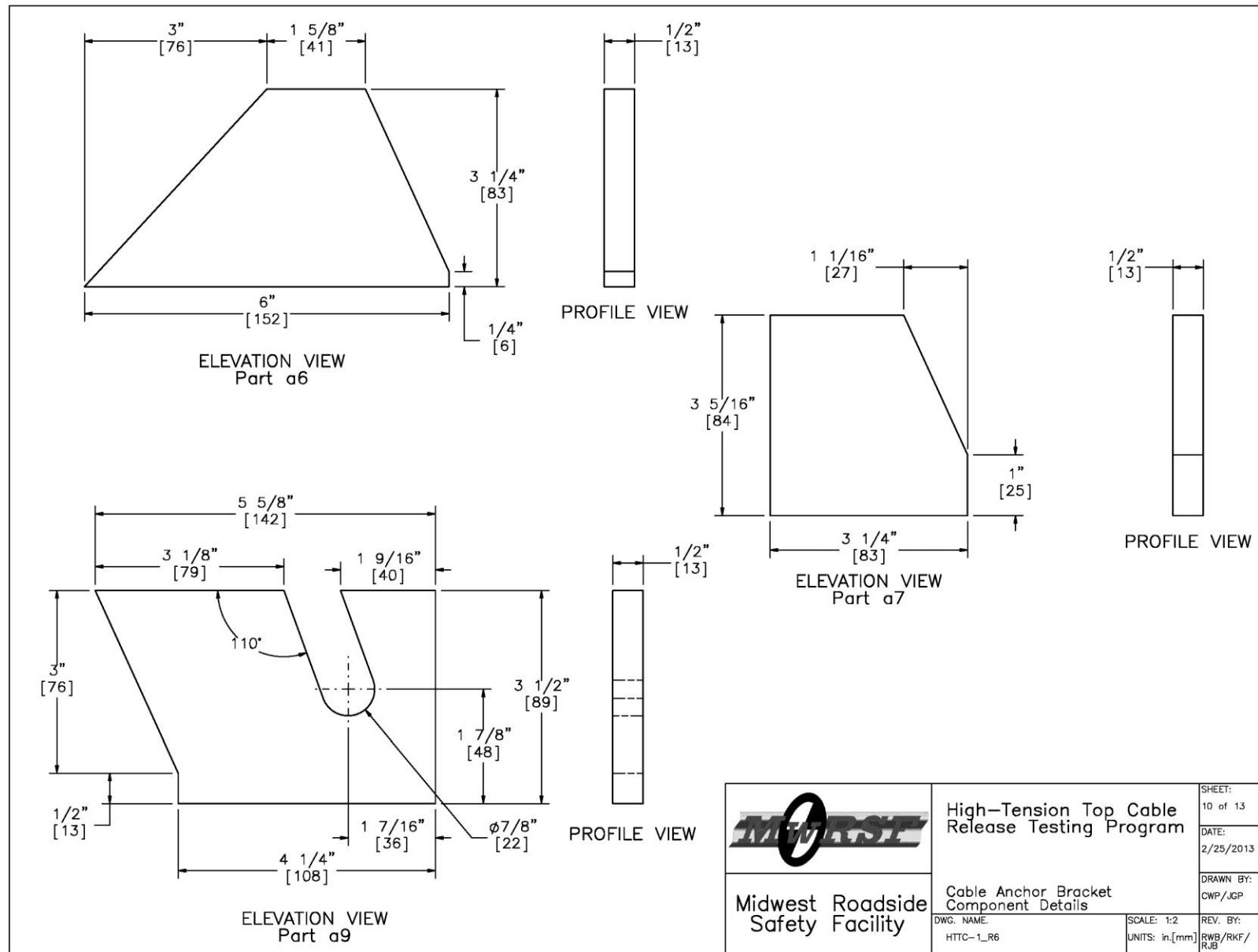


Figure 443. Cable Anchor Bracket Component Details, Test No. HTTC-1

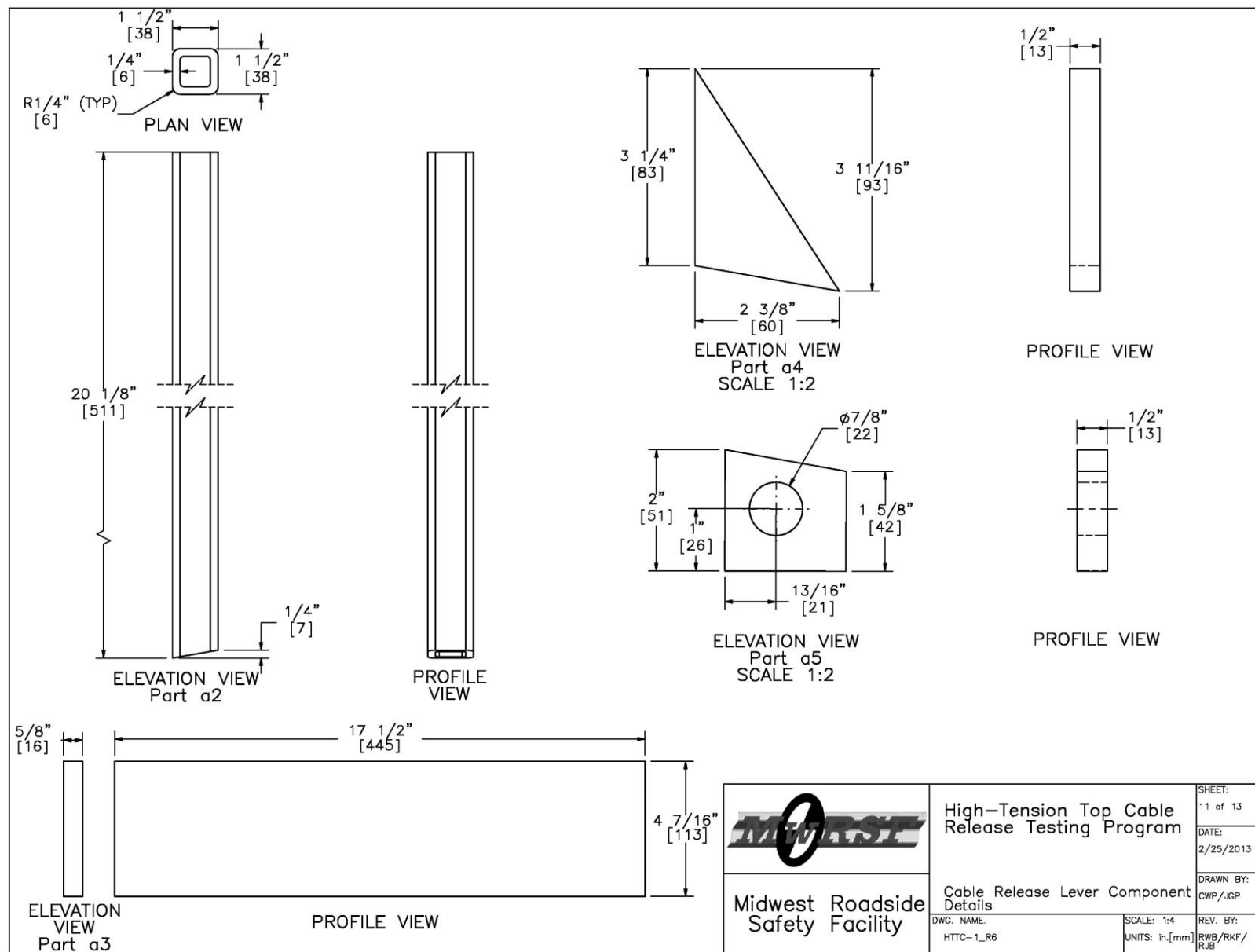


Figure 444. Cable Release Lever Component Details, Test No. HTTC-1

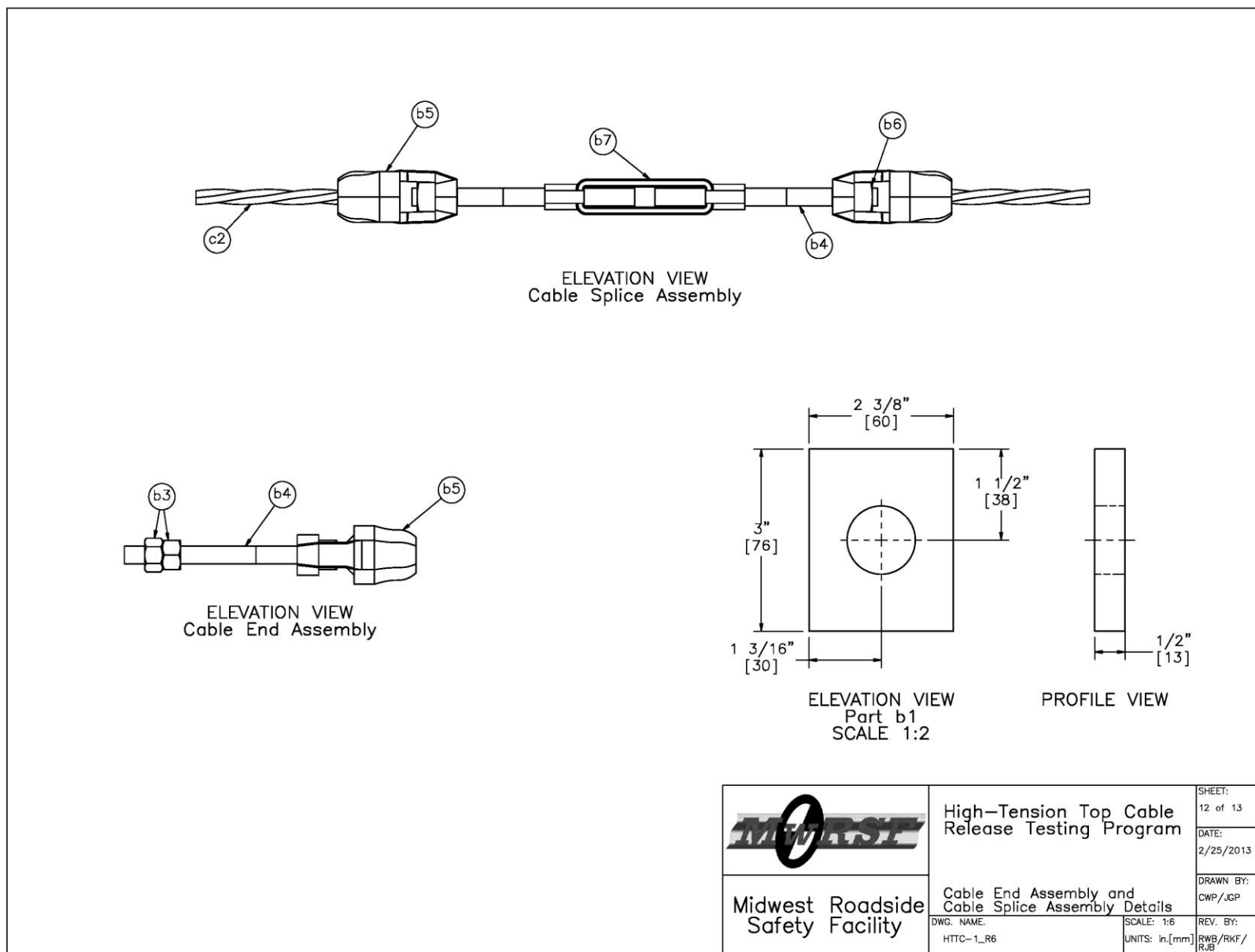


Figure 445. Cable End Assembly and Cable Splice Assembly Details, Test No. HTTC-1


Item No.	QTY.	Description	Material Specifications	Hardware Guide
a1	2	Cable Anchor Bracket Base Plate, 19 3/4" x 10 1/4" x 1/2" [502 x 260 x 12.7]	ASTM A36 Steel	—
a2	4	Cable Release Lever Impact Tube, 1 1/2" x 1 1/2" x 1/4" [38 x 38 x 6.4]	ASTM A500 Gr. B	—
a3	2	Cable Release Lever Base Plate, 17 1/2" x 4 7/16" x 5/8" [445 x 113 x 15.9]	ASTM A36 Steel	—
a4	4	Cable Release Lever Support Gusset, 3 11/16" x 2 3/8" x 1/2" [93 x 60 x 12.7]	ASTM A36 Steel	—
a5	4	Cable Release Lever Rotation Bracket, 2" x 2" x 1/2" [51 x 51 x 12.7]	ASTM A36 Steel	—
a6	4	Cable Anchor Bracket Exterior Gusset, 6" x 3 1/4" x 1/2" [152 x 83 x 12.7]	ASTM A36 Steel	—
a7	6	Cable Anchor Bracket Interior Gusset, 3 5/16" x 3 1/4" x 1/2" [84 x 83 x 12.7]	ASTM A36 Steel	—
a8	2	Cable Anchor Bracket Cable Plate, 19 3/4" x 3 5/8" x 5/8" [502 x 92 x 15.9]	ASTM A36 Steel	—
a9	4	Cable Anchor Bracket Rotation Bracket, 5 5/8" x 3 1/2" x 1/2" [142 x 89 x 12.7]	ASTM A36 Steel	—
a10	2	3/4" [19] Dia. UNC, 20" [508] Long Hex Bolt* and Nut	ASTM A307	—
a11	16	3/4" [19] Dia. UNC Heavy Hex Nut	ASTM A563 Gr. A	—
a12	16	3/4" [19] Dia. UNC, 13 3/4" [349] Long Threaded Rod	ASTM A449/ASTM A193 Gr. B7 Galv. or Stainless/SAE Gr. 5	—
a13	20	3/4" [19] Dia. Plain Round Washer	ASTM F844/ SAE Gr. 2	FWC20a
b1	8	CMB High Tension Anchor Plate Washer, 3" x 2 3/8" x 1/2" [76 x 60 x 12.7]	ASTM A36 Steel	—
b2	1	3/4" [19] Dia. Cable	AASHTO M30 Type 1 Class A	—
b3	16	7/8" [22] Dia. UNC Heavy Hex Nut	ASTM A563 Gr. C	RCE03
b4	10	7/8" [22] Dia. UNC, 11" [279] Long Threaded Rod	ASTM A449/ASTM A193 Gr. B7 Galv. or Stainless/SAE Gr. 5	RCE03
b5	10	Bennet Cable End Fitter	ASTM A47	RCE03
b6	10	7/8" [22] Dia. UNC Square Nut	SAE Gr. 5	FNS20
b7	1	Bennet Short Threaded Turnbuckle	As Supplied	—
c1	5	S3x5.7 [S76x8.5] Post, 58 7/8" [1495] Long	ASTM A572 GR50-07, ASTM A709 GR50-09A, ASTM A992-06A	—
d1	5	Straight Rod — ϕ 1/8" [3] Cable Clip	ASTM B16 Brass C36000 Half Hard (H02), ROUND. TS \geq 68.0 ksi, YS \geq 52.0 ksi	—
<p>* A 22" [559] long threaded rod may be substituted for the part no. a10 if necessary. Use of threaded will require two extra hex nuts and flat washers.</p> <p>Notes: (1) Mill Test Report for part d1 stock material has TS=81 ksi, YS=62 ksi.</p>				
 <p>Midwest Roadside Safety Facility</p>			<p>High-Tension Top Cable Release Testing Program</p> <p>Bill of Materials</p> <p>DWG. NAME: HTTC-1_R6</p> <p>SCALE: NONE</p> <p>UNITS: in.[mm]</p> <p>REV. BY: RWB/RKF/RJB</p>	<p>SHEET: 13 of 13</p> <p>DATE: 2/25/2013</p> <p>DRAWN BY: CWP/JGP</p>

Figure 446. Bill of Materials, Test No. HTTC-1

20.3 Test Facility

Physical testing was conducted at the MwRSF outdoor testing facility, which is located at the Lincoln Air Park on the northwest side of the Lincoln Municipal Airport. The facility is approximately 5 miles (8 km) northwest from the University of Nebraska-Lincoln's city campus.

20.4 Equipment and Instrumentation

Several types of equipment and instrumentation were utilized for this test and to collect and record data, including a bogie vehicle, accelerometers, an optic speed trap, pressure tape switches, high-speed and standard speed digital video, and digital still cameras.

20.4.1 Bogie

A rigid-frame bogie vehicle was used for this test. A variable-height, detachable impact head was used in the testing. The bogie head was constructed of 8-in. (203-mm) diameter, 1/2-in. (13-mm) thick standard steel pipe, with 3/4-in. (19-mm) neoprene belting wrapped around the pipe. The impact head was bolted to the bogie vehicle, thus creating a rigid frame with an impact height of 26-3/4 in. (673 mm). The bogie with the impact head is shown in Figure 447. The weight of the bogie with the addition of the mountable impact head and accelerometers was 1,877 lb (851 kg).



Figure 447. Rigid-Frame Bogie Aligned for Test No. HTTC-1

A pickup truck with a reverse cable tow system was used to propel the bogie to a target impact speed of 45 mph (72 km/h). When the bogie approached the end of the guidance system, it was released from the tow cable, allowing it to be free rolling when it impacted the post. A remote-control braking system was installed on the bogie, thus allowing it to be brought safely to rest after the test.

20.4.2 Accelerometers

An accelerometer system was mounted on the bogie vehicle near its center of gravity to measure the acceleration in the longitudinal, lateral, and vertical directions. However, only the longitudinal acceleration was processed and reported. Two environmental shock and vibration sensor/recorder systems were used to measure the accelerations in the longitudinal, lateral, and vertical directions. Both of the accelerometers were mounted near the center of gravity of the test vehicles. The electronic accelerometer data obtained in dynamic testing was filtered using the

SAE Class 60 and the SAE Class 180 Butterworth filter conforming to the SAE J211/1 specifications [73].

The first accelerometer system was a two-arm piezoresistive accelerometer system manufactured by Endevco of San Juan Capistrano, California. Three accelerometers were used to measure each of the longitudinal, lateral, and vertical accelerations independently at a sample rate of 10,000 Hz. The accelerometers were configured and controlled using a system developed and manufactured by Diversified Technical Systems, Inc. (DTS) of Seal Beach, California. More specifically, data was collected using a DTS Sensor Input Module (SIM), Model TDAS3-SIM-16M. The SIM was configured with 16 MB SRAM and 8 sensor input channels with 250 kB SRAM/channel. The SIM was mounted on a TDAS3-R4 module rack. The module rack was configured with isolated power/event/communications, 10BaseT Ethernet and RS232 communication, and an internal backup battery. Both the SIM and module rack were crashworthy. The “DTS TDAS Control” computer software program and a customized Microsoft Excel worksheet were used to analyze and plot the accelerometer data.

The second system, Model EDR-3, was a triaxial piezoresistive accelerometer system manufactured by IST of Okemos, Michigan. The EDR-3 was configured with 256 kB of RAM, a range of ± 200 g's, a sample rate of 3,200 Hz, and a 1,120 Hz low-pass filter. The “DynaMax 1 (DM-1)” computer software program and a customized Microsoft Excel worksheet were used to analyze and plot the accelerometer data.

Accelerometer data was collected, but never processed. It was determined to be unnecessary for the evaluation of the top cable-to-post attachments.

20.4.3 Optic Speed Trap

The retroreflective optic speed trap was used to determine the speed of the bogie vehicle before impact. Three retroreflective targets, spaced at 18-in. (457-mm) intervals, were applied to

the side of the bogie vehicle and reflect the beam of light. When the emitted beam of light was returned to the Emitter/Receiver, a signal was sent to the Optic Control Box, which in turn sent a signal to the data computer as well as activated the External LED box. The computer recorded the signals and the time each occurred. The speed was then calculated using the spacing between the retroreflective targets and the time between the signals. LED lights and high-speed digital video analysis are only used as a backup in the event that vehicle speeds cannot be determined from the electronic data.

20.4.4 Pressure Tape Switches

Three pressure tape switches, spaced at approximately 18-in. (457-mm) intervals and placed near the end of the bogie track, were used to determine the speed of the bogie before the impact. As the left-front tire of the bogie passed over each tape switch, a strobe light was fired sending an electronic timing signal to the data acquisition system. The system recorded the signals and the time each occurred. The speed was then calculated using the spacing between the sensors and the time between the signals. Strobe lights and high-speed video analysis are used only as a backup in the event that vehicle speeds cannot be determined from the electronic data. Due to technical difficulties, the pressure tape switches were not used to calculate bogie speed.

20.4.5 Digital Photography

Three AOS X-PRI high-speed digital video cameras and three JVC digital video cameras were used to document each test. The AOS high-speed camera had a frame rate of 500 frames per second and the JVC digital video camera had a frame rate of 29.97 frames per second. Both cameras were placed laterally from the post, with a view perpendicular to the bogie's direction of travel. A Nikon D50 digital still camera was also used to document pre- and post-test conditions.

21 TOP CABLE-TO-POST ATTACHMENT—TEST RESULTS

21.1 Test No. HTTC-1 and Results

One bogie impact test was performed to evaluate the performance of 1/8-in. (3.2-mm) diameter, C360 brass, straight rods with bent ends as top cable-to-post attachment for the high-tension, cable barrier system. The small-scale cable barrier system consisted of five S3x5.7 (S76x8.5) steel posts, two cable terminals—one at each end—and a cable. A pre-test photograph of the entire system is shown in Figure 448.



Figure 448. Pre-Test Photograph of Cable Barrier System, Test No. HTTC-1

For test no. HTTC-1, the 1,877-lb (851-kg) steel-framed bogie impacted the barrier system at the center post, traveling 49.4 mph (79.5 km/h) and at a 25-degree angle. The post began to rotate backward immediately. High-speed video footage clearly showed that the cable was free from the post at a time of 0.008 sec after impact. The cable deflected slightly before

releasing away from the post, thus causing a wave to propagate along the length of the cable. As a result of the wave, the top cable-to-post attachments immediately upstream and downstream of the post sustained some damage, but they did not allow the cable to release from the posts. The impacted post yielded at the ground line and bent all the way over as the bogie overran it. The bogie went under the released cable. The test was considered a success. Pre- and post-test photographs for the posts that were impacted are shown in Figures 449 through 451. Sequential photographs from each of the high-speed video cameras are shown in Figures 452 through 454.



Figure 449. Pre-Test and Post-Test Photographs for Post No. 3, Test No. HTTC-1



Figure 450. Pre-Test and Post-Test Photographs for Post No. 4, Test No. HTTC-1



Figure 451. Pre-Test and Post-Test Photographs for Post No. 5, Test No. HTTC-1



Figure 452. Sequential Photographs for Camera AOS5, Test No. HTTC-1



Figure 453. Sequential Photographs for Camera AOS6, Test No. HTTC-1

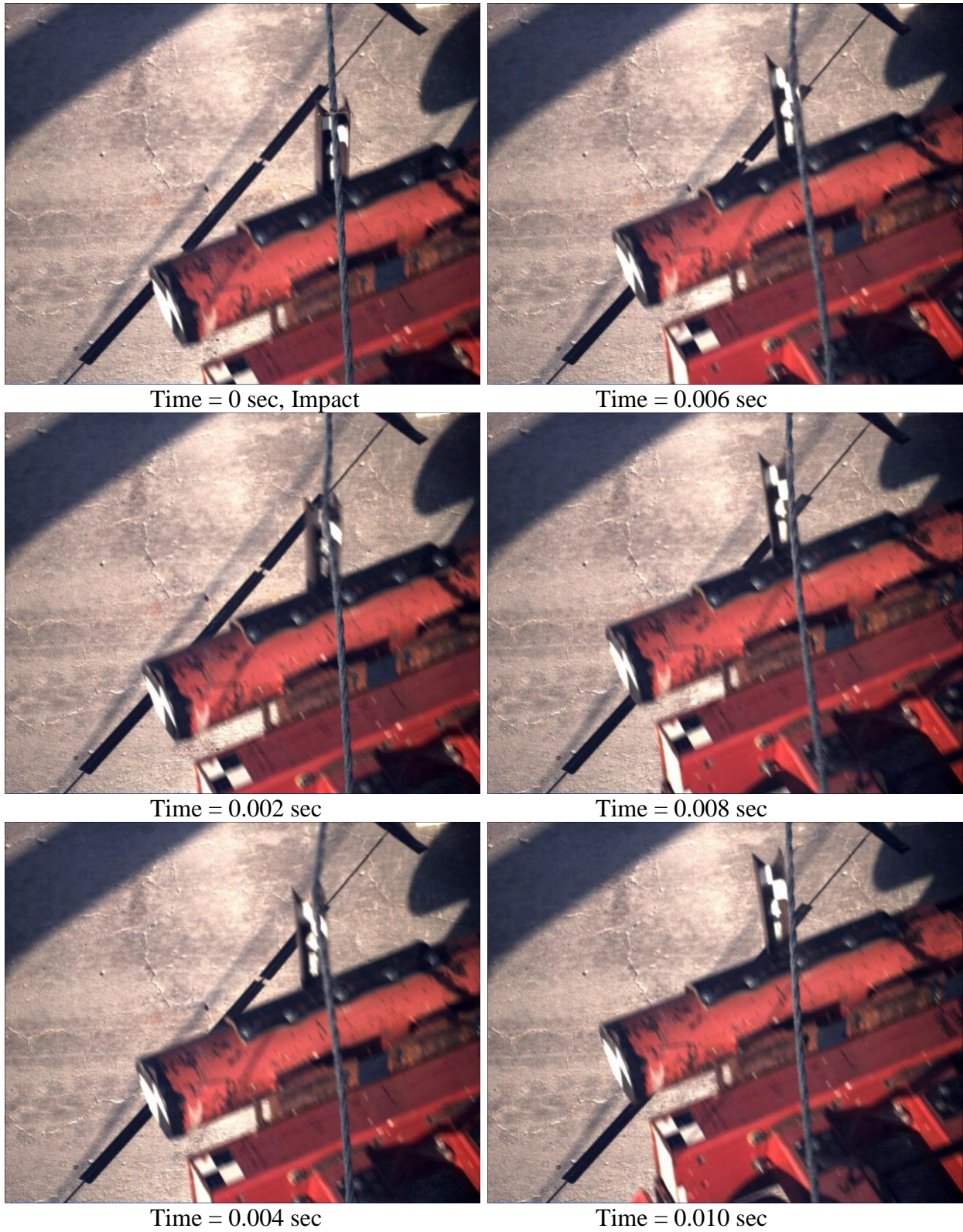


Figure 454. Sequential Photographs for Camera AOS7, Test No. HTTC-1

21.2 Discussion, Summary, Conclusions, and Recommendations

The 1/8-in. (3.2-mm) diameter, C360 brass, straight rod with bent ends was chosen for dynamic testing and evaluation due to: (1) its static vertical release load of 175.2 lb (779.3 N) was in the target range of 100 to 200 lb (445 to 890 N) and (2) it could be reasoned through engineering judgment and hand calculations that its static lateral release load would be similar to the static vertical release load. Ultimately, test no. HTTC-1 was considered a success. The cable was fully released away from the impacted post approximately 0.008 sec after impact, and the bogie did not overrun the cable. Furthermore, the upstream and downstream cable-to-post attachments absorbed the stress wave caused by the impact event to the tensioned cable without releasing it, which was a secondary concern. Thus, the 1/8-in. (3.2-mm) diameter, C360 brass, straight rod with bent ends was recommended for implementation as the new top cable-to-post attachment in the high-tension, 4-cable median barrier.

When using Equation 4.13 to select the cable tension and post spacing, a conservatively low estimate of the top cable-to-post attachment's lateral cable release load should be used. MwRSF recommends using a value of 150 lb (667 N).

22 SUMMARY, CONCLUSIONS, AND RECOMMENDATIONS

22.1 Summary and Conclusions

22.1.1 Research Objective

The research objective of the portion of the project reported herein was to design new cable-to-post attachments to improve the safety performance of the non-proprietary, high-tension, 4-cable median barrier system. The modified cable barrier system would be designed for use in median ditches with 6V:1H or flatter side slopes and using a 0 to 4 ft (0 to 1.2 m) lateral placement away from the edge of the shoulder or slope break point. However, the state DOTs may desire to select the system configuration so that the barrier would provide satisfactory safety performance when positioned anywhere in a 6V:1H or flatter median ditch. In addition, it was hopeful that the cable barrier system could later be modified for use in 4V:1H sloped medians, including at 0 to 4 ft (0 to 1.2 m) as well as anywhere in the ditch. Finally, the modified cable barrier system would be designed to meet the Test Level 3 impact safety standards provided in MASH.

22.1.2 Research Approach

The research objective was completed in four steps: (1) determine the minimum design loads associated with horizontal and vertical curves as a function of post spacing; (2) determine target capacities for the vertical and lateral cable release out of the cable-to-post attachments at all four cable heights; (3) design and test cable-to-post attachments for the bottom three cables; and (4) design and test cable-to-post attachments for the top cable. Steps 3 and 4 were ongoing, with cable-to-post attachments constantly being designed, tested, modified and re-tested until final recommendations were ready to be made.

22.1.3 Determination of Design Loads

Cable barriers installed along roadways with changes in vertical and horizontal alignment will encounter load conditions which tend to push cables against the post, pull cables away from posts, lift cables up, or push cables down at the cable-to-post attachment. In order to design the cable-to-post attachments, it was necessary to determine these design loads. The resulting load equations were a function of the cable tension, post spacing, and curve parameters. Vertical and horizontal curve parameters were obtained from the AASHTO Green Book [72].

The vertical loads are given by Equation 4.11.

$$(R_V)_{Max} = T \frac{s}{100K} \quad (4.11)$$

Where T = cable tension
 s = post spacing
 K = horizontal length per percent algebraic difference
 in intersecting grades

The K-value for a sag vertical curve on a highway with a design speed of 40 mph (72 km/h) is 64 ft (19.5 m). For an 8-kip (36-kN) cable tension, the change in the slope of the cable between two adjacent, 16-ft (4.9-m) post spans, on a 40-mph (64 km/h) sag vertical curve, will produce a 20-lb (89-N) uplift force at the cable-to-post attachments. For comparison, the weight of a 16-ft (4.9-m) length of cable is approximately 13 lb (58 N). The design speed for most highways will be greater than 40 mph (64 km/h), so the K-values will be greater than 64 ft (19.5 m), resulting in even smaller vertical forces on the cable-to-post attachments.

The lateral loads are given by Equation 4.13.

$$F = T \left(\frac{s}{R} \right) \quad (4.13)$$

Where F = lateral load on the cable-to-post attachment
 T = cable tension
 s = post spacing
 R = horizontal curve radius

Equation 4.13 is a useful relationship for determining the maximum allowable post spacing on a horizontal curve. For a design cable tension of 8 kips (36 kN) and lateral cable-to-post attachment strength, F , the maximum allowable post spacing as a function of the curve radius is shown in Figure 455.

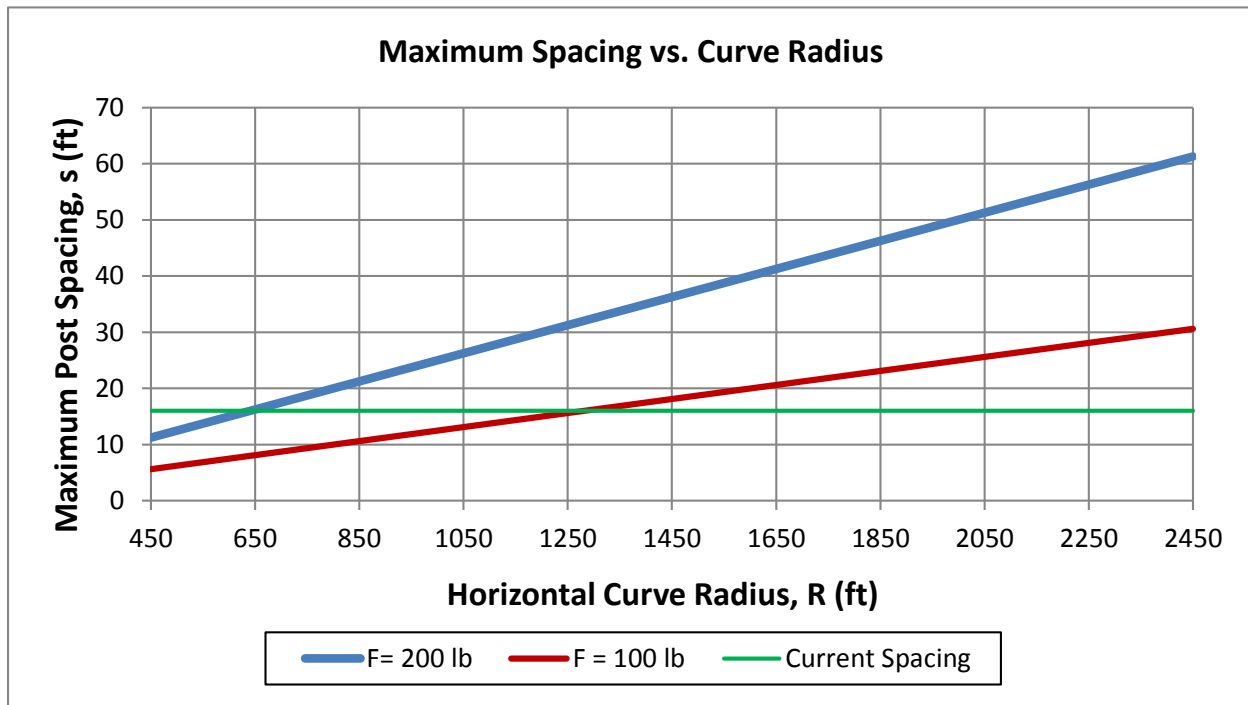


Figure 455. Maximum Post Spacing vs. Horizontal Curve Radius

22.1.4 Determining the Target Capacities

As a starting point, a target vertical cable release of 225 lb (1.00 kN) was chosen for the lower three cable-to-post attachments. This value reflected a significant reduction from the 1.18- kip (5.25-kN) vertical resistance of the keyway bolts used in the most recent designs. The goal was to ensure that if a vehicle's A-pillar became positioned under the cable and began to push up on it (as observed in full scale crash test no. 4CMBLT-1), the cable would quickly release away from the post, introducing slack to the cable so that the normal force exerted by the cable on the A-pillar would not crush the A-pillar.

In addition to the targeted vertical cable release load, the lower three cable-to-post attachments would be designed with a targeted lateral release load of 6.00 kips (26.7 kN). The goal was for the cable-to-post attachments to be able to develop the full moment capacity of the post when loaded laterally. Bogie tests, as described in Chapter 6, were used to evaluate potential prototypes for cable-to-post attachments for the lower three cables.

The top cable-to-post attachments would need to hold the cable in place before an impact, but easily and quickly release the cable when a post was impacted and began to rotate backward and downward. Using Equation 4.13 and assuming a maximum cable tension of 8.00 kips (35.6 kN), a horizontal curve radius of 960 ft (293 m), the minimum curve radius for a roadway with a 55-mph (89-km/h) design speed, and a post spacing between 12 and 24 ft (3.7 and 7.3 m), the target lateral cable release load for designing the top cable-to-post attachments was set in the range of 100 to 200 lb (445 to 890 N).

22.1.5 Keyway Bolts

Once the desired vertical and lateral cable release loads were selected for the cable-to-post attachments, the next step was to design and test new cable-to-post attachments for the lower three cables. This process began with the keyway bolts. A total of twenty-eight bogie tests were performed on different keyway bolt concepts. For example, the bolt material was varied from the stronger A449 steel to the weaker C1018 steel. In addition, the shape of the keyway and of the bolt was explored. During this re-design effort, an ideal cable-to-post attachment behavior was refined. Ideally, when a cable-to-post attachment is pulled laterally, the bolt head will become caught in the narrow part of the keyway, thus forcing the attachment to fail. When pulled vertically, the attachment will bend and its head will rotate up and out of the wider part of the keyway without scraping against the inside of the flange. This behavior was first observed in some preliminary LS-DYNA simulations that were conducted on extended keyway bolts as part

of an academic effort. In actual bogie tests, modified extended keyway bolts were found to have lateral and vertical cable release loads of 6.47 kips (28.8 kN) and 486 lb (2.16 kN), respectively.

22.1.6 Tabbed Brackets

In addition to improved keyway bolts, prototype tabbed brackets were designed and tested for consideration as cable-to-post attachments for the lower three cables. Tabbed brackets were fabricated from grade 50 sheet steel. A total of 42 bogie tests were performed on different tabbed bracket concepts. Ten different versions were tested. There were two different variations of tabbed brackets—crimp-in-place and bolted, which referenced the method of attachment to the post. Ideal keyway attachment behavior could not be achieved with the crimp-in-place tabbed brackets. Head scraping against the inside of the flange caused the vertical cable release loads to be as high as 2.87 kips (12.8 kN). Therefore, crimp-in-place tabbed brackets were discarded in favor of the bolted variation.

Several equations were derived to guide the design process as well as to determine the dimensions of prototype bolted tabbed brackets. These equations were refined over the course of the design process and are presented here in their final form. The dimensions, idealized load orientations, and assumed failure locations that were used in the development of the design equations, are shown in Figures 456 and 457.

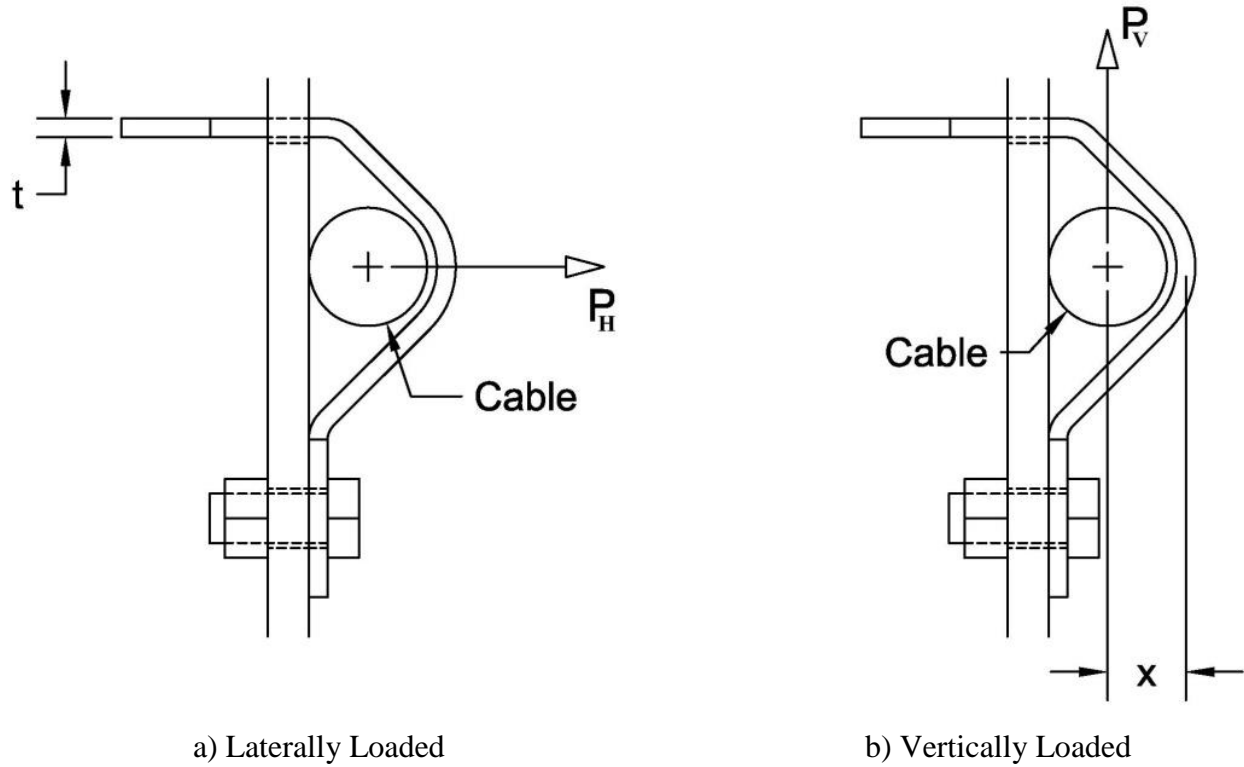


Figure 456. Bolted Tabbed Bracket—(a) Laterally Loaded and (b) Vertically Loaded

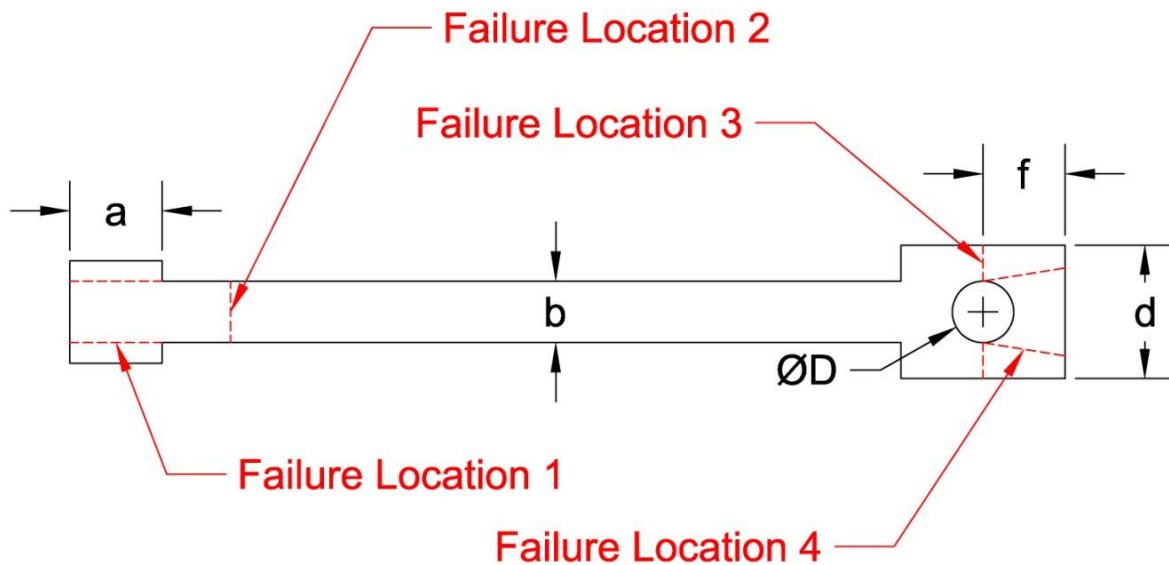


Figure 457. Bolted Tabbed Bracket Dimensions

For the lateral loading condition, as shown in Figure 456a, four failure locations were assumed in the bracket, as shown in Figure 457, thus resulting in four separate equations. In the

derivation of the following equations, one half of the applied lateral load, P_H , was assumed to be distributed to each end, as shown in Figure 458. It should be noted that dynamic magnification factors were not used in the derivation of the lateral load equations as they were not deemed necessary.



Figure 458. End Reactions for Use in the Design Equations

The applied lateral load needed to cause failure at location 1 was calculated using Equation 14.1. Failure location 1 was assumed to be a pure shear fracture in which two surfaces provided shear resistance to the end reaction of $P_H/2$. The right side of the equation includes a factor of 5/6 to account for the difference in the predicted versus observed lateral loads from the bolted tabbed brackets in Round 2.

$$P_{H_1} = \left(\frac{5}{6}\right) \frac{4}{\sqrt{3}} at\sigma_u = \frac{10}{3\sqrt{3}} at\sigma_u \quad (14.1)$$

Where, t = thickness (see Figure 456a)
 σ_u = ultimate tensile stress
 a = length of head (see Figure 457)

The applied lateral load needed to cause failure at location 2 was calculated using Equation 14.2. Failure location 2 was assumed to be a pure tensile fracture in which one surfaces provided tensile resistance to the end reaction of $P_H/2$. The right side of the equation includes a factor of 5/6 to account for the difference in the predicted versus observed lateral loads from the bolted tabbed brackets in Round 2.

$$P_{H_2} = \left(\frac{5}{6}\right) 2bt\sigma_u = \frac{5}{3}bt\sigma_u \quad (14.2)$$

Where, b = width of neck (see Figure 457)

The applied lateral load needed to cause failure at location 3 was calculated using Equation 14.3. Failure location 3 was assumed to be a pure tensile fracture in which a cross-section through the center of the bolt provided tensile resistance to the end reaction of $P_H/2$. The diameter of bolt hole was assumed to be 1/16 in. (1.6 mm) larger than the diameter of the bolt, and the drilling or punching operation was assumed to affect an additional 1/16 in. (1.6 mm) of material around the hole, further reducing the tensile area. The right side of the equation includes a factor of 5/6 to account for the difference in the predicted versus observed lateral loads from the bolted tabbed brackets in Round 2.

$$P_{H_3} = \left(\frac{5}{6}\right) 2(d - D - v)t\sigma_u = \frac{5}{3}(d - D - v)t\sigma_u = \frac{5}{3}(d - d_b - \mu)t\sigma_u \quad (14.3)$$

Where d = width of bottom tab (see Figure 457)
 D = diameter of hole (see Figure 457)
 v = 1/16 in. (1.6 mm)
 d_b = diameter of bolt
 μ = 1/8 in. (3.2 mm)

The applied lateral load needed to cause failure at location 4 was calculated using Equation 14.4. Failure location 4 was assumed to be tearing failure according to AISC Equation J3-6a [76]. The right side of the equation includes a factor of 5/6 to account for the difference in the predicted versus observed lateral loads from the bolted tabbed brackets in Round 2.

$$P_{H_4} = \left(\frac{5}{6}\right) 2.4 \left(f - \frac{D}{2}\right) t\sigma_u = 2 \left(f - \frac{D}{2}\right) t\sigma_u = 2 \left(f - \frac{d_b + v}{2}\right) \quad (14.4)$$

Where f = distance from the center of the bolt hole to the bottom edge of the bolted tabbed bracket (see Figure 457)

The vertical release load was assumed to occur in pure, plastic bending. The idealized vertical loading used to derive Equation 14.5 was shown in Figure 456b. A dynamic

magnification factor of 1.5 was incorporated into the vertical release load equation. The moment arm, x , was measured between the center of the cable and the mid-plane of the outer bracket, as shown in Figure 456b.

$$P_V = \frac{1.5M_P}{x} = \frac{1.5Z\sigma_y}{x} = \frac{1.5\left(\frac{bt^2}{4}\right)\sigma_y}{x} = \frac{3bt^2\sigma_y}{8x} \quad (14.5)$$

Where M_P = plastic moment
 Z = plastic section modulus where bending occurs
 x = length of the moment arm (see Figure 456b)
 σ_y = yield stress
 b = cross-sectional width where bending occurs (see Figure 457)

Equations 14.1 through 14.5 used the actual yield and tensile strengths of the material, not the minimum values. MwRSF recommends using grade 50 sheet steel with yield and tensile strengths similar to the steel used to fabricate the prototype tabbed brackets. The ASTM A1011 HSLA Grade 50 sheet steel that was used had yield and tensile strengths of 56 ksi (386 MPa) and 69 ksi (476 MPa), respectively.

In general, Equations 14.1 through 14.4 predicted the lateral release loads very well, especially if the failure observed in the component test was by pure tensile fracture at failure locations 2 or 3. Equation 14.5 was also useful, but it tended to under-predict the vertical release loads.

Bolted tabbed brackets performed much better than the crimp-in-place variation. Based on the results of the component tests, tabbed bracket Version 10 was recommended for the cable-to-post attachment for the lower three cables. However, it should be noted that bolted tabbed bracket Version 8 as well as the extended keyway bolt may both be viable options.

22.1.7 Top Cable-to-Post Attachments

A total of 45 static tests were performed on potential top cable-to-post attachments. Based on the static test results, one attachment was chosen for a bogie impact test to verify that it would easily and quickly release the cable when the post was impacted by a vehicle and rotated backward and downward. The bogie impact test successfully demonstrated that the 1/8-in. (3.2-mm) diameter, C360 brass, straight rod with bent ends performed very well as the top cable-to-post attachment. The static tests, which were used to evaluate prototypes for the top cable-to-post attachment, investigated vertical cable release capacities. From the results and using engineering judgment, it was reasoned that the lateral cable release loads would be very similar the vertical cable release loads due to notch geometry.

22.2 Recommendations

Tabbed bracket Version 10 is recommended as the preferred cable-to-post attachment for the lower three cables. It is to be secured to the flange of the post with a 5/16-in. (7.9-mm), SAE grade 5, hex cap screw and nut. Tabbed bracket Version 10 had lateral and vertical cable release loads of 6.10 kips (27.1 kN) and 346 lb (1.54 kN), respectively.

The 1/8-in. (3.2-mm) diameter, C360 brass, straight rod with bent ends is recommended as the preferred top cable-to-post attachment. The cable is to sit in a V-notch on top of the post and the straight rod is to be inserted through the designated holes in the flanges so that it restrains the cable within the post. From static testing, the vertical cable release load of the recommended straight rod with bent ends was 175 lb (778 N). The 1/8-in. (3.2-mm) diameter C360 brass that was used for the prototypes had a 7.2% elongation at failure, and yield and tensile strengths of 62 ksi (427 MPa) and 81 ksi (558 MPa), respectively. It may be possible to use galvanized carbon steel instead of C360 brass for the straight rod with bent ends, as long as the yield, tensile strength, and ductility are similar. Further testing may be required in those cases.

When using Equation 14.13 to select the cable tension and post spacing, a conservatively low estimate of the top cable-to-post attachment's lateral cable release load should be used. MwRSF recommends using a value of 150 lb (667 N).

23 REFERENCES

1. *Manual for Assessing Safety Hardware (MASH)*, American Association of State Highway and Transportation Officials (AASHTO), Washington, D.C., 2009.
2. Johnson, E.A., Sicking, D.L., Faller, R.K., Lechtenberg, K.A., Rohde, J.R., Bielenberg, R.W., Reid, J.D., Rosenbaugh, S.K., *Phase I Development of a Non-Proprietary, Four-Cable, High-Tension Median Barrier*, Final Report to the Midwest States' Regional Pooled Fund Program, Transportation Research Report No. TRP-03-213-11, Project No.: SPR-3(017), Project Code: RPFP-04-01 and RPFP-08-02 – Years 14, 16, and 18, Midwest Roadside Safety Facility, University of Nebraska-Lincoln, December 28, 2011.
3. Schmidt, J.D., Sicking, D.L., Faller, R.K., Lechtenberg, K.A., Bielenberg, R.W., Reid, J.D., and Rosenbaugh, S.K., *Phase II Development of a Non-Proprietary, Four-Cable, High-Tension Median Barrier*, Final Report to the Midwest States' Regional Pooled Fund Program, Transportation Research Report No. TRP-03-253-12, Project No. TPF-5(091) Supplement #1, Project Code: RPFP-09-01 – Year 19, Midwest Roadside Safety Facility, University of Nebraska-Lincoln, March 21, 2012.
4. Kampschneider, L.R., Homan, D. H., Lechtenberg, K.A., Faller, R.K., Bielenberg, R.W., Sicking, D.L., Reid, J.D., and Rosenbaugh, S.K., *Evaluation of a Non-Proprietary, High-Tension, 4-Cable Median Barrier on Level Terrain*, Final Report to the Midwest States' Regional Pooled Fund Program, Transportation Research Report No. TRP-03-258-12, Project Nos. TPF-5(091) Supplement #1, TPF-5(193) Supplement #20, #44, and #45, Project Codes: RPFP-09-01, RPFP-10-CABLE-2, and RPFP-12-CABLE-1&2—Years 19, 20 and 22, Midwest Roadside Safety Facility, University of Nebraska-Lincoln, November 29, 2012.
5. Stolle, C.S., *Cable Median Barrier Failure Analysis and Remediation*, Doctoral Dissertation, University of Nebraska-Lincoln, December 2012.
6. Hunter, W.W., J.R. Stewart, K.A. Eccles, H.F. Huang, F.M. Council, and D.L. Harkey. "Three-Strand Cable Median Barrier in North Carolina: An In-Service Evaluation," Paper No. 01-0375, Presented at the Transportation Research Board Annual Meeting, January 2001.
7. Gabler, H.C., Gabauer, D.J., and Bowen, D., *Evaluation of Cross-Median Crashes*, Final Report to the New Jersey Department of Transportation, Report No. FHWA–NJ–2005-04, Rowan University, February 2005.
8. Stolle, C.S., Reid, J.D., Lechtenberg, K.A., *Update to Cable Barrier Literature Review*, Transportation Research Report No.: TRP-03-227-10, Project No.: TPF-5(193), Sponsoring Agency Code: RPFP-09-01, Midwest Roadside Safety Facility, University of Nebraska-Lincoln, Lincoln, Nebraska, August 12, 2010.
9. Thiele, J.C., Bielenberg, R.W., Faller, R.K., Sicking, D.L., Rohde, J.R., Reid, J.D., Polivka, K.A., and Holloway, J.C., *Design and Evaluation of High-Tension Cable Barrier Hardware*, Final Report to the Midwest States' Regional Pooled Fund Program,

Transportation Research Report No. TRP-03-200-08, Project No.: SPR-3(017), Project Code: RPFP-01-05, RPFP-04-01, RPFP-06, and RPFP-08-02 - Years 11, 14, 16, and 18, Midwest Roadside Safety Facility, University of Nebraska-Lincoln, February 25, 2008.

10. Graham, M.D., Burnett, W.C., Gibson, J.L., and Freer, R.H., *New Highway Barriers: The Practical Application of Theoretical Design*, Highway Research Record No. 174, New York State Department of Transportation, 1967, pp. 88-167.
11. *A Guide to Standardized Highway Barrier Hardware*, American Association of State Highway and Transportation Officials, Task Force 13, On-line Guide, Designators SGR01a-b, FBH01-03, and FBH04, Accessed February 28, 2013, <<https://www.aashtotf13.org/Barrier-Hardware.php>>.
12. Ross, H.E., Sicking, D.L., Zimmer, R.A., and Michie, J.D., *Recommended Procedures for the Safety Performance Evaluation of Highway Features*, National Cooperative Highway Research Program (NCHRP) Report 350, Transportation Research Board, Washington, D.C., 1993.
13. Horne, D.A., FHWA NCHRP Report No. 350 eligibility letter B-64 of nonproprietary guardrails and median barriers, Memorandum to Resource Center Directors, Division Administrators, and Federal Lands Highway Division Engineers, February 14, 2000.
14. Baxter, J.R., FHWA NCHRP Report No. 350 eligibility letter B-64sup of generic cable barriers, Memorandum to Resource Center Managers, Division Administrators, and Federal Land Highway Division Engineers, September 12, 2005.
15. *Resource Charts*, PDF document created by KLS Engineering, FHWA Contract DTFH61-10-D-00021, Roadside Safety Systems Installers and Designers Mentors Program, February, 2013.
16. “Brifen Wire Rope Safety Fence”, Brifen USA, Inc., Accessed February 28, 2013, <<http://www.brifenus.com>>.
17. Wright, F.G., FHWA NCHRP Report No. 350 eligibility letter B-82 of 4-strand Brifen Wire Rope Safety Fence (WRSF) at TL-3, To Graham Sharp, Brifen Ltd., Mansfield, Nottinghamshire, United Kingdom, April 10, 2001.
18. Baxter, J.R., FHWA NCHRP Report No. 350 eligibility letter B-82B of 4-strand Brifen WRSF at TL-4, To Derek W. Muir, Hill & Smith Ltd., Bilston, Wolverhampton, West Midlands, United Kingdom, March 27, 2005.
19. Baxter, J.R., FHWA NCHRP Report No. 350 eligibility letter B-82C of 3-strand Brifen WRSF at TL-3, To Derek W. Muir, Hill & Smith Ltd., Bilston, Wolverhampton, West Midlands, United Kingdom, May 26, 2005.
20. Baxter, J.R., FHWA NCHRP Report No. 350 eligibility letter B-82C1 of 3-strand Brifen WRSF with reduced post spacing at TL-3, To Derek W. Muir, Hill & Smith Ltd., Bilston, Wolverhampton, West Midlands, United Kingdom, April 13, 2006.

21. Baxter, J.R., FHWA NCHRP Report No. 350 eligibility letter B-82B1 of 4-strand Brifen WRSF on 4V:1H slopes at TL-3, To Derek W. Muir, Hill & Smith Ltd., Bilston, Wolverhampton, West Midlands, United Kingdom, May 9, 2006.
22. “Brifen WRSF NCHRP 350 TL-4”, Revision No. 1, Revised February 8, 2013, Drawings Received via Email on February 27, 2013, Email requestdrawings@brifenusa.com for a copy.
23. “Gibraltar Cable Barrier System”, Gibraltar Cable Barrier Systems, L.P., Accessed February 27, 2013, <<http://gibraltartx.com/cable-barriers/overview>>.
24. Baxter, J.R., FHWA NCHRP Report No. 350 eligibility letter B-137 of 3-strand Gibraltar cable barrier at TL-3, To Bill Neusch, Gibraltar, Burnet, TX, June 13, 2005.
25. Baxter, J.R., FHWA NCHRP Report No. 350 eligibility letter B-137A of 3-strand Gibraltar cable barrier at TL-4, To Bill Neusch, Gibraltar, Burnet, TX, September 9, 2005.
26. Baxter, J.R., FHWA NCHRP Report No. 350 eligibility letter B-137B of alternative post spacing for 3-strand Gibraltar cable barrier at TL-4, To Bill Neusch, Gibraltar, Burnet, TX, April 3, 2006.
27. Baxter, J.R., FHWA NCHRP Report No. 350 eligibility letter B-147A of Gibraltar cable to W-beam transition at TL-3, To Bill Neusch, Gibraltar, Burnet, TX, June 16, 2006.
28. Baxter, J.R., FHWA NCHRP Report No. 350 eligibility letter B-137C (HSA) of 3-strand Gibraltar cable barrier placed on 4V:1H slope at TL-3, To Bill Neusch, Gibraltar, Burnet, TX, July 12, 2006.
29. Baxter, J.R., FHWA NCHRP Report No. 350 eligibility letter B-137A1 of 4-strand Gibraltar cable barrier at TL-4, To Bill Neusch, Gibraltar, Burnet, TX, October 27, 2006.
30. Nicol, D.A., FHWA NCHRP Report No. 350 eligibility letter B-137C (HSSD) of revised anchor design for 4-strand Gibraltar cable barrier at TL-4, To Bill Neusch, Gibraltar, Burnet, TX, January 8, 2008.
31. Nicol, D.A., FHWA NCHRP Report No. 350 eligibility letter B-137D of 4-point anchorage to 4-strand Gibraltar cable barrier at TL-4, To Bill Neusch, Gibraltar, Burnet, TX, February 8, 2008.
32. “Gibraltar Cable Barrier Installation Guide”, Version 5.4, Updated May 2009, Accessed February 27, 2013, <<http://gibraltartx.com/assets/uploads/pdf/gibraltar-installation.pdf>>.
33. “Nu-Cable Cable Barrier Systems Installation Manual: Test Level 4”, Version 2011.09A, Accessed February 27, 2013, <http://nucorhighway.com/files/NU-CABLE_DOCUMENT_INSTALLATIONMANUAL_TL4.pdf>.
34. Jacoby, C.H., FHWA NCHRP Report No. 350 eligibility letter B-96 of 3-strand guardrail with Marion Steel U-Channel posts at TL-3, To Rick Mauer, Marion Steel Company, Greenland, NH, August 30, 2002.

35. Baxter, J.R., FHWA NCHRP Report No. 350 eligibility letter B-96A of variations on 3-strand guardrail with Marion Steel U-channel posts at TL-3, To Rick Mauer, Nucor Steel Marion Inc., Marion, OH, October 12, 2005.
36. Nicol, D.A., FHWA NCHRP Report No. 350 eligibility letter B-167 of 4-strand Nucor Wire Rope Barrier System at TL-4, To Rick Mauer, Nucor Steel Marion Inc., Marion, OH, January 24, 2008.
37. Nicol, D.A., FHWA NCHRP Report No. 350 eligibility letter B-183 of Nu-Cable systems using plastic or steel sockets at TL-3 and TL-4, To Rick Mauer, Nucor Steel Marion Inc., Greenland, NH, November 26, 2008.
38. Nicol, D.A., FHWA NCHRP Report No. 350 eligibility letter B-184 of revised hanging clip for Nucor steel posts at TL-4, To Rick Mauer, Nucor Steel Marion Inc., Greenland, NH, December 9, 2008.
39. Nicol, D.A., FHWA NCHRP Report No. 350 eligibility letter B-193 (REVISED) of 4-strand Nu-Cable system on 4V:1H slope at TL-3, To Rick Mauer, Nucor Steel Marion Inc., Greenland, NH, July 27, 2009.
40. Nicol, D.A., FHWA NCHRP Report No. 350 eligibility letter B-184A of 4-strand Nu-Cable with 20-ft spacing at TL-4, To Rick Mauer, Nucor Steel Marion Inc., Greenland, NH, September 23, 2009.
41. "SAFENCE Wire Rope Safety Fence System", Accessed February 27, 2013, <<http://www.gregorycorp.com/docpdf/highway/safence/SRB001-009.pdf>>.
42. Wright F.G., FHWA NCHRP Report No. 350 eligibility letter B-88 of 4-strand Safence at TL-3, To Mats Heinevik, Blue Systems AB, 426 58 V. Frolunda, Sweden, July 13, 2001.
43. Baxter, J.R., FHWA NCHRP Report No. 350 eligibility letter B-88A of 4-strand Safence for roadside applications at TL-3, To Michael Kempen, Safence, Inc., Douglaston, NY, January 28, 2004.
44. Baxter, J.R., FHWA NCHRP Report No. 350 eligibility letter B-88B of 4-strand Safence with posts set in concrete footings at TL-3, To Mats Heinevik, Blue Systems AB, 426 58 V. Frolunda, Sweden, June 8, 2004.
45. Baxter, J.R., FHWA NCHRP Report No. 350 eligibility letter B-88C of 4-strand Safence with alternative posts at TL-3, To Michael Kempen, Safence, Inc., Douglaston, NY, May 26, 2005.
46. Baxter, J.R., FHWA NCHRP Report No. 350 eligibility letter B-88D of 3-strand Safence at TL-4, To Michael Kempen, Safence, Inc., Douglaston, NY, December 27, 2006.
47. Rice, G.E., FHWA NCHRP Report No. 350 eligibility letter B-88E of 4-strand Safence with different cable heights at TL-4, To Michael Kempen, Safence, Inc., Douglaston, NY, July 31, 2007.

48. Nicol, D.A., FHWA NCHRP Report No. 350 eligibility letter B-88F of 3-strand Safence on 4V:1H slope at TL-3, To Jesper Sorensen, Safence, Inc., Seattle, WA, December 23, 2008.
49. Stolle, C.S., Faller, R.K., Lechtenberg, K.A., Sicking, D.L., Bielenberg, R.W., Reid, J.D., and Holloway, J.C., *Evaluation of the Modified Three Cable Guardrail System Installed on a 4:1 Fill Slope*, Final Report to SAFENCE Inc., Transportation Research Report No.: TRP-03-246-10, Midwest Roadside Safety Facility, University of Nebraska-Lincoln, Lincoln, Nebraska, December 14, 2010.
50. "CASS Cable Safety System Test Level 3/Test Level 4 Instruction Manual", Revised May 14, 2009, Accessed February 27, 2013, <http://www.highwayguardrail.com/products/pdfs/CASS_TL3TL4-Installation.pdf>.
51. Griffith, M.S., FHWA NCHRP Report No. 350 eligibility letter B-119 of 3-strand CASS at TL-3, To Rodney A. Boyd, Trinity Highway Safety Products Division, Dallas, TX, May 13, 2003.
52. Griffith, M.S., FHWA NCHRP Report No. 350 eligibility letter B-119A of 3-strand CASS with 5-m post spacing at TL-3, To Rodney A. Boyd, Trinity Highway Safety Products Division, Dallas, TX, May 15, 2003.
53. Baxter, J.R., FHWA NCHRP Report No. 350 eligibility letter B-119B of 3-strand CASS with 2-m post spacing and concrete footings at TL-3, To Rodney A. Boyd, Trinity Highway Safety Products Division, Dallas, TX, August 28, 2003.
54. Baxter, J.R., FHWA NCHRP Report No. 350 eligibility letter B-141 of 3-strand CASS TL-3 and CASS TL-4 with S4x7.7 driven posts at TL-3 and TL-4, To Stephen L. Brown, Trinity Highway Safety Products, Inc., Dallas, TX, November 17, 2005.
55. Baxter, J.R., FHWA NCHRP Report No. 350 eligibility letter B-141A of 3-strand CASS TL-3 with driven posts at 20-ft post spacing at TL-3, To Stephen L. Brown, Trinity Highway Safety Products, Inc., Dallas, TX, May 2, 2006.
56. Baxter, J.R., FHWA NCHRP Report No. 350 eligibility letter B-141B of 3-strand CASS TL-3 with 32.5-ft post spacing at TL-3, To Stephen L. Brown, Trinity Highway Safety Products, Inc., Dallas, TX, May 8, 2006.
57. Baxter, J.R., FHWA NCHRP Report No. 350 eligibility letter B-157 of 3-strand CASS TL-3 with S4x7.7 posts & terminal at TL-4, To Stephen L. Brown, Trinity Highway Products, LLC, Dallas, TX, April 23, 2007.
58. Nicol, D.A., FHWA NCHRP Report No. 350 eligibility letter B-141C of 3-strand CASS on 4V:1H slope at TL-3, To Brian Smith, Trinity Highway Products, LLC, Dallas, TX, November 14, 2008.
59. Nicol, D.A., FHWA NCHRP Report No. 350 eligibility letter B-141E of 4-strand CASS with C-channel posts at TL-3, To Brian Smith, Trinity Highway Products, LLC, Dallas, TX, April 8, 2009.

60. Nicol, D.A., FHWA NCHRP Report No. 350 eligibility letter B-141D of 3-strand CASS on 6V:1H or flatter slopes at TL-4, To Brian Smith, Trinity Highway Products, LLC, Dallas, TX, March 19, 2009.
61. Griffith, M.S., FHWA MASH eligibility letter B-232 of CASS S3 on 4V:1H slope at TL-3, To Brian Smith, Trinity Highway Products, LLC, Dallas, TX, May 4, 2012.
62. "CASS C Shaped Posts", Accessed February 27, 2013, <<http://www.highwayguardrail.com/products/cass.html>>.
63. "Installation Manual Armorwire Cable Barrier TL-3 and TL-4 Systems", Accessed February 27, 2013, <<http://www.armorflex.co.nz/Armorflex/files/8c/8c14a887-c7e0-483c-8981-a17c511ec6a1.pdf>>.
64. Griffith, M.S., FHWA NCHRP Report No. 350 eligibility letter B-222 of 3- and 4-strand Armorwire Barrier at TL-3 and TL-4, To Dallas James, Armorflex International Ltd., Auckland, New Zealand, January 27, 2012.
65. FHWA Safety Web Site, Keyword: Cable Barrier, Accessed March 4, 2013, <http://safety.fhwa.dot.gov/roadway_dept/policy_guide/road_hardware/barriers/>.
66. *Laboratory Test Procedure for FMVSS No. 216a, Roof Crush Resistance*, National Highway Traffic Safety Administration (NHTSA), TP-216a-00, May 6, 2009, Accessed March 6, 2013 <<http://www.nhtsa.gov/Vehicle+Safety/Test+Procedures?procedurePage=1>>.
67. *Crashworthiness Evaluation Roof Strength Test Protocol (Version II)*, Insurance Institute for Highway Safety (IIHS), December, 2012, Accessed March 6, 2013, <http://www.iihs.org/ratings/protocols/pdf/test_protocol_roof.pdf>.
68. *Laboratory Test Procedure for FMVSS No. 216, Roof Crush Resistance*, National Highway Traffic Safety Administration (NHTSA), TP-216-05, November 16, 2006, Accessed March 6, 2013 <<http://www.nhtsa.gov/Vehicle+Safety/Test+Procedures?procedurePage=1>>.
69. Murphy, T., "New A-Pillars Enhance Safety But Impede Visibility", Wards Auto, July 13, 2011, Accessed November 18, 2012, <http://wardsauto.com/ar/roof_standards_expansive_110713>.
70. Molacek, K.J., Lechtenberg, K.A., Faller, R.K., Rohde, J.R., Sicking, D.L., Bielenberg, R.W., Reid, J.D., Stolle, C.J., Johnson, E.A., and Stolle, C.S., *Design and Evaluation of a Low-Tension Cable Median Barrier System*, Final Report to the Midwest State's Regional Pooled Fund Program, Transportation Research Report No. TRP-03-195-08, Project No.: SPR-3(017), Project Code: RPPF-01-05 - Year 12, Midwest Roadside Safety Facility, University of Nebraska-Lincoln, Lincoln, Nebraska, December 8, 2008.
71. Dickey, B.J., Stolle, C.S., Bielenberg, R.W., Faller, R.K., Sicking, D.L., Reid, J.D., Lechtenberg, K.A., Rosenbaugh, S.K., *Design and Evaluation of a High-Tension Cable Median Barrier Attachment*, Final Report to the Midwest States' Regional Pooled Fund

Program, Transportation Research Report No. TRP-03-228-11, Project No. TPF-5(193), Project Code: RPFP-09-01 - Year 19, Midwest Roadside Safety Facility, University of Nebraska-Lincoln, May 11, 2011.

72. *A Policy on Geometric Design of Highways and Streets*, 6th Edition, American Association of State Highway and Transportation Officials (AASHTO), Washington, D.C., 2011, pp. 3-32 and 3-161.
73. Society of Automotive Engineers (SAE), *Instrumentation for Impact Test—Part 1—Electronic Instrumentation*, SAE/J211/1 MAR95, New York City, NY, July 2007.
74. Stolle, C.S., Reid, J.D., Bielenberg, R.W., *Improved Models of Cable-To-Post Attachments for High-Tension Cable Barriers*, Final Report to the Mid-America Transportation Center (MATC), Transportation Research Report No. TRP-03-267-12, Midwest Roadside Safety Facility, University of Nebraska-Lincoln, April 24, 2012.
75. Boresi, A.P., Schmidt, R.J., *Advanced Mechanics of Materials*, 6th Edition, Copyright 2003, John Wiley and Sons, Inc.
76. American Institute of Steel Construction (AISC), *Specification for Structural Steel Buildings*, Chicago, IL, June 22, 2010.

24 APPENDICES






Appendix A. Proprietary Cable Barrier Systems

A resource chart is provided in Figure A-1 which provides researchers and designers with basic information on several federally-approved cable barrier systems. Researchers and designers are encouraged to visit the manufacturers' web sites for more information on the specific proprietary systems.

Cable Barriers

September 26, 2012

* Systems can be installed on 1V:6H and 1V:4H slopes, but cable configuration and offsets from the roadway edge and from the ditch bottom must be in accordance with test results and manufacturers' recommendations.

NAME	MANUFACTURER	TEST LEVEL		POST TYPE	CABLE	DISTINGUISHING CHARACTERISTICS
		NCHRP 350	MASH			
Generic Weak-post Cable Guardrail (Low Tension)	 Generic	3		I-Beam Post Flanged steel U-Channel Post Weakened rounded Timber Posts	3 cable configuration. Cables placed on one side of post; the side closer to the road - Roadside Application. Two cables are placed on one side of the post and the other cable is placed on the opposite side - Median Application.	Cables are attached with hook bolts. Uses a crashworthy generic terminals. Typical Post Spacing 4 ft to 16 ft.
Brifen Wire Rope Safety Fence (WRSF) http://www.brifenus.com	 Brifen	3 and 4		Z Shaped Posts	3 and 4 cable configuration. Interweaving of cables between adjacent post.	Top cable is placed in a slot at the center of the post. Other 2 or 3 cables are weaved around post. Uses proprietary terminal. Posts can be driven or socketed. Typical Post spacing 10.5 ft to 21 ft.
Gibraltar http://gibraltartx.com	 Gibraltar	3 and 4		C Channel Posts	3 and 4 cable configuration. Pre-stretched or Non-pre-stretched.	Cables are attached using a single steel hair pin. Posts are placed such that adjacent post are on opposite sides of the cable. Uses proprietary terminal. Posts can be driven or socketed. Typical Post spacing 10 ft to 30 ft.
Nucor Steel Marion Cable Barrier System http://nucorhighway.com/nucable.html	 Nucor Steel Marion	3 and 4		U Channel Posts	3 and 4 cable configuration. Pre-stretched or Non-pre-stretched.	Cables are attached using locking hook bolts or hook bolts and a strap. 2 of 4 cable are placed on one side of post and the other two are placed on the opposite side. Uses proprietary terminal. Posts can be driven or socketed. Typical Post spacing 6.6 ft. to 20 ft.
Safence http://www.gregorycorp.com/highway/safence.cfm	 Gregory Highway Products	3 and 4		C-shaped Posts	3 and 4 cable configuration.	All cables are inserted in a slot at the center of the post and separated by plastic spacers. Uses proprietary terminal. Posts can be driven or socketed. Typical Post spacing 6.5 ft to 33.2 ft.
CASS http://www.highwayguardrail.com/products/cb.html	 Trinity Highway Products, LLC	3 and 4		C-shaped and I-Beam Post (S3 & S4)	3 and 4 cable configuration. Pre-stretched or Non-pre-stretched configuration.	Cables are placed in a wave-shaped slot at the center of the post and separated by plastic spacers. Some versions also have cables that are supported on the flanges of the post. Uses proprietary terminal. Posts can be driven or socketed. Typical Post spacing 6.5 ft to 32.5 ft.



U.S. Department of Transportation
Federal Highway Administration

The safety systems shown on this chart are eligible for reimbursement under the Federal-Aid Highway Program. This reference is for informational purposes only, and was created by KLS Engineering under FHWA Contract, DTFH61-10-D-00021, Roadside Safety Systems Installers and Designers Mentor Program. For further information on an individual system please refer to the manufacturers' website.



Page 1 of 1

Figure A-1. Cable Barrier Resource Chart [15]

August 29, 2013
MWRSF Report No. TRP-03-285-13

Appendix B. Full-Scale Crash Test Summary Sheets—Cable Barrier Testing

A summary sheet for each full-scale crash test on low- and high-tension cable barrier systems that have been performed by MwRSF is provided in this section. Summary sheets contain general information about the system and its components, test layout, as well as test results. For more information about these tests, it is recommended to review the noted references.

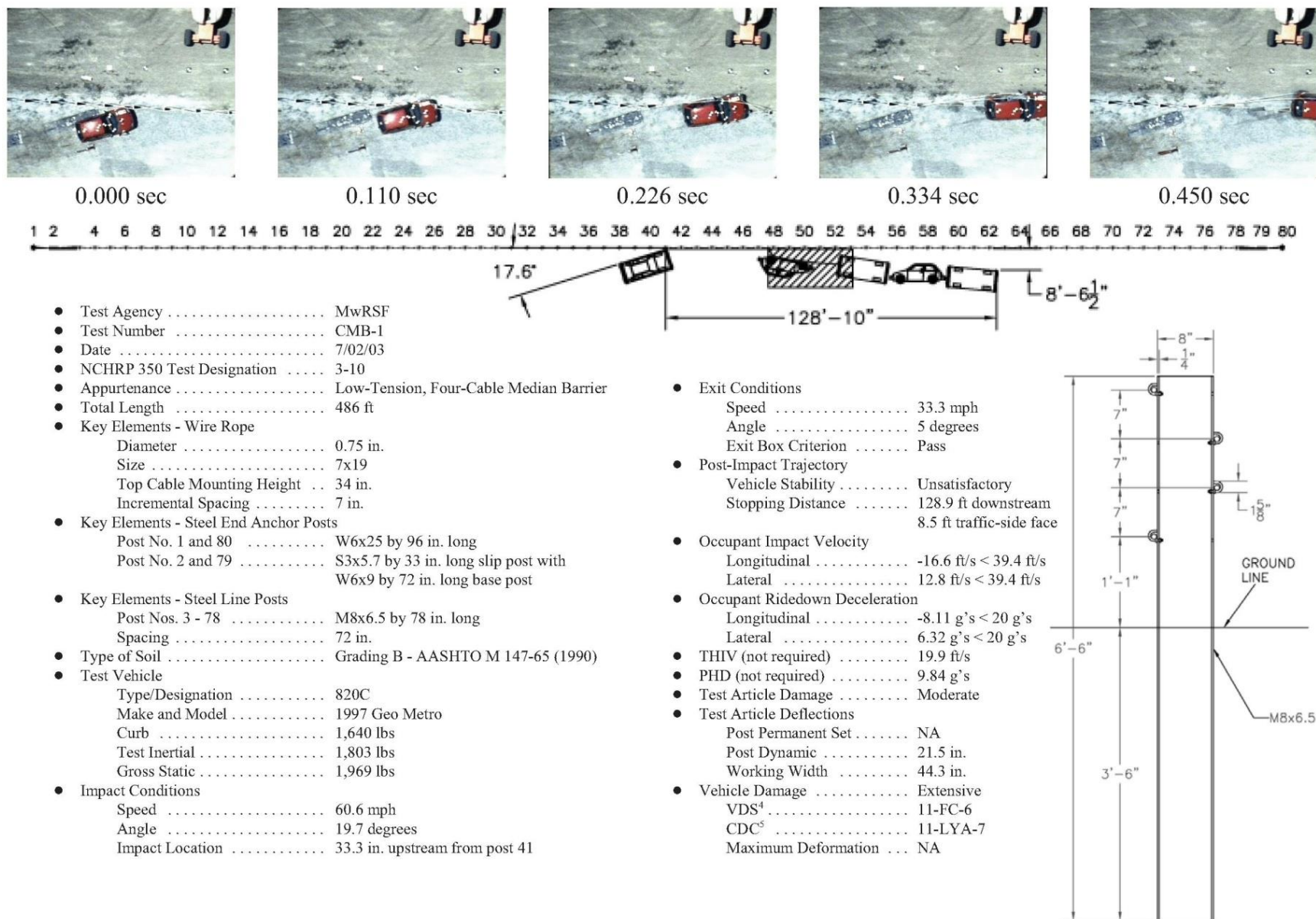


Figure B-1. Test Results Summary (English), Test No. CMB-1 [70]

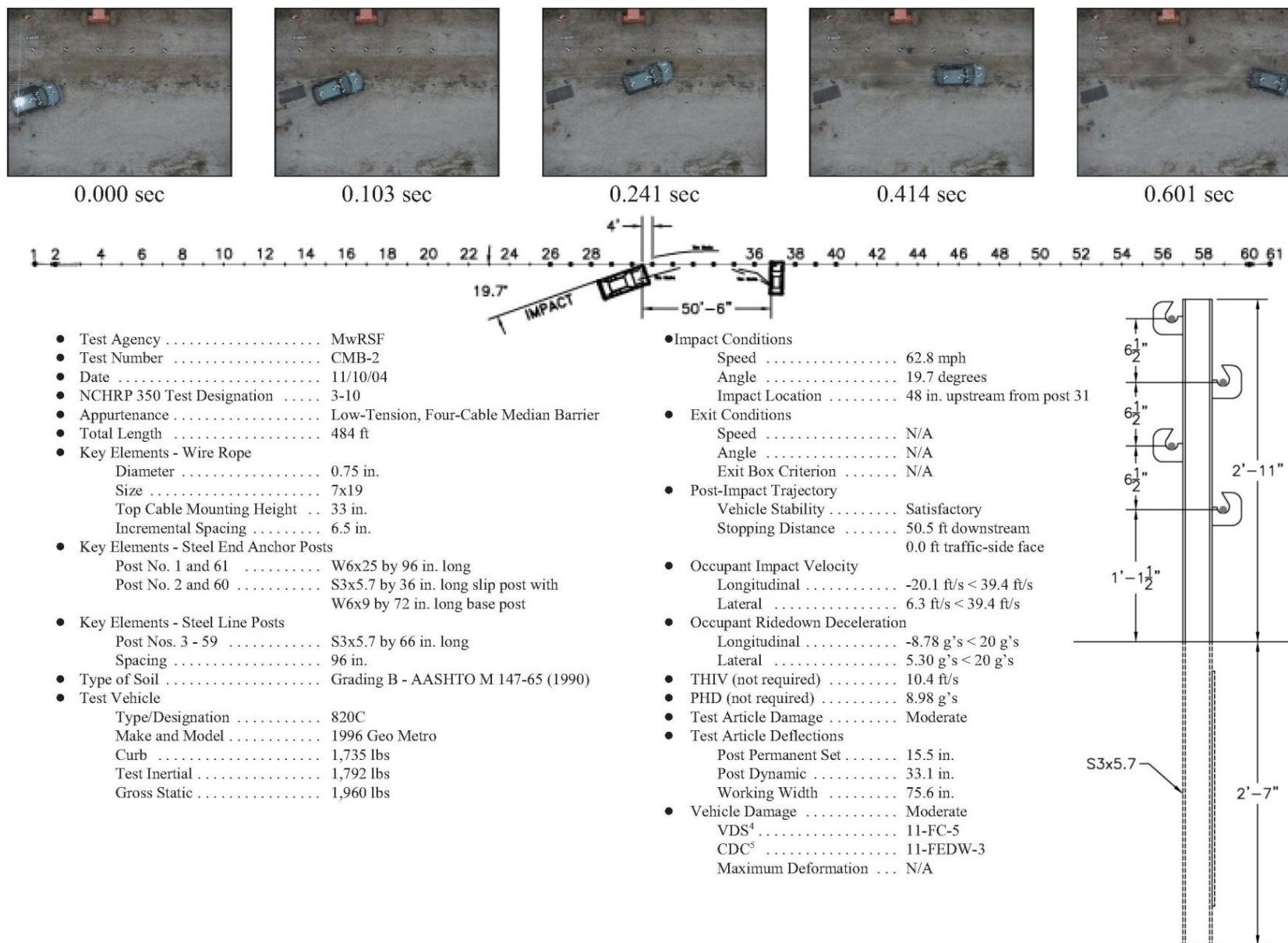


Figure B-2. Test Results Summary (English), Test No. CMB-2 [70]

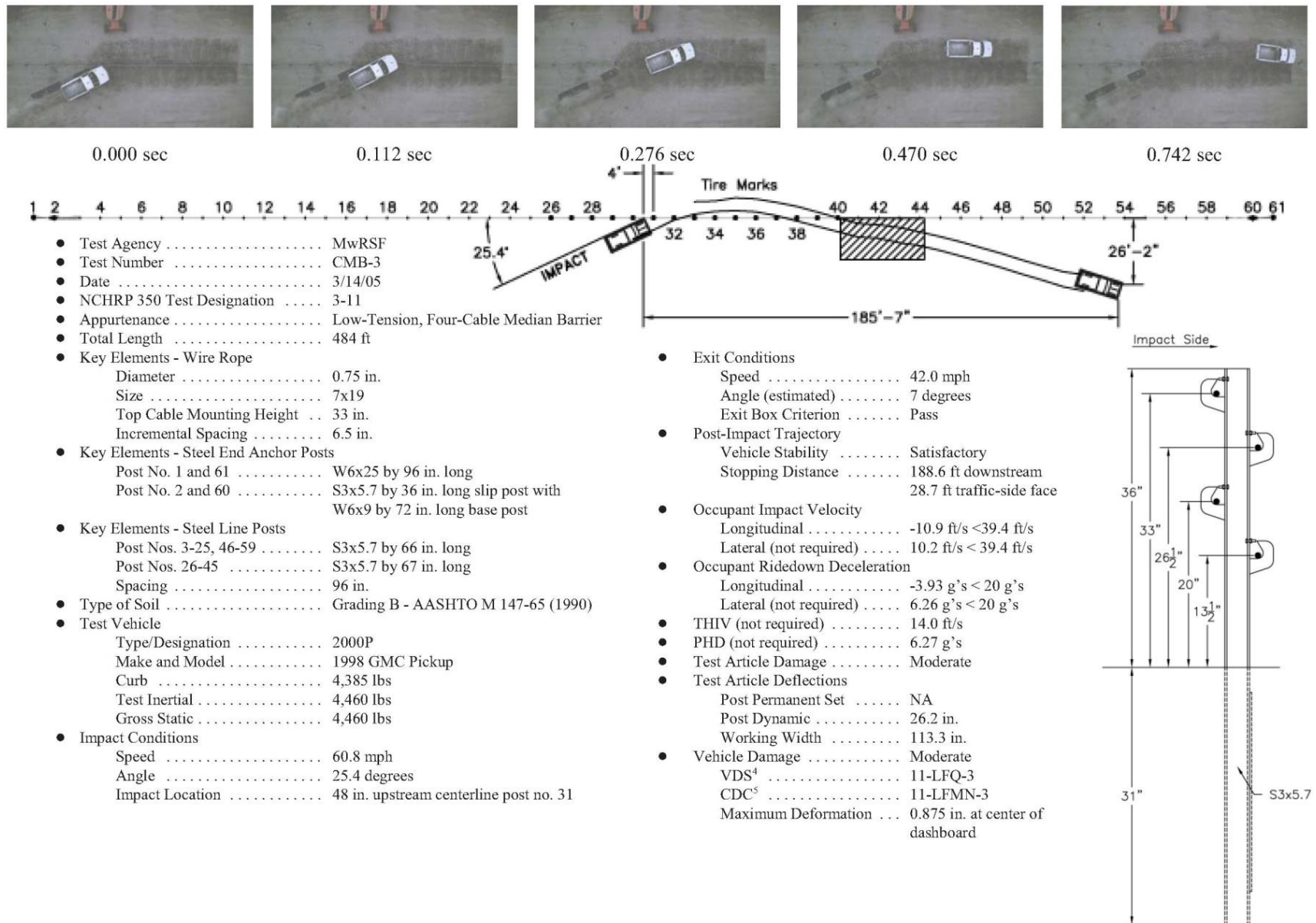


Figure B-3. Test Results Summary (English), Test No. CMB-3 [70]

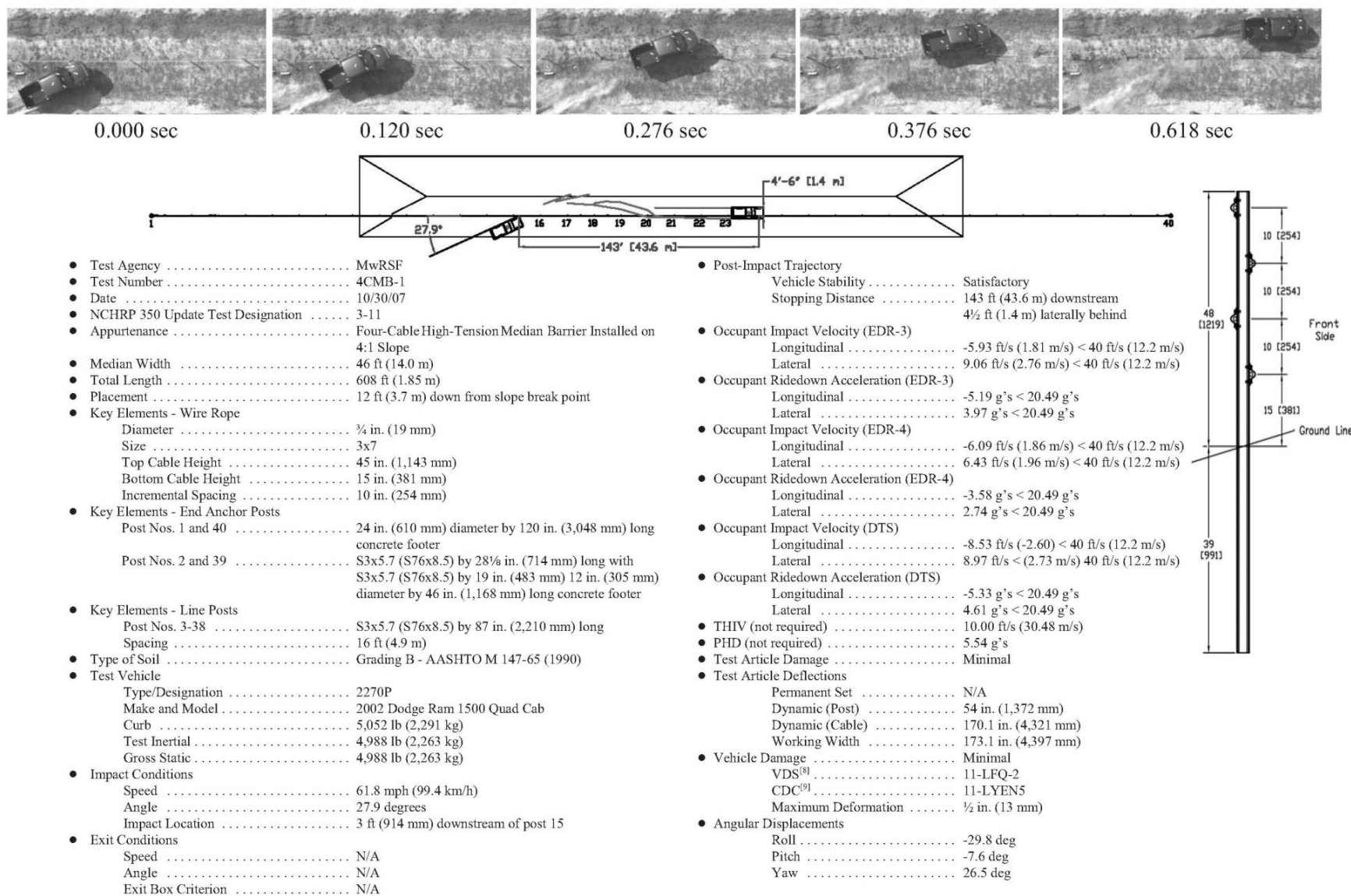


Figure B-4. Test Results Summary (English), Test No. 4CMB-1 [2]

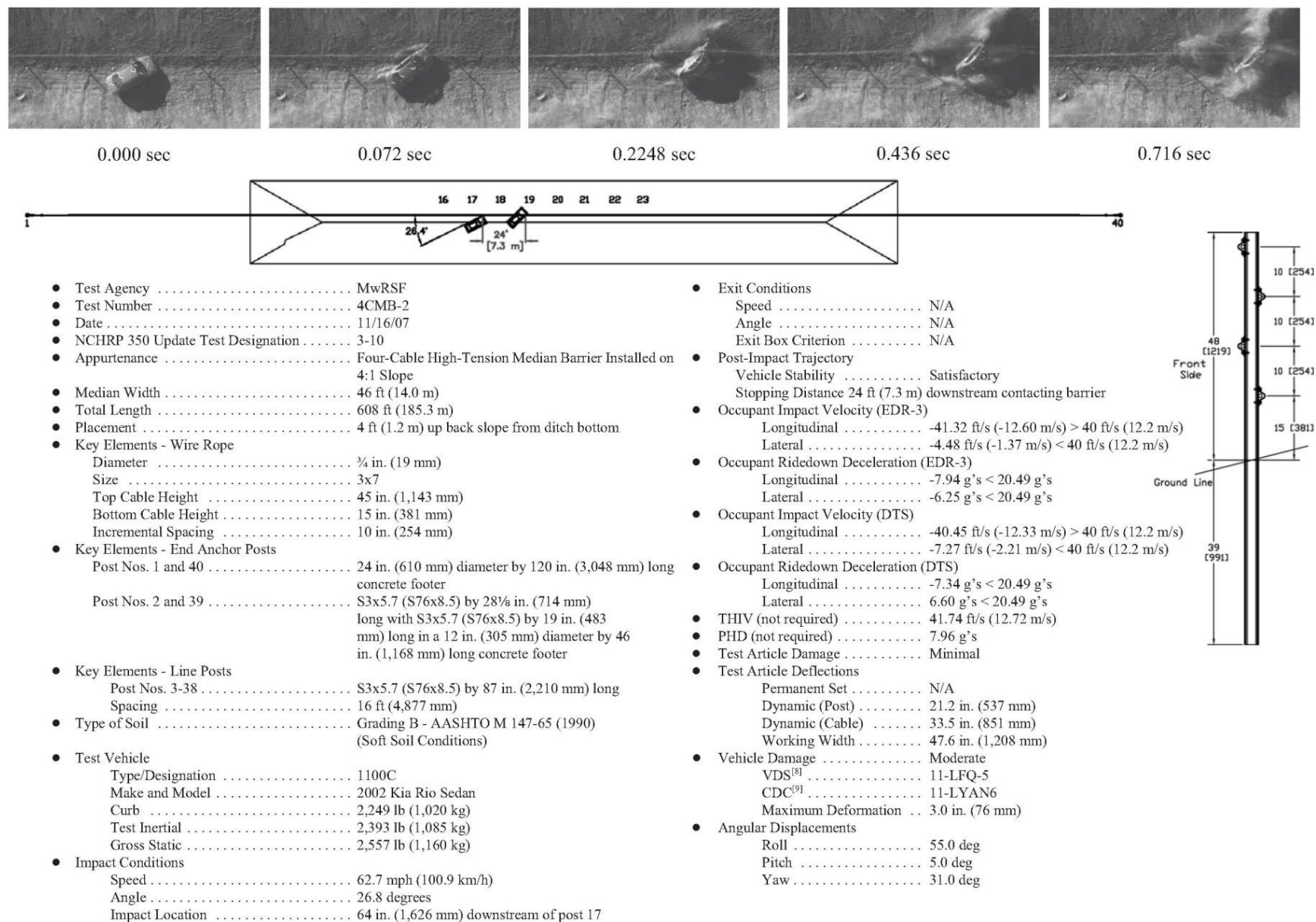
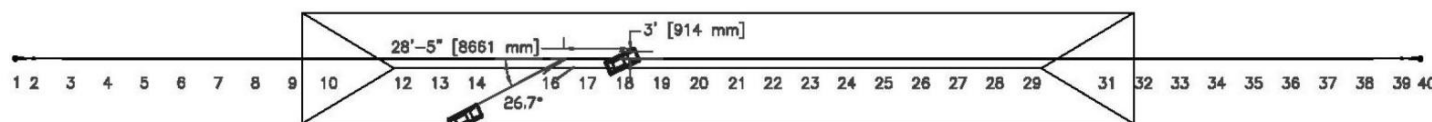
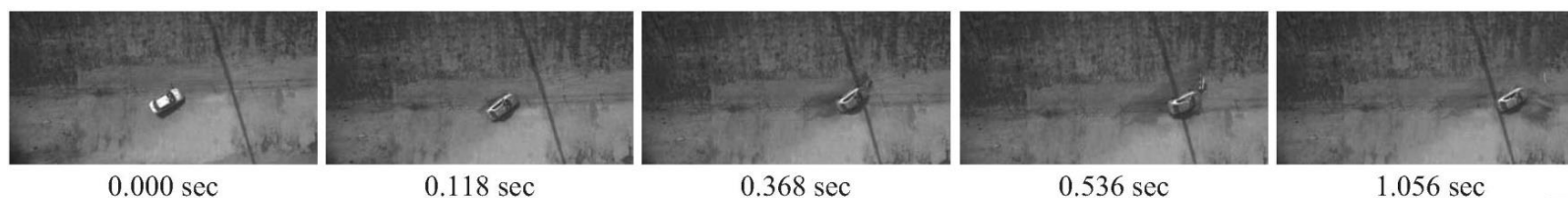


Figure B-5. Test Results Summary (English), Test No. 4CMB-2 [2]



- Test Agency MwRSF
- Test Number 4CMB-3
- Date 8/25/08
- MASH Test Designation 3-10
- Appurtenance Four-Cable High-Tension Median Barrier Installed on on 4:1 Slope
- Median Width 46 ft (14.0 m)
- Total Length 608 ft (185.3 m)
- Placement 4 ft (1.2 m) up back slope from ditch bottom
- Key Elements - Wire Rope
 - Diameter ¾ in. (19 mm)
 - Size 3x7
 - Top Cable Height 45 in. (1,143 mm)
 - Bottom Cable Height 13½ in. (343 mm)
 - Incremental Spacing 10½ in. (267 mm)
- Key Elements - End Anchor Posts
 - Post Nos. 1 and 40 24 in. (610 mm) diameter by 120 in. (3,048 mm) long concrete footer
 - Post Nos. 2 and 39 S3x5.7 (S76x8.5) by 28⅞ in. (714 mm) long with S3x5.7 (S76x8.5) by 19 in. (483 mm) long in a 12 in. (305 mm) diameter by 46 in. (1,164 mm) long concrete footer
- Key Elements - Line Posts
 - Post Nos. 3-38 S3x5.7 (S76x8.5) by 90 in. (2,286 mm) long
 - Spacing 16 ft (4.88 m)
- Type of Soil Grading B - AASHTO M 147-65 (1990) (Strong/stiff soil condition)
- Test Vehicle
 - Type/Designation 1100C
 - Make and Model 2002 Kia Rio Sedan
 - Curb 2,402 lb (1,090 kg)
 - Test Inertial 2,411 lb (1,094 kg)
 - Gross Static 2,586 lb (1,173 kg)
- Impact Conditions
 - Speed 62.0 mph (99.8 km/h)
 - Angle 27.2 degrees
 - Impact Location 64 in. (1,626 mm) downstream of post 16

- Exit Conditions
 - Speed NA
 - Angle NA
 - Exit Box Criterion NA
- Post-Impact Trajectory
 - Vehicle Stability Satisfactory
 - Stopping Distance 28 ft - 5 in. (8.66 m) downstream
3 ft (914 mm) laterally behind
- Occupant Impact Velocity (EDR-3)
 - Longitudinal -31.17 ft/s (-9.50 m/s) < 40 ft/s (12.2 m/s)
 - Lateral -2.85 ft/s (-0.87 m/s) < 40 ft/s (12.2 m/s)
- Occupant Ridedown Deceleration (EDR-3)
 - Longitudinal -6.51 g's < 20.49 g's
 - Lateral -6.86 g's < 20.49 g's
- Occupant Impact Velocity (DTS)
 - Longitudinal -27.30 ft/s (-8.32 m/s) < 40 ft/s (12.2 m/s)
 - Lateral -4.37 ft/s (-1.33 m/s) < 40 ft/s (12.2 m/s)
- Occupant Ridedown Deceleration (DTS)
 - Longitudinal -6.19 g's < 20.49 g's
 - Lateral -7.53 g's < 20.49 g's
- THIV (not required) NA
- PHD (not required) NA
- Test Article Damage Moderate
- Test Article Deflections
 - Permanent Set N/A
 - Dynamic (Post) 13.5 in. (343 mm)
 - Dynamic (Cable) 50.3 in. (1,278 mm)
 - Working Width 64.5 in. (1,638 mm)
- Vehicle Damage Severe
 - VDS^[8] 11-LFQ-6
 - CDC^[9] 11-LYAW8
 - Maximum Deformation 10½ in. (267 mm)
- Angular Displacements
 - Roll -20.63 deg
 - Pitch 14.38 deg
 - Yaw 22.02 deg

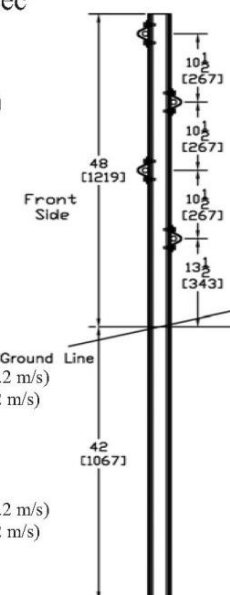


Figure B-6. Test Results Summary (English), Test No. 4CMB-3 [2]

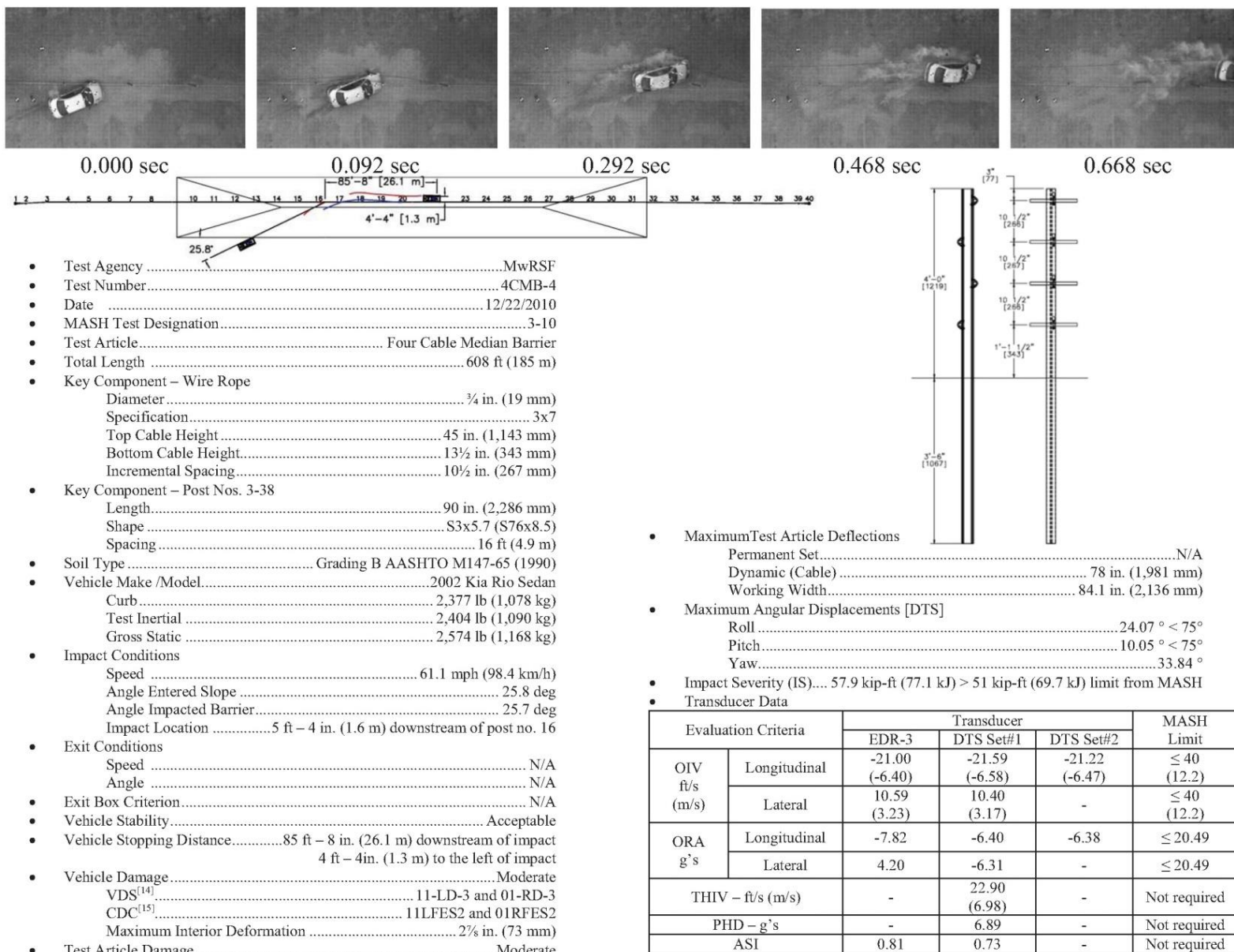


Figure B-7. Test Results Summary (English), Test No. 4CMB-4 [3]

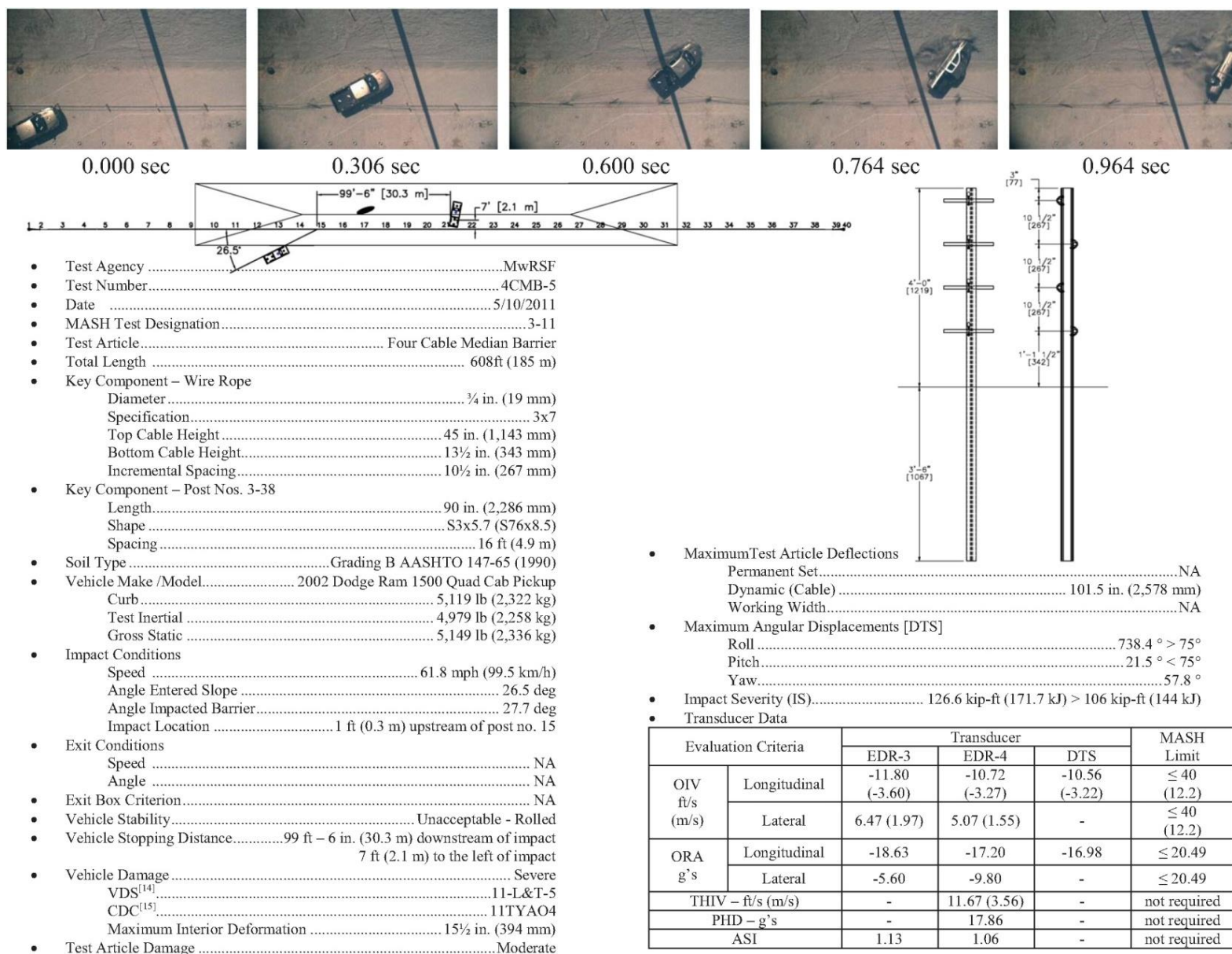


Figure B-8. Test Results Summary (English), Test No. 4CMB-5 [3]

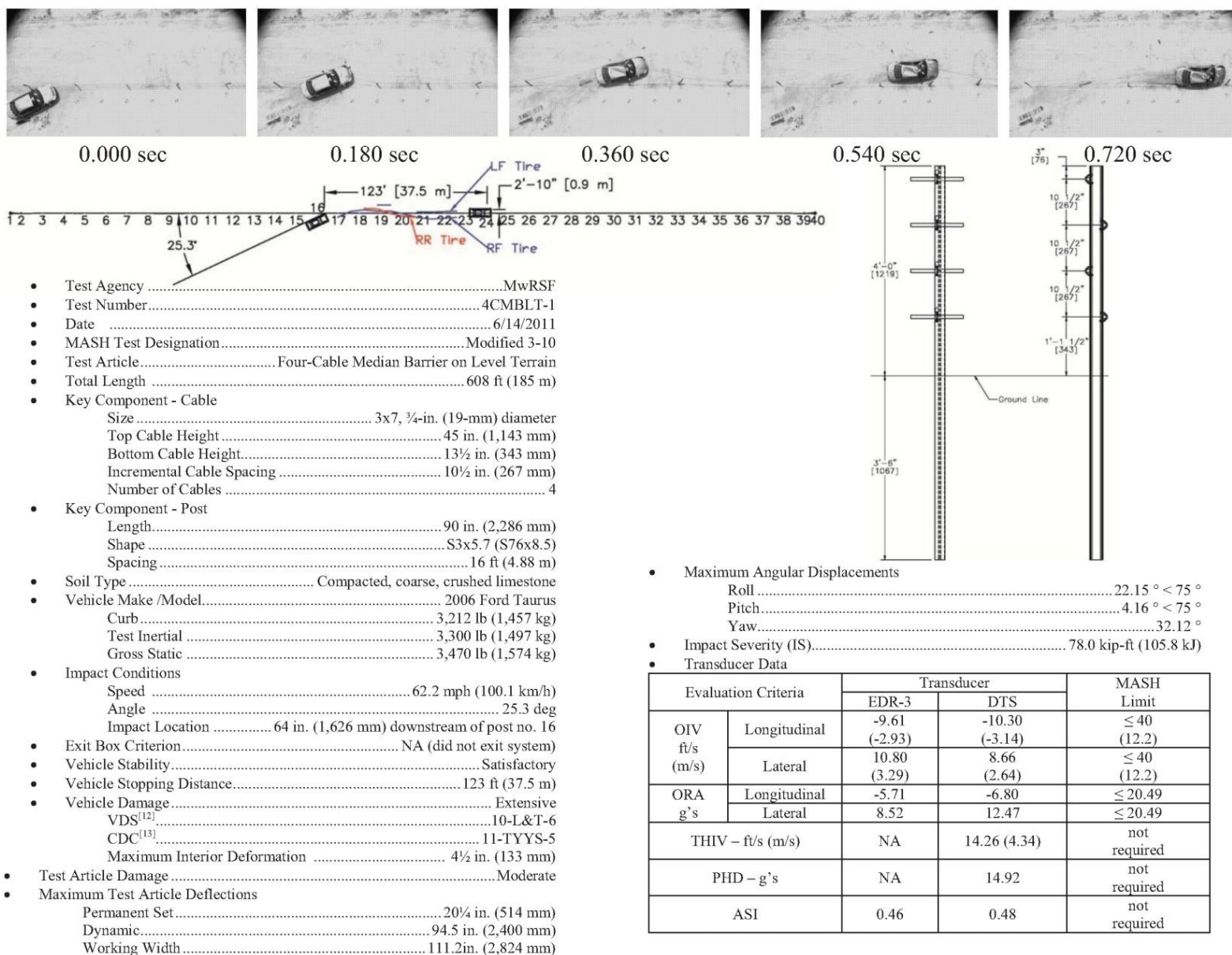


Figure B-9. Test Results Summary (English), Test No. 4CMBLT-1 [4]

Appendix C. Derivation of Cable Slope Changes

This section contains the derivation of an equation that was used in Chapter 4, Section 4.3, to determine the vertical loads applied to cable-to-post attachments based on changes in the vertical roadway alignment.

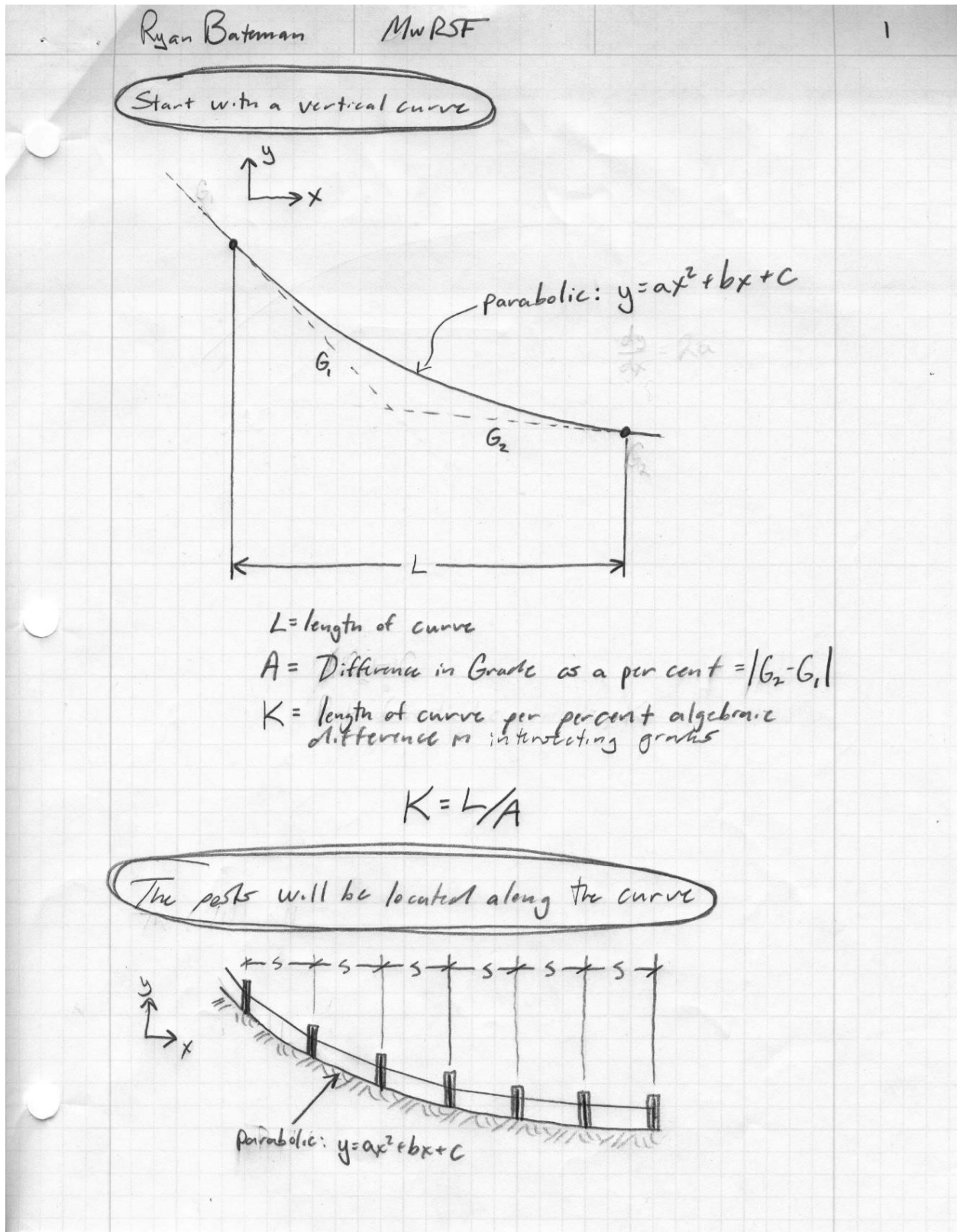


Figure C-1. Derivation of Slope Change, Sheet ¼

Ryan Bateman	MwRSF	2
--------------	-------	---

$$y = ax^2 + bx + c$$
$$\frac{dy}{dx} = 2ax + b \quad ; \quad \frac{dy}{dx} \Big|_{x=0} = b$$

Recall that K is the length of curve per percent algebraic difference in intersecting grades

$$\frac{dy}{dx} \Big|_{x=K} = b + \frac{1}{100}$$

set that equal to $\frac{dy}{dx} \Big|_{x=K} = 2aK + b$

$$2aK + b = b + \frac{1}{100}$$
$$a = \frac{1}{200K}$$

Figure C-2. Derivation of Slope Change, Sheet 2/4

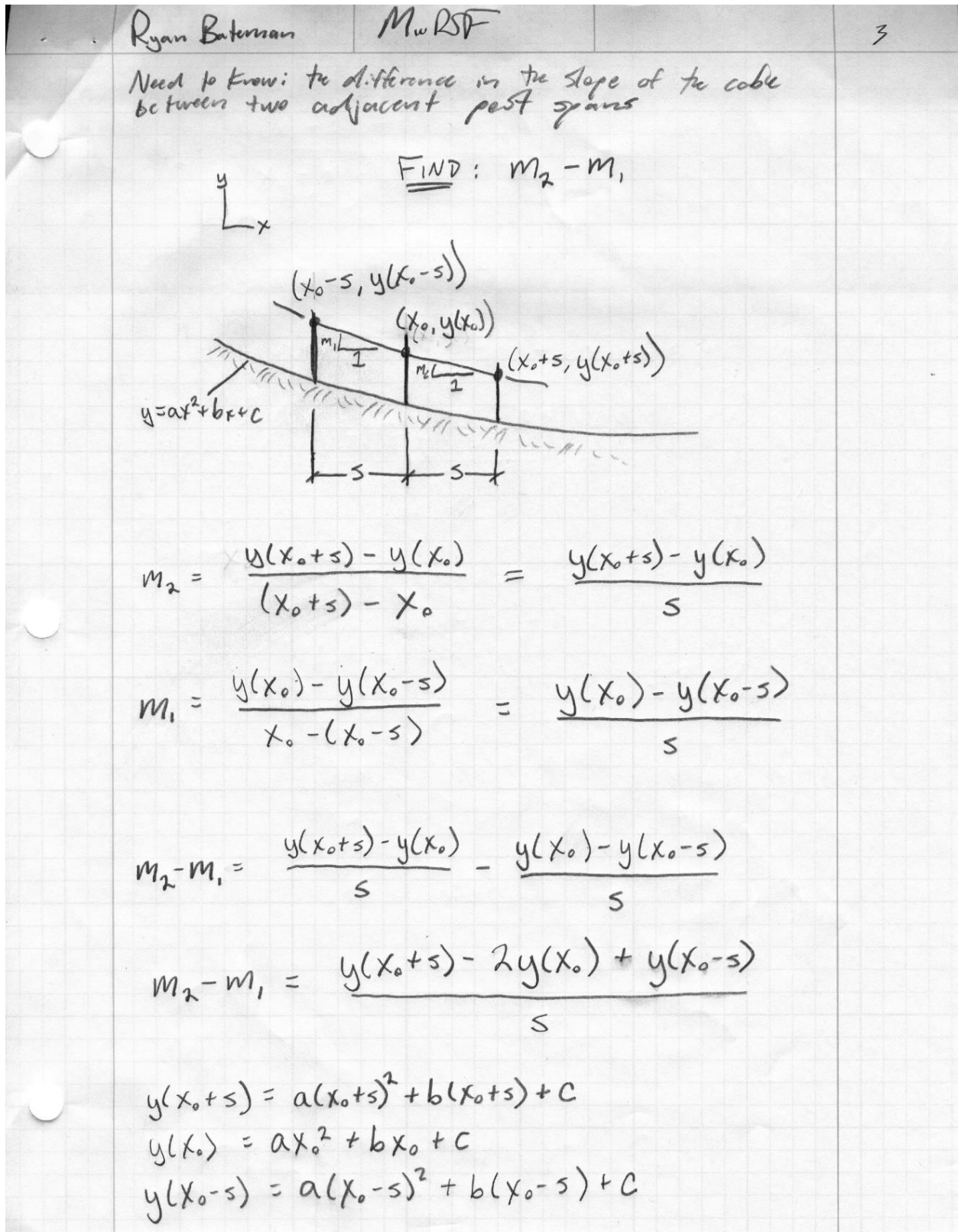


Figure C-3. Derivation of Slope Change, Sheet ¾

Ryan Bateman MwRSF 4

$$y(x_0+s) = ax_0^2 + 2ax_0s + as^2 + bx_0 + bs + c$$
$$y(x_0) = ax_0^2 + bx_0 + c \Rightarrow 2y(x_0) = 2ax_0^2 + 2bx_0 + 2c$$
$$y(x_0-s) = ax_0^2 - 2ax_0s + as^2 + bx_0 - bs + c$$
$$m_2 - m_1 = \frac{ax_0^2 + 2ax_0s + as^2 + bx_0 + bs + c - 2ax_0^2 - 2bx_0 - 2c + ax_0^2 - 2ax_0s + as^2 + bx_0 - bs + c}{s}$$
$$m_2 - m_1 = \frac{2as^2}{s} = 2as$$

Recall that $a = \frac{1}{200K}$

$$m_2 - m_1 = 2\left(\frac{1}{200K}\right)s ; \boxed{m_2 - m_1 = \frac{s}{100K}}$$

Figure C-4. Derivation of Slope Change, Sheet 4/4

Appendix D. CAD Details for Top Cable-to-Post Attachments

CAD details for the top cable-to-post attachment concepts, as denoted in Chapter 17, are provided in this section. These details were used for in-house fabrication and do not constitute a formal set of drawings.

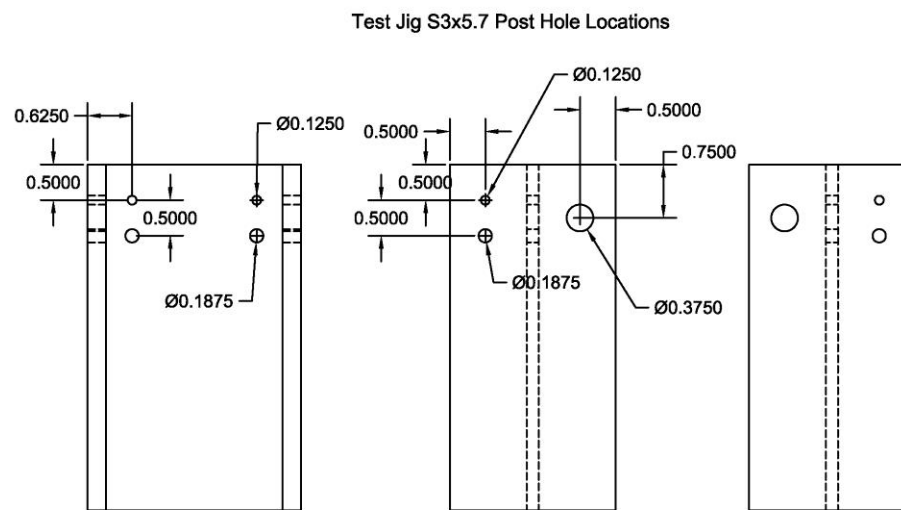


Figure D-1. S3x5.7 (S76x8.5) Section Hole Details

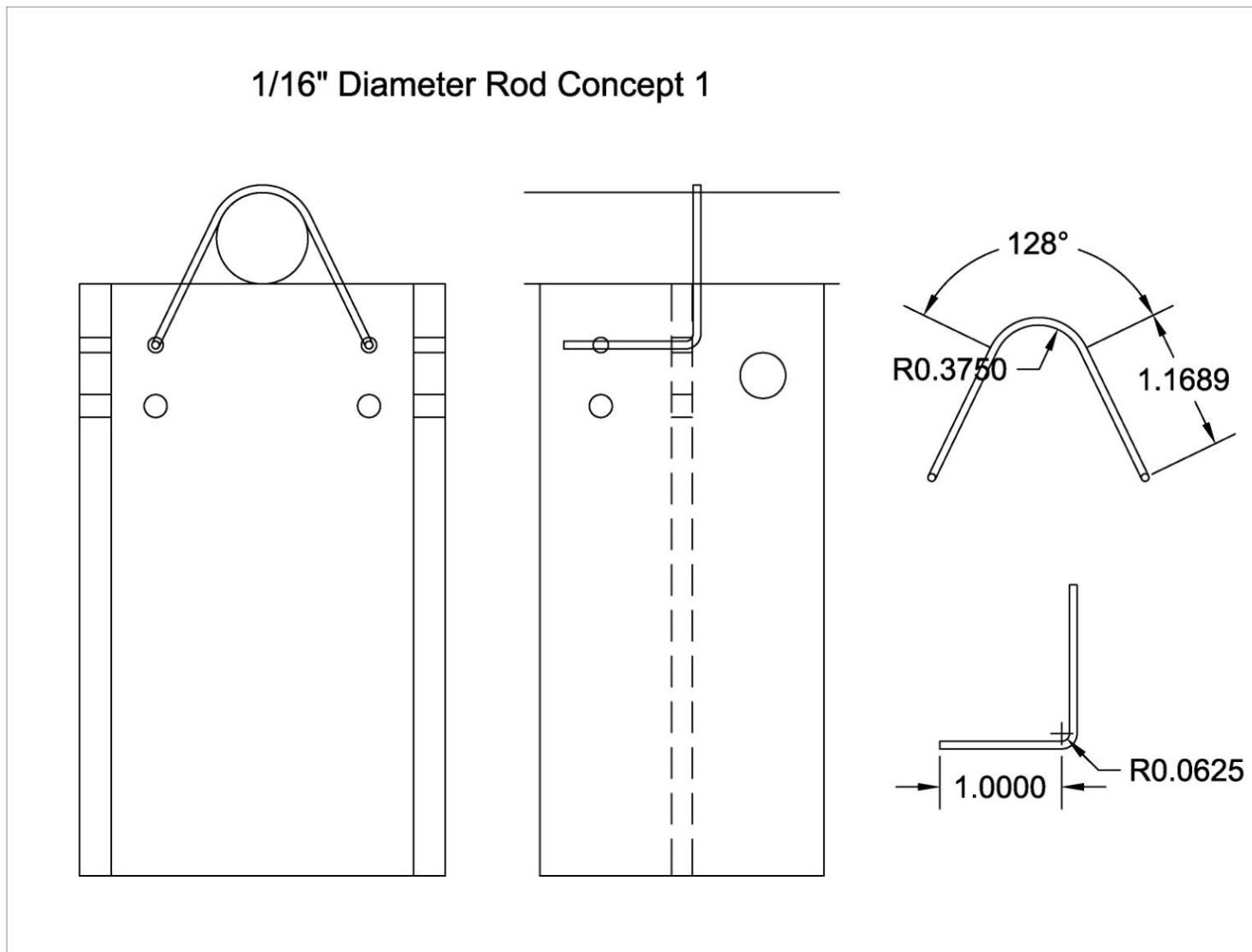


Figure D-2. 1/16 in. (1.6 mm) Diameter, Web-Inserted Curved Rod Detail

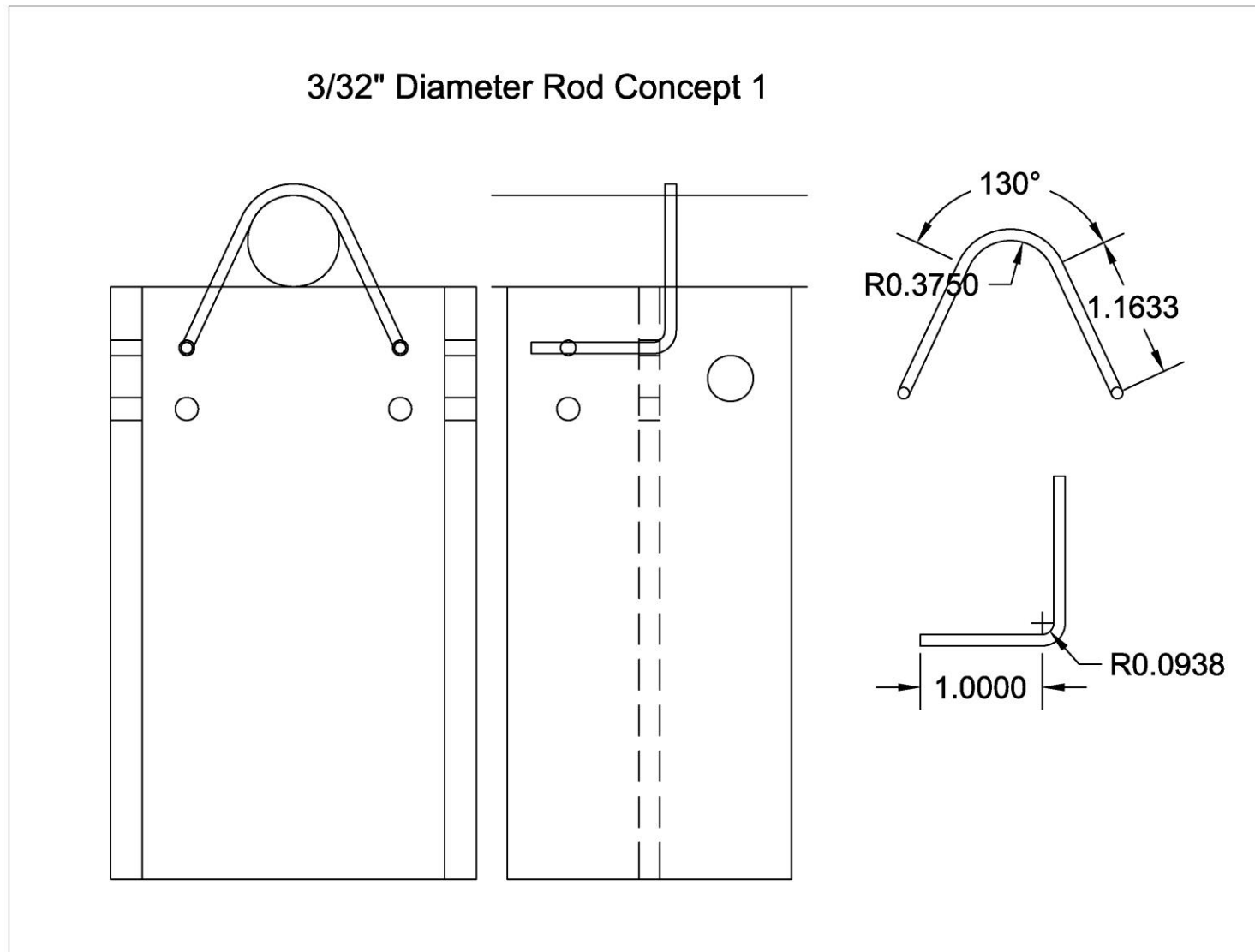


Figure D-3. 3/32 in. (2.4 mm) Diameter, Web-Inserted Curved Rod Detail

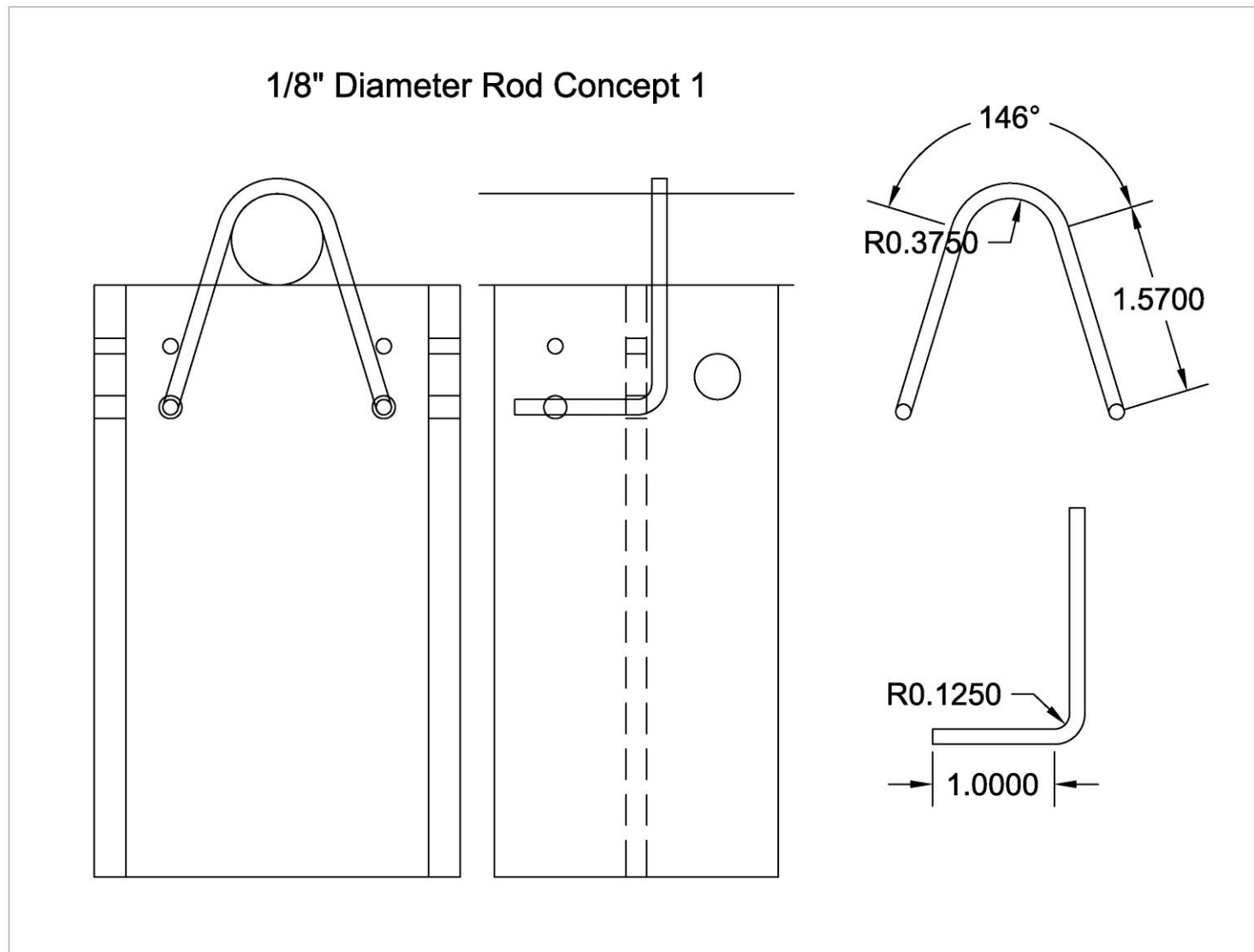


Figure D-4. 1/8 in. (3.2 mm) Diameter, Web-Inserted Curved Rod Detail

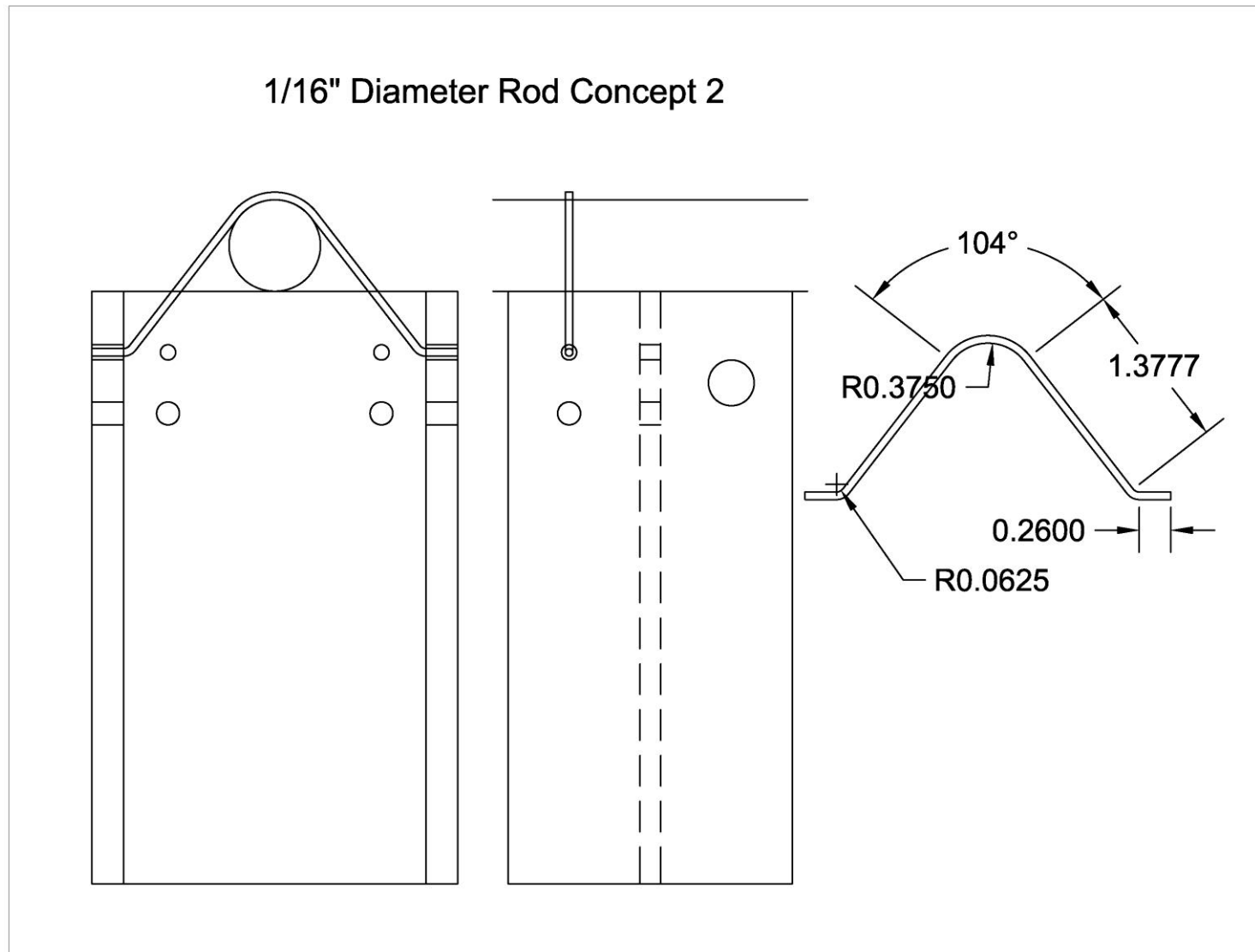


Figure D-5. 1/16 in. (1.6 mm) Diameter, Squeeze-In-Place Curved Rod Detail

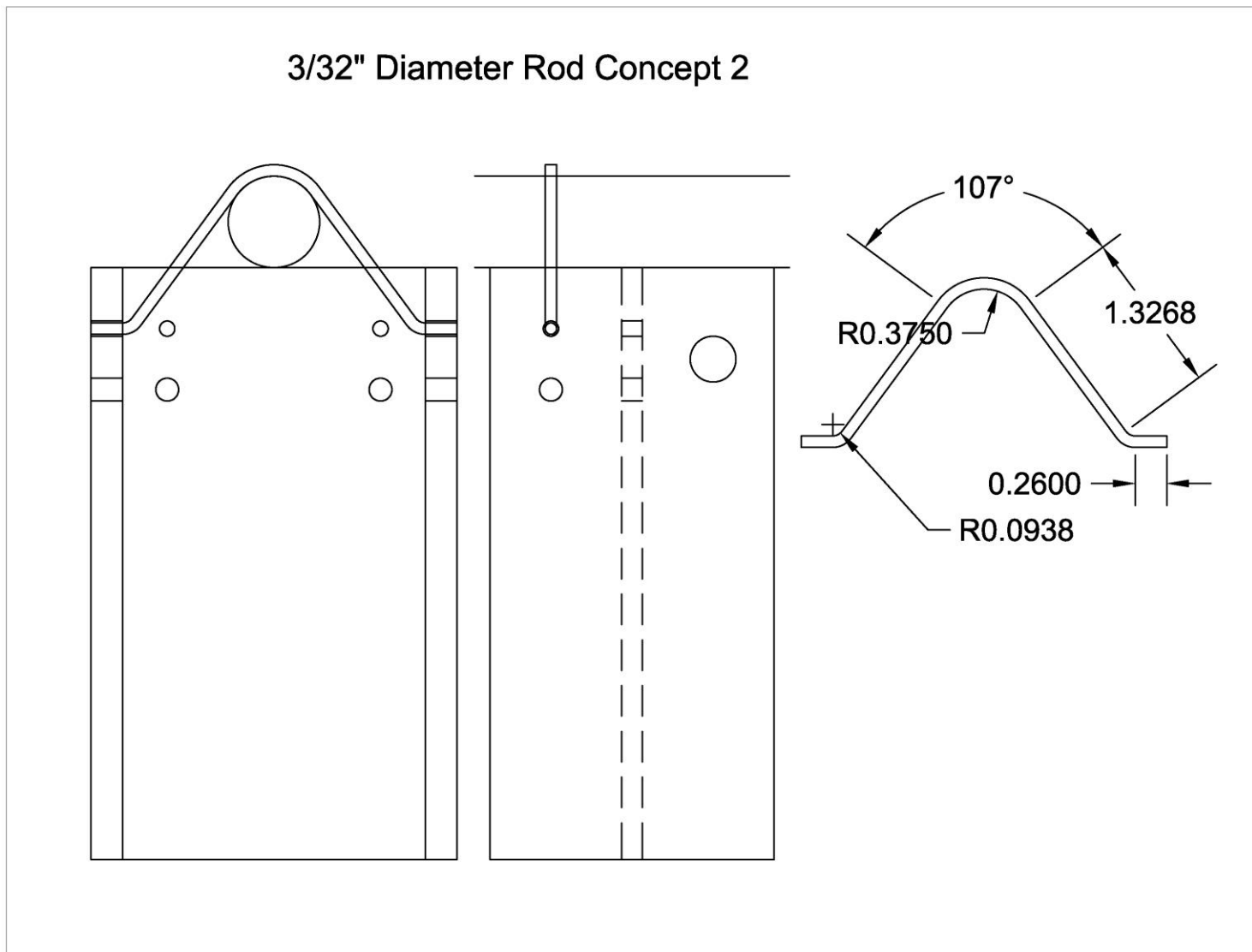


Figure D-6. 3/32 in. (2.4 mm) Diameter, Squeeze-In-Place Curved Rod Detail

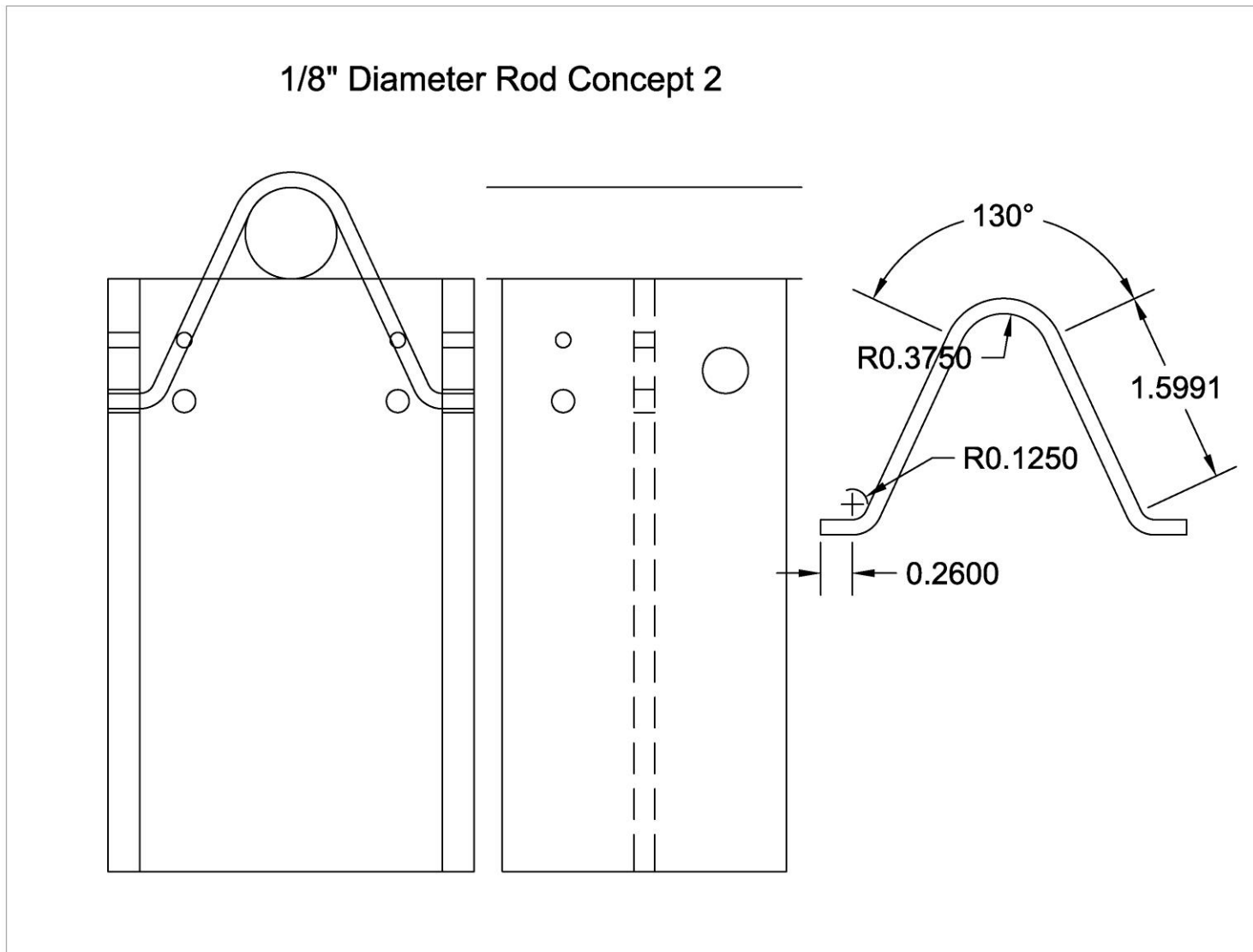


Figure D-7. 1/8 in. (3.2 mm) Diameter, Squeeze-In-Place Curved Rod Detail

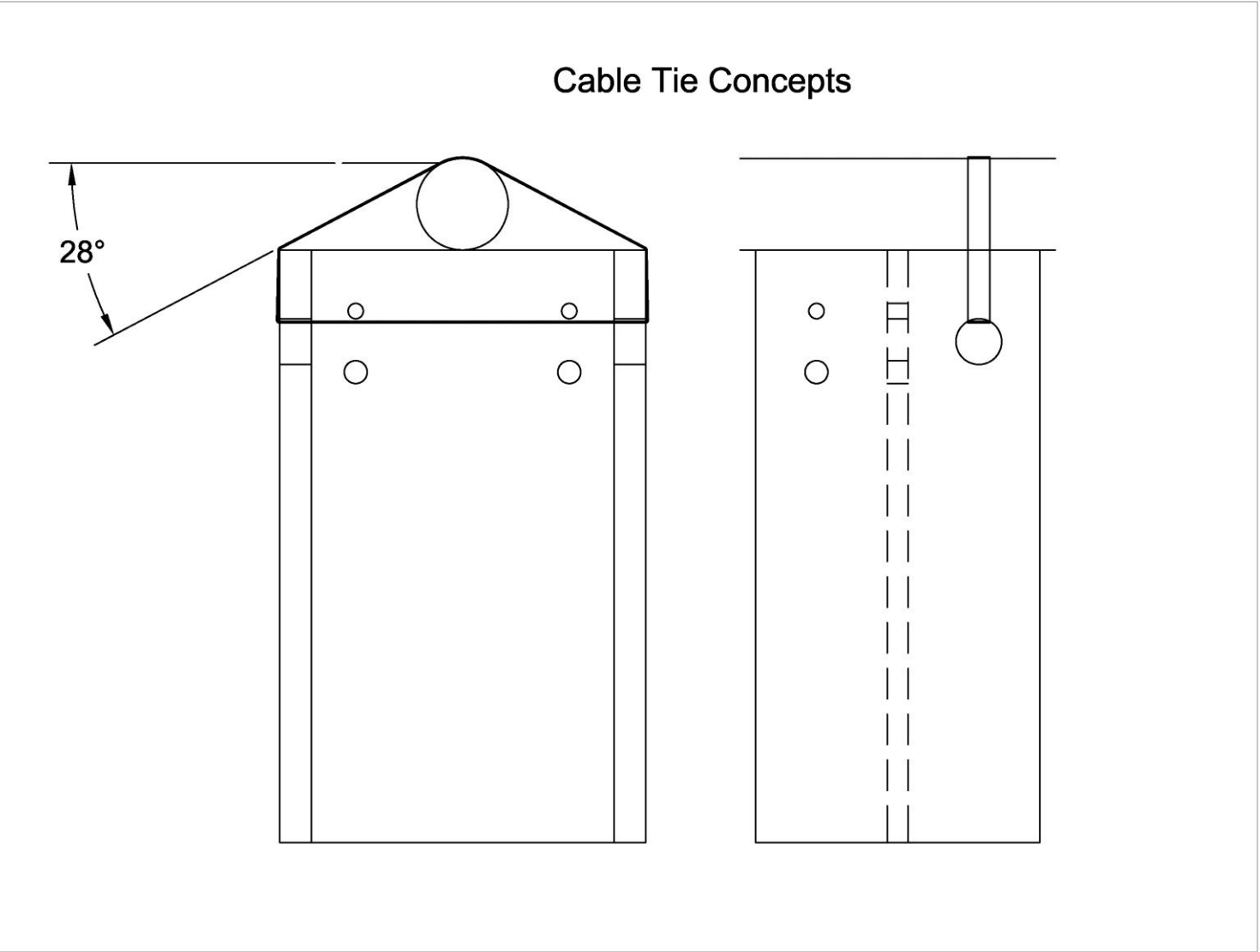


Figure D-8. Cable Tie Concepts

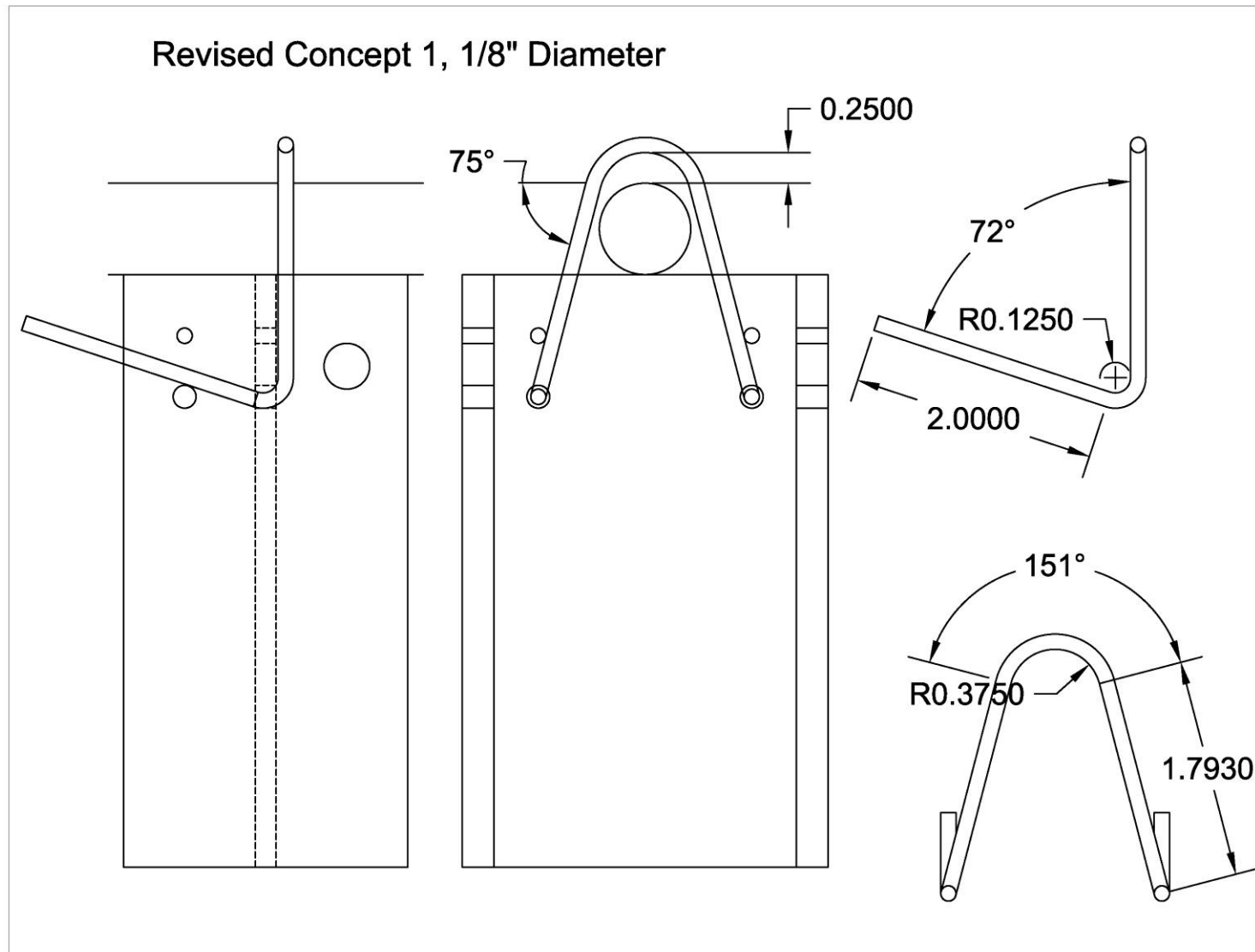


Figure D-9. 1/8 in. (3.2 mm) Diameter, Revised Web-Inserted Curved Rod Detail

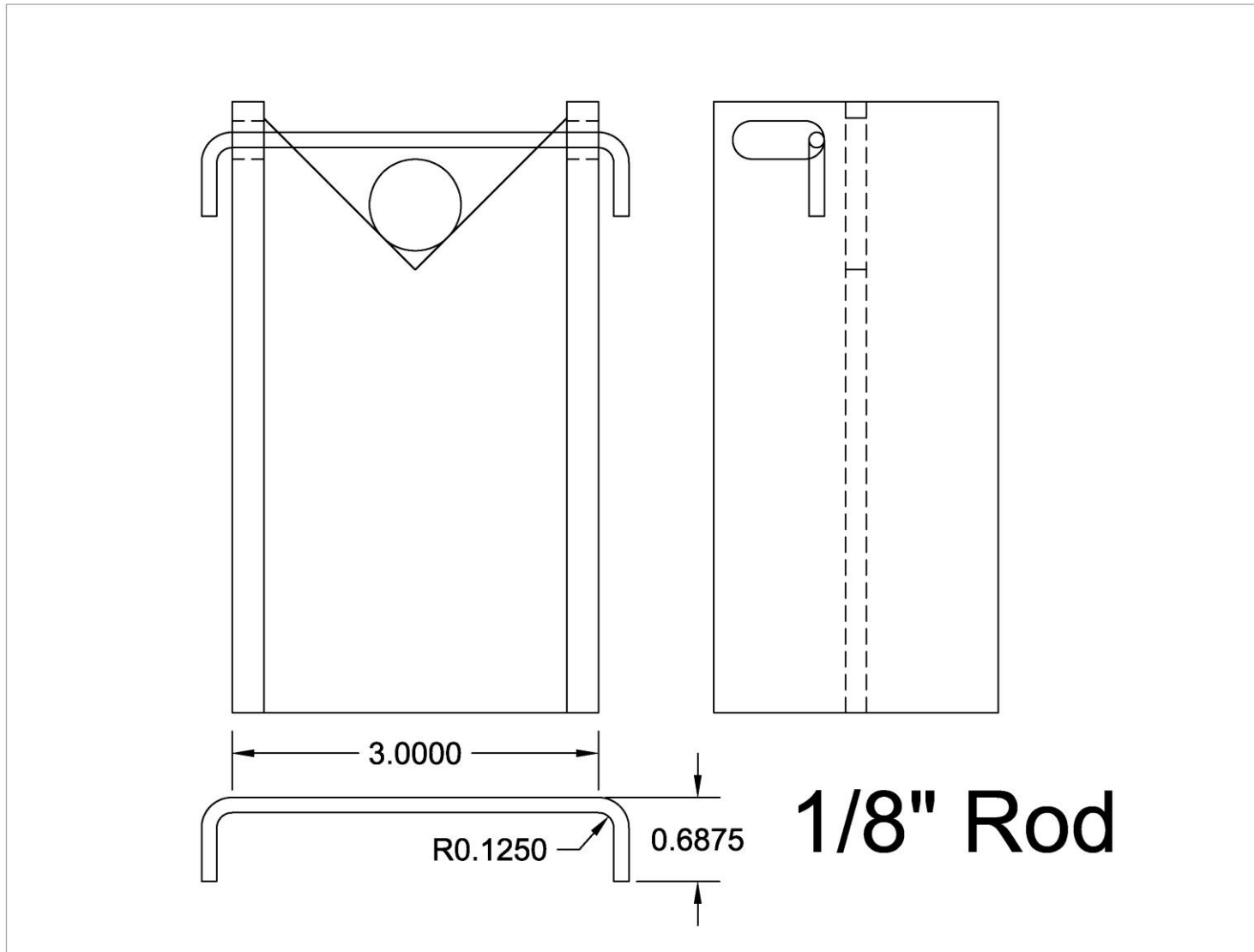


Figure D-10. 1/8 in. (3.2 mm) Diameter, Straight Rod with Bent Ends Detail

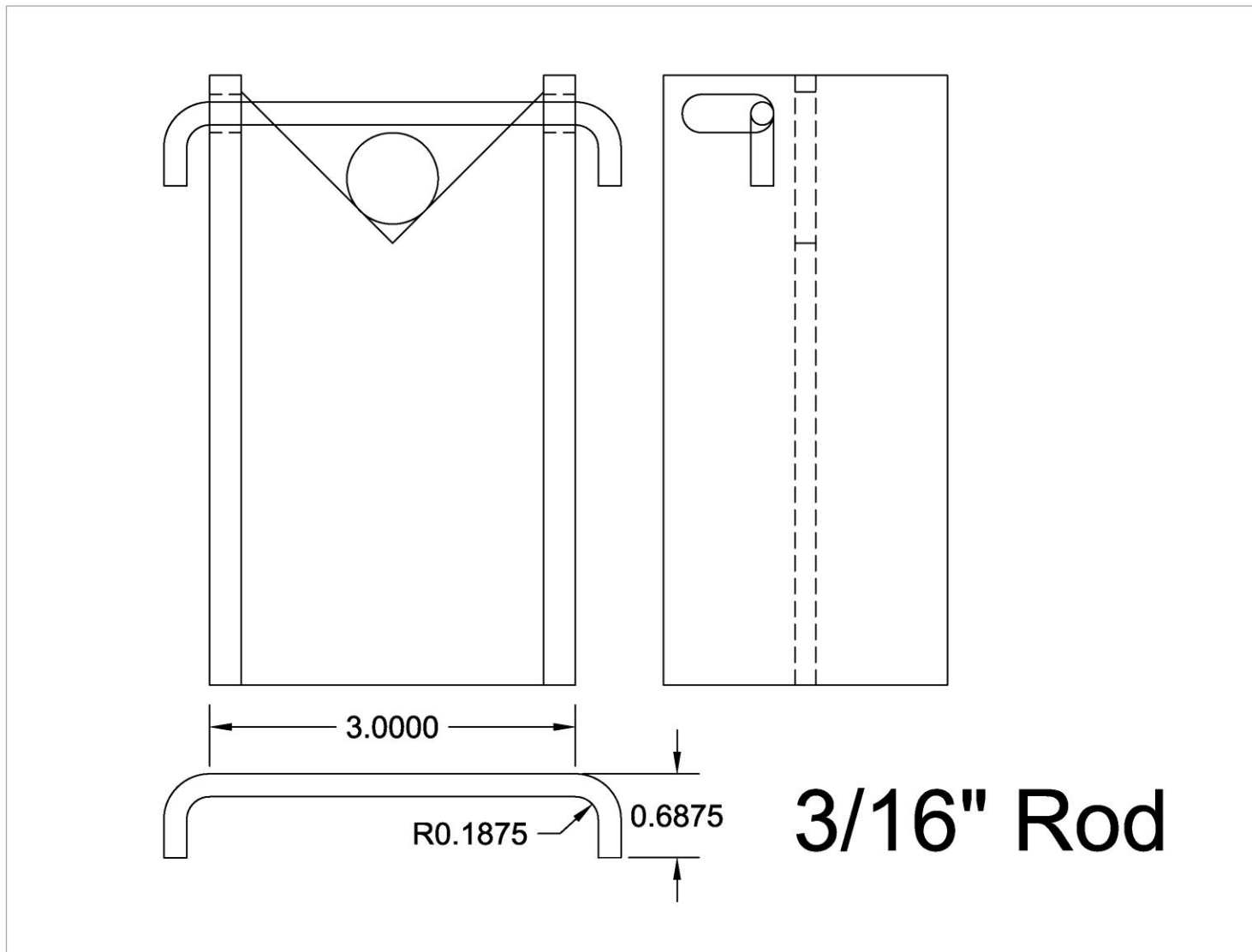


Figure D-11. 3/16 in. (4.8 mm) Diameter, Straight Rod with Bent Ends Detail

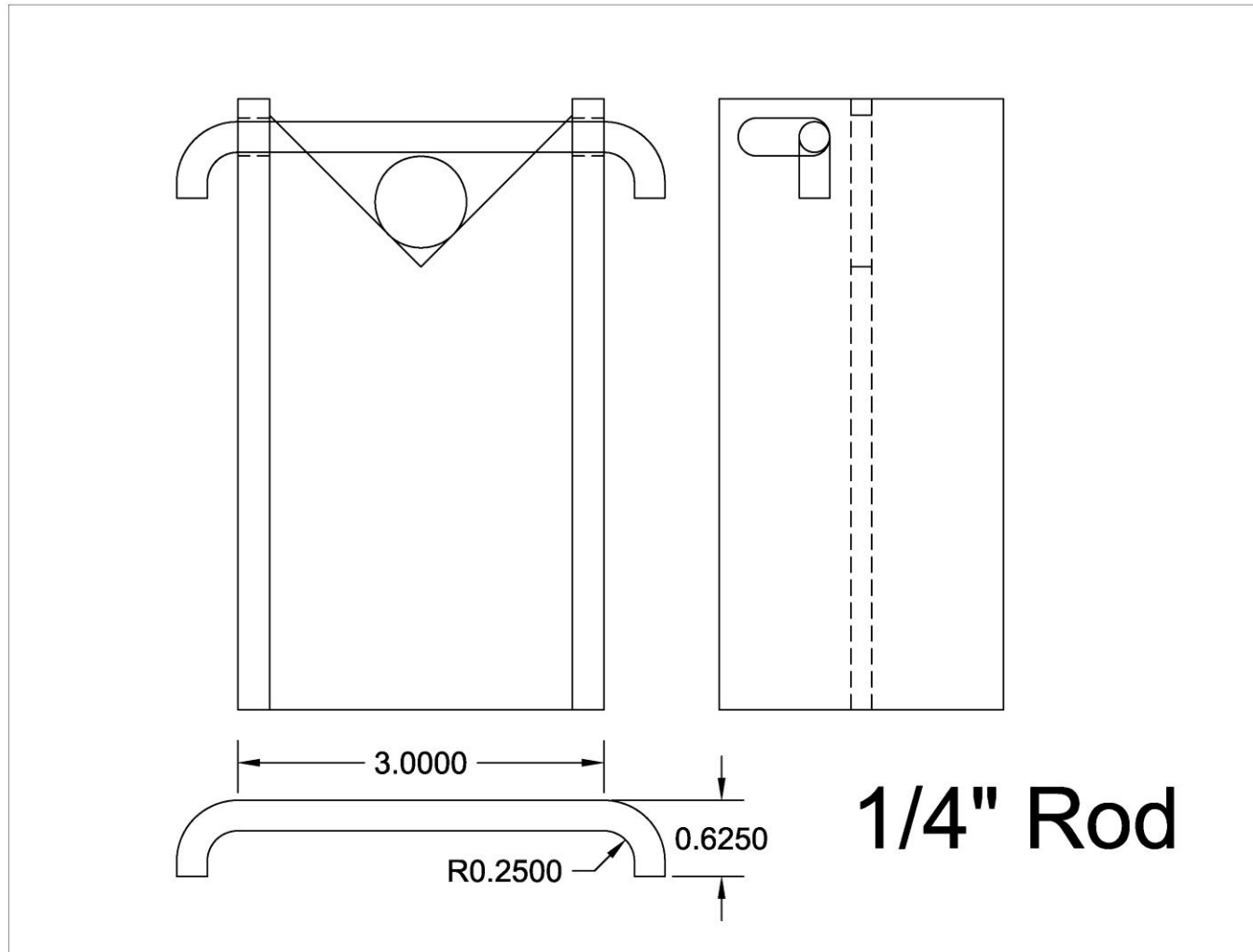



Figure D-12. 1/4 in. (6.4 mm) Diameter, Straight Rod with Bent Ends Detail

Appendix E. Material Specifications

Mill certificates for the keyway bolts, the sheet steel for the tabbed brackets, and the brass and stainless steel round rods and bars for the top cable-to-post attachments are provided in this section. Mill certificates provide information about chemical composition, applicable ASTM standards, mechanical properties, and other items of interest for engineers.

Service in Metals Since 1953

Murphy and Nolan, Inc. 

BAR and TUBING SPECIALISTS

www.murphynolan.com

P.O. BOX 6689, 340 PEAT ST.
SYRACUSE, N.Y. 13217-6689
(315) 474-8203
1-800-836-6385
FAX (315) 474-8208

07/26/05

55 INDUSTRIAL PARK CIRCLE
ROCHESTER, N.Y. 14624-2493
(585) 426-1420
1-800-333-0827
FAX (585) 247-1962

BENNETT BOLT WORKS
P.O. BOX 922
JORDAN, NY 13080

Order Number: 325647
Your PO: 75210
Ship Date:
Fax Number: 315-689-3999

Ln.	Description	Heat Number	Certificate of Mill Test Reports				
CARBON STEEL ROUND BAR 1018 C F ASTM A108 (RED)							
8 PC(S) (16#) 1/4" RD x 10/12' R/L							
Heat Number: A78762							
Chemical Composition							
	C	SI	MN	P	S		
	0.1700	0.1700	0.6700	0.0080	0.0110		
	AL						
	0.0050						
Mechanical Properties							
	Yield Strng	Tensile Strng	% Elong	Brinell Hardness	Hardness		
	54.000	64.000	15		126		

Figure E-1. AISI C1018 Keyway Bolts



MUELLER BRASS CO.

Control No: 705583

LOCATIONS:

2199 LAPEER AVENUE
PORT HURON, MICHIGAN 48060

302 ASHFIELD STREET
BELDING, MICHIGAN 48809

Certified Test Report

Sold: 00061067 Ship: 00059225
To: COPPER & BRASS SALES To: COPPER & BRASS SALES-
ATTENTION: ACCOUNTS PAYABLE 8001 THYSSENKRUPP PARKWAY
P.O. BOX #5116 NORTHWOOD, OH 43619
SOUTHFIELD, MI 48086-5116

Cust PO: 5400146354 MBCo SO: 352441 Ln 70 Cert Lvl: 2
Cust Part: CURD00527 Part Nbr: 0250RD601200XX1 FC
Type: ROD Size: RND 0.250 Qty Shpd: 3,085 UM: Lbs
Cust Spec: ASTM B16/16M-10 BOL: 50471286 Shpd: 06/05/12

Mechanical Properties

Lot Number: 1375756		Temper: H020 1/2 H		CDA Alloy: C36000	
Yield Strength ()		Tensile Strength ()		Elongation % in 2 Inches	
				Hardness RB	

Chemical Analysis (%)

	Cu	Pb	Fe	Zn					
ASTM B16/16M-10	60.0-63.0	2.5-3.0	0.35 Max	REM					
Lot Number: 1375756	61.6	2.7	0.13	REM.					

OTHER EACH MAX: .50

We hereby certify to the chemical and mechanical properties reported herewith and to the fact that they were determined in conformance with the specification noted above or any exceptions to this specification we have granted. We also hereby certify that the material furnished on this order is free from mercury contamination and that no mercury bearing equipment was used in the manufacture of these items.

Melted and Manufactured in USA
ISO9001:2008 registered QMS

Produced in Compliance with:
EN10204 3.1
EU Directives:
2002/95/EC (RoHS Compliant)
2000/53/EC

By: *Stephanie Goodell* 06/05/12
Stephanie Goodell
Metallurgist

From: Copper and Brass Sales
Cust: ONLINE METALS
Part: 1257
Wgt: 86.000 LB

Del: 2401949744
PO: 76155
Date: 07/09/2012

James K Baber

Figure E-2. 1/4 in. (6.4 mm) Diameter, C360 Brass Round Bar

VIRAJ PROFILES LIMITED

10 Imperial Chambers, 1st Floor,
Wilson Road, Mumbai 400 038
INDIA



TEST CERTIFICATE

CUSTOMER SUMMIT STAINLESS STEEL, LLC 2001 ELIZABETH ST. NO. BRUNSWICK, NJ 08902 USA	ORDER NO VJ11470	PACKING LIST NO IMP/925319/5	INSPECTION NO 100001085328 GRADE 304/304L	DATE 29.04.2011 HEAT No 22816
--	----------------------------	--	--	--

BUNDLE NO :
5186990

DESCRIPTION
STAINLESS STEEL BRIGHT BARS

COLD DRAWN

SIZE	SHAPE	TOLERANCE	LENGTH	PIECES	WEIGHT
1/8"	ROUND	ASTM A484	12' (-0/+2")	1820	922.000 LB

CHEMICAL ANALYSIS

%C	%Mn	%Si	%S	%P	%Cr	%Ni	%Cu	%Mo	%Co	%N2
0.0140	1.900	0.440	0.0200	0.0390	18.440	8.080	0.370	0.230	0.150	0.07600

TEST RESULTS

0.2% yield strength ksi	Tensile Strength ksi	Elongation %	Reduction Of Area %	Hardness BHN	Grain Size NOS
97.0	113.0	41.0	70.0	231.0	7.0

SPECIFICATION:

MATERIAL CONFORMS TO ASTM A276-06 COND A, A479/A479M-06a COND A, AMS QQ-S-763 B-06(EXCEPT MARKING), SAB AMS 5639H/5647H(EXCEPT MARKING), ASME SA 479/A479M-98 COND A, JOE TEST SATISFACTORY AS PER ASTM A262-02a PRACTICE E, ASTM A 182/182M-06 P304/304L, A 193/193M-98 B4 CL 1, A314-97, MIL-S162B, ASME SA 182/182M-98 F304/304L, SA 193/193M-98 B4 CL 1, MIL-S162B, DOD-F24669/6, (FOR CHEM. AND MICH. ONLY) NACE-MR-0175, GRAIN SIZE AS PER ASTM B112-96a1. IMPROVED MACHINABILITY QUALITY. UNS-S-30400/S-30403 CERTIFICATE AS PER EN 10204-3.1.

REMARKS

MATERIAL IS FREE FROM MERCURY CONTAMINATION, FREE FROM WELD OR WELD REPAIRS, MICRO-FREE FROM CONTINUOUS CARBIDE NETWORK ON GRAIN BOUNDARIES. MACRO-GOOD, MINIMUM SOLUTION ANNEALING TEMPERATURE 1050C, SOAKING TIME 01hr/each, WATER QUENCHED. MELT SOURCE: AOD. WE CONFIRM THAT THE MATERIAL HAS BEEN TESTED AND FOUND TO BE FREE FROM RADIOACTIVE CONTAMINATION MELTED AND PRODUCED IN INDIA.

We hereby certify that the material described above has been tested and complies with the terms of order/contract.

YARDE METALS, INC. CERTIFIES THAT
THIS IS A TRUE COPY OF THE ORIGINAL
MILL TEST REPORT NOW ON FILE
RECEIVED AND INSPECTED

MAR 15 2012

BY Melissa Gagnier
Melissa Gagnier, Certification Engineer

WORKS INSPECTOR
K R R MURTHY

YARDE METALS Inc 05-09-12

S20509SL011-3 ONLINE METALS.C PO: 73782 Part #:
100.00PC 51.00LB

Figure E-3. 1/8 in. (3.2 mm) Diameter, T-304 Stainless Steel Round Bar

KME Brass Italy S.r.l.

KME

TEST REPORT

Certificate Nr	: 336254	Groupe Nr	: 1157685
Customer	: COPPER AND BRASS		
Customer Ref.	: KMA 111019 06 PO 5400120		
Job Number	: 511938/3	Item EM	: 0044519
Material Desc.	: ROD FREE MACHINING ASTM B16 - Brass C36000 - H02 -		
	: RND 3 16 IN L. 12 FT - Pointed/Chamfered		
Part Number	: CURD00477		
Quantity	: LB 6093.6		

Chemical Composition: ASTM B16 C36000

%	Cu	Pb	Zn	Fe	Other Imp.
Min	60.0	2.5		0.0	0.0
Max	63.0	3.0		0.35	0.5
	60.2589	2.7831	p.d.	0.2092	0.2954

Physical Characteristics: ASTM B16 H02

Test	Elong. 5.65	Tensile Streng.	Yield St.
	1	kpsi	0.5 kpsi
Min	7.0	57	25
Max			
12076783	15.2	68	63

Dimensional Characteristics: ASTM B249

Test	Size
	Inch
Min	0.1860
Max	0.1890
12076783	0.1874

Serravalle Scrivia 01/02/2012

Company with the quality management system certified by IGQ according to ISO 9001-2008

Document complying to EN 10204 2.2 standard, issued under computerized control.

Signature not required. The Quality Manager Mr. Orazio Ruggieri. - MADE IN ITALY -

KME Brass Italy S.r.l. a tutti i sensi
Attestato di Qualita' Prodotto
Materie Plastiche e Metalliche
Serravalle Scrivia
Via dei Riformati, 2

Contatto Prodotto/Qualita' Prodotto
Numero Verde 800-20-1111
Fax 0584-5411240
Email: kme@kme.it

Logo della IGQ 01/02/2012
Il Sig. Orazio Ruggieri
Qualita' Prodotto/Qualita' Prodotto
Materie Plastiche e Metalliche
Serravalle Scrivia

Attestato di Qualita' Prodotto/Qualita' Prodotto
Materie Plastiche e Metalliche
Serravalle Scrivia

From: Copper and Brass Sales

Cust: ONLINE METALS

Part: 4345

Wgt: 90.000 LB

Del: 2401967075

PO: 76614

Date: 07/19/2012

James K. Baber

Figure E-4. 3/16 in. (4.8 mm) Diameter, C360 Brass Round Bar

TRI STAR METALS, LLC.
1201 S. ADAMS AVE.
FREEPORT, IL 61032
An ISO 9001:2008 Registered Company

CERTIFICATE DATE: October 27, 2011 **CUSTOMER:** Copper & Brass Sales
ORDER#: 180196 **CUSTOMER PO#:** 5400118635-R02
MATERIAL: 303 **DESCRIPTION:** .0937" x 12'
HEAT NUMBER: 3P354 **QTY. SHIPPED:** 1,109 LBS
 PART #: SSRD00004

CHEMICAL COMPOSITION

C	Mn	Si	S	P	Ni	Cr	Mo	Other Elements
.064	1.960	.190	.3187	.024	8.010	17.720	.100	Cu=.730 Co=.180 N=.0305

MECHANICAL VALUES

TENSILE (KSI)	YIELD (KSI)	ELONGATION (%)	REDUCTION OF AREA (%)	HARDNESS
105	77	34	62	222 HB

ADDITIONAL REMARKS:

This material meets the chemistry specifications for: ASTM A582/A 582M.2005
RoHS COMPLIANT SE AMS 5640/U ACTUAL CHEMISTRY/ACT. PHYSICAL.

MATERIAL IS FREE FROM MERCURY CONTAMINATION. EN10204 3.1.B
MELT ORIGIN: TAIWAN

MATERIAL IS MANUFACTURED IN THE UNITED STATES OF AMERICA

I hereby certify that this data is correct as contained in the records of this company.

QUALITY CONTROL REPRESENTATIVE:
Form# 7.9.0.0.4 Rev C

Janie Wells
Janie Wells - QA Certification Technician

Figure E-5. 3/32 in. (2.4 mm) Diameter, T-303 Stainless Steel Round Bar

KME Brass Italy S.r.l.



TEST REPORT

Certificate Nr	: 337841	Group Nr:	1157687
Customer	: COPPER AND BRASS		
Customer Ref.	: KMA 111019 07 PO 5400120		
Job Number	: 511964/1	Item EM:	5057291
Material Desc.	: ROD FREE MACHINING ASTM B16 - Brass C36000 - H02 -		
	: RND 3/32 IN B L. 12 FT - Pointed/Chamfered		
Part Number	: CURD00528		
Quantity	: LB 2405.2		

Chemical Composition: ASTM B16 C36000

%	Cu	Pb	Zn	Fe	Other Imp.				
Min	60.0	2.5		0.0	0.0				
Max	63.0	3.0		0.35	0.5				
000000	60.2	2.86	p.d.	0.25	0.0				

Physical Characteristics: ASTM B16 H02

Test	Elong. S. 65	Tensile Streng.							
	%	ksi							
Min	7.0	57							
Max									
12077129	14.0	73							

Dimensional Characteristics: ASTM B16B B

Test	Size								
	inch								
Min	0.0928								
Max	0.0938								
12077129	0.0935								

Note

Serravalle Scrivia 21/02/2012

Company with the quality management system certified by ICQ according to ISO 9001-2008

Document complying to EN 10204 3.1 standard, issued under computerized control.

Signature not required. The Quality Manager Mr. Orazio Ruggieri. - MADE IN ITALY -

KME Brass Italy S.r.l. e anche uniche
Member of the KME Group
Sede Legale e Uff. Amministrativi
00127 Roma
Via del Risorgimento, 2

Chiusa Pubblica 2006 Firenze
Phone +39 055-4471.1
Fax +39 055-4471.243
Email: kme.italy@kme.it

Cap. Soc. € 1.000.000.000.000.000
Cod. Fiscale e Reg. Imprese
di Firenze n° 0085840450
Partita IVA 0085840450
RCA n° 008584

Stipendi e compensi: Direzione e amministrazione: KME Italy S.p.A. - Firenze (FI)

Figure E-6. 3/32 in. (2.4 mm) Diameter, C360 Brass Round Bar

Certificate of Test

Customer COPPER AND BRASS SALES INC.
 Invoice No 148 - 1520411K11
 P.O. No SEE BELOW
 Mill & Melting BOOYOUNG INDUSTRY, KOREA

No 2011BY0404A1-3
 Date 04/04/11
 Commodity FREE CUTTING BRASS C36000 HALF HARD IN 12 FT L
 Spec PER ASTM B 16/16M REV 2005, ROHS COMPLIANT

Job No.	Lot No.	Size	Quantity	Temper	Remarks	B/D No.	Mat No.	Inspection Result
P.O. No.	Lot No.	Size	Quantity	Temper	Remarks	B/D No.	Mat No.	Inspection Result
5400086487	BY0404A1-3-3	1/2" X 3-1/2", RECTANGLE	2,170	H02	RECTANGLE		CUREC00137	GOOD
5400095315	BY0404A1-4-5	0.0625" DIA, ROUND	1,243	H02	ROUND		CURD01351	GOOD
5400095315	BY0404A1-3-4	1/4" X 1/2", RECTANGLE, AS EXTRUDED, W/F	1,093	H02	RECTANGLE		CUREC00598	GOOD
5400095315	BY0404A1-3-5	1/4" X 4", RECTANGLE, AS EXTRUDED, W/F	974	H02	RECTANGLE		CUREC01043	GOOD
5400095319	BY0404A1-3-6	1/8" X 1", RECTANGLE, AS EXTRUDED, W/F	1,074	H02	RECTANGLE		CUREC01085	GOOD
5400095320	BY0404A1-3-7	3/8" X 2-1/2", RECTANGLE	1,138	H02	RECTANGLE		CUREC00265	GOOD
5400095309	11S00606	5-1/4" DIA, ROUND, CAST/TURNED, 4.26 FT	2,072	H02	ROUND, CAST/TURNED		CURD01398	GOOD
5400095309	11W00369	6-1/2" DIA, ROUND, CAST/TURNED, 4.26 FT	1,063	H02	ROUND, CAST/TURNED		CURD00066	GOOD
Chemical/Physical	Element	Cu	Pb	Fe	Zn		T.S., Ksi	EL, %
Composition, %	Spec							HRB
5400086487	BY0404A1-3-3	60.200	2.700	0.200	Rem.			
5400095315	BY0404A1-4-5	60.870	2.740	0.220	Rem.		51.16	44.24
5400095315	BY0404A1-3-4	60.800	2.630	0.220	Rem.		80.21	42.26
5400095315	BY0404A1-3-5	60.200	2.700	0.200	Rem.		59.90	43.21
5400095319	BY0404A1-3-6	60.700	2.620	0.200	Rem.		54.29	43.82
5400095320	BY0404A1-3-7	60.200	2.600	0.220	Rem.		59.91	43.20
5400095309	11S00606	60.240	2.880	0.260	Rem.		54.62	43.78
5400095309	11W00369	60.580	2.850	0.250	Rem.		N/A	N/A

SIGNED FOR BOOYOUNG IND.

Lloyds Pacific International, Inc.

From: Copper and Brass Sales

Cust: ONLINE METALS

Part: 4745

Wgt: 12.000 LB

Del: 2401724595

PO: 70543

Date: 02/28/2012

James K. Baber

Figure E-7. 1/16 in. (1.6 mm) Diameter, C360 Brass Round Bar

CERTIFICATE OF TEST

Customer COPPER AND BRASS SALES INC.

No 2011-11-23-055

Invoice No 401202K11

Date 11/23/11

P.O. No 5400121368

Commodity CDA 360 FREE CUTTING BRASS ROD IN 12 FT L

Mil & Melting DAECHEUNG, KOREA

Spec PER ASTM B 15/B16M, RV. 2010, ROHS COMPLIANT

Job No.	11-04-	DESCRIPTION	Quantity	Temper	Remarks	B/D No.	Mat No.	Inspection Result
Line No.	Lot No.	SIZE	Pieces	WTL, Lbs				Dimension Surface
0010	11-08-A1107-103	3/16" (+/-0.003) DPS, HEXAGON, S.C., W/PACK	1,003	H02	HEX.S.C.		CUHEX00002	GOOD GOOD
0020	33003-1	7/64" (+/-0.0013) DIA, ROUND, W/PACKING	1,909	H02	ROUND		CURD01212	GOOD GOOD
0030	33004-1	1/8" (+/-0.0013) DIA, ROUND, W/PACKING	1,966	H02	ROUND		CURD00223	GOOD GOOD
0040	33006-1	13/64" (+/-0.0015) DIA, ROUND, W/PACKING	979	H02	ROUND		CURD00082	GOOD GOOD
0050	33007-1	13/64" (+/-0.0015) DIA, ROUND, W/PACKING	2,971	H02	ROUND		CURD00082	GOOD GOOD
0100	11-08-A1107-103	3/16" (+/-0.003) DPS, HEXAGON, S.C., W/PACK	2,162	H02	HEX.S.C.		CUHEX00002	GOOD GOOD
0110	33005-1	5/32" (+/-0.0015) DIA, ROUND, W/PACKING	1,953	H02	ROUND		CURD01263	GOOD GOOD
0120	33008-1	13/64" (+/-0.0015) DIA, ROUND, W/PACKING	952	H02	ROUND		CURD00282	GOOD GOOD
0130	33065-1	3/8" (+/-0.0015) DIA, ROUND	1,942	H02	ROUND		CURD00231	GOOD GOOD
0140	33066-1	1/2" (+/-0.0015) DIA, ROUND	2,334	H02	ROUND		CURD00895	GOOD GOOD
0150	33031-1	5/8" (+/-0.002) DIA, ROUND	1,565	H02	ROUND		CURD00452	GOOD GOOD
0160	33045-1	3/4" (+/-0.002) DIA, ROUND	2,979	H02	ROUND		CURD00117	GOOD GOOD
0170	33052-1	1" (+/-0.002) DIA, ROUND	1,940	H02	ROUND		CURD01087	GOOD GOOD
0180	32948-1	1-1/2" (+/-0.0025) DIA, ROUND	1,799	H02	ROUND		CURD00360	GOOD GOOD
0190	11-08-A1118-129	3/16" (+/-0.0035) DPS, SQUARE, W/PACKING	2,167	H02	SQUARE		CUSQ00007	GOOD GOOD
0200	33204-1	2-3/4" (+/-0.025) DPS, SQUARE	1,984	H02	SQUARE		CUSQ00024	GOOD GOOD
Chemical/Physical Element								
		Cu	Pb	Fe			Zn	
Composition, %	Spec	60.0-63.0	2.50-3.00	0.35 max			T.S., Ksi	Y.S., Ksi
								E/L (%)
0010	11-08-A1107-103	60.357	2.743	0.163			75	54
0020	33003-1	60.562	2.711	0.218			80	57
0030	33004-1	60.562	2.711	0.218			81	62
0040	33006-1	60.296	2.790	0.222			78	68
0050	33007-1	60.296	2.790	0.222			81	69
0100	11-08-A1107-103	60.357	2.743	0.163			75	54
0110	33005-1	60.296	2.790	0.222			82	66
0120	33008-1	60.296	2.790	0.222			77	64
0130	33065-1	60.690	2.788	0.201			64	49
0140	33066-1	60.690	2.788	0.201			64	42
0150	33031-1	60.889	2.855	0.218			59	43
0160	33045-1	60.769	2.669	0.218			57	34
0170	33052-1	60.645	2.879	0.214			59	40
0180	32948-1	60.433	2.725	0.181			52	32
0190	11-08-A1118-129	60.565	2.776	0.155			74	53
0200	33204-1	60.940	2.694	0.181			51	21

SIGNED FOR DAE CHANG IND.

Lloyds Pacific International, Inc.

Lloyds Pacific Materials NA, Inc.
Copper and Brass Sales Div sold to:
CUSTOMER: *Online Metals*
YOUR PO#: *72159*
CBS ORDER#: *1701088109*
QTY: *100 PC*
BY: *WJ* DATE: *9/20/12*

Cust: ONLINE METALS
Part: 1255
Wgt: 54.240 LB

PO: 70154
Date: 02/21/2012
Del: 2401711062

Paul D. Hill

Figure E-8. 1/8 in. (3.2 mm) Diameter C360 Brass Round Bar



METALLURGICAL TEST REPORT

6870 Highway 42 East
Ghent, KY 41045-9615
(502) 347-6000

Certificate: 747042 05 Mail To: Ship To: Date: 6/19/2012 Page: 1 Of 1
COPPER AND BRASS SALES, INC. COPPER AND BRASS SALES, INC.
ATTN: ACCOUNTS PAYABLE 8001 MURPHY WAY
SOUTHFIELD MI 48086- NORTHWOOD OH 43619
Customer: 0925 045 Leg Length: Steel: 304/304L
NAS Order: LN 84917 8 Length: 144.00 in
Your Order: 5400144908 Corrosion: ASTM A262 Prac A/E OK
Item Code:

PRODUCT DESCRIPTION:

Round Bar, Annealed, Cold Draw
UNS 30400/30403 EN 10204 3.1, ASTM A484/10
ASTM A276/10, ASTM A479/11, ASTM A182/10 CHEM ONLY,
ASME SA479/10a, ASME SA182/10 CHEM ONLY
AMS 5639H, AMS 5647J, AMS QQS-763B, QQS-763F
SOLUTION ANNEAL TEMP 1900F MIN

REMARKS:

COMPLIES W/REQUIREMENTS OF DFARS EU DIRECTIVE 2002.95.
EC. RoHS. EAF+AOD+CC. NO WELD REPAIR. MELTED AND MFG IN USA
FREE FROM MERCURY AND LOW MELTING ALLOY CONTAMINATION

Bundle Weight	Bundle Weight	Bundle Weight	Bundle Weight	Bundle Weight	Bundle Weight	Bundle Weight	Bundle Weight	Bundle Weight
BE68874	785	BE68882	1184					

CHEMICAL ANALYSIS

Heat	Supplier #	CM	C %	CO %	CR %	CU %	MN %	MO %	N %	NI %	P %	S %
C7H1		US	.013	.15	18.14	.36	1.45	.29	.084	8.51	.031	.0230
SI %			.32									

MECHANICAL PROPERTIES

	Id	HB	.2YS	UTS	RA	Elong
	o i	No.	KSI	KSI	%	% 2"
BE68874	R L	231.0	97.60	114.36	72.89	38.50
BE68882	R L	231.0	97.60	114.36	72.89	38.50

NAS hereby certifies that the analysis on this certification is correct. Based upon the results and the accuracy of the test methods used, the material meets the specifications stated. These results relate only to the items tested and this report cannot be reproduced, except in its entirety, without the written approval of NAS

Technical
Dept. Mgr.

ERIC HESS

James K. Baber

Del: 2401972572

PO: 76771

Date: 07/23/2012

From: Copper and Brass Sales

Cust: ONLINE METALS

Part: 73

Wgt: 102.000 LB

Figure E-9. 1/4 in. (6.4 mm) Diameter, T-304 Stainless Steel Round Bar



**NORTH AMERICAN
STAINLESS**

METALLURGICAL TEST REPORT

6870 Highway 42 East
Ghent, KY 41045-9615
(502) 347-6000

Certificate: 729117 03	Mail To: COPPER AND BRASS SALES, INC. ATTN: ACCOUNTS PAYABLE SOUTHFIELD MI 48086-	Ship To: COPPER AND BRASS SALES, INC. CUSTOMER PICKUP GHENT KY 41045	Date: 4/16/2012 Page: 1 OF 1 Steel: 304/304L Finish: Cold Draw Dia/Thk: .1875 in Leg Length: Length: 144.00 in Corrosion: ASTM A262 Frac A/E OK
Customer: 0925 022			
NAS Order: LN 82470 1			
Your Order: 5400136908	Item Code: SSRD00618		

PRODUCT DESCRIPTION:

Round Bar, Annealed, Cold Draw
UNS 30400/30403 EN 10204 3.1, ASTM A484/10
ASTM A276/10, ASTM A479/10a, ASTM A182/10 CHEM ONLY,
ASME SA479/10a, ASME SA182/10 CHEM ONLY
AMS 5639H, AMS 5647J, AMS QQS-763B, QQS-763F
SOLUTION ANNEAL TEMP 1900F MIN

REMARKS:

COMPLIES W/REQUIREMENTS OF DFARS EU DIRECTIVE 2002.95.
EC. RoHS. EAF+AOD+CC. NO WELD REPAIR. MELTED AND MFG IN USA
FREE FROM MERCURY AND LOW MELTING ALLOY CONTAMINATION

Bundle Weight	Bundle Weight	Bundle Weight	Bundle Weight	Bundle Weight	Bundle Weight	Bundle Weight	Bundle Weight	Bundle Weight
BE54079 1248	BE54080 1041	BE54081 1192	BE54082 1172					

CHEMICAL ANALYSIS CM(Country of Melt) ES(Spain) US(United States) ZA(South Africa) JP(Japan)

Heat	Supplier #	CM	C	CO	CR	CU	MN	MO	N	NI	P	S
COP5		US	.029	.25	18.16	.50	1.33	.37	.072	8.53	.030	.0250
			SI									
			.27									

MECHANICAL PROPERTIES

	1 d o i c r	HB No.	.2YS KSI	UTS KSI	RA %	Elong % 2"
BE54079	R L	238.0	98.20	114.52	81.21	30.72
BE54080	R L	238.0	98.20	114.52	81.21	30.72
BE54081	R L	238.0	98.20	114.52	81.21	30.72
BE54082	R L	238.0	98.20	114.52	81.21	30.72

NAS hereby certifies that the analysis on this certification is correct and the material meets the specifications stated.

Technical Dept. Mgr.

ERIC HESS

Figure E-10. 3/16 in. (4.8 mm) Diameter, T-304 Stainless Steel Round Bar

Certified Report Of Chemical Analysis And Mechanical Tests

Date Shipped: 5/26/2009

Sales Order: 423794001
 Sold To: STATE STEEL SUPPLY CO
 214 COURT STREET P.O. BOX 3224 SIOUX CITY IA
 STATE STEEL SUPPLY CO(RAIL)
 Ship To: 214 COURT STREET - RAIL SIOUX CITY IA

Customer PO: P90323BL002/4

Product Description: ASTM A1011 GRD 50XF

Hot Band Prime ASTM A1011 GRD 50XF 0.1290 Min x 80.2500 in

Heat Chemistry %

Heat	C	Mn	P	S	Si	Cu	B	Cr	V	Ti	Co	Al	N	Ni	Mo	Ca	SN
88471	0.06	0.87	0.008	0.007	0.025	0.01	0.000	0.02	0.001	0.017	0.018	0.039	0.0059	0	0.01	0.004	0.002

Heat Physicals

Yield PSI	Yield MPa	UTS PSI	UTS MPa	Elongation %	Direction
54200	374	65200	449	32.2	L
56300	388	66500	458	31.3	L

Shipment Tags Represented By Preceding Heat Results

Tag #	Load	Gauge	Width	Length
06582707	01325949	0.129	60.25	Coil

All tests were performed by ArcelorMittal - Indiana Harbor, unless specified, in accordance with the following: chemical analysis per ASTM E415 and E1019; mechanical test per ASTM E8 and E646, JIS Z2241, 2253 and 2254, EN 10002-1; Rockwell hardness per ASTM E18; coating weight per ASTM A754, A90, and A428. All tests are performed to the current version of the standard, unless otherwise noted. All tensile testing performed with gauge length of 2 inches. These results relate only to the items tested. Information about measurement uncertainty, when applicable, is available upon request. ArcelorMittal - Indiana is A2LA certified. Charpy testing is performed by ArcelorMittal - Burns Harbor, an A2LA certified facility.

We hereby certify the above is correct as contained in the records of the corporation.
 ArcelorMittal, Indiana Harbor West - Quality Assurance Department

Peter D. Carey

20

Gauge 10 Sheet Steel

Figure E-11. 10-Gauge Sheet Steel

Arcelor

ArcelorMittal
 Indiana Harbor West
 3001 Dickey Road
 East Chicago, IN 46312



ESSAR Steel Algoma Inc. 105 West Street, Sault Ste. Marie, Ontario Canada P6A 7B4

CUSTOMER PURCHASE ORDER NUMBER P90728BL002	ENTRY DATE 2009/07/31	SHIP DATE 2009/09/08	INVOICE NUMBER 140719	SUPPLIER'S NO. 03-5628	CARRIER GTW	PAGE -187955
---	--------------------------	-------------------------	--------------------------	---------------------------	----------------	-----------------

CHANGE TO CUSTOMER NAME AND ADDRESS

STATE STEEL SUPPLY CO.
214 COURT STREET
SIOUX CITY IOWA 51102
P.O. BOX 3224

SHIP TO CUSTOMER NAME AND ADDRESS

STATE STEEL SUPPLY CO.
214 COURT STREET
SIOUX CITY, IOWA 51102
IOWA

MILL TEST REP

ESSAR STEEL ALGOMA INC. CERTIFIES THAT THE MATERIAL DESCRIBED WAS MADE AND ACCORDANCE WITH THE RLA SPECIFICATION SHOWN. ALL ARE RETAINED IN ACCORDANCE WITH COMPANY'S STANDARD RECORD PRACTICES.

J. JOHNSTON
MANAGING METALLURGIST

THIS MILL TEST REPORT MAY BE REPRODUCED EXCEPT IN FULL WRITTEN APPROVAL OF ESSAR ALGOMA INC. IF YOU RECEIVE DOCUMENT AND ARE NOT THE RECEIVER, PLEASE CALL (70) COLLECT FOR INSTRUCTIONS OF DISPOSAL OF DOCUMENT.

SUPPLEMENTARY INSTRUCTIONS

TEST CERT 1: BOB LANSWORTH 712-277-3306 TEST CERT 2: PLATE TE ST COUPON:

GROUP TEST REPORTS REQUIRED 2000115860 WS

CUSTOMER USE RESALE 2009/09/18 12:32

MEETS EN 10204 3.1
HEATS INDICATED WITH (+) MADE IN CANADA WITH DOMESTIC AND NORTH AMERICAN MATERIALS

***** PRODUCT SHIPPED *****

CUSTOMER ITEM 00002 OUR ITEM 001 DIMENSIONS .112 MIN X 60.25 X COIL

COIL NUMBER	HEAT	NO. PIECES	WEIGHT	COIL NUMBER	HEAT	NO. PIECES	WEIGHT
63526011	6946J-01	1	40600	63526012	6946J-51	1	40740

***** MECHANICAL PROPERTIES *****

TENSILE TESTS:

HEAT	SAMPLE	GAUGE	COND	METH	DIR	YIELD	TENSILE	% ELONG	LAB
6946J	SRCE	.1120	AR	.2	L	55.5	68.0	32(2")	ALG

***** CHEMICAL PROPERTIES *****

HEAT	(WT %)	C	MN	P	S	SI	CR	NI	CU	MO	AL	CB	V	B
6946J +		.06	.46	.007	.003	.02	.02	.02	.05	.00	.021	.006	.031	.00280

****WARNING**** THE TEST RESULTS AND VALUES REPORTED HEREIN INDICATE ONLY THAT (1) THE PARTICULAR STEEL FOR WHICH THIS CERTIFICATE IS ISSUED MEETS THE MINIMUM SPECIFIED YIELD STRENGTH AND (2) THE CHEMICAL ANALYSIS AND PHYSICAL PROPERTIES OF SUCH STEEL ARE IN CONFORMANCE WITH THE REQUIREMENTS OF THE SPECIFICATION INDICATED. THE RESULTS OR VALUES REPORTED HEREIN CAN NOT BE USED TO QUALIFY THE STEEL FOR ANY SPECIFICATION OTHER

Gauge 11 Sheet Steel

Figure E-12. 11-Gauge Sheet Steel

ESSAR Steel Algoma Inc. 105 West Street, Sault Ste. Marie, Ontario Canada P6A 7B4

CUSTOMER PURCHASE ORDER NUMBER: P90728BL002 ENTRY DATE: 2009/07/31 SHIP DATE: 2009/09/08 TALLY NUMBER: 140893 SHIPPER'S NO.: - CAUSE: IC -299670

CHARGE TO CUSTOMER NAME AND ADDRESS: STATE STEEL SUPPLY CO. 214 COURT STREET SIOUX CITY IOWA 51102 P.O. BOX 3224

SHIP TO CUSTOMER NAME AND ADDRESS: STATE STEEL SUPPLY CO. 214 COURT STREET SIOUX CITY, IOWA 51102 IOWA

MILL TEST REPORT
ESSAR STEEL ALGOMA INC. CERTIFIES THAT THE PARTS DESCRIBED WAS MADE AND ACCORDANCE WITH THE AISI SPECIFICATION SHOWN. ALL ARE RETAINED IN ACCORDANCE WITH COMPANY'S STANDARD RECORD PRACTICES.

J. JOHNSTON
MANAGING METALLURGIST

CUSTOMER SPECIFICATION
HOT ROLLED STEEL SHEET - HSLA - ASTM A1011 GR 50 HSLA-F (07) - DO - TEMPER ROLLED - CUT EDGE ACCEPTABLE - RESTRICTED GAUGE 1/2 TOLERANCE - HSLA MODERATE FORMING SEMI-CRIT SURFACE STD SHPE

SUPPLEMENTARY INSTRUCTIONS
TEST CERT 1: BOB LANSWORTH 712-277-3306 TEST CERT 2: PLATE TE ST COUPON:

QUANTITY: TEST REPORTS REQUIRED 2000115881 WS
CUST USE: RESALE 2009/09/09 15:55

MEETS EN 10204 3.1
HEATS INDICATED WITH (+) MELTED AND ROLLED IN CANADA WITH IMPORTED AND DOMESTIC PARTS

***** PRODUCT SHIPPED *****

CUSTOMER ITEM 00001 OUR ITEM 002 DIMENSIONS .097 MIN X 60.25 X COIL

COIL NUMBER	HEAT	NO. PIECES	WEIGHT	COIL NUMBER	HEAT	NO. PIECES	WEIGHT
63526025	6947J-03	1	38990				

***** MECHANICAL PROPERTIES *****

TENSILE TESTS:

HEAT	SRC	GAGE	COND	METH	DIR	YIELD KSI	TENSILE KSI	% ELONG	LAB
6947J	DSPC	.0970	AR	.2	L	55.5	66.5	36(2")	ALC

***** CHEMICAL PROPERTIES *****

HEAT	(WT %)	C	MN	P	S	SI	CR	NI	CU	MO	AL	CB	V	B
6947J +		.05	.49	.009	.004	.02	.03	.02	.07	.06	.017	.006	.031	.00303

PAGE 3 OF 3

WARNING THE TEST RESULTS AND VALUES REPORTED HEREIN INDICATE ONLY THAT (1) THE PARTICULAR STEEL FOR WHICH THIS CERTIFICATE IS ISSUED MEETS THE MINIMUM SPECIFIED YIELD STRENGTH AND (2) THE CHEMICAL ANALYSIS AND PHYSICAL PROPERTIES OF SUCH STEEL ARE IN CONFORMANCE WITH THE REQUIREMENTS OF THE SPECIFICATION INDICATED. THE RESULTS OR VALUES REPORTED HEREIN CAN NOT BE USED TO QUALIFY THE STEEL FOR ANY SPECIFICATION OTHER THAN THAT FOR WHICH THIS CERTIFICATE IS ISSUED.

Gauge 12 Sheet Steel

Figure E-13. 12-Gauge Sheet Steel

ESSAR Steel Algoma Inc.		105 West Street, Sault Ste. Marie, Ontario Canada P6A 7B4			
CUSTOMER PURCHASE ORDER NUMBER P00420ER006	ENTRY DATE 2010/04/29	SHIP DATE 2010/05/21	TALLY NUMBER 178714	SHIPMENTS NO. -	CARRIER CM
PAGE					-187144
CHARGE TO CUSTOMER NAME AND ADDRESS STATE STEEL SUPPLY CO. 214 COURT STREET SIOUX CITY IOWA 51102 P.O. BOX 3224			SHIP TO CUSTOMER NAME AND ADDRESS STATE STEEL SUPPLY CO. 214 COURT STREET SIOUX CITY, IOWA 51102 IOWA		
CUSTOMER SPECIFICATION HOT ROLLED STEEL SHEET - HSLA - ASTM A1011 GR 50 HSLAS-P (07) - DQ - RESTRICTED GAUGE 1/2 TOLERANCE - HSLA MODERATE FORMING SEMI-CRIT SURFACE STD SHPE					MILL TEST REP ESSAR STEEL ALGOMA INC. CERTIFIES THAT THE MATERIAL DESCRIBED WAS MADE AND ACCORDANCE WITH THE RUL. SPECIFICATION SHOWS ALL ARE ASSURED IN ACCORDANCE COMPANY'S STANDARD RECORD PRACTICES. J. JOHNSTON MANAGING METALLURGIST THIS MILL TEST REPORT MAY REPRODUCE EXCEPT IN FULL WRITTEN APPROVAL OF ESSAR ALGOMA INC. IF YOU RECEIVE DOCUMENT AND ARE NOT THE RECEIVER, PLEASE CALL FOR COLLECT FOR INSTRUCTIONS OF DISPOSAL OF DOCUMENT
SUPPLEMENTARY INSTRUCTIONS TEST CERT 1: ERIC.RUBEL@STATESTEEL.COM TEST CERT 2: PLATE TES T COUPON:					
SHIP TO TEST REPORTS REQUIRED			2000146922 CM		
SHIP USE RESALE			2010/05/23 11:33		
MEETS EN 10204 3.1 ISO QUALITY AND ENVIRONMENTAL CERTIFICATES AVAILABLE AT WWW.ESSARSTEELALGOMA.COM HEATS INDICATED WITH (+) MADE IN CANADA WITH DOMESTIC AND NORTH AMERICAN MATERIALS					
***** PRODUCT SHIPPED *****					
CUSTOMER ITEM 00001 OUR ITEM 001 DIMENSIONS .071 MIN X 48.125 X COIL					
COIL NUMBER 9321171	HEAT-MS 4283K-05	NO. PIECES 1	WEIGHT 42500	COIL NUMBER 9500068	HEAT-MS 4283K-55
		NO. PIECES 1	WEIGHT 39850		
***** MECHANICAL PROPERTIES *****					
TENSILE TESTS:					
HEAT 4283K	* SAMPLE *	* TEST *	YIELD TENSILE	LAB	
	SRCE GAUGE	COND METH DIR	KSI KSI % ELONG	ALG	
	DSPC .0710	AR .2 L	53.3 70.0 31(2")		
***** CHEMICAL PROPERTIES *****					
HEAT (WT %)	C	MN	P	S	SI
	TI	SN	N	AS	CR
	.06	.46	.015	.004	.03
	.001		.0111		.04
				.03	.03
				.06	.01
				.022	
				.006	.032
					.00230

PAGE 3 OF 3

WARNING THE TEST RESULTS AND VALUES REPORTED HEREIN INDICATE ONLY THAT (1) THE PARTICULAR STEEL FOR WHICH THIS CERTIFICATE IS ISSUED MEETS THE MINIMUM SPECIFIED YIELD STRENGTH AND (2) THE CHEMICAL ANALYSES AND PHYSICAL PROPERTIES OF SUCH STEEL ARE IN CONFORMANCE WITH THE REQUIREMENTS OF THE SPECIFICATION INDICATED. THE RESULTS OR VALUES REPORTED HEREIN CAN NOT BE USED TO QUALIFY THE STEEL FOR ANY SPECIFICATION OTHER THAN THE ONE INDICATED AND CAN NOT BE RELIED UPON FOR ANY PURPOSE (INCLUDING DESIGN OR CALCULATIONS) AS REPRESENTING THE ACTUAL STRENGTH OF SUCH STEEL.

Gauge 14 Sheet Steel

Figure E-14. 14-Gauge Sheet Steel

END OF DOCUMENT